ABIOTIC STRESSES IN AGROECOLOGY: A CHALLENGE FOR WHOLE PLANT PHYSIOLOGY

EDITED BY: Urs Feller, Alison H. Kingston-Smith and Mauro Centritto
PUBLISHED IN: Frontiers in Plant Science and Frontiers in Environmental Science

frontiers Research Topics

frontiers

ISSN 1664-8714
ISBN 978-2-88945-204-0
DOI 10.3389/978-2-88945-204-0

About Frontiers

Frontiers is more than just an open-access publisher of scholarly articles: it is a pioneering approach to the world of academia, radically improving the way scholarly research is managed. The grand vision of Frontiers is a world where all people have an equal opportunity to seek, share and generate knowledge. Frontiers provides immediate and permanent online open access to all its publications, but this alone is not enough to realize our grand goals.

Frontiers Journal Series

The Frontiers Journal Series is a multi-tier and interdisciplinary set of open-access, online journals, promising a paradigm shift from the current review, selection and dissemination processes in academic publishing. All Frontiers journals are driven by researchers for researchers; therefore, they constitute a service to the scholarly community. At the same time, the Frontiers Journal Series operates on a revolutionary invention, the tiered publishing system, initially addressing specific communities of scholars, and gradually climbing up to broader public understanding, thus serving the interests of the lay society, too.

Dedication to Quality

Each Frontiers article is a landmark of the highest quality, thanks to genuinely collaborative interactions between authors and review editors, who include some of the world's best academicians. Research must be certified by peers before entering a stream of knowledge that may eventually reach the public - and shape society; therefore, Frontiers only applies the most rigorous and unbiased reviews.
Frontiers revolutionizes research publishing by freely delivering the most outstanding research, evaluated with no bias from both the academic and social point of view.
By applying the most advanced information technologies, Frontiers is catapulting scholarly publishing into a new generation.

What are Frontiers Research Topics?

Frontiers Research Topics are very popular trademarks of the Frontiers Journals Series: they are collections of at least ten articles, all centered on a particular subject. With their unique mix of varied contributions from Original Research to Review Articles, Frontiers Research Topics unify the most influential researchers, the latest key findings and historical advances in a hot research area! Find out more on how to host your own Frontiers Research Topic or contribute to one as an author by contacting the Frontiers Editorial Office: **researchtopics@frontiersin.org**

ABIOTIC STRESSES IN AGROECOLOGY: A CHALLENGE FOR WHOLE PLANT PHYSIOLOGY

Topic Editors:
Urs Feller, University of Bern, Switzerland
Alison H. Kingston-Smith, Aberystwyth University, UK
Mauro Centritto, National Research Council, Italy

Corn (Zea mays L.) leaves exposed to a severe drought period. Leaf rolling and anticipated/atypical senescence are major visible symptoms of insufficient water supply. Drought may affect yield even when leaves recover after the stress period.
Picture: Urs Feller

Cover image by Mauro Centritto - Argan (Argania spinosa) is an endemic tree of south-western Morocco where it is resistant to harsh conditions (poor soils, high radiative load and extreme drought, i.e. in a region where rainfall rarely exceeds 300 mm y-1, and at times is less than 120 mm y-1), where it plays a vital role in protecting the land from degradation.

Understanding plant responses to abiotic stresses is central to our ability to predict the impact of global change and environmental pollution on the production of food, feed and forestry. Besides increasing carbon dioxide concentration and rising global temperature, increasingly frequent and severe climatic events (e.g. extended droughts, heat waves, flooding) are expected in the coming decades. Additionally, pollution (e.g. heavy metals, gaseous pollutants such as ozone or sulfur dioxide) is an important factor in many regions, decreasing plant productivity and product quality.

This Research topic focuses on stress responses at the level of whole plants, addressing biomass-related processes (development of the root system, root respiration/fermentation, leaf expansion, stomatal regulation, photosynthetic capacity, leaf senescence, yield) and interactions between organs (transport via xylem and phloem, long-distance signaling and secondary metabolites). Comparisons between species and between varieties of the same species are helpful to evaluate the potential for species selection and genetic improvement.

This research topic is focused on the following abiotic stresses and interactions between them:

- Increased carbon dioxide concentration in ambient air is an important parameter influenced by global change and affects photosynthesis, stomatal regulation, plant growth and finally yield.
- Elevated temperature: both the steady rise in average temperature and extreme events of shorter duration (heat waves) must be considered in the context of alterations in carbon balance through increased photorespiration, decreased Rubisco activation and carboxylation efficiency, damage to photosynthetic apparatus, as well as loss of water via transpiration and stomatal sensitivity.
- Low temperatures (late frosts, prolonged cold phases, freezing temperature) can decrease overwintering survival rates, productivity of crop plants and species composition in meadows.
- Water availability: More frequent, severe and extended drought periods have been predicted by climate change models. The timing and duration of a drought period is crucial to determining plant responses, particularly if the drought event coincides with an increase in temperature. Drought causes stomatal closure, decreasing the cooling potential of transpiration and potentially leading to thermal stress as leaf temperature rises. Waterlogging may become also more relevant during the next decades and is especially important for seedlings and young plants. It is not the presence of water itself that causes the stress, but the exclusion of oxygen from the soil which causes a decrease in respiration and an increase in fermentation rates followed by a period of potential oxidative stress as water recedes.
- Salinity: high salt concentration in soil influences soil water potential, the water status of the plant and hence affects productivity. Salt tolerance will become an important trait driven by increased competition for land and the need to exploit marginal lands.

Citation: Feller, U., Kingston-Smith, A. H., Centritto, M., eds. (2017). Abiotic Stresses in Agroecology: A Challenge for Whole Plant Physiology. Lausanne: Frontiers Media.
doi: 10.3389/978-2-88945-204-0

Table of Contents

frontiers in Environmental Science

EDITORIAL
published: 20 April 2017
doi: 10.3389/fenvs.2017.00013

Editorial: Abiotic Stresses in Agroecology: A Challenge for Whole Plant Physiology

Urs Feller[1]*, *Alison H. Kingston-Smith*[2] *and Mauro Centritto*[3]

[1] *Institute of Plant Sciences and Oeschger Centre for Climate Change Research, University of Bern, Bern, Switzerland,* [2] *Institute of Biological, Environmental and Rural Sciences, Aberystwyth University, Aberystwyth, UK,* [3] *Tree and Timber Institute, National Research Council, Florence, Italy*

Keywords: climate change, salt, temperature, water availability, whole plant physiology

Editorial on the Research Topic

Abiotic Stresses in Agroecology: A Challenge for Whole Plant Physiology

Abiotic stresses in agroecology are caused by climatic factors (e.g., temperature and precipitation extremes), pollutants (e.g., heavy metals, gaseous pollutants) and salinity. In the context of global change, climatic factors become particularly important. The alarming, progressive alterations in climate caused by rising levels of carbon dioxide (CO_2) and other greenhouse gases in the atmosphere are linked to well-known consequences of climate change; increase in average global temperature and the melting of the polar ice caps (IPCC, 2014). In addition to these global problems, increased frequencies and severities of extreme events including heat waves, drought periods or waterlogging have significant impacts at local and regional levels (Schär et al., 2004; IPCC, 2012; Kelley et al., 2015; Knutti et al., 2016). Such events may strongly influence crop yields and the quality of agricultural products. The effects of stresses imposed by these factors individually and in combination are relevant in the context of agroecology and in developing new agricultural concepts taking into account soil quality, biodiversity, sustainability as well as social and economic aspects (Tomich et al., 2011; Lai, 2015). This Research Topic focuses on the impacts of abiotic stress at the whole plant level, the mechanisms involved in the stress responses and the potential to increase stress tolerance in field crops and trees.

Elevated CO_2 in the atmosphere caused by human activities is the major driver for global climate change that affects ambient temperature and precipitation patterns on global and regional scales, and water availability in soils as well as the frequency and severity of extreme events (IPCC, 2012, 2014). Atmospheric CO_2 may also directly influence primary metabolism and thereby plant growth and productivity as reported by Long et al. (2006), Centritto et al. (2011), Hasegawa et al. (2013), Haworth et al., Haworth et al., Martinez-Lüscher et al. Free-air CO_2 enrichment (FACE) facilities have been used to establish the impact of elevated CO_2 on the efficiency of radiation, water and nitrogen utilization, overall crop yields (Dugas and Pinter, 1994; Long et al., 2006), and the interactions between sink structures (Hasegawa et al., 2013). In this Research Topic, Martinez-Lüscher et al. investigated interactions between elevated CO_2 levels, ambient temperature and water availability in grapevine (*Vitis vinifera* L.) phenology from bud break to fruit maturation, while Haworth et al. addressed interactions between elevated CO_2, stomatal control and photosynthetic performance. Haworth et al. argue that because of the tendency in free-air CO_2 (FACE) experiments to publish more of significant results and less of nonsignificant results, the meta-analyses of results of such studies might lead to overestimation of the physiological impacts of rising CO_2 levels in the atmosphere. Therefore while the direction and significance of impacts

Edited and reviewed by:
P. K. Ramachandran Nair, University of Florida, USA

***Correspondence:**
Urs Feller
urs.feller@ips.unibe.ch

Specialty section:
This article was submitted to Agroecology and Land Use Systems, a section of the journal Frontiers in Environmental Science

Received: *31 January 2017*
Accepted: *27 March 2017*
Published: *20 April 2017*

Citation:
Feller U, Kingston-Smith AH and Centritto M (2017) Editorial: Abiotic Stresses in Agroecology: A Challenge for Whole Plant Physiology. Front. Environ. Sci. 5:13. doi: 10.3389/fenvs.2017.00013

reported in individual studies are not questioned by these considerations (Haworth et al.), caution is recommended when extrapolating such findings to world-wide productivity, especially as the interactions between atmospheric CO_2 levels and other environmental factors (e.g., temperature, water availability) and the physiological mechanisms behind these interactions remain to be further elucidated.

Water availability in the soil and water relations of plants are key parameters predicted to be influenced by global climate change through altered regional precipitation patterns. This subject was addressed in several papers (Jian et al.; Kunert et al.; Martinez-Lüscher et al.; Polania et al.; Zarrouk et al.). Drought effects on root architecture and nodule properties in legumes with symbiotic nitrogen fixation as well as the possibilities for genetic improvements were reviewed by Kunert et al. Extended drought periods not only affect the development and physiological functions of roots and vegetative shoots, but also influence redistribution of nutrients to pods and seeds of maturing beans (Polania et al.) or to ripening grape berries (Zarrouk et al.). From these reports it is evident that source/sink relationships are highly relevant in plants exposed to drought and perturbation affects the quantity and quality of yield. Salt stress is an important consideration in many regions (especially coastal zones) and while not directly related to global climatic change, there are some similarities to drought stress and interactions with other abiotic stress factors (Wang et al., 2003; Munns and Tester, 2008), for example microRNAs were found to be important for the germination of rapeseed (*Brassica napus* L.) seeds under drought or salt stress (Jian et al.). Transport processes across membranes are important for subcellular compartmentation (e.g., sequestration into the vacuole) as well as for long-distance transport processes (e.g., release into the root xylem followed by acropetal transport in the transpiration stream). A salt-specific mechanism was investigated in soybean (*Glycine max* (L.) Merr.) by Wei et al. These authors found that a Cl^-/H^+ antiporter (*GmCLC1*) contributed to salt tolerance and was involved in the retention of Cl^- ions in the roots and in decreasing the release to the shoot.

Besides the steady increase in average temperature caused by the elevated CO_2 concentration in the air, more frequent and more severe extreme events including heat waves and also cold phases have been predicted by climate models (Schär et al., 2004; IPCC, 2012). Elevated temperature may influence photosynthetic performance (e.g., via decreased Rubisco activase activity as reported by Scafaro et al., 2016), stomatal regulation (Reynolds-Henne et al., 2010; Feller and Vaseva, 2014), floret fertility (Prasad et al.) or ripening berries (Zarrouk et al.). These effects, which are all related to the source/sink network, have been clearly documented, but the overall effects of heat on various plant species and the mechanisms behind these effects are not yet well understood. A perspective paper on limitations to grassland productivity by low temperature was contributed by Wingler and Hennessy to this Research Topic and addresses issues of seasonality, breeding and epigenetic changes. The risk for freezing damage in woody perennial plants was evaluated in the context of global climate change in an opinion paper contributed by Arora and Taulavuori. These authors refer to cold acclimation prior to the cold season, dormancy and deacclimation (including the risk of premature deacclimation) and discuss physiological processes involved as well as their regulation.

Cytokinin may play an important role in the perception of environmental stresses (Argueso et al., 2009). Two papers in this Research topic are focused on the role of cytokinin in the response of plants to abiotic stresses (Golan et al.; Paul et al.). Transgenic *Arabidopsis* plants characterized by an overproduction of cytokinin were found to be less drought-susceptible and to be more productive under drought than control plants (Golan et al.). The avoidance of premature senescence in these drought-stressed plants and the mechanisms involved in the beneficial cytokinin effects were investigated. Paul et al. presented good evidence that cytokinin is important for the maintenance of meristematic functions in plants subjected to abiotic stress and that this protective effect in poplar (*Populus* × *canescens* (Aiton) Sm.) is important during the summer as well as during winter.

The response of plants to various abiotic stresses or to combinations of stresses is of practical relevance, since environmental disturbances are often characterized by coincidence of several factors (e.g., drought and elevated temperature) (Wang et al., 2003). Responses of plants to various stresses and combinations of stresses were addressed in several papers of this Research Topic (Gangadhar et al.; Martinez-Lüscher et al.; Zarrouk et al.). Gangadhar et al. characterized the functions of the thermo-tolerance gene *StnsLTP1* in enhancing the activation of the antioxidant defense system, thus contributing to tolerance to multiple abiotic stresses in potato. Kopecky et al. explored the evolution of polyploidy within the fescue [*Festuca pratensis* subsp. *apennina* (De Not.) Hegi] species and how this knowledge can contribute to improved stress tolerance in *Festulolium* cultivars to produce climate change resilient grasses. As mentioned by these authors as well as by others, the elucidation of breeding strategies is a key aspect to support farmers in a changing climate with more frequent and more severe extreme events (Humphreys et al., 2014).

All aspects presented in this Research Topic are relevant in the context of the impact of abiotic stress, but not all relevant aspects could be included in this Research Topic. The following aspects remain to be addressed or further emphasized in the future:

(a) Additional abiotic stresses not included here (e.g., pollution, unbalanced nutrient supply).
(b) Timing of stress phases (starting time, duration, single phase or multiple phases).
(c) Interplay between various abiotic stresses including the mechanisms behind the interactions.
(d) Further integration of processes at the whole-plant level including recovery phases.
(e) Separation of species-specific and more general effects.

(f) Identification of key proteins/genes for breeding (potential for improvements).
(g) Biophysical limits of crops to climatic extremes.

AUTHOR CONTRIBUTIONS

UF, AHK-S, and MC co-wrote this editorial based on the various contributions to this Research Topic.

ACKNOWLEDGMENTS

We thank all authors of contributions to this Research Topic for preparing high-quality manuscripts under a tight time schedule and the reviewers for critically evaluating the papers and for further improving them with their questions, comments, and suggestions. AHK-S acknowledges strategic support to IBERS, Aberystwyth University, from the Biotechnology and Biological Sciences Research Council (BBSRC).

REFERENCES

Argueso, C. T., Ferreira, F. J., and Kieber, J. J. (2009). Environmental perception avenues: the interaction of cytokinin and environmental response pathways. *Plant Cell Environ.* 9, 1147–1160. doi: 10.1111/j.1365-3040.2009.01940.x

Centritto, M., Tognetti, R., Leitgeb, E., Střelcová, K., and Cohen, S. (2011). "Above ground processes: anticipating climate change influences," in *Forest Management and the Water Cycle: An Ecosystem-Based Approach*, vol. 212, Ecological Studies, eds M. Bredemeier, S. Cohen, D. L. Godbold, E. Lode, V. Pichler, and P. Schleppi (Dordrecht: Springer), 31–64.

Dugas, W. A., and Pinter, P. J. Jr. (1994). Introduction to the free-air carbon dioxide enrichment (FACE) cotton project. *Agric. For. Meteorol.* 70, 1–2. doi: 10.1016/0168-1923(94)90043-4

Feller, U., and Vaseva, I. I. (2014). Extreme climatic events: impacts of drought and high temperature on physiological processes in agronomically important plants. *Front. Environ. Sci.* 2:39. doi: 10.3389/fenvs.2014.00039

Hasegawa, T., Sakai, H., Tokida, T., Nakamura, H., Zhu, C., Usui, Y., et al. (2013). Rice cultivar responses to elevated CO_2 at two free-air CO_2 enrichment (FACE) sites in Japan. *Funct. Plant Biol.* 40, 148–159. doi: 10.1071/FP12357

Humphreys, M., O'Donovan, S., Farrell, M., Gay, A., and Kingston-Smith, A. H. (2014). The potential of novel *Festulolium* (2n = 4x = 28) hybrids as productive, nutrient-use-efficient fodder for ruminants. *Food Energy Secur.* 3, 98–110. doi: 10.1002/fes3.50

IPCC (2012). "Summary for policymakers," in *Managing the Risks of Extreme Events and Disasters to Advance Climate Change Adaptation. A Special Report of Working Groups I and II of the Intergovernmental Panel on Climate Change,* eds C. B. Field, V. Barros, T. F. Stocker, D. Qin, D. J. Dokken, K. L. Ebi, M. D. Mastrandrea, K. J. Mach, G.-K. Plattner, S. K. Allen, M. Tignor, and P. M. Midgley (Cambridge, MA: Cambridge University Press), 1–19.

IPCC (2014). "Climate change 2014: mitigation of climate change," in *Contribution of Working Group III to the Fifth Assessment. Report of the Intergovernmental Panel on Climate Change*, eds O. Edenhofer, R. Pichs-Madruga, Y. Sokona, E. Farahani, S. Kadner, K. Seyboth, A. Adler, I. Baum, S. Brunner, P. Eickemeier, B. Kriemann, J. Savolainen, S. Schlömer, C. von Stechow, T. Zwickel, and J. C. Minx (Cambridge, MA: Cambridge University Press), 1–1435.

Kelley, C. P., Mohtadi, S., Cane, M. A., Seager, R., and Kushnir, Y. (2015). Climate change in the fertile crescent and implications of the recent syrian drought. *Proc. Natl. Acad. Sci. U.S.A.* 112, 3241–3246. doi: 10.1073/pnas.1421533112

Knutti, R., Rogelj, J., Sedláček, J., and Fischer, E. M. (2016). A scientific critique of the two-degree climate change target. *Nat. Geosci.* 9, 13–19. doi: 10.1038/NGEO2595

Lai, R. (2015). Restoring soil quality to mitigate soil degradation. *Sustainability* 7, 5875–5895. doi: 10.3390/su7055875

Long, S. P., Ainsworth, E. A., Leakey, A. D., Nösberger, J., and Ort, D. R. (2006). Food for thought: lower-than-expected crop yield stimulation with rising CO_2 concentrations. *Science* 312, 1918–1921. doi: 10.1126/science.1114722

Munns, R., and Tester, M. (2008). Mechanisms of salinity tolerance. *Annu. Rev. Plant Biol.* 59, 651–681. doi: 10.1146/annurev.arplant.59.032607.092911

Reynolds-Henne, C. E., Langenegger, A., Mani, J., Schenk, N., Zumsteg, A., and Feller, U. (2010). Interactions between temperature, drought and stomatal opening in legumes. *Environ. Exp. Bot.* 68, 37–43. doi: 10.1016/j.envexpbot.2009.11.002

Scafaro, A. P., Gallé, A., Van Rie, J., Carmo-Silva, E., Salvucci, M. E., and Atwell, B. J. (2016). Heat tolerance in a wild *Oryza* species is attributed to maintenance of Rubisco activation by a thermally stable Rubisco activase ortholog. *New Phytol.* 211, 899–911. doi: 10.1111/nph.13963

Schär, C., Vidale, P. L., Lüthi, D., Frei, C., Häberli, C., Liniger, M. A., et al. (2004). The role of increasing temperature variability in European summer heatwaves. *Nature* 427, 332–336. doi: 10.1038/nature02300

Tomich, T. P., Brodt, S., Ferris, H., Galt, R., Horwath, W. R., Kebreab, E., et al. (2011). Agroecology: a review from a global-change perspective. *Annu. Rev. Environ. Resour.* 36, 193–222. doi: 10.1146/annurev-environ-012110-121302

Wang, W. X., Vinocur, B., and Altman, A. (2003). Plant responses to drought, salinity and extreme temperatures: towards genetic engineering for stress tolerance. *Planta* 218, 1–14. doi: 10.1007/s00425-003-1105-5

Conflict of Interest Statement: The authors declare that the research was conducted in the absence of any commercial or financial relationships that could be construed as a potential conflict of interest.

frontiers in Environmental Science

ORIGINAL RESEARCH
published: 12 July 2016
doi: 10.3389/fenvs.2016.00048

Sensitivity of Grapevine Phenology to Water Availability, Temperature and CO_2 Concentration

Johann Martínez-Lüscher[1, 2], Tefide Kizildeniz[3], Višnja Vučetić[4], Zhanwu Dai[5], Eike Luedeling[6, 7], Cornelis van Leeuwen[5], Eric Gomès[5], Inmaculada Pascual[3], Juan J. Irigoyen[3], Fermín Morales[8] and Serge Delrot[5]*

[1] School of Agriculture, Policy and Development, University of Reading, Reading, UK, [2] Genetics and Crop Improvement Program, East Malling Research, East Malling, UK, [3] Grupo de Fisiología del Estrés en Plantas, Departamento de Biología Ambiental (Unidad Asociada al CSIC, EEAD, Zaragoza e ICVV, Logroño, Spain), Facultades de Ciencias y Farmacia, Universidad de Navarra, Pamplona, Spain, [4] Meteorological Research and Development Division, Agrometeorological Department, Meteorological and Hydrological Service, Zagreb, Croatia, [5] UMR 1287, EGFV, Bordeaux Sciences Agro, Institut National de la Recherche Agronomique, Université de Bordeaux, Villenave d'Ornon, France, [6] World Agroforestry Centre, Nairobi, Kenya, [7] Centre for Development Research (ZEF), University of Bonn, Bonn, Germany, [8] Departamento de Nutrición Vegetal, Estación Experimental de Aula Dei, CSIC, Zaragoza, Spain

OPEN ACCESS

Edited by:
Urs Feller,
University of Bern, Switzerland

Reviewed by:
Claudio Lovisolo,
University of Turin, Italy
Maren Müller,
University of Barcelona, Spain

***Correspondence:**
Johann Martínez-Lüscher
jmluscher@gmail.com

Specialty section:
This article was submitted to Agroecology and Land Use Systems, a section of the journal Frontiers in Environmental Science

Received: *29 April 2016*
Accepted: *09 June 2016*
Published: *12 July 2016*

Citation:
Martínez-Lüscher J, Kizildeniz T, Vučetić V, Dai Z, Luedeling E, van Leeuwen C, Gomès E, Pascual I, Irigoyen JJ, Morales F and Delrot S (2016) Sensitivity of Grapevine Phenology to Water Availability, Temperature and CO_2 Concentration. Front. Environ. Sci. 4:48. doi: 10.3389/fenvs.2016.00048

In recent decades, mean global temperatures have increased in parallel with a sharp rise in atmospheric carbon dioxide (CO_2) levels, with apparent implications for precipitation patterns. The aim of the present work is to assess the sensitivity of different phenological stages of grapevine to temperature and to study the influence of other factors related to climate change (water availability and CO_2 concentration) on this relationship. Grapevine phenological records from 9 plantings between 42.75°N and 46.03°N consisting of dates for budburst, flowering and fruit maturity were used. In addition, we used phenological data collected from 2 years of experiments with grapevine fruit-bearing cuttings with two grapevine varieties under two levels of water availability, two temperature regimes and two levels of CO_2. Dormancy breaking and flowering were strongly dependent on spring temperature, while neither variation in temperature during the chilling period nor precipitation significantly affected budburst date. The time needed to reach fruit maturity diminished with increasing temperature and decreasing precipitation. Experiments under semi-controlled conditions revealed great sensitivity of berry development to both temperature and CO_2. Water availability had significant interactions with both temperature and CO_2; however, in general, water deficit delayed maturity when combined with other factors. Sensitivities to temperature and CO_2 varied widely, but higher sensitivities appeared in the coolest year, particularly for the late ripening variety, 'White Tempranillo'. The knowledge gained in whole plant physiology and multi stress approaches is crucial to predict the effects of climate change and to design mitigation and adaptation strategies allowing viticulture to cope with climate change.

Keywords: climate change, viticulture, fruit development, ripening, chilling, dormancy, partial least squares regression

INTRODUCTION

Evolution of Environmental Factors Linked to Climate Change

Analyses of historic climatic changes indicate an increase in mean land surface temperature by 1.06°C over a period of more than 100 years, with the lion's share of this amount—0.85°C—occurring over the past two decades (IPCC, 2014b). Climate projections for the end of the 21st century forecast increases in temperature within a rather wide range, from stabilization at 1.5°C higher than the current reference period to a more than 4°C increase in average global temperature, depending on the mitigation measures adopted (IPCC, 2014a). The main driver of the temperature increase has been human emission of greenhouse gases. Among these, CO_2 is the most relevant in volume and global effect (IPCC, 2014a), with its concentrations increasing from a preindustrial level of 280 $\mu L\ L^{-1}$ to currently more than 400 $\mu L\ L^{-1}$ in 2016, with predictions for the end of the century ranging from 421 to a 936 $\mu L\ L^{-1}$ (Meinshausen et al., 2011). Rainfall in many major wine growing regions of the world has decreased and is expected to decrease further in the future (IPCC, 2014b).

Dependence of Grapevine on Temperature

Important effects of temperature on grapevine (*Vitis vinifera* L.) have long been recognized as influencing plant physiology, berry composition and ultimately wine characteristics (Jones et al., 2005; Bonada and Sadras, 2015). Thermal time integrals are even used as one of the main criteria to assess the suitability of a given cultivar to a given location (Gladstones, 1992). Premium commercial vineyards have been traditionally distributed across a relatively wide range of latitudes, ranging from the subtropics to temperate climates like the south of England (at 53°N). Across this range, temperature during dormancy and growing season varies widely (Jones, 2006, 2007). However, the distribution of grape growing regions is not necessarily aligned with the acclimation or adaptation thresholds of the species, and in the case of quality wine production, the upper temperature limits are hard to assess even at the variety level (van Leeuwen et al., 2013). Evidence of the plasticity of this species and the apparent lack of thermal restrictions for growing grapes is the recent increase in production of both table and wine grapes in subtropical and tropical areas (Demir, 2014).

Temperature Thresholds for Wine Typicity

Although basic climatic conditions for grape growing are easily satisfied, rising temperatures may make it difficult to consistently fulfill specific criteria required for grape quality in many places without adjusting variety, clone or accession within a given variety, or changing management practices. This is especially relevant for wine grapes, as most wine appellations in the world aim to deliver a very specific product, resulting from the wine-making, grapevine genetic material (cultivar and clone), cultural practices, edaphic factors and climatic conditions (van Leeuwen et al., 2004). Final grape composition results from numerous processes leading to accumulation and/or decay of metabolites, which are affected to a considerable degree by climatic conditions (Kuhn et al., 2014). Consequently, aromas, aroma precursors, phenolic compounds, organic acids, and sugars have very different accumulation patterns throughout grape development and, what is most relevant, their responses to increasing temperatures may differ in magnitude. The best example is that temperature increases can enhance both sugar accumulation and organic acid decay, but acidity is more affected than sugar levels. This results in lower acidity for the same sugar level in grapes grown under warmer conditions (Lakso and Kliewer, 1975; Sweetman et al., 2009; Etienne et al., 2013). This decoupling has been reported for other relevant metabolites, such as anthocyanins (decreasing the anthocyanin/sugar ratio) (Sadras and Moran, 2012; Martínez-Lüscher et al., 2016), proanthocyanidins (Cohen et al., 2012) and aromas (Bonada et al., 2015). In contrast, a decoupling of anthocyanins and sugars was reported with increasing water stress, in favor of anthocyanins in Cabernet Sauvignon (Sadras et al., 2007). During the ripening period, in summer, elevated temperature and drought occur simultaneously, and therefore, the effects on the decoupling of anthocyanins and sugars can be moderate due to the contrasting responses elicited by these two factors. In this sense, Sadras and Moran (2012) reported that restricted water supply during berry development can contribute to partially restore anthocyanin/sugar ratios disrupted by high temperature.

Relationship between Wine Composition and Altered Phenology

Despite the scarcity of data, some attempts have been undertaken to relate grape composition to records of environmental conditions (Bonada and Sadras, 2015). Grapevine phenology records, however, are relatively abundant and can be a good proxy for altered grape composition in response to environmental factors (Sadras and Moran, 2013; Bonada and Sadras, 2015). The duration of the phenophases can affect metabolite dynamics (Kuhn et al., 2014; Martínez-Lüscher et al., 2016), but it is also likely that advancing phenology shifts the ripening period toward the warmest part of the year (Webb et al., 2007; Duchene et al., 2010), which is not compatible with the production of high quality table wines (van Leeuwen and Seguin, 2006). Other factors, such as water deficit and elevated CO_2, did not affect significantly grape development speed of 'Red Tempranillo' fruit-bearing cuttings when applied individually (Salazar Parra, 2011). Only, a significant hastening in grape ripening was observed when these two factors were applied simultaneously from veraison to maturity.

Annual Cycle of Grapevine Development

Most temperate fruit crops need a period of cool temperatures before they can produce flowers (Campoy et al., 2011; Considine and Considine, 2016). Satisfaction of the chilling requirement influences the timing of budburst, flowering and subsequent phenological stages (Luedeling, 2012). However, grapevine flowering and veraison can be modeled quite successfully using spring temperatures as the only predictor variable (Parker et al., 2011), suggesting a weak effect of temperatures during bud dormancy (Garcia de Cortazar-Atauri et al., 2009). While the period from the breaking of dormancy to flowering is

strongly determined by temperature, flowering to veraison is often influenced by other abiotic factors such as water deficit (Davies et al., 1994; Antolin et al., 2003; Martínez-Lüscher et al., 2015a), and the correlation is usually weaker (Duchene et al., 2010). This becomes even more evident for the period from flowering or veraison to fruit maturity, which is influenced by an even larger number of factors (Petrie and Sadras, 2008; Webb et al., 2012). Even though ripeness is defined by subjective criteria, and therefore is not a phenological event strictly, it can be reliably measured in relation to metabolite concentrations, such as sugars, anthocyanins and organic acids (Bonada and Sadras, 2015). For instance, regarding the implications of sugar content for the potential alcohol content of resulting wine, the concentration of total soluble solids (TSS) is a straightforward and reliable marker for the progress of ripening (Bonada and Sadras, 2015).

Aim of the Study

In recent years, phenology responses of perennial crops to projected future climates have been assessed. These projections have often focused on response to temperature, with a few cases including water availability, but they have not convincingly considered CO_2. The present study aims to give an overview of the effect of climate change-related phenomena (water deficit, increasing temperature and elevated CO_2) on the phenology of grapevine, a temperate perennial woody crop. For this purpose, we evaluated historical data of phenological records and conducted some experiments under controlled conditions. The combination of these two data sources—historical records and fruit-bearing cuttings under controlled conditions—allows immediate extrapolation to the field when analyzing historical data, but it also allows studying the direct effects of these environmental factors at reasonable cost, when performing experiments under semi-controlled conditions.

MATERIALS AND METHODS

Field Phenology Records

Grapevine phenological records of Croatia were obtained from the pan European phenology project (PEP725 Pan European Phenology Data; dataset accessed on 2015-09-23 at http://www.pep725.eu). Croatia has a long tradition in phenological observations carried out by the Meteorological and Hydrological Service from 1951, which was extended to vineyards in 1958. In this study, the records were used to calculate the time elapsed between March 1st and the beginning of budburst (BBCH 7), budburst to beginning of flowering (BBCH 60) and from flowering to fruit maturity (BBCH 87), to test the influence of temperature on grapevine development (Lorenz et al., 1995). The database consisted of 307 seasonal records collected between 1961 and 2013 from nine commercial vineyards in five phenological stations in Croatia (Mandicevac, Daruvar, KriZevCi, Cepic and Trsteno). These sites, which are distributed between latitudes 42.75°N and 46.03°N and between longitudes 14.13°E and 19.23°E, are representative of the average latitude for the distribution of northern hemisphere vineyards. The nine plots had different climate and soil conditions but none were irrigated. Most of them were in south-orientated hills. In the continental part (Mandicevac, Daruvar and KriZevCi) and the northern Adriatic Coast (Cepic), vines were trained with trellis, distance between rows varied from 1.6 to 2.2 m, and distance within plants in a row ranged from 0.7 to 1.2 m. In the southern Adriatic Coast (Trsteno), there was no training, and separation between plants was 1 × 1 m. The white varieties observed in the vineyards were 'Chasselas Dore,' present in Mandicevac, KriZevCi and Trsteno; 'Riesling Italico,' present in Mandicevac, KriZevCi and Daruvar; and 'Istrian Malmsey,' present in Cepic. 'Plavac Mali,' an autochthonous red variety present in Trsteno, was also observed.

Temperature and Rainfall Records

Field temperature and rainfall records were extracted from the E-OBS European gridded data set (Haylock et al., 2008). As this database contains daily minimum and maximum temperatures, hourly records were constructed with procedures contained in the chillR package (Luedeling, 2016), for R programming language (R Development Core Team, 2016). These procedures follow the recommendations of Linvill (1990). Sunrise, sunset and day length data for this method were modeled using each site latitude (Spencer, 1971; Almorox et al., 2005).

Identification of Chilling and Warming Periods

Partial Least Squares (PLS) regression was used at one of the locations (Mandicevac) to correlate variation in daily chill and heat accumulation to grapevine budburst dates. Daily chill accumulation (in Chill Portions) was calculated according to the so-called Dynamic Model (Fishman et al., 1987), which is regarded as the most accurate under a wide range of circumstances (Campoy et al., 2011). Daily heat accumulation (in Growing Degree Hours) was calculated according to Anderson et al. (1986), with a curvilinear model using a base temperature of 4°C and an optimum temperature of 26°C, which are representative of grapevine response to temperature (Parker et al., 2011). Formulas for each model are given in Luedeling and Brown (2011) and Luedeling et al. (2009), respectively. Eleven-day running means were constructed to facilitate interpretation of the results (Luedeling and Gassner, 2012). Forty-one datasets were created, consisting of 694 independent variables—daily heat and chill accumulation from June 1st (of the year preceding the year of recorded budburst) to May 14th, which was the latest budburst date recorded at the site (data for May 14th were omitted in leap years)—and one bud break date each. PLS regression outputs—variable importance in the projection (VIP) and model coefficients—were used to delineate the periods where an increase in daily chill accumulation indicated a bloom-advancing effect (negative correlation between chill accumulation and budburst date; this was interpreted as the chilling phase) and where an increase in daily heat accumulation implied a bloom-advancing effect (negative correlation; warming phase). The VIP threshold for importance was set to 0.8, which is commonly adopted by other studies (Wold et al., 2001). Further details of the procedures are described in Luedeling et al. (2013). Once these periods were identified, three-dimensional

interpolation (Kriging) was used to illustrate the differential effects of temperature during the chilling and warming periods on budburst dates. This aims to facilitate the interpretation of the effect of two predictor variables that are highly correlated. The angle of the contour lines that are generated indicates, which one of the two factors is dominant in determining budburst dates (Guo et al., 2015).

Plant Material and Growth Conditions

Dormant cuttings of *Vitis vinifera* L. cvs 'Red Tempranillo' (accession T43, Clone RJ-43) and 'White Tempranillo' (accession CI-101 in the "La Grajera" germplasm bank, Government of Rioja, Spain) were collected in January of 2014 and 2015 from an experimental vineyard of the Institute of Sciences of Vine and Wine (ICVV) in Logroño (La Rioja, Spain).

Three node cuttings of *V. vinifera* L. cv. 'Red Tempranillo' and 'White Tempranillo' were selected to produce fruit-bearing cuttings according to Mullins (1966), as described in Kizildeniz et al. (2015). Rooting was induced using indole butyric acid (300 mg L^{-1}) in a heated moist-bed (25–27°C) kept in a cool chamber (5°C). After 1 month, the rooted cuttings were planted in 0.8 L plastic pots containing a mixture of sand, perlite and vermiculite (1:1:1, v/v) and transferred to the greenhouse. At fruit set, plants were planted in 13 L plastic pots containing a mixture of peat and perlite (2:1, v/v). Only a single flowering stem was allowed to develop on each plant, resulting in only one grape bunch per plant. Pruning was used to control vegetative growth until fruit set, thus allowing only 4 leaves per plant to grow. Growth conditions in the greenhouse were 26/15°C and 60/80% relative humidity (RH) (day/night), with a photoperiod of 15 h with natural daylight supplemented with high-pressure metal halide lamps (OSRAM®, Augsburg, Germany). The supplemental system was triggered when photosynthetically active radiation (PAR) dropped below a photosynthetic flux density (PPFD) of 900 μmol m^{-2} s^{-1}, providing a PPFD of 500 μmol m^{-2} s^{-1} at inflorescence level. Plants were irrigated with the nutrient solution described by Ollat et al. (1998): NH_4NO_3 (64.5 mg L^{-1}), $(NH_4)_2HPO_4$ (75 mg L^{-1}), KNO_3 (129 mg L^{-1}), $MgSO_4.7H_2O$ (125 mg L^{-1}), $Ca(NO_3)_2.4H_2O$ (248 mg L^{-1}), $(NH_4)_2SO_4$ (66 mg L^{-1}), Fe (EDDHA) (280 mg L^{-1}), H_3BO_3 (2.86 mg L^{-1}), $MnCL_2.4H_2O$ (1.81 mg L^{-1}), $ZnSO_4.7H_2O$ (0.22 mg L^{-1}), $CuSO_4.5H_2O$ (0.08 mg L^{-1}) and $(NH_4)_6Mo_7O_{24}.4H_2O$ (0.016 mg L^{-1}). Plants grew under these conditions until fruit set (from March to May, both in 2014 and 2015).

Temperature Gradient Greenhouse Experiment Design and Analyses

Treatments were applied in the temperature gradient greenhouses (TGGs), located at the University of Navarra (42.80°N, 1.67°W) in Pamplona (Navarra, Spain), from June to August (i.e., from fruit set to maturity) in 2014 and 2015. TGGs are designed as temperature gradient tunnels (Rawson, 1995), which allows investigating the effects on plants of environmental changes, such as elevated temperature, elevated CO_2 and drought, acting separately or in combination. They were constructed with a modular design with three temperature modules, which creates a temperature gradient ranging from near-ambient temperature in module 1 to ambient temperature +4°C in module 3. CO_2 can be injected into the greenhouse to increase the air CO_2 concentration as desired (more details in Morales et al., 2014). When fruit set was complete for all plants, fruit-bearing cuttings of 'Red Tempranillo' and 'White Tempranillo' cultivars were subjected to a combination of two temperature regimes (ambient and ambient +4°C, no experimental plants were set in module 2 with intermediate temperature) and two CO_2 concentrations (current ca. 400 μL L^{-1} and elevated ca. 700 μL L^{-1}) until maturity (defined as TSS = 21–23°Brix). Each treatment consisted of 10 plants, which were selected on the basis of similar grape bunch sizes. Plants were maintained with free vegetative growth. CO_2 concentration, temperature, relative humidity and radiation were measured and/or controlled by an automated monitoring system. Data were analyzed with XLStat (Addinsoft, Paris, France) by a factorial ANOVA (2 × 2 × 2 × 2 × 2). Only main factors and two-level interaction *P*-values were presented.

RESULTS

Effect of Temperature on Grapevine Dormancy Breaking Under Field Conditions

PLS regression results for budburst dates (**Figure 1**) showed several periods with significant variable importance in the projection (VIP) scores (>0.8) and negative coefficients between September 23rd and February 27th, suggesting that during this period, increases in chilling were correlated to advanced budburst. Although there was a period of negative correlations before this period—between August 31st and September 8th—and a large period of significant scores and positive coefficients from October 25th to November 26th, it seemed reasonable to interpret the period between September 23rd and February 27th as the chilling phase, in agreement with studies showing the effectiveness of chilling in October (Dokoozlian, 1999; Li and Dami, 2016). Days with significant VIP scores coupled with negative correlation coefficients for daily heat accumulation were also discontinuous, but they were concentrated in two major periods: January 4th to January 16th and January 22nd to May 1st, with only a brief interruption, during which model coefficients did not remain negative every day. In addition, mean heat accumulation during the first period—January 4th to January 16th—was very low and most likely did not have a strong effect in most years. It must be noted that this species may fulfill its critical chilling requirement much earlier than most perennial crops, and therefore, important and negative scores for heat accumulation could be expected at any time of the chilling period when adequate temperature levels are reached. We delineated the warming phase as the period between January 22nd and May 1st.

The delineation of chilling and warming phases allowed calculation of mean temperature during these phases. Results showed a weak effect of changes in temperature during the

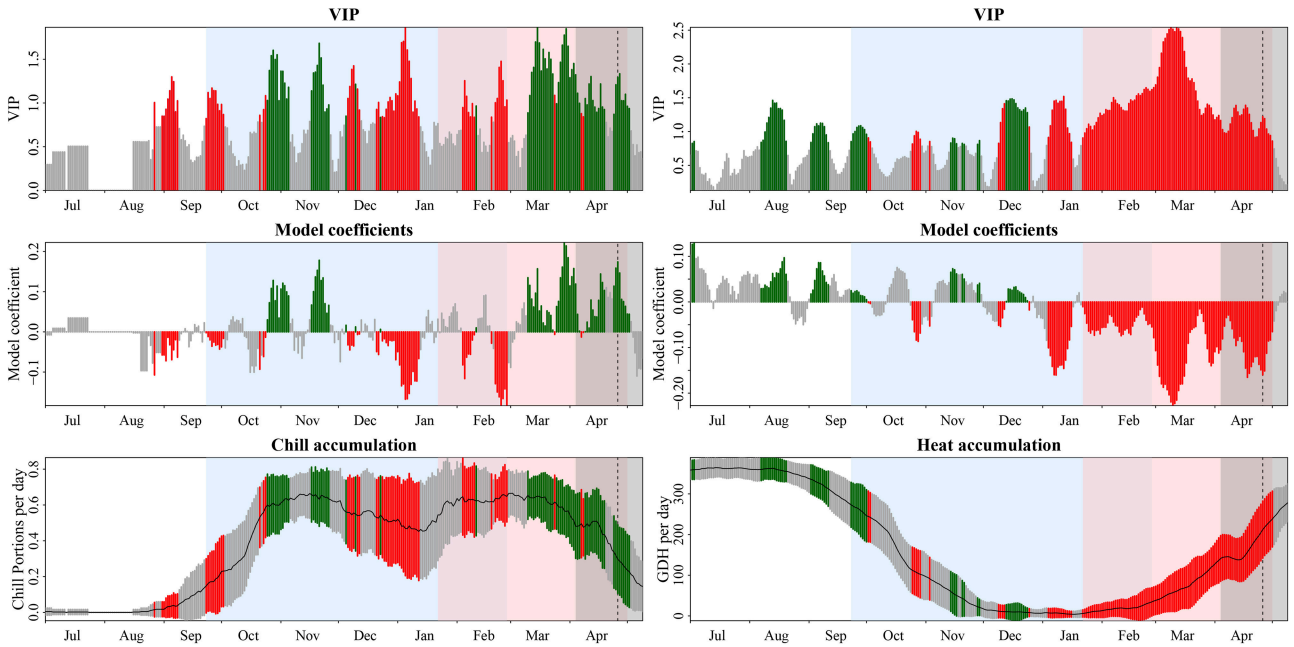

FIGURE 1 | Results of Partial Least Squares (PLS) regression analysis for budburst dates of grapevine cv. 'Riesling Italico' in Mandicevac (Croatia), using the Dynamic Model and the GDH Model for quantifying chill and heat accumulation, respectively (historical data from 1961 to 2013). Color bars in the figures indicate VIP above 0.8, the threshold for considering variables important. Green and red bars represent, besides importance, a positive and negative relationship, respectively, between budburst and daily chilling and heat accumulation. In the lower graphs (chill accumulation and heat accumulation), bars represent the standard deviation of daily chill and heat accumulation, with colors following the same pattern as for the variable importance in the projection (VIP) and model coefficients. Blue, red, and gray shaded areas and dashed lines represent the designated chilling and warming period, range in budburst dates and average budburst date, respectively. GDH, Growing Degree Hours.

chilling phase on budburst date (**Figure 2**). Taking into account the angle and the separation of the contour lines in **Figure 2**, the sensitivity of budburst date to changes in temperature during the chilling period was small (0.03 d $^{\circ}C^{-1}$), compared to −4.38 d $^{\circ}C^{-1}$ for temperatures during the warming phase. The almost horizontal contour lines of the interpolation surface suggest that temperature during the warming period strongly affected budburst date compared to the effect of temperatures during the chilling period. In addition, variation in mean temperature during the delineated chilling phase is much lower than during the warming phase (ranges of −4.2 to 3.9°C and 3.0 to 9.2°C, respectively).

Decoupling of the Effects of Water Availability and Temperature on Grapevine Phenophases under Field Conditions

The linear regression trend determined for all sites (**Figure 3**) shows that the sensitivity is −4.49 days change in budburst date for each degree of temperature increase (d $^{\circ}C^{-1}$) from March 1st to budburst. This sensitivity is higher than for any other phenophase displayed, as the stage from budbreak to flowering had a sensitivity of −3.29 d $^{\circ}C^{-1}$ and the stage from flowering to harvest had a sensitivity of −2.57 d $^{\circ}C^{-1}$. When the effect of temperature on field phenological data was decoupled from rainfall (**Figure 4**), precipitation showed a differential effect on phenological periods. The interpolation surface of the period from March 1st to budburst (**Figure 4A**) shows some delaying effects in rainy years and advancing effects in dry years, but this was not a general trend and it resulted in a high degree of patchiness. Contrarily, the period from budburst to flowering and flowering to ripe fruit resulted in smoother interpolation surfaces (**Figures 4B,C**, respectively). In the case of budburst to flowering (**Figure 4B**), only temperature and not rainfall showed an advancing effect. This is suggested by decreasing values of contour lines and interpolation surface with increasing temperature, but not with rainfall. However, in the case of the period from flowering to ripe fruit (**Figure 4C**), this effect was shared by increases in temperatures and decreases in precipitation.

Effects of Water Availability, Temperature, CO_2 Concentration and their Interactions under Semi-Controlled Conditions

The two varieties ('Red Tempranillo' and 'White Tempranillo') showed different sensivities to increasing temperatures (**Figure 5**). The figures obtained were −1.52 d $^{\circ}C^{-1}$ in 2014 and 0.15 d $^{\circ}C^{-1}$ in 2015 for 'Red Tempranillo' and −2.03 d $^{\circ}C^{-1}$ in 2014 and −0.90 d $^{\circ}C^{-1}$ in 2015 for 'White Tempranillo'. The lower sensitivity to temperature observed in 2015 for both varieties was most likely associated with higher temperatures recorded in that year and a higher number of days with temperatures above 35°C (**Table 1**). Atmospheric

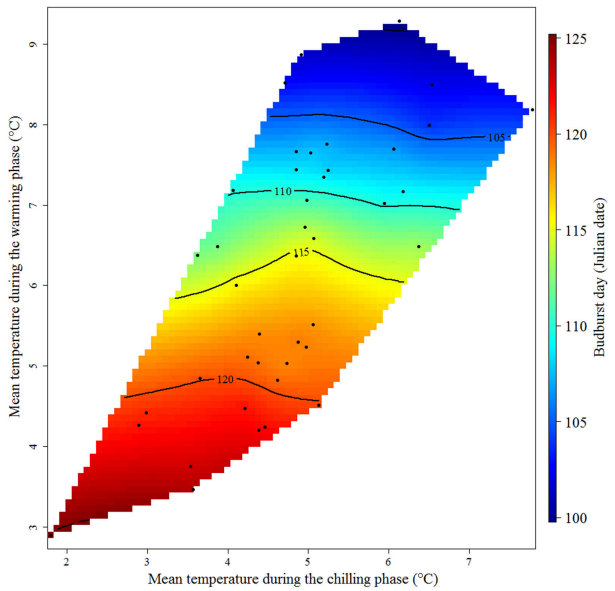

FIGURE 2 | Response of the budburst date of grapevine cv. 'Riesling Italico' in Mandicevac (Croatia) to average temperatures during the chilling and warming periods (September 23rd to February 27th and January 22nd to May 1st, respectively (historical data from 1961 to 2013). Colors and contour lines represent predicted flowering dates expressed in Julian dates (days of the year) using observed data points of grapevine budburst dates in Mandicevac (Croatia; black dots).

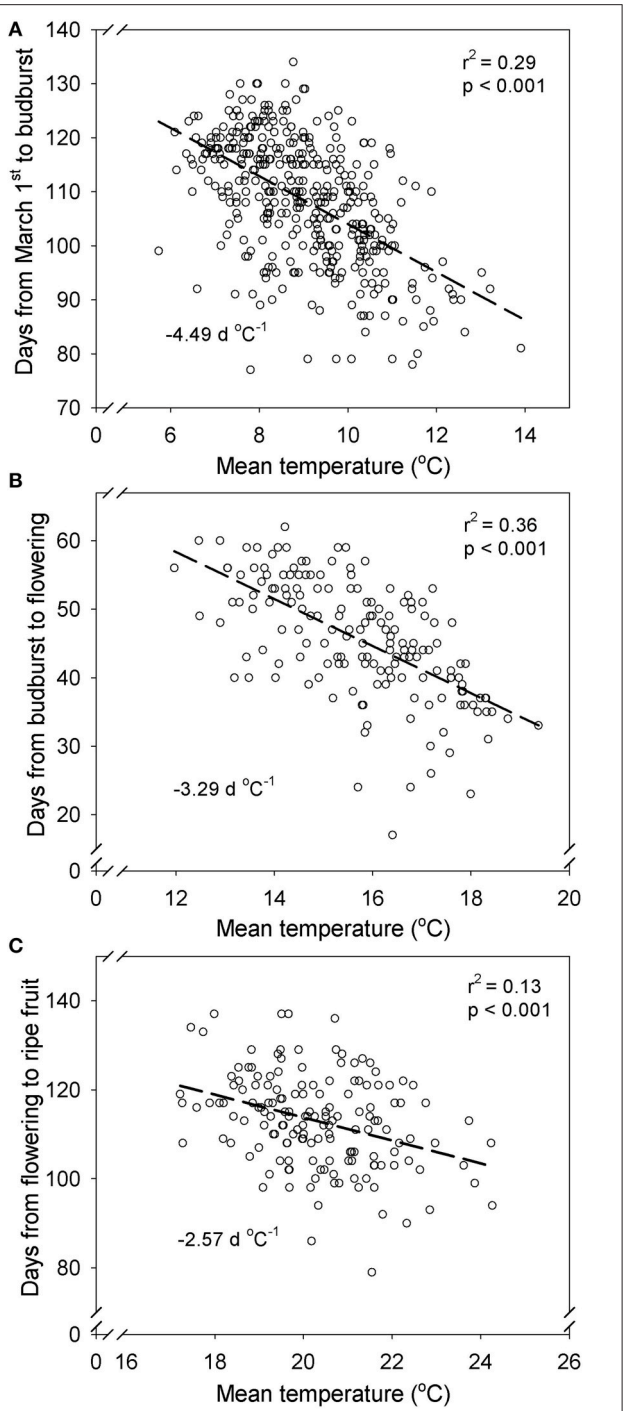

FIGURE 3 | Time from March 1st to budburst (A), budburst to flowering (B) and flowering to ripe fruit stage (C) vs. mean temperature for that period for each year and place. Data from 9 plantings in Daruvar, Cepic, KriZevCi, Mandicevac and Trsteno (Croatia) (historical data from 1961 to 2013).

CO_2 did not change the sensitivity to temperature in any case, and this is supported by the lack of interactions in the two-way ANOVA analysis. The overall effect of CO_2 and temperature was highly significant [$p(CO_2) < 0.001$ and $p(Temp) = 0.001$], with elevated CO_2 having an advancing effect of 4.37 d and 3.54 d in T and T+4°C treatments, respectively. However, looking at the varieties separately, the effect was not significant for the 'Red Tempranillo' variety [$p(CO_2)$ and $p(Temp) > 0.05$], whereas the effect for 'White Tempranillo' was strong [$p(CO_2) < 0.001$ and $p(Temp) = 0.005$]. Considering all years and varieties, high CO_2 advanced phenology by 6.75 d and 4.06 d in the T and T+4°C treatments, respectively.

It must be noted that several two-level interactions were significant for time from fruit set to veraison, veraison to harvest and fruit set to harvest (**Table 2**). Therefore, the significance of the main effects must be interpreted with caution. For instance, 5 out of 11 interactions involved the Year main effect, which reflects the inconsistency of some factor effects from year to year. Other important interactions were found between the Cultivar and CO_2 for time from veraison to maturity and fruit set to maturity. These findings point out the higher susceptibility of the white cultivar under all the combinations of conditions. Still, it must be noted that for most combinations of treatments, elevated CO_2 plants completed fruit development and ripening earlier than their ambient CO_2 homolog. Interactions between environmental factors were also found, including between water deficit and temperature and between water deficit and CO_2. In the main effect comparisons, water deficit extended the ripening period by an average of 3 days. However, looking at the effect of water deficit combined with other factors, cyclic drought (CD) had an advancing effect (i.e., 'Red Tempranillo' under T–E CO_2 in 2015 and 'White Tempranillo' under T–E CO_2 in 2014 and

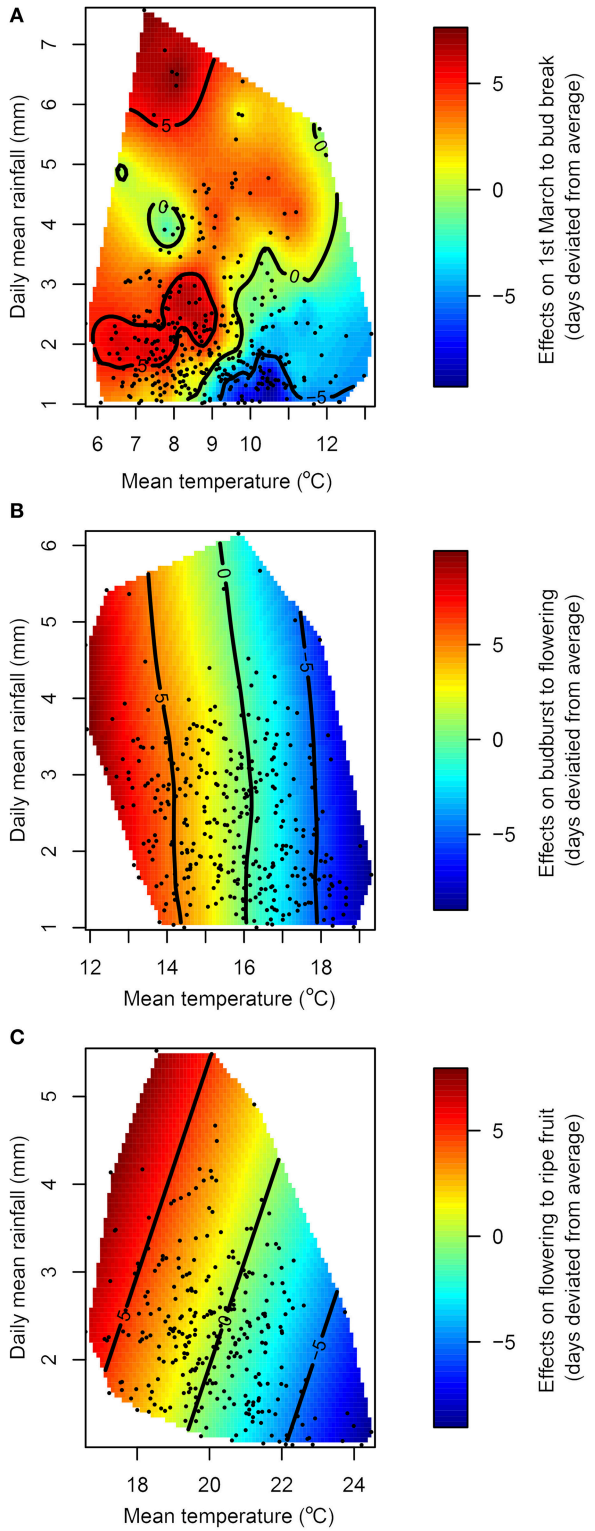

FIGURE 4 | Response of the length of the periods March 1st to budburst (A), budburst to flowering (B) and flowering to ripe fruit (C) to mean temperature and mean rainfall for each planting and year (historical data from 1961 to 2013). Colors and contour lines represent predicted deviation from the average length of each period expressed in days using observed data points of the length of each phenophase (black dots).

2015), which explains the significant interactions between water availability and temperature and CO_2.

DISCUSSION

Effect of Temperature

Many studies have reported the accelerating effects of rising temperatures on phenology based on events typically occurring in spring (i.e., budburst, leaf unfolding, and flowering). While most species show a clear advance in phenology, an exception to this general trend may be those species that are starting to experience difficulties in meeting their chilling requirements (Guo et al., 2015). In this respect, grapevine (*Vitis vinifera* L.) is presented in the literature as a species with a low chill requirement, despite its tendency to burst and flower rather late (Mullins et al., 1992). Although they are believed to need a very small exposure to chilling temperatures to resume growth and flower normally, incremental exposure to chilling temperatures reduces the time to respond to high temperatures and increases the percentage of budburst, which suggests some sensitivity to chilling (Dokoozlian, 1999). In the present study, grapevines do not show a major change in budburst date in response to changes in temperature during the chilling period. Instead, temperature during the warming period was the overriding factor influencing this phenophase (**Figure 2**). The high variable importance in the projection (VIP) values and negative coefficients for heat accumulation observed at the beginning of March highlight the importance of taking into account this period for the prediction of budburst and flowering. These results support previous studies that find best model performance for models using the March 1st as a start date for the accumulation of thermal time, instead of the classical approach of taking into account temperatures from January 1st (Garcia de Cortazar-Atauri et al., 2009; Duchene et al., 2010; Parker et al., 2011).

For later phenological events, such as onset of ripening, thermal time models have proven to be valuable tools. However, as the growing season goes on, the level of complexity increases and factors such as yield, cultural practices and water availability may also influence the timing of phenophases (Petrie and Sadras, 2008; Sadras and Petrie, 2011; Martínez de Toda et al., 2013). Simply, the ripening of non-climacteric fruits relies to a great extent on photoassimilation in the leaves, translocation and storage of photoassimilates, which are reactions greatly enhanced by temperature (Greer and Weedon, 2013). Historical data also support the relationship between temperature and commercial ripeness in grapes (Chuine et al., 2004; Daux et al., 2012). In the historical data used in this study, the effect of temperature on the time between flowering and harvest was visible, but—as expected—the correlation was weaker than for the completion of previous stages, such as budburst or flowering. This advancement of the ripening period, shifting dates from September to August in the northern hemisphere, has the additional effect of shifting this period to what is usually the warmest part of the year (Webb et al., 2007; Duchene et al., 2010). In this study, this effect resulted in an increase of the temperature during the ripening period by 1.27°C for each °C increase in the average temperature (Figure S1).

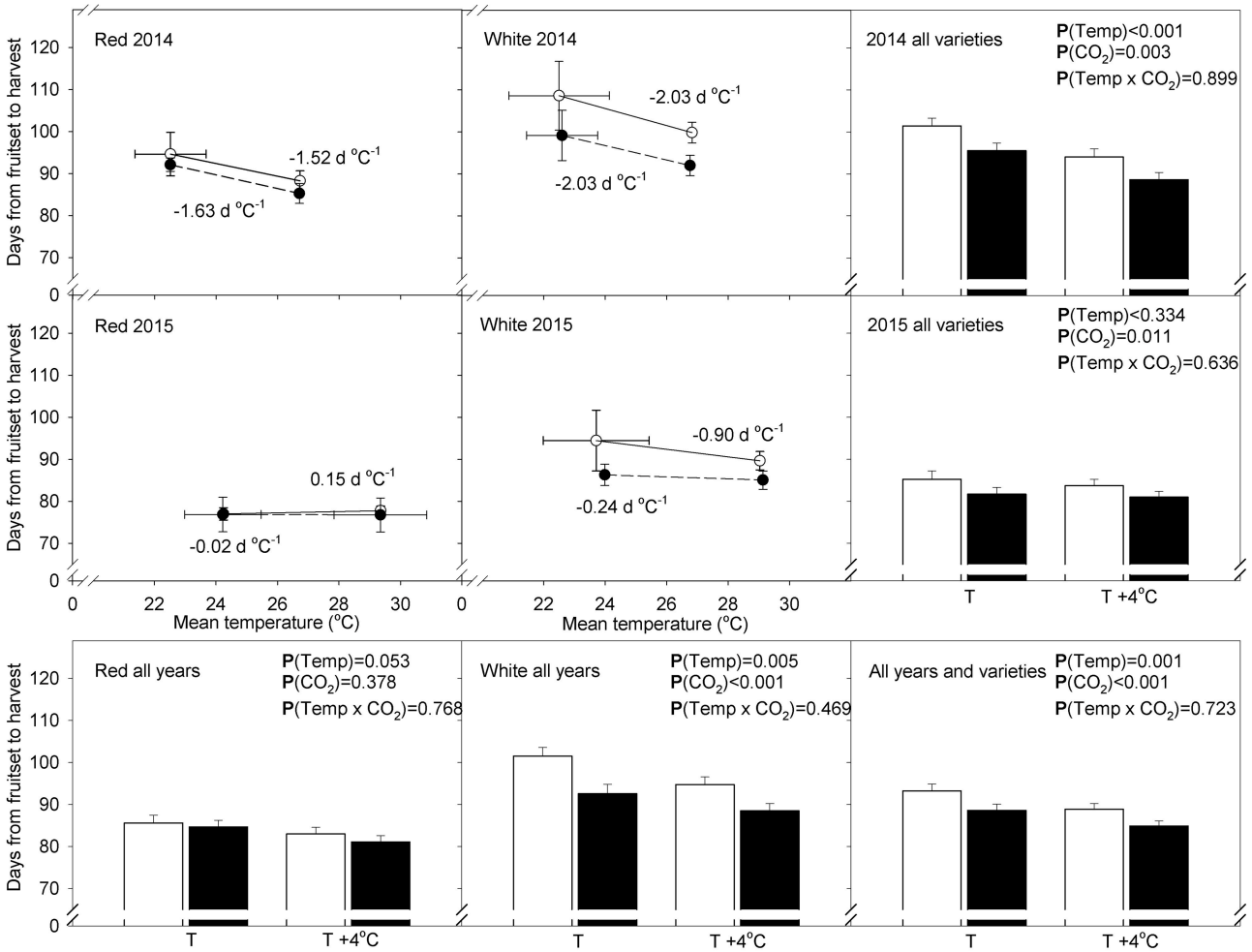

FIGURE 5 | Days to complete fruit development (from fruit set to designated maturity) vs. mean temperature between the phenophases in 'Red Tempranillo' and 'White Tempranillo' grapevine grown under two CO_2 concentrations (ambient CO_2 or 700 μL L^{-1} CO_2; white and black points and bars, respectively) and two temperature regimes (ambient temperature, T or ambient temperature +4°C, T+4°C). Points and bars represent means ± standard error (n = 16–20). *P*-values based on four-way ANOVA taking as main factors: cultivar, temperature, CO_2 concentration and water availability.

TABLE 1 | Temperature recorded in the temperature gradient greenhouse experiments with 'Red Tempranillo' and 'White Tempranillo' grapevine.

Year	2014		2015	
Temperature regime	**T**	**T+4°C**	**T**	**T+4°C**
Mean daily minimum (°C)	14.8	18.8	15.4	19.65
Daily mean (°C)	22.1	26.5	22.9	27.1
Mean daily maximum (°C)	28.7	33.5	29.7	35.11
Days above 30°C	46	85	44	77
Days above 35°C	8	42	19	50

T, ambient temperature and T+4°C, ambient temperature +4°C.

Effect of Water Availability in Relation to Temperature

Our studies show differences in the effects of rainfall depending on the phenological period. Whereas events occurring before berry development do not show a clear dependence on rainfall, berry development shows a higher dependence both on temperature and water availability (**Figure 4**). Mild water deficit has proven to enhance ripening through several processes, such as altering plant abscisic acid (ABA) signaling, reduction in berry size or concentrating berry contents (i.e., anthocyanins and sugars) (Deluc et al., 2009; van Leeuwen et al., 2009; Chaves et al., 2010). In fact, environmental cues such as water deficit, as well as solar radiation, and even heat within the suboptimal range of temperature of a variety, may promote signaling mechanisms, such as ABA biosynthesis, and enhance ripening (Kuhn et al., 2014). ABA signaling during grape ripening interacts with plant responses to exogenous stresses, by regulating the process of plant adaptation (Ferrandino and Lovisolo, 2014). Many key genes involved in flavonoid biosynthesis are up-regulated during ripening, therefore ABA accumulation induced by stress conditions may induce the activation of these key

TABLE 2 | Days to complete phenological periods: fruit set to veraison, veraison to designated maturity and fruit set to designated maturity in 'Red Tempranillo' and 'White Tempranillo' grapevine grown under two water availability levels (FI, full irrigation or CD, cyclic drought), two temperature regimes (ambient temperature, T or ambient temperature +4°C, T+4°C) and two CO_2 concentrations (A CO_2, ambient CO_2, or E CO_2, 700 μL L^{-1} CO_2).

Cultivar	Water availability	Temperature	CO_2 level	Years	Fruit set to veraison	Veraison to maturity	Fruit set to maturity
Red	FI	T	A CO_2	2014	64.1 ± 1.5	29.8 ± 3.4	93.9 ± 3.0
				2015	53.0 ± 1.1	25.6 ± 2.3	78.6 ± 2.5
			E CO_2	2014	57.9 ± 1.3	31.5 ± 1.9	89.4 ± 2.5
				2015	51.6 ± 1.1	27.0 ± 1.8	79.1 ± 1.8
		T+4	A CO_2	2014	56.2 ± 1.1	25.3 ± 1.3	81.5 ± 1.8
				2015	54.2 ± 1.5	20.8 ± 2.3	75.0 ± 1.1
			E CO_2	2014	54.9 ± 1.5	27.1 ± 2.2	82.0 ± 3.6
				2015	51.1 ± 1.0	24.5 ± 1.4	75.6 ± 1.7
	CD	T	A CO_2	2014	68.7 ± 2.3	27.8 ± 2.2	95.4 ± 2.0
				2015	48.7 ± 1.5	26.7 ± 1.3	75.4 ± 1.6
			E CO_2	2014	57.5 ± 1.7	37.3 ± 2.3	94.8 ± 1.7
				2015	51.4 ± 0.9	23.0 ± 1.4	74.3 ± 1.1
		T+4	A CO_2	2014	66.5 ± 2.2	28.5 ± 1.8	95.0 ± 3.3
				2015	54.8 ± 1.7	25.7 ± 2.1	80.5 ± 1.5
			E CO_2	2014	57.0 ± 1.4	31.5 ± 2.4	88.5 ± 2.8
				2015	50.2 ± 1.4	27.8 ± 1.7	78.0 ± 0.9
White	FI	T	A CO_2	2014	66.5 ± 2.4	40.1 ± 2.0	106.6 ± 3.0
				2015	50.4 ± 0.7	39.4 ± 3.5	90.0 ± 3.7
			E CO_2	2014	56.9 ± 0.6	47.5 ± 3.0	104.4 ± 3.4
				2015	49.5 ± 0.9	41.2 ± 3.6	90.7 ± 3.7
		T+4	A CO_2	2014	58.9 ± 1.3	31.8 ± 1.6	90.7 ± 0.9
				2015	51.5 ± 1.6	40.7 ± 4.3	92.2 ± 3.3
			E CO_2	2014	55.0 ± 0.5	30.3 ± 1.0	85.3 ± 1.1
				2015	51.5 ± 1.4	33.1 ± 2.1	84.6 ± 2.8
	CD	T	A CO_2	2014	62.9 ± 2.1	50.4 ± 3.2	111.1 ± 3.3
				2015	49.6 ± 0.8	49.2 ± 2.6	98.9 ± 2.6
			E CO_2	2014	59.6 ± 1.1	37.0 ± 4.2	93.3 ± 5.1
				2015	48.3 ± 0.5	33.6 ± 3.0	81.9 ± 2.9
		T+4	A CO_2	2014	60.9 ± 0.9	48.1 ± 2.5	109.0 ± 2.5
				2015	48.8 ± 0.6	38.3 ± 3.2	87.1 ± 2.8
			E CO_2	2014	58.3 ± 1.2	40.4 ± 3.4	98.7 ± 3.6
				2015	48.1 ± 0.5	37.4 ± 3.7	85.5 ± 3.5
Means of main factors			'Red Tempranillo'		56.1 ± 0.6	27.5 ± 0.6	83.6 ± 0.8
			'White Tempranillo'		54.8 ± 0.5	39.9 ± 0.9	94.4 ± 1.0
			Full irrigation		55.2 ± 0.5	32.2 ± 0.8	87.5 ± 0.9
			Water deficit		55.7 ± 0.6	35.2 ± 0.9	90.5 ± 1.1
			Ambient temperature		56.0 ± 0.6	35.4 ± 0.9	91.1 ± 1.1
			Elevated temperature		54.9 ± 0.5	32.0 ± 0.8	86.8 ± 0.9
			Ambient CO_2		57.2 ± 0.6	34.3 ± 0.9	91.3 ± 1.1
			Elevated CO_2		53.7 ± 0.4	33.1 ± 0.8	86.6 ± 0.9
			2014		60.1 ± 0.5	35.3 ± 0.8	95.0 ± 1.0
			2015		50.8 ± 0.3	32.1 ± 0.9	83.0 ± 0.8
ANOVA P of main factors			**P**(Cult)		<0.001	<0.001	<0.001
			P(WA)		n.s.	0.005	0.01

(Continued)

TABLE 2 | Continued

Cultivar	Water availability	Temperature	CO_2 level	Years	Fruit set to veraison	Veraison to maturity	Fruit set to maturity
			P(Temp)		0.014	<0.001	<0.001
			P(CO_2)		<0.001	n.s.	<0.001
			P(Year)		<0.001	0.001	<0.001
			P(Cult) × **P**(WA)		n.s.	n.s.	n.s.
ANOVA 2 level interactions			**P**(Cult) × **P**(Temp)		n.s.	n.s.	n.s.
			P(Cult) × **P**(CO_2)		n.s.	<0.001	0.004
			P(Cult) × **P**(Year)		n.s.	n.s.	n.s.
			P(WA) × **P**(Temp)		n.s.	0.007	<0.001
			P(WA) × **P**(CO_2)		n.s.	0.028	0.014
			P(WA) × **P**(Year)		<0.001	n.s.	<0.001
			P(Temp) × **P**(CO_2)		n.s.	n.s.	n.s.
			P(Temp) × **P**(Year)		<0.001	n.s.	0.002
			P(CO_2) × **P**(Year)		<0.001	n.s.	n.s.

Values are elapsed time (days) mean ± SE, n = 8–10. Cult, Cultivar; Temp, Temperature; WA, water availability and n.s., not significant.

genes (Nicolas et al., 2014), thus improving berry quality (Ferrandino and Lovisolo, 2014). For example, despite hastening fruit ripening, mild water deficit normally has a desirable effect, increasing the concentration of some phenolic compounds in the grapes (Chaves et al., 2010). However, as climate change continues, places experiencing a risk of severe water deficit may encounter contrasting effects. Severe water deficit can induce stomatal closure, greatly reduce carbon fixation, and subsequently, impair berry ripening (Martínez-Lüscher et al., 2015a). This may explain the results obtained with fruit-bearing cuttings, where a water deficit appeared to generally delay maturity. In addition, water availability had significant interactions with both temperature and CO_2 concentration. For conditions such as ambient temperature and elevated CO_2, where plants were presumably less stressed, the general tendency of cyclic drought to delay ripening was reverted. Contrasting effects of water deficit have also been reported by Cook and Wolkovich (2016) in large scale field data analyses, where precipitation correlates positively with harvest date anomalies in France, while they correlate negatively in the drier vineyards of Spain. Cook and Wolkovich (2016) highlight that the relationship between water deficit and early harvest has weakened in recent decades in central Europe due to the decoupling of the incidence of high temperatures and drought.

The influence of temperature and water availability on grape ripening may depend on other factors, such as soil type, variety and rootstock, among others. Soil is a key factor for vine productivity and fruit quality, and the response of *V. vinifera* to water deficit may depend on the soil water retention capacity (Oliveira et al., 2003). In addition, the increase in phenolic concentrations observed in higher clay soils were greater in wet and intermediate years than in dry years when abundant ABA biosynthesis controls plant responses to drought, independently from soil properties (references in Lovisolo et al., 2016). Soils with moderate water retention capacity induced mild water stress, thus favoring fruit ripening, compared with soils with either very low or unlimited water availability (Tramontini et al., 2013). Also, they stated that water availability in the soil overrides differences due to cultivar in determining the vineyard productive potential. van Leeuwen et al. (2004), who studied the effect of weather, soil and cultivar simultaneously, found that soil had little effect on phenology (1 day change in flowering-harvest) compared with weather and cultivar (up to 14 and 9 day difference in the flowering-harvest period, respectively). For fruit quality, however, impacts of weather and soil were greater than that of cultivar, with effects being mediated through their influence on vine water status. Concerning rootstocks, a small and possibly insignificant 3-day difference for the time between flowering and harvest in a comparison among three different rootstocks was reported by Dias Tofanelli et al. (2011). In contrast, Corso et al. (2016), using a selection of the most representative rootstocks and scions of mid-latitude vineyards, showed a rather strong effect of rootstocks on ripening rates. Varieties can also differ in their response to increased temperatures and water deficit. Based on the results under controlled conditions, late ripening varieties may be more sensitive than early ones. Probably, early ripening varieties may be more predetermined to ripen during the warmest part of the year, reaching a threshold of precocity where further advances are not possible, whereas late ripening varieties may be advanced to a greater extent, and therefore, the increase in ambient temperature during their ripening period may be greater.

Effect of CO_2 Concentration in Relation to Temperature

Grapevine fruit-bearing cuttings grown under semi-controlled conditions showed similar sensitivities to increasing temperatures compared to field grown vines, although sensitivities were lower in the warmer year, 2015, and for the early cultivar, 'Red Tempranillo.' The change induced by elevated CO_2 followed similar variation, but this effect was greater than the effect of the 4°C increase. In recent studies with grapevine fruit-bearing cuttings, a correlation between

carbon fixation rates and grape development rates has been reported (Martínez-Lüscher et al., 2015b). This behavior has been described under field conditions as well, where leaf removal treatments, which presumably reduce overall grapevine carbon fixation, resulted in a delay in grape maturity (Martínez de Toda et al., 2013; Parker et al., 2014, 2015). Plants exposed to elevated CO_2 often show photosynthetic acclimation, which is characterized by an initial increase in carbon fixation rates and reduction to initial levels or even lower after a mid-term exposure (Leakey et al., 2009). However, this is not a generalized response and, even if this were the case, it would not mean that plant performance and fruit yield would be strongly affected (Idso and Kimball, 1991; Leakey et al., 2009). One of the greatest efforts to study the effect of elevated CO_2 on fruiting woody perennials is a 17-year experiment on sour orange trees (*Citrus aurantium* L.) with open-top-chambers, which showed a constant increase in yield despite photosynthetic acclimation (Kimball et al., 2007). To the best of our knowledge, a paper by Bindi et al. (2001) is the only FACE experiment study in the literature, where an increase in sugar accumulation in the grapes was reported. Although this effect was diluted in the latest stages of ripening, this is evidence for accelerated ripening in grapes grown under elevated CO_2. In previous reports, Salazar Parra et al. (2010) and Martínez-Lüscher et al. (2016) showed how grapes grown under both elevated CO_2 and increased temperature met the sugar criteria for harvest much earlier, and this led to a decrease in anthocyanin concentration. In contrast, Kizildeniz et al. (2015), who studied the interaction between elevated CO_2 and increasing temperature, reported that elevated CO_2 showed mitigating effects, generally increasing anthocyanin concentration and increasing either grape organic acid concentration or decreasing grape pH, probably related to the precocity of these treatments. Thus, due to its complexity, the relationship between different environmental factors and grape composition should be assessed with caution, as phenology-mediated effects are likely.

Martínez de Toda and Balda Manzanos (2013) and Martínez de Toda et al. (2013) showed that cultural practices, such as canopy density reduction, can have an opposite effect to that resulting from high temperature, reducing TSS concentration for a fixed date. However, in that case, this contributed to restore grape pH, but reduced anthocyanin concentration. Interestingly, Martínez de Toda et al. (2014), in a similar experiment but harvesting grapes at a designated TSS concentration, found that delayed phenological development contributed to increasing anthocyanin concentration. These findings suggest that carbon translocation into the grapes can be controlled, thus altering the timing of phenological stages, which can contribute to mitigating the effects of climate change.

CONCLUSIONS

The results of the present study suggest that temperature, water deficit and CO_2 levels representative of the conditions expected for the end of the 21st century may strongly advance budburst, flowering, and berry designated maturity. Some uncertainties still exist, such as whether the delaying effect of severe water deficit or the decreasing sensitivity under extreme temperature, which have been observed both in fruit-bearing cuttings in the present study and in other field studies, will be generally observable in vineyards in the future. Future efforts should be directed to investigating how grapevine whole-plant physiology may be altered in response to climate change-related factors, and to uncoupling the effects of environmental factors such as temperature, water deficit and CO_2, from their potential effects on berry phenology. These are crucial topics to establish successful mitigation and adaptive strategies for viticulture in a changing environment.

AUTHOR CONTRIBUTIONS

JM performed the analysis and elaborated the draft of the manuscript. ZD and EL designed the analysis of the field data. IP, JI, and FM designed the TGG experiments, TK performed the TGG experiments. VV provided the field data and reviewed the manuscript. JM, TK, ZD, EL, CV, EG, IP, JI, FM, and SD contributed to the interpretation of the results and elaboration of the final manuscript.

FUNDING

This work was funded by the Land Settlement Association, the University of Reading Research Endowment Trust and East Malling Trust, European Union (INNOVINE Call FP7-KBBE-2011-6, Proposal N○311775), Ministerio de Ciencia e Innovación of Spain (MCINN BFU 2011-26989), Ministerio de Economía y Competitividad of Spain (AGL2014-56075-C2-1-R), Aragón Government (A03 research group) and Asociación de Amigos de la Universidad de Navarra (grant to TK).

ACKNOWLEDGMENTS

We acknowledge the members of the PEP725 project making possible accessing the field data, the E-OBS dataset from the EU-FP6 project ENSEMBLES (http://ensembles-eu.metoffice.com) and the data providers in the ECA&D project (http://www.ecad.eu). Special thanks to Amadeo Urdiain, Hector Santesteban and Mónica Oyarzun for technical assistance in the TGG experiments.

SUPPLEMENTARY MATERIAL

The Supplementary Material for this article can be found online at: http://journal.frontiersin.org/article/10.3389/fenvs.2016.00048

REFERENCES

Almorox, J., Hontoria, C., and Benito, M. (2005). Statistical validation of daylength definitions for estimation of global solar radiation in Toledo, Spain. *Energy Conv. Manag.* 46, 1465–1471. doi: 10.1016/j.enconman.2004.07.007

Anderson, J. L., Richardson, E. A., and Kesner, C. D. (1986). Validation of chill unit and flower bud phenology models for "Montmercy" sour cherry. *Acta Hortic.* 184, 71–78. doi: 10.17660/ActaHortic.1986.184.7

Antolin, M. C., Baigorri, H., De Luis, I., Aguirrezabal, F., Geny, L., Broquedis, M., et al. (2003). ABA during reproductive development in non-irrigated grapevines (*Vitis vinifera* L. *cv. Tempranillo). Aust. J. Grape Wine Res.* 9, 169–176. doi: 10.1111/j.1755-0238.2003.tb00266.x

Bindi, M., Fibbi, L., and Miglietta, F. (2001). Free Air CO_2 Enrichment (FACE) of grapevine (*Vitis vinifera* L.): II. Growth and quality of grape and wine in response to elevated CO_2 concentrations. *Eur. J. Agron.* 14, 145–155. doi: 10.1016/S1161-0301(00)00093-9

Bonada, M., Jeffery, D. W., Petrie, P. R., Moran, M. A., and Sadras, V. O. (2015). Impact of elevated temperature and water deficit on the chemical and sensory profiles of Barossa Shiraz grapes and wines. *Aust. J. Grape Wine Res.* 21, 240–253. doi: 10.1111/ajgw.12142

Bonada, M., and Sadras, V. O. (2015). Review: critical appraisal of methods to investigate the effect of temperature on grapevine berry composition. *Aust. J. Grape Wine Res.* 21, 1–17. doi: 10.1111/ajgw.12102

Campoy, J. A., Ruiz, D., and Egea, J. (2011). Dormancy in temperate fruit trees in a global warming context: a review. *Sci. Hortic.* 130, 357–372. doi: 10.1016/j.scienta.2011.07.011

Chaves, M. M., Zarrouk, O., Francisco, R., Costa, J. M., Santos, T., Regalado, A. P., et al. (2010). Grapevine under deficit irrigation: hints from physiological and molecular data. *Ann. Bot.* 105, 661–676. doi: 10.1093/aob/mcq030

Chuine, I., Yiou, P., Viovy, N., Seguin, B., Daux, V., and Le Roy Ladurie, E. (2004). Historical phenology: grape ripening as a past climate indicator. *Nature* 432, 289–290. doi: 10.1038/432289a

Cohen, S. D., Tarara, J. M., Gambetta, G. A., Matthews, M. A., and Kennedy, J. A. (2012). Impact of diurnal temperature variation on grape berry development, proanthocyanidin accumulation, and the expression of flavonoid pathway genes. *J. Exp. Bot.* 63, 2655–2665. doi: 10.1093/jxb/err449

Considine, M. J., and Considine, J. A. (2016). On the language and physiology of dormancy and quiescence in plants. *J. Exp. Bot.* 67, 3189–3203. doi: 10.1093/jxb/erw138

Cook, B. I., and Wolkovich, E. M. (2016). Climate change decouples drought from early wine grape harvests in France. *Nat. Clim.* doi: 10.1038/nclimate2960. [Epub ahead of print].

Corso, M., Vannozzi, A., Ziliotto, F., Zouine, M., Nicolato, T., Maza, E., et al. (2016). Grapevine rootstocks differentially affect the rate of ripening and modulate auxin-related genes in Cabernet Sauvignon berries. *Front. Plant Sci.* 7:69. doi: 10.3389/fpls.2016.00069

Daux, V., de Cortazar-Atauri, I. G., Yiou, P., Chuine, I., Garnier, E., Ladurie, E. L., et al. (2012). An open-access database of grape harvest dates for climate research: data description and quality assessment. *Climate Past* 8, 1403–1418. doi: 10.5194/cp-8-1403-2012

Davies, W. J., Tardieu, F., and Trejo, C. L. (1994). How do chemical signals work in plants that grow in drying soil. *Plant Physiol.* 104, 309–314.

Deluc, L. G., Quilici, D. R., Decendit, A., Grimplet, J., Wheatley, M. D., Schlauch, K. A., et al. (2009). Water deficit alters differentially metabolic pathways affecting important flavor and quality traits in grape berries of Cabernet Sauvignon and Chardonnay. *BMC Genomics* 10:212. doi: 10.1186/1471-2164-10-212

Demir, K. (2014). A review on grape growing in tropical regions. *Turk. J. Agric. Nat. Sci.* 6, 1236–1241.

Dias Tofanelli, M. B., Vasconcelos Botelho, R., Paioli Pires, E. J., Ferreira Vilela, L. A., and Oliveira Ribeiro, D. (2011). Phehology of "Niagara Rosada" grepevines grafted on different rootstocks grown on Cerrado (Brazilian savanna) of Goiás State, Brazil. *Afr. J. of Biotechnol.* 10, 3387–3392.

Dokoozlian, N. K. (1999). Chilling temperature and duration interact on the budbreak of "Perlette" grapevine cuttings. *HortScience* 34, 1054–1056.

Duchene, E., Huard, F., Dumas, V., Schneider, C., and Merdinoglu, D. (2010). The challenge of adapting grapevine varieties to climate change. *Clim. Res.* 41, 193–204. doi: 10.3354/cr00850

Etienne, A., Genard, M., Lobit, P., Mbeguie-A-Mbeguie, D., and Bugaud, C. (2013). What controls fleshy fruit acidity? A review of malate and citrate accumulation in fruit cells. *J. Exp. Bot.* 64, 1451–1469. doi: 10.1093/jxb/ert035

Ferrandino, A., and Lovisolo, C. (2014). Abiotic stress effects on grapevine (*Vitis vinifera* L.): Focus on abscisic acid-mediated consequences on secondary metabolism and berry quality. *Environ. Exp. Bot.* 103, 138–147. doi: 10.1016/j.envexpbot.2013.10.012

Fishman, S., Erez, A., and Couvillon, G. A. (1987). The temperature dependence of dormancy breaking in plants: mathematical analysis of a two-step model involving a cooperative transition. *J. Theor. Biol.* 124, 473–483. doi: 10.1016/S0022-5193(87)80221-7

García de Cortázar-Atauri, I., Brisson, N., and Gaudillere, J. P. (2009). Performance of several models for predicting budburst date of grapevine (*Vitis vinifera* L.). *Int. J. Biometeorol.* 53, 317–326. doi: 10.1007/s00484-009-0217-4

Gladstones, J. S. (1992). *Viticulture and Environment: A Study of the Effects of Environment on Grapegrowing and Wine Qualities, with Emphasis on Present and Future Areas for Growing Winegrapes in Australia*. Adelaide, SA: Winetitles.

Greer, D. H., and Weedon, M. M. (2013). The impact of high temperatures on *Vitis vinifera* cv. Semillon grapevine performance and berry ripening. *Front. Plant. Sci.* 4:491. doi: 10.3389/fpls.2013.00491

Guo, L., Dai, J., Wang, M., Xu, J., and Luedeling, E. (2015). Responses of spring phenology in temperate zone trees to climate warming: a case study of apricot flowering in China. *Agric. For. Meteorol.* 201, 1–7. doi: 10.1016/j.agrformet.2014.10.016

Haylock, M. R., Hofstra, N., Klein Tank, A. M. G., Klok, E. J., Jones, P. D., and New, M. (2008). A European daily high-resolution gridded data set of surface temperature and precipitation for 1950–2006. *J. Geophys. Res.* 113:D20119. doi: 10.1029/2008jd010201

Idso, S. B., and Kimball, B. A. (1991). Downward regulation of photosynthesis and growth at high CO_2 levels No evidence for either phenomenon in three-year study of sour orange trees. *Plant Physiol.* 96, 990–992. doi: 10.1104/pp.96.3.990

IPCC (2014a). *Climate Change 2014: Mitigation of Climate Change. Contribution of Working Group III to the Fifth Assessment Report of the Intergovernmental Panel on Climate Change*. Cambridge; New York, NY: Cambridge University Press.

IPCC (2014b). "Climate Change 2014: Synthesis Report," in *Contribution of Working Groups I, II and III to the Fifth Assessment Report of the Intergovernmental Panel on Climate Change*, eds Core Writing Team, R. K. Pachauri, and L. A. Meyer (Geneva: IPCC), 151.

Jones, G. (2006). "Climate and terroir: impacts of climate variability and change on wine," in *Fine Wine and Terroir-The Geoscience Perspective*, eds R. W. Macqueen and L. D. Meinert (St John's, NL: Geological Association of Canada), 1–14.

Jones, G. V. (2007). Climate change: observations, projections, and general implications for viticulture and wine production. *Econ. Depart. Working Paper* 7, 15.

Jones, G. V., White, M. A., Cooper, O. R., and Storchmann, K. (2005). Climate change and global wine quality. *Clim. Change* 73, 319–343. doi: 10.1007/s10584-005-4704-2

Kimball, B. A., Idso, S. B., Johnson, S., and Rillig, M. C. (2007). Seventeen years of carbon dioxide enrichment of sour orange trees: final results. *Global Change Biol.* 13, 2171–2183. doi: 10.1111/j.1365-2486.2007.01430.x

Kizildeniz, T., Mekni, I., Santesteban, H., Pascual, I., Morales, F., and Irigoyen, J. J. (2015). Effects of climate change including elevated CO_2 concentration, temperature and water deficit on growth, water status, and yield quality of grapevine (*Vitis vinifera* L.) cultivars. *Agric. Water Manag.* 159, 155–164. doi: 10.1016/j.agwat.2015.06.015

Kuhn, N., Guan, L., Dai, Z. W., Wu, B. H., Lauvergeat, V., Gomès, E., et al. (2014). Berry ripening: recently heard through the grapevine. *J. Exp. Bot.* 65, 4543–4559. doi: 10.1093/jxb/ert395

Lakso, A. N., and Kliewer, W. M. (1975). The influence of temperature on malic acid metabolism in grape berries: I. Enzyme responses. *Plant Physiol.* 56, 370–372. doi: 10.1104/pp.56.3.370

Leakey, A. D. B., Ainsworth, E. A., Bernacchi, C. J., Rogers, A., Long, S. P., and Ort, D. R. (2009). Elevated CO_2 effects on plant carbon, nitrogen, and water relations: six important lessons from FACE. *J. Exp. Bot.* 60, 2859–2876. doi: 10.1093/jxb/erp096

Li, S., and Dami, I. E. (2016). Responses of *Vitis vinifera* 'Pinot gris' grapevines to exogenous abscisic acid (ABA): I. yield, fruit quality, dormancy, and freezing tolerance. *J. Plant Growth Regul.* 35, 245–255. doi: 10.1007/s00344-015-9529-2

Linvill, D. E. (1990). Calculating chilling hours and chill units from daily maximum and minimum temperature observations. *Hortscience* 25, 14–16.

Lorenz, D. H., Eichhorn, K. W., Bleiholder, H., Klose, R., Meier, U., and Weber, E. (1995). Growth stages of the grapevine: phenological growth stages of the grapevine (*Vitis vinifera* L. ssp. vinifera)—Codes and descriptions according to the extended BBCH scale†. *Aust. J. Grape Wine Res.* 1, 100–103. doi: 10.1111/j.1755-0238.1995.tb00085.x

Lovisolo, C., Lavoie-Lamoureux, A., Tramontini, S., and Ferrandino, A. (2016). Grapevine adaptations to water stress: new perspectives about soil/plant interactions. *Theor. Exp. Plant. Physiol.* 28, 53–66. doi: 10.1007/s40626-016-0057-7

Luedeling, E. (2012). Climate change impacts on winter chill for temperate fruit and nut production: a review. *Sci. Hortic.* 144, 218–229. doi: 10.1016/j.scienta.2012.07.011

Luedeling, E. (2016). *chillR: Statistical Methods for Phenology Analysis in Temperate Fruit Trees*. R package version 0.62. Available online at: http://cran.r-project.org/web/packages/chillR/

Luedeling, E., and Brown, P. H. (2011). A global analysis of the comparability of winter chill models for fruit and nut trees. *Int. J. Biometeorol.* 55, 411–421. doi: 10.1007/s00484-010-0352-y

Luedeling, E., and Gassner, A. (2012). Partial Least Squares Regression for analyzing walnut phenology in California. *Agric. For. Meteorol.* 158–159, 43–52. doi: 10.1016/j.agrformet.2011.10.020

Luedeling, E., Kunz, A., and Blanke, M. M. (2013). Identification of chilling and heat requirements of cherry trees–a statistical approach. *Int. J. Biometeorol.* 57, 679–689. doi: 10.1007/s00484-012-0594-y

Luedeling, E., Zhang, M., McGranahan, G., and Leslie, C. (2009). Validation of winter chill models using historic records of walnut phenology. *Agric. For. Meteorol.* 149, 1854–1864. doi: 10.1016/j.agrformet.2009.06.013

Martínez de Toda, F., and Balda Manzanos, P. (2013). Delaying berry ripening through manipulating leaf area to fruit ratio. *Vitis* 52, 171–176.

Martínez de Toda, F., Sancha González, J. C., and Balda Manzanos, P. (2013). Reducing the sugar and pH of the grape (*Vitis vinifera* L. cvs. Grenache and Tempranillo) through a single shoot trimming. *S. Afr. J. Enol. Vitic.* 34, 246–251.

Martínez de Toda, F., Sancha, J. C., Zheng, W., and Balda, P. (2014). Leaf area reduction by trimming, a growing technique to restore the anthocyanins: sugars ratio decoupled by the warming climate. *Vitis* 53, 189–192.

Martínez-Lüscher, J., Morales, F., Delrot, S., Sánchez-Díaz, M., Gomès, E., Aguirreolea, J., et al. (2015a). Characterization of the adaptive response of grapevine (cv. Tempranillo) to UV-B radiation under water deficit conditions. *Plant Sci.* 232, 13–22. doi: 10.1016/j.plantsci.2014.12.013

Martínez-Lüscher, J., Morales, F., Delrot, S., Sánchez-Díaz, M., Gomès, E., Aguirreolea, J., et al. (2015b). Climate change conditions (elevated CO_2 and temperature) and UV-B radiation affect grapevine (*Vitis vinifera* cv. Tempranillo) leaf carbon assimilation, altering fruit ripening rates. *Plant Sci.* 236, 168–176. doi: 10.1016/j.plantsci.2015.04.001

Martínez-Lüscher, J., Sánchez-Díaz, M., Delrot, S., Aguirreolea, J., Pascual, I., and Gomès, E. (2016). Ultraviolet-B alleviates the uncoupling effect of elevated CO_2 and increased temperature on grape berry (*Vitis vinifera* cv. Tempranillo) anthocyanin and sugar accumulation. *Aust. J. Grape Wine Res.* 22, 87–95. doi: 10.1111/ajgw.12213

Meinshausen, M., Smith, S. J., Calvin, K., Daniel, J. S., Kainuma, M. L. T., Lamarque, J.-F., et al. (2011). The RCP greenhouse gas concentrations and their extensions from 1765 to 2300. *Clim. Change* 109, 213–241. doi: 10.1007/s10584-011-0156-z

Morales, F., Pascual, I., Sánchez-Díaz, M., Aguirreolea, J., Irigoyen, J. J., Goicoechea, N., et al. (2014). Methodological advances: using greenhouses to simulate climate change scenarios. *Plant Sci.* 226, 30–40. doi: 10.1016/j.plantsci.2014.03.018

Mullins, M. G. (1966). Test-plant for investigations of the physiology of fruiting in *Vitis vinifera* L. *Nature* 209, 419–420. doi: 10.1038/209419a0

Mullins, M. G., Bouquet, A., and Williams, L. E. (1992). *Biology of the Grapevine*. Cambridge, UK: Cambridge University Press.

Nicolas, P., Lecourieux, D., Kappel, C., Cluzet, S., Cramer, G., Delrot, S., et al. (2014). The basic leucine zipper transcription factor ABSCISIC ACID RESPONSE ELEMENT-BINDING FACTOR2 is an important transcriptional regulator of abscisisic acid-dependent grape ripening processes. *Plant Physiol.* 164, 365–383. doi: 10.1104/pp.113.231977

Oliveira, C., Silva Ferreira, A. C., Mendes Pinto, M., Hogg, T., Alves, F., and Guedes de Pinho, P. (2003). Carotenoid compounds in grapes and their relationship to plant water status. *J. Agric. Food Chem.* 51, 5967–5971. doi: 10.1021/jf034275k

Ollat, N., Geny, L., and Soyer, J. (1998). Les boutures fructifères de vigne: validation d'un modèle d'étude du development de la physiologie de la vigne. I. Caracteristiques de l'appareil vegetatif. *J. Int. Sci. Vigne Vin* 32, 1–8.

Parker, A. K., de Cortazar-Atauri, I. G., van Leeuwen, C., and Chuine, I. (2011). General phenological model to characterise the timing of flowering and veraison of *Vitis vinifera* L. *Aust. J. Grape Wine Res.* 17, 206–216. doi: 10.1111/j.1755-0238.2011.00140.x

Parker, A. K., Hofmann, R. W., van Leeuwen, C., McLachlan, A. R. G., and Trought, M. C. T. (2014). Leaf area to fruit mass ratio determines the time of veraison in Sauvignon Blanc and Pinot Noir grapevines. *Aust. J. Grape Wine Res.* 20, 422–431. doi: 10.1111/ajgw.12092

Parker, A. K., Hofmann, R. W., van Leeuwen, C., McLachlan, A. R. G., and Trought, M. C. T. (2015). Manipulating the leaf area to fruit mass ratio alters the synchrony of total soluble solids accumulation and titratable acidity of grape berries. *Aust. J. Grape Wine Res.* 21, 266–276. doi: 10.1111/ajgw.12132

Petrie, P. R., and Sadras, V. O. (2008). Advancement of grapevine maturity in Australia between 1993 and 2006: putative causes, magnitude of trends and viticultural consequences. *Aust. J. Grape Wine Res.* 14, 33–45. doi: 10.1111/j.1755-0238.2008.00005.x

Rawson, H. M. (1995). Yield responses of 2 wheat genotypes to carbon-dioxyde and temperature in-field studies using temperature-gradient tunnels. *Aust. J. Plant Physiol.* 22, 23–32. doi: 10.1071/PP9950023

R Development Core Team (2016). *R: A Language and Environment for Statistical Computing*. Vienna: R Foundation for Statistical Computing. Available online at: http://www.R-project.org

Sadras, V. O., and Moran, M. A. (2012). Elevated temperature decouples anthocyanins and sugars in berries of Shiraz and Cabernet Franc. *Aust. J. Grape Wine Res.* 18, 115–122. doi: 10.1111/j.1755-0238.2012.00180.x

Sadras, V. O., and Moran, M. A. (2013). Nonlinear effects of elevated temperature on grapevine phenology. *Agric. For. Meteorol.* 173, 107–115. doi: 10.1016/j.agrformet.2012.10.003

Sadras, V. O., and Petrie, P. R. (2011). Climate shifts in south-eastern Australia: early maturity of Chardonnay, Shiraz and Cabernet Sauvignon is associated with early onset rather than faster ripening. *Aust. J. Grape Wine Res.* 17, 199–205. doi: 10.1111/j.1755-0238.2011.00138.x

Sadras, V. O., Stevens, R., Pech, J., Taylor, E., Nicholas, P., and McCarthy, M. (2007). Quantifying phenotipic plasticity of berry traits using an allometric-type approach: a case study on anthocyanins and sugars in berries of Cabernet Sauvignon. *Aust. J. Grape Wine Res.* 13, 72–80. doi: 10.1111/j.1755-0238.2007.tb00237.x

Salazar Parra, C. (2011). *Vid y Cambio Climático. Estudio del Proceso de Maduración de la baya en Esquejes Fructíferos de Tempranillo, en Respuesta a la Interacción de CO_2 Elevado, Estrés Hídrico y Temperatura Elevada*. PhD Thesis. University of Navarra. Spain

Salazar Parra, C., Aguirreolea, J., Sánchez-Díaz, M., Irigoyen, J. J., and Morales, F. (2010). Effects of climate change scenarios on *Tempranillo grapevine* (*Vitis vinifera* L.) ripening: response to a combination of elevated CO_2 and temperature, and moderate drought. *Plant Soil* 337, 179–191. doi: 10.1007/s11104-010-0514-z

Spencer, J. W. (1971). Fourier series representation of the position of the sun. *Search* 2, 172.

Sweetman, C., Deluc, L. G., Cramer, G. R., Ford, C. M., and Soole, K. L. (2009). Regulation of malate metabolism in grape berry and other developing fruits. *Phytochemistry* 70, 1329–1344. doi: 10.1016/j.phytochem.2009.08.006

Tramontini, S., van Leeuwen, C., Domec, J.-C., Destrac-Irvine, A., Basteau, C., Vitali, M., et al. (2013). Impact of soil texture and water availability on the hydraulic control of plant and grape-berry development. *Plant Soil* 368, 215–230. doi: 10.1007/s11104-012-1507-x

van Leeuwen, C., Friant, P., Choné, X., Tregoat, O., Koundouras, S., and Dubourdieu, D. (2004). Influence of climate, soil, and cultivar on terroir. *Am. J. Enol. Vitic.* 55, 207–217.

van Leeuwen, C., Schultz, H. R., Garcia de Cortazar-Atauri, I., Duchene, E., Ollat, N., Pieri, P., et al. (2013). Why climate change will not dramatically decrease viticultural suitability in main wine-producing areas by 2050. *Proc. Natl. Acad. Sci. U.S.A.* 110, E3051–E3052. doi: 10.1073/pnas.1307927110

van Leeuwen, C., and Seguin, G. (2006). The concept of terroir in viticulture. *J. Wine Res.* 17, 1–10. doi: 10.1080/09571260600633135

van Leeuwen, C., Tregoat, O., Choné, X., Bois, B., Pernet, D., and Gaudillere, J. P. (2009). Vine water status is a key factor in grape ripening and vintage quality for red Bordeaux wine. How can it be assessed for vineyard management purposes? *J. Int. Sci. Vigne Vin* 43, 121–134. doi: 10.20870/oeno-one.2009.43.3.798

Webb, L. B., Whetton, P. H., and Barlow, E. W. R. (2007). Modelled impact of future climate change on the phenology of winegrapes in Australia. *Aust. J. Grape Wine Res.* 13, 165–175. doi: 10.1111/j.1755-0238.2007.tb00247.x

Webb, L. B., Whetton, P. H., Bhend, J., Darbyshire, R., Briggs, P. R., and Barlow, E. W. R. (2012). Earlier wine-grape ripening driven by climatic warming and drying and management practices. *Nature Climate Change* 2, 259–264. doi: 10.1038/nclimate1417

Wold, S., Sjöström, M., and Eriksson, L. (2001). PLS-regression: a basic tool of chemometrics. *Chem. Intell. Lab. Syst.* 58, 109–130. doi: 10.1016/S0169-7439(01)00155-1

Conflict of Interest Statement: The authors declare that the research was conducted in the absence of any commercial or financial relationships that could be construed as a potential conflict of interest.

frontiers in Plant Science

ORIGINAL RESEARCH
published: 25 October 2016
doi: 10.3389/fpls.2016.01568

Impaired Stomatal Control Is Associated with Reduced Photosynthetic Physiology in Crop Species Grown at Elevated [CO_2]

Matthew Haworth[1], Dilek Killi[2], Alessandro Materassi[3], Antonio Raschi[3] and Mauro Centritto[1]*

[1] National Research Council – Tree and Timber Institute, Florence, Italy, [2] Department of Agrifood Production and Environmental Sciences, University of Florence, Florence, Italy, [3] National Research Council – Institute of Biometeorology, Florence, Italy

Physiological control of stomatal conductance (G_s) permits plants to balance CO_2-uptake for photosynthesis (P_N) against water-loss, so optimizing water use efficiency (WUE). An increase in the atmospheric concentration of carbon dioxide ([CO_2]) will result in a stimulation of P_N and reduction of G_s in many plants, enhancing carbon gain while reducing water-loss. It has also been hypothesized that the increase in WUE associated with lower G_s at elevated [CO_2] would reduce the negative impacts of drought on many crops. Despite the large number of CO_2-enrichment studies to date, there is relatively little information regarding the effect of elevated [CO_2] on stomatal control. Five crop species with active physiological stomatal behavior were grown at ambient (400 ppm) and elevated (2000 ppm) [CO_2]. We investigated the relationship between stomatal function, stomatal size, and photosynthetic capacity in the five species, and then assessed the mechanistic effect of elevated [CO_2] on photosynthetic physiology, stomatal sensitivity to [CO_2] and the effectiveness of stomatal closure to darkness. We observed positive relationships between the speed of stomatal response and the maximum rates of P_N and G_s sustained by the plants; indicative of close co-ordination of stomatal behavior and P_N. In contrast to previous studies we did not observe a negative relationship between speed of stomatal response and stomatal size. The sensitivity of stomata to [CO_2] declined with the ribulose-1,5-bisphosphate limited rate of P_N at elevated [CO_2]. The effectiveness of stomatal closure was also impaired at high [CO_2]. Growth at elevated [CO_2] did not affect the performance of photosystem II indicating that high [CO_2] had not induced damage to the photosynthetic physiology, and suggesting that photosynthetic control of G_s is either directly impaired at high [CO_2], sensing/signaling of environmental change is disrupted or elevated [CO_2] causes some physical effect that constrains stomatal opening/closing. This study indicates that while elevated [CO_2] may improve the WUE of crops under normal growth conditions, impaired stomatal control may increase the vulnerability of plants to water deficit and high temperatures.

Keywords: stomatal behavior, stomatal evolution, stomatal sensitivity, drought, photosynthetic down-regulation, food security

OPEN ACCESS

Edited by:
Peter Thorburn, Commonwealth Scientific and Industrial Research Organisation, Australia

Reviewed by:
Hazem M. Kalaji, Warsaw University of Life Sciences, Poland
Alex Wu, University of Queensland, Australia

****Correspondence:***
Matthew Haworth
haworth@ivalsa.cnr.it

Specialty section:
This article was submitted to Agroecology and Land Use Systems, a section of the journal Frontiers in Plant Science

Received: *30 May 2016*
Accepted: *05 October 2016*
Published: *25 October 2016*

Citation:
Haworth M, Killi D, Materassi A, Raschi A and Centritto M (2016) Impaired Stomatal Control Is Associated with Reduced Photosynthetic Physiology in Crop Species Grown at Elevated [CO_2]. Front. Plant Sci. 7:1568. doi: 10.3389/fpls.2016.01568

INTRODUCTION

Stomatal pores act as the interface between the plant and the atmosphere, regulating the uptake of CO_2 for photosynthesis (P_N) and the loss of water via transpiration. Photosynthesis rates are positively related to stomatal conductance (G_s; Wong et al., 1979; Flexas and Medrano, 2002), and effective stomatal control through morphological changes to the number of stomata and physiological regulation of stomatal aperture size allows the optimal balance of CO_2-uptake and water-loss over a range of favorable and sub-optimal growth conditions (Flexas et al., 2002; Lauteri et al., 2014; Haworth et al., 2015). Physiological regulation of the size of the stomatal pore aperture ranges from 'active' to 'passive' stomatal behavior. Active stomatal behavior involves rapid alteration of stomatal aperture following an external stimulus as ions are actively pumped across guard cell membranes to alter guard cell turgor. Alternatively, where guard cell turgor, and as a result pore area, follows whole leaf turgor, stomatal behavior is considered to be passive (Chater et al., 2013). The development of crop species has involved the selection of more productive and faster growing varieties over multiple generations (Evans, 1980; Roche, 2015). These selected varieties often possess greater leaf area rates of P_N than their less productive counterparts (Zelitch, 1982; Fischer et al., 1998; Gu et al., 2014). As a result, the vast majority of crops currently cultivated possess active stomatal physiological behavior that permits the levels of G_s required to sustain high P_N, but also the capacity to respond rapidly to a change in environmental conditions (Kalaji and Nalborczyk, 1991; Haworth et al., 2015; Roche, 2015). However, it is unclear how active physiological stomatal behavior in crop plants can be affected by changes in the atmospheric concentration of $[CO_2]$, and whether growth at elevated $[CO_2]$ can induce a loss of stomatal control.

Rising atmospheric $[CO_2]$ is considered to have a beneficial effect on the carbon balance of plants though CO_2-fertilization and reduced transpirative water-loss generally associated with lower G_s that results in an increase in water use efficiency (WUE; Centritto et al., 2002; Wullschleger et al., 2002; Haworth et al., 2016). Nonetheless, climate change will also result in an increase in the frequency, severity and duration of drought, and increased temperature events (Ciais et al., 2005). In these cases, effective stomatal control is crucial to the plant stress response (e.g., Bunce, 2000; Shah and Paulsen, 2003; Killi et al., 2016), particularly in fast-growing crop species with high maximum rates of G_s. It has been suggested that smaller stomata are able to open and close more rapidly, thus affording greater responsiveness to a change in growth conditions (Hetherington and Woodward, 2003; Drake et al., 2013). Plants with large numbers of small stomata are also able to maintain greater levels of G_s (de Boer et al., 2016), potentially as an adaptation to declining $[CO_2]$ over the Cenozoic (Franks and Beerling, 2009). It may therefore be expected that stomatal size, the speed of stomatal closure and maximal rates of P_N and G_s are closely associated in fast-growing plants with active stomatal behavior. Nevertheless, the impact of growth at elevated $[CO_2]$ on the regulation of stomatal aperture is largely unknown.

Stomatal aperture is regulated by network of interlinked signals (Hetherington and Woodward, 2003) incorporating photosynthesis in the light (Messinger et al., 2006) and the physiological status of the plant (e.g., Lauteri et al., 2014). Beech (*Fagus sylvatica*), chestnut (*Castanea sativa*), and oak (*Quercus robur*) all exhibit an inverse relationship between G_s and leaf to air vapor pressure deficit (VPD) under light conditions when grown at ambient $[CO_2]$. However, when grown in atmospheres enriched in $[CO_2]$ to 710 ppm, oak and chestnut showed reduced stomatal sensitivity to VPD, while beech no longer altered G_s to VPD (Heath, 1998). Growth at elevated $[CO_2]$ did not induce a reduction of G_s in beech, but also reduced the speed ($\sim$−25% after 4 days) and tightness ($\sim$−22% over a soil water potential range of −200 to −250 hPa) of stomatal closure in response to soil drying. This impaired stomatal control was associated with reduced stomatal sensitivity to the drought stress hormone ABA in the beech plants grown at elevated $[CO_2]$. Furthermore, an increase in leaf area, alongside the loss of stomatal control incurred at high $[CO_2]$, made the beech trees more susceptible to drought stress when grown in atmospheres enriched in $[CO_2]$ (Heath and Kerstiens, 1997). The cycad *Lepidozamia peroffskyana* and broad-leaved conifer *Nageia nagi* both exhibit active stomatal control when grown at ambient $[CO_2]$ under well-watered conditions. However, when grown at elevated $[CO_2]$ of 1500 ppm, both species no longer adjusted G_s in response to an instantaneous change in external $[CO_2]$ (C_a; Haworth et al., 2013), indicative of a loss of stomatal control. Hollyfern (*Cyrtomium fortunei*) also showed a loss of stomatal sensitivity to C_a and impaired stomatal closure during darkness when grown in atmospheres of 2000 ppm $[CO_2]$ (Haworth et al., 2015). Such a loss of stomatal control at high $[CO_2]$ would impair the capacity of plants to limit water-loss associated with P_N during episodes of high transpirative demand.

Effective stomatal control is not only important during light-driven assimilation of CO_2, but also when conditions are not favorable for P_N (Killi et al., 2016). At night many plants do not close their stomata to their full extent, resulting in transpirative water-loss in the absence of P_N. Night-time G_s in Eucalyptus (*Eucalyptus sideroxylon*) is 30% of levels recorded in the day-time (Zeppel et al., 2012), and can be as high as 250 mmol m^{-2} s^{-1} in many plants (Caird et al., 2007), thus representing a significant loss of water. The ecological function of night-time G_s is unclear, but is hypothesized to be related to the maintenance of root mass-flow of water to ensure the uptake of mobile nutrients such as nitrogen (Caird et al., 2007). Under elevated $[CO_2]$ of 640 ppm and not experiencing drought, Eucalyptus exhibited a 17% increase in night-time G_s, but levels of G_s during the day-time were identical at ambient and elevated $[CO_2]$ (Zeppel et al., 2012); possibly as an adaptation to enhance nutrient uptake due to reduced root mass-flow of water under elevated $[CO_2]$ (Van Vuuren et al., 1997). Under optimal growth conditions, during the night plant water potential generally equilibrates with that of soil water potential (Hinckley et al., 1978; Donovan et al., 2001). Increased night-time G_s may impair the equilibration of leaf and soil water potentials, or in the case of promoting root mass-flow to

enhance nutrient uptake may indicate some underlying nutrient deficiency in the plants. This increase in night-time G_s under elevated [CO_2] may seem somewhat incongruous, as an increase in [CO_2] is widely considered likely to reduce G_s (Centritto et al., 1999; Ainsworth and Rogers, 2007). However, a rise in [CO_2] may impair stomatal function, resulting in stomatal pores that close more slowly and less tightly (e.g., Haworth et al., 2015), potentially accounting for observations of increased night-time G_s at elevated [CO_2] (Zeppel et al., 2012). Measurement of the speed of the stomatal response of plants grown under elevated [CO_2] to darkness (i.e., conditions no longer conducive to P_N) and the tightness of stomatal closure (Haworth et al., 2015) may provide indications of any loss of stomatal function associated with high [CO_2].

The loss of stomatal control represented by the reduced capacity and speed of stomatal closure at elevated [CO_2] may render plants vulnerable to desiccation during episodes of drought or high transpirative demand. This is counter to the prevailing consensus that an increase in [CO_2] would improve WUE (Centritto et al., 2002; Ainsworth and Rogers, 2007) and mitigate drought by reducing water-loss (Wall, 2001). A loss of stomatal control and increased vulnerability to drought and heat-waves would have severe implications for crops such as wheat (e.g., Stratonovitch and Semenov, 2015). However, there is comparatively little information regarding the impact of elevated [CO_2] on stomatal control in crop species. Photosynthesis in the mesophyll layer and G_s are closely co-ordinated via C_i in the presence of red light (Messinger et al., 2006; Engineer et al., 2016). It is possible that any effect of elevated [CO_2] may have an effect upon the regulation of stomatal aperture via a direct effect on P_N. To study the mechanistic effects of elevated [CO_2] on stomatal control in C3 crop plants we grew oat (*Avena sativa*), sunflower (*Helianthus annuus*), cotton (*Gossypium hirsutum*), barley (*Hordeum vulgare*), and wheat (*Triticum aestivum*) under ambient (400 ppm) and elevated (2000 ppm) [CO_2]. As comparatively little is known about how growth at elevated [CO_2] can affect stomatal control, a higher [CO_2] level was chosen for the elevated treatment than concentrations predicted by the IPCC (2007) models, but not in the context of atmospheric [CO_2] over the last 200 million years (Berner, 2009), as this would clearly demonstrate whether growth at elevated [CO_2] has a mechanistic effect on stomatal function. The effect of growth at elevated [CO_2] on stomatal control (tightness of closure following a cessation of illumination and sensitivity to instantaneous changes in C_a: reported in a previous study, with the exception of wheat, of Haworth et al., 2015) and the interaction with photosynthetic physiology were investigated. We hypothesize that these fast-growing crop species with high rates of P_N will exhibit a high degree of stomatal control, but that this stomatal control may become impaired at elevated [CO_2]. This study aims to: (i) investigate potential correlations between stomatal pore size and the speed of stomatal closure, and whether species with 'fast' stomata possess greater maximum rates of G_s and P_N; (ii) determine how stomatal control in crop plants with active physiological stomatal behavior is affected by growth at elevated [CO_2] through analysis of speed and tightness of stomatal closure following the cessation of illumination and stomatal sensitivity to instantaneous increases in C_a; (iii) assess whether adjustment of the photosynthetic physiology may affect stomatal control at high [CO_2] either through alteration of the 'photosynthetic' stomatal response to [CO_2], or damage to the photosynthetic apparatus incurred by growth at elevated [CO_2], and; (iv) explore the possible implications of any change in stomatal control for crop plants growing in a future high [CO_2] and water-limited world.

MATERIALS AND METHODS

Plant Growth Conditions

The plants were potted in 6 dm^3 square pots using a 5:1 mixture of commercial compost and vermiculite and placed in two large walk-in growth rooms with full control of light, temperature, [CO_2] (one chamber maintained ambient atmospheric [CO_2] of 400 ppm and the second an elevated [CO_2] level of 2000 ppm) and humidity for 16-week (technical details of the plant growth chambers are given in Materassi et al., 2005). The plants were watered to pot capacity every 2 days and provided weekly with a commercial liquid plant fertilizer (COMPO Concime Universale, NPK 7-5-7, B, Cu, Fe, Mn, Mo, Zn: COMPO Italia, Cesano Maderno, Italy) to facilitate nutrient availability at free access rates. The growth chambers maintained conditions of 16 h of daylight (14 h at full *PAR* levels of 1000 $\mu mol\ m^{-2}\ s^{-1}$ with two 1-h periods of simulated dawn/dusk where light intensity was incrementally increased/decreased), a day and night-time temperature regime of 25/18°C and constant relative humidity of 50%. To avoid potential chamber effects, the growth rooms were alternated every 2 weeks – no significant differences were observed in the measurements conducted under the same conditions in different growth chambers. Timings of day/night programs on the plant growth chambers were staggered to allow the maximum number of plants to be analyzed at the optimal time of the day/night program for photosynthetic activity (07:00–11:00 h), and thus avoid the influence of circadian stomatal behavior; particularly where stomata close at midday or during the early afternoon when leaf water potentials may decrease. Four replicates of each species were grown under ambient and elevated [CO_2], and a minimum of three replicates were used for the measurement of stomatal sensitivity to C_a and closure in response to darkness.

Leaf Gas-Exchange Analysis of Stomatal Control

A PP-Systems Ciras-2 attached to a PLC6(U) leaf cuvette and LED light unit (PP-Systems, Amesbury, MA, USA) was used to gauge the physiological response of stomata to darkness and C_a. All physiological measurements were conducted on the same leaf per plant (no more than one measurement was performed on each plant over 48 h) in a well-ventilated air-conditioned room maintained at 25°C. The newest fully expanded leaf was consistently used for analysis (in grasses this was the leaf below

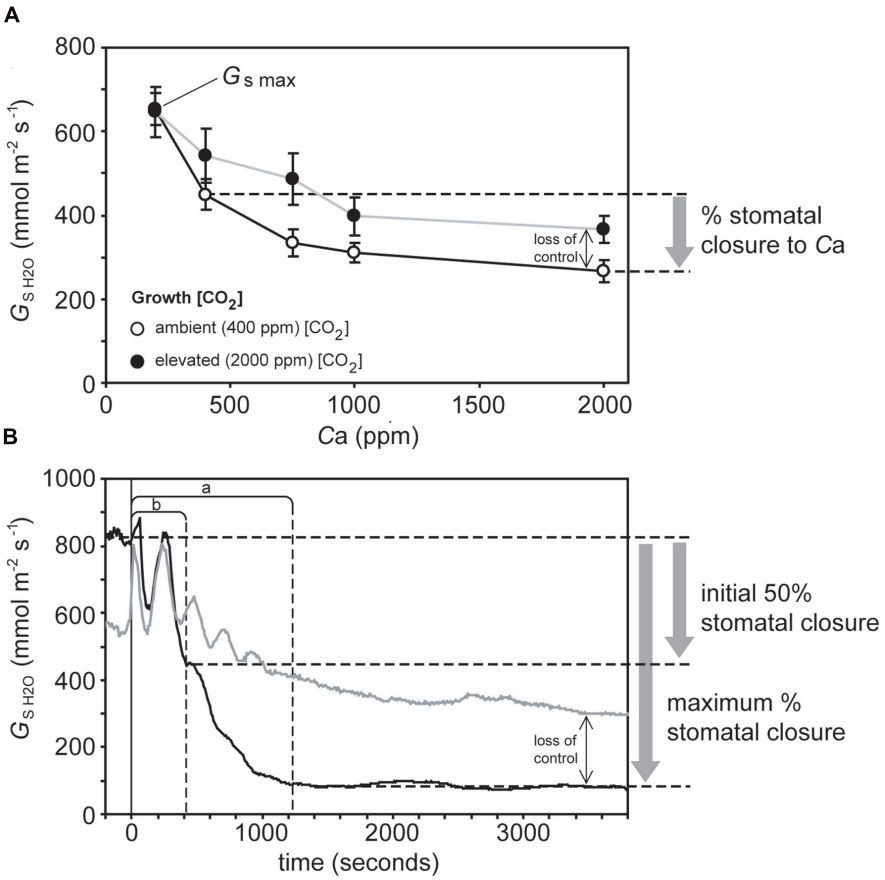

FIGURE 1 | Illustration of gas exchange measurements in sunflower to determine: (A) Stomatal sensitivity to C_a – plants grown in atmospheres of 400 ppm (open symbols, black line) and 2000 ppm (closed symbols, gray line) were exposed to instantaneous increases in C_a. Stomatal conductance was allowed to stabilize at each C_a before data was logged. The difference between G_s values at C_a values of 400 and 2000 ppm [CO_2] is used to infer stomatal closure. **(B)** Stomatal closure to darkness – the leaves of plants grown in atmospheres of 400 ppm (black line) and 2000 ppm (gray line) were placed in a cuvette, after G_s had remained stable for 10 min the light in the cuvette and room were simultaneously switched off (represented by the vertical black line). Fifty percent of the maximum and maximum stomatal closure are marked by dashed horizontal lines. The speed of stomatal closure at 50% and maximum stomatal closure are marked by dashed vertical lines labeled *a* and *b*, respectively. The lack of stability in G_s values immediately after the cessation of illumination may be an artifact related to changes in the temperature of the leaf cuvette affecting the measurement of relative humidity of the air within the cuvette. For clarity, the points taken to illustrate the determination of stomatal closure are only showed in relation to the plants grown at 400 ppm [CO_2] (black lines). Plants grown at 2000 ppm (gray lines) are included to illustrate the impact of [CO_2] on stomatal control, with the black arrow indicating the loss of stomatal control incurred by growth at elevated [CO_2].

the flag leaf) to avoid any age-related effects regarding stomatal functionality. To assess the physiological stomatal behavioral responses of the plants to C_a, the level of [CO_2] within the leaf cuvette was increased in a number of stages (200, 400, 750, 1000, and 2000 ppm CO_2) while temperature (25°C), VPD (1.6–1.8 KPa ± 0.1 KPa), and light intensity (2000 μmol m^{-2} s^{-1}) remained constant. At each [CO_2] step, the stomatal conductance of water vapor ($G_{s\ H2O}$) was allowed to stabilize and then remain stable for 5–10 min before being recorded. Maximum stomatal conductance ($G_{s\ max}$) was considered to be $G_{s\ H2O}$ recorded at a [CO_2] of 50 ppm to induce full stomatal opening (Centritto et al., 2003). Stomatal closure was expressed as the percentage of $G_{s\ H2O}$ values at 2000 ppm CO_2 relative to those recorded at an ambient [CO_2] of 400 ppm (**Figure 1**). To measure the stomatal response to darkness, a leaf was placed in the leaf cuvette with a temperature of 25°C, *PAR* of 2000 μmol m^{-2} s^{-1} and 400 ppm [CO_2]. After $G_{s\ H2O}$ had remained stable for 15 min the lights in both the cuvette and the room were simultaneously switched off and $G_{s\ H2O}$ was recorded every 10 s for a minimum of 1 h (Meidner and Mansfield, 1965). Vapor pressure deficit in the cuvette was maintained between 1.6 to 1.8 KPa ± 0.1 KPa throughout the measurement of the stomatal response to darkness. Stomatal closure in response to the cessation of illumination was expressed as the percentage $G_{s\ H2O}$ after 1-h of darkness. The speed of stomatal closure is not uniform after the onset of darkness (Haworth et al., 2015); the reduction in $G_{s\ H2O}$ per second over the first 50% reduction in $G_{s\ H2O}$, and also over the time to reach the maximum extent of stomatal closure was therefore determined (**Figure 1**). Measurements of stomatal pore length (SPL) of the plants under ambient and elevated [CO_2] were taken from Haworth et al. (2015).

Leaf Gas-Exchange and Chlorophyll Fluorescence Analysis of Photosynthetic Physiology

Response curves of P_N to increasing internal sub-stomatal [CO_2] (C_i) under a saturating light intensity of 2000 μmol m^{-2} s^{-1} (C_a sequence of 350, 250, 150, 50, 100, 200, 300, 400, 600, 800, 1000, 1200, 1400, 1600, 1800, and 2000 ppm) at a standard cuvette temperature of 25°C were recorded on the same leaves used to assess stomatal control using the same Ciras-2 photosynthesis system. The maximum carboxylation rate of RubisCO (Vc_{max}), the maximum rate of electron transport for regeneration of ribulose-1,5-bisphosphate (J_{max}) and mesophyll conductance to CO_2 (G_{mCO2}) were calculated from the P_N/C_i response curves following Ethier and Livingston (2004). The 'curve fitting' method of Ethier and Livingston (2004) estimates G_{mCO2} from the response of P_N to increasing partial pressure of CO_2 in the sub-stomatal air-space assuming a constant G_{mCO2} across the range of C_i values (cf. Flexas et al., 2007). Total conductance to CO_2 (G_{totCO2}) was calculated as:

$$G_{tot\,co2} = \frac{(G_{s\,co2} * G_{m\,co2})}{(G_{s\,co2} + G_{m\,co2})}$$

Where G_{sCO2} is the stomatal conductance to CO_2 – in the present manuscript to further aid differentiation between measurement of stomatal conductance to H_2O and CO_2, $G_{s\ H2O}$ is expressed as mmol m^{-2} s^{-1}, while $G_{s\ CO2}$ is expressed as mol m^{-2} s^{-1}. The maximum rate of photosynthesis ($P_{N\ max}$) was considered to be P_N at a saturating light intensity of 2000 μmol m^{-2} s^{-1} and [CO_2] of 2000 ppm. The maximum (F_v/F_m) and actual (ΦPSII: $\Delta F/F'm$) quantum efficiency of photosystem II was recorded using a Hansatech FMS-2 (saturating pulse of 10,000 μmol m^{-2} s^{-2}) and dark adaptation clips (Hansatech, King's Lynn, UK) after 30 min of dark adaptation and exposure to actinic light of 1000 μmol m^{-2} s^{-1} for a minimum of 10 min after the first saturating pulse (Genty et al., 1989; Kalaji et al., 2014).

Statistical Analyses

Statistical analyses were performed using SPSS 20 (IBM, New York, NY, USA). To test [CO_2] treatment effects a one-way ANOVA was used to assess differences in variance between samples. A two-way ANOVA was used to assess species and [CO_2] effects on G_{smax} (**Figure 3**). The relative change (Δ) in parameters was expressed as a percentage of the values recorded at 2000 ppm [CO_2] relative to control values measured at 400 ppm [CO_2]. Linear regression was used to investigate potential relationships between stomatal characteristics such as stomatal pore length and speed of stomatal closure and whether relative changes in stomatal behavior (i.e., Δ G_s change to [CO_2] or darkness) were associated with the relative change in photosynthetic physiology.

RESULTS

The rate of P_N in the five crop species grown in atmospheres of ambient and elevated [CO_2] was positively related to G_{sCO2} and G_{totCO2} when measured at a common [CO_2] level of 400 ppm (**Figure 2**). However, P_N did not correlate to G_{mCO2} measured using the curve fitting approach. Stomatal conductance to water vapor was 18.5–48.9% lower at elevated [CO_2] in four of the species when measured at their respective growth

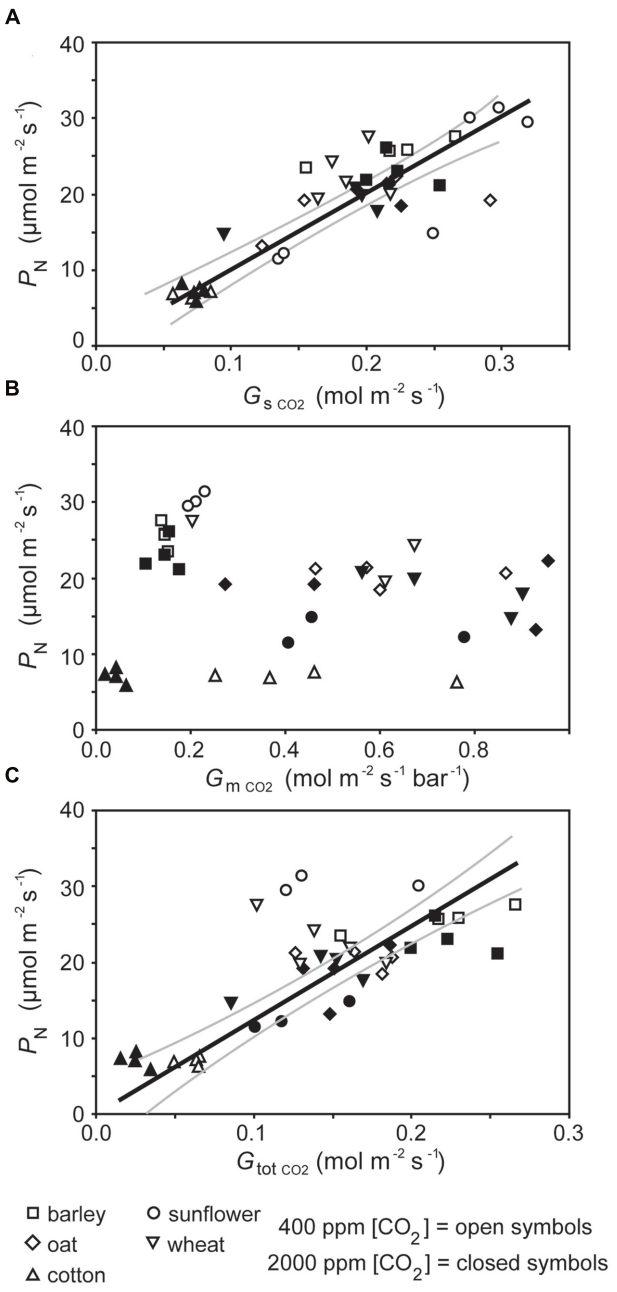

FIGURE 2 | The relationship between photosynthesis (P_N) and (A) stomatal conductance to CO_2 (G_{sCO2}; linear regression $F_{1,37} = 107.922$; $P = 1.607 \times 10^{-12}$; $R^2 = 0.863$), (B) mesophyll conductance to CO_2 (G_{mCO2}; linear regression $F_{1,37} = 0.052$; $P = 0.821$), and (C) total conductance to CO_2 (G_{totCO2}; linear regression $F_{1,37} = 46.763$; $P = 4.659 \times 10^{-8}$; $R^2 = 0.747$). Solid black line indicates best fit, gray lines either side indicate 95% confidence intervals of the mean.

$[CO_2]$ levels. Cotton showed no change in $G_{s\ H2O}$ when grown at 400 and 2000 ppm $[CO_2]$ (**Table 1**; **Figure 2**). Positive relationships were observed between the speed of stomatal closure to darkness and P_N max (**Figures 3A,B**). The maximum rate of stomatal conductance was significantly correlated to the speed of stomatal closure during the initial 50% reduction in $G_{s\ H2O}$ (**Figure 3C**), but not to the maximum extent of stomatal closure (**Figure 3D**). In plants grown at an ambient $[CO_2]$ of 400 ppm, no relationship was observed between SPL and the speed of stomatal closure during the initial 50% reduction in $G_{s\ H2O}$ (**Figure 4A**). However, a positive relationship was observed between SPL and the speed of stomatal closure to the maximum extent of stomatal closure at ambient $[CO_2]$ (**Figure 4C**). Positive relationships were observed between the speed of stomatal closure and SPL in the five crop plants grown at elevated $[CO_2]$ (**Figures 4B,D**).

Growth at elevated $[CO_2]$ resulted in significant declines in V_{cmax} in cotton and sunflower (**Table 1**). This coincided with lower stomatal closure to darkness (**Figure 5**). Sunflower showed lower V_{cmax} and J_{max} that coincided with impaired stomatal closure to darkness and stomatal sensitivity to C_a; however, ΔV_{cmax} in all five species did not correlate to Δstomatal closure to C_a (**Figure 6A**). Oat, wheat, and barley did not exhibit any significant correlations between photosynthetic physiology and stomatal control (**Figure 5**). However, when the relative change in photosynthetic parameters was compared to the relative change in stomatal control a highly significant positive correlation was observed between ΔV_{cmax} and Δstomatal closure to darkness (**Figure 6B**). In effect, those species that retain V_{cmax} (i.e., a ΔV_{cmax} close to 100%) also tend to maintain stomatal closure (i.e., a Δstomatal closure to darkness close to 100%) at high $[CO_2]$; while species that exhibit reduced V_{cmax} at high $[CO_2]$ also show lower ability to close stomata in response to the cessation of illumination. Less robust positive correlations were also observed between ΔJ_{max} with Δstomatal closure to $[CO_2]$ (**Figure 6C**) and Δstomatal closure to darkness (**Figure 6D**).

TABLE 1 | The effect of growth at ambient (400 ppm) and elevated (2000 ppm) $[CO_2]$ on maximum rate of carboxylation of ribulose-1,5-bisphosphate carboxylase/oxygenase (V_{cmax}), the maximum rate of electron transport required for ribulose-1,5-bisphosphate regeneration (J_{max}), stomatal conductance of water vapor (G_{sH2O}) and chlorophyll fluorescence parameters of the maximum (F_v/F_m) and actual (ΦPSII) quantum efficiency of photosystem II.

Species	V_{cmax} (μmol m^{-2} s^{-1})		J_{max} (μmol m^{-2} s^{-1})		$G_{s\ H2O}$ (mmol m^{-2} s^{-1})		F_v/F_m		ΦPSII	
	Amb $[CO_2]$	Elev $[CO_2]$	Amb $[CO_2]$	Elev $[CO_2]$	Amb $[CO_2]$	Elev $[CO_2]$	Amb $[CO_2]$	Elev $[CO_2]$	Amb $[CO_2]$	Elev $[CO_2]$
Oat	87.8 ± 8.6^a	70.7 ± 6.7^a	144.6 ± 7.5^a	123.5 ± 10.2^a	669.7 ± 10.7^a	439.4 ± 62.4^b	0.842 ± 0.002^a	0.858 ± 0.017^a	0.427 ± 0.020^a	0.436 ± 0.035^a
Wheat	133.0 ± 4.0^a	121.9 ± 6.8^a	174.9 ± 11.1^a	148.0 ± 8.8^a	511.2 ± 26.5^a	416.4 ± 57.0^a	0.838 ± 0.004^a	0.837 ± 0.003^a	0.505 ± 0.034^a	0.494 ± 0.015^a
Cotton	68.4 ± 8.8^a	34.2 ± 2.7^b	73.5 ± 2.9^a	75.1 ± 5.2^a	138.3 ± 6.3^a	137.7 ± 5.6^a	0.827 ± 0.003^a	0.823 ± 0.001^a	0.233 ± 0.004^a	0.338 ± 0.013^b
Sunflower	123.4 ± 10.7^a	61.1 ± 13.2^b	173.3 ± 24.5^a	96.9 ± 4.2^b	976.5 ± 122.1^a	498.6 ± 93.6^b	0.854 ± 0.003^a	0.858 ± 0.006^a	0.566 ± 0.019^a	0.560 ± 0.030^a
Barley	72.4 ± 0.9^a	66.9 ± 3.5^a	137.0 ± 1.0^a	120.8 ± 8.7^a	874.0 ± 60.4^a	585.5 ± 18.4^b	0.845 ± 0.004^a	0.840 ± 0.004^a	0.438 ± 0.033^a	0.397 ± 0.012^a

Values are the mean of four to six replicates. ± indicates standard error. Letters indicate significant difference determined with a one-way ANOVA.

DISCUSSION

Co-ordination of Photosynthesis and Stomatal Control

Photosynthesis of the crop plants grown at ambient and elevated $[CO_2]$ when measured at a common $[CO_2]$ was closely related to stomatal and total conductance to CO_2 (**Figures 2A,C**). However, $G_{m\ CO2}$ derived from the curve fitting method (Ethier and Livingston, 2004) did not show any significant relationship to P_N either at a common C_a (**Figure 2B**) or the respective growth $[CO_2]$ levels of the plants (data not shown). The curve fitting approach calculates a single G_m value along the P_N – C_i curve. The efficacy of this approach is reliant upon G_m remaining constant at a range of C_i values (Tazoe et al., 2009, 2011), however, measurement of G_m using the variable J method of Harley et al. (1992) across a C_i gradient suggests that rates of G_{mCO2} may not be uniform and instead vary with the availability of CO_2 in relation to rates of P_N and

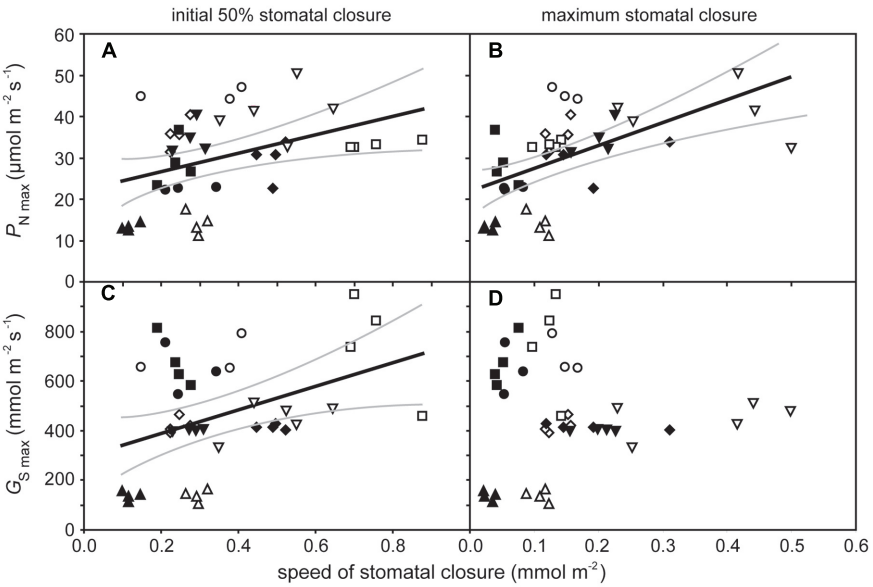

FIGURE 3 | The relationship between maximum rates of photosynthesis ($P_{N\,max}$) and speed of stomatal closure during the initial 50% closure (A) (linear regression $F_{1,37} = 6.814$; $P = 0.0130$; $R^2 = 0.394$) and to the maximum extent of stomatal closure, (B) (linear regression $F_{1,37} = 17.654$; $P = 0.00016$; $R^2 = 0.568$); and the relationship between maximum rates of stomatal conductance (G_{smax}) and speed of stomatal closure during the initial 50% closure, (C) (linear regression $F_{1,37} = 7.235$; $P = 0.0107$; $R^2 = 0.404$) and to the maximum extent of stomatal closure, and (D) (linear regression $F_{1,37} = 0.058$; $P = 0.811$). Solid black line indicates best fit, gray lines either side indicate 95% confidence intervals of the mean. Symbols as in **Figure 2**.

respiration (Flexas et al., 2007). The curve fitting method has been successfully applied to the determination of G_{mCO2} in plants grown at identical [CO_2] but different levels of water availability (Miyazawa et al., 2008). However, no relationship was observed between P_N and G_{mCO2} of the crop plants grown at different levels of [CO_2] in the present study (**Figure 2B**). This may suggest that there is no effect of growth at elevated [CO_2] on G_{mCO2} in the crop species analyzed as there were limited reductions in photosynthetic capacity of four of the five species due to the free availability of nutrients (Kitao et al., 2015), or a limitation in the effectiveness of the method due to the size of the cuvette employed (2 cm^2; Pons et al., 2009). Movement of CO_2 within the leaf is unlikely to have affected the P_N – C_i curves (Pons et al., 2009), as the species analyzed in this study possess heterobaric leaves (Nikolopoulos et al., 2002).

The speed of stomatal closure showed a positive relationship to $P_{N\cdot max}$ and $G_{s\cdot max}$ (**Figure 3**). This suggests that species with high potential rates of P_N and G_s require a high degree of stomatal control to reduce transpirative water-loss and prevent desiccation when conditions are not conducive to P_N. This relationship may be indicative of natural selective pressures induced by declining [CO_2] during the Cenozoic (65 Ma to present; Haworth et al., 2011) and artificial selective pressures during the domestication of crop species (Evans, 1980; Roche, 2015) favoring highly effective physiological stomatal control alongside high rates of P_N and G_s. The trend of declining [CO_2] during much of the past 65 million years (Berner, 2006) is considered to have favored species with large numbers of small stomata as the most effective arrangement of the epidermal surface to achieve maximum rates of gas exchange (Franks and Beerling, 2009; de Boer et al., 2016) in conjunction with rapid stomatal opening and closing (Hetherington and Woodward, 2003; Raven, 2014). In contrast to previous observations of a negative relationship between stomatal size and the speed of the adjustment in the size of stomatal aperture in closely related species with identical stomatal complex morphology (Drake et al., 2013), this study showed a positive relationship between stomatal size and the speed of the stomatal response to darkness (**Figure 4**). However, this positive relationship reflects the diversity in stomatal complex morphologies of the five plants studied. The dicots, cotton, and sunflower, both have stomatal complexes composed of 'kidney-shaped' guard cells; whereas the monocot grasses, oat, wheat, and barley, have larger 'dumb-bell' type guard cells (Haworth et al., 2015). The dumb-bell stomatal complexes of grasses may open and close more rapidly than kidney-shaped stomatal complexes. Stomatal opening relies upon an increase in guard cell turgor as ions are pumped across cell membranes to reduce water potential; however, to effectively open the larger dumb-bell guard cell pairs there needs to be a corresponding loss of turgor in the surrounding cell epidermal subsidiary cells to accommodate an increase in stomatal aperture (Franks and Farquhar, 2007). This rapid control and co-ordination of changes in cell turgor may account for the generally faster rates of stomatal closure observed in the grasses analyzed in this study (**Figure 4**), and ability of grasses to support larger stomatal pore apertures than species with kidney-shaped stomatal complexes.

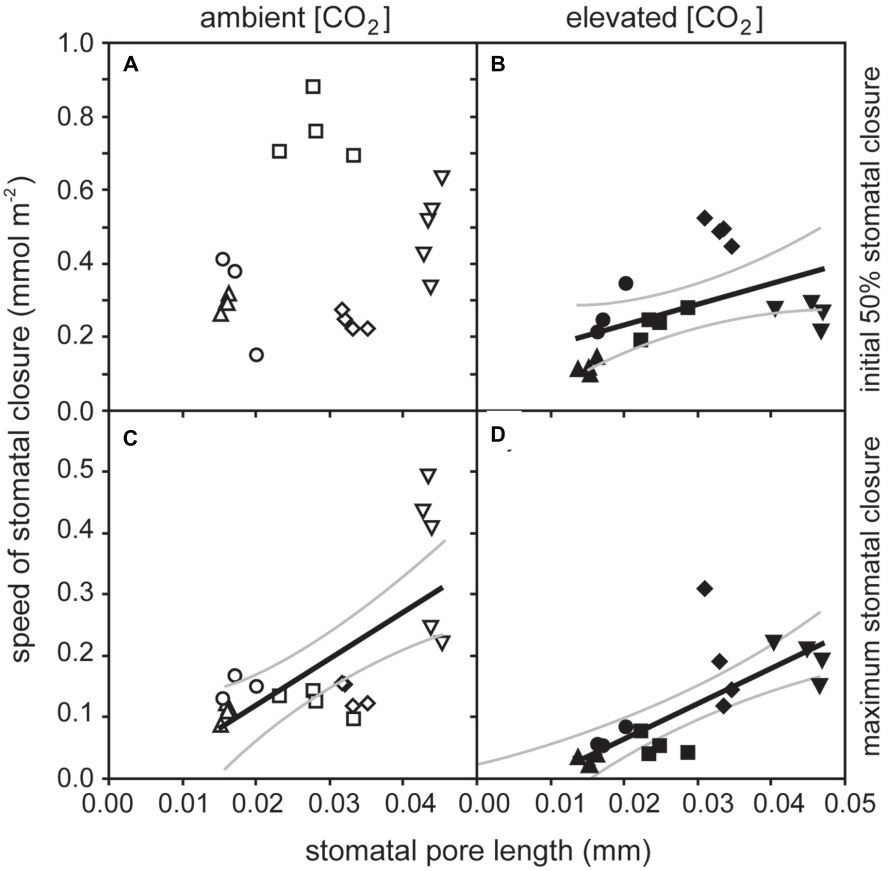

FIGURE 4 | The relationship between the stomatal pore length (SPL) and speed of stomatal closure to darkness: (A) speed of stomatal closure during the initial 50% of closure versus SPL of plants grown at 400 ppm [CO_2] (linear regression $F_{1,37} = 1.358$; $P = 0.259$); (B) speed of stomatal closure during the initial 50% of closure versus SPL of plants grown at 2000 ppm [CO_2] (linear regression $F_{1,37} = 0.0331$; $P = 5.378$; $R^2 = 0.490$); (C) speed of stomatal closure during the time taken to achieve maximum closure versus SPL of plants grown at 400 ppm [CO_2] (linear regression $F_{1,37} = 16.304$; $P = 0.0008$; $R^2 = 0.689$), and (D) speed of stomatal closure during the time taken to achieve maximum closure versus SPL of plants grown at 2000 ppm [CO_2] (linear regression $F_{1,37} = 24.190$; $P = 0.0001$; $R^2 = 0.766$). Solid black line indicates best fit, gray lines either side indicate 95% confidence intervals of the mean. Symbols as in **Figure 2**.

The Effect of Elevated [CO_2] on Active Stomatal Behavior

Regulation of stomatal aperture size is achieved through a complex hierarchical sensory and signaling network (Hetherington and Woodward, 2003; Kim et al., 2010; Merilo et al., 2014). The results of this study (**Figure 6**) and others (e.g., Heath and Kerstiens, 1997; Heath, 1998; Zeppel et al., 2012) suggest that growth at elevated [CO_2] may affect either the network of stomatal sensing/signaling or the physical function of stomata. Physiological stomatal control may occur via a signal from the mesophyll to the guard cells (Mott et al., 2008; Fujita et al., 2013), or as a result of metabolic changes within the guard cells (Talbott and Zeiger, 1998). It is not possible from the present dataset to definitively state whether the reduction in photosynthetic physiology and impaired stomatal function at high [CO_2] are causally linked or co-incidental. Quantitative trait loci responsible for P_N and stomatal control occur within the same region of the genome in sunflower (Hervé et al., 2001), indicating the importance of their co-ordination in plant responses to environmental change. The mesophyll is the site where the majority of P_N occurs and mesophyll P_N and G_s are closely linked (Messinger et al., 2006). The results of this study may suggest that the effects on photosynthetic capacity and stomatal control at high [CO_2] are associated. Growth at high [CO_2] can cause damage (Madsen, 1971), inhibition (Van Oosten et al., 1994), and feedback limitations (Sage et al., 1989) to the photosynthetic physiology. However, the species studied in this experiment all exhibit fairly rapid growth that would reduce the impact of sink limitations (Manderscheid et al., 2010), and did not experience any limitations in nutrient availability that might promote any reduction of photosynthetic capacity at elevated [CO_2] (Farage et al., 1998). Three of the five crops showed no effect of growth at elevated [CO_2] on $P_N - C_i$ curves, and none of the five crops exhibited lower F_v/F_m or ΦPSII values at the higher [CO_2] that might indicate some impairment or loss of performance of PSII corresponding to damage to the thylakoid

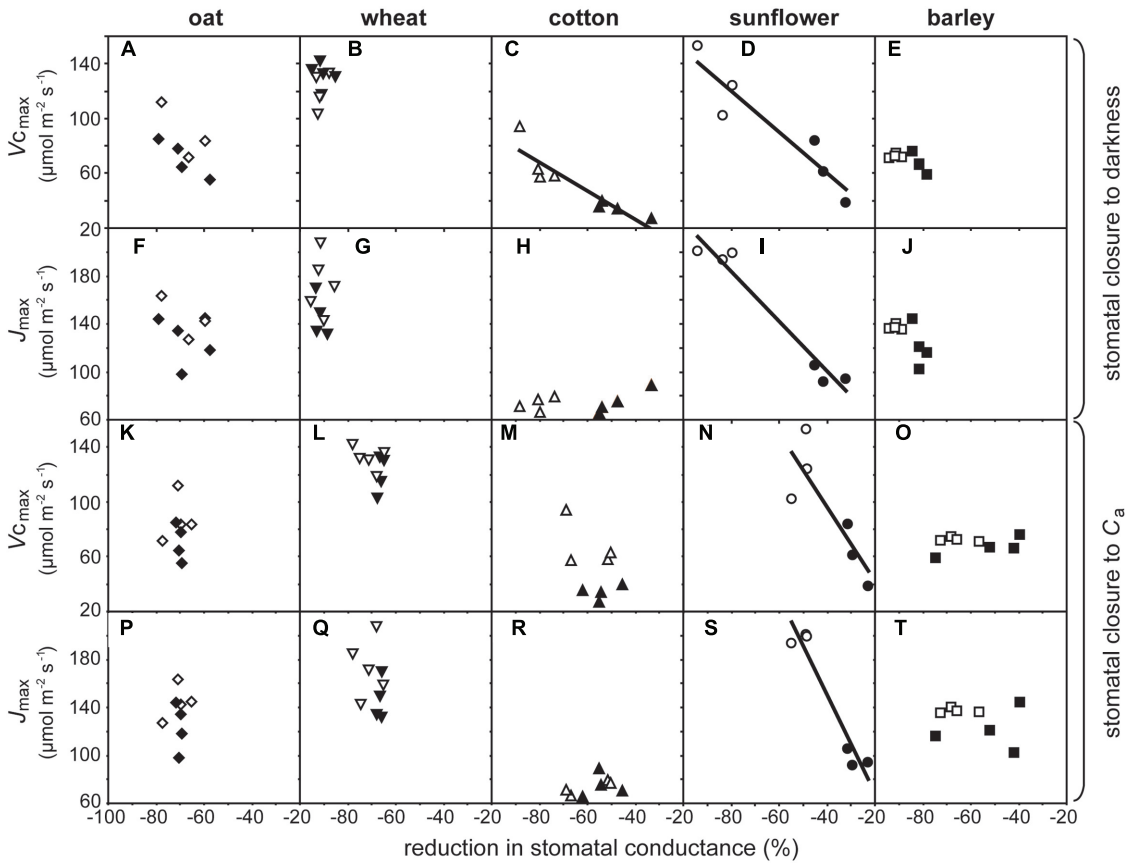

FIGURE 5 | The impact of growth at an elevated [CO_2] of 2000 ppm on photosynthetic physiology and stomatal sensitivity to C_a and closure to darkness. Linear regression was used to calculate *F* and *P* values are as follows: **(A)** $F_{1,6} = 2.889$, $P = 0.140$; **(B)** $F_{1,7} = 0.079$, $P = 0.787$; **(C)** $F_{1,6} = 29.981$, $P = 0.00155$, $R^2 = 0.913$; **(D)** $F_{1,4} = 28.643$, $P = 0.00587$, $R^2 = 0.877$; **(E)** $F_{1,6} = 0.312$, $P = 0.597$; **(F)** $F_{1,6} = 0.726$, $P = 0.427$; **(G)** $F_{1,7} = 0.0252$, $P = 0.878$; **(H)** $F_{1,6} = 1.430$, $P = 0.277$; **(I)** $F_{1,4} = 81.006$, $P = 0.0008$, $R^2 = 0.953$; **(J)** $F_{1,6} = 5.604$, $P = 0.0557$; **(K)** $F_{1,6} = 0.0325$, $P = 0.863$; **(L)** $F_{1,7} = 1.549$, $P = 0.253$; **(M)** $F_{1,6} = 1.600$, $P = 0.253$; **(N)** $F_{1,4} = 9.705$, $P = 0.0357$, $R^2 = 0.708$; **(O)** $F_{1,6} = 0.312$, $P = 0.597$; **(P)** $F_{1,6} = 0.108$, $P = 0.754$; **(Q)** $F_{1,7} = 0.378$, $P = 0.558$; **(R)** $F_{1,6} = 1.309$, $P = 0.296$; **(S)** $F_{1,4} = 46.374$, $P = 0.00243$, $R^2 = 0.921$; **(T)** $F_{1,6} = 0.184$, $P = 0.682$. Symbols as in **Figure 2**.

membranes (Shaw et al., 2014; Kalaji et al., 2016) that may account for the patterns observed in P_N and stomatal control reported in this study.

An increase in [CO_2] commonly induces a reduction in stomatal aperture in plants with active physiological stomatal control (Morison and Gifford, 1983; Haworth et al., 2013). Separation of the epidermis and mesophyll layers suggests that this is the result of a signal derived from the mesophyll such as sucrose or malate (Mott et al., 2008; Fujita et al., 2013) regulated by carbonic anhydrase within the mesophyll (Hu et al., 2010). An increase in transport of sucrose to the apoplastic space surrounding the guard cells may act as a signal to induce stomatal closure and limit water-loss during episodes where levels of photosynthetic sugar production exceed rates of transport from the photosynthetic organs (Outlaw, 2003). The plants grown at 2000 ppm [CO_2] in this study exhibited stomatal sensitivity to an increase in C_a from 400 to 2000 ppm; however, the degree of closure in cotton and sunflower was lower, possibly indicating impairment of the mesophyll to guard cell signal, or physical damage to the stomata constraining the ability to close. The leaves of plants grown at high [CO_2] frequently contain greater concentrations of soluble sugars due to CO_2-fertilization and the accumulation of photosynthate if the capacity to transport sugars is exceeded (Van Oosten et al., 1994; Paul and Driscoll, 1997). Such an increase in soluble sugars in the apoplast at high [CO_2] may impair the efficacy of a sucrose mesophyll derived signal, or the sensitivity of guard cells to apoplastic fluctuations in sucrose concentrations. The concentration of sugars such as sucrose derived from guard cell P_N may also play a role in maintaining guard cell turgor after the influx of potassium ions responsible for stomatal opening (Talbott and Zeiger, 1998). Disruption to carbohydrate metabolism may also influence guard and subsidiary cell osmotic balance, thus affecting the mechanics of stomatal opening/closing (e.g., Franks and Farquhar, 2007) and possibly accounting for impaired stomatal control in sunflower and cotton (**Figure 5**).

Stomatal opening in response to sub-ambient [CO_2] occurs in isolated epidermal strips without the mesophyll, but stomatal closure induced by [CO_2] levels above ambient requires chemical contact between the mesophyll and epidermal layers, suggesting

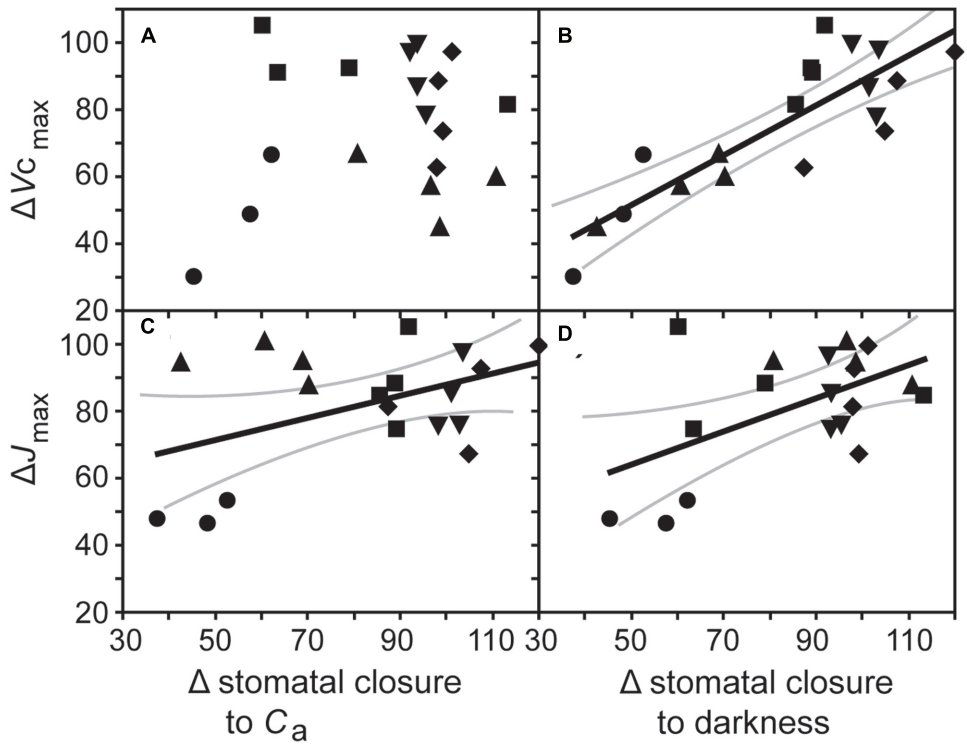

FIGURE 6 | The relationship between the proportional change in the maximum rate of carboxylation of ribulose-1,5-bisphosphate carboxylase/oxygenase (ΔVc_{max}) with (A) the change in stomatal closure to a change in C_a from 400 to 2000 ppm [CO_2] (Δstomatal closure to C_a; linear regression $F_{1,17} = 0.819$; $P = 0.378$), and (B) stomatal closure to darkness in plants grown at an elevated [CO_2] of 2000 ppm (Δstomatal closure to darkness; linear regression $F_{1,17} = 44.454$; $P = 3.966 \times 10^{-6}$; $R^2 = 0.851$), and the relationship between the proportional change in the maximum rate of electron transport required for ribulose-1,5-bisphosphate regeneration (ΔJ_{max}) with (C) Δstomatal closure to C_a (linear regression $F_{1,17} = 7.244$; $P = 0.0154$; $R^2 = 0.547$), and (D) Δstomatal closure to darkness (linear regression $F_{1,17} = 4.506$; $P = 0.0488$; $R^2 = 0.458$). Solid black line indicates best fit, gray lines either side indicate 95% confidence intervals of the mean. Symbols as in **Figure 2**.

the operation of a diffusible signal (Fujita et al., 2013). No difference was observed in G_{smax} values recorded at a C_a of 50 ppm [CO_2] (two-way ANOVA: CO_2, $F_{1,38} = 1.580$, $P = 0.219$; species $F_{4,38} = 52.511$, $P = 7.160 \times 10^{-13}$) of plants grown at 400 and 2000 ppm [CO_2] (**Figure 3C**). However, G_s sensitivity to an instantaneous increase in [CO_2] from 400 to 2000 ppm did alter between species; indicative of differential stomatal control mechanisms to sense and signal sub-ambient [CO_2] (Fujita et al., 2013) and the photosynthetic control of [CO_2] at higher levels of [CO_2] (Messinger et al., 2006). The results of this study suggest that control of G_s by mesophyll P_N via C_i is influenced via the effect of growth at elevated [CO_2] on photosynthetic physiology in cotton and sunflower with kidney-shaped stomatal complexes (**Figure 6**). The similarity in stomatal response to a sub-ambient C_a of 50 ppm, but difference in stomatal sensitivity to super-ambient C_a may indicate that growth at elevated [CO_2] does not affect the physical aspects of stomatal opening/closing but rather disrupts the photosynthetic control of G_s. In essence, the photosynthetic mesophyll to guard cell signaling mechanism appears to be operating in the same manner, but at high [CO_2] the fine control of stomatal behavior is impaired. Stomatal aperture during P_N is linked to C_i (Roelfsema et al., 2002). Stomatal conductance in cocklebur (*Xanthium strumarium*) showed a gradual change when P_N was CO_2-limited and a more dramatic reduction with C_i when P_N was limited by the regeneration of ribulose-1,5-bisphosphate (Messinger et al., 2006). This may account for the lack of correlation between ΔVc_{max} and stomatal sensitivity to [CO_2] (**Figure 6A**) and the negative correlation between ΔJ_{max} and Δstomatal closure to [CO_2] (**Figure 6C**) observed in this study; suggesting that alteration of photosynthetic capacity may influence the photosynthetic determination of stomatal aperture in response to fluctuations in C_i.

The pronounced reduction in the effectiveness of stomatal closure to darkness with Vc_{max} (**Figure 6B**) may also be suggestive of a link between P_N and physiological stomatal behavior or impaired physical operation of the stomata. A diverse range of stomatal morphologies (Franks and Farquhar, 2007) and physiological behaviors (Haworth et al., 2013, 2015) are observed in evolutionarily diverse plants. The species utilized in this study all exhibit active physiological behavior (Haworth et al., 2015), but possess contrasting stomatal morphologies. The monocot grass species with dumb-bell guard cells generally retained the ability to close stomata, while the kidney-shaped stomata of the two dicots closed less effectively at high [CO_2] (**Figure 6C**). Dumb-bell guard cells exhibit larger and faster changes in turgor

than kidney-shaped guard cells (Franks and Farquhar, 2007). The guard cells of grasses do not possess chloroplasts (Brown and Johnson, 1962) and possibly reply upon the movement of potassium for stomatal opening (Fairley-Grenot and Assmann, 1992). To accommodate the rapid and large change in dumb-bell guard cell turgor, the surrounding subsidiary cells also undergo osmotic adjustment (Franks and Farquhar, 2007). This may suggest that the differential effect of elevated [CO_2] on stomata of grasses and dicots found in this is due to differences in the biochemistry of stomatal opening related to the presence/absence of guard cell chloroplasts, stomatal signaling or photosynthetic control of stomatal aperture.

Implications of Reduced Stomatal Control at High [CO_2]

The results of this study suggest that one unexpected impact of elevated [CO_2] may be a loss of stomatal function in some C3 herbaceous crop species. This impaired stomatal control corresponded to reduced carboxylation capacity, consistent with linkage between G_s and P_N. Growth at elevated [CO_2] generally reduced $G_{s\ H2O}$ (**Table 1**). This lower $G_{s\ H2O}$ was not associated with a decrease in stomatal density, but a reduction in stomatal aperture via physiological stomatal control (Haworth et al., 2015). Under normal growth conditions this lower $G_{s\ H2O}$ will result in reduced water-loss and correspondingly greater WUE, consistent with observations of enhanced WUE in other experimental studies of elevated [CO_2] (Centritto et al., 2002; Wullschleger et al., 2002; Ainsworth and Rogers, 2007). However, loss of stomatal function at elevated [CO_2] may impair the ability of crop plants with active physiological stomatal behavior to exert stomatal control in the event of a change in growth conditions. Specifically, the reduced ability of stomata to close at elevated [CO_2] may have significant implications for the capacity of crops to tolerate drought and heat stress in the future (e.g., Killi et al., 2016) and warranting further experimental investigation.

The aim of this study was to investigate the effects of elevated [CO_2] on stomatal control by using a very high [CO_2] level of 2000 ppm. This concentration is beyond the range of the IPCC worst case scenario (IPCC, 2007), but not above levels of [CO_2] that have occurred over Earth history since the origination of vascular plants (e.g., Berner, 2009; Haworth et al., 2011). To investigate the loss of stomatal function under more realistic levels of [CO_2] for the next 50–100 years further work should be undertaken in controlled environment chambers and free air CO_2 enrichment (FACE) systems. However, many FACE systems do not increase [CO_2] at night for economic reasons, instead operating enrichment only during daylight hours when P_N occurs. In terms of gauging the effect of elevated [CO_2] on stomatal control it would be necessary for the plants to experience the most realistic simulation of future atmospheric conditions possible via continuous enrichment of [CO_2] levels. The number and duration of heat-waves and drought events are predicted to increase in the future (e.g., Schär et al., 2004; Vautard et al., 2007). The capacity of crop plants to respond to and resist these adverse growth conditions is largely dependent upon effective stomatal control (Killi et al., 2016). At elevated [CO_2], WUE may be higher and delay/mitigate the impact of drought (Wall, 2001; Wullschleger et al., 2002), but the results of our study and that of Heath and Kerstiens (1997) suggests that at severe drought the loss of stomatal function in C3 plants with kidney-shaped stomatal complexes could impair tolerance to drought. Further experimental work at [CO_2] levels equivalent to those predicted in the next 100 years is required to assess whether the loss of stomatal control at high [CO_2] may have negative implications for food security in a water-limited world.

AUTHOR CONTRIBUTIONS

MH and AR: Designed the experiments. MH, DK, and AM: Conducted the experiments. MH, DK, and MC: Processed data. MH, DK, AM, AR, and MC: Wrote the manuscript.

ACKNOWLEDGMENTS

The authors gratefully acknowledge funding from an EU Marie Curie IEF (2010-275626) and the EU FP7 project 3–4 (289582). The comments of two anonymous reviewers significantly improved this manuscript.

REFERENCES

Ainsworth, E. A., and Rogers, A. (2007). The response of photosynthesis and stomatal conductance to rising [CO2]: mechanisms and environmental interactions. *Plant Cell Environ.* 30, 258–270. doi: 10.1111/j.1365-3040.2007.01641.x

Berner, R. A. (2006). GEOCARBSULF: a combined model for Phanerozoic atmospheric O2 and CO2. *Geochim. Cosmochim. Acta* 70, 5653–5664. doi: 10.1016/j.gca.2005.11.032

Berner, R. A. (2009). Phanerozoic atmospheric oxygen: new results using the geocarbsulf model. *Am. J. Sci.* 309, 603–606. doi: 10.2475/07.2009.03

Brown, W. V., and Johnson, C. (1962). The fine structure of the grass guard cell. *Am. J. Bot.* 49, 110–115. doi: 10.2307/2439025

Bunce, J. A. (2000). Acclimation of photosynthesis to temperature in eight cool and warm climate herbaceous C3 species: temperature dependence of parameters of a biochemical photosynthesis model. *Photosynth. Res.* 63, 59–67. doi: 10.1023/A:1006325724086

Caird, M. A., Richards, J. H., and Donovan, L. A. (2007). Night-time stomatal conductance and transpiration in C3 and C4 plants. *Plant Physiol.* 143, 4–10. doi: 10.1104/pp.106.092940

Centritto, M., Loreto, F., and Chartzoulakis, K. (2003). The use of low [CO2] to estimate diffusional and non-diffusional limitations of photosynthetic capacity of salt-stressed olive saplings. *Plant Cell Environ.* 26, 585–594. doi: 10.1046/j.1365-3040.2003.00993.x

Centritto, M., Lucas, M. E., and Jarvis, P. G. (2002). Gas exchange, biomass, whole-plant water-use efficiency and water uptake of peach (*Prunus persica*) seedlings in response to elevated carbon dioxide concentration and water availability. *Tree Physiol.* 22, 699–706. doi: 10.1093/treephys/22.10.699

Centritto, M., Magnani, F., Lee, H. S., and Jarvis, P. G. (1999). Interactive effects of elevated [CO2] and drought on cherry (*Prunus avium*) seedlings II. Photosynthetic capacity and water relations. *New Phytol.* 141, 141–153. doi: 10.1046/j.1469-8137.1999.00326.x

Chater, C., Gray, J. E., and Beerling, D. J. (2013). Early evolutionary acquisition of stomatal control and development gene signalling networks. *Curr. Opin. Plant Biol* 16, 638–646. doi: 10.1016/j.pbi.2013.06.013

Ciais, P., Reichstein, M., Viovy, N., Granier, A., Ogée, J., Allard, V., et al. (2005). Europe-wide reduction in primary productivity caused by the heat and drought in 2003. *Nature* 437, 529–533. doi: 10.1038/nature03972

de Boer, H. J., Price, C. A., Wagner-Cremer, F., Dekker, S. C., Franks, P. J., and Veneklaas, E. J. (2016). Optimal allocation of leaf epidermal area for gas exchange. *New Phytol.* 210, 1219–1228. doi: 10.1111/nph.13929

Donovan, L., Linton, M., and Richards, J. (2001). Predawn plant water potential does not necessarily equilibrate with soil water potential under well-watered conditions. *Oecologia* 129, 328–335. doi: 10.1007/s004420100738

Drake, P. L., Froend, R. H., and Franks, P. J. (2013). Smaller, faster stomata: scaling of stomatal size, rate of response, and stomatal conductance. *J. Exp. Bot.* 64, 495–505. doi: 10.1093/jxb/ers347

Engineer, C. B., Hashimoto-Sugimoto, M., Negi, J., Israelsson-Nordström, M., Azoulay-Shemer, T., Rappel, W.-J., et al. (2016). CO2 sensing and CO2 regulation of stomatal conductance: advances and open questions. *Trends Plant Sci.* 21, 16–30. doi: 10.1016/j.tplants.2015.08.014

Ethier, G. J., and Livingston, N. J. (2004). On the need to incorporate sensitivity to CO2 transfer conductance into the Farquhar–von Caemmerer–Berry leaf photosynthesis model. *Plant Cell Environ.* 27, 137–153. doi: 10.1111/j.1365-3040.2004.01140.x

Evans, L. T. (1980). The natural history of crop yield: a combination of improved varieties of crop plants and technological innovations continues to increase productivity, but the highest yields are approaching limits set by biological constraints. *Am. Sci.* 68, 388–397.

Fairley-Grenot, K., and Assmann, S. (1992). Whole-cell K+ current across the plasma membrane of guard cells from a grass: *Zea mays*. *Planta* 186, 282–293. doi: 10.1007/BF00196258

Farage, P. K., McKee, I. F., and Long, S. P. (1998). Does a low nitrogen supply necessarily lead to acclimation of photosynthesis to elevated CO2? *Plant Physiol.* 118, 573–580. doi: 10.1104/pp.118.2.573

Fischer, R., Rees, D., Sayre, K., Lu, Z.-M., Condon, A., and Saavedra, A. L. (1998). Wheat yield progress associated with higher stomatal conductance and photosynthetic rate, and cooler canopies. *Crop Sci.* 38, 1467–1475. doi: 10.2135/cropsci1998.0011183X003800060011x

Flexas, J., Bota, J., Escalona, J. M., Sampol, B., and Medrano, H. (2002). Effects of drought on photosynthesis in grapevines under field conditions: an evaluation of stomatal and mesophyll limitations. *Funct. Plant Biol.* 29, 461–471. doi: 10.1071/PP01119

Flexas, J., Diaz-Espejo, A., Galmés, J., Kaldenhoff, R., Medrano, H., and Ribas-Carbo, M. (2007). Rapid variations of mesophyll conductance in response to changes in CO2 concentration around leaves. *Plant Cell Environ.* 30, 1284–1298. doi: 10.1111/j.1365-3040.2007.01700.x

Flexas, J., and Medrano, H. (2002). Drought-inhibition of photosynthesis in C3 plants: stomatal and non–stomatal limitations revisited. *Ann. Bot.* 89, 183–189. doi: 10.1093/aob/mcf027

Franks, P. J., and Beerling, D. J. (2009). CO2 forced evolution of plant gas exchange capacity and water-use efficiency over the Phanerozoic. *Geobiology* 7, 227–236. doi: 10.1111/j.1472-4669.2009.00193.x

Franks, P. J., and Farquhar, G. D. (2007). The mechanical diversity of stomata and its significance in gas-exchange control. *Plant Physiol.* 143, 78–87. doi: 10.1104/pp.106.089367

Fujita, T., Noguchi, K., and Terashima, I. (2013). Apoplastic mesophyll signals induce rapid stomatal responses to CO2 in *Commelina communis*. *New Phytol.* 199, 395–406. doi: 10.1111/nph.12261

Genty, B., Briantais, J.-M., and Baker, N. R. (1989). The relationship between the quantum yield of photosynthetic electron transport and quenching of chlorophyll fluorescence. *Biochim. Biophys. Acta Gen. Subj.* 990, 87–92. doi: 10.1016/S0304-4165(89)80016-9

Gu, J., Yin, X., Stomph, T. J., and Struik, P. C. (2014). Can exploiting natural genetic variation in leaf photosynthesis contribute to increasing rice productivity? A simulation analysis. *Plant Cell Environ.* 37, 22–34. doi: 10.1111/pce.12173

Harley, P. C., Loreto, F., Dimarco, G., and Sharkey, T. D. (1992). Theoretical considerations when estimating the mesophyll conductance to CO2 flux by analysis of the response of photosynthesis to CO2. *Plant Physiol.* 98, 1429–1436. doi: 10.1104/pp.98.4.1429

Haworth, M., Elliott-Kingston, C., and McElwain, J. C. (2011). Stomatal control as a driver of plant evolution. *J. Exp. Bot.* 62, 2419–2423. doi: 10.1093/jxb/err086

Haworth, M., Elliott-Kingston, C., and McElwain, J. (2013). Co-ordination of physiological and morphological responses of stomata to elevated [CO2] in vascular plants. *Oecologia* 171, 71–82. doi: 10.1007/s00442-012-2406-9

Haworth, M., Killi, D., Materassi, A., and Raschi, A. (2015). Co-ordination of stomatal physiological behavior and morphology with carbon dioxide determines stomatal control. *Am. J. Bot.* 102, 677–688. doi: 10.3732/ajb.1400508

Haworth, M., Moser, G., Raschi, A., Kammann, C., Grünhage, L., and Müller, C. (2016). Carbon dioxide fertilisation and supressed respiration induce enhanced spring biomass production in a mixed species temperate meadow exposed to moderate carbon dioxide enrichment. *Funct. Plant Biol.* 43, 26–39.

Heath, J. (1998). Stomata of trees growing in CO2-enriched air show reduced sensitivity to vapour pressure deficit and drought. *Plant Cell Environ.* 21, 1077–1088. doi: 10.1046/j.1365-3040.1998.00366.x

Heath, J., and Kerstiens, G. (1997). Effects of elevated CO2 on leaf gas exchange in beech and oak at two levels of nutrient supply: consequences for sensitivity to drought in beech. *Plant Cell Environ.* 20, 57–67. doi: 10.1046/j.1365-3040.1997.d01-13.x

Hervé, D., Fabre, F., Berrios, E. F., Leroux, N., Al Chaarani, G., Planchon, C., et al. (2001). QTL analysis of photosynthesis and water status traits in sunflower (*Helianthus annuus* L.) under greenhouse conditions. *J. Exp. Bot.* 52, 1857–1864. doi: 10.1093/jexbot/52.362.1857

Hetherington, A. M., and Woodward, F. I. (2003). The role of stomata in sensing and driving environmental change. *Nature* 424, 901–908. doi: 10.1038/nature01843

Hinckley, T. M., Lassoie, J. P., and Running, S. W. (1978). Temporal and spatial variations in the water status of forest trees. *For. Sci.* 24, 1–72.

Hu, H., Boisson-Dernier, A., Israelsson-Nordstrom, M., Bohmer, M., Xue, S., Ries, A., et al. (2010). Carbonic anhydrases are upstream regulators of CO2 controlled stomatal movements in guard cells. *Nat. Cell Biol.* 12, 87–93. doi: 10.1038/ncb2009

IPCC (2007). *Climate Change 2007: Impacts, Adaptation and Vulnerability. Contribution of Working Group II to the Fourth Assessment Report of the Intergovernmental Panel on Climate Change*. Cambridge: Cambridge University Press.

Kalaji, H., and Nalborczyk, E. (1991). Gas exchange of barley seedlings growing under salinity stress. *Photosynthetica* 25, 197–202.

Kalaji, H. M., Jajoo, A., Oukarroum, A., Brestic, M., Zivcak, M., Samborska, I. A., et al. (2016). Chlorophyll a fluorescence as a tool to monitor physiological status of plants under abiotic stress conditions. *Acta Physiol. Plant.* 38, 1–11. doi: 10.1007/s11738-016-2113-y

Kalaji, H. M., Schansker, G., Ladle, R. J., Goltsev, V., Bosa, K., Allakhverdiev, S. I., et al. (2014). Frequently asked questions about in vivo chlorophyll fluorescence: practical issues. *Photosynth. Res.* 122, 121–158. doi: 10.1007/s11120-014-0024-6

Killi, D., Bussotti, F., Raschi, A., and Haworth, M. (2016). Adaptation to high temperature mitigates the impact of water deficit during combined heat and drought stress in C3 sunflower and C4 maize varieties with contrasting drought tolerance. *Physiol. Plant.* doi: 10.1111/ppl.12490 [Epub ahead of print].

Kim, T.-H., Böhmer, M., Hu, H., Nishimura, N., and Schroeder, J. I. (2010). Guard cell signal transduction network: advances in understanding abscisic acid, CO2 and Ca2+ signaling. *Annu. Rev. Plant Biol.* 61, 561–591. doi: 10.1146/annurev-arplant-042809-112226

Kitao, M., Yazaki, K., Kitaoka, S., Fukatsu, E., Tobita, H., Komatsu, M., et al. (2015). Mesophyll conductance in leaves of Japanese white birch (*Betula platyphylla* var. japonica) seedlings grown under elevated CO2 concentration and low N availability. *Physiol. Plant.* 155, 435–445. doi: 10.1111/ppl.12335

Lauteri, M., Haworth, M., Serraj, R., Monteverdi, M. C., and Centritto, M. (2014). Photosynthetic diffusional constraints affect yield in drought stressed rice cultivars during flowering. *PLoS ONE* 9:e109054. doi: 10.1371/journal.pone.0109054

Madsen, E. (1971). Cytological changes due to the effect of carbon dioxide concentration on the accumulation of starch in chloroplasts of tomato leaves. *R. Vet. Agric. Univ. Yearb.* 191–194.

Manderscheid, R., Pacholski, A., and Weigel, H.-J. (2010). Effect of free air carbon dioxide enrichment combined with two nitrogen levels on growth, yield and yield quality of sugar beet: evidence for a sink limitation of beet growth under elevated CO2. *Eur. J. Agron.* 32, 228–239. doi: 10.1016/j.eja.2009.12.002

Materassi, A., Fasano, G., and Arca, A. (2005). Climatic chamber for plant physiology: a new project concept. *Riv. Ingegneria Agrar. (Italy)* 4, 79–87.

Meidner, H., and Mansfield, T. A. (1965). Stomatal responses to illumination. *Biol. Rev.* 40, 483–508. doi: 10.1111/j.1469-185X.1965.tb00813.x

Merilo, E., Jõesaar, I., Brosché, M., and Kollist, H. (2014). To open or to close: species-specific stomatal responses to simultaneously applied opposing environmental factors. *New Phytol.* 202, 499–508. doi: 10.1111/nph.12667

Messinger, S. M., Buckley, T. N., and Mott, K. A. (2006). Evidence for involvement of photosynthetic processes in the stomatal response to CO2. *Plant Physiol.* 140, 771–778. doi: 10.1104/pp.105.073676

Miyazawa, S.-I., Yoshimura, S., Shinzaki, Y., Maeshima, M., and Miyake, C. (2008). Deactivation of aquaporins decreases internal conductance to CO2 diffusion in tobacco leaves grown under long-term drought. *Funct. Plant Biol.* 35, 553–564. doi: 10.1071/FP08117

Morison, J. I., and Gifford, R. M. (1983). Stomatal sensitivity to carbon dioxide and humidity a comparison of two C3 and two C4 grass species. *Plant Physiol.* 71, 789–796. doi: 10.1104/pp.71.4.789

Mott, K. A., Sibbernsen, E. D., and Shope, J. C. (2008). The role of the mesophyll in stomatal responses to light and CO2. *Plant Cell Environ.* 31, 1299–1306. doi: 10.1111/j.1365-3040.2008.01845.x

Nikolopoulos, D., Liakopoulos, G., Drossopoulos, I., and Karabourniotis, G. (2002). The relationship between anatomy and photosynthetic performance of heterobaric leaves. *Plant Physiol.* 129, 235–243. doi: 10.1104/pp.010943

Outlaw, W. H. (2003). Integration of cellular and physiological functions of guard cells. *Crit. Rev. Plant Sci.* 22, 503–529. doi: 10.1080/713608316

Paul, M., and Driscoll, S. (1997). Sugar repression of photosynthesis: the role of carbohydrates in signalling nitrogen deficiency through source: sink imbalance. *Plant Cell Environ.* 20, 110–116. doi: 10.1046/j.1365-3040.1997.d01-17.x

Pons, T. L., Flexas, J., von Caemmerer, S., Evans, J. R., Genty, B., Ribas-Carbo, M., et al. (2009). Estimating mesophyll conductance to CO2: methodology, potential errors, and recommendations. *J. Exp. Bot.* 60, 2217–2234. doi: 10.1093/jxb/erp081

Raven, J. A. (2014). Speedy small stomata? *J. Exp. Bot.* 65, 1415–1424. doi: 10.1093/jxb/eru032

Roche, D. (2015). Stomatal conductance is essential for higher yield potential of C3 crops. *Crit. Rev. Plant Sci.* 34, 429–453. doi: 10.1080/07352689.2015.1023677

Roelfsema, M. R. G., Hanstein, S., Felle, H. H., and Hedrich, R. (2002). CO2 provides an intermediate link in the red light response of guard cells. *Plant J.* 32, 65–75. doi: 10.1046/j.1365-313X.2002.01403.x

Sage, R. F., Sharkey, T. D., and Seemann, J. R. (1989). Acclimation of photosynthesis to elevated CO2 in five C3 species. *Plant Physiol.* 89, 590–596. doi: 10.1104/pp.89.2.590

Schär, C., Vidale, P. L., Lüthi, D., Frei, C., Häberli, C., Liniger, M. A., et al. (2004). The role of increasing temperature variability in European summer heatwaves. *Nature* 427, 332–336. doi: 10.1038/nature02300

Shah, N., and Paulsen, G. (2003). Interaction of drought and high temperature on photosynthesis and grain-filling of wheat. *Plant Soil* 257, 219–226. doi: 10.1023/A:1026237816578

Shaw, A. K., Ghosh, S., Kalaji, H. M., Bosa, K., Brestic, M., Zivcak, M., et al. (2014). Nano-CuO stress induced modulation of antioxidative defense and photosynthetic performance of Syrian barley (*Hordeum vulgare* L.). *Environ. Exp. Bot.* 102, 37–47. doi: 10.1016/j.envexpbot.2014.02.016

Stratonovitch, P., and Semenov, M. A. (2015). Heat tolerance around flowering in wheat identified as a key trait for increased yield potential in Europe under climate change. *J. Exp. Bot.* 66, 3599–3609. doi: 10.1093/jxb/erv070

Talbott, L. D., and Zeiger, E. (1998). The role of sucrose in guard cell osmoregulation. *J. Exp. Bot.* 49, 329–337. doi: 10.1093/jexbot/49.suppl_1.329

Tazoe, Y., von Caemmerer, S., Badger, M. R., and Evans, J. R. (2009). Light and CO2 do not affect the mesophyll conductance to CO2 diffusion in wheat leaves. *J. Exp. Bot.* 60, 2291–2301. doi: 10.1093/jxb/erp035

Tazoe, Y., Von Caemmerer, S., Estavillo, G. M., and Evans, J. R. (2011). Using tunable diode laser spectroscopy to measure carbon isotope discrimination and mesophyll conductance to CO2 diffusion dynamically at different CO2 concentrations. *Plant Cell Environ.* 34, 580–591. doi: 10.1111/j.1365-3040.2010.02264.x

Van Oosten, J. J., Wilkins, D., and Besford, R. T. (1994). Regulation of the expression of photosynthetic nuclear genes by CO2 is mimicked by regulation by carbohydrates–a mechanism for the acclimation of photosynthesis to high CO2. *Plant Cell Environ.* 17, 913–923. doi: 10.1111/j.1365-3040.1994.tb00320.x

Van Vuuren, M. M. I., Robinson, D., Fitter, A. H., Chasalow, S. D., Williamson, L., and Raven, J. A. (1997). Effects of elevated atmospheric CO2 and soil water availability on root biomass, root length, and N, P and K uptake by wheat. *New Phytol.* 135, 455–465. doi: 10.1046/j.1469-8137.1997.00682.x

Vautard, R., Yiou, P., D'andrea, F., De Noblet, N., Viovy, N., Cassou, C., et al. (2007). Summertime European heat and drought waves induced by wintertime mediterranean rainfall deficit. *Geophys. Res. Lett.* 34, L07711. doi: 10.1029/2006GL028001

Wall, G. W. (2001). Elevated atmospheric CO2 alleviates drought stress in wheat. *Agric. Ecosyst. Environ.* 87, 261–271. doi: 10.1016/S0167-8809(01)00170-0

Wong, S. C., Cowan, I. R., and Farquhar, G. D. (1979). Stomatal conductance correlates with photosynthetic capacity. *Nature* 282, 424–426. doi: 10.1038/282424a0

Wullschleger, S. D., Tschaplinski, T. J., and Norby, R. J. (2002). Plant water relations at elevated CO2–implications for water-limited environments. *Plant Cell Environ.* 25, 319–331. doi: 10.1046/j.1365-3040.2002.00796.x

Zelitch, I. (1982). The close relationship between net photosynthesis and crop yield. *Bioscience* 32, 796–802. doi: 10.2307/1308973

Zeppel, M. J. B., Lewis, J. D., Chaszar, B., Smith, R. A., Medlyn, B. E., Huxman, T. E., et al. (2012). Nocturnal stomatal conductance responses to rising [CO2], temperature and drought. *New Phytol.* 193, 929–938. doi: 10.1111/j.1469-8137.2011.03993.x

Conflict of Interest Statement: The authors declare that the research was conducted in the absence of any commercial or financial relationships that could be construed as a potential conflict of interest.

frontiers in Plant Science

PERSPECTIVE
published: 03 August 2016
doi: 10.3389/fpls.2016.01153

Has the Impact of Rising CO_2 on Plants been Exaggerated by Meta-Analysis of Free Air CO_2 Enrichment Studies?

Matthew Haworth[1], Yasutomo Hoshika[2] and Dilek Killi[3]*

[1] Tree and Timber Institute, National Research Council (CNR-IVALSA), Firenze, Italy, [2] National Research Council, Firenze, Italy, [3] Department of Agrifood Production and Environmental Sciences, University of Florence, Florence, Italy

Meta-analysis is extensively used to synthesize the results of free air CO_2 enrichment (FACE) studies to produce an average effect size, which is then used to model likely plant response to rising [CO_2]. The efficacy of meta-analysis is reliant upon the use of data that characterizes the range of responses to a given factor. Previous meta-analyses of the effect of FACE on plants have not incorporated the potential impact of reporting bias in skewing data. By replicating the methodology of these meta-analytic studies, we demonstrate that meta-analysis of FACE has likely exaggerated the effect size of elevated [CO_2] on plants by 20 to 40%; having significant implications for predictions of food security and vegetation response to climate change. Incorporation of the impact of reporting bias did not affect the significance or the direction of the [CO_2] effect.

Keywords: photosynthesis, stomatal conductance, yield, food security, atmospheric CO_2, elevated CO_2

OPEN ACCESS

Edited by:
Urs Feller,
University of Bern, Switzerland

Reviewed by:
Eero Nikinmaa,
University of Helsinki, Finland
Matthew Paul,
Rothamsted Research, UK

****Correspondence:***
Matthew Haworth
haworth@ivalsa.cnr.it

Specialty section:
This article was submitted to Agroecology and Land Use Systems, a section of the journal Frontiers in Plant Science

Received: *14 June 2016*
Accepted: *19 July 2016*
Published: *03 August 2016*

Citation:
Haworth M, Hoshika Y and Killi D (2016) Has the Impact of Rising CO_2 on Plants been Exaggerated by Meta-Analysis of Free Air CO_2 Enrichment Studies? Front. Plant Sci. 7:1153. doi: 10.3389/fpls.2016.01153

Meta-analysis is a statistical approach that combines the findings of multiple experimental studies to quantify a population effect (Field and Gillett, 2010; Quintana, 2015). This technique has become increasingly popular to gage plant responses to carbon dioxide (Long et al., 2004; Ainsworth and Long, 2005; Ainsworth and Rogers, 2007), ozone (Feng et al., 2008), nutrient status (Koricheva et al., 1998), herbivory (Hawkes and Sullivan, 2001) and drought (Pinheiro and Chaves, 2011). The synthesis of pools of data from related studies should in theory permit more accurate prediction of the impact of environmental change on plants. Indeed, the results of meta-analytic studies are increasingly used to model plant responses to climate change and inform perspectives on the likely impacts on photosynthesis, carbon sequestration, and food security (Long et al., 2004, 2006; Ainsworth, 2008; Wu et al., 2011). Here, we illustrate how the limitations of this approach are not being critically applied in the plant sciences. One area where meta-analysis has been widely utilized is in the study of plant responses to increased atmospheric carbon dioxide concentration ([CO_2]) in free air [CO_2] enrichment (FACE) studies (e.g., Long et al., 2004; Ainsworth and Long, 2005; Ainsworth and Rogers, 2007; Bishop et al., 2014). We use the meta-analysis of FACE experiments as an example of the limitations inherent in this approach that result in an overemphasis of the effect of [CO_2], and thus distort our understanding of crop responses to [CO_2]. We acknowledge that growth under FACE has a direct impact upon photosynthesis and growth through CO_2-fertilization; however, meta-analytic approaches have exaggerated the predicted impact of rising [CO_2].

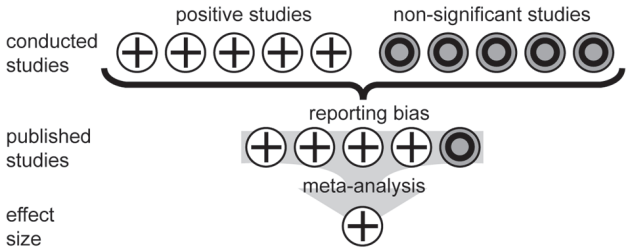

FIGURE 1 | An illustration of the development of reporting bias in the published literature and its possible effect on the outcome of a meta-analytic study.

Meta-analysis utilizes the effect size of numerous studies to produce an average effect size for a given factor (Field and Gillett, 2010; Quintana, 2015). As such, the meta-analysis is entirely dependent upon the input of studies, and whether those studies represent a true reflection of the treatment effect size. The most highly cited (Long et al., 2004; Ainsworth and Long, 2005; Ainsworth and Rogers, 2007) and recent meta-analytic studies (Bishop et al., 2014; Baig et al., 2015) of plant responses to FACE rely upon data from peer-reviewed studies indexed in the *ISI Web of Science* and/or *Scopus*. However, the possibility of reporting bias influencing the selection of studies is not considered. The issue of reporting bias is widely acknowledged in medicinal science; it is estimated that studies that demonstrate a positive

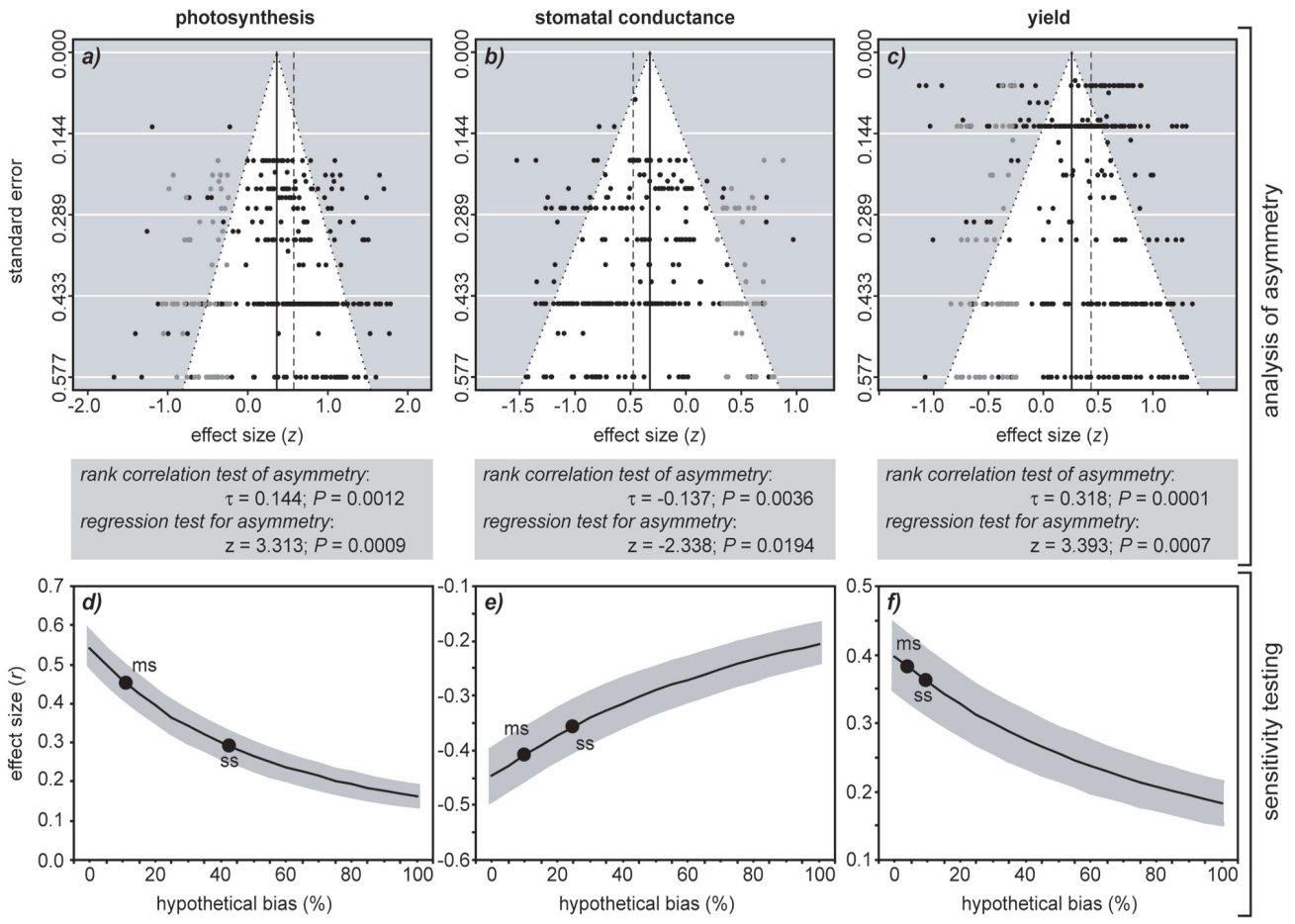

FIGURE 2 | The impact of reporting bias on the outcome of meta-analysis of the effect of FACE on C3 herbaceous plants. All articles were peer-reviewed and listed within the *ISI Web of Knowledge*. Funnel plots of photosynthesis ($n = 265$) **(a)**, stomatal conductance ($n = 243$) **(b)** and yield ($n = 302$) **(c)** show the distribution of data. Data from the studies used in the meta-analysis is represented by solid black circles. To balance asymmetry in the funnel plot the trim and fill method (Duval and Tweedie, 2000) uses the existing data to impute estimated 'missing studies' that are represented as gray symbols. The black solid vertical line indicates the mean effect size of the meta-analysis after the trim and fill. The dashed vertical line indicates the mean effect size computed by the meta-analysis before the 'missing studies' were imputed. The difference between the black solid line and dashed vertical line represents the effect of *reporting bias* on effect size as indicated by the trim and fill method. The gray box below the funnel plot shows the Begg – Mazumdar (Begg and Mazumdar, 1994) rank correlation coefficient using Kendall's τ and Egger's regression test (Egger et al., 1997) to assess the probability of publication bias within the datasets. To gage the impact of hypothetical publication bias in the literature on the meta-analysis of photosynthesis **(d)**, stomatal conductance **(e)** and yield **(f)** we included increasing numbers of studies with randomly generated small effect sizes (r) of −0.1 to 0.1 (Cohen, 1992). The black solid line indicates the mean effect size for the meta-analysis and the gray shading either side represents 95% confidence intervals. Solid circles indicate the points where moderate (labeled ms) and severe (labeled ss) selection calculated using the model of Vevea and Woods (2005) would occur.

effect are 94% more likely to be submitted (Greenwald, 1975) and then published (Coursol and Wagner, 1986) in leading journals. These journals are most likely to be indexed and their studies included in meta-analyses (**Figure 1**). This skew toward positive studies is driven by publication bias (where journals prefer to publish positive studies), data availability bias (studies with a large effect size are more likely to be written up in comparison to those where the replication is insufficient to demonstrate a significant effect) and reviewer bias (where reviewers favor manuscripts reporting strong treatment effects confirming a prevailing consensus; Dwan et al., 2013). Funnel plots are one of the most common methods to observe possible reporting bias in meta-analysis datasets. Asymmetry in funnel plots is indicative of bias and can be assessed using regression (Egger et al., 1997), rank correlation (Begg and Mazumdar, 1994) and the 'trim and fill' method [where estimated 'missing studies' are imputed to create a more symmetrical funnel plot (Duval and Tweedie, 2000)].

To test for and assess the possible impacts of bias in FACE studies, we followed the methodology of previous meta-analysis of FACE by analysing data from studies indexed in the *ISI Web of Science* (Long et al., 2004; Ainsworth and Long, 2005; Ainsworth and Rogers, 2007; Bishop et al., 2014; Baig et al., 2015). We compiled photosynthesis, stomatal conductance and yield data from 103 studies of C3 herbaceous plants to FACE (a full list of articles and species used in the meta-analysis is given in Supplementary Information). We then performed a random effects meta-analysis using the metafor package (Viechtbauer, 2010) in *R* statistical software following Field and Gillett (2010) and Quintana (2015) (**Figure 2**). Bias in the dataset was assessed using regression (Egger et al., 1997), rank correlation (Begg and Mazumdar, 1994), trim and fill (Duval and Tweedie, 2000) and weighting analysis of the studies (Vevea and Woods, 2005).

Begg and Mazumdar's (1994) rank correlation and Egger's et al. (1997) regression test indicated significant asymmetry in the funnel plots suggestive of reporting bias for all three parameters. The inclusion of estimated missing studies using the trim and fill method (Duval and Tweedie, 2000) resulted in a more balanced spread of the data and also reduced the effect size of FACE on photosynthesis by 43%, stomatal conductance by 32% and yield by 41%. The model of Vevea and Woods (2005) performs a sensitivity analysis, applying weight functions of the effect sizes of studies within a meta-analysis to determine the impact of moderate or severe reporting bias on effect size. Assuming that our dataset has experienced moderate selection, this would indicate that reporting bias has induced 5 to 15% increases in effect size.

It is particularly difficult to quantify the true effect of bias on a meta-analysis (Field and Gillett, 2010; Quintana, 2015). It is possible to survey non-indexed so-called 'gray' literature that is not subject to peer-review, directly approach researchers for non-significant unpublished data or submit contrasting 'sample' articles or questionnaires to journals to quantify rates of acceptance/rejection. However, all of these methods are time consuming and subject to limitations. We therefore decided to assess the potential impact of bias on meta-analysis of FACE by incorporating an increasing proportion of studies showing small effect sizes (randomly generated r values of −0.1 to 0.1: Cohen (1992) and re-running the meta-analyses as a 'sensitivity test' of the published data). Assuming that the current published literature is not subject to any bias, photosynthesis ($r = 0.542$), stomatal conductance ($r = -0.447$), and yield ($r = 0.398$) all showed significant effects of elevated [CO_2], and the significance of this effect remained even at the highest levels of hypothetical reporting bias. A hypothetical publication bias of 30% induced reductions in [CO_2] effect size of 43.7% in photosynthesis, 27.6% in stomatal conductance and 27.5% in yield. The decline in effect size becomes more apparent at the 80–90% level found in medicinal science (Greenwald, 1975; Coursol and Wagner, 1986). Such reductions in effect size will have critical implications for studies where the output of meta-analyses are used to predict the photosynthetic (Ainsworth and Rogers, 2007) and yield (Long et al., 2006; Bishop et al., 2014; Challinor et al., 2014) responses of plants to rising [CO_2].

Our analysis is indicative of high levels of bias within published meta-analytic studies of plant responses to FACE that have resulted in over-estimation of the effect size of elevated [CO_2]. As a result the outputs of these studies should be treated with a degree of caution. We propose that sensitivity testing of meta-analytic studies of plant responses to FACE be undertaken as standard in the future (e.g., Vevea and Woods, 2005), and efforts made to further encourage the publication of studies reporting non-significant outcomes and compilation of non-significant data for researchers wishing to undertake meta-analysis.

AUTHOR CONTRIBUTIONS

MH and YH conceived the study. MH and YH collected the data. DK performed statistical analysis. MH drew the figures. MH, YH, and DK wrote the manuscript.

ACKNOWLEDGMENT

We are grateful for funding from the EU FP7 project 3 to 4 (289582).

SUPPLEMENTARY MATERIAL

The Supplementary Material for this article can be found online at: http://journal.frontiersin.org/article/10.3389/fpls.2016.01153

REFERENCES

Ainsworth, E. A. (2008). Rice production in a changing climate: a meta-analysis of responses to elevated carbon dioxide and elevated ozone concentration. *Glob. Chang. Biol.* 14, 1642–1650. doi: 10.1111/j.1365-2486.2008.01594.x

Ainsworth, E. A., and Long, S. P. (2005). What have we learned from 15 years of free-air CO2 enrichment (FACE)? a meta-analytic review of the responses of photosynthesis, canopy. *New Phytol.* 165, 351–371. doi: 10.1111/j.1469-8137.2004.01224.x

Ainsworth, E. A., and Rogers, A. (2007). The response of photosynthesis and stomatal conductance to rising [CO2]: mechanisms and environmental interactions. *Plant Cell Environ.* 30, 258–270. doi: 10.1111/j.1365-3040.2007.01641.x

Baig, S., Medlyn, B. E., Mercado, L. M., and Zaehle, S. (2015). Does the growth response of woody plants to elevated CO2 increase with temperature? a model-oriented meta-analysis. *Glob. Chang. Biol.* 21, 4303–4319. doi: 10.1111/gcb.12962

Begg, C. B., and Mazumdar, M. (1994). Operating characteristics of a rank correlation test for publication bias. *Biometrics* 50, 1088–1101. doi: 10.2307/2533446

Bishop, K. A., Leakey, A. D. B., and Ainsworth, E. A. (2014). How seasonal temperature or water inputs affect the relative response of C3 crops to elevated [CO2]: a global analysis of open top chamber and free air CO2 enrichment studies. *Food Energy Secur.* 3, 33–45. doi: 10.1002/fes3.44

Challinor, A., Watson, J., Lobell, D., Howden, S., Smith, D., and Chhetri, N. (2014). A meta-analysis of crop yield under climate change and adaptation. *Nat. Clim. Chang.* 4, 287–291. doi: 10.1038/nclimate2153

Cohen, J. (1992). A power primer. *Psychol. Bull.* 112, 155–158. doi: 10.1037/0033-2909.112.1.155

Coursol, A., and Wagner, E. E. (1986). Effect of positive findings on submission and acceptance rates: a note on meta-analysis bias. *Prof. Psychol. Res. Pr.* 17, 136–137. doi: 10.1037/0735-7028.17.2.136

Duval, S., and Tweedie, R. (2000). Trim and fill: a simple funnel-plot–based method of testing and adjusting for publication bias in meta-analysis. *Biometrics* 56, 455–463. doi: 10.1111/j.0006-341X.2000.00455.x

Dwan, K., Gamble, C., Williamson, P. R., and Kirkham, J. J. (2013). Systematic review of the empirical evidence of study publication bias and outcome reporting bias—an updated review. *PLoS ONE* 8:e66844. doi: 10.1371/journal.pone.0066844

Egger, M., Smith, G. D., Schneider, M., and Minder, C. (1997). Bias in meta-analysis detected by a simple, graphical test. *Br. Med. J.* 315, 629–634. doi: 10.1136/bmj.315.7109.629

Feng, Z., Kobayashi, K., and Ainsworth, E. A. (2008). Impact of elevated ozone concentration on growth, physiology, and yield of wheat (*Triticum aestivum* L.): a meta-analysis. *Glob. Change Biol.* 14, 2696–2708.

Field, A. P., and Gillett, R. (2010). How to do a meta-analysis. *Br. J. Math. Stat. Psychol.* 63, 665–694. doi: 10.1348/000711010X502733

Greenwald, A. G. (1975). Consequences of prejudice against the null hypothesis. *Psychol. Bull.* 82, 1–20. doi: 10.1037/h0076157

Hawkes, C. V., and Sullivan, J. J. (2001). The impact of herbivory on plants in different resource conditions: a meta-analysis. *Ecology* 82, 2045–2058. doi: 10.1890/0012-9658(2001)082[2045:TIOHOP]2.0.CO;2

Koricheva, J., Larsson, S., Haukioja, E., and Keinänen, M. (1998). Regulation of woody plant secondary metabolism by resource availability: hypothesis testing by means of meta-analysis. *Oikos* 83, 212–226. doi: 10.2307/3546833

Long, S. P., Ainsworth, E. A., Leakey, A. D. B., Nösberger, J., and Ort, D. R. (2006). Food for thought: lower-than-expected crop yield stimulation with rising CO2 concentrations. *Science* 312, 1918–1921. doi: 10.1126/science.1114722

Long, S. P., Ainsworth, E. A., Rogers, A., and Ort, D. R. (2004). Rising atmospheric carbon dioxide: plants face the future. *Annu. Rev. Plant Biol.* 55, 591–628. doi: 10.1146/annurev.arplant.55.031903.141610

Pinheiro, C., and Chaves, M. M. (2011). Photosynthesis and drought: can we make metabolic connections from available data? *J. Exp. Bot.* 62, 869–882. doi: 10.1093/jxb/erq340

Quintana, D. S. (2015). From pre-registration to publication: a non-technical primer for conducting a meta-analysis to synthesize correlational data. *Front. Psychol.* 6:1549. doi: 10.3389/fpsyg.2015.01549

Vevea, J. L., and Woods, C. M. (2005). Publication bias in research synthesis: sensitivity analysis using a priori weight functions. *Psychol. Methods* 10, 428–443. doi: 10.1037/1082-989X.10.4.428

Viechtbauer, W. (2010). Conducting meta-analyses in R with the metafor package. *J. Statist. Softw.* 36, 1–48. doi: 10.18637/jss.v036.i03

Wu, Z., Dijkstra, P., Koch, G. W., Peñuelas, J., and Hungate, B. A. (2011). Responses of terrestrial ecosystems to temperature and precipitation change: a meta-analysis of experimental manipulation. *Glob. Chang. Biol.* 17, 927–942. doi: 10.1111/j.1365-2486.2010.02302.x

Conflict of Interest Statement: The authors declare that the research was conducted in the absence of any commercial or financial relationships that could be construed as a potential conflict of interest.

frontiers in Plant Science

MINI REVIEW
published: 12 July 2016
doi: 10.3389/fpls.2016.01015

Drought Stress Responses in Soybean Roots and Nodules

Karl J. Kunert[1], Barend J. Vorster[1], Berhanu A. Fenta[2], Tsholofelo Kibido[1], Giuseppe Dionisio[3] and Christine H. Foyer[4]*

[1] Department Plant Production and Soil Science, Forestry and Agricultural Biotechnology Institute, University of Pretoria, Pretoria, South Africa, [2] Melkassa Agricultural Research Centre, Ethiopian Institute of Agricultural Research, Adama, Ethiopia, [3] Faculty of Science and Technology, Research Centre Flakkebjerg, Department of Molecular Biology and Genetics, Aarhus University, Aarhus, Denmark, [4] Centre for Plant Sciences, School of Biology, Faculty of Biological Sciences, University of Leeds, Leeds, UK

Drought is considered to be a major threat to soybean production worldwide and yet our current understanding of the effects of drought on soybean productively is largely based on studies on above-ground traits. Although the roots and root nodules are important sensors of drought, the responses of these crucial organs and their drought tolerance features remain poorly characterized. The symbiotic interaction between soybean and rhizobia facilitates atmospheric nitrogen fixation, a process that provides essential nitrogen to support plant growth and development. Symbiotic nitrogen fixation is important for sustainable agriculture, as it sustains plant growth on nitrogen-poor soils and limits fertilizer use for crop nitrogen nutrition. Recent developments have been made in our understanding of the drought impact on soybean root architecture and nodule traits, as well as underpinning transcriptome, proteome and also emerging metabolome information, with a view to improve the selection of more drought-tolerant soybean cultivars and rhizobia in the future. We conclude that the direct screening of root and nodule traits in the field as well as identification of genes, proteins and also metabolites involved in such traits will be essential in order to gain a better understanding of the regulation of root architecture, bacteroid development and lifespan in relation to drought tolerance in soybean.

Keywords: ***Glycine max*, root architecture, nodule traits, soybean omics, water stress**

OPEN ACCESS

Edited by:
Urs Feller,
University of Bern, Switzerland

Reviewed by:
Prateek Tripathi,
The Scripps Research Institute, USA
Dominique Job,
Centre National de la Recherche Scientifique, France
Thomas Seth Davis,
California Polytechnic State University, USA

****Correspondence:***
Karl J. Kunert
karl.kunert@up.ac.za

Specialty section:
This article was submitted to Agroecology and Land Use Systems, a section of the journal Frontiers in Plant Science

Received: *29 April 2016*
Accepted: *27 June 2016*
Published: *12 July 2016*

Citation:
Kunert KJ, Vorster BJ, Fenta BA, Kibido T, Dionisio G and Foyer CH (2016) Drought Stress Responses in Soybean Roots and Nodules. Front. Plant Sci. 7:1015. doi: 10.3389/fpls.2016.01015

INTRODUCTION

The world-wide soybean production in 2015/2016 will be 320.15 million metric tons (Global soybean production.com, 2016). Sustainability of soybean yields is, however, threatened by predicted climatic changes with persistent droughts over many parts of the world (Dai, 2013; Foyer et al., 2016). Selection of more drought-tolerant soybean cultivars is therefore required to address this imminent threat to food and protein security (Ku et al., 2013).

Recent advances in current understanding of the effects of drought on soybean growth have predominantly been based on evaluation of above-ground (shoot) traits, with flowering and seed stages particularly sensitive to drought stress. In contrast, drought effects on soybean roots, and specifically root nodules, has been less studied. Moreover, relatively little information is available

concerning how drought affects the symbiotic relationship between nitrogen fixing soil rhizobia and the host plant (Ferguson et al., 2010). This unique symbiotic relationship is initiated by the plant through release of root flavonoids into the rhizosphere, recognized by compatible *Rhizobium sp.* Flavonoid signaling results in bacterial production of specific lipochito-oligosaccharides (Nod factors) secreted by rhizobia (Kondorosi et al., 2013). Nod factors are in turn recognized by specific LysM receptor-like kinases located on root epidermal cells. Nod factor binding results in genetic and metabolic signaling cascades that are mediated, at least in part, by cell specific nuclear Ca^{2+} oscillations (Charpentier and Oldroyd, 2013). The signaling cascade results in increased division of cortical cells within the root infection area with formation of composite structures derived from the two symbiotic partners (Gage, 2004). This bacterial infection thread allows rhizobia penetrating deep into the dividing cellular profile resulting in a new organ, the N-fixing 'nodule,' housing infected rhizobia replicating within nodule cells (Oldroyd et al., 2011; Oldroyd, 2013). Inside infected cells, rhizobia are encapsulated with a plant-derived membrane forming the facultative organelle, the symbiosome (Oldroyd, 2013). The symbiosome provides strict plant control on movement of nutrients from bacteria and regulates rhizobial activity and persistence. The symbiosis is facultative and initiated by nitrogen starvation of the host plant (Maróti and Kondorosi, 2014). Within the symbiosome, bacteria differentiate into an endosymbiotic form (bacteroids) for fixing N_2 into ammonium. This energy-requiring process is dependent on photosynthate supplied by the shoots. Fixation is catalyzed by the bacterial enzyme nitrogenase requiring a low, but stable, oxygen environment achieved in part through activity of a nodule localized oxygen diffusion barrier. Continual oxygen flux to support bacteroid respiration is finally ensured by the nodule expressed protein leghaemoglobin.

The purpose of this mini-review is to provide an update on the recent developments that have enhanced our understanding of how drought influences soybean roots/nodules, with a particular focus on root and nodule phenome and symbiotic nitrogen fixation. Effects of drought on the soybean root/nodule transcriptome, proteome and metabolome are also outlined as illustrated in **Figures 1** and **2**.

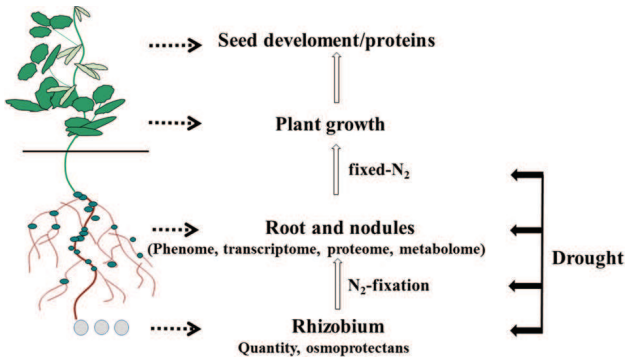

FIGURE 1 | Below-ground plant organs affected by drought that can be analyzed using omics technologies, including the rhizobia that form symbiotic relationships with soybean roots.

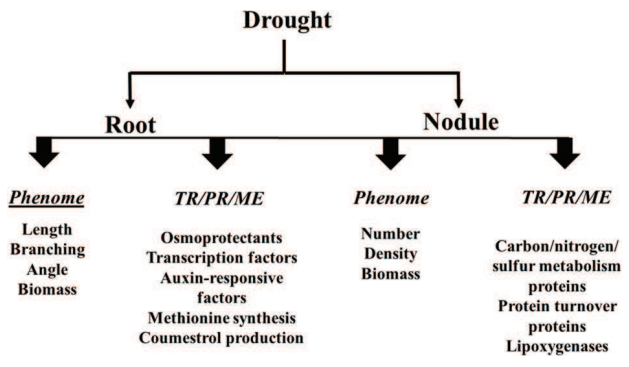

FIGURE 2 | Effects of drought on the soybean root and nodule phenome, transcriptome (TR), proteome (PR) and metabolome (ME).

DROUGHT-INDUCED CHANGES TO THE ROOT PHENOME

Soybean has an allorhizic root system consisting of a primary root (tap root) and lateral (basal) roots (Ao et al., 2010; Fenta et al., 2014). Decreased root lengths and dry biomass accumulation have been reported in many soybean accessions under drought conditions (Thu et al., 2014). Drought not only changes root architecture (root depth, root branching density, and root angle) but also partitioning of root to shoot biomass with an increase in root mass (Franco et al., 2011; Fenta et al., 2014). Several studies have provided strong evidence that root types either penetrating deep into the soil and attaining greater "root mass at depth" (Lopes et al., 2011; Ali et al., 2016) or roots with large xylem diameters and/or larger lateral root systems with more root hairs are advantageous under drought conditions (Tanaka et al., 2014; Vadez, 2014). Such roots tend to have a greater total surface area, which facilitate maximal moisture and nutrient extraction to maintain photosynthesis (Blum, 2011; Lopes et al., 2011; Comas et al., 2013). The soybean cultivar Jackson is an excellent example possessing this type of root system with long roots growing deep into the soil allowing better water uptake than other more drought-sensitive cultivars (Serraj et al., 1997; Fenta et al., 2014). However, identification of soybean cultivars with improved root architecture characteristics still remains challenging. Classic root phenotyping approaches including analysis of soil cores and applying standard excavation techniques to determine root traits are still the methods of choice (Fenta et al., 2014). Future more accurate non-destructive methods under development are transparent tubes (mini-rhizotrons), to measure with a camera various root characteristics around the outside walls of the tubes, or *in situ* tomographic measurements of the root system with X-rays (Mooney et al., 2012; Eberbach et al., 2013).

CHANGES IN THE ROOT TRANSCRIPTOME AND PROTEOME

Transcriptome analysis and Next-Generation Sequencing (NGS) are current strategies to particularly study plant responses to abiotic stress (Fan et al., 2013). Identification of genes underpinning root traits and related drought responses have recently received intensive interest (Manavalan et al., 2009; Libault et al., 2010; Comas et al., 2013; Thao et al., 2013; Satbhai et al., 2015). Among 3,000 genes strongly up-regulated in roots by drought were several transcription factors, receptor-like kinases, calcium signaling components as well as jasmonate and abscisic acid biosynthetic genes (Tripathi et al., 2016). Transcriptome responses to drought are also highly dependent on stress intensity and duration as well as species and organs investigated. In the case of soybean roots, 145 root genes were for example differentially expressed due to drought. Identified gene functions demonstrated a complex drought response with genes involved in different multiple biochemical pathways related to drought adaptation (Stolf-Moreira et al., 2011). Applying the deep SuperSAGE method, increased expression of 1,127 unitags in a stress-tolerant soybean accession were associated with responses to hormone stimuli, water stress, as well as oxidative stresses (Neto et al., 2013). Other transcriptome studies were carried out with soybean cultivars W82 and DT2008. The genome of W82, often used as a model cultivar, was sequenced several years ago (Schmutz et al., 2010). DT2008, an economically important soybean cultivar and widely grown in Vietnam (Vinh et al., 2010; Sulieman et al., 2015), has high drought tolerance (Ha et al., 2013; Sulieman et al., 2015) and better nodule development under drought when compared to W82 (Sulieman et al., 2015). By comparing the root transcriptomes of DT2008 and W82, seedlings under normal and dehydration conditions (2 and 10 h treatment), 38172 soybean genes, which changed in expression, could be annotated with high confidence (Ha et al., 2015). Data suggested that higher drought tolerability of DT2008 roots, when compared to W82, might be attributed to a higher number of root genes induced by early dehydration than by prolonged dehydration. The higher drought tolerability of DT2008 vs. W82 might be further attributed to differential expression of genes associated in osmo-protectant biosynthesis, detoxification, cell wall-related proteins, kinases, transcription factors as well as phosphatase 2C proteins (Ha et al., 2015). In particular, the levels of transcripts encoding the auxin responsive factors (ARFs) *GmARF33* and *GmARF50* were greatly increased in shoots and roots. For example, *GmARF50* transcripts were rapidly increased by 15- and 30-fold after 2 and 10 h of dehydration, respectively (Ha et al., 2013). Further, subjecting Williams 82 to increasing drought conditions caused the total differential expression of 6609 transcripts including many genes involved in hormone (auxin/ethylene), carbohydrate, cell wall-related secondary metabolism as well as transcription factors controlling root growth (Song et al., 2016). However, a more in-depth functional characterization is still required to determine how these transcripts will lead to better drought tolerance.

Several proteomics study have also been carried out to unravel the abiotic stress response mechanism in soybean (Hossain et al., 2013) and root proteins, changed in abundance due to drought, were involved in osmotic-stress responses (Toorchi et al., 2009). These proteomics studies also highlighted again the key role of root genes involved in osmo-protection and encoding kinases and transcription factors in the drought response. Interestingly, decreased amounts of methionine synthase were also found as a response to drought (Mohammadi et al., 2012; Oh and Komatsu, 2015). This enzyme catalyzes the conversion of cysteine into methionine in sulfur metabolism. This protein, of central importance in sulfur metabolism, might therefore be a drought responsive protein underpinning possible epigenetic controls that are triggered in drought response. Lower methionine synthase activity under drought might further negatively affect soybean growth due to less available methionine for protein biosynthesis. Furthermore, a great number of root metabolites, such as coumestrol, also change during drought (Tripathi et al., 2016). Coumestrol possibly stimulates mycorrhizal colonization and there is emerging evidence that mycorrhizal plants have improved drought tolerance (Armada et al., 2016).

EXPLORING THE NODULE PHENOME

Soybean has determinate nodules formed by the symbiotic interaction of a soybean plant with *Bradyrhizobium* (Herridge et al., 2008). Despite symbiotic N_2 fixation is adequate to meet the nitrogen needs of the soybean crop, high-yielding soybeans benefit from supplemental N applications, since N_2 fixation capacities are not always sufficient to produce high yields. However, nodule numbers are only decreased when soybean plants are subjected to severe drought conditions (Fernandez-Luquen et al., 2008; Márquez-García et al., 2015). Nodule drought tolerance has been linked to the ability to sustain a supply of photosynthate to the nodules during drought and to greater nodule biomass (King and Purcell, 2001). The relationships between the frequency and intensity of nodulation and root growth and architecture are, however, still poorly understood, particularly the factors that control nodule density per unit root length in the absence and presence of stress. Furthermore, although nitrate is required for root development, it has a negative impact on nodulation (Ferguson et al., 2010). Therefore, improving root and nodule development under drought requires in the future a better understanding of the consequences of the signaling of nitrate and related nutrients, such as phosphate, on root development together with the impact of drought-induced changes on nutrient availability on symbiotic nitrogen fixation.

Exposure to severe drought also impairs nitrogenase activity. This may be caused by several factors including impairment of the supply of photosynthate to the nodules to drive symbiotic nitrogen fixation and breakdown of the oxygen diffusion barrier or loss of leghemoglobin (King and Purcell, 2006; Arrese-Igor et al., 2011). In exchange for photosynthate, soybean nodules deliver reduced nitrogen in form of ureides (allantoin and allantonic acid), mediated by UPS1 transporter proteins (Collier and Tegeder, 2012), to the plant, providing the nitrogen that

is required for biomass production and finally seed protein production. However, the molecular mechanisms that support ureide export to the plant via the xylem have so far not been fully characterized.

EXPLORING THE NODULE TRANSCRIPTOME AND PROTEOME

Studies on nodule transcriptome profiles have largely focused on the early stages of nodule development. The release of the complete soybean genome (Schmutz et al., 2010) and the RNAseq atlas of genes expressed in fourteen different soybean tissues, including nodules, (Severin et al., 2010) provide currently a useful genetic resource to also study single nodule genes, or gene networks, after drought exposure with automated bioinformatics methods predicting also gene regulatory networks (Zhu et al., 2013). A recently predicted soybean nodulation-related regulatory gene network, consisting of 10 regulatory modules, might be also applicable to investigate drought effects on nodule gene expression. Transcriptome studies have been generally limited by poor genome annotation, but the situation is gradually improving with the growing annotated soybean genome database (Severin et al., 2010). The previous application of Suppression Subtractive Hybridisation (SSH) technology on soybean nodules, in the absence and presence of drought, largely identified sequences with unknown functions. Only relatively few drought-responsive transcripts had known functions applying this technology including ferritins and metallothionins involved in metal detoxification, particularly in response to oxidative stress (Clement et al., 2008). We recently also explored the nodule cysteine protease transcriptome during developmental nodule senescence. Several papain-like and legumain-like cysteine proteases, also called vacuolar processing enzymes (VPEs), were identified to be strongly expressed during nodule senescence (Van Wyk et al., 2014). In nodules, papain-like cysteine proteases have known functions in the regulation of bacterial symbiosis and nitrogen fixation, they target for example leghemoglobin (Van de Velde et al., 2006; Li et al., 2008). We have recently also found that inhibition of papain-like cysteine protease activity can improve soybean tolerance to drought and favors increased nodulation (Quain et al., 2014, 2015). VPEs are involved in developmental senescence and activation of pre-proteases. With their caspase-like activity, they further play an important role in programmed cell death (PCD) (Hara-Nishimura et al., 2005; Roberts et al., 2012). Other such identified cysteine proteases with caspase-1 like activity include the 20S proteasome beta subunit 1 (PBA1; casapase-3 like activity), DEVDase (Hatsugai et al., 2009; Gu et al., 2010; Han et al., 2012), YVADase (Hara-Nishimura et al., 2005), VKMDase (Bonneau et al., 2008), VEIDase, and TATDase (Chichkova et al., 2010). Cathepsin B, also with caspase-3 activity and responsible for PCD, is normally bound to an endogenous cysteine protease inhibitor but is released upon perception of PCD triggers (Ge et al., 2016). An interesting aspect would be therefore to investigate in the future if exposure to drought may compromise such protease-inhibitor interactions and hence lead to PCD.

Proteome analyses on legume nodules have not only been carried out to better understand the soybean symbiosome (Clarke et al., 2015), but also to find drought-induced proteome changes. The nodule proteomes of *Medicago truncatula* and *Glycine max* were recently compared under drought and drought caused the down-regulation of the entire nodule proteome. Particular proteins down-regulated were lipoxygenases and proteins involved in carbon, nitrogen and sulfur metabolism, similar to the root proteome, and proteins involved in protein turnover (Gil-Quintana et al., 2015). The study also highlighted a high degree of similarity between both legume proteomes. Research carried out on *M. truncatula* might be, therefore, also directly applicable to other economically important legume crops, such as soybean. Applicable findings include that drought induces a major change in the metabolic profile of *M. truncatula* nodules with accumulation of amino acids (Pro, His, and Trp) and carbohydrates (sucrose, galactinol, raffinose, and trehalose) associated with a decline of bacteroid proteins involved in C-metabolism (Larrainzar et al., 2009). Further applicable findings are that in *M. truncatula* nodules methionine biosynthesis is particularly affected by drought and that, despite sufficient S-availability, the nitrogen fixation rate in response to drought declines. Such decline is associated with a down-regulation of proteins involved in biosynthesis of methionine and *S*-adenosyl-L-methionine (SAM), a precursor in ethylene biosynthesis, as well as ethylene biosynthesis (Larrainzar et al., 2014). These results provide strong evidence for a central importance of sulfur metabolism in the drought response. Also, the recent finding of significant delay in drought-induced leaf senescence in nodulated *M. truncatula* plants with nodulated plants recovering more effectively from drought, relative to non-nodulated plants, might also be applicable to soybean (Staudinger et al., 2016).

FOCUS AREAS FOR INTENSIVE EXPLORATION

Technology development is key to future progress. In particular, a major focus must be more accurate, non-invasive monitoring of root architecture and nodulation in the field. Extraction of the entire root system from field-grown plants ("shovelomics") to determine drought-induced changes in root architecture is often laborious and requires destructive root excavation (Fenta et al., 2014). Scientists are often reluctant to work in the field with such system. High throughput root and nodule phenotyping under field conditions by direct screening of root and nodule systems in the soil, without the need for excavation, is therefore very likely crucial for any future soybean improvement.

An exciting future task will also be the development of root and nodule transcriptome, proteome as well as metabolome maps in relation to drought (Nguyen, 2016). However, this should also include more in-depth functional characterization of transcripts/proteins/metabolites and how they lead to better drought tolerance. Transcriptomic and proteomics studies

already indicate that up-regulation of genes involved in osmo-protection and coding for kinases and transcription factors are playing a key role in the drought response in addition to down-regulation of genes coding for proteins involved in nitrogen and sulfur metabolism. Deeper understanding of drought-induced changes in gene/protein/metabolite expression patterns will provide information on gene/protein/metabolite networks underpinning phenotypic traits relevant to stress tolerance and also how they ultimately link to phenome changes allowing new insights into changes required for drought recovery.

Improving the soybean-rhizobia symbiosis might also contribute to better drought tolerance. More robust rhizobia with better osmo-tolerance of rhizobia to persist for longer in droughted soils might thereby be a contributor (Mhadhbi et al., 2013). Recent research has also provided evidence that plant growth-promoting rhizobacterium (PGPR) improve plant adaptation to drought by stimulating lateral root formation and increasing shoot growth (Rolli et al., 2015) with stimulation partly caused by bacterium-produced volatile organic compounds (Wintermans et al., 2016). Also, salicylic acid to assemble a better root microbiome might play a role, since salicylic acid can modulate colonization of the root by specific bacterial families (Lebeis et al., 2015). Pyrrolizidine alkaloids (PAs), involved in plant cell re-programming for micro-symbiont entry, might be further a contributor and a target for investigation. A plant-homo-spermidine synthase (HSS), the first pathway-specific enzyme of PA biosynthesis, is exclusively localized in nodules (Irmer et al., 2015) suggesting that the plant is the main PA producer. Investigation how drought affects expression of soybean nodule HSS (Glyma.06g126700) might be therefore interesting.

Drought might finally also affect expression of nodule specific cysteine-rich antimicrobial peptides (NCR AMPs) essential for bacteroid development and found in legumes with indeterminate nodules (Mergaert et al., 2003; Horváth et al., 2015). In *M. truncatula* nodules, the bacteria undergo an irreversible differentiation process producing elongated polyploid bacteroids that cannot resume cell division. This differentiation process is controlled by nodule specific NCRs (Van de Velde et al., 2010; Haag et al., 2011, 2012; Frendo et al., 2013; Horváth et al., 2015). Although 138 NCRs were recently detected in *M. truncatula* bacteroids (Durgo et al., 2015) such NCRs, or peptides with similar antimicrobial functions, have so far not been found in soybean. Search for similar peptides in soybean and characterizing them under drought might be therefore an interesting future task.

AUTHOR CONTRIBUTIONS

KK has overall organized the paper and has written the draft paper. BV contributed with knowledge about proteolytic events in nodules and transcriptome analysis. BF contributed with his knowledge about root architecture, nodule characterization and recent developments in root and nodule screening. TK contributed with her knowledge about rhizobia screening for drought tolerance. GD contributed with his knowledge about legumains. CF contributed with her knowledge about nodule biology and and was involved in final writing of the paper.

ACKNOWLEDGMENTS

This work was funded by the International Foundation of Science (IFS grant C/5151-1), the NRF Incentive funding for rated researchers (90779) and the NRF National Bioinformatics Functional Genomics program (86947). Funding received from the Genomic Research Institute (GRI), University of Pretoria, is also acknowledged. TK thanks the NRF/DST in South Africa for a bursary. CF thanks BBSRC (UK) for financial support (BB/K501839/1).

REFERENCES

Ali, M. L., Luetchens, J., Singh, A., Shaver, T. M., Kruger, G. R., and Lorenz, A. J. (2016). Greenhouse screening of maize genotypes for deep root mass and related root traits and their association with grain yield under water-deficit conditions in the field. *Euphytica* 207, 79–94. doi: 10.1007/s10681-015-1533-x

Ao, J., Fu, J., Tian, J., Yan, X., and Liao, H. (2010). Genetic variability for root morph-architecture traits and root growth dynamics as related to phosphorus efficiency in soybean. *Funct. Plant Biol.* 37, 304–312. doi: 10.1071/FP09215

Armada, E., Probanza, A., Roldán, A., and Azcón, R. (2016). Native plant growth promoting bacteria *Bacillus thuringiensis* and mixed or individual mycorrhizal species improved drought tolerance and oxidative metabolism in *Lavandula dentata* plants. *J. Plant Physiol.* 192, 1–12. doi: 10.1016/j.jplph.2015.11.007

Arrese-Igor, C., González, E. M., Marino, D., Ladrera, R., Larrainzar, E., and Gil-Quintana, E. (2011). Physiological response of legumes nodules to drought. *Plant Stress* 5, 24–31.

Blum, A. (2011). Drought resistance – is it really a complex trait? *Funct. Plant Biol.* 38, 753–757. doi: 10.1071/FP11101

Bonneau, L., Ge, Y., Drury, G. E., and Gallois, P. (2008). What happened to plant caspases? *J. Exp. Bot.* 59, 491–499. doi: 10.1093/jxb/erm352

Charpentier, M., and Oldroyd, G. E. D. (2013). Nuclear calcium signaling in plants. *Plant Physiol.* 163, 496–503. doi: 10.1104/pp.113.220863

Chichkova, N. V., Shaw, J., Galiullina, R. A., Drury, G. E., Tuzhikov, A. I., Kim, S. H., et al. (2010). Phytaspase, a relocalisable cell death promoting plant protease with caspase specificity. *EMBO J.* 29, 1149–1161. doi: 10.1038/emboj.2010.1

Clarke, V. C., Loughlin, P. C., Gavrin, A., Chen, C., Brear, E. M., Day, D. A., et al. (2015). Proteomic analysis of the soybean symbiosome identifies new symbiotic proteins. *Mol. Cell Proteomics* 14, 1301–1322. doi: 10.1074/mcp.M114.043166

Clement, M., Lambert, A., Herouart, D., and Boncompagni, E. (2008). Identification of new up-regulated genes under drought stress in soybean nodules. *Gene* 426, 15–22. doi: 10.1016/j.gene.2008.08.016

Collier, R., and Tegeder, M. (2012). Soybean ureide transporters play a critical role in nodule development, function and nitrogen export. *Plant J.* 72, 355–367. doi: 10.1111/j.1365-313X.2012.05086.x

Comas, L. H., Becker, S. R., Cruz, V. M. V., Byrne, P. F., and Dierig, D. A. (2013). Root traits contributing to plant productivity under drought. *Front. Plant Sci.* 4:442. doi: 10.3389/fpls.2013.00442

Dai, A. (2013). Increasing drought under global warming in observations and models. *Nat. Climate Change* 3, 52–58. doi: 10.1038/nclimate1811

Durgo, H., Klement, E., Hunyadi-Gulyas, E., Szucs, A., Kereszt, A., Medzihradszky, K. F., et al. (2015). Identification of nodule-specific cysteine-rich plant peptides in endosymbiotic bacteria. *Proteomics* 15, 2291–2295. doi: 10.1002/pmic.201400385

Eberbach, P. L., Hoffmann, J., Moroni, S. J., Wade, L. J., and Weston, L. A. (2013). Rhizo-lysimetry: facilities for the simultaneous study of root behavior and resource use by agricultural crop and pasture systems. *Plant Methods* 9, 3. doi: 10.1186/1746-4811-9-3

Fan, X. D., Wang, J. Q., Yang, N., Dong, Y. Y., Liu, L., Wang, F. W., et al. (2013). Gene expression profiling of soybean leaves and roots under salt, saline-alkali and drought stress by high-throughput Illumina sequencing. *Gene* 512, 392–402. doi: 10.1016/j.gene.2012.09.100

Fenta, B. A., Beebe, S. E., Kunert, K. J., Burridge, J. D., Barlow, K. M., Lynch, P. J., et al. (2014). Field phenotyping of soybean roots for drought stress tolerance. *Agronomy* 4, 418–435. doi: 10.3390/agronomy4030418

Ferguson, B. J., Indrasumunar, A., Hayashi, S., Lin, M. H., Lin, Y. H., Reid, D. E., et al. (2010). Molecular analysis of legume nodule development and autoregulation. *J. Integr. Plant Biol.* 52, 61–76. doi: 10.1111/j.1744-7909.2010.00899.x

Fernandez-Luquen, F., Dendooven, L., Munive, A., Corlay-Chee, L., Serrano-Covarrubias, L. M., and Espinosa-Victoria, D. (2008). Micro-morphology of common bean (*Phaseolus vulgaris* L.) nodules undergoing senescence. *Acta Physiol. Plant.* 30, 545–552. doi: 10.1007/s11738-008-0153-7

Foyer, C. H., Lam, H.-M., Nguyen, H. T., Siddique, K. H. M., Varshney, R., et al. (2016). Neglecting legumes has compromised global food and nutritional security. *Nat. Plants* (in press).

Franco, J. A., Bañón, S., Vicente, M. J., Miralles, J., and Martínez-Sánchez, J. J. (2011). Root development in horticultural plants grown under abiotic stress conditions-a review. *J. Hortic. Sci. Biotechnol.* 86, 543–556. doi: 10.1080/14620316.2011.11512802

Frendo, P., Matamoros, M. A., Alloing, G., and Becana, M. (2013). Thiol-based redox signaling in the nitrogen-fixing symbiosis. *Front. Plant Sci.* 4:376. doi: 10.3389/fpls.2013.00376

Gage, D. J. (2004). Infection and invasion of roots by symbiotic, nitrogen-fixing rhizobia during nodulation of temperate legumes. *Microbiol. Mol. Biol. Rev.* 68, 280–300. doi: 10.1128/MMBR.68.2.280-300.2004

Ge, Y., Cai, Y. M., Bonneau, L., Rotari, V., Danon, A., Mckenzie, E. A., et al. (2016). Inhibition of cathepsin B by caspase-3 inhibitors blocks programmed cell death in *Arabidopsis*. *Cell Death Differ.* doi: 10.1038/cdd.2016.34 [Epub ahead of print].

Gil-Quintana, E., Lyon, D., Staudinger, C., Wienkoop, S., and González, E. M. (2015). *Medicago truncatula* and *Glycine max*: different drought tolerance and similar local response of the root nodule proteome. *J. Proteome Res.* 14, 5240–5251. doi: 10.1021/acs.jproteome.5b00617

Global soybean production.com (2016). *Global Soybean Production April 2016*. Available at: http://www.globalsoybeanproduction.com/ [accessed June 19, 2016].

Gu, C., Kolodziejek, I., Misas-Villamil, J., Shindo, T., Colby, T., Verdoes, M., et al. (2010). Proteasome activity profiling: a simple, robust and versatile method revealing subunit-selective inhibitors and cytoplasmic, defense-induced proteasome activities. *Plant J.* 62, 160–170. doi: 10.1111/j.1365-313X.2009.04122.x

Ha, C. V., Le, D. T., Nishiyama, R., Watanabe, Y., Sulieman, S., Tran, U. T., et al. (2013). The auxin response factor transcription factor family in soybean: genome-wide identification and expression analyses during development and water stress. *DNA Res.* 20, 511–524. doi: 10.1093/dnares/dst027

Ha, C. V., Watanabe, Y., Tran, U. T., Le, D. T., Tanaka, M., Nguyen, K. H., et al. (2015). Comparative analysis of root transcriptomes from two contrasting drought-responsive Williams 82 and DT2008 soybean cultivars under normal and dehydration conditions. *Front. Plant Sci.* 6:551. doi: 10.3389/fpls.2015.00551

Haag, A. F., Baloban, M., Sani, M., Kerscher, B., Pierre, O., Farkas, A., et al. (2011). Protection of Sinorhizobium against host cysteine-rich antimicrobial peptides is critical for symbiosis. *PLoS Biol.* 9:e1001169. doi: 10.1371/journal.pbio.1001169

Haag, A. F., Kerscher, B., Dall'Angelo, S., Sani, M., Longhi, R., Baloban, M., et al. (2012). Role of cysteine residues and disulfide bonds in the activity of a legume root nodule-specific, cysteine-rich peptide. *J. Biol. Chem.* 287, 10791–10798. doi: 10.1074/jbc.M111.311316

Han, J. J., Lin, W., Oda, Y., Cui, K. M., Fukuda, H., and He, X. Q. (2012). The proteasome is responsible for caspase-3-like activity during xylem development. *Plant J.* 72, 129–141. doi: 10.1111/j.1365-313X.2012.05070.x

Hara-Nishimura, I., Hatsugai, N., Nakaune, S., Kuroyanagi, M., and Nishimura, M. (2005). Vacuolar processing enzyme: an executor of plant cell death. *Curr. Opin. Plant Biol.* 8, 404–408. doi: 10.1016/j.pbi.2005.05.016

Hatsugai, N., Iwasaki, S., Tamura, K., Kondo, M., Fuji, K., Ogasawara, K., et al. (2009). A novel membrane fusion-mediated plant immunity against bacterial pathogens. *Genes Dev.* 23, 2496–2506. doi: 10.1101/gad.1825209

Herridge, D. F., Peoples, M. B., and Boddey, R. M. (2008). Global inputs of biological nitrogen fixation in agricultural systems. *Plant Soil* 311, 1–18. doi: 10.1007/s11104-008-9668-3

Horváth, B., Domonkos, A., Kereszt, A., Szücs, A., Ábrahám, E., and Ayaydin, F. (2015). Loss of the nodule-specific cysteine rich peptide, NCR169, abolishes symbiotic nitrogen fixation in the *Medicago truncatula* dnf7mutant. *Proc. Natl. Acad. Sci. U.S.A.* 112, 15232–15237. doi: 10.1073/pnas.1500777112

Hossain, Z., Khatoon, A., and Komatsu, S. (2013). Soybean proteomics for unraveling abiotic stress response mechanism. *J. Proteome Res.* 12, 4670–4684. doi: 10.1021/pr400604b

Irmer, S., Podzun, N., Langel, D., Heidemann, F., Kaltenegger, E., Schemmerling, B., et al. (2015). New aspect of plant – rhizobia interaction: alkaloid biosynthesis in Crotalaria depends on nodulation. *Proc. Natl. Acad. Sci. U.S.A.* 112, 4164–4169. doi: 10.1073/pnas.1423457112

King, C. A., and Purcell, L. C. (2001). Soybean nodule size and relationship to nitrogen fixation response to water deficit. *Crop Sci.* 41, 1099–1107. doi: 10.2135/cropsci2001.4141099x

King, C. A., and Purcell, L. C. (2006). Genotypic variation for shoot N concentration and response to water deficits in soybean. *Crop Sci.* 46, 2396–2402. doi: 10.2135/cropsci2006.03.0165

Kondorosi, E., Mergaert, P., and Kereszt, A. (2013). A paradigm for endosymbiotic life: cell differentiation of *Rhizobium* bacteria provoked by host plant factors. *Annu. Rev. Microbiol.* 67, 611–628. doi: 10.1146/annurev-micro-092412-155630

Ku, Y.-S., Au-Yeung, W.-K., Yung, Y.-L., Li, M.-W., Wen, C.-Q., Liu, X., et al. (2013). "Drought stress and tolerance in soybean," in *A Comprehensive Survey of International Soybean Research - Genetics, Physiology, Agronomy and Nitrogen Relationships*, ed. J. E. Board (New York, NY: InTech), 209–237.

Larrainzar, E., Molenaar, J. A., Wienkoop, S., Gil-Quintana, E., Alibert, B., Limami, A. M., et al. (2014). Drought stress provokes the down-regulation of methionine and ethylene biosynthesis pathways in *Medicago truncatula* roots and nodules. *Plant Cell and Environment* 37, 2051–2063. doi: 10.1111/pce.12285

Larrainzar, E., Wienkoop, S., Scherling, C., Kempa, S., Ladrera, R., Arrese-Igor, C., et al. (2009). Carbon metabolism and bacteroid functioning are involved in the regulation of nitrogen fixation in *Medicago truncatula* under drought and recovery. *Mol. Plant Microbe Interact.* 22, 1565–1576. doi: 10.1094/MPMI-22-12-1565

Lebeis, S. L., Paredes, S. H., Lundberg, D. S., Breakfield, N., Gehring, J., McDonald, M., et al. (2015). PLANT MICROBIOME. Salicylic acid modulates colonization of the root microbiome by specific bacterial taxa. *Science* 349, 860–864. doi: 10.1126/science.aaa8764

Li, Y., Zhou, L., Chen, D., Tan, X., Lei, L., and Zhou, J. (2008). A nodule-specific plant cysteine proteinase, AsNODF32, is involved in nodule senescence and nitrogen fixation activity of the green manure legume *Astragalus* sinicus. *New Phytol.* 180, 185–192. doi: 10.1111/j.1469-8137.2008.02562.x

Libault, M., Farmer, A., Joshi, T., Takahashi, K., Langley, R. J., Franklin, L. D., et al. (2010). An integrated transcriptome atlas of the crop model *Glycine max*, and its use in comparative analyses in plants. *Plant J.* 63, 86–99. doi: 10.1111/j.1365-313X.2010.04222.x

Lopes, M. S., Araus, J. L., van Heerden, P. D. R., and Foyer, C. H. (2011). Enhancing drought tolerance in C4 crops. *J. Exp. Bot.* 62, 3135–3153. doi: 10.1093/jxb/err105

Manavalan, L. P., Guttikonda, S. K., Phan Tran, L.-S., and Nguyen, H. T. (2009). Physiological and molecular approaches to improve drought resistance in soybean. *Plant Cell Physiol.* 50, 1260–1276. doi: 10.1093/pcp/pcp082

Maróti, G., and Kondorosi, E. (2014). Nitrogen-fixing *Rhizobium*-legume symbiosis: are polyploidy and host peptide-governed symbiont differentiation general principles of endosymbiosis? *Front. Microbiol.* 5:326. doi: 10.3389/fmicb.2014.00326

Márquez-García, B., Shaw, D., Cooper, J. W., Karpinska, B., Quain, M. D., Makgopa, E. M., et al. (2015). Redox markers for drought-induced nodule senescence, a process occurring after drought-induced senescence of the

lowest leaves in soybean (*Glycine max* Merr.). *Annals Bot.* 116, 497–510. doi: 10.1093/aob/mcv030

Mergaert, P., Nikovics, K., Kelemen, Z., Maunoury, N., Vaubert, D., Kondorosi, A., et al. (2003). A novel family in *Medicago truncatula* consisting of more than 300 nodule-specific genes coding for small, secreted polypeptides with conserved cysteine motifs. *Plant Physiol.* 132, 161–173. doi: 10.1104/pp.102.018192

Mhadhbi, H., Chihaoui, S., Mhamdi, R., Mnasri, B., and Jebara, M. (2013). A highly osmotolerant rhizobial strain confers a better tolerance of nitrogen fixation and enhances protective activities to nodules of *Phaseolus vulgaris* under drought stress. *Afr. J. Biotechnol.* 10, 4555–4563.

Mohammadi, P. P., Moieni, A., Hiraga, S., and Komatsu, S. (2012). Organ-specific proteomic analysis of drought-stressed soybean seedlings. *J. Proteomics* 75, 1906–1923. doi: 10.1016/j.jprot.2011.12.041

Mooney, S. J., Pridmore, T. P., Helliwell, J., and Bennett, M. J. (2012). Developing X-ray computed tomography to non-invasively image 3-D root systems architecture in soil. *Plant Soil* 352, 1–22. doi: 10.1007/s11104-011-1039-9

Neto, J. R. C. F., Pandolfi, V., Guimaraes, F. C., Benko-Iseppon, A. M., Romero, C., Silva, R. L., et al. (2013). Early transcriptional response of soybean contrasting accessions to root dehydration. *PLoS ONE* 8:e83466. doi: 10.1371/journal.pone.0083466

Nguyen, H. (2016). *Soybean Genetics and Genomics Laboratory*. Available at: http://soybeangenomics.missouri.edu/research/functional_genomics.htm [Accessed April 26, 2016].

Oh, M. W., and Komatsu, S. (2015). Characterization of proteins in soybean roots under flooding and drought stress. *J. Proteomics* 114, 161–181. doi: 10.1016/j.jprot.2014.11.008

Oldroyd, G. E. (2013). Speak, friend, and enter: signalling systems that promote beneficial symbiotic associations in plants. *Nat. Rev. Microbiol.* 11, 252–263. doi: 10.1038/nrmicro2990

Oldroyd, G. E., Murray, J. D., Poole, P. S., and Downie, J. A. (2011). The rules of engagement in the legume-rhizobial symbiosis. *Annu. Rev. Genet.* 45, 119–144. doi: 10.1146/annurev-genet-110410-132549

Quain, M. D., Makgopa, M. E., Cooper, J. W., Kunert, K. J., and Foyer, C. H. (2015). Ectopic phytocystatin expression increases nodule numbers and influences the responses of soybean (*Glycine max*) to nitrogen deficiency. *Phytochemistry* 112, 179–187. doi: 10.1016/j.phytochem.2014.12.027

Quain, M. D., Makgopa, M. E., Márquez-García, B., Comadira, G., Fernandez-Garcia, N., Olmos, E., et al. (2014). Ectopic phytocystatin expression leads to enhanced drought stress tolerance in soybean (*Glycine max*) and *Arabidopsis thaliana* through effects on strigolactone pathways and can also result in improved seed traits. *Plant Biotechnol. J.* 12, 903–913. doi: 10.1111/pbi.12193

Roberts, I. N., Caputo, C., Criado, M. V., and Funk, C. (2012). Senescence-associated proteases in plants. *Physiol. Plant.* 145, 130–139. doi: 10.1111/j.1399-3054.2012.01574.x

Rolli, E., Marasco, R., Vigani, G., Ettoumi, B., Mapelli, F., Deangelis, M. L., et al. (2015). Improved plant resistance to drought is promoted by the root-associated microbiome as a water stress-dependent trait. *Environ. Microbiol.* 17, 316–331. doi: 10.1111/1462-2920.12439

Satbhai, S. B., Ristova, D., and Busch, W. (2015). Underground tuning: quantitative regulation of root growth. *J. Exp. Bot.* 66, 1099–1112. doi: 10.1093/jxb/eru529

Schmutz, J., Cannon, S. B., Schlueter, J., Ma, J., Mitros, T., Nelson, W., et al. (2010). Genome sequence of the palaeopolyploid soybean. *Nature* 463, 178–183. doi: 10.1038/nature08670

Serraj, R., Bona, S., Purcell, L. C., and Sinclair, T. R. (1997). Nitrogen accumulation and nodule activity of field-grown 'Jackson' soybean in response to water deficits. *Field Crops Res.* 52, 109–116. doi: 10.1016/S0378-4290(96)01068-4

Severin, A. J., Woody, J. L., Bolon, Y. T., Joseph, B., Diers, B. W., Farmer, A. D., et al. (2010). RNA-Seq Atlas of *Glycine max*: a guide to the soybean transcriptome. *BMC Plant Biol.* 10:160. doi: 10.1186/1471-2229-10-160

Song, L., Prince, S., Valliyodan, B., Joshi, T., Maldonado dos Santos, J. V., et al. (2016). Genome-wide transcriptome analysis of soybean primary root under varying water deficit conditions. *BMC Genomics* 17:57. doi: 10.1186/s12864-016-2378-y

Staudinger, C., Mehmeti-Tershani, V., Gil-Quintana, E., Gonzalez, E. M., Hofhansl, F., Bachmann, G., et al. (2016). Evidence for a rhizobia-induced drought stress response strategy in *Medicago truncatula*. *J. Proteomics* 136, 202–213. doi: 10.1016/j.jprot.2016.01.006

Stolf-Moreira, R., Lemos, E. G. M., Carareto-Alves, L., Marcondes, J., and Pereira, S. S. (2011). Transcriptional profiles of roots of different soybean genotypes subjected to drought stress. *Plant Mol. Biol. Rep.* 29, 19–34. doi: 10.1186/1471-2164-14-687

Sulieman, S., Van Ha, C., Nasr Esfahani, M., Watanabe, Y., Nishiyama, R., Pham, C. T., et al. (2015). DT2008: a promising new genetic resource for improved drought tolerance in soybean when solely dependent on symbiotic N2 fixation. *BioMed Res. Int.* 2015:7. doi: 10.1155/2015/687213

Tanaka, N., Kato, M., Tomioka, R., Kurata, R., Fukao, Y., Aoyama, T., et al. (2014). Characteristics of a root hair-less line of *Arabidopsis thaliana* under physiological stresses. *J. Exp. Bot.* 65, 1497–1512. doi: 10.1093/jxb/eru014

Thao, N. P., Thu, N. B., Hoang, X. L., Van Ha, C., and Tran, L. S. (2013). Differential expression analysis of a subset of drought-responsive GmNAC genes in two soybean cultivars differing in drought tolerance. *Int. J. Mol. Sci.* 14, 23828–23841. doi: 10.3390/ijms141223828

Thu, N. B., Nguyen, Q. T., Hoang, X. L., Thao, N. P., and Tran, L. S. (2014). Evaluation of drought tolerance of the Vietnamese soybean cultivars provides potential resources for soybean production and genetic engineering. *BioMed Res. Int.* 2014:9. doi: 10.1155/2014/809736

Toorchi, M., Yukawa, K., Nouri, M. Z., and Komatsu, S. (2009). Proteomics approach for identifying osmotic-stress-related proteins in soybean roots. *Peptides* 30, 2108–2117. doi: 10.1016/j.peptides.2009.09.006

Tripathi, P., Rabara, R. C., Reese, R. N., Miller, M. A., Rohila, J. S., Subramanian, S., et al. (2016). A toolbox of genes, proteins, metabolites and promoters for improving drought tolerance in soybean includes the metabolite coumestrol and stomatal development genes. *BMC Genomics* 17:102. doi: 10.1186/s12864-016-2420-0

Vadez, V. (2014). Root hydraulics: the forgotten side of roots in drought adaptation. *Field Crops Res.* 165, 15–24. doi: 10.1016/j.fcr.2014.03.017

Van de Velde, W., Guerra, J. C., De Keyser, A., De Rycke, R., Rombauts, S., Maunoury, N., et al. (2006). Aging in legume symbiosis. A molecular view on nodule senescence in *Medicago truncatula*. *Plant Physiol.* 141, 711–720. doi: 10.1104/pp.106.078691

Van de Velde, W., Zehirov, G., Szatmari, A., Debreczeny, M., Ishihara, H., Kevei, Z., et al. (2010). Plant peptides govern terminal differentiation of bacteria in symbiosis. *Science* 327, 1122–1126. doi: 10.1126/science.1184057

Van Wyk, S. G., Du Plessis, M., Cullis, C., Kunert, K. J., and Vorster, B. J. (2014). Cysteine protease and cystatin expression and activity during soybean nodule development and senescence. *BMC Plant Biol.* 14:294. doi: 10.1186/s12870-014-0294-3

Vinh, M. Q., Chung, P. T. B., Manh, N. V., and Hong, L. T. A. (2010). Results of research, creation, drought-tolerant soybean variety, DT2008. *Vietnam J. Sci. Technol.* 6, 46–50.

Wintermans, P. C., Bakker, P. A., and Pieterse, C. M. (2016). Natural genetic variation in *Arabidopsis* for responsiveness to plant growth-promoting rhizobacteria. *Plant Mol. Biol.* 90, 623–634. doi: 10.1007/s11103-016-0442-2

Zhu, M., Dahmen, J. L., Stacey, G., and Cheng, J. (2013). Predicting gene regulatory networks of soybean nodulation from RNA-Seq transcriptome data. *BMC Bioinformatics* 14:278. doi: 10.1186/1471-2105-14-278

Conflict of Interest Statement: The authors declare that the research was conducted in the absence of any commercial or financial relationships that could be construed as a potential conflict of interest.

frontiers in Plant Science

ORIGINAL RESEARCH
published: 12 May 2016
doi: 10.3389/fpls.2016.00660

Effective Use of Water and Increased Dry Matter Partitioned to Grain Contribute to Yield of Common Bean Improved for Drought Resistance

Jose A. Polania[1,2]*, *Charlotte Poschenrieder*[2], *Stephen Beebe*[1] and *Idupulapati M. Rao*[1]*

[1] Centro Internacional de Agricultura Tropical, Santiago de Cali, Colombia, [2] Lab Fisiología Vegetal, Facultad de Biociencias, Universidad Autónoma de Barcelona, Bellaterra, Spain

OPEN ACCESS

Edited by:
Urs Feller,
University of Bern, Switzerland

Reviewed by:
Bingcheng Xu,
Chinese Academy of Sciences and Ministry of Water Resources, China
Jorge Alberto Acosta-Gallegos,
Instituto Nacional de Investigaciones Forestales, Agrícolas y Pecuarias, Mexico
James Kelly,
Michigan State University, USA

***Correspondence:**
Jose A. Polania
j.a.polania@cgiar.org;
Idupulapati M. Rao
i.rao@cgiar.org

Specialty section:
This article was submitted to Agroecology and Land Use Systems, a section of the journal Frontiers in Plant Science

Received: 30 March 2016
Accepted: 29 April 2016
Published: 12 May 2016

Citation:
Polania JA, Poschenrieder C, Beebe S and Rao IM (2016) Effective Use of Water and Increased Dry Matter Partitioned to Grain Contribute to Yield of Common Bean Improved for Drought Resistance. Front. Plant Sci. 7:660. doi: 10.3389/fpls.2016.00660

Common bean (*Phaseolus vulgaris* L.) is the most important food legume in the diet of poor people in the tropics. Drought causes severe yield loss in this crop. Identification of traits associated with drought resistance contributes to improving the process of generating bean genotypes adapted to these conditions. Field studies were conducted at the International Center for Tropical Agriculture (CIAT), Palmira, Colombia, to determine the relationship between grain yield and different parameters such as effective use of water (EUW), canopy biomass, and dry partitioning indices (pod partitioning index, harvest index, and pod harvest index) in elite lines selected for drought resistance over the past decade. Carbon isotope discrimination (CID) was used for estimation of water use efficiency (WUE). The main objectives were: (i) to identify specific morpho-physiological traits that contribute to improved resistance to drought in lines developed over several cycles of breeding and that could be useful as selection criteria in breeding; and (ii) to identify genotypes with desirable traits that could serve as parents in the corresponding breeding programs. A set of 36 bean genotypes belonging to the Middle American gene pool were evaluated under field conditions with two levels of water supply (irrigated and drought) over two seasons. Eight bean lines (NCB 280, NCB 226, SEN 56, SCR 2, SCR 16, SMC 141, RCB 593, and BFS 67) were identified as resistant to drought stress. Resistance to terminal drought stress was positively associated with EUW combined with increased dry matter partitioned to pod and seed production and negatively associated with days to flowering and days to physiological maturity. Differences in genotypic response were observed between grain CID and grain yield under irrigated and drought stress. Based on phenotypic differences in CID, leaf stomatal conductance, canopy biomass, and grain yield under drought stress, the lines tested were classified into two groups, water savers and water spenders. Pod harvest index could be a useful selection criterion in breeding programs to select for drought resistance in common bean.

Keywords: canopy biomass, carbon isotope discrimination, pod harvest index, terminal drought stress, water use efficiency

INTRODUCTION

Common bean (*Phaseolus vulgaris* L.) is the most important food legume in the tropics of Latin America and eastern and southern Africa. Beans are predominantly cultivated by small farmers in these two regions where climate variability and limited use of inputs frequently reduce productivity (Beebe, 2012; Beebe et al., 2013). The yield of beans is affected by various constraints (Thung and Rao, 1999). Among those drought is responsible for losses between 10 and 100%. About 60% of the bean-producing regions have prolonged periods of water shortage and drought is the second most important factor in yield reduction after diseases (Thung and Rao, 1999; Rao, 2014). The development of bean varieties resistant to drought stress conditions through breeding is a useful strategy to increase food security in marginal areas. Breeding programs for improving resistance to drought usually select the best genotypes based on grain yield under drought stress (Rosales et al., 2012). A physiological approach using morpho-physiological traits as selection criteria can increase the possibility of combining parents with complementary traits, provided the germplasm is characterized more thoroughly than just testing for yield (Reynolds and Trethowan, 2007; Mir et al., 2012). A useful trait must exhibit higher heritability, enough genetic variability, correlation with yield, and its evaluation must be fast, easy and cheap (Jackson et al., 1996; Araus et al., 2002; Beebe et al., 2013).

Three key processes, among others, have been related to improved drought resistance: (i) acquiring greater amount of water by the root system from the soil profile to facilitate transpiration, (ii) acquiring more carbon (biomass) in relation to water transpired, and (iii) increased mobilization of accumulated carbon to the harvestable economic product (Condon et al., 2004). Previous research identified several traits that contribute to improved resistance of common bean to drought and these include earliness, deep rooting, and greater ability to partition dry matter to grain production (Hall, 2004; Beebe et al., 2013; Rao et al., 2013; Rao, 2014). Water use efficiency (WUE), or "more crop per drop" is considered as an important component of drought resistance in different crops (Blum, 2009; Sinclair, 2012; Vadez et al., 2014). Increased WUE reduces the rate of transpiration and crop water use, processes that are crucial for carbon assimilation, biomass production, and yield (Blum, 2009; Sinclair, 2012). However, the reduction in water use is generally achieved by plant traits and environmental responses that could also reduce yield potential (Blum, 2005). WUE is a complex trait and difficult to phenotype, preventing many breeding programs from using WUE directly (Araus et al., 2002; Easlon et al., 2014). In contrast to WUE, effective use of water (EUW) implies maximal soil moisture capture for transpiration, and also involves decreased non-stomatal transpiration and minimal water loss by soil evaporation (Blum, 2009). EUW is relevant when there is still soil water available at maturity or when deep-rooted genotypes access water deep in the soil profile that is not normally available (Araus et al., 2002). Ideotypes of plants have been proposed by Blum (2015) for targeting in plant breeding according to agro-ecological zones and types of drought such as, the isohydric ("water saving") plant model and the anisohydric ("water spending") plant model. The water saving model might have an advantage in the harshest environments, whereas the water spending model will perform relatively better under more moderate drought conditions.

One plant attribute that has been associated with WUE is carbon isotope discrimination (CID), based on the inverse relationship between CID and WUE (greater ^{13}C discrimination being associated with lower values of WUE, or conversely, more water use and transpiration). Selection for low ^{13}C discrimination has been proposed as a screening method to improve WUE in breeding C_3 crops (Araus et al., 2002; Khan et al., 2007; Easlon et al., 2014). Use of CID presented some advantages by reflecting integration over long periods of gas exchange during crop development, high throughput sampling, relatively low cost, and high heritability (Easlon et al., 2014). In bush bean under moderate droughts or non-arid environments, it has been observed that there is a positive relationship between CID, root length density and grain yield (Sponchiado et al., 1989; White et al., 1990; White, 1993; Hall, 2004; Polania et al., 2012). Increased water use is associated with increased accumulation of carbon and plant growth. However, improved harvest index (HI) or enhanced mobilization of photosynthates to grain production plays an essential role in increase of yield under stress. In most environments with drought, water deficit occurs during reproductive development, reducing HI (Blum, 2009). Several studies in common bean have shown that increased dry matter partitioned to pod and seed formation contributes to better grain yield under drought as well as low soil fertility stress (Rao, 2014). Therefore, assimilate partitioning is an important attribute to evaluate adaptation to abiotic stress in common bean (Rosales-Serna et al., 2004; Beebe et al., 2008, 2013; Klaedtke et al., 2012; Polania et al., 2012, 2016; Rosales et al., 2012; Assefa et al., 2013; Rao et al., 2013; Rao, 2014).

The main objectives of this study were: (i) to identify specific morpho-physiological traits that contribute to improved resistance to drought in lines developed over several cycles of breeding and that could be useful as selection criteria in breeding beans for drought resistance; and (ii) to identify genotypes with desirable traits that could serve as parents in breeding programs that are aimed to improve drought resistance.

MATERIALS AND METHODS

Experimental Site and Meteorological Conditions

Two field trials were conducted during the dry season (from June to September in both 2012 and 2013), at the main experiment station of the International Center for Tropical Agriculture (CIAT) in Palmira, Colombia, located at 3° 29″ N latitude, 76° 21″ W longitude and at an altitude of 965 m. Basic characteristics of this field site were described previously (Beebe et al., 2008). The soil is a Mollisol (Aquic Hapludoll) with adequate nutrient supply and is estimated to permit storage of 100 mm of available water (assuming 1.0 m of effective root growth with −0.03 and −1.5 MPa as upper and lower limits for soil matric potential). During the crop-growing season, maximum and minimum air

temperatures in 2012 were 31.0 and 19.0°C, and in 2013 were 30.2 and 19.2°C, respectively. Total rainfall during the active crop growth was 85.8 mm in 2012 and 87.7 mm in 2013. The potential pan evaporation was of 385.2 mm in 2012 and 351.0 mm in 2013. Two levels of water supply (irrigated and rainfed) were applied to simulate well-watered (control) and drought stress treatments respectively. Trials were furrow irrigated (∼35 mm of water per irrigation). The drought stress treatment under rainfed conditions in 2012 received three irrigations (at 3 days before planting and at 5 and 23 days after planting) and in 2013 also received three irrigations (at 3 days before planting and at 4 and 15 days after planting). In both years, irrigation was suspended after the third irrigation to induce terminal drought stress conditions. The irrigated control treatment received five irrigations in 2012 and six irrigations in 2013 to ensure adequate soil moisture for crop growth and development.

Plant Material and Experimental Design

For this study 36 bush bean genotypes belonging to the Middle American gene pool were selected: 22 elite lines of common bean (BFS 10, BFS 29, BFS 32, BFS 67, MIB 778, NCB 226, NCB 280, RCB 273, RCB 593, SCR 16, SCR 2, SCR 9, SEN 56, SER 118, SER 119, SER 125, SER 16, SER 48, SER 78, SMC 141, SMC 43, and SXB 412); five interspecific lines between elite line SER 16 and *Phaseolus coccineus* (ALB 6, ALB 60, ALB 74, ALB 88, and ALB 213); one landrace of tepary bean (*Phaseolus acutifolius*) G40001 from Veracruz-Mexico, and two interspecific lines between tepary bean and common bean (INB 841 and INB 827 developed from five cycles of congruity backcrossing of tepary with ICA Pijao). BFS (small red) lines were developed to improve adaptation to low soil fertility and drought. SER and SCR (small red), SEN (small black), and NCB (small black) lines were developed for improved adaptation to drought. ALB (small red) lines were developed for improved adaptation to drought and aluminum toxicity. RCB (small red) lines were developed for improved yield potential, disease resistance, and commercial grain. SEA 15 and BAT 477 were included as drought resistant checks, and three commercial cultivars of common bean (DOR 390, Pérola and Tio Canela) as drought sensitive materials. BAT 477 NN was included as a non-nodulating bean genotype. In the 2 years, a 6 × 6 partially balanced lattice design with three replications was used. Experimental units consisted of 4 rows with 3.72 m row length with a row-to-row distance of 0.6 m and plant-to-plant spacing of 7 cm (equivalent to 24 plants m^{-2}). Trials were managed by controlling weeds with application of herbicides (Fomesafen, Fluazifop-p-butil, and Bentazon) and pests and diseases by spraying with insecticides (Thiametoxam, Clorpirifos, Imidacloprid, Abamectina, Cyromazine, and Milbemectin) and fungicides (Benomil and Carboxin) as needed.

Yield Measurements and Phenological Assessment

Grain was harvested from two central rows after discarding end plants in both the irrigated and drought plots. Mean yields per hectare were corrected for 0% moisture in grain. Days to flowering (DF) and days to physiological maturity (DPM) were recorded for each plot. DF is defined as the number of days after planting until 50% of the plants have at least one open flower. DPM is the number of days after planting until 50% of plants have at least one pod losing its green pigmentation. The geometric mean (GM) of grain yield was determined as $(NS \times DS)^{1/2}$ where NS is no stress (irrigated) and DS is drought stress. The drought response index (DRI) was calculated as indicator of drought resistance as described before (Bidinger et al., 1987; Krishnamurthy et al., 2010), using DF under rainfed conditions for every individual plot and yield potential as arithmetic mean of grain yield under irrigated conditions across replications.

Physiological Measurements

At mid-pod filling, a 50 cm segment of the row (equivalent to an area of 0.3 m^2) from each plot with about seven plants was used for destructive sampling to measure total canopy biomass (CB) and leaf area index (LAI). Leaf area was measured using a leaf area meter (model LI-3000, LI-COR, NE, USA) and the LAI was calculated as leaf area per unit land area. Also, at mid-pod filling the stomatal conductance was measured with a portable leaf porometer (Decagon SC-1) on a fully expanded young leaf of one plant within each replication. Measurements were made late in the morning $(10 a.m.–12 noon) on clear, sunny days with minimal wind. At the time of harvest, plants in 50 cm of a row from each plot were cut and dry weights of stem, pod, seed, and pod wall, seed number per area (SNA), and pod number per area (PNA) were recorded. The following attributes were determined according to Beebe et al. (2013): harvest index (HI) (%): seed biomass dry weight at harvest/total shoot biomass dry weight at mid-pod filling × 100; pod harvest index (PHI) (%): seed biomass dry weight at harvest/pod biomass dry weight at harvest × 100; pod partitioning index (PPI) (%): pod biomass dry weight at harvest/total canopy biomass dry weight at mid-pod filling × 100. HI and PPI were estimated using the CB value at mid-pod filling growth stage which is assumed to be the time that reflects the maximum vigor of the genotype. It is assumed that from this time common bean begins to lose canopy biomass through leaf fall, especially under terminal drought stress. Shoot and seed total nonstructural carbohydrates (TNC) concentrations were determined according to the method described by Kang and Bringk (1995).

One plant of each genotype from each plot (irrigated and drought) was selected for destructive sampling at mid-pod filling. A random sample of grain per experimental unit was selected, washed thoroughly and ground. The ground samples of plants at mid-pod filling and grain at harvest were sent to UC Davis Stable Isotope Facility in USA for ^{13}C analysis. CID ($\Delta^{13}C$ in ‰) was calculated according to the following equation, where $\delta^{13}Cs$ and $\delta^{13}Ca$ are sample and atmospheric concentrations of ^{13}C, respectively, and carbon isotope composition of atmosphere is assumed to be −8.0‰(Farquhar et al., 1989). Isotopic discrimination between ^{13}C and ^{12}C (Δ) in shoot and grain was related to whole plant water use (Farquhar et al., 1989).

$$\Delta\ 13C\ (CID)\ = \frac{[\delta 13Ca - \delta 13Cs]}{[1 + (\delta 13Cs/1000)]}$$

Statistical Analysis

All data were analyzed using the SAS (v 9.0) PROC MIXED and PROC CORR (SAS Institute Inc., 2008). The adjusted means for each genotype and the environment (irrigated and rainfed) were obtained using the mixed models theory together with the MIXED procedure considering the effects of the replications and blocks within replications as random and genotypes as fixed. Correlation coefficients were calculated by the PROC CORR. Values reported with *, **, or *** are statistically significant at probability levels of 5, 1, and 0.1%, respectively.

RESULTS

Grain Yield

The data on rainfall distribution, water applied through irrigation, and pan evaporation in both trials indicated that the crop suffered terminal drought stress during crop development under rainfed treatment conditions. The mean value of grain yield under drought conditions decreased by 56% compared with irrigated conditions (**Table 1**). Under drought conditions the grain yield of 36 genotypes ranged from 59 to 1526 kg ha^{-1} (**Table 1**). Among the genotypes tested, the lines BFS 29, NCB 280, SEN 56, BFS 10, SEA 15, and NCB 226 were superior in their resistance to drought stress. The relationship between grain yield of drought and irrigated treatments indicated that BFS 29, NCB 280, SEN 56, BFS 10, and NCB 226 were not only drought resistant but were also responsive to irrigation (**Table 1**). Among the 36 genotypes tested, the biofortified line MIB 778, was the most sensitive to drought stress. MIB 778 is an interspecific progeny of common bean and *P. dumosus*, which may explain its extreme sensitivity to drought. The genotypes Pérola, DOR 390, SMC 43, and ALB 88 were also sensitive to drought stress (**Table 1**).

Leaf Stomatal Conductance and Carbon Isotope Discrimination

Leaf stomatal conductance presented a significant positive correlation with grain yield under both irrigated (0.24**) and drought stress (0.31***) conditions (**Table 3**). The lines NCB 280, SEN 56, SCR 16, SMC 141, NCB 226, SEA 15, and BFS 10, combined higher values of leaf stomatal conductance with better grain yield under drought stress (**Tables 1, 2**). The lines MIB 778, Pérola, SMC 43, and DOR 390 presented lower values of stomatal conductance combined with lower grain yield under drought stress (**Tables 1, 2**). Similarly correlations and differences in genotypic response were observed between grain CID and grain yield under irrigated and drought stress conditions (**Table 3**). The accession of *P. acutifolius* G 40001 and the lines SER 16, ALB 6, and ALB 60 presented lower values of leaf stomatal conductance and grain CID (lower use of water) combined with moderate plant growth and grain yield under drought stress (**Tables 1, 2**).

Canopy Biomass (CB), Pod Partitioning Index (PPI), and Pod Harvest Index (PHI)

A positive and significant correlation was observed between CB and grain yield under both irrigated and drought conditions, 0.39*** and 0.59***, respectively (**Table 3**). The drought resistant lines combined higher CB production with higher grain yield under drought stress conditions. The drought susceptible lines presented lower values of both CB and grain yield under drought conditions (**Table 1**). It is important to note that the sampled area to determine CB at mid-pod filling was small and this could overestimate the total CB values per hectare. This small area was selected to facilitate comparison of large number of genotypes. Lines with superior grain yield showed higher values of LAI under drought stress (**Table 3**). The PPI reflects the biomass partitioned to pods at harvest as a proportion of the total CB at mid-pod filling growth stage. This ratio and HI may be overestimated because we used the CB values at mid-pod filling growth stage with the assumption that this growth stage reflects the maximum vigor. The values of CB may be underestimated if vegetative growth continues between mid-pod filling to physiological maturity due to irrigation or intermittent rainfall. Correlation coefficients between grain yield and PPI were positive and highly significant under drought conditions (**Table 3**). Also, the drought resistant lines combined higher value of PPI and grain yield under drought stress conditions while the drought susceptible lines showed lower ability in partitioning of dry matter to pod production under drought conditions (**Table 1**). The lines SMC 141 and SER 118 were outstanding in dry matter partitioning to pod production, but the CB values of these lines were lower under drought stress (**Table 1**).

The PHI value reflects the biomass partitioned to seed as a proportion of total pod biomass. A positive and highly significant correlation of PHI with grain yield was observed under both irrigated and drought conditions (**Table 3**). The lines identified as drought resistant were superior in PHI, resulting in a higher grain yield under drought conditions. The drought susceptible lines described previously showed lower ability in partitioning of dry matter from plant structures to pod production (PPI) and from podwall to seed production (PHI) resulting in poor performance under drought stress (**Figure 2**, **Table 1**). The accession of *P. acutifolius* (G 40001) and the lines INB 841 and SER 118 likewise presented higher values of PHI under drought stress. A weak positive correlation between grain yield and seed TNC was observed under both irrigated and drought stress conditions (**Table 3**). The drought resistant lines combined higher seed TNC concentration with higher grain yield under drought stress. The drought susceptible lines presented lower seed TNC concentration and grain yield under drought stress.

Days to Flowering (DF), Days to Physiological Maturity (DPM), Pod Number Per Area (PNA), Seed Number Per Area (SNA), and 100 Seed Weight

Results on the analysis of DRI showed that the lines SMC 141, BFS 10, BAT 477, NCB 280, SEA 15, SCR 16, BFS 67, NCB 226, SEN 56, and SER 78 were drought resistant with higher values of DRI, while Pérola, RCB 273, ALB 74, BFS 32, DOR 390, SMC 43, ALB 88, INB 841, and MIB 778 were highly drought sensitive with lower values of DRI (**Table 1**). A negative and significant correlation was observed between DF and grain yield under both irrigated and drought conditions, −0.51*** and

TABLE 1 | Phenotypic differences in canopy biomass, pod partitioning index, grain yield and drought response index (DRI) of 36 genotypes of common bean grown under irrigated and drought conditions in 2012 and 2013 at Palmira, Colombia.

Genotype	Canopy biomass (kg ha^{-1})		Pod partitioning index (%)		Grain yield (kg ha^{-1})			DRI
	Irrigated	Drought	Irrigated	Drought	Irrigated	Drought	GM	
NCB 280	4695	3165	87	74	2922	1457	2117	0.70
BFS 29	4391	3788	87	65	2971	1526	2012	0.31
NCB 226	3742	3051	101	69	2973	1316	2000	0.56
SEN 56	4988	3063	80	74	2898	1330	1996	0.54
BFS 10	4074	2944	84	66	2700	1409	1905	0.76
SCR 2	4554	3636	76	66	2495	1272	1887	0.61
SEA 15	4188	3377	92	70	2243	1451	1867	0.64
SER 118	4215	2367	70	94	2508	798	1816	0.35
ALB 74	4318	2871	80	55	2127	971	1776	0.06
ALB 6	4240	2727	91	68	2469	1006	1743	0.06
BFS 67	4763	2992	74	62	2662	1163	1739	0.57
RCB 593	4560	3329	74	52	2519	1321	1691	0.35
SER 48	4448	3455	81	57	2368	1046	1677	0.02
SMC 43	3967	2534	57	47	1682	442	1670	1.00
BFS 32	4525	2655	99	67	2918	1037	1670	−0.75
SCR 9	4161	2990	90	57	2312	1053	1656	−0.04
SER 125	4901	3710	66	59	2432	1178	1647	0.45
SER 78	4892	3374	61	73	2345	1116	1591	−0.34
SER 119	4228	3480	80	55	2459	1120	1572	−0.06
SCR 16	4709	2935	86	74	2744	1310	1536	−0.27
G 40001	3810	3073	71	52	2233	1035	1522	−0.31
INB 827	4847	3181	64	63	2247	1069	1512	0.40
RCB 273	4552	3025	90	57	2425	934	1497	−0.61
ALB 60	4671	2899	76	44	2669	1162	1488	−0.33
INB 841	3268	2408	112	61	2316	845	1447	−1.06
SXB 412	3814	2680	89	65	2507	937	1436	0.14
BAT 477	4501	2982	71	61	2131	983	1435	0.71
SER 16	4443	3694	84	43	2502	1252	1381	−0.27
ALB 88	3826	2346	65	53	2018	544	1334	−0.66
Tío Canela 75	4148	2401	70	78	1936	805	1219	0.21
ALB 213	4641	2874	72	57	2659	1262	1092	−0.90
SMC 141	3894	2298	82	87	2592	1189	939	−0.88
DOR 390	4411	2452	64	32	2259	505	871	−0.81
BAT 477 NN	2212	2382	99	44	1078	771	845	0.30
Pérola	3523	2120	87	49	1838	413	837	−0.39
MIB 778	4108	2102	60	15	828	59	288	−1.07
Mean	4256	2927	80	60	2361	1030	1520	0
Sig. diff.	*	*	NS	*	*	*	*	*

*Values reported are mean for two seasons. GM = geometric mean. *Significant difference at 0.05 level as estimated from the MIXED procedure.*

-0.53^{***}, respectively (**Table 3**). The lines identified as drought resistant described previously combined shorter DF with higher grain yield under drought stress conditions (**Tables 1, 2**). The drought susceptible checks Tío Canela, Pérola, and DOR 390 and the lines MIB 778 and SMC 43 showed sensitivity to drought stress with greater DF under drought conditions (**Table 2**). The same response was observed in DPM (**Table 2**), that showed a negative and highly significant correlation with grain yield under both irrigated and drought treatments (**Table 3**). The drought resistant lines with shorter DF also showed shorter DPM with superior grain yield than the other genotypes under drought stress (**Tables 1, 2**). A negative and significant correlation was observed between DF and CB ($r = -0.18^{**}$ and $r = -0.35^{***}$) and DPM and CB ($r = -0.13^{*}$ and $r = -0.20^{**}$) under irrigated and drought conditions, respectively. The PNA, SNA, and 100 seed weight showed a positive and highly significant correlation with grain yield under both irrigated and drought treatments (**Table 3**). The lines BFS 29, BFS 10, NCB 280, SEN 56, SCR 16, SCR 2, and NCB 226 showed higher values of PNA than the other genotypes under drought stress conditions (data not

TABLE 2 | Phenotypic differences in days to flowering, days to physiological maturity and leaf stomatal conductance of 36 genotypes of common bean grown under irrigated and drought conditions in 2012 and 2013 at Palmira, Colombia.

Genotype	Days to flowering		Days to physiological maturity		Leaf stomatal conductance (mmol m^{-2} s^{-1})	
	Irrigated	Drought	Irrigated	Drought	Irrigated	Drought
ALB 6	34	34	60	62	351	317
ALB 60	32	32	56	57	309	342
ALB 74	33	33	59	59	354	398
ALB 88	34	35	61	62	375	441
ALB 213	32	33	59	60	361	366
BAT 477	36	37	62	61	265	357
BAT 477 NN	37	38	63	62	373	508
BFS 10	32	33	57	58	382	408
BFS 29	31	31	58	57	410	320
BFS 32	31	32	57	56	282	399
BFS 67	35	36	60	62	311	485
DOR 390	38	39	65	63	378	346
G 40001	32	32	55	55	288	345
INB 827	35	36	62	61	384	393
INB 841	31	30	57	55	305	258
MIB 778	39	40	66	67	351	277
NCB 226	31	33	64	62	331	442
NCB 280	30	31	56	57	417	629
Pérola	39	40	68	67	360	268
RCB 273	32	33	60	60	324	321
RCB 593	31	33	56	58	357	328
SCR 2	32	32	61	60	436	395
SCR 9	32	33	59	57	447	331
SCR 16	33	34	59	59	372	506
SEA 15	32	30	58	57	271	429
SEN 56	32	32	60	58	335	492
SER 16	31	32	56	57	383	310
SER 48	32	33	59	57	348	344
SER 78	34	35	59	59	300	363
SER 118	34	36	62	60	404	331
SER 119	33	33	59	59	364	361
SER 125	32	32	56	57	360	377
SMC 43	35	36	59	59	337	246
SMC 141	37	38	62	63	327	510
SXB 412	36	37	60	60	350	234
Tío Canela 75	37	38	64	64	315	348
Mean	34	34	60	60	350	376
Sig. diff.	*	*	*	*	NS	*

*Values reported are mean for two seasons. *Significant difference at 0.05 level as estimated from the MIXED procedure.*

shown). These lines also presented higher values of SNA. The line SEA 15 showed the highest value of 100 seed weight under drought stress followed by NCB 226, SCR 2, SCR 16, NCB 280, and BFS 10. The genotypes ALB 88, DOR 390, SMC 43, Pérola, and MIB 778 produced less pods and seeds under drought stress.

DISCUSSION

This study permitted evaluating a diverse set of elite common bean breeding lines recently developed for improving resistance to drought stress. It was conducted in the light of past experience with shoot traits such as CID, stomatal conductance, canopy biomass, and indices of dry matter partitioning such as PPI, PHI, and HI. The lines were derived from crosses among bean races (Beebe et al., 2008), as well as interspecific crosses with introgression from *P. coccineus* (Butare et al., 2012) or *P. acutifolius* (Beebe, 2012). The lines NCB 280, NCB 226, SEN 56, SCR 2, SCR 16, SMC 141, RCB 593, BFS 67, SER 16, ALB 60, ALB 6, BFS 10, and BFS 29 developed over several cycles of breeding to drought limitation were found to be remarkably drought resistant. These lines also showed values of grain yield that doubles the values under drought stress of three leading commercial cultivars in Latin America:

TABLE 3 | Correlation coefficients (r) between final grain yield (kg ha^{-1}) and other shoot attributes of 36 genotypes of common bean grown under irrigated and drought stress conditions in 2012 and 2013 at Palmira, Colombia.

Plant traits	Irrigated	Drought
Leaf area index (m^2/m^2)	0.12	0.43***
Canopy biomass (kg ha^{-1})	0.39***	0.59***
Leaf stomatal conductance (mmol m^{-2} s^{-1})	0.24***	0.31***
Pod partitioning index (%)	0.14*	0.29***
Harvest index (%)	0.24***	0.39***
Pod harvest index (%)	0.61***	0.48***
Shoot TNC content (mg g^{-1})	−0.21**	0.05
Seed TNC content (mg g^{-1})	0.21**	0.16*
Days to flowering	−0.51***	−0.53***
Days to physiological maturity	−0.37***	−0.36***
Pod number per area (no. m^{-2})	0.32***	0.55***
Seed number per area (no. m^{-2})	0.36***	0.63***
100 seed weight (g)	0.44***	0.25***
Shoot CID (‰)	−0.12	0.15*
Grain CID (‰)	0.37***	0.36***

Mean values of two seasons were used for correlation analysis., **, *** Significant at the 0.05, 0.01, and 0.001 probability levels, respectively.*

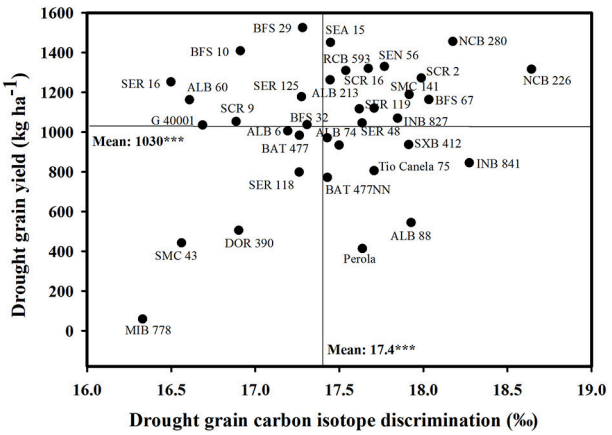

FIGURE 1 | Relationship between grain yield and grain carbon isotope discrimination (CID) under drought stress. Mean values for two seasons (2012, 2013) were used. Water spenders with higher grain yield and greater values of CID were identified in the upper, right hand quadrant. Water savers with higher grain yield and lower values of CID were identified in the upper, left hand quadrant.

DOR 390, Perola, and Tío Canela. We removed the effects of drought escape (early flowering) and yield potential (optimally irrigated yield) by estimating DRI through analysis. We found a relationship between genotypes with higher values of grain yield under drought stress and higher values of DRI. This positive relationship indicates that genotypes with higher values of grain yield under drought stress are physiologically responsive to drought stress. This analysis also allowed us to examine drought resistance that can be explained by physiological measurements made in this study and discussed below.

Grain Yield and Carbon Isotope Discrimination (CID)

The relationship between different tissues sampled for CID and grain yield, showed that using grain sample is more relevant than CB sample at mid-pod filling in the determination of CID for common bean under drought conditions. We consider that the use of grain sample for CID determination makes more sense in the case of common bean under terminal drought stress. This is because it is taken at maturity, and it would reflect an integrated effect of gas exchange during a critical and important crop growth stage which is grain filling. In our experimental conditions the effect of terminal drought is stronger at harvest than at mid-pod filling. A relationship was observed between stomatal conductance and grain CID under rainfed conditions, with differences in performance among some genotypes (**Figure 1**, **Table 2**). Stomatal conductance and CID are useful measurements to track plant responses to drought but these depend on different processes. CID depends on variation in photosynthetic biochemistry, conductance of CO_2 to the leaf interior and the chloroplasts, or a combination of these (Seibt et al., 2008; Easlon et al., 2014). After evaluating 36 advanced lines over two seasons, several drought resistant genotypes showed a clear evidence of superior access to soil moisture, and a few drought resistant genotypes showed a contrasting pattern for using less water. These results allowed us to classify the genotypes into two groups: water savers (isohydric plants) and water spenders (anisohydric) and this could facilitate targeting genotypes suitable to different agro-ecological zones (Blum, 2015). We classify NCB 280, SMC 141, SCR 16, SEN 56, BFS 67, and NCB 226 as water spenders that are able to access more water and show better water status during their canopy growth and grain development, resulting in higher grain yield. Our results also indicate that these lines maximize their capture of soil water for transpiration and maintain adequate gas exchange rates thus contributing to improved growth and greater proportion of biomass partitioned to grain (**Figure 1**, **Tables 1**, **2**). We consider that these lines were drought resistant through EUW as proposed by Blum (2009). These genotypes should be useful for cultivation in areas exposed to intermittent drought stress in Central America, South America, and Africa, particularly in agro-ecological regions where rainfall is intermittent during the season and soils that can store greater amount of available water deep in the soil profile.

We also identified a few genotypes that are combining lower values of grain CID and stomatal conductance with better grain yield under rainfed conditions, and we classified these genotypes as water savers, which are BFS 10, SER 16, ALB 6, ALB 60, and G 40001 (**Figure 1**, **Tables 1**, **2**). The line G 40001 (*P. acutifolius*) of tepary bean presents different traits related to drought resistance confirming its behavior as water saver with a combination of morpho-physiological characteristics such as greater ability for partitioning dry matter to grain, fine roots, smaller leaves for reduced water use, and reduced stomatal conductance (Mohamed et al., 2005; Butare et al., 2011; Rao et al., 2013; Beebe et al., 2014). Our classification of the line SER

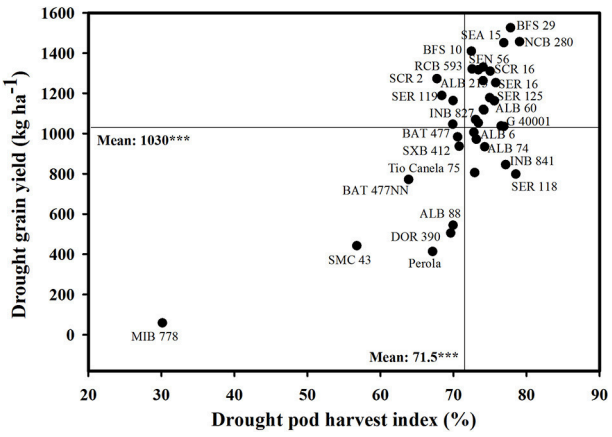

FIGURE 2 | Identification of genotypes with greater values of grain yield and pod harvest index (PHI) under drought stress. Mean values for two seasons (2012, 2013) were used. Higher yielding genotypes with greater values of PHI were identified in the upper, right hand quadrant.

16 as water saver is consistent with a previous study conducted under greenhouse conditions where this line was characterized as responsive to soil drying by closing its stomata sooner than the other genotypes during progressive soil drying (Devi et al., 2013). The water savers could be more suitable to bean farmers in semiarid to dry environments, dominated by terminal type of drought stress in Central America, Africa, northern Mexico, and north-east Brazil.

We also identified a group of genotypes (BFS 29, SEA 15, SER 125, and RCB 593) with intermediate response in terms of either as water spenders or as water savers with higher grain yield and these genotypes may be suitable for improving yield stability in drought-prone areas. The correlation between grain CID and grain yield under drought stress was weak but positive (**Table 3**). This is because of a few water saving genotypes that influenced the correlation. The values of grain CID are useful to classify genotypes as either water spenders or water savers together with other morpho-physiological attributes such as leaf stomatal conductance.

Grain Yield, Canopy Biomass, and Indices of Dry Matter Partitioning

Total shoot biomass or CB can be understood in a physiological sense as the result of accumulated net photosynthesis of the crop, and it is shown to be related to yield in several crops (Araus et al., 2002). Several drought resistant lines were outstanding in CB production and grain yield under drought stress. Also these lines were superior in leaf area development under drought stress. These lines were able to access more water, as reflected in the values of grain CID. This, combined with increased dry matter partitioned to grain (HI and PHI), resulted in improved resistance to drought (Muñoz-Perea et al., 2007; Polania et al., 2012, 2016; Assefa et al., 2013; Rao et al., 2013; Beebe et al., 2014; Rao, 2014). Compared with the drought-sensitive checks DOR 390, Pérola, and Tio Canela, most of the bred lines showed a higher accumulation of CB at mid-pod filling growth stage. These results show significant progress in breeding for improved CB accumulation and enhanced dry matter partitioning toward pod and grain production. Previous research suggested that the drought resistance in common bean is associated with a more efficient dry matter partitioning to pod formation and grain production (Hall, 2004; Rosales-Serna et al., 2004; Cuellar-Ortiz et al., 2008; Klaedtke et al., 2012; Rosales et al., 2012; Assefa et al., 2013; Beebe et al., 2013, 2014; Rao et al., 2013; Rao, 2014). The positive and significant correlations between grain yield and biomass partitioning indices (PPI, HI, and PHI) under drought stress (**Table 3**) highlight the importance of improved dry matter partitioning from plant biomass to pod formation (PPI) and grain production (PHI). Genotypes that increased the proportion of dry matter partitioned to grain also showed higher values of TNC in seed (results not shown). The lines BFS 29, SEA 15, BFS 10, NCB 280, SEN 56, SCR 16, and SMC 141 showed greater grain yield under drought and were superior in their ability to partition greater proportion of biomass to pod and grain production (**Figure 2**, **Table 1**). The lines INB 841 and SER 118 showed especially higher values of PPI and PHI across years under stress, and both are excellent parents. Breeding programs should focus on the selection of best-performing materials that combine greater values of CB as a result of EUW with greater ability to partition dry matter toward pod development and grain filling. PHI could serve as a useful selection criterion for improving drought resistance because of its simplicity in measurement and its significant correlation with grain yield under both irrigated and drought conditions (Assefa et al., 2013).

Grain Yield, Phenology, and Yield Components

Early maturing genotypes were more adapted to drought stress and responsive to irrigation. Farmers have multiple reasons for preferring short season varieties, one of them is to minimize exposure to drought (White and Singh, 1991; Beebe, 2012). Early maturity has been a standard mechanism to confront drought in breeding programs, and it is a trait that may be more useful where terminal drought predominates (Beebe et al., 2014). However, previous results indicated that a shorter growth cycle can reduce grain yield potential per day by an estimated 74 kg ha^{-1} (White and Singh, 1991). In contrast, recent results show that early maturing genotypes with increased dry matter partitioned to grain can compensate this effect, indicating that high yielding lines had higher grain yield per day compared with low yielding genotypes under drought (Klaedtke et al., 2012; Rao et al., 2013; Beebe et al., 2014). We also observed a negative and significant correlation between phenology (DF and DPM) and CB and phenology and SNA under both irrigated and drought stress conditions. These phenotypic correlations suggest that a rapid accumulation of CB due to EUW, combined with an efficient remobilization of these reserves to the pod and grain formation (higher values of grain yield per day and SNA), is an important adaptive strategy of early maturing and drought resistant genotypes. Significant positive associations between grain yield and PPI, PHI and 100 seed weight under both irrigated and drought conditions suggest that increased

dry matter partitioning toward grain, or sink strength, is an important factor in determining grain yield under drought stress (Polania et al., 2016). Greater values of SNA and PNA likewise are consistent with the hypothesis that drought resistant lines have greater sink strength.

An important role for EUW in drought resistance implies that the understanding of the factors controlling the deep rooting and water status of the plant would be of great importance to improve drought resistance. In this scenario, traits such as grain CID related with EUW, CB, PPI, PHI, PNA, and SNA should be also considered as useful plant traits to be included in bean breeding programs aimed for improving drought resistance. Some of these traits are easier to implement in a breeding program due to their simplicity and relatively low analytical cost: PHI, grain CID, PNA, and SNA. Since these parameters could be determined at harvest time, it may be easier for breeders to integrate into on-going breeding efforts.

CONCLUSIONS

Our results demonstrate that drought resistance in common bean is related to EUW to produce greater canopy biomass, combined with an increased dry matter partitioned from vegetative structures to the pods and subsequently to grain production resulting in higher values of pod and SNA. Several lines (BFS 29, SEA 15, BFS 10, NCB 280, SEN 56, SCR 16, and SMC 141) expressed this desirable combination of traits. Resistance to terminal drought stress was found to be positively associated with EUW combined with superior ability to partition greater proportion of dry matter toward pod and seed production and negatively associated with days to flowering and DPM. Based on phenotypic differences in grain CID, leaf stomatal conductance, canopy biomass and grain yield under drought stress, the lines tested were classified into two groups, water savers and water spenders. We suggest that pod harvest index could be a useful selection criterion in breeding programs to select for drought resistance in common bean.

AUTHOR CONTRIBUTIONS

JP, CP, SB, and IR designed the experiments and contributed to data interpretation. JP collected and analyzed the data. JP, CP, SB, and IR wrote the paper. All authors read and approved the final manuscript.

ACKNOWLEDGMENTS

The authors acknowledge the support of the Bill and Melinda Gates Foundation (BMGF), and the CGIAR research program on grain legumes for financial support of research on improving drought resistance in common bean. We also thank Miguel Grajales, Cesar Cajiao, Mariela Rivera, and bean breeding and physiology teams at CIAT, Colombia for their contribution.

REFERENCES

Araus, J. L., Slafer, G. A., Reynolds, M. P., and Royo, C. (2002). Plant breeding and drought in C3 cereals: what should we breed for? *Ann. Bot.* 89, 925–940. doi: 10.1093/aob/mcf049

Assefa, T., Beebe, S., Rao, I. M., Cuasquer, J., Duque, M. C., Rivera, M., et al. (2013). Pod harvest index as a selection criterion to improve drought resistance in white pea bean. *Field Crop Res.* 148, 24–33. doi: 10.1016/j.fcr.2013.04.008

Beebe, S. (2012). Common bean breeding in the tropics. *Plant Breed. Rev.* 36, 357–426. doi: 10.1002/9781118358566.ch5

Beebe, S., Rao, I. M., Blair, M. W., and Acosta-Gallegos, J. A. (2013). Phenotyping common beans for adaptation to drought. *Front. Physiol.* 4:35. doi: 10.3389/fphys.2013.00035

Beebe, S., Rao, I. M., Cajiao, C., and Grajales, M. (2008). Selection for drought resistance in common bean also improves yield in phosphorus limited and favorable environments. *Crop Sci.* 48, 582. doi: 10.2135/cropsci2007.07.0404

Beebe, S., Rao, I. M., Devi, M., and Polania, J. (2014). Common beans, biodiversity, and multiple stress: challenges of drought resistance in tropical soils. *Crop Pasture Sci.* 65, 667–675. doi: 10.1071/CP13303

Bidinger, F. R., Mahalakshimi, V., and Rao, G. D. P. (1987). Assessment of drought resistance in pearl millet [*Pennisetum americanum* (L.) Leeke]. I Factors affecting yields under stress. *Aust. J. Agric. Res.* 38, 37–48. doi: 10.1071/AR9870037

Blum, A. (2005). Drought resistance, water-use efficiency, and yield potential - are they compatible, dissonant, or mutually exclusive? *Aust. J. Agric. Res.* 56, 1159–1168. doi: 10.1071/AR05069

Blum, A. (2009). Effective use of water (EUW) and not water-use efficiency (WUE) is the target of crop yield improvement under drought stress. *Field Crops Res.* 112, 119–123. doi: 10.1016/j.fcr.2009.03.009

Blum, A. (2015). Towards a conceptual ABA ideotype in plant breeding for water limited environments. *Funct. Plant Biol.* 42, 502. doi: 10.1071/FP14334

Butare, L., Rao, I. M., Lepoivre, P., Cajiao, C., Polania, J., Cuasquer, J., et al. (2012). Phenotypic evaluation of interspecific recombinant inbred lines (RILs) of *Phaseolus* species for aluminium resistance and shoot and root growth response to aluminium-toxic acid soil. *Euphytica* 186, 715–730. doi: 10.1007/s10681-011-0564-1

Butare, L., Rao, I. M., Lepoivre, P., Polania, J., Cajiao, C., Cuasquer, J., et al. (2011). New genetic sources of resistance in the genus *Phaseolus* to individual and combined aluminium toxicity and progressive soil drying stresses. *Euphytica* 181, 385–404. doi: 10.1007/s10681-011-0468-0

Condon, A. G., Richards, R. A., Rebetzke, G. J., and Farquhar, G. D. (2004). Breeding for high water-use efficiency. *J. Exp. Bot.* 55, 2447–2460. doi: 10.1093/jxb/erh277

Cuellar-Ortiz, S. M., De La Paz Arrieta-Montiel, M., Acosta-Gallegos, J. A., and Covarrubias, A. A. (2008). Relationship between carbohydrate partitioning and drought resistance in common bean. *Plant Cell Environ.* 31, 1399–1409. doi: 10.1111/j.1365-3040.2008.01853.x

Devi, M., Sinclair, T. R., Beebe, S., and Rao, I. M. (2013). Comparison of common bean (*Phaseolus vulgaris* L.) genotypes for nitrogen fixation tolerance to soil drying. *Plant Soil* 364, 29–37. doi: 10.1007/s11104-012-1330-4

Easlon, H. M., Nemali, K. S., Richards, J. H., Hanson, D. T., Juenger, T. E., and McKay, J. K. (2014). The physiological basis for genetic variation in water use efficiency and carbon isotope composition in *Arabidopsis thaliana*. *Photosynth. Res.* 119, 119–129. doi: 10.1007/s11120-013-9891-5

Farquhar, G. D., Ehleringer, J. R., and Hubick, K. T. (1989). Carbon isotope discrimination and photosynthesis. *Annu. Rev. Plant Physiol. Plant Mol. Biol.* 40, 503–537. doi: 10.1146/annurev.pp.40.060189.002443

Hall, A. E. (2004). "Comparative ecophysiology of cowpea, common bean and peanut," in *Physiology and Biotechnology Integration for Plant Breeding*, eds H. T. Nguyen and A. Blum (New York, NY: Marcel Dekker Inc.), 271–325.

Jackson, P., Robertson, M., Cooper, M., and Hammer, G. (1996). The role of physiological understanding in plant breeding; from a breeding perspective. *Field Crops Res.* 49, 11–37. doi: 10.1016/S0378-4290(96)01012-X

Kang, J. H., and Bringk, G. E. (1995). White clover morphology and physiology in response to defoliation interval. *Crop Sci.* 35, 264–269. doi: 10.2135/cropsci1995.0011183X003500010048x

Khan, H. U. R., Link, W., Hocking, T. J., and Stoddard, F. L. (2007). Evaluation of physiological traits for improving drought tolerance in faba bean *(Vicia faba L.). Plant Soil* 292, 205–217. doi: 10.1007/s11104-007-9217-5

Klaedtke, S. M., Cajiao, C., Grajales, M., Polania, J., Borrero, G., Guerrero, A., et al. (2012). Photosynthate remobilization capacity from drought-adapted common bean (*Phaseolus vulgaris* L.) lines can improve yield potential of interspecific populations within the secondary gene pool. *J. Plant Breed. Crop Sci.* 4, 49–61. doi: 10.5897/JPBCS11.087

Krishnamurthy, L., Kashiwagi, J., Gaur, P. M., Upadhyaya, H. D., and Vadez, V. (2010). Sources of tolerance to terminal drought in the chickpea (*Cicer arietinum L.*) minicore germplasm. *Field Crops Res.* 119, 322–330. doi: 10.1016/j.fcr.2010.08.002

Mir, R. R., Zaman-Allah, M., Sreenivasulu, N., Trethowan, R. M., and Varshney, R. K. (2012). Integrated genomics, physiology and breeding approaches for improving drought tolerance in crops. *Theor. Appl. Genet.* 125, 625–645. doi: 10.1007/s00122-012-1904-9

Mohamed, F., Mohamed, M., Schmitz-Eiberger, N., Keutgen, and Noga, G. (2005). Comparative drought postponing and tolerance potentials of two tepary bean lines in relation to seed yield. *Afr. Crop Sci. J.* 13, 49–60.

Muñoz-Perea, C. G., Allen, R. G., Westermann, D. T., Wright, J. L., and Singh, S. P. (2007). Water use efficiency among dry bean landraces and cultivars in drought-stressed and non-stressed environments. *Euphytica* 155, 393–402. doi 10.1007/s10681-006-9340-z

Polania, J., Rao, I. M., Cajiao, C., Rivera, M., Raatz, B., and Beebe, S. (2016). Physiological traits associated with drought resistance in Andean and Mesoamerican genotypes of common bean (*Phaseolus vulgaris* L.). *Euphytica*. doi: 10.1007/s10681-016-1691-5. [Epub ahead of print].

Polania, J., Rao, I. M., Mejía, S., Beebe, S., and Cajiao, C. (2012). Características morfo-fisiológicas de frijol común (*Phaseolus vulgaris* L.) relacionadas con la adaptación a sequía. *Acta Agron.* 61, 197–206.

Rao, I. M. (2014). "Advances in improving adaptation of common bean and Brachiaria forage grasses to abiotic stresses in the tropics," in *Handbook of Plant and Crop Physiology*, ed M. Pessarakli (Boca Raton, FL: CRC Press; Taylor and Francis Group), 847–889.

Rao, I. M., Beebe, S., Polania, J., Ricaurte, J., Cajiao, C., Garcia, R., et al. (2013). Can tepary bean be a model for improvement of drought resistance in common bean? *Afr. Crop Sci. J.* 21, 265–281.

Reynolds, M. P., and Trethowan, R. M. (2007). "Physiological interventions in breeding for adaptation to abiotic stress," in *Scale and Complexity in Plant Systems Research, Gene–Plant–Crop Relations*, eds J. H. J. Spiertz, P. C. Struik, and. H. H. Van Laar (Wageningen: UR Frontis Series), 127–144.

Rosales, M. A., Ocampo, E., Rodríguez-Valentín, R., Olvera-Carrillo, Y., Acosta-Gallegos, J. A., and Covarrubias, A. A. (2012). Physiological analysis of common bean (*Phaseolus vulgaris* L.) cultivars uncovers characteristics related to terminal drought resistance. *Plant Physiol. Biochem.* 56, 24–34. doi: 10.1016/j.plaphy.2012.04.007

Rosales-Serna, R., Kohashi-Shibata, J., Acosta-Gallegos, J. A., Trejo-López, C., Ortiz-Cereceres, J., and Kelly, J. D. (2004). Biomass distribution, maturity acceleration and yield in drought-stressed common bean cultivars. *Field Crops Res.* 85, 203–211. doi: 10.1016/S0378-4290(03)00161-8

SAS Institute Inc. (2008). *SAS/STAT® 9.2*. Cary, NC: SAS Institute Inc.

Seibt, U., Rajabi, A., Griffiths, H., and Berry, J. A. (2008). Carbon isotopes and water use efficiency: sense and sensitivity. *Oecologia* 155, 441–454. doi: 10.1007/s00442-007-0932-7

Sinclair, T. R. (2012). Is transpiration efficiency a viable plant trait in breeding for crop improvement? *Funct. Plant Biol.* 39, 359–365. doi: 10.1071/FP11198

Sponchiado, B. N., White, J. W., Castillo, J. A., and Jones, P. G. (1989). Root growth of four common bean cultivars in relation to drought tolerance in environments with contrasting soil types. *Exp. Agric.* 25, 249. doi: 10.1017/S0014479700016756

Thung, M., and Rao, I. M. (1999). "Integrated management of abiotic stresses," in *Common Bean Improvement in the Twenty-First Century*, ed S. P. Singh (Dordrecht: Springer), 331–370.

Vadez, V., Kholova, J., Medina, S., Kakkera, A., and Anderberg, H. (2014). Transpiration efficiency: new insights into an old story. *J. Exp. Bot.* 65, 6141–6153. doi: 10.1093/jxb/eru040

White, J. W. (1993). "Implications of carbon isotope discrimination studies for breeding common bean under water deficits," in *Stable Isotopes and Plant Carbon-Water Relations*, eds J. R. Ehleringer, A. E. Hall, and G. D. Farquhar (San Diego, CA: Academic press), 387–398.

White, J. W., Castillo, J. A., and Ehleringer, J. R. (1990). Associations between productivity, root growth and carbon isotope discrimination in *Phaseolus vulgaris* under water deficit. *Aust. J. Plant Physiol.* 17, 189–198. doi: 10.1071/PP9900189

White, J. W., and Singh, S. P. (1991). Sources and inheritance of earliness in tropically adapted indeterminate common bean. *Euphytica* 55, 15–19. doi: 10.1007/BF00022554

Conflict of Interest Statement: The authors declare that the research was conducted in the absence of any commercial or financial relationships that could be construed as a potential conflict of interest.

frontiers in Plant Science

ORIGINAL RESEARCH
published: 15 November 2016
doi: 10.3389/fpls.2016.01640

Grape Ripening Is Regulated by Deficit Irrigation/Elevated Temperatures According to Cluster Position in the Canopy

Olfa Zarrouk[1], Cecilia Brunetti[2,3], Ricardo Egipto[4], Carla Pinheiro[1,5]*, Tânia Genebra[1], Antonella Gori[2,3], Carlos M. Lopes[4], Massimiliano Tattini[6] and M. Manuela Chaves[1,4]*

[1] Instituto de Tecnologia Química e Biológica, Universidade NOVA de Lisboa, Oeiras, Portugal, [2] Trees and Timber Institute, The National Research Council of Italy, Florence, Italy, [3] Department of Plant, Soil and Environmental Sciences, University of Florence, Florence, Italy, [4] Linking Landscape, Environment, Agriculture and Food (LEAF), Instituto Superior de Agronomia, Universidade de Lisboa, Lisboa, Portugal, [5] Faculdade de Ciências e Tecnologia, Universidade NOVA de Lisboa, Caparica, Portugal, [6] Department of Biology, Agriculture and Food Sciences, Institute for Sustainable Plant Protection, The National Research Council of Italy, Florence, Italy

The impact of water deficit on berry quality has been extensively investigated during the last decades. Nonetheless, there is a scarcity of knowledge on the performance of varieties exposed to a combination of high temperatures/water stress during the growing season and under vineyard conditions. The objective of this research was to investigate the effects of two irrigation regimes, sustained deficit irrigation (SDI, 30% ET_C) and regulated deficit irrigation (RDI, 15% ET_C) and of two cluster positions within the canopy (east- and west-exposed sides) on berry ripening in red Aragonez (Tempranillo) grapevines. The study was undertaken for two successive years in a commercial vineyard in South Portugal, monitoring the following parameters: pre-dawn leaf water potential, berry temperature, sugars, polyphenols, abscisic acid (ABA) and related metabolites. Additionally, expression patterns for different transcripts encoding for enzymes responsible for anthocyanin and ABA biosynthesis (*VviUFGT*, *VvNCED1*, *VvβG1, VviHyd1, VviHyd2*) were analyzed. In both years anthocyanin concentration was lower in RDI at the west side (RDIW- the hottest one) from *véraison* onwards, suggesting that the most severe water stress conditions exacerbated the negative impact of high temperature on anthocyanin. The down-regulation of *VviUFGT* expression revealed a repression of the anthocyanin synthesis in berries of RDIW, at early stages of berry ripening. At full-maturation, anthocyanin degradation products were detected, being highest at RDIW. This suggests that the negative impact of water stress and high temperature on anthocyanins results from the repression of biosynthesis at the onset of ripening and from degradation at later stages. On the other hand, berries grown under SDI displayed a higher content in phenolics than those under RDI, pointing out for the attenuation of the negative temperature effects under SDI. Irrigation regime and berry position had small effect on free-ABA concentration. However, ABA catabolism/conjugation process and ABA biosynthetic pathway were affected by water and heat stresses. This indicates the role of ABA-GE and catabolites in berry ABA homeostasis under abiotic stresses. Principal component analysis (PCA) showed that

OPEN ACCESS

Edited by:
Urs Feller,
University of Bern, Switzerland

Reviewed by:
Claudio Lovisolo,
University of Turin, Italy
Amarendra Narayan Misra,
Central University of Jharkhand, India

***Correspondence:**
Olfa Zarrouk
zolfa@itqb.unl.pt
Carla Pinheiro
pinheiro@itqb.unl.pt

Specialty section:
This article was submitted to Agroecology and Land Use Systems, a section of the journal Frontiers in Plant Science

Received: *17 June 2016*
Accepted: *18 October 2016*
Published: *15 November 2016*

Citation:
Zarrouk O, Brunetti C, Egipto R, Pinheiro C, Genebra T, Gori A, Lopes CM, Tattini M and Chaves MM (2016) Grape Ripening Is Regulated by Deficit Irrigation/Elevated Temperatures According to Cluster Position in the Canopy. Front. Plant Sci. 7:1640. doi: 10.3389/fpls.2016.01640

the strongest influence in berry ripening is the deficit irrigation regime, while temperature is an important variable determining the improvement or impairment of berry quality by the deficit irrigation regime. In summary, this work shows the interaction between irrigation regime and high temperature on the control of berry ripening.

Keywords: ABA metabolism, anthocyanins, flavonols, heat stress *Vitis vinifera*, water stress

INTRODUCTION

The effect of water stress on grape berry ripening and quality has been extensively investigated during the last decades (for reviews, see Chaves et al., 2010; Kuhn et al., 2013). Overall, berry quality benefits from mild to moderate water deficit (Chaves et al., 2010) and the reduction in berry development was early proposed as mostly responsible for the improvement of berry quality by water deficits (Matthews and Anderson, 1988). However, more recently water deficit was shown to profoundly alter berry secondary metabolism, particularly of flavonoids, thus greatly regulating the ripening process (development and composition) (Castellarin et al., 2007a,b). The regulation of genes and proteins of the various metabolic pathways is either the consequence of a direct effect of water shortage and/or indirect via the changing of the light environment around grape clusters due to the impairment of vine vegetative growth.

The matter is far from being conclusively addressed, two major causes can be highlighted: the experimental set-ups adopted in the majority of experiments, namely the water stress timing and conditions; the diversity of varieties (Zarrouk et al., 2016). It was shown that pre-*véraison* water stress promotes the accumulation of anthocyanins, as a consequence of both reduced berry development and enhanced expression of flavonoid genes, thus leading (Basile et al., 2011; Intrigliolo et al., 2012; Romero et al., 2013) to earlier grape ripening (Castellarin et al., 2007a,b). In contrast, water stress imposed at post-*véraison* just increased the proportion of seeds and skin relative to whole-berry fresh mass, without significant effects on secondary metabolism (Roby and Matthews, 2004).

On the other hand, several reports (Deluc et al., 2009; Girona et al., 2009; Niculcea et al., 2014) have shown that the effect of water deficit on the biosynthesis of phenolics and berry growth is strongly cultivar dependent. The differential increase of anthocyanin compounds in berries under pre- or post-*véraison* deficit irrigation was primarily attributed to large differences in abscisic acid (ABA) sensitivity displayed by different varieties (Ferrandino and Lovisolo, 2013). Grape varieties may have either isohydric or anisohydric strategy to cope with water stress, as a consequence of large differences in the ability to regulate water losses through chemical (i.e., ABA) signaling (Deluc et al., 2009; Lovisolo et al., 2010; Balint and Reynolds, 2013; Niculcea et al., 2014). In addition, ABA was reported to strongly control key events of grape ripening through regulation of primary (sugars) and secondary metabolite biosynthesis (e.g., anthocyanins) (Davies et al., 1997; Peppi and Fidelibus, 2008). ABA levels peak around *véraison* stage (Owen et al., 2009; Wheeler et al., 2009), following the up-regulation of gene transcription and proteins expression related to ABA biosynthesis (Deluc et al., 2007; Giribaldi et al., 2007). These findings support the idea that ripening of non-climacteric grapes is, to a certain extent, ABA-regulated (Davies et al., 1997; Jia et al., 2011; Niculcea et al., 2014). Nonetheless, the expression of 9-cis-epoxycarotenoid dioxygenase (NCED), the enzyme involved in the first committed step of ABA (Qin and Zeevaart, 2002) is not always correlated with the concentration of free-ABA in berries (Deluc et al., 2009; Wheeler et al., 2009). This suggests that products of ABA catabolism/conjugation (Nambara and Marion-Poll, 2003) may be also involved in berry ripening. Free-ABA, the active form of this hormone, may be oxidized by ABA 8′-hydroxylase to phaseic (PA) and dihydrophaseic acids (DPA) or conjugated with glucose to form ABA-glucosylester (ABA-GE), through the action of ABA glucosyltransferase (ABA-GTase). ABA-GE plays an important role in the regulation of ABA content since it releases free-ABA through β-D-glucosidase and it has been proposed to be involved in long-distance transport of ABA.

Several reports showed the impact of water shortage on the hormonal balance of grape berry during ripening (Deluc et al., 2009; Niculcea et al., 2013) and on the ABA catabolites concentrations (Balint and Reynolds, 2013). Zarrouk et al. (2012) showed that both free ABA and ABA-GE are involved in the enhancement of ripening process in stressed berries.

In this context, Coombe (1989) attributes the promotion of sugar accumulation in water stressed berries to a direct effect of ABA signaling on fruit ripening. More recently, Niculcea et al. (2014) observed that the imposition of both types of deficit irrigation (pre- and post-*véraison*), altered the pattern of ABA accumulation, and relates the improvement of sugar concentration, phenolic substances and anthocyanins to the persistence of ABA production over time in post-*véraison*-stressed berries. Nonetheless, the enhancement of berry ABA content by water stress is not always accompanied by an increase in sugars or in secondary metabolites. In our previous investigation (Zarrouk et al., 2012), a negative effect of moderate deficit irrigation on grape berry anthocyanin concentration was observed, despite the increase in ABA concentration at *véraison,* suggesting a decoupling on the ripening process parameters due to other external factor than water deficit. Climate condition, namely high temperature along the growing season is considered a putative constraint to the implementation and success of the deficit irrigation regime (Shellie, 2011). Also, the interaction between elevated temperature and water deficit is considered the main cause of variability in field experiments results (Bonada et al., 2015) namely in what concerns the ripening of wine grapes (Real et al., 2015).

In this context, Fernandes de Oliveira and Nieddu (2013) showed that high temperature at mid-ripening coupled

with moderate deficit irrigation (25% of Etc) reduced total anthocyanin content, possibly by degrading these compounds or/and inhibiting their biosynthesis. Bonada et al. (2015) related an advance of the onset of berry net water loss by elevated temperature under water deficit, which hastened berry ripening and altered the balance of sensory traits.

The effect of temperature on berry composition has been studied extensively and the negative impact of high temperature on anthocyanin content was reported (Spayd et al., 2002; Mori et al., 2007; Sadras and Moran, 2012; Bonada and Sadras, 2014; Bonada et al., 2015). Nonetheless, to date, there appears to be a scarcity of knowledge of the performance of different varieties exposed to a combination of high temperatures and water stress during the growing seasons and under vineyard conditions (Greer and Weedon, 2013).

Portugal is the 11th highest wine-producing country worldwide (OIV, 2016), with strong influence of wine industry on the economic stability and development of the country (Fraga et al., 2016). Recent climate studies in Portugal highlight an increase in the temperature during grape growing season (Fraga et al., 2012), with increase in minimum temperature during the ripening period (Malheiro et al., 2010; Fraga et al., 2012) and an acute dryness in summer (Santos et al., 2012). This compromise the optimal climatic conditions to grow most current varieties particularly in southern Portugal (Real et al., 2015), with likely negative impact in wine characteristics. Irrigation is being used to maintain winegrape yield and overcome the negative impact of water stress incidence during the grapevine reproductive season, but the effects of different kinds of irrigation systems on berry and wine quality are still largely unknown.

In this investigation we analyzed the combined effect of water and heat stress in grape berry ripening process. Our experiments with Aragonez variety (syn. Tempranillo) over two consecutive seasons aimed at the revelation of the existence of differences in the accumulation and the biosynthesis of different parameters that define ripening in relation to the cluster position within the canopy and the irrigation regime applied. For this, the effect of two different irrigation regimes on grape berry skin during development was examined. The study focused on sugar accumulation in the berry, anthocyanin and flavonol accumulation in skin, endogenous ABA and ABA metabolites, as well as expression patterns for different transcripts encoding for enzymes responsible for anthocyanin and ABA biosynthesis (*VviUFGT*, *VvNCED1*, *VvβG1, VviHyd1, VviHyd2*).

MATERIALS AND METHODS

Vineyard Site, Experimental Design, and Berry Temperature Measurements

Experiments were conducted over 2013-2014 in a commercial vineyard (Herdade do Esporão), located at Reguengos de Monsaraz, Alentejo winegrowing region, Southern Portugal (lat. 38° 23′ 55.00″ N; long. 7° 32′ 46.00″ W). The climate is of Mediterranean type, with hot and dry summers and mild rainy winters. Soil texture is a sandy-loam to silty-clay-loam, with a pH of 7.0–7.6, a low content in organic matter (10.5 g kg^{-1}) and high P_2O_5 and K_2O values (110 and 173 mg kg^{-1}, respectively). The 11-year-old grapevines of the red variety Aragonez (syn. Tempranillo) were grafted on 1103 Paulsen rootstock. Vines were spaced 1.5 m within and 3.0 m between rows, on a north-south orientation, trained on a vertical shoot positioning and spur-pruned on a bilateral Royat Cordon system. All vines were uniformly pruned with 15–16 nodes per vine. The experimental layout was a randomized complete block design with two treatments and four replications per treatment. The elemental plot comprised three adjacent rows (two buffer rows and a central one for data collection) of 10 vines each. Climate data (air temperature and precipitation) were obtained from an automatic meteorological station located in the experimental orchard, near the vineyard (at ∼900 m).

Two irrigation treatments were applied: Sustained Deficit Irrigation (SDI), usually applied by winegrower, and Regulated Deficit Irrigation (RDI). The drip line was positioned along the row close to the vine trunks and consisted of pressure compensating 2.2 L/h drip emitters with 1.0 m spacing. Irrigation started on June, 14th and was ended at September, 6th in 2013; in 2014 it started on June, 12th and stopped on August, 23th. Watering was applied according to the crop evapotranspiration (ET_c) and soil water content. ET_c was estimated from the reference evapotranspiration (ET_0) using the crop coefficients proposed by Allen et al. (1998). During irrigation, the average fraction of ET_c applied was *ca* 0.3 in SDI and 0.15 in RDI. Water was applied 1–2 times a week. The total amount of water supplied until commercial harvest to SDI plants was 111 and 57 mm in 2013 and 2014 respectively (∼30% ET_c), while the supply on RDI was 53 mm in 2013 and 38 mm in 2014 (∼15% ET_c) (Supplementary Table 1). Standard cultural practices in the region were applied to all treatments. To characterize the vine water status, pre-dawn leaf water potential (Ψ_{pd}) was measured before each sampling date. Measurements were carried out on an adult leaf from eight replicate plants from each treatment, using a Scholander pressure chamber (Model 1000; PMS instrument Co., Corvallis, OR, USA). In order to estimate accumulated water stress, pre-dawn water stress integral ($S\Psi_{pd}$) was determined for each phenological stage accordingly to Myers (1988), using a −0.2 MPa maximum threshold. Berry temperature was monitored continuously (at 30-min-intervals) using a dual channel temperature data logger to which a two-junction, fine wires copper-constantan thermocouples were attached. These probes were positioned on berry surface (avoiding direct sun exposure) of a sample of clusters located in different canopy positions (exposed and internal; facing east and west) of 2 vines per treatment.

In order to quantify the incidence of berry temperature on anthocyanin accumulation at each side of the canopy (east and west), the Rustioni et al. (2011) approach was used. Berry temperature was averaged each hour and then converted into normal heat hours (NHH) and cumulated per phenological period. NHH computing procedure was done as described by Rustioni et al. (2011), based on a function that varies from 0 to 1 and gives 0 for temperatures outside minimum and maximum cardinals ($T_{min} = 10°C$ and $T_{max} = 35°C$) and 1 for temperatures at optimum ($T_{opt} = 25°C$).

Grape Berry Analysis

Berries were collected at different developmental stages during summer (from June to August). Four stages were considered: end of pea size (PS, 5–6 weeks after anthesis), *véraison* (V, 9–10 weeks after anthesis), mid-ripening (MR, 12 weeks after anthesis) and full maturation (FM, 14 weeks after anthesis). During 2013, only three stages were sampled (pea size, *véraison* and full maturation) as a consequence of unusual early berry maturation and an acceleration of sugar accumulation and acid breakdown. At each sampling date a representative sample of 50 bunches per treatment from 10 vines per replicate (30-40 plants per treatment) was randomly collected from the experimental vineyard. Bunches from each east side and west side of the vine (East side and West side) were collected separately. Four sample groups were generated: SDI east (SDIE), SDI west (SDIW), RDI east (RDIE), and RDI west (RDIW). A sub-sample of 20 bunches was collected and stored at 4°C. Three independent replicates of 50 berries each were weighed to determine berry weight and diameter, and the juice was extracted to determine total soluble solids (TSS, °Brix) and titratable acidity (TA, g tartaric acid L^{-1}). The concentration of TSS was measured using a manual refractometer (ITREF 32, Instrutemp). The TA was assessed according to Office International de la Vigne et du Vin (OIV, 1990) procedure. The second sub-sample of 30 bunches was immediately frozen in liquid nitrogen from which three to four independent pools of 30-40 frozen berries were carefully selected, peeled and the seeds removed. Skins were removed, weighted and ground in liquid nitrogen to a fine powder and stored at −80°C until successive analysis.

ABA and Related Metabolites Analysis

ABA, ABA-GE, PA, and DPA concentrations in berry skin were simultaneously analyzed by HPLC MS/MS. Before starting the extraction procedure, 40 ng of each deuterium-labeled internal standards were added (ABA-d6, ABA-GE-d5, PA-d3, DPA-d3, all from National Research Council of Canada, Saskatoon, SK, Canada) per 300 mg of freeze dried skin powder. The tissue was extracted with 3 mL of CH_3OH:H_2O (50:50 adjusted to pH 2.5 with HCOOH) for 30 min at 4°C. The supernatant was partitioned three times with 3 mL of n-exane. The methanolic fraction was purified using Sep-Pak C18 cartridges (Waters, Massachusetts, USA), and the eluate was dried under nitrogen and rinsed with 250 μL of CH_3OH:H_2O acidified at pH 2.5. Identification and quantification of free-ABA, ABA-GE, PA and DPA was performed through the injection of 3 μL of sample solution in a LC-ESI-MS/MS equipment, consisting of a LC-MS-8030 triple quadrupole mass spectrometer operating in negative ion mode equipped with electrospray ionization source (ESI) and coupled with a Nexera HPLC system (all from Shimadzu, Kyoto, Japan). Compounds were separated in an Agilent Poroshell C18 column (3.0 × 100 mm, 2.7 μm) eluted with a linear gradient solvent, at a flow rate of 0.3 mL min-1, from 95% H_2O (with the addition of 0.1% of HCOOH, solvent A) to 100% CH_3CN/MeOH (50/50, with the addition of 0.1% of HCOOH, solvent B) over a 30-min run. Quantification of free-ABA, ABA-GE, PA, and DPA was conducted in multiple reaction monitoring (MRM) with the corresponding transitions for each analyte (ABA: 263/153; d6-ABA: 269/159; ABA-GE: 425/263; d5-ABA-GE: 430/268; PA: 279/139; d3-PA: 282/142; DPA: 281/171; d3-DPA: 284/174).

Phenylpropanoids Analysis

Freeze dried skins (300–350 mg) were ground in a mortar under liquid nitrogen and the obtained powder was extracted with 70% of aqueous ethanol acidified to pH 2 by HCOOH (3 × 5 mL) and sonicated for 30 min. The supernatant was partitioned with 3 × 5 mL of n-Hexane, reduced to dryness under vacuum and rinsed with CH_3OH/H_2O (50/50, pH 2). Aliquots of 5 μL were injected into Perkin Elmer Flexar HPLC equipped with a quaternary 200Q/410 pump and a LC 200 photodiode array detector (Perkin Elmer, Bradford, CT, USA). Metabolites were separated in a 4.6 × 250 mm Hypersil SB-C_{18} column (5 μm) (Agilent Technologies, Milan, Italy), operating at 30°C and eluted at a flow rate of 1 mL min^{-1}. Anthocyanins were separated using a gradient solvent system consisting of H_2O (plus 5% HCOOH) (A), CH_3OH (plus 5% HCOOH) (B), CH_3CN (plus 5% HCOOH (C), during a 47 min run: 0–2 min 80% A, 15% B, 5% C; 2–17 min to 70% A, 20% B, 10% C; 17–32 min to 55% A, 30% B, 15% C; 32–37 min 55% A, 30% B, 15% C; 37–42 min to 20% A, 40% B, 40% C; 42–47 min 20% A, 40% B, 40% C. Flavonoids and hydroxycinnamic acids were separated using a linear gradient solvent system consisting of solvent A (90% H_2O with the addition of 0.1% formic acid, 10% CH_3CN) and solvent B (90% CH_3CN and 10% of H_2O with the addition of 0.1% formic acid). The chromatographic run lasted 45 min starting from 100% solvent A and arriving to 100% solvent B. Individual metabolites were identified on the basis of their retention times, UV-spectral characteristics and mass-spectrometric data. HPLC-MS-MS analysis was performed with a LC-MS-8030 triple quadrupole mass spectrometer operating in the electrospray ionization (ESI) mode and a Nexera HPLC system (all from Shimadzu, Kyoto, Japan). The mass spectrometer operated in negative ion scan mode for hydroxycinnamic derivatives and flavonoids detection, and in positive ion scan mode for anthocyanin detection. Product ion spectra were obtained using Argon as collision gas at a pressure of 230 kPa. Quantification of anthocyanins was performed at 530 nm using calibration curves of cyanidin 3-*O*-glucoside chloride, delphinidin 3-*O*-glucoside chloride, petunidin 3-*O*-glucoside chloride, malvidin 3-*O*-glucoside chloride (Extrasynthese). Quantification of flavonoids and hydroxycinnamic acid derivatives was performed at 350 and 330 nm respectively using the calibration curve of quercetin 3-*O*-glucoside, rutin, myricetin 3-*O*-glucoside, *trans*-caftaric acid and *trans*-coutaric acid; gallic acid, protocatechuic acid, vanillic acid and syringic acidwere quantified at 280 nm.

Analysis of Degradation Products of Anthocyanins

Degradation products of anthocyanins were quantified on the samples extracted for phenylpropanoids analysis following the protocol reported in Seeram et al. (2001) and Sadilova et al. (2007) with some modifications. Aliquots of 20 μL were injected into Perkin Elmer Flexar HPLC reported above and analyzed on a 4.6 × 250 mm Hypersil SB-C_{18} column (5 μm) (Agilent Technologies, Milan, Italy), operating at

30°C and eluted at a flow rate of 1 mL min^{-1}. Degradation products of anthocyanins were detected at 235 nm and quantified using authentic standards of protocatechuic acid and phloroglucinaldehyde (Sigma Aldrich, Milan, Italy).

RNA Extraction and cDNA Synthesis

Total RNA extractions were performed in 1.5 mL tube, using the method of Reid et al. (2006). Briefly, skin tissue of 20 berries was ground to a fine powder in liquid nitrogen using a mortar and pestle. The extraction buffer, pre-warmed (65°C) (300 mM Tris HCl pH 8.0, 25 mM EDTA, 2 M NaCl, 2% (w/v) CTAB, 2% (w/v) PVPP, 0.05% (w/v) spermidine trihydrochloride and 2% (v/v) β-mercaptoethanol just prior use) was added to powder and shaken vigorously. Tubes were subsequently incubated at 65°C with shaking for 10 min. Mixtures were extracted twice with equal volumes of chloroform:isoamyl alcohol (24:1) and centrifuged at 16,100 g for 10 min at 4°C. To the supernatant add 100 µl 3 M NaOAc (pH 5.2) and 600 µl isopropanol were added, mixed, and stored at −80 °C for 25 min. Nucleic acid pellets were collected by centrifugation at 16,100 g for 30 min at 4°C. The pellet was dissolved in 250 µL TE (pH 7.5) and adds 94 µL of 8 M LiCl and stored at 4°C overnight. RNA was pelleted by centrifugation at 16,100 g for 30 min at 4°C, then washed with 1 µl of ice cold 70% ethanol, air dried, and dissolved in RNase-free water. Total RNA was purified using an RNeasy® Mini kit (Qiagen) with the addition of an on-column DNAse I digestion (RNase-Free DNase Set; Qiagen). RNA concentration was determined before and after DNase I digestion using a Nanodrop ND-1000 spectrophotometer (Nanodrop Technologies) in 260/280 nm ratio. RNA integrity was evaluated by 1% (w/v) agarose gel electrophoresis. First-strand cDNA was synthesized using the Omniscript® Reverse Transcription kit (Qiagen) according to the manufacture's instructions. The cDNA was prepared from 1000 ng of total RNA and synthesized at 37°C for 60 min and the cDNA stored at −80°C.

Quantitative Real-Time PCR Analysis

Quantitative real-time PCR was performed in the iQ5 2.0 Standard Edition (Bio-Rad), sequence detection system in a 96-well reaction plate. Each reaction (20 µl) contained 250 nM of each primer, 5 µL of 1/50 diluted cDNA, and 10 µl of Power SYBR Green Master Mix (Bio-Rad). Thermal cycling conditions were 95°C for 10 min followed by 95°C for 10 s, 60°C for 10 s, and 72°C for 10 s for 40 cycles. Dissociation curves for each amplicon were then analyzed to verify the specificity of each amplification reaction; the dissociation curve was obtained by heating the amplicon from 55 to 95°C. Each PCR was run in triplicate within the same plate, and the cycle threshold (Ct) values obtained from the technical replicates were averaged. Gene transcripts were quantified by comparing the Ct of the target gene with that of actin (Reid et al., 2006). Gene expression was expressed as mean and standard error calculated from the three biological replicates. Primer pairs for *VviUFGT* were retrieved from Jeong et al. (2004), *VviNCED1* and *VviβG1* from Sun et al. (2010), *VviHyd1 and VviHyd2* from Speirs et al. (2013).

Data Analysis

Measurements were conducted of four biological replicates. Data of each season were subjected to analysis of variance (ANOVA) using SPSS 12.0 (SPSS Inc., Chicago, USA). Means were separated by Duncan's multiple range test ($p \leq 0.05$). Principal component analysis (PCA) was also performed on all measured skin parameters, using the R software (version 3.2.5, R Development Core Team 2011) and the ade4 package (Culhane et al., 2002; Chessel et al., 2004; Thioulouse and Dray, 2009).

RESULTS

Vine Water Status and Cluster Zone Microclimate

Water applied in RDI treatment from pea-size berry to full maturation was similar in both years, while SDI treated-plants in 2014 received ∼65% of water than in 2013 (Supplementary Table 1). The cumulative pre-dawn water stress ($S\Psi_{pd}$) was higher in 2014. In RDI and SDI treatments, accumulated stress from pea-size berry to *véraison* was 2–13 times higher in 2014 than in 2013, respectively (**Table 1**). The accumulated stress from *véraison* to full maturation was similar in both years in RDI treatment, while accumulated stress in SDI treatment in 2014 was 1.5 times higher than in 2013 (**Table 1**). Berry temperature (T_{berry}) on west-exposed clusters was always higher than in east-exposed berries, irrespective of the phenological stage, irrigation treatment and year (**Table 2**; Supplementary Figure 1). Air temperature (T_{air}) measured from *véraison* to full maturity was, on average, 2°C higher in 2013 than in 2014 (Supplementary Table 2). In the same period, maximum T_{air} was 0.4°C higher in 2014, while minimum temperature in 2013 was 1.0 °C higher than in 2014. In both years, the T_{air} never went below 10 °C. In 2013, an accumulated period of 121 h with T_{air} above 35°C was observed, whereas in 2014 only 83 h had T_{air} above 35°C. Though accumulated hours with $T_{air} > 35$°C in 2013 was higher, the duration of $T_{berry} > 35$°C observed in 2013 was lower than in 2014, irrespective of irrigation and cluster exposure.

Slight differences were observed between irrigation treatments in T_{berry} from clusters from the same canopy side in both years (**Table 2**). While the west-exposed clusters displayed maximum

TABLE 1 | Pre-dawn water stress integral (SΨpd), according to Myers (1988) in sustained deficit irrigation (SDI) and regulated deficit irrigation (RDI) treatments during the periods pea size -*véraison* (PS-V), *véraison*-mid-ripening (V-MR), mid-ripening-full maturation (MR-FM) and *véraison*-full maturation (V-FM) in 2013 and 2014 growing seasons.

		$S\Psi_{pd}$(MPa.day)	
		RDI	**SDI**
2013	PS—V (DOY 191–210)	3.52	0.38
	V—FM (DOY 211–230)	6.43	3.75
2014	PS—V (DOY 167–195)	7.12	5.05
	V—MR (DOY 196–210)	7.95	6.05
	MR—FM (DOY 211–223)	5.87	4.79

DOY: day of the year.

TABLE 2 | Maximum (T_{berry} max), Minimum (T_{berry} min) and Average (T_{berry} avg) berry temperature and Number of hours with temperature below 10°C (T_{berry} < 10°C)* and above 35°C (T_{berry} > 35°C) of east- and west-exposed clusters in sustained deficit irrigation (SDI) and regulated deficit irrigation (RDI) treatments during *véraison* (PS-V), mid-Ripening (V-MR), full maturation (MR-FM) and from *véraison* to full maturation (V-FM) period in 2013 and 2014 growing seasons.

Year	Phenology	SDIE				SDIW				RDIE				RDIW			
		T_{berry} max (°C)	T_{berry} min (°C)	T_{berry} avg (°C)	T_{berry} > 35°C (Hours)	T_{berry} max (°C)	T_{berry} min (°C)	T_{berry} avg (°C)	T_{berry} > 35°C (Hours)	T_{berry} max (°C)	T_{berry} min (°C)	T_{berry} avg (°C)	T_{berry} > 35°C (Hours)	T_{berry} max (°C)	T_{berry} min (°C)	T_{berry} avg (°C)	T_{berry} > 35°C (Hours)
2013	PS-V	39.2	10.6	24.3	22	47.2	10.3	24.5	45	37	10.6	24.1	10	46.2	10.4	24.9	48
	V-FM	42.5	12.6	26.4	88	48.2	12.4	26.7	112	40	12.7	26	73	47.8	12.3	26.8	106
	PS-FM	42.5	10.6	25.5	110	48.2	10.3	25.8	157	40	10.6	25.2	83	47.8	10.4	26	154
2014	PS-V	40.6	9.8	22.3	48	45.5	10.7	22.5	51	40.8	10.9	22.3	44	43.3	11	22.1	44
	V-MR	42.8	12.2	25.4	70	47.7	12.6	25.7	73	40	13.1	25.1	49	46.5	13.1	25.4	69
	MR-FM	38.4	12.2	25.3	35	46.9	12.2	24.9	48	36.6	12.9	25.1	20	42.8	12.8	25.3	56
	PS-FM	42.8	9.8	23.8	153	47.1	10.7	23.9	172	40.8	10.9	23.7	113	46.5	11	23.7	169

*Except for SDIE regime in 2014 the number of hours with temperature below 10°C (T_{berry} < 10°C) were null. For SDIE regime in 2014 it was 1 at PS-V.

T_{berry} higher than the east exposed clusters, the amplitude was larger in the RDI treatment (T_{berry} 5–8°C and 2.5–9°C higher in SDI and RDI, respectively). Regarding for the number of hours with T_{berry} > 35°C, the berries of the RDI treatment were shown to accumulate more hours with T_{berry} > 35°C than the berries of the SDI treatment. Although in 2014, the accumulated hours of berry temperature above 35°C was lower than the observed in 2013 (**Table 2**).

Berry Composition

The trend of the TSS and TA accumulation both in 2013 and 2014 is presented in **Figure 1**. There was a significant season effect ($P < 0.01$) on both TSS and TA. TSS was higher in 2013 (25°Brix) than in 2014 (22°Brix), the reverse being observed for TA (∼3.4 g L^{-1} in 2013 vs. ∼4.9 g L^{-1} in 2014). In 2013, no significant TSS differences between irrigation treatments and side of the canopy were observed.

In 2014, differences between treatments and side of the canopy started to be observed at *véraison*. TSS starts to accumulate at *véraison* in berries from east-side followed by the west side both in SDI and RDI. This trend was also observed at mid-ripening, and at full maturation in SDI. At full maturation RDI presents higher TSS as compared with SDI, being highest at RDIW. The breakdown of TA was observed since *véraison* stage, especially in RDI. Differences in TA content were not observed between east and west berries at both pea size and *véraison* stages. On the contrary, from mid-ripening to full maturation, west side berries had lower TA content east side berries, in both SDI and RDI.

Grape Skin Anthocyanin Composition and Accumulation

A wide range of cyanidin, delphinidin, malvidin, petunidin, and peonidin derivatives were identified in either years of experimentation (**Table 3**), but their concentration was higher in 2014 than in 2013. Irrespective of the year, the concentration of anthocyanins increased since *véraison* to reach maximum levels at full maturation in all treatments (**Figure 2**). Anthocyanin levels were lower in RDI than SDI. West-exposed berries displayed lower anthocyanin concentration than east-exposed berries, irrespective of irrigation. In 2013, no differences in the trend of accumulation of anthocyanin were observed at *véraison*, except for RDIE which was significantly higher as compared with all other treatments. In contrast, at full maturation SDIE showed higher anthocyanin concentration as compared to SDIW and RDIW. Methoxylated anthocyanins (peonidin, petunidin, and malvidin) were highest in east exposed clusters in both irrigation regimes at full maturation (**Figure 2**). The ratio of methoxylated to non-methoxylated anthocyanins was the highest in RDIE, as well as in east sided than in west sided berries (**Table 3**).

In 2014 the level of anthocyanins since *véraison* stage was higher in east than in west-exposed barriers, irrespective of irrigation regime (**Figure 2**). This trend was even more evident at mid-ripening and at full maturation. Differences in anthocyanin concentration were not recorded between SDI and RDI at mid-ripening stage, whereas at full maturation RDI had lower anthocyanin content than SDI, irrespective of canopy position (**Figure 2**). The ratio of methoxylated

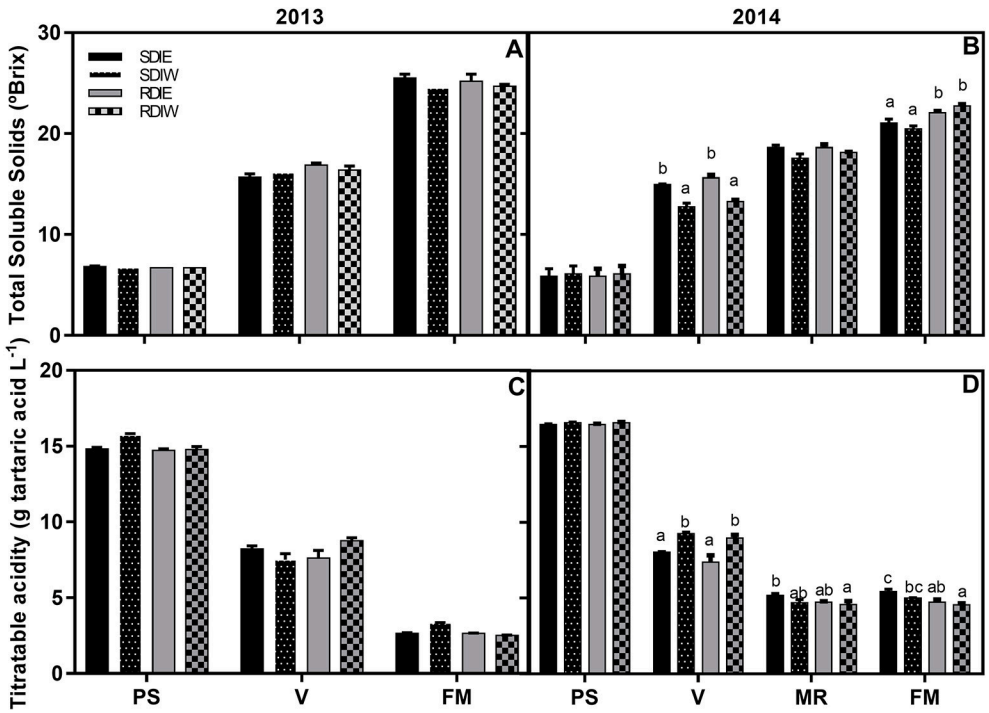

FIGURE 1 | Total soluble solids (TSS) (A,B) and titratable acidity (TA) **(C,D)** in grape berries growing under sustained deficit irrigation (SDI) and regulated deficit irrigation (RDI) vines from two cluster position east (E) and west (W) in the seasons of 2013 and 2014. Values are mean ± SE ($n \geq 3$). Different letters suffix indicate significant differences among treatments at the same date using Duncan test ($p \leq 0.05$).

to non-methoxylated anthocyanin ratio in SDI exceeded that in RDI at *véraison*, the reverse being observed at mid-ripening.

Grape Skin Phenylpropanoids Composition and Accumulation

Different derivatives of hydroxycinnamic acid, such as caftaric and coutaric acid, and of quercetin and myricetin were identified in berry skin (**Table 4**). Traces of benzoic acids, e.g., gallic acid, protocatechuic acid, vanillic acid and syringic acid were also detected in 2013, but not in 2014. In general, phenolic acids (hydrocinnamic acids and benzoic acids) concentrations decreased along berry development and were higher in SDI as compared with RDI at all studied phenological stages, and in both seasons. In addition, phenolic acids were higher at west side than the east side at pea-size and *véraison*. The flavonol content was higher at west side than the east side (independent on irrigation treatment) since the pea size stage. The concentration of phenylpropanoids was greater in 2014 than in 2013.

Grape Skin Anthocyanin Degradation Products

Products of anthocyanin degradation, such as protocatechuic acid and phloroglucinaldehyde were only detected at full maturation (**Figure 3**), the concentration of which in west-exposed berries exceeded that in east-exposed berries. The degradation of anthocyanins was higher in berries under RDI.

Free ABA and Related Metabolites Accumulation in Grape Skin

Free-ABA concentration sharply increased at *véraison* in both years (**Figure 4**). There were no significant differences at pea size and *véraison* in ABA skin concentration in 2014. In 2013, ABA was highest at west side independently from irrigation at pea size stage, and lowest in RDIE at *véraison*. In 2013, SDI treatment presented highest free ABA at full maturation stage, where east side presents highest values. In 2014, SDI treatment presented higher ABA both at mid-ripening and full maturation stages. In contrast with 2013, in 2014 west side presented the highest free ABA at mid-ripening and full maturation stages. DPA was the pre-dominant ABA catabolite present while PA concentration was significantly lower. PA and DPA concentrations showed the same trend of accumulation and decreased along berry ripening. During 2013, PA and DPA were highest at pea size and decreases thereafter. At this stage, RDI was higher than SDI and west side presented highest content. During 2014, no differences were observed at pea size, and PA and DPA showed a sharp increase at *véraison* stage in SDIW and RDIW while decreases at east side in both irrigation treatments. This highest content at west side was maintained at mid-ripening being SDIW with higher content than RDIW (**Figure 4**). Contrarily to PA and DPA, the ABA-GE increased along berry development in both

TABLE 3 | Anthocyanin concentration in berry skins (μmol g^{-1} dry weight) of east- and west-exposed clusters under sustained deficit irrigation (SDI) and regulated deficit irrigation (RDI) along the berry development and during the seasons of 2013 and 2014.

		Véraison				Mid-ripening				Full maturation			
		SDIE	SDIW	RDIE	RDIW	SDIE	SDIW	RDIE	RDIW	SDIE	SDIW	RDIE	RDIW
ANTHOCYANINS (μmol g^{-1} DW)													
Delphinidin-3-*O*-glucoside	2013	1.07 ± 0.04	1.17 ± 0.07	2.44 ± 0.20	0.86 ± 0.03	nd	nd	nd	nd	4.67 ± 0.42	3.28 ± 0.17	5.02 ± 0.18	3.77 ± 0.10
	2014	1.34 ± 0.05	0.56 ± 0.05	1.30 ± 0.09	1.08 ± 0.43	5.78 ± 0.52	3.43 ± 0.11	4.46 ± 0.84	3.54 ± 0.24	7.60 ± 0.35	8.58 ± 0.14	5.17 ± 1.03	6.23 ± 0.49
Cyanidin-3-*O*-glucoside	2013	0.36 ± 0.01	0.33 ± 0.01	0.74 ± 0.02	0.31 ± 0.03	nd	nd	nd	nd	0.58 ± 0.03	0.39 ± 0.03	0.87 ± 0.04	0.68 ± 0.02
	2014	0.30 ± 0.01	0.12 ± 0.02	0.32 ± 0.04	0.28 ± 0.02	0.80 ± 0.08	0.48 ± 0.01	0.53 ± 0.07	0.41 ± 0.05	0.84 ± 0.02	0.98 ± 0.03	0.68 ± 0.08	0.76 ± 0.07
Petunidin-3-*O*-glucoside	2013	0.59 ± 0.02	0.70 ± 0.06	1.47 ± 0.13	0.49 ± 0.02	nd	nd	nd	nd	3.40 ± 0.24	2.33 ± 0.12	3.41 ± 0.12	2.51 ± 0.05
	2014	1.11 ± 0.05	0.47 ± 0.05	0.99 ± 0.08	0.81 ± 0.37	4.61 ± 0.39	2.80 ± 0.08	3.83 ± 0.10	3.25 ± 0.24	6.31 ± 0.13	6.55 ± 0.09	4.61 ± 0.36	4.74 ± 0.24
Peonidin-3-*O*-glucoside	2013	0.29 ± 0.01	0.32 ± 0.01	0.65 ± 0.03	0.26 ± 0.02	nd	nd	nd	nd	0.95 ± 0.07	0.55 ± 0.03	1.01 ± 0.03	0.77 ± 0.02
	2014	0.58 ± 0.02	0.29 ± 0.05	0.58 ± 0.02	0.48 ± 0.04	1.51 ± 0.12	1.02 ± 0.01	1.24 ± 0.06	0.88 ± 0.06	1.77 ± 0.03	1.86 ± 0.05	1.85 ± 0.34	1.67 ± 0.02
Malvidin-3-*O*-glucoside	2013	0.85 ± 0.04	1.13 ± 0.11	1.96 ± 0.18	0.74 ± 0.03	nd	nd	nd	nd	7.79 ± 0.60	4.75 ± 0.22	5.95 ± 0.19	4.09 ± 0.07
	2014	3.52 ± 0.09	1.74 ± 0.23	2.73 ± 0.22	2.38 ± 1.05	13.26 ± 1.08	8.95 ± 0.28	13.76 ± 1.55	9.96 ± 0.42	21.80 ± 0.45	19.37 ± 0.42	18.45 ± 1.19	15.58 ± 0.16
Delphinidin-3-*O*-acetylglucoside	2013	0.03 ± 0.00	0.03 ± 0.00	0.07 ± 0.01	0.02 ± 0.00	nd	nd	nd	nd	0.16 ± 0.01	0.14 ± 0.01	0.15 ± 0.00	0.15 ± 0.00
	2014	0.00 ± 0.00	0.01 ± 0.00	0.03 ± 0.01	0.01 ± 0.00	0.20 ± 0.02	0.16 ± 0.00	0.20 ± 0.01	0.17 ± 0.02	0.29 ± 0.02	0.36 ± 0.00	0.25 ± 0.04	0.27 ± 0.02
Peonidin-3-*O*-acetylglucoside	2013	0.00 ± 0.00	0.00 ± 0.00	0.00 ± 0.00	0.00 ± 0.00	nd	nd	nd	nd	0.02 ± 0.01	0.03 ± 0.00	0.04 ± 0.00	0.03 ± 0.00
	2014	0.00 ± 0.00	0.00 ± 0.00	0.00 ± 0.00	0.00 ± 0.00	nd	nd	nd	nd	nd	nd	nd	nd
Malvidin-3-*O*-acetylglucoside	2013	0.03 ± 0.00	0.05 ± 0.01	0.08 ± 0.01	0.03 ± 0.00	nd	nd	nd	nd	0.52 ± 0.04	0.41 ± 0.02	0.36 ± 0.02	0.29 ± 0.01
	2014	0.25 ± 0.01	0.16 ± 0.03	0.19 ± 0.02	0.22 ± 0.08	0.97 ± 0.06	0.89 ± 0.08	1.28 ± 0.06	1.05 ± 0.00	1.96 ± 0.02	1.93 ± 0.05	1.98 ± 0.07	1.42 ± 0.03
Delphinidin-3-*O*-(6″-O-coumaroyl)glucoside (*cis* isomer)	2013	0.05 ± 0.01	0.07 ± 0.01	0.12 ± 0.01	0.05 ± 0.00	nd	nd	nd	nd	0.71 ± 0.08	0.60 ± 0.03	0.55 ± 0.03	0.50 ± 0.02
	2014	0.25 ± 0.01	0.12 ± 0.04	0.22 ± 0.03	0.26 ± 0.09	0.93 ± 0.11	0.94 ± 0.10	1.48 ± 0.05	1.16 ± 0.09	2.02 ± 0.05	2.26 ± 0.09	1.61 ± 0.37	1.66 ± 0.04
Cyanidin-3-*O*-(6″-O-coumaroyl)glucoside (*trans* isomer)	2013	0.04 ± 0.00	0.04 ± 0.00	0.07 ± 0.01	0.03 ± 0.00	nd	nd	nd	nd	0.13 ± 0.01	0.12 ± 0.01	0.15 ± 0.01	0.14 ± 0.01
	2014	0.09 ± 0.01	0.05 ± 0.00	0.08 ± 0.01	0.11 ± 0.01	0.17 ± 0.03	0.13 ± 0.02	0.23 ± 0.02	0.18 ± 0.00	0.33 ± 0.00	0.38 ± 0.01	0.24 ± 0.05	0.29 ± 0.02
Petunidin-3-*O*-(6″-O-coumaroyl)glucoside (*trans* isomer)	2013	0.04 ± 0.00	0.05 ± 0.01	0.10 ± 0.01	0.03 ± 0.00	nd	nd	nd	nd	0.60 ± 0.06	0.51 ± 0.02	0.49 ± 0.02	0.40 ± 0.01
	2014	0.23 ± 0.01	0.12 ± 0.01	0.18 ± 0.02	0.20 ± 0.08	0.92 ± 0.08	0.83 ± 0.02	1.18 ± 0.19	1.08 ± 0.04	1.73 ± 0.04	1.80 ± 0.02	1.41 ± 0.07	1.37 ± 0.03
Peonidin-3-*O*-(6″-O-coumaroyl)glucoside (*cis* isomer)	2013	0.00 ± 0.00	0.00 ± 0.00	0.01 ± 0.00	0.00 ± 0.00	nd	nd	nd	nd	0.01 ± 0.00	0.01 ± 0.00	0.01 ± 0.00	0.01 ± 0.00
	2014	nd	nd	nd	nd	nd	nd	nd	nd	nd	nd	nd	nd
Malvidin-3-*O*-(6″-O-coumaroyl)glucoside (*cis* isomer)	2013	0.01 ± 0.00	0.01 ± 0.00	0.01 ± 0.00	0.01 ± 0.00	nd	nd	nd	nd	0.05 ± 0.01	0.05 ± 0.00	0.05 ± 0.00	0.04 ± 0.00
	2014	0.07 ± 0.02	0.03 ± 0.00	0.04 ± 0.01	0.04 ± 0.01	0.18 ± 0.01	0.16 ± 0.02	0.24 ± 0.02	0.20 ± 0.01	0.23 ± 0.01	0.28 ± 0.03	0.29 ± 0.04	0.21 ± 0.03
Peonidin-3-*O*-(6″-O-coumaroyl)glucoside (trans isomer) + Malvidin-3-O-(6″-O-coumaroyl)glucoside (trans isomer)	2013	0.11 ± 0.01	0.15 ± 0.02	0.25 ± 0.03	0.09 ± 0.01	0.00 ± 0.00	0.00 ± 0.00	0.00 ± 0.00	0.00 ± 0.00	1.97 ± 0.15	1.44 ± 0.00	1.38 ± 0.08	0.96 ± 0.03
	2014	1.10 ± 0.04	0.59 ± 0.05	0.75 ± 0.07	0.71 ± 0.14	3.95 ± 0.32	3.38 ± 0.09	4.68 ± 0.26	4.21 ± 0.13	8.19 ± 0.16	6.94 ± 0.14	9.10 ± 0.93	5.59 ± 0.00
Methoxylated/non-Methoxylated Ratio	2013	1.50 ± 0.01	1.58 ± 0.01	3.31 ± 0.03	1.23 ± 0.01	nd	nd	nd	nd	5.54 ± 0.07	3.93 ± 0.04	6.18 ± 0.04	4.74 ± 0.02
	2014	3.46 ± 0.01	3.99 ± 0.02	2.83 ± 0.03	2.80 ± 0.10	3.23 ± 0.12	3.51 ± 0.03	3.80 ± 0.08	3.78 ± 0.07	3.79 ± 0.04	3.08 ± 0.03	4.75 ± 0.11	3.32 ± 0.07

nd, non-detected; Values presented are mean ± SD (n ≥ 3).

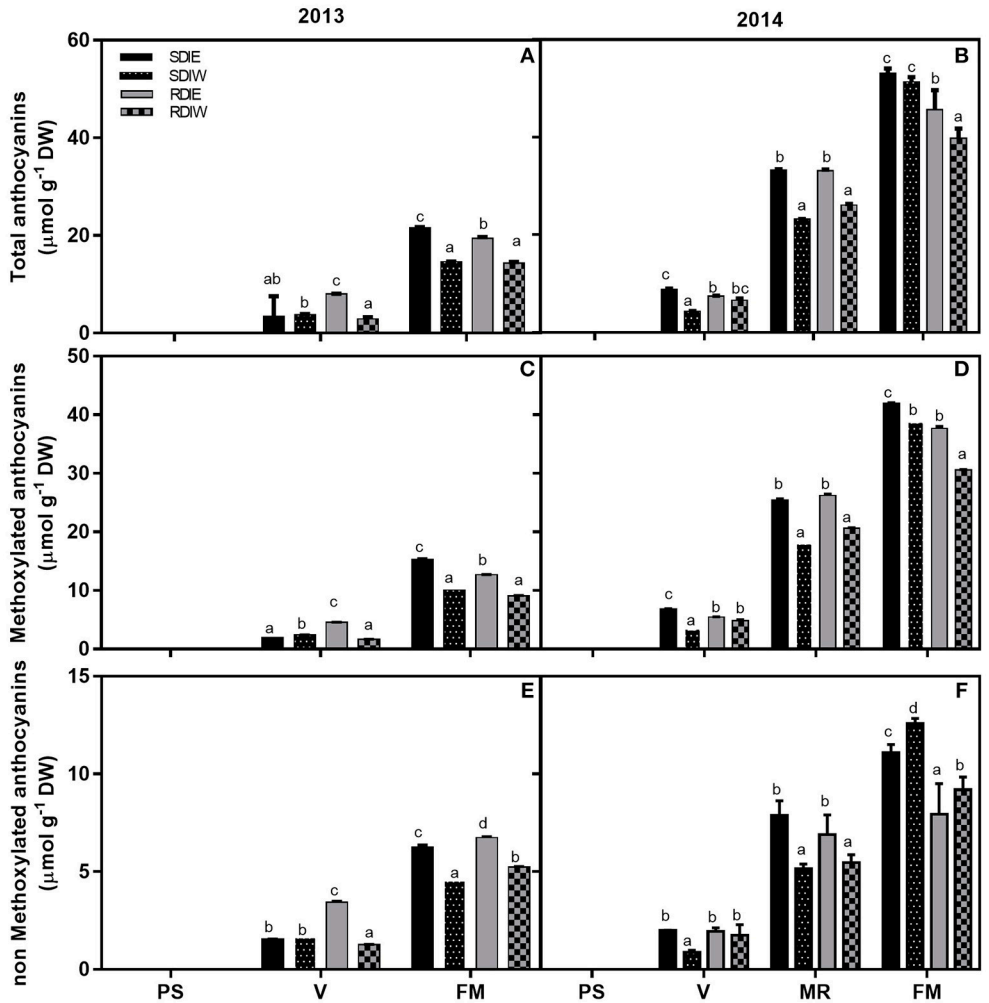

FIGURE 2 | Total anthocyanin (A,B), methoxylated **(C,D)**, and non-methoxylated **(E,F)** anthocyanin accumulation in grape berry skin growing under sustained deficit irrigation (SDI) and regulated deficit irrigation (RDI) vines from two cluster position east (E) and west (W) in the seasons of 2013 and 2014. Values are mean ± SD ($n \geq 3$). Different letters suffix indicate significant differences among treatments at the same date using Duncan test ($p \leq 0.05$).

years and its concentration was lower in RDI and at the west side.

Expression of *VviUFGT*, *VviNCED1*, *Vviβ G1*, *VviHyd1,* and *VviHyd2* Genes in Grape Berry Skin

The expression profile of *VviUFGT* was transiently up-regulated in all treatments at *véraison* stage during skin development (**Figure 5**). This increase in *VviUFGT* expression coincides with the onset of anthocyanin accumulation. Differences among treatments in the expression were observed from *véraison* until full maturation, where *VviUFGT* showed the maximum expression under SDI when compared with RDI. *VviUFGT* expression was also repressed at the west side both in SDI and RDI at *véraison*. However, at full maturation, *VviUFGT* was highest at SDIE while no differences due to the side were observed in RDI. *VviNCED1*, was studied at different phenological stages (**Figure 6**). A peak of expression was detected at *véraison* in both irrigation treatments. The expression of *VviNCED1* decreases from véraison onward, being more expressed at the west side of both irrigation treatments at mid-ripeningand at full maturation stages. In skin, *VviβG1* peaked at *véraison* stage. *VviβG1* expression was up-regulated at the west side of the canopy at pea size stage and in RDI at mid-ripening. Although no significant differences were recorded, a tendency in highest expression of *VviβG1* in RDI and at the west side of the canopy was recorded at *véraison*. The trend of expression of two genes encoding ABA 8′-hydroxylases (*VviHyd1* and *VviHyd2*) was studied along berry ripening (**Figure 6**). *VviHyd1* expression was higher at pea size stage but no statistical differences were recorded between east and west side of the canopy. Although, *VviHyd1* expression decreased thereafter, it maintained a statistical high expression level both in SDIW and RDIW at *véraison* coincident with high PA and

TABLE 4 | Flavonol concentration in berry skins (μmol g^{-1} dry weight) of east- and west-exposed clusters under sustained deficit irrigation (SDI) and regulated deficit irrigation (RDI) along the berry development and during the seasons of 2013 and 2014.

		Pea-size			Véraison				Mid-ripening				Full maturation			
		SDIE	SDIW	RDIE	RDIW	SDIE	SDIW	RDIE	RDIW	SDIE	SDIW	RDIE	RDIW	SDIE	SDIW	RDIE	RDIW
FLAVONOLS (μmol g^{-1} DW)																	
trans-caftaric acid	2013	5.73 ± 0.18	7.04 ± 0.39	6.00 ± 0.21	6.23 ± 0.15	2.50 ± 0.05	2.95 ± 0.07	2.04 ± 0.25	2.52 ± 0.07	nd	nd	nd	nd	1.40 ± 0.06	1.35 ± 0.03	1.13 ± 0.03	1.22 ± 0.04
	2014	8.26 ± 0.20	8.97 ± 0.20	8.26 ± 0.20	8.97 ± 0.20	3.48 ± 0.04	3.82 ± 0.27	3.80 ± 0.28	6.10 ± 0.71	2.45 ± 0.97	2.71 ± 0.27	2.44 ± 0.31	2.73 ± 0.17	2.31 ± 1.30	1.52 ± 0.12	1.70 ± 0.15	1.57 ± 0.01
Gallic acid + Protocatechuic acid + Vanillic acid + Syringic acid	2013	0.32 ± 0.02	0.38 ± 0.04	0.29 ± 0.00	0.30 ± 0.01	0.60 ± 0.04	0.61 ± 0.04	0.51 ± 0.01	0.53 ± 0.05	nd	nd	nd	nd	0.25 ± 0.02	0.20 ± 0.02	0.46 ± 0.02	0.39 ± 0.01
	2014	nd	nd	nd	nd	nd	nd	nd	nd	nd	nd	nd	nd	nd	nd	nd	nd
trans-coutaric acid	2013	5.72 ± 0.16	6.59 ± 0.51	5.63 ± 0.23	6.12 ± 0.13	2.85 ± 0.08	3.47 ± 0.10	2.23 ± 0.26	2.86 ± 0.19	nd	nd	nd	nd	1.70 ± 0.13	1.46 ± 0.10	1.35 ± 0.06	1.21 ± 0.09
	2014	7.58 ± 0.23	8.59 ± 0.17	7.58 ± 0.23	8.59 ± 0.17	2.97 ± 0.15	3.29 ± 0.33	3.48 ± 0.31	5.95 ± 0.31	2.17 ± 0.81	2.17 ± 0.81	2.35 ± 0.24	2.71 ± 0.57	2.20 ± 0.92	2.49 ± 1.31	1.45 ± 0.16	1.30 ± 0.12
Rutin + Quercetin-3-O-glucoside	2013	1.89 ± 0.12	1.85 ± 0.31	2.53 ± 0.03	2.50 ± 0.04	1.47 ± 0.04	1.32 ± 0.11	0.86 ± 0.04	1.19 ± 0.05	nd	nd	nd	nd	0.90 ± 0.05	1.34 ± 0.09	1.17 ± 0.09	1.30 ± 0.10
	2014	1.59 ± 0.32	2.44 ± 0.07	1.59 ± 0.32	2.44 ± 0.07	3.36 ± 0.04	2.57 ± 0.25	3.62 ± 0.39	3.85 ± 0.17	3.74 ± 0.32	2.07 ± 0.27	2.24 ± 0.35	2.11 ± 0.05	1.47 ± 0.24	2.77 ± 0.11	1.13 ± 0.15	2.84 ± 0.03
Myricetin 3-O-glucoside	2013	0.67 ± 0.05	0.54 ± 0.11	0.98 ± 0.04	0.90 ± 0.12	0.74 ± 0.02	0.63 ± 0.05	0.45 ± 0.05	0.64 ± 0.04	nd	nd	nd	nd	1.31 ± 0.12	1.45 ± 0.13	1.66 ± 0.12	1.48 ± 0.13
	2014	0.30 ± 0.16	0.57 ± 0.07	0.30 ± 0.16	0.57 ± 0.07	1.11 ± 0.03	0.88 ± 0.34	1.23 ± 0.12	1.27 ± 0.26	2.51 ± 0.16	1.08 ± 0.23	1.25 ± 0.24	1.26 ± 0.40	0.85 ± 0.07	3.63 ± 0.56	0.91 ± 0.35	2.97 ± 0.04

nd, non-detected; Values presented are mean ± SD (n ≥ 3).

DPA concentrations at this stage. *VviHyd2* presented a similar trend of expression than *VviHyd1*. However, *VviHyd2* was higher-expressed at the west side of the canopy at all phenological stages studied and in RDI treatment since *véraison* stage.

Interaction between Deficit Irrigation and Cluster Position with Berry Ripening and Quality Traits

PCA performed on cumulative water stress ($S\Psi_{pd}$), NHH and AEBT at *véraison* and full maturation separated the SDI from RDI as well as cluster position in both years (Supplementary Figure 2). In order to decipher the "vintage effect," PCA was performed combining all data from both years (**Figure 7A**). This analysis showed that most traits contribute to the separation along the first axis and explain 67% of the variability (Supplementary Table 3), contributing thereby to a strong "vintage effect." In addition, both deficit irrigation regime and cluster position, were discriminated along the 2nd and 3rd axis (13 and 11% respectively) in the 2 years (**Figure 7A**). Nonetheless, PCA showed difference between both studied years, being the impact of deficit irrigation regime greater in 2013, while in 2014 the cluster position had more influence (**Figure 7A**). ABA-GE parameter contributed for the separation along the 2nd and 3rd axis (Supplementary Table 3). Taking into consideration the data from **Figure 7B** (PCA for 2013) and 7C (PCA for 2014), we could further indicate that ABA-GE discriminated between deficit irrigation systems (**Figure 7B**, along 1st axis; **Figure 7C**, along 2nd axis) (Supplementary Table 3). In both cases, ABA-GE contributed for the separation SDI vs. RDI. However, only in 2014 it discriminates east vs. west cluster position. A distinctive response of ABA and ABA metabolism to both the irrigation treatment and the cluster position is observed in 2014 (**Figure 8**). It is important to note, that the first and the second axis explain 68–69% of observed variability and that the second axis contributes with at least a ½ to ¾ of the first axis.

Also for 2014, PCA shows (**Figure 7C**), that the parameters associated with cluster position discrimination (east vs. west) were the different chemical forms of malvidin (Malvidin-3-O-glucoside, Malvidin-3-O-acetylglucoside, and Peonidin-3-O-(6″-O-coumaroyl)glucoside + Malvidin-3-O-(6″-O-coumaroyl)glucoside), flavonols (rutin and quercetin-3-O-glucoside and myricetin), and degradation products of anthocyanins. These molecules, in a year with low water availability (high $S\Psi_{pd}$), were able to discriminate east-west position and responded to the berry temperature. In contrast, in 2013, the separation according to cluster position was only achieved along the 4th axis (7%) and none of above mentioned parameters contributed significantly for such separation (Supplementary Table 3). This indicates that in 2013, other factors in addition to water stress and T_{berry} are impacting on berry skin metabolism. It appears that in wet years, vines could cope with high T_{air} in a way that made difficult to separate the effects of irrigation from cluster position.

In order to explain the effect of water stress and/or cluster position on berry ripening and composition, we explore for the existence of correlations. To our surprise, neither anthocyanins

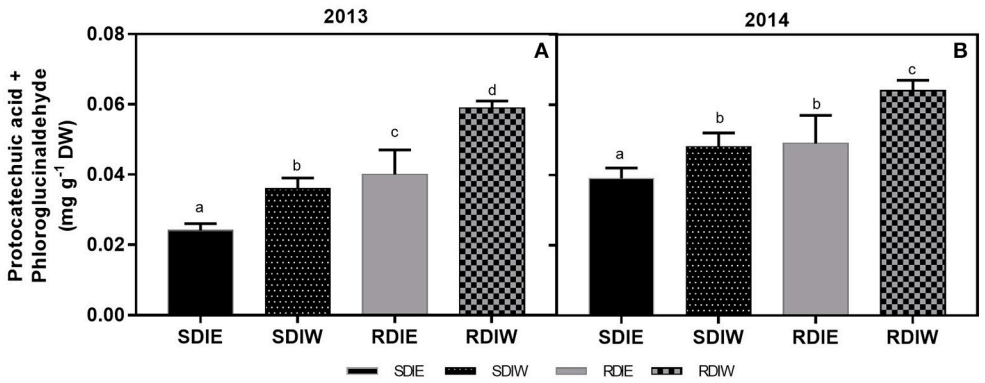

FIGURE 3 | Protocatechuic acid and phloroglucinaldehyde content (mg g^{-1} dry weight) in berry skin growing under sustained deficit irrigation (SDI) and regulated deficit irrigation (RDI) vines from two cluster position east (E) and west (W) in the seasons of 2013 (A) and 2014 **(B)**. Values are mean ± *SD* ($n \geq 3$). Different letters suffix indicate significant differences among treatments at the same date using Duncan test ($p \leq 0.05$).

nor ABA correlated with $S\Psi_{pd}$ in both years. Nonetheless, a highly significant and negative correlation between free-ABA and total anthocyanins was observed for both irrigation treatments ($r = -0.76$, $p \leq 0.0001$) in the 2 years. Interestingly, a weaker correlation was observed on the west side as compared with the east side (east $r = -0.84$, $p \leq 0.001$ vs. west $r = -0.67$, $p \leq 0.05$) indicating that high temperature affect negatively ripening process, namely anthocyanin accumulation. In addition, a thermal disruption of the anthocyanins/ABA relationship among the different irrigations and cluster positions was observed, being the RDIW showing the larger difference, suggesting the higher susceptibility of RDI to high temperature as compared with SDI.

DISCUSSION

Ripening is a complex process leading to several physiological and metabolic changes including softening, and sugar and anthocyanin accumulation. In contrast to climacteric fruits in which the control of ripening is well established, in non-climacteric grape berries, ripening is, still, poorly understood.

Hormones, particularly ABA, are long known to participate in the ripening process of grape berry (Jeong et al., 2004; Symons et al., 2006; Wheeler et al., 2009; Koyama et al., 2010; Sun et al., 2010; Böttcher and Davies, 2012). Deficit irrigation has been proposed as suitable viticultural practice to influence berry ripening, through the stimulation of sugar and anthocyanin biosynthesis under a mild to moderate water deficits (Castellarin et al., 2007a; Gambetta et al., 2010). However, deficit irrigation has been shown to increase (Basile et al., 2011; Santesteban et al., 2011) decrease (Intrigliolo et al., 2012; Zarrouk et al., 2012) or to have negligibly affect (Castellarin et al., 2007a,b; Girona et al., 2009) on anthocyanin biosynthesis. Mechanisms through which water deficit affects berry ripening require further elucidation, mostly because increases in sugars and anthocyanins in berries exposed to pre- or post-véraison deficit irrigation depends greatly on the sensitivity of berry developmental growth and cultivar's sensitivity to ABA signaling (Ferrandino and Lovisolo, 2013).

Air temperature, namely high temperatures, may also have a strong impact on berry quality, leading to a drop in berry acidity and an increase in sugar content (Keller, 2010), while reducing anthocyanin content (Mori et al., 2007; Tarara et al., 2008; Greer and Weedon, 2013) and varietal aroma (Jones and Goodrich, 2008; Bonada et al., 2015). Our study aimed at evaluating the combined effect of changes in water availability and berry temperature (by sampling berries located on different sides in the canopy) on grape berry ripening and composition.

Interactive Effects of Irrigation Regime and Berry Temperature on the Biosynthesis, Accumulation, and Degradation of Anthocyanins

Water deficit has been considered to impact on the accumulation of anthocyanins through the stimulation of anthocyanin hydroxylation (Castellarin et al., 2007b), which converts hydroxylated anthocyanins (cyanidin and delphinidin) into their methoxylated derivates (peonidin, petunidin, and malvidin) (Kennedy et al., 2002; Castellarin et al., 2007a,b). In contrast, high temperature was shown to reduce anthocyanin hydroxylation in grape berries (Tarara et al., 2008). Our study shows that methoxylated anthocyanins accumulated from mid-ripening to full maturation stages in berries located on the east canopy side, irrespective of year and irrigation regime. The ratio of methoxylated to non-methoxylated anthocyanin was higher in RDI than SDI vines, as reported previously (Castellarin et al., 2007a,b; Deluc et al., 2009). On the other hand, the ratio of methoxylated to non-methoxylated anthocyanins was higher in berries located at the west than at the east side, confirming previous findings of high temperature influence on the anthocyanin forms (Tarara et al., 2008).

Methoxylation of anthocyanins greatly affects berry color and stability (Jackman and Smith, 1996). Our data suggests that anthocyanin methoxylation might represent a strategy adopted by grapes to cope with the combined effects of water shortage and heat stress. Increasing anthocyanin stability

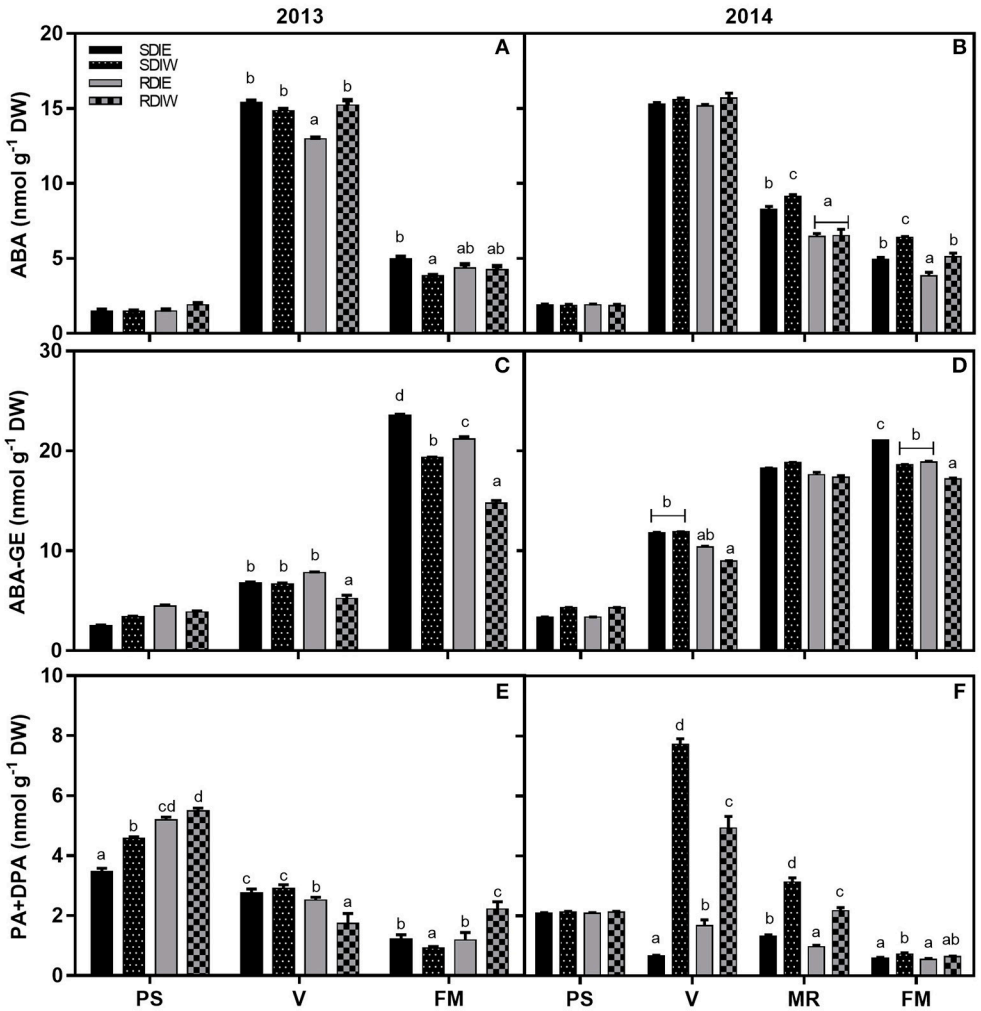

FIGURE 4 | Effect of irrigation regime: sustained deficit irrigation (SDI) and regulated deficit irrigation (RDI) and cluster position east (E) and west (W) on ABA (A,B), ABA-GE **(C,D)**, and PA+DPA **(E,F)** concentration in grape berry skins during the seasons of 2013 and 2014. Values are mean ± *SD* ($n \geq 3$). Different letters suffix indicate significant differences among treatments at the same date using Duncan test ($p \leq 0.05$).

through methoxylation may partly compensate for reduced anthocyanin biosynthesis when carbon assimilation is severely constrained under severe stress (i.e., the combined effect of water deficit and heat stress). The concentration of anthocyanins was significantly repressed in west-exposed berries, both in SDI and RDI during ripening in 2013. In 2014, no differences in anthocyanin concentrations between sides were observed in SDI at full maturation suggesting that more irrigated SDI vines are less sensitive to high temperatures during ripening in coolest years or/and years with less hours of extreme temperature which corroborates recent studies of Romero et al. (2016). In contrast, RDI showed statistically lower concentration at the west side than at the east side and lower than SDI. Our findings suggest that the most severe stress conditions, i.e., RDI treatment, exacerbated the negative impact of high temperature on anthocyanin biosynthesis and/or degradation. Our hypothesis is further corroborated by the observation that the expression of *VviUFGT,* which is involved in late steps of anthocyanin biosynthesis, was down-regulated in RDI as compared to SDI at the onset of ripening. This also supports the negative effect of higher pre-*véraison* $S\Psi_{pd}$ on anthocyanin biosynthesis. The expression of *VviUFGT* was also repressed at the west side in both irrigation treatments, possibly due to greater heat stress incidence in this side (**Table 2**). In contrast, *VviUFGT* expression was higher at west side than in east side in both treatments at full maturation, suggesting the possibility of an enhancement of anthocyanin biosynthesis at this stage. However, this enhancement was not translated into higher anthocyanin concentrations in the berries located at the west side. This may be due to the highest rate of degradation registered on the west side of the canopy in both irrigation treatments (**Figure 4**). Our results suggest that the negative impact of water stress and high temperature on anthocyanin content likely results from the repression of anthocyanin biosynthesis at the onset of ripening. We also provide evidence that accumulation

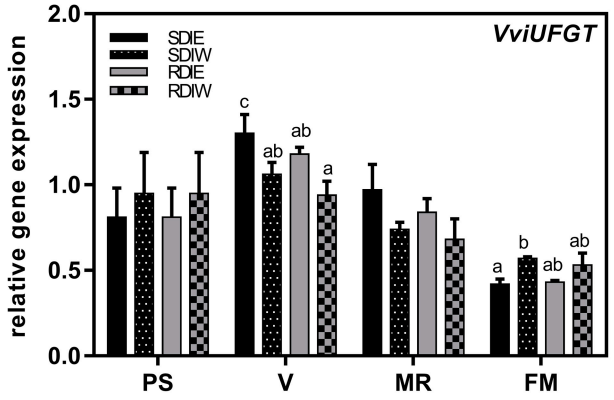

FIGURE 5 | Expression of the UDP-glucose:flavonoid 3-O-glucosyltransferase gene (*VviUFGT*), in berry skin growing under sustained deficit irrigation (SDI) and regulated deficit irrigation (RDI) vines from two cluster position east (E) and west (W) in the seasons of 2013 and 2014. Values are mean ± SE ($n \geq 3$). Different letters suffix indicate significant differences among treatments at the same date using Duncan test ($p \leq 0.05$).

of anthocyanins at full maturation is negatively affected by water/heat stress possibly because of the higher degradation rate of these compounds at later stages of berry ripening.

Interactive effects of water deficit and side of the canopy on berry quality are clearly exposed in our study. There is compelling evidence that the negative impact of water deficit on berry quality greatly depends on temperature (Tarara et al., 2008; Bonada et al., 2013; Fernandes de Oliveira and Nieddu, 2013). In our experiment, an annual effect on anthocyanin accumulation was observed, 2013 exhibiting lower concentrations than in 2014, in spite of 2013 showing lower accumulated water stress ($S\Psi_{pd}$). The high temperatures observed in the growing season of 2013 (2°C higher than 2014) could explain these results. On the other hand, in 2013, berries accumulated more hours with T_{air} above the threshold of >35°C during the ripening period, as compared with 2014. This could explain the acceleration of sugar accumulation (TSS) and acid breakdown (TA) observed in 2013 with regards to 2014. While TSS was higher in 2013 than in 2014 at full maturation, anthocyanins were lower in 2013. This result corroborates the fact that high temperature promotes sugar concentration in detriments of other quality attributes of berries, leading to poorly balanced wines with reduced varietal characteristics (Mira de Orduña, 2010). Sugar accumulation was reported to be required for anthocyanin biosynthesis in grape berries (Gollop et al., 2002; Castellarin et al., 2007a). Although no differences were observed in TSS due to irrigation treatments and cluster position in 2013, anthocyanins were repressed at the west side of the canopy. In 2014, TSS was lower at west side at *véraison*, which corroborates with low anthocyanin concentration results. However, at full maturation, TSS was higher in RDI (both sides of the canopy) as compared with SDI, while anthocyanins were lower in RDI treatments (east and west). Taking into account the more stressful temperature conditions in 2013, and higher cumulative heat stress from pea size to full maturation at west exposure in 2014, these results suggest a decoupling of anthocyanin/sugar as a consequence of high temperature (Sadras and Moran, 2012; Bonada et al., 2013).

Differential Regulation of Flavonol and Other Phenylpropanoid Accumulation during Berry Development by Irrigation and Cluster Position

The influence of water and heat stress on flavonol profile in grapes is still unclear, in contrast with compelling evidence reported for anthocyanin biosynthesis (Ferrandino and Lovisolo, 2013). Our study offers the first evidence that the combined effect of water and temperatures stress is distinct from those reported for water- or heat stressed grapes alone (Spayd et al., 2002; Castellarin et al., 2007a,b; Azuma et al., 2012; Zarrouk et al., 2012).

Deficit irrigation did not enhance the concentration of flavonol compounds, and no differences were observed between SDI and RDI berries. The data corroborates Deluc et al. (2009), which showed that flavonol content is not affected by water stress in a red grapevine variety but it is in a white one. Nevertheless, flavonols were higher at the west side of both SDI and RDI treatments, suggesting an enhancement of their accumulation/biosynthesis under heat stress. The results suggest that the same climactic conditions that influence anthocyanin biosynthesis/accumulation at west side of the canopy may also affect flavonols since they share the same biosynthetic pathway. In this sense, the present study may suggest that the increase of flavonol concentration is promoted by the decrease in the UDP-glucose:flavonoid 3-O-glucosyltransferase activity by heat stress. We found that the transcript of this enzyme (*VviUFGT*) is down-regulated, suggesting that more substrate is available for flavonol biosynthesis via flavonol synthase activity. The competition for substrates (that both enzymes share) supports it. These results show also the differential impact of irrigation is dependent upon the stage of berry growth and the year, and suggest the multiple roles of flavonols during development, as previously reported by Cohen et al. (2008). In addition, the accumulation of phenolic acids at west side, may account for a protective effect against oxidative stress thanks to their chemical structures. Phenolic acids are able to scavenge free radicals (Blokhina et al., 2003), which are expected to be generated by high temperatures.

Water Deficit and Cluster Position Modulate ABA Metabolism in the Berry

ABA is a key signal in the trigger of berry ripening, as suggested by the increase of berry ABA content around *véraison* (Wheeler et al., 2009; Giribaldi et al., 2010; Sun et al., 2010; Zifkin et al., 2012; Karppinen et al., 2013; Niculcea et al., 2013). However, the effect of water stress on ABA concentration in grape berries is far from being conclusively addressed (Deluc et al., 2009; Balint and Reynolds, 2013; Niculcea et al., 2013, 2014). In addition, contrasting findings have been reported in studies exploring the effect of heat stress on ABA metabolism (Azuma et al., 2012; Carbonell-Bejerano et al., 2013; Rienth et al., 2014) which appear to be particularly dependent on grape berry phenology.

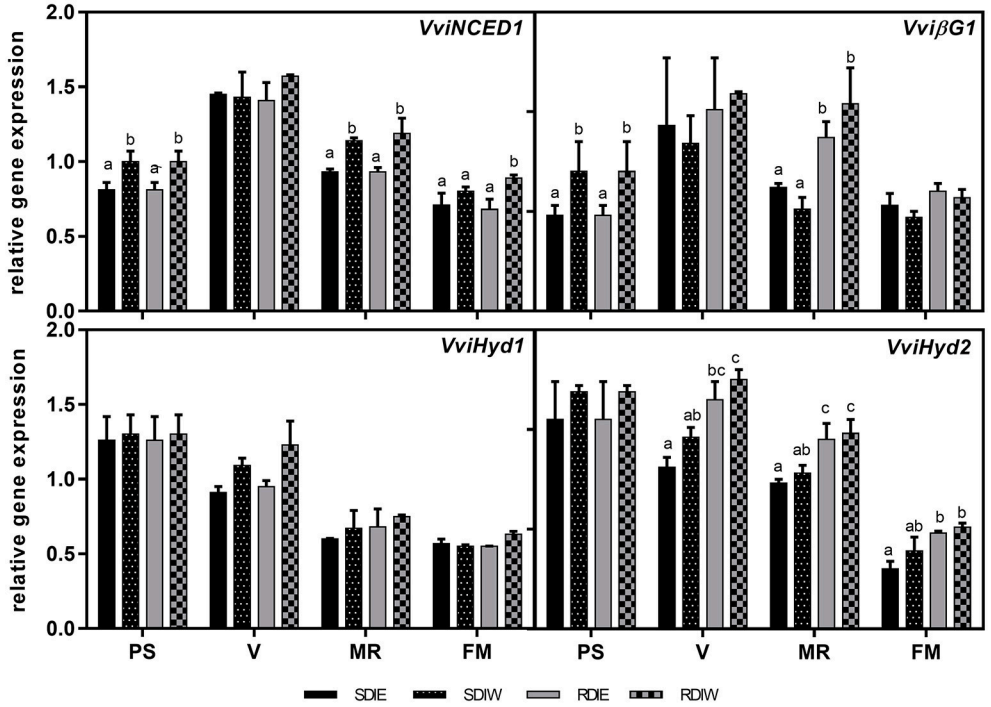

FIGURE 6 | Expression of several genes of the ABA pathway in berry skin growing under sustained deficit irrigation (SDI) and regulated deficit irrigation (RDI) vines from two cluster position east (E) and west (W) in the seasons of 2013 and 2014. β-glucosidase (*VvβG1*), 9-cis-epoxycarotenoid dioxygenase (*VviNCED1*), ABA 8′ hydroxylase 1 (*VviHyd1*) and ABA 8′ hydroxylase 2 (*VviHyd2*). Values are mean ± SD ($n \geq 3$). Different letters suffix indicate significant differences among treatments at the same date using Duncan test ($p \leq 0.05$).

In this sense, Rienth et al. (2014) showed that ABA synthesis was repressed by heat stress at the beginning of *véraison* and enhanced at the end of this developmental stage.

In our study, free-ABA concentration increased at *véraison* in both years, concomitantly with the sharp increase in transcripts of ABA biosynthesis genes, *VviNCED1* and *VviβG1*. This enhancement of ABA-biosynthetic genes coincided with a steep increase in berry sugars and anthocyanins. Irrigation regime and berry position had little effect on free-ABA levels at *véraison*, in contrast with their effects on sugar and anthocyanin. Additionally, although the strong correlation found between free-ABA and total anthocyanins on both sides of the canopy, the west side showed a weaker correlation as compared with the east side. We hypothesize that high temperature account for the differential modulation of these metabolites, since it was demonstrated to uncouple some ripening-related traits (Sadras and Moran, 2012; Carbonell-Bejerano et al., 2013; Sadras et al., 2013).

The biological function of ABA in grape ripening requires a transient increase at *véraison* as well as the subsequent decrease, which seems to be under developmental control (Wheeler et al., 2009). This hypothesis is reinforced by our study since ABA concentration in skins was found to not respond to vine water status ($S\Psi_{pd}$). On the other hand, the ABA increase coincides with the decrease in the PA and DPA, suggesting that this increase is caused by a decreased catabolism rate (Castellarin et al., 2015) and increased biosynthesis. Our results also point out to the effect of environmental conditions on ABA catabolism, since effects of irrigation and cluster position on PA and DPA were recorded. The molecular regulation of PA and DPA shows a complex pattern. The genes encoding ABA 8′-hydroxylases (*VviHyd1* and *VviHyd2*) were expressed equally in berry skin, but only *VviHyd2* was modulated by water stress, being up-regulated under RDI treatment.

The decrease of ABA after *véraison* may be due to several processes of degradation and oxidation. ABA-GE increased from pea size, reaching maximum content at full maturation, being higher in SDI treatment and repressed in west side of the canopy. This suggests that ABA-GE responds negatively to high temperatures and water stress intensity, contrasting with previous reports analysing ABA-GE under water stress (Deluc et al., 2009; Zarrouk et al., 2012; Balint and Reynolds, 2013). This highlights the need to carefully monitor water stress imposition and progression in order to be able to compare data sets originated from distinct experimental setups.

Grape berry can also modulate it ABA concentration via the release of ABA-GE by β-glucosidase (Lee et al., 2006; Sun et al., 2010; Zhang et al., 2013). *VvβG1* transcript increased around *véraison*, coincident with ABA accumulation, which indicates that β-glucosidase might play a role in regulating the level of ABA during the ripening at this stage. At mid-ripening, *VvβG1* transcript was up-regulated in RDI skins, suggesting a high

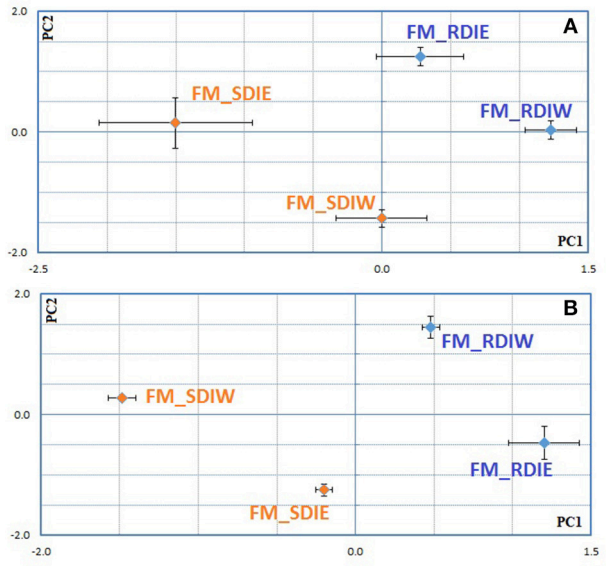

FIGURE 7 | Principal components analysis considering all data set from both growing seasons 2013–2014 (A), and individual growing season 2013 **(B)** and 2014 **(C)** for *Tempranillo* cv. at full maturation stage. **(A)** PC1 = 67%; PC2 = 13%; **(B)** PC1 = 50%; PC2 = 39%; **(C)** PC1 = 48%; PC2 = 26%. The plots were constructed using the row normed scores obtained with the ade4 package.

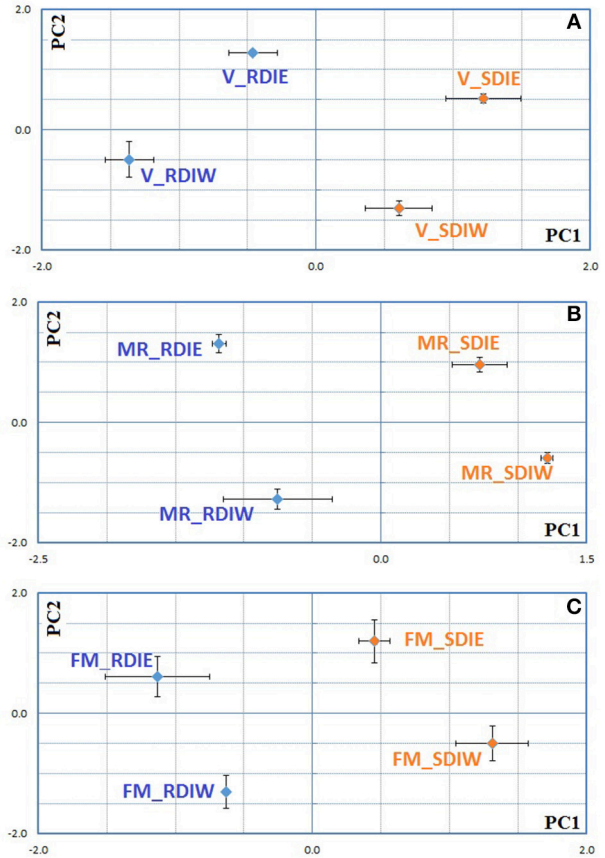

FIGURE 8 | Principal components analysis followed by between groups analysis considering ABA metabolites data set from 2014 growing seasons for Tempranillo cv. for véraison (A), mid-ripening **(B)**, and full maturation stages **(C)**. **(A)** PC1 = 39%; PC2 = 30% **(B)** PC1 = 44%; PC2 = 24% **(C)** PC1 = 39%; PC2 = 29%. The plots were constructed using the row normed scores obtained with the ade4 package.

release of free ABA from ABA-GE in this treatment. This latter result may also explain in part the lower ABA-GE concentrations at full maturation in RDI. Altogether, these results indicate that ABA found in skin along berry development may be also derived from the de-conjugation process of ABA-GE at later stages of berry development. These findings support a role for β-glucosidase in the modulation of ABA content during grape berries development and in response to dehydration.

The accumulation pattern of the different ABA related products provided evidence that endogenous ABA content is modulated by a dynamic balance between biosynthesis and catabolism. It appears that in grape berry, the ABA homeostasis is achieved by degradation before *véraison*, while after *véraison* ABA homeostasis is realized by conjugation. In addition, changes in ABA catabolism/conjugation along berry development were affected by water stress particularly when also submitted to heat stress, indicating that ABA-GE and ABA catabolites play an essential role in ABA homeostasis under environmental constraints.

CONCLUSION

Our work shows that the impact of irrigation regime and high temperature interaction in the control of berry ripening is quite complex and dynamic. Multivariate analysis showed that the strongest parameter influencing the berry ripening is the deficit irrigation system, in spite of some differences observed between the 2 years. Nonetheless, berry temperature is an important variable conditioning the deficit irrigation effect on berry quality. Deficit irrigation has a positive effect on berry composition only when the high temperature is not a limiting factor. Seasons with increased water stress, lead to a larger impact of high temperatures on the berry ripening and composition. Our results also show that the negative impact of water stress and high temperature on anthocyanins results from the repression of biosynthesis at the onset of ripening and from degradation at later stages Independently from the effect of water stress and cluster position, the increase in free ABA took place at the same stage as anthocyanin and sugar accumulation in the skin. Water and heat stresses do not affect free ABA, but do alter ABA catabolism/conjugation. This suggests that the homeostasis of berry ABA under abiotic stresses is mostly controlled by of catabolism/oxidation processes. Besides the observed *season*-specific effect on the accumulation and biosynthesis of different metabolites in the grape berry, and in general, SDI gives rise to berries with greater concentrations of phenolics than RDI, with the additional advantage of attenuating heat incidence at the west side of the canopy.

AUTHOR CONTRIBUTIONS

OZ and MC conceived and planned the study. CB, AG, and MT performed the HPLC analysis of flavonoids and ABA. CB and MT performed the data integration and processing for the above compounds. RE and CL implemented and maintained the viticultural treatments and monitored the vineyard. RE did the climatic and irrigation data processing and analysis. CP performed PCAs data analysis. OZ and TG did the sampling and the processing and analysis of the berry samples. OZ and CP performed data analysis. OZ, CP, and MC drafted the initial manuscript, all authors contributed to the final manuscript.

ACKNOWLEDGMENTS

This work was supported by the European Community's Seventh Framework Programme (FP7/2007-2013) under the grant agreement n° FP7-311775, Project INNOVINE and was integrated into the COST (European Cooperation in Science and Technology) Action FA1106 "Quality fruit." This work was also supported by the Ministero dell'Istruzione, dell'Università e della Ricerca of Italy: PRIN 2010–2011 "PRO-ROOT" and Progetto Premiale 2012 "Aqua." RE had a scholarship from INNOVINE. OZ was supported by postdoctoral fellowships from INNOVINE and FCT (SFRH/BPD/111693/2015). This work was supported by FCT, through R&D Unit, UID/Multi/04551/2013 (GreenIT). Authors acknowledge Herdade do Esporão (Reguengos de Monsaraz, Alentejo, Portugal) for the experimental vineyard facilities and Agri-Ciência-Consultores de Engenharia, Lda for providing berry temperature data.

SUPPLEMENTARY MATERIAL

The Supplementary Material for this article can be found online at: http://journal.frontiersin.org/article/10.3389/fpls.2016.01640/full#supplementary-material

REFERENCES

Allen, R. G., Pereira, L. S., Raes, D. and Smith, M. (1998). *Crop Evapotranspiration-Guidelines for Computing Crop Water Requirements.* FAO Irrigation and Drainage Paper 56. FAO, Rome, 300, D05109.

Azuma, A., Yakushiji, H., Koshita, Y., and Kobayachi, S. (2012). Flavonoid biosynthesis-related genes in grape skin are differentially regulated by temperature and light conditions. *Planta* 236, 1067–1080. doi: 10.1007/s00425-012-1650-x

Balint, G., and Reynolds, A. G. (2013). Impact of irrigation strategies on abscisic acid and its catabolites profiles in leaves and berries of Baco noir grapes. *J. Plant Growth Regul.* 32, 884–900. doi: 10.1007/s00344-013-9354-4

Basile, B., Marsal, J., Mata, M., Vallverdú, X., Bellvert, J., and Girona, J. (2011). Phenological sensitivity of Cabernet Sauvignon to water stress: vine physiology and berry composition. *Am. J. Enol. Vitic.* 62, 452–461. doi: 10.5344/ajev.2011.11003

Blokhina, O., Virolainen, E., and Fagerstedt, K. V. (2003). Antioxidants, oxidative damage and oxygen deprivation stress: a review. *Ann. Bot.* 91, 179–194. doi: 10.1093/aob/mcf118

Bonada, M., Jeffrey, D. W., Petrie, P. R., Moran, M. A., and Sadras, V. O. (2015). Impact of elevated temperature and water deficit on the chemical and sensory profiles of Barossa Shiraz grapes and wines. *Aust. J. Grape. Wine Res.* 21, 240–253. doi: 10.1111/ajgw.12142

Bonada, M., Sadras, V., Moran, M., and Fuentes, S. (2013). Elevated temperature and water stress accelerate mesocarp cell death and shrivelling, and decouple sensory traits in Shiraz berries. *Irrig. Sci.* 31, 1317–1331. doi: 10.1007/s00271-013-0407-z

Bonada, M., and Sadras, V. O. (2014). Review: critical appraisal of methods to investigate the effect of temperature on grapevine berry composition. *Aust. J. Grape. Wine Res.* 21, 1–17. doi: 10.1111/ajgw.12102

Böttcher, C., and Davies, C. (2012). "Hormonal control of grape berry development and ripening," in *The Biochemistry of the Grape Berry*, Vol. 1, eds H. Gerós, M. M. Chaves, and S. Delrot (Sharjah: Bentham Science), 194–217.

Carbonell-Bejerano, P., Santa María, E., Torres-Pérez, R., Royo, C., Lijavetzky, D., Bravo, G., et al. (2013). Thermotolerance responses in ripening berries of *Vitis vinifera* L. cv Muscat Hamburg. *Plant Cell Physiol.* 54, 1200–1216. doi: 10.1093/pcp/pct071

Castellarin, S. D., Gambetta, G. A., Wada, H., Krasnow, M. N., Cramer, G. R., Peterlunger, E., et al. (2015). Characterization of major ripening events during softening in grape: turgor, sugar accumulation, abscisic acid metabolism, colour development, and their relationship with growth. *J. Exp. Bot.* 67, 709–722. doi: 10.1093/jxb/erv483

Castellarin, S. D., Matthews, M. A., Di Gaspero, G., and Gambetta, G. A. (2007a). Water deficits accelerate ripening and induce changes in gene expression regulating flavonoid biosynthesis in grape berries. *Planta* 227, 101–112. doi: 10.1007/s00425-007-0598-8

Castellarin, S. D., Pfeiffer, A., Sivilotti, P., Degan, M., Peterlunger, E., and Di Gaspero, G. (2007b). Transcriptional regulation of anthocyanin biosynthesis in ripening fruits of grapevine under seasonal water deficit. *Plant Cell Environ.* 30, 1381–1399. doi: 10.1111/j.1365-3040.2007.01716.x

Chaves, M. M., Zarrouk, O., Francisco, R., Costa, J. M., Santos, T., Regalado, A. P., et al. (2010). Grapevine under deficit irrigation: hints from physiological and molecular data. *Ann. Bot.* 105, 661–676. doi: 10.1093/aob/mcq030

Chessel, D., Dufour, A.-B., and Thioulouse, J. (2004). The ade4 package-I- one-Table methods. *R. News* 4, 5–1.

Cohen, S. D., Tarara, J. M., and Kennedy, J. A. (2008). Assessing the impact of temperature on grape phenolic metabolism. *Anal. Chim. Acta* 621, 57–67. doi: 10.1016/j.aca.2007.11.029

Coombe, B. G. (1989). The grape berry as a sink. *Acta Hort.* 239, 149–158. doi: 10.17660/ActaHortic.1989.239.20

Culhane, A. C., Perrière, G., Considine, E. C., Cotter, T. G., and Higgins, D. G. (2002). Between-group analysis of microarray data. *Bioinformatics* 18, 1600–1608. doi: 10.1093/bioinformatics/18.12.1600

Davies, C., Boss, P. K., and Robinson, S. P. (1997). Treatment of grape berries, a nonclimacteric fruit with a synthetic auxin, retards ripening and alters the expression of developmentally regulated genes. *Plant. Physiol.* 115, 1155–1161. doi: 10.1104/pp.115.3.1155

Deluc, L. G., Grimplet, J., Wheatley, M. D., Tillett, R. L., Quilici, D. R., Osborne, C., et al. (2007). Transcriptomic and metabolite analyses of Cabernet Sauvignon grape berry development. *BMC Genomics* 8:429. doi: 10.1186/1471-2164-8-429

Deluc, L. G., Quilici, D. R., Decendit, A., Grimplet, J., Wheatley, D., Schlauch, A., et al. (2009). Water deficit alters differentially metabolic pathways affecting important flavour and quality traits in grape berries of Cabernet Sauvignon and Chardonnay. *BMC Genomics* 10:212. doi: 10.1186/1471-2164-10-212

Fernandes de Oliveira, A., and Nieddu, G. (2013). Deficit irrigation strategies in Vitis vinifera L. *cv.* Cannonau under Mediterranean climate. Part II - cluster microclimate and anthocyanin accumulation patterns. *S. Afr. J. Enol. Vitic.* 34, 184–195.

Ferrandino, A., and Lovisolo, C. (2013). Abiotic stress effects on grapevine (*Vitis vinifera* L.): focus on abscisic acid-mediated consequences on secondary metabolism and berry quality. *Environ. Exp. Bot.* 103, 138–147. doi: 10.1016/j.envexpbot.2013.10.012

Fraga, H., Malheiro, A. C., Moutinho-Pereira, J., and Santos, J. A. (2012). An overview of climate change impacts on European viticulture. *Food. Ener. Secur.* 1, 94–110. doi: 10.1002/fes3.14

Fraga, H., Santos, J. A., Malheiro, A. C., Oliveira, A. A., Moutinho-Perreira, J., and Jones, G. V. (2016). Climatic suitability of Portuguese grapevine varieties and climate change adaptation. *Int. J. Climatol.* 36, 1–12. doi: 10.1002/joc.4325

Gambetta, G. A., Matthews, M. A., Shaghasi, T. H., McElrone, A. J., and Castellarin, S. D. (2010). Sugar and abscisic acid signaling orthologs are activated at the onset of ripening in grape. *Planta* 232, 219–234. doi: 10.1007/s00425-010-1165-2

Giribaldi, M., Gény, L., Delrot, S., and Schubert, A. (2010). Proteomic analysis of the effects of ABA treatments on ripening *Vitis vinifera* berries. *J. Exp. Bot.* 61, 2447–2458. doi: 10.1093/jxb/erq079

Giribaldi, M., Perugini, I., Sauvage, F. X., and Shubert, A. (2007). Analysis of protein changes during grape berry ripening by 2-DE and MALDI-TOF. *Proteomics* 7, 3154–3170. doi: 10.1002/pmic.200600974

Girona, J., Marsal, J., Mata, M., del Campo, J., and Basile, B. (2009). Phenological sensitivity of berry growth and composition of Tempranillo grapevines (*Vitis vinifera* L.) to water stress. *Aust. J. Grape. Wine Res.* 15, 268–277. doi: 10.1111/j.1755-0238.2009.00059.x

Gollop, R., Even, S., Colova-Tsolova, V., and Perl, A. (2002). Expression of the grape dihydroflavonol reductase gene and analysis of its promoter region. *J. Exp. Bot.* 53, 1397–1409. doi: 10.1093/jexbot/53.373.1397

Greer, D. H., and Weedon, M. M. (2013). The impact of high temperatures on *Vitis vinifera* cv. Semillon grapevine performance and berry ripening. *Front. Plant Sci.* 4:491. doi: 10.3389/fpls.2013.00491

Intrigliolo, D. S., Pérez, D., Risco, D., Yeves, A., and Castel, J. R. (2012). Yield components and grape composition responses to seasonal water deficits in Tempranillo grapevines. *Irrig. Sci.* 30, 339–349. doi: 10.1007/s00271-012-0354-0

Jackman, R. L., and Smith, J. L. (1996). "Anthocyanins and betalains," in *Natural Food Colorants,* 2nd Edn., eds G. A. F. Hendry and J. D. Houghton (London: Chapman & Hall) 244–309.

Jeong, S. T., Goto-Yamamoto, N., Kobayashi, S., and Esaka, M. (2004). Effects of plant hormones and shading on the accumulation of anthocyanins and the expression of anthocyanin biosynthetic genes in grape berry skins. *Plant Sci.* 167, 247–252. doi: 10.1016/j.plantsci.2004.03.021

Jia, H. F., Chai, Y. M., Li, C. L., Lu, D., Luo, J. J., Qin, L., et al. (2011). Abscisic acid plays an important role in the regulation of strawberry fruit ripening. *Plant Physiol.* 157, 188–199. doi: 10.1104/pp.111.177311

Jones, G. V., and Goodrich, G. B. (2008). Influence of climate variability on wine region in the western USA and on wine in the Napa valley. *Clim. Res.* 35, 241–254. doi: 10.3354/cr00708

Karppinen, K., Hirvelä, E., Nevala, T., Sipari, N., Suokas, M., and Jaakola, L. (2013). Changes in the abscisic acid levels and related gene expression during fruit development and ripening in bilberry (*Vaccinium myrtillus* L.). *Phytochemistry* 95, 217–134. doi: 10.1016/j.phytochem.2013.06.023

Keller, M. (2010). Managing grapevines to optimise fruit development in a challenging environment: a climate change primer for viticulturists. *Aust. J. Grape Wine Res.* 16, 56–69. doi: 10.1111/j.1755-0238.2009.00077.x

Kennedy, J. A., Matthews, M. A., and Waterhouse, A. L. (2002). Effect of maturity and vine water status on grape skin and wine flavonoids. *Am. J. Enol. Vitic.* 53, 268–274.

Koyama, K., Sadamatsu, K., and Goto-Yamamoto, N. (2010). Abscisic acid stimulated ripening and gene expression in berry skins of the Cabernet Sauvignon grape. *Funct. Integr. Gen.* 10, 367–381. doi: 10.1007/s10142-009-0145-8

Kuhn, N., Guan, L., Dai, Z. W., Wu, B. H., Lauvergeat, V., Gomès, E., et al. (2013). Berry ripening, recently heard through the grapevine. *J. Exp. Bot.* 65, 4543–4559. doi: 10.1093/jxb/ert395

Lee, K. H., Piao, H. L., Kim, H. Y., Choi, S. M., Jiang, F., Hartung, W., et al. (2006). Activation of glucosidase via stress-induced polymerization rapidly increases active pools of abscisic acid. *Cell* 126, 1109–1120. doi: 10.1016/j.cell.2006.07.034

Lovisolo, C., Perrone, I., Carra, A., Ferrandino, A., Flexas, J., Medrano, H., et al. (2010). Drought-induced changes in development and function of grapevine (*Vitis* spp.) organs and in their hydraulic and non-hydraulic interactions at the whole-plant level: a physiological and molecular update 2010. *Funct. Plant Biol.* 37, 98–116. doi: 10.1071/FP09191

Malheiro, A. C., Santos, J. A., Fraga, H., and Pinto, J. G. (2010). Climate change scenarios applied to viticultural zoning in Europe. *Clim. Res.* 43, 163–177. doi: 10.3354/cr00918

Matthews, M. A., and Anderson, M. M. (1988). Fruit ripening in *Vitis vinifera* L.: responses to seasonal water deficits. *Am. J. Enol. Vitic.* 39, 313–320.

Myers, B. J. (1988). Water stress integral - a link between short-term stress and long-term growth. *Tree Physiol.* 4, 315–323. doi: 10.1093/treephys/4.4.315

Mira de Orduña, R. (2010). Climate change associated effects on grape and wine quality and production. *Food Res. Inter.* 43, 1844–1855. doi: 10.1016/j.foodres.2010.05.001

Mori, K., Goto-Yamamoto, N., Kitayama, M., and Hashizume, K. (2007). Loss of anthocyanins in red-wine grape under high temperature. *J. Exp. Bot.* 58, 1935–1945. doi: 10.1093/jxb/erm055

Nambara, E., and Marion-Poll, A. (2003). ABA action and interactions in seeds. *Trends Plant Sci.* 8, 213–217. doi: 10.1016/S1360-1385(03)00060-8

Niculcea, M., Lopez, J., Sanchez-Diaz, M., and Antolin, M. C. (2014). Involvement of berry hormonal content in the response to pre- and post-veraison water deficit in different grapevine (*Vitis vinifera* L.) cultivars. *Aust. J. Grape Wine Res.* 20, 281–291. doi: 10.1111/ajgw.12064

Niculcea, M., Martinez-Lapuente, L., Guadalupe, Z., Sánchez-Díaz, M., Morales, F., Ayestarán, B., et al. (2013). Effects of water deficit irrigation on hormonal content and nitrogen compounds in developing berries of *Vitis vinifera* L. cv. Tempranillo. *J. Plant Growth Reg.* 32, 551–563. doi: 10.1007/s00344-013-9322-z

OIV (1990). *Recueil des Méthodes Internationales D'analyse Des Vins et Des Moûts*, Vol. 2. Available online at: http://www.oiv.int/en/normes-et-documents-techniques/methodes-danalyse/recueil-des-methodes-internationales-danalyse-des-vins-et-des-mouts-2-vol

OIV (2016). *State of the Vitiviniculture World Market*. Available online at: http://www.oiv.int/public/medias/4587/oiv-noteconjmars2016-en.pdf

Owen, S. J., Lafond, M. D., Bowen, P., Bogdanoff, C., Usher, K., and Abrams, S. R. (2009). Profiles of abscisic acid and its catabolites in developing Merlot grape (*Vitis vinifera*) berries. *Am. J. Enol. Vitic.* 60, 277–284.

Peppi, M. C., and Fidelibus, M. W. (2008). Effects of Forchlorfenuron and abscisic acid on the quality of 'Flame Seedless' grapes. *HortScience* 43, 173–176.

Qin, X., and Zeevaart, J. A. D. (2002).Overexpression of a 9-cis-epoxycarotenoid dioxygenase gene in *Nicotiana plumbaginifolia* increases abscisic acid and phaseic acid levels and enhances drought tolerance. *Plant Physiol.* 128, 544–551. doi: 10.1104/pp.010663

Real, A. C., Borges, J., Sarsfield Cabral, J., and Jones, G. V. (2015). Partitioning the grapevine growing season in the Douro Valley of Portugal: accumulated heat better than calendar dates. *Int. J. Biometeorolo.* 59, 1045–1059. doi: 10.1007/s00484-014-0918-1

Reid, K. E., Olsson, N., Schlosser, J., Peng, F., and Lund, S. T. (2006). An optimized grapevine RNA isolation procedure and statistical determination of reference genes for real-time RT-PCR during berry development. *BMC Plant Biol.* 6:27. doi: 10.1186/1471-2229-6-27

Rienth, M., Torregosa, L., Luchaire, N., Chatbanyong, R., Lecourieux, D., Kelly, M. T., et al. (2014). Day and night heat stress trigger different transcriptomic responses in green and ripening grapevine (*Vitis vinifera*) fruit. *BMC Plant Biol.* 14:108. doi: 10.1186/1471-2229-14-108

Roby, G., and Matthews, M. A. (2004). Relative proportions of seed, skin and flesh, in ripe berries from Cabernet Sauvignon grapevines grown in a vineyard either well irrigated or under water deficit. *Aust. J. Grape Wine Res.*10, 74–82. doi: 10.1111/j.1755-0238.2004.tb00009.x

Romero, P., Fernández, J. I., and Botía, P. (2016). Interannual climatic variability effects on yield,berry and wine quality indices in long-term deficit irrigated grapevines, determined by multivariate analysis. *Inter. J. Wine Res.* 8, 3–17. doi: 10.2147/IJWR.S107312

Romero, P., Gil-Muñoz, R., del Amor, F. M., Valdés, E., Fernández, J. I., and Martinez-Cutillas, A. (2013). Regulated deficit irrigation based upon optimum water status improves phenolic composition in Monastrell grapes and wines. *Agric. Water. Manag.* 121, 85–101. doi: 10.1016/j.agwat.2013.01.007

Rustioni, L., Rossoni, M., Cola, G., Mariani, L., and Failla, O. (2011). Bunch exposure to direct solar radiation increases ortho-diphenol anthocyanins in norther Italy climate conditions. *J. Int. Sci. Vigne Vin* 45, 85–99. doi: 10.20870/oeno-one.2011.45.2.1489

Sadilova, E., Carle, R., and Stintzing, F. C. (2007). Thermal degradation of anthocyanins and its impact on colour and *in vitro* antioxidant capacity. *Mol. Nutr. Food Res.* 51, 1461–1471. doi: 10.1002/mnfr.200700179

Sadras, V. O., and Moran, M. A. (2012). Elevated temperature decouples anthocyanins and sugars in berries of Shiraz and Cabernet Franc. *Aust. J. Grape Wine Res.* 18, 115–122. doi: 10.1111/j.1755-0238.2012.00180.x

Sadras, V. O., Moran, M. A., and Bonada, M. (2013). Effects of elevated temperature in grapevine. I Berry sensory traits. *Aust. J Grape Wine Res.* 19, 95–106. doi: 10.1111/ajgw.12007

Santesteban, L. G., Miranda, C., and Royo, J. B. (2011). Regulated deficit irrigation effects on growth, yield, grape quality and individual anthocyanin composition in *Vitis vinifera* L. cv. Tempranillo. *Agric. Water Manag.* 98, 1171–1179. doi: 10.1016/j.agwat.2011.02.011

Santos, J. A., Grätsch, S. D., Karremann, M. K., Jones, G. V., and Pinto, J. G. (2012). Ensemble projections for wine production in the Douro Valley of Portugal. *Clim. Change* 117, 211–225. doi: 10.1007/s10584-012-0538-x

Seeram, N. P., Momin, R. A., Nair, M. G., and Bourquin, L. D. (2001). Cyclooxygenase inhibitory and antioxidant cyanidin glycosides in cherries and berries. *Phytomedicine* 8, 362–369. doi: 10.1078/0944-7113-00053

Shellie, K. C. (2011). Interactive effects of deficit irrigation and berry exposure aspect on Merlot and Cabernet Sauvignon in an arid climate. *Am. J. Enol. Vitic.* 62, 462–470.

Spayd, S. E., Tarara, J. M., Mee, D. L., and Ferguson, J. C. (2002). Separation of sunlight and temperature effects on the composition of *Vitis vinifera* cv. Merlot berries. *Am. J. Enol. Vitic.* 53, 171–182.

Speirs, J., Binney, A., Collins, M., Edwards, E., and Loveys, B. (2013). Expression of ABA synthesis and metabolism genes under different irrigation strategies and atmospheric VPDs is associated with stomatal conductance in grapevine (*Vitis vinifera* L. cv Cabernet Sauvignon). *J. Exp. Bot.* 64, 1907–1916. doi: 10.1093/jxb/ert052

Sun, L., Zhang, M., Ren, J., Qi, J., Zhang, G., and Leng, P. (2010). Reciprocity between abscisic acid and ethylene at the onset of berry ripening and after harvest. *BMC Plant Biol.* 10:257. doi: 10.1186/1471-2229-10-257

Symons, G. M., Davies, C., Shavrukov, Y., Dry, I. B., Reid, J. B., and Thomas, M. R. (2006). Grapes on steroids. Brassinosteroids are involved in grape berry ripening. *Plant Physiol.* 140, 150–158. doi: 10.1104/pp.105.070706

Tarara, J. M., Lee, J., Spayd, S. E., and Scagel, C. F. (2008). Berry temperature and solar radiation alter acylation, proportion, and concentration of anthocyanin in Merlot grapes. *Am. J. Enol. Vitic.* 59, 235–247.

Thioulouse, J., and Dray, S. (2009). *ade4TkGUI: ade4 Tcl/Tk Graphical User Interface*. R package version 0.2-5. Available online at: http://CRAN.R-project.org/package=ade4TkGUI

Wheeler, S., Loveys, B., Ford, C., and Davis, C. (2009). The relationship between the expression of abscisic acid biosynthesis genes, accumulation of abscisic acid and the promotion of *Vitis vinifera* L. berry ripening by abscisic acid. Aust. *J. Grape Wine Res.* 15, 195–204. doi: 10.1111/j.1755-0238.2008.00045.x

Zarrouk, O., Costa, J. M., Francisco, R., Lopes, C., and Chaves, M. M. (2016). "Drought and water management in Mediterranean vineyards," in *Grapevine in a Changing Environment: A Molecular and Ecophysiological Perspective*, eds S. Delrot, M. Chaves, H. Gerós, and H. Medrano (Chichester: Wiley-Blackwell), 38–67.

Zarrouk, O., Francisco, R., Pinto-Marijuan, M., Brossa, R., Santos, R. R., Pinheiro, C., et al. (2012).Impact of irrigation regime on berry development and flavonoids composition in Aragonez (Syn. Tempranillo) grapevine. *Agric. Water Manag.* 114, 18–29. doi: 10.1016/j.agwat.2012.06.018

Zhang, G., Duan, C., Wang, Y., Wang, Y., Ji, K., Xu, H., et al. (2013). The expression pattern of β-glucosidase genes *(VvβGs)* during grape berry maturation and dehydration stress. *Plant Growth Reg.* 70, 105–114. doi: 10.1007/s10725-012-9782-3

Zifkin, M., Jin, A., Ozga, J. A., Zaharia, L. I., Schernthaner, J. P., Gesell, A., et al. (2012). Gene expression and metabolite profiling of developing hidhbush bluberry fruit indicates transcriptional regulation of flavonoid metabolism and activation of abscisic acid metabolism. *Plant Physiol.* 158, 200–224. doi: 10.1104/pp.111.180950

Conflict of Interest Statement: The authors declare that the research was conducted in the absence of any commercial or financial relationships that could be construed as a potential conflict of interest.

frontiers in Plant Science

ORIGINAL RESEARCH
published: 13 May 2016
doi: 10.3389/fpls.2016.00658

Identification of Rapeseed MicroRNAs Involved in Early Stage Seed Germination under Salt and Drought Stresses

*Hongju Jian †, Jia Wang †, Tengyue Wang, Lijuan Wei, Jiana Li and Liezhao Liu **

Chongqing Engineering Research Center for Rapeseed, College of Agronomy and Biotechnology, Southwest University, Chongqing, China

Drought and salinity are severe and wide-ranging abiotic stresses that substantially affect crop germination, development and productivity, and seed germination is the first critical step in plant growth and development. To comprehensively investigate small-RNA targets and improve our understanding of miRNA-mediated post-transcriptional regulation networks during *Brassica napus* seed imbibition under drought and salt stresses, we constructed three small-RNA libraries from *B. napus* variety ZS11 embryos exposed to salt (200 mM NaCl, denoted "S"), drought (200 g L^{-1} PEG-6000, denoted "D"), and distilled water (denoted "CK") during imbibition and sequenced them using an Illumina Genome Analyzer. A total of 11,528,557, 12,080,081, and 12,315,608 raw reads were obtained from the CK, D, and S libraries, respectively. Further analysis identified 85 known miRNAs belonging to 31 miRNA families and 882 novel miRNAs among the three libraries. Comparison of the D and CK libraries revealed significant down-regulation of six miRNA families, miR156, miR169, miR860, miR399, miR171, and miR395, whereas only miR172 was significantly up-regulated. In contrast, comparison of the S library with the CK library showed significant down-regulation of only two miRNA families: miRNA393 and miRNA399. Putative targets for 336, 376, and 340 novel miRNAs were successfully predicted in the CK, D, and S libraries, respectively, and 271 miRNA families and 20 target gene families [including disease resistance protein (DIRP), drought-responsive family protein (DRRP), early responsive to dehydration stress protein (ERD), stress-responsive alpha-beta barrel domain protein (SRAP), and salt tolerance homolog2 (STH2)] were confirmed as being core miRNAs and genes involved in the seed imbibition response to salt and drought stresses. The sequencing results were partially validated by quantitative RT-PCR for both conserved and novel miRNAs as well as the predicted target genes. Our data suggest that diverse and complex miRNAs are involved in seed imbibition, indicating that miRNAs are involved in plant hormone regulation, and may play important roles during seed germination under salt- or drought-stress conditions.

Keywords: drought stress, salt stress, microRNA, *Brassica napus*, seed germination

OPEN ACCESS

Edited by:
Alison Kingston-Smith, Aberystwyth University, UK

Reviewed by:
Shirish Anand Ranade, CSIR-National Botanical Research Institute, India
Anyela Valentina Camargo Rodriguez, Aberystwyth University, UK

****Correspondence:***
Liezhao Liu
liezhao2003@126.com

† These authors have contributed equally to this work.

Specialty section:
This article was submitted to Agroecology and Land Use Systems, a section of the journal Frontiers in Plant Science

Received: *14 October 2015*
Accepted: *29 April 2016*
Published: *13 May 2016*

Citation:
Jian H, Wang J, Wang T, Wei L, Li J and Liu L (2016) Identification of Rapeseed MicroRNAs Involved in Early Stage Seed Germination under Salt and Drought Stresses. Front. Plant Sci. 7:658. doi: 10.3389/fpls.2016.00658

INTRODUCTION

Drought and salinity are severe and wide-ranging abiotic stresses that substantially affect the germination, development, and productivity of crops. Unlike most animals, plants are sessile organisms that have evolved mechanisms to cope with a wide range of changes in the environment and climate through the regulation of gene expression (Sunkar, 2010). These mechanisms involve complicated biological processes that finely coordinate molecular signaling pathways. To prevent cellular damage and to aid in recovery, specific genes, or proteins are activated at the molecular level by various stresses (Chinnusamy et al., 2007; Shinozaki and Yamaguchi-Shinozaki, 2007). Although there are specific pathways for each stress, certain key genes, or proteins act as nodal components that are integral in stress responsive signal transduction pathways (Knight and Knight, 2001; Fujita et al., 2006). Much effort has been devoted to elucidating gene expression in plants exposed to dry and brackish conditions; however, the mechanisms underlying the regulation of gene expression under these conditions remain largely unknown.

Various types of short and long non-coding RNAs (ncRNAs) are of great interest to molecular biologists. Among ncRNA subclasses, microRNAs (miRNAs), which are endogenous, non-coding RNAs ∼21 nucleotides in length that negatively regulate gene expression at the transcriptional, post-transcriptional, and translational levels in both plants and animals (Bartel, 2004; Brodersen et al., 2008; Yang X. Y. et al., 2013), are the most thoroughly characterized (Bartel, 2009). The first discovered miRNAs were *lin-4* and *let-7*, which control developmental timing in *Caenorhabditis elegans* and were later identified in almost all multicellular eukaryotes (Lee et al., 1993). In plants, miRNAs are involved in controlling many biological and metabolic processes, including organ maturation (Juarez et al., 2004; Guo et al., 2005), hormone signaling (Liu et al., 2009), developmental timing (Achard et al., 2004), and responses to pathogens (Sullivan and Ganem, 2005; Navarro et al., 2006) as well as to environmental abiotic stresses such as drought (Zhao et al., 2007), salinity (Zhao et al., 2009), heavy metals (Huang et al., 2009), and cold (Zhou et al., 2008). For example, miR159 and miR160 have been shown to be involved in the regulation of seed germination through effects on the sensitivity of seeds to abscisic acid (ABA) and auxin, suggesting that these miRNAs may function in the seed germination process (Reyes and Chua, 2007; Nonogaki, 2010). Many other miRNAs have also been shown to act under conditions of environmental stress, such as miR169 with high salt (Zhao et al., 2009), miR395 with sulfate starvation (Jones-Rhoades and Bartel, 2004), and miR398 with heavy metal toxicity (Sunkar et al., 2006). To date, more than 40 miRNA families have been observed to be involved in responses to abiotic stresses in plants (Sunkar, 2010), many of which are involved in responses to salt and drought stresses (Xiong et al., 2006; Peng et al., 2014). In addition, some miRNAs have been identified in more than one plant species (Sunkar et al., 2007), suggesting that their function in response to stress might be conserved among species, whereas others, called non-conserved or novel microRNAs, are species or tissue specific.

Brassica napus L. (AACC, $2n = 38$), commonly known as rapeseed, is an amphidiploid species that originated from interspecies crosses between *Brassica rapa* (AA, $2n = 20$) and *Brassica oleracea* (CC, $2n = 18$). *B. napus* is the third most economically important member of the genus *Brassica*, provides many useful products, and is grown worldwide (Dalton-Morgan et al., 2014). Similar to all crops, exposure to soil salinity and drought stresses at specific developmental stages in *Brassica* leads to compromised growth, development, and seed production. Although miRNAs and their targets have been widely studied in model plants, there is only limited knowledge to date on the small-RNA population of rapeseed. In the first report of miRNAs in *Brassica*, Xie et al. (2007) identified 21 miRNAs in *B. napus* using computational methods (Xie et al., 2007). Pant et al. (2009) performed the first deep sequencing of small-RNA libraries to identify phosphate deprivation-responsive miRNAs in *B. rapa* and *Arabidopsis* (Pant et al., 2009). A study of the global miRNA response to phosphate deficiency and cadmium stress in *B. napus* was conducted by Huang et al. (2010), validating *BnAPS3*, *BnAPS4,* and *BnSultr2:1* as targets of miR395. Subsequently, both conserved and *Brassica*-specific miRNAs were reported in studies of *B. rapa* (Kim et al., 2012; Wang F. D. et al., 2012; Yu et al., 2012), *B. napus* (Korbes et al., 2012; Wang J. Y. et al., 2012; Xu et al., 2012; Zhao et al., 2012; Zhou et al., 2012), *B. oleracea* (Wang J. Y. et al., 2012), and *Brassica juncea* (Yang J. H. et al., 2013).

Seed germination is the first critical step in plant growth and development. Plant development is determined by a multitude of factors that include genetic makeup and both biological and non-biological challenges. As abiotic stresses, such as drought, salt, heat, cold, and heavy metals, are major factors affecting seed germination, it is important to study the regulatory molecules and associated gene networks of seed germination under drought and salt stresses to improve crop yields via biotechnology, particularly with respect to the possible small RNA-mediated regulation of seed germination under such stress (Martin et al., 2010). miRNA expression during seed germination has been characterized in maize (Wang et al., 2011) and *Arabidopsis thaliana* (Jung and Kang, 2007; Kim et al., 2010) by analyzing conserved miRNAs derived from miRBase (Griffiths-Jones et al., 2008) through high-throughput sequencing. Since the initial report on rapeseed miRNAs, many conserved and rapeseed-specific miRNAs in different tissues have been identified as being involved in different biological processes (Buhtz et al., 2008; Huang et al., 2010; Korbes et al., 2012; Xu et al., 2012; Zhao et al., 2012; Zhou et al., 2012). However, the roles of miRNAs during *B. napus* seed germination under drought and salt stresses remain largely unknown. Potential information about miRNA mediated regulation under salt and drought stresses in rapeseed which may help to explore genomics behind stress mediated response.

To investigate small-RNA targets comprehensively and to further understand the miRNA-mediated post-transcriptional regulation network during rapeseed germination under drought and salt stresses, we constructed three small-RNA libraries from embryos of *B. napus* variety ZS11 seeds undergoing 60 h of imbibition under salt (S) or drought (D) stress compared to distilled water (CK) and then performed miRNA sequencing.

The miRNAs and targets identified in this study may facilitate an understanding of the molecular mechanisms of stress signaling.

MATERIALS AND METHODS

Plant Material, RNA Isolation, and Small-RNA High-Throughput Sequencing

Healthy *B. napus* ZS11 seeds were surface sterilized and soaked using filter paper as the underlay in distilled water, 200 mM NaCl, or 200 g L^{-1} PEG-6000 solution, marked CK, S, and D, respectively; three replicates were performed. The seeds were incubated at 22°C in darkness for 60 h until the hypocotyl emerged but the length was <2 mm. The embryo and hypocotyl together were frozen in liquid nitrogen immediately after collection and then stored at −80°C. Total RNA was isolated using TRIzol H (Invitrogen, USA) according to the manufacturer's instructions. The quality of the RNA samples was evaluated as described previously (Han et al., 2014). Three RNA samples were sent to BGI (Shenzhen, China) for sRNA library construction and Solexa sequencing using the Illumina HiSeq 2000 platform according to the manufacturer's protocols (Liang et al., 2010).

Small-RNA Data Analysis

Small-RNA reads of each sample were filtered with the SOAPnuke software (http://soap.genomics.org.cn/) (Li et al., 2009), developed by the Beijing Genome Institute (BGI), to remove low-quality reads, reads smaller than 18 nt, adaptor sequences, and contamination formed by adaptor–adaptor ligation according to the software's default settings (http://soap.genomics.org.cn). The Rfam database (http://www.sanger.ac.uk/software/Rfam) (Griffiths-Jones et al., 2005) and the GenBank noncoding RNA database (http://www.ncbi.nlm.nih.gov/) were used to annotate these perfectly matched sequences, which might include noncoding RNAs (e.g., tRNA, rRNA, snRNA, and snoRNA) or mRNA degradation fragments. Subsequently, small RNAs were aligned to miRNA precursors of rapeseed in miRBase 21.0 (Kozomara and Griffiths-Jones, 2014) to obtain known miRNAs with the following two criteria: (1) the small RNA tags align to the miRNA precursors in miRBase with no mismatches; (2) after fulfilling the first criterion, the tags align to mature miRNAs in miRBase with at least 16 nt of overlap, allowing for offsets. Those miRNAs that satisfied both the above criteria were counted to determine the expression of known miRNAs. In addition, sequencing data of three samples were uploaded to NIH Short Read Archive with accession number SRP073343.

Prediction of Novel miRNAs

To identify novel miRNAs in rapeseed, small-RNA sequences were aligned to the *B. napus* genome sequence to obtain precursor sequences. Novel miRNA candidates were identified with the Mireap program developed by the BGI. The sequences were regarded as novel miRNA candidates only if their structures met the previously reported criteria (Allen et al., 2005; Wang et al., 2011). Briefly, the secondary structures of filtered pre-miRNA sequences were checked using Mfold (Wiese and Hendriks, 2006). In each case, only the structure exhibiting the minimum free energy was selected for manual inspection.

Target Gene Prediction

The psRobot software (Wu et al., 2012) was used to predict the potential targets of newly identified miRNAs responsive to salt and drought stresses. All predicted target genes were assessed using the scoring system and according to previously described criteria (Srivastava et al., 2014). Genes with a score <2.5 were considered miRNA targets.

Expression Analysis of Rapeseed miRNAs Using qRT-PCR

Samples of embryos were collected from the CK, D, and S treatments via the same method used for miRNA library construction. Total RNA from each sample was extracted as described above. miRNA abundance was checked by qPCR according to previous reports (Shi and Chiang, 2005). The addition of poly(A) tails to sRNAs by poly(A) polymerase and cDNA synthesis was carried out using miRcute miRNA First-Strand cDNA Synthesis Kit (TIANGEN, Beijing, China), and qPCR was performed with miRcute miRNA qPCR Detection Kit according to the manufacturer's instructions. qPCR was performed using a CFX96 Real-time System (BIO-RAD, USA) with SYBR® Premix (TIANGEN, Beijing, China). The miRNA-specific forward primer for each miRNA was designed based on the entire miRNA sequence with the Tm adjusted to 60°C (**Table S1**).The universal reverse primer was designed based on the adapter sequence, which was provided with the miRNA cDNA synthesis kit (TIANGEN, Beijing, China). The *B. napus* U6 gene was used as the internal control to normalize the qPCR data, as previously described (Huang et al., 2010). The PCR conditions were as follows: 95°C for 2 min, followed by 40 cycles of 95°C for 20 s and 60°C for 30 s. A final ramping stage of 65–95°C was performed to confirm the absence of multiple products and primer dimers. The fold-changes in miRNA expression level were calculated using the comparative Ct ($2^{-\Delta\Delta Ct}$) method and normalized against the expression level in the CK sample. Triplicate biological and technological replicates were performed for the three samples.

Validation of Predicted miRNA Target Gene Expression Profiles by Quantitative RT-PCR

Predicted target genes were obtained from the *B. napus* Sequence database (http://www.genoscope.cns.fr/brassicanapus/). The software Primer Premier 5.0 (PREMIER Biosoft Int., Palo Alto, CA, USA) was used to design specific primers for quantitative RT-PCR (**Table S2**), and qPCR was performed using a CFX96 Real-time System (BIO-RAD, USA) with SYBR® Premix (TIANGEN, Beijing, China). Briefly, each 20 μL PCR reaction contained ∼100 ng cDNA, 8 μL 2.5× RealMasterMix/20× SYBR solution, and 200 nM each primer. The PCR conditions were as follows: 94°C for 2 min, followed by 40 cycles of 94°C for 15 s and 60 °C for 30 s. A final ramping stage of 65–95°C was performed to confirm the absence of multiple products and primer dimers. Actin was used for each sample as an endogenous control. All samples were subjected to at least three technical

replicates. Data were analyzed using the Ct ($2^{-\Delta\Delta Ct}$) method described above. Moreover, the software SPSS19.0 (SPSS Inc., Chicago, IL, USA) was used for statistical analysis in this study.

RESULTS

Sequence Analysis of Short RNAs

To identify and characterize conserved and novel miRNAs involved in *B. napus* seed germination in response to salt and drought stresses, we constructed three small-RNA libraries and obtained sequence reads by Illumina high-throughput sequencing. A total of 11,528,557, 12,080,081, and 12,315,608 raw reads were obtained from the control, drought, and salt stress treatments, respectively. After the removal of low-quality reads, 3′ adapters and 5′ adapters, reads shorter than 18 nt, and other contaminating sequences, 11,317,915 (98.68%), 11,917,020 (99.17%), and 12,087,933 (98.66%) clean reads representing 3,754,707, 4,246,335, and 3,658,598 unique sequences were obtained, respectively (**Table S3**). Additionally, we annotated all 18–28 nt reads from the CK, D, and S libraries and obtained 4,534,861, 5,095,273, and 4,454,112 unique reads, respectively (**Table 1**). Approximately 2.74, 1.59, and 2.24% of the unique reads matched noncoding RNAs (rRNAs, tRNAs, snRNAs, snoRNAs), accounting for 11.06, 10.84, and 16.05% of the total reads in the CK, D, and S libraries, respectively (**Table 1**). Subsequently, ∼15.38, 14.99, and 15.54% of the reads in CK, D, and S libraries, respectively, were mapped to coding sequences, which may constitute RNA degradation products, whereas a very small percentage of reads were mapped to intron sequences, which may be able to produce pre-miRNAs.

The distribution of various sizes of the small RNAs was not homogeneous. The most abundant were small RNAs 20–24 nt in length (**Figure 1**), among which sequences 24 nt long were in the greatest abundance, accounting for 39.42, 47.82, and 38.69% of the sequences in the control, drought, and salt libraries, respectively. These results are similar to those in other plant species, including *A. thaliana* (Rajagopalan et al., 2006), *Arachis hypogaea* (Zhao et al., 2010), *Oryza sativa* (Morin et al., 2008), *Populus* spp. (Lu et al., 2005), and *Zea mays* (Wang et al., 2011). The second most abundant sequences were 23 nt in length, accounting for 13.81% of the sequences in the drought stress library, whereas sequences with a length of 20 nt were the second most abundant in the control and salt stress libraries, accounting for 19.50 and 18.16%, respectively.

Identification of Conserved miRNAs in the Three Libraries

Conserved miRNA families found in many species are responsive to many changes in the plant life cycle. To identify such conserved miRNAs in the three libraries, unique reads (minus reads mapping to snRNAs, snoRNAs, tRNAs, intron sequences, and coding sequences) from the libraries were subjected to a homolog search against miRBase21.

In the CK, D, and S libraries, 85, 81, and 81 known miRNAs, respectively, were found, belonging to 29, 29, and 28 different miRNA families, respectively, with an average of 3 miRNA members per family among the three libraries (**Table S4**). The miRNA members of known families were highly divergent. Briefly, the miR169 family was the most abundant, with 14 members distinguished by internal nucleotide differences in the CK, S, and D small-RNA libraries, and 6–7 members of the miR156, miR166, miR171, and miR395 families were also found. Of the remaining miRNA families, 7 families had 2–4 members and 15 families had a single member in at least one library (**Figure 2**).

TABLE 1 | Distribution of small RNAs among different categories in three libraries.

Locus class	CK				D				S			
	Total		Unique		Total		Unique		Total		Unique	
NONPROTEIN-CODING RNAs												
snoRNA	5352	0.05%	2239	0.05%	6645	0.06%	2802	0.05%	5057	0.04%	2252	0.05%
snRNA	8346	0.07%	3384	0.07%	9371	0.08%	3646	0.07%	9674	0.08%	3586	0.08%
tRNA	216,253	1.91%	7683	0.17%	167,375	1.40%	7226	0.14%	267,363	2.21%	8886	0.20%
rRNA	1,021,790	9.03%	65,548	1.45%	1,108,552	9.30%	67,536	1.33%	1,657,908	13.72%	84,936	1.91%
SMALL RNAs MATCHING PROTEIN-CODING GENES												
exon_antisense	242,071	2.14%	106,937	2.36%	278,336	2.34%	120,562	2.37%	248,569	2.06%	108,882	2.44%
exon_sense	533,661	4.72%	148,056	3.26%	525,008	4.41%	160,432	3.15%	567,580	4.70%	159,510	3.58%
intron_antisense	368,034	3.25%	175,881	3.88%	430,309	3.61%	195,244	3.83%	366,290	3.03%	169,262	3.80%
intron_sense	722,449	6.38%	266,756	5.88%	809,310	6.79%	287,415	5.64%	705,803	5.84%	254,553	5.72%
miRNA	2,131,604	18.83%	503	0.01%	1,556,356	13.06%	511	0.01%	2,123,566	17.57%	496	0.01%
repeat	5537	0.05%	3060	0.07%	6978	0.06%	3521	0.07%	6125	0.05%	3114	0.07%
unannotation	6,062,818	53.57%	3,754,707	82.80%	7,018,780	58.90%	4,246,335	83.34%	6,129,998	50.71%	3,658,598	82.14%
Total	11,317,915	100%	4,534,754	100%	11,917,020	100%	5,095,230	100%	12,087,933	100%	4,454,075	100%

CK, control; D, drought stress; S, salt stress.

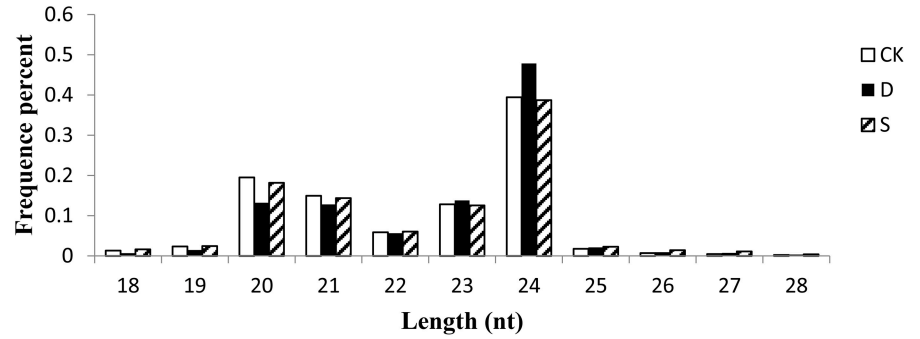

FIGURE 1 | Size distribution of small RNAs in CK, D, and S libraries from rapeseed. CK, control; D, drought stress; S, salt stress.

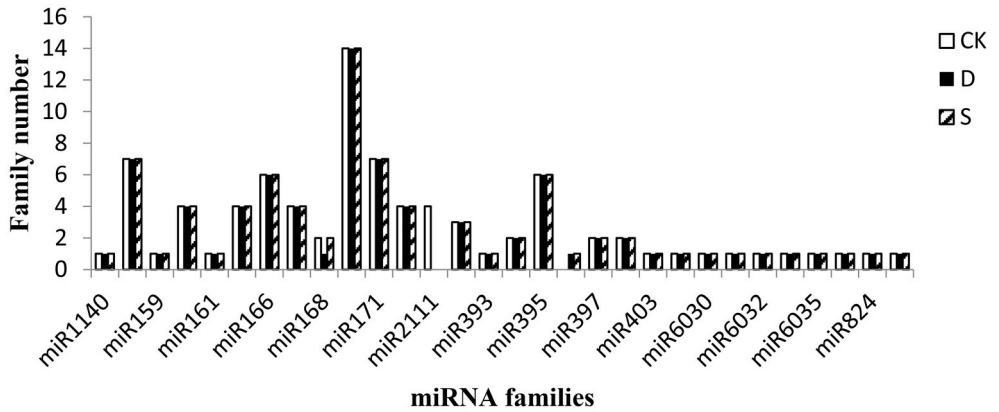

FIGURE 2 | Number of family members per miRNA family detected in the three libraries. Candidate miRNA families were considered together and grouped by their miRBase numerical identifiers. CK, control; D, drought stress; S, salt stress.

The relative abundance of miRNAs can be estimated by the number of reads revealed by high-throughput sequencing. Intriguingly, the rapeseed miRNA abundance exhibited substantial variation. For example, miR156, with 6,955,462, 4,784,853, and 6,920,959 redundancies in the CK, D, and S libraries, respectively, was the miRNA most frequently sequenced in the three libraries; in contrast, many miRNAs (e.g., miR6035, miR393, miR6034, miR2111, miR6036, and miR396) were sequenced <20 times (**Figure 3**, **Table 2**). Our sequence analysis indicated that the abundance of certain members of miRNA families can vary dramatically among the three libraries, suggesting functional variation within each family. As an example, the abundance of the miR168 family in the CK library varied from 1 read (miR168b) to 12,878 reads (miR168a) based on deep sequencing. Similar instances were found in other miRNA families, such as the miR156 (62,938–1,698,631 reads), miR167 (2785–240,853 reads), miR169 (8–2565 reads), and miR171 (6–592 reads) families. Such variation was similar in the other two libraries (**Table S5**), suggesting that distinct members in the same miRNA family have dramatically different levels of expression, likely due to tissue-specific, developmental stage-specific, or environment-specific expression.

Based on the criterion, $|\log_2$ fold change$| \geq 1.0$ and $P \leq 0.05$, the expression of miR166, miR167, and miR390, which were among the top 10 most expressed miRNAs, did not show significant differential expression. Indeed, only six miRNAs (miR156, miR169, miR171, miR395, miR399, and miR860), which were sequenced <50 times, were significantly differentially expressed between the drought stress and control treatments. Compared with salt stress, four miRNAs (miR171, miR393, miR395, and miR860) were markedly differentially expressed in the D library, and miR393 and miR399 were significantly differentially expressed in the CK library (**Table 2**). The miRNA family groups with similar expression patterns were then classified using Heatmap clustering. For instance, miR161, miR394, miR395, and miR403 were down-regulated by salt stress, whereas miR171, miR393, and miR824 were up-regulated by drought stress (**Figure S1**).

To explore the roles of these conserved miRNAs in evolution, further analyses focusing on broader comparisons against known conserved miRNAs in Viridiplantae, including Brassicaceae, Malvaceae, Rutaceae, Solanaceae, Salicaceae, Rhizophoraceae, and Lamiales, and even monocotyledons, Embryophyta, Coniferophyta, and Chlorophyta, were performed. Based on BLAST analysis, some miRNA families, such as miR156/157, miR159, miR160, miR165/166, miR171, and miR396, were found to be highly conserved (**Table S6**). For example, miR156/157 is highly expressed during the seedling stage in different species.

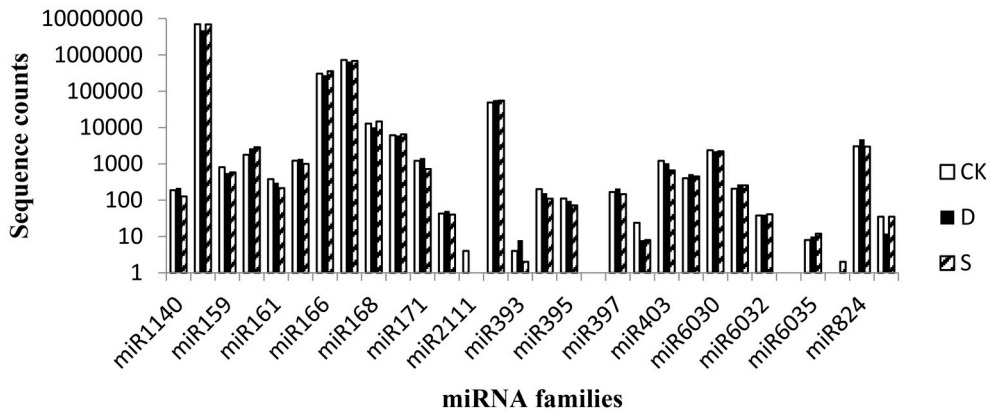

FIGURE 3 | Abundance of conserved miRNAs in the CK, D, and S libraries in rapeseed. CK, control; D, drought stress; S, salt stress.

Identification of Novel miRNAs in Rapeseed

Each species possesses species-specific miRNAs (Zhao et al., 2010; Chi et al., 2011; Li et al., 2011; Schreiber et al., 2011; Song et al., 2011; Gao et al., 2012; Guo et al., 2012; Lertpanyasampatha et al., 2012; Lv et al., 2012), and the characteristic hairpin structures of miRNA precursors, the Dicer cleavage site, and the minimum free energy are important factors for predicting novel miRNAs. Many papers have reported the prediction of novel miRNAs using Mireap according to strict criteria (Li et al., 2013), and based on these criteria, 882 novel miRNAs were predicted from the three libraries (**Table S7**). The lengths of the novel miRNAs were 20–23 nt, with 23 nt being the most common length in the three libraries (**Table S8**). More than half of the novel predicted miRNAs begin with a 5′ uridine, and these miRNAs accounted for more than eighty percent of small RNAs 20 and 21 nt in length (**Table S7**) (Bonnet et al., 2004; Zhang et al., 2006). According to Mfold3.2, the average negative minimal folding free energy of these miRNA precursors is approximately −245 to −18 kcal mol^{-1}, which was similar to miRNA precursors in other species (Wang et al., 2011). Compared with known miRNA families, the abundance of novel miRNAs was very low, and the majority of these miRNAs were present <100 times. Nonetheless, these miRNAs comprised 87.79% (367/418), 88.83% (382/430), and 88.92% (369/415) of the CK, D, and S libraries, respectively. The most abundant novel miRNA was novel_mir_34, which was sequenced 58,924, 70,723, and 60,320 times in the CK, D, and S libraries, respectively. Unlike conserved miRNAs, different types of novel miRNAs were expressed in the three independent libraries. Of the novel miRNAs identified, 199, 216, and 204 were specific to the CK, D, and S libraries, respectively, and only 118 were shared among the libraries. In the CK and D libraries, 170 novel miRNAs were shared, whereas 167 and 162 miRNAs were shared between the CK and S and D and S libraries, respectively (**Figure 4**).

Using the criteria of $|\log_2$ fold change$| \geq 1.0$ and $P \leq 0.05$, 268, 242, and 273 miRNAs exhibited significantly different expression between the CK and D, CK and S, and S and D libraries, respectively. Two novel miRNAs—bna-miR25 and bna-miR385—were significantly up-regulated under drought stress and down-regulated under salt stress, respectively (**Figure 5**).

Target Prediction of Rapeseed miRNAs

As the identification of mRNA targets is necessary for an understanding of the biological roles of *B. napus* miRNAs (Korbes et al., 2012), psRobot software was used to predict the targets of conserved and novel miRNAs. The cut-off threshold was set at 2.5, and 610 and 4133 putative targets were found for the conserved and 656 novel miRNA families, respectively (**Tables S9**, **S10**). However, no target genes were found for 226 of the novel miRNA families (**Table S11**). Various transcription factors, including SBP, MYB, ARF, NAM, NAC, CBF, TCP, NF-YA, and GRF, were among the majority of the conserved miRNA targets identified in different species, including *Arabidopsis* (Adai et al., 2005), grape (Carra et al., 2009), mustard (Xie et al., 2007), poplar (Lu et al., 2008), rice (Sunkar et al., 2005), soybean (Subramanian et al., 2008), and wheat (Jin et al., 2008). F-box protein, ATP sulfurylase, CCHC-type zinc finger protein, NAD(P)-binding protein, and Poly(ADP-ribose) polymerase, proteins involved in the regulation of metabolic processes, were also identified as conserved miRNA targets. In our datasets, miRNA156 showed the highest abundance, followed by miRNA167, miRNA166, and miRNA390, during the very early stage of seed germination under salt and drought stresses. miRNA156 is involved in floral development and phase change through down-regulation of the SQUAMOSA promoter binding protein-like (SPL) family of transcription factor genes, which are up-regulated in the juvenile phase and down-regulated in the adult phase (Wu et al., 2009; Zhang et al., 2009; Yang et al., 2011). Many studies have emphasized that the transcription factor HD-ZIP participates in plant leaf morphogenesis, and *ATHB15*, a member of the HD-ZIP family targeted by miRNA166, may play a role in plant vascular development because it is predominantly expressed in vascular tissues (Ohashi-Ito and Fukuda, 2003). The miRNA156 and miRNA166 families are very important in seed germination

TABLE 2 | The miRNA abundance of conserved miRNA families among control (CK), salt (S), and drought (D) treatments.

miR_name	Count			Fold change log_2 Ratio normalized			Significance		
	CK	D	S	D/CK	S/CK	S/D	D/CK	S/CK	S/D
bna-miR156f	1,698,631	1,178,297	1,692,709	−0.58	−0.11	0.48			
bna-miR156d	1,691,684	1,172,845	1,685,873	−0.58	−0.11	0.48			
bna-miR156a	1,690,785	1,172,163	1,685,001	−0.58	−0.11	0.48			
bna-miR156e	1,685,364	1,167,914	1,679,624	−0.59	−0.11	0.48			
bna-miR167a	240,853	217,836	228,063	−0.20	−0.18	0.02			
bna-miR167b	240,853	217,836	228,062	−0.20	−0.18	0.02			
bna-miR167c	240,687	217,691	227,973	−0.20	−0.18	0.02			
bna-miR156b	63,030	31,238	59,290	−1.07	−0.19	0.88	*		
bna-miR156c	63,030	31,237	59,289	−1.07	−0.19	0.88	*		
bna-miR156g	62,938	31,159	59,173	−1.07	−0.19	0.88	*		
bna-miR166e	58,893	53,340	68,334	−0.20	0.11	0.31			
bna-miR166b	58,893	53,337	68,334	−0.20	0.11	0.31			
bna-miR166c	58,893	53,337	68,333	−0.20	0.11	0.31			
bna-miR166a	58,877	53,342	68,310	−0.20	0.11	0.31			
bna-miR166d	58,786	53,247	68,200	−0.20	0.11	0.31			
bna-miR390b	16,224	19,115	18,376	0.18	0.08	−0.10			
bna-miR390a	16,222	19,111	18,371	0.18	0.08	−0.10			
bna-miR390c	16,222	19,111	18,371	0.18	0.08	−0.10			
bna-miR168a	12,878	10,166	14,762	−0.40	0.10	0.49			
bna-miR166f	11,544	10,656	13,676	−0.17	0.14	0.31			
bna-miR824	3047	4751	2977	0.58	−0.14	−0.72			
bna-miR167d	2785	2116	2489	−0.45	−0.26	0.19			
bna-miR169n	2565	3057	2933	0.20	0.09	−0.11			
bna-miR6030	2363	2238	2211	−0.13	−0.20	−0.06			
bna-miR169a	1310	1275	1439	−0.10	0.03	0.13			
bna-miR169b	1299	1269	1436	−0.09	0.04	0.13			
bna-miR403	1216	1048	661	−0.27	−0.98	−0.71			
bna-miR159	807	561	583	−0.58	−0.57	0.01			
bna-miR171f	592	673	344	0.13	−0.88	−1.01			*
bna-miR171g	592	673	344	0.13	−0.88	−1.01			*
bna-miR164a	493	546	403	0.09	−0.39	−0.48			
bna-miR160b	454	682	729	0.53	0.58	0.05			
bna-miR160d	454	682	729	0.53	0.58	0.05			
bna-miR160a	453	686	731	0.54	0.59	0.05			
bna-miR160c	426	613	683	0.47	0.58	0.11			
bna-miR6029	400	521	453	0.33	0.08	−0.25			
bna-miR161	380	303	216	−0.38	−0.92	−0.53			
bna-miR164b	245	278	199	0.13	−0.40	−0.53			
bna-miR164d	245	278	199	0.13	−0.40	−0.53			
bna-miR164c	243	277	199	0.13	−0.39	−0.52			
bna-miR6031	208	273	257	0.34	0.20	−0.13			
bna-miR1140	189	219	127	0.16	−0.68	−0.83			
bna-miR169g	148	68	106	−1.18	−0.58	0.59	*		
bna-miR169h	148	68	106	−1.18	−0.58	0.59	*		
bna-miR169k	148	68	106	−1.18	−0.58	0.59	*		
bna-miR169i	147	68	105	−1.17	−0.59	0.58	*		
bna-miR169j	147	68	105	−1.17	−0.59	0.58	*		
bna-miR169l	147	68	105	−1.17	−0.59	0.58	*		
bna-miR394a	101	78	55	−0.43	−0.98	−0.55			

(Continued)

TABLE 2 | Continued

miR_name	Count			Fold change log_2Ratio normalized			Significance		
	CK	D	S	D/CK	S/CK	S/D	D/CK	S/CK	S/D
bna-miR394b	100	78	55	−0.41	−0.96	−0.55			
bna-miR397a	84	105	73	0.27	−0.30	−0.57			
bna-miR397b	84	105	73	0.27	−0.30	−0.57			
bna-miR169m	40	31	23	−0.42	−0.90	−0.48			
bna-miR6032	38	40	41	0.02	0.01	−0.01			
bna-miR395a	35	31	21	−0.23	−0.84	−0.61			
bna-miR395b	35	31	21	−0.23	−0.84	−0.61			
bna-miR395c	35	31	21	−0.23	−0.84	−0.61			
bna-miR860	35	12	35	−1.60	−0.10	1.50	*		*
bna-miR172b	24	24	19	−0.06	−0.44	−0.38			
bna-miR399a	12	4	4	−1.64	−1.69	−0.05	*	*	
bna-miR399b	12	4	4	−1.64	−1.69	−0.05	*	*	
bna-miR172c	11	15	8	0.39	−0.56	−0.95			
bna-miR6035	8	10	12	0.27	0.48	0.22			
bna-miR169c	8	4	6	−1.06	−0.52	0.54	*		
bna-miR169d	8	4	6	−1.06	−0.52	0.54	*		
bna-miR169e	8	4	6	−1.06	−0.52	0.54	*		
bna-miR169f	8	4	6	−1.06	−0.52	0.54	*		
bna-miR171d	7	22	7	1.60	−0.10	−1.70	*		*
bna-miR171e	7	22	7	1.60	−0.10	−1.70	*		*
bna-miR171b	7	20	8	1.46	0.09	−1.37	*		*
bna-miR172a	7	8	11	0.14	0.55	0.41			
bna-miR171a	6	20	7	1.68	0.12	−1.56	*		*
bna-miR171c	6	20	7	1.68	0.12	−1.56	*		*
bna-miR393	4	8	2	0.94	−1.10	−2.05		*	*
bna-miR395d	2	1	3	−1.06	0.48	1.54	*		*
bna-miR395e	2	1	3	−1.06	0.48	1.54	*		*
bna-miR395f	2	1	3	−1.06	0.48	1.54	*		*
bna-miR172d	1	4	2	1.94	0.90	−1.05	*		*
bna-miR6036	1	1	2	−0.06	0.90	0.95			
bna-miR6034	1	1	0	−0.06	–	–			
bna-miR168b	1	0	1	–	−0.10	–			
bna-miR2111a-5p	1	0	0	–	–	–			
bna-miR2111b-3p	1	0	0	–	–	–			
bna-miR2111b-5p	1	0	0	–	–	–			
bna-miR2111d	1	0	0	–	–	–			
bna-miR396a	0	1	1	–	–	–			

Significant (*) if $|log_2$ fold change$| \geq 1.0$ and $P \leq 0.05$; otherwise insignificant. CK, control; D, drought stress; S, salt stress.

not only due to their high abundance but also because of the large size of those miRNA families compared to other miRNA families. Studies have demonstrated cross-talk regulation between ABA and auxin during seed germination (Weitbrecht et al., 2011), and miRNA167 and miRNA160 have been shown to be involved in inhibiting auxin response factors ARF6 and ARF8 (Wu et al., 2006) and ARF10, ARF16, and ARF17 (Mallory et al., 2005; Wang et al., 2005), respectively. Additionally, miRNA159 has been shown to be involved in the regulation of seed dormancy and germination by inhibiting *MYB33* and *MYB101*, two positive regulators of ABA response during germination.

To gain further insight into the functions of novel miRNAs in rapeseed during seed germination under salt and drought

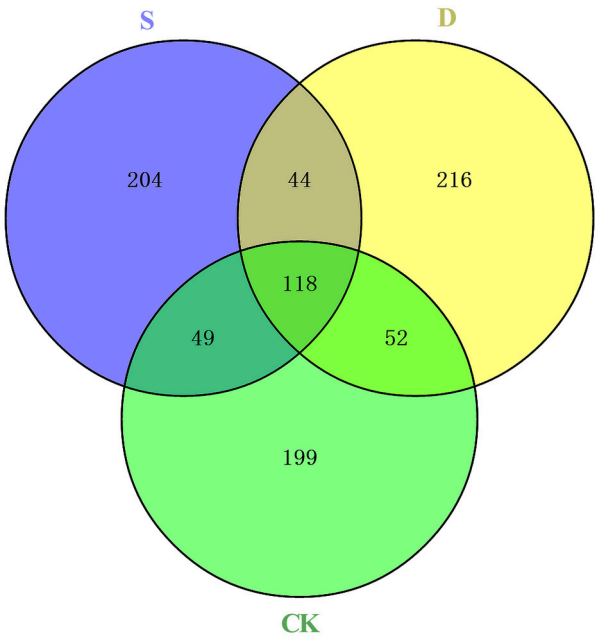

FIGURE 4 | Diagram of novel miRNAs identified in three libraries. CK, control; D, drought stress; S, salt stress.

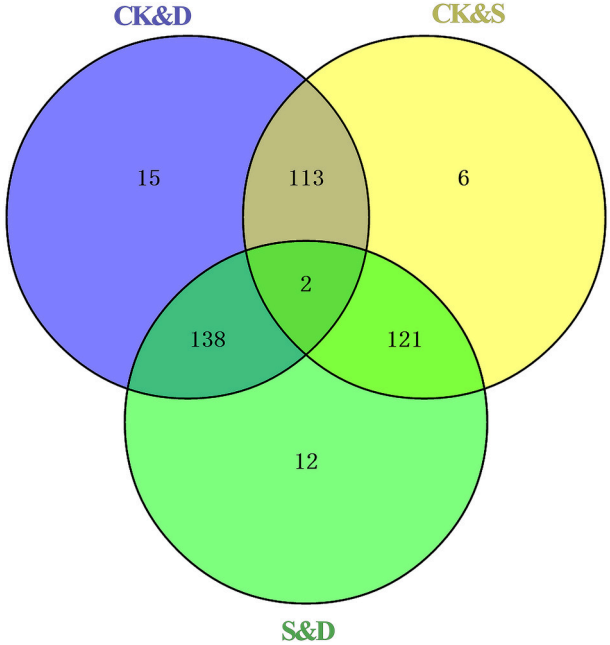

FIGURE 5 | Diagram of significantly different expression novel miRNAs between CK&D, CK&S, and S&D. CK, control; D, drought stress; S, salt stress.

stresses, putative targets of the 656 newly identified miRNAs were predicted, revealing various functions, including transcription, metabolism, transport, kinases, oxidative reduction and isomerase and helicase activities. According to miRNA regulatory network analysis using Cytoscape (http://www.cytoscape.org/), 271 miRNA families and 20 target gene families in rapeseed were confirmed to be core miRNAs and genes involved in response to salt and drought stresses. Direct stress-responsive gene families, such as disease resistance protein (DIRP), drought-responsive family protein (DRRP), early responsive to dehydration stress protein (ERD), stress-responsive alpha-beta barrel domain protein (SRAP), and salt tolerance homolog2 (STH2), were also predicted in our analysis. Overall, miRNA regulatory mechanisms responsive to salt and drought stresses are highly sophisticated in rapeseed, and these miRNAs and their targets related to stress response add to our knowledge of stress resistance and the stress tolerance mechanism in this plant.

Expression Profiles of miRNAs and Their Targets in Response to Salt and Drought Stresses

To confirm the expression patterns of miRNAs in response to salt and drought stresses, quantitative RT-PCR (qRT-PCR) was performed for 6 conserved miRNAs (miR1140, miR403, miR824, miR164a, miR166e, and miR169n) and 9 novel ones (bna-miR17, bna-miR37, bna-miR77, bna-miR122, bna-miR144, bna-miR290, bna-miR485, bna-miR516, and bna-miR700). As expected, the qRT-PCR results were consistent with the expression profiles obtained by RNA-seq (**Figure 6**). qRT-PCR was also performed on target genes of 17 randomly selected miRNAs, of which 8 are from known miRNA families (miR156b, miR403, miR160a, miR164a, miR166e miR171f, miR6030, and miR169n) and 9 from novel miRNA families (bna-miR17, bna-miR37, bna-miR77, bna-miR122, bna-miR144, bna-miR290, bna-miR485, bna-miR700, and bna-miR814). However, as illustrated in **Figure 7**, the expression profiles of 19 target genes showed an inverse relationship with the expression profiles of their corresponding miRNAs, suggesting that the miRNAs indeed target those genes.

DISCUSSION

Seed germination is a critical step in plant growth and development. However, abiotic stresses such as drought and salt are major factors affecting the seed germination rate. Thus, understanding this process as a whole—from early seed germination to the establishment of the seedling—can help us to engineer and select more robust crop species and increase crop yield and quality. In this study, three sRNA libraries from imbibed seed embryos under control, salt, and drought treatments were constructed, and miRNAs were sequenced using high-throughput sequencing.

Many miRNAs Participate in Rapeseed Germination

High-throughput sequencing has been applied to study miRNAs at the whole-genome level in many plant species. However,

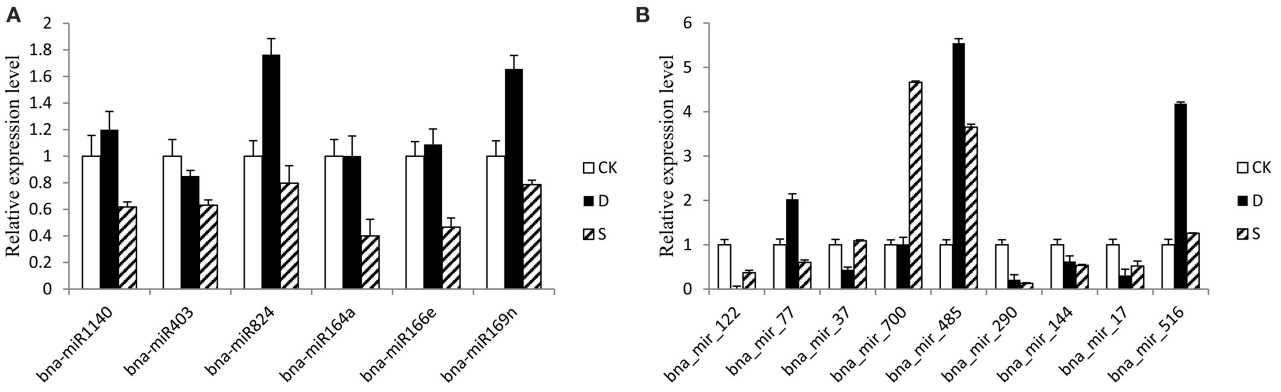

FIGURE 6 | Quantitative RT-PCR validation of mature miRNAs. The expression profiles of mature miRNAs were consistent with the results obtained by small-RNA deep sequencing. The expression values presented are the means of three technical replicates. U6 was used for each sample as an endogenous control. **(A,B)** Represent the expression pattern of mature conserved and novel miRNAs, respectively.

the means by which miRNA families function in plant development, stress responses, and other processes in *B. napus*, one of the most important oil crops in the world, are not very clear. In our study, the three libraries contained 35,322,868 clean reads and 14,084,059 unique small-RNA reads. Two of the three libraries shared from 65.27 to 67.88% of the total clean reads; however, they shared only 14.34–14.68% of the unique small-RNA reads, a phenomenon also observed in maize (Li et al., 2013). These findings suggest that the shared reads have high expression levels and the library-specific small RNAs low expression levels. The low expression levels of these specific unique small RNAs may indicate that they function in specific and unique regulation pathways.

Successful seed germination and the establishment of a normal seedling are essential. Although the evidence is fragmentary, there are several sources that emphasize miRNAs as a very important component of seed germination (Li et al., 2013; Zhang et al., 2013). For instance, Weitbrecht et al. (2011) highlighted that ABA and gibberellin acid (GA) play vital roles in seed germination. Briefly, ABA levels generally decrease during imbibition, whereas GA levels increase during the transition to germination. In *Arabidopsis*, two positive ABA regulators, *MYB33* and *MYB101*, which are negatively regulated by miR159, play key roles in seed germination. In the present study, *BnaA04g18810D* and *BnaC04g43020D*, homologs of *AtMYB101*, were predicted to be target genes of miR159. In the absence of miR159, *MYB33,* and *MYB101* up-regulated genes are deregulated during seed germination (Alonso-Peral et al., 2010); thus, *MYB-like* genes participate in GA-induced pathways via miR159-mediated regulation during seed germination. AUXIN RESPONSIVE FACTORs (ARFs), which are pivotal for translating auxin signals into transcriptional responses, comprise a class of targets for the miRNA160/167 families. Indeed, studies have shown that the negative regulation of ARF10 by miR160 plays an important role in seed germination (Liu et al., 2007), and miR167 regulates ARF6 and ARF8 in adventitious rooting in *Arabidopsis* (Gutierrez et al., 2009) and in cultured rice cells (Yang et al., 2006). The crosstalk between ABA and auxin in imbibed mature seeds has been discussed by Liu et al. (2007), and studies have indicated that ABA sensitivity would decrease in mature seeds via the down-regulation of auxin signal transduction. Regardless, the mechanisms of ABA-auxin crosstalk during seed germination remain enigmatic. Laccases, which are involved in the lignification and thickening of the cell wall during secondary cell growth (Constabel et al., 2000), were found to be down-regulated by miR397, suggesting that miR397 plays a vital role in decreasing the thickness of the cell wall during the transition from a dormant embryo to a germinated embryo by causing laccase mRNA cleavage. Other miRNA families have been reported to be involved in seed germination in other species, such as miR166 (*HD-ZIP*), miR164 (*NAC1*), and miR396 (*GRF*) (Tahir et al., 2006; Li et al., 2013; Zhang et al., 2013). These findings indicate the existence of complex mechanisms of gene regulation involving miRNAs during seed germination.

Potential Roles of miRNAs in Seed Germination Response to Salt and Drought Stresses

Many conserved and novel miRNAs are aberrantly expressed in drought stress in different crops, such as cowpea (Barrera-Figueroa et al., 2011), tobacco (Frazier et al., 2011), wheat (Kantar et al., 2011), soybean (Kulcheski et al., 2011), and bean (Arenas-Huertero et al., 2009). miR169, one of the most important miRNAs involved in drought stress, was down-regulated in our study. Similarly, the expression of miR169a and miR169c in *Arabidopsis* decreased under drought stress, and the miR169-target gene *NFYA5*, a member of the *Arabidopsis* family of CCAAT-box nuclear transcription factors functioning in drought resistance, was strongly induced (Li et al., 2008). However, miR169 was found to be up-regulated in rice and tomato under drought conditions (Zhao et al., 2007; Zhang et al., 2011). The three nuclear factor Y subunit genes (SlNF-YA1/2/3) targeted by miR169

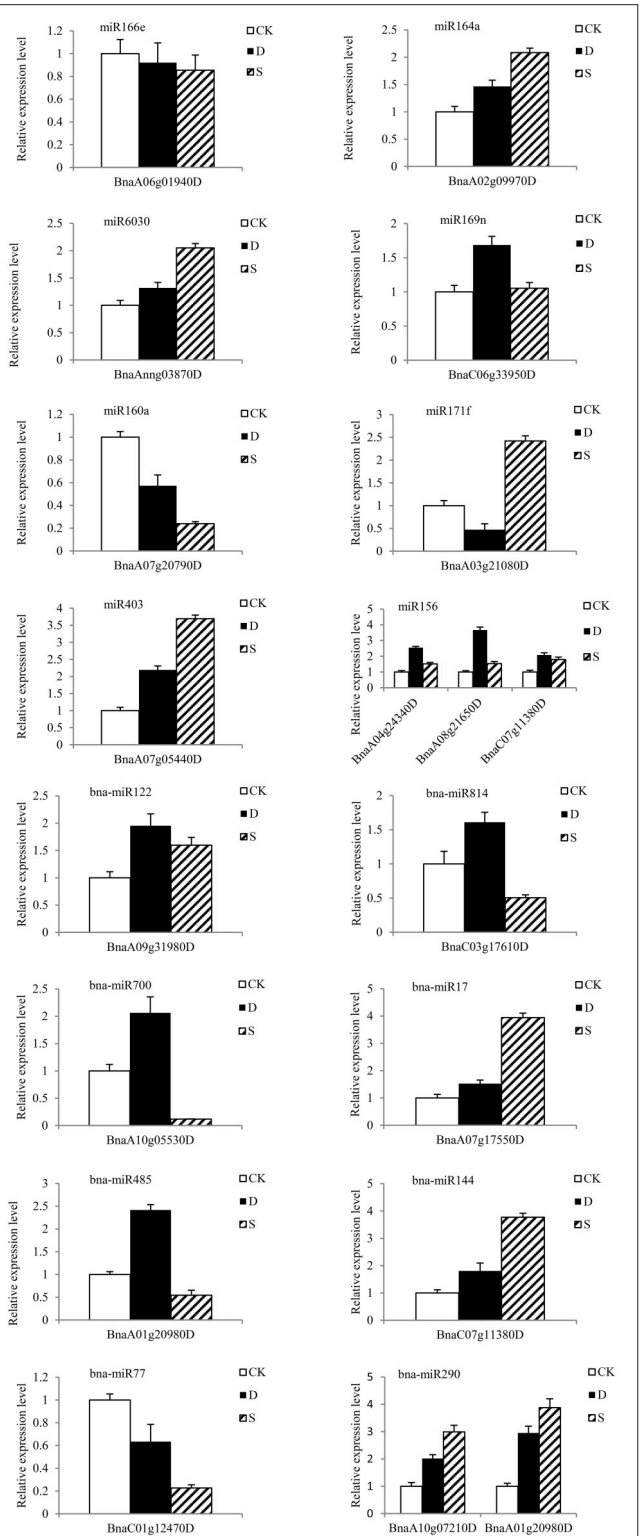

FIGURE 7 | Quantitative RT-PCR analyses of relative expression levels of various predicted target genes. The rapeseed housekeeping gene actin7 was used as the internal control. The values presented are the means of three technical replicates.

were also down-regulated. Moreover, overexpressing miR169c in tomato plants resulted in better tolerance to drought. In *Arabidopsis*, miR157, miR167, miR168, miR171, miR408, miR393, and miR396 were reported to be up-regulated in response to drought stress (Liu et al., 2008). In our study, miR156b/c/g, miR171a/d/e, and miR172d were significantly up-regulated, whereas miR860, miR399a/b, and miR395d/e/f were down-regulated.

Although plants invoke similar cellular and metabolic responses to salt and drought stresses (Munns, 2005), the genes and pathways involved vary (Bartels and Sunkar, 2005; Golldack et al., 2011). In our study, miR393 and miR399, both are involved in phosphate homeostasis, were significantly down-regulated. However, miR399 was up-regulated under low phosphate in *Arabidopsis* (Fujii et al., 2005) and rice (Wang et al., 2009). When plants suffer from phosphate starvation, mature miR399 activated by the PHR1 transcription factor cleaves target PHO2 mRNA (Pant et al., 2008). In addition, mRNAs of TIR1/AFB2 auxin receptors (TAARs), regulators of auxin signaling homeostasis, are targeted and cleaved by up-regulated miR393 during salt and drought stresses in *O. sativa*, *A. thaliana*, *M. truncatula,* and *Phaseolus vulgaris* (Dharmasiri et al., 2005; Chen et al., 2011; Si-Ammour et al., 2011; Windels and Vazquez, 2011). miR393 also functions in the root development response to nitrate treatment by cleaving TAAR transcripts, which are positive regulators of auxin signaling (Vidal et al., 2010). It is easy to understand the crucial rule of miR393 in response to different stresses because auxin is involved in almost every aspect of plant life (Windels and Vazquez, 2011). These miRNAs may increase drought or salt tolerance through unknown mechanisms associated with crosstalk regulation in plants, and future studies in rapeseed involving miRNA over-expression for functional annotation are warranted.

AUTHOR CONTRIBUTIONS

LL conceived and designed the experiments. HJ and JW performed the experiments. HJ, JW, and TW analyzed the data. LW, JL, and LL contributed reagents/materials/analysis tools. HJ wrote the paper.

FUNDING

This study was supported by National Natural Science Foundation of China (31371655), 973 Program (2015CB150201), and Chongqing graduate student research innovation project (CYB2015063).

SUPPLEMENTARY MATERIAL

The Supplementary Material for this article can be found online at: http://journal.frontiersin.org/article/10.3389/fpls.2016.00658

Table S1 | The primers used for mature miRNAs qRT-PCR.

Table S2 | The primers used for predicted miRNAs targets qRT-PCR.

Table S3 | Raw data analysis for the three libraries.

Table S4 | The number of conserved miRNA family members.

Table S5 | The miRNA abundance of conserved miRNA families among the control (CK), salt (S), and drought (D) treatments.

Table S6 | Conserved miRNAs from *B. napus* and their homologs in selected other species. +, detected in this species; −, not detected in this species.

Table S7 | The miRNA abundance of novel miRNA families among the control (CK), salt (S), and drought (D) treatments.

Table S8 | Size distribution of novel miRNAs in the rapeseed CK, D, and S libraries.

Table S9 | Predicted targets of conserved miRNAs in the CK, D, and S libraries.

Table S10 | Predicted targets of novel miRNAs in the CK, D, and S libraries.

Table S11 | Novel miRNAs with no targets predicted in the CK, D, and S libraries.

Figure S1 | Heat map of conserved miRNA read abundance in the *B. napus* control, salt, and drought libraries.

REFERENCES

Achard, P., Herr, A., Baulcombe, D. C., and Harberd, N. P. (2004). Modulation of floral development by a gibberellin-regulated microRNA. *Development* 131, 3357–3365. doi: 10.1242/dev.01206

Adai, A., Johnson, C., Mlotshwa, S., Archer-Evans, S., Manocha, V., Vance, V., et al. (2005). Computational prediction of miRNAs in *Arabidopsis thaliana*. *Genome Res.* 15, 78–91. doi: 10.1101/gr.2908205

Allen, E., Xie, Z. X., Gustafson, A. M., and Carrington, J. C. (2005). microRNA-directed phasing during trans-acting siRNA biogenesis in plants. *Cell* 121, 207–221. doi: 10.1016/j.cell.2005.04.004

Alonso-Peral, M. M., Li, J., Li, Y., Allen, R. S., Schnippenkoetter, W., Ohms, S., et al. (2010). The microRNA159-regulated GAMYB-like genes inhibit growth and promote programmed cell death in Arabidopsis. *Plant Physiol.* 154, 757–771. doi: 10.1104/pp.110.160630

Arenas-Huertero, C., Perez, B., Rabanal, F., Blanco-Melo, D., De la Rosa, C., Estrada-Navarrete, G., et al. (2009). Conserved and novel miRNAs in the legume *Phaseolus vulgaris* in response to stress. *Plant Mol. Biol.* 70, 385–401. doi: 10.1007/s11103-009-9480-3

Barrera-Figueroa, B. E., Gao, L., Diop, N. N., Wu, Z. G., Ehlers, J. D., Roberts, P. A., et al. (2011). Identification and comparative analysis of drought-associated microRNAs in two cowpea genotypes. *BMC Plant Biol.* 11:127. doi: 10.1186/1471-2229-11-127

Bartel, D. P. (2004). MicroRNAs: genomics, biogenesis, mechanism, and function. *Cell* 116, 281–297. doi: 10.1016/S0092-8674(04)00045-5

Bartel, D. P. (2009). MicroRNAs: target recognition and regulatory functions. *Cell* 136, 215–233. doi: 10.1016/j.cell.2009.01.002

Bartels, D., and Sunkar, R. (2005). Drought and salt tolerance in plants. *CRC. Crit. Rev. Plant Sci.* 24, 23–58. doi: 10.1080/07352680590910410

Bonnet, E., Wuyts, J., Rouze, P., and Van de Peer, Y. (2004). Evidence that microRNA precursors, unlike other non-coding RNAs, have lower folding free energies than random sequences. *Bioinformatics* 20, 2911–2917. doi: 10.1093/bioinformatics/bth374

Brodersen, P., Sakvarelidze-Achard, L., Bruun-Rasmussen, M., Dunoyer, P., Yamamoto, Y. Y., Sieburth, L., et al. (2008). Widespread translational inhibition by plant miRNAs and siRNAs. *Science* 320, 1185–1190. doi: 10.1126/science.1159151

Buhtz, A., Springer, F., Chappell, L., Baulcombe, D. C., and Kehr, J. (2008). Identification and characterization of small RNAs from the phloem of *Brassica napus*. *Plant J.* 53, 739–749. doi: 10.1111/j.1365-313X.2007.03368.x

Carra, A., Mica, E., Gambino, G., Pindo, M., Moser, C., Pe, M. E., et al. (2009). Cloning and characterization of small non-coding RNAs from grape. *Plant J.* 59, 750–763. doi: 10.1111/j.1365-313X.2009.03906.x

Chen, Z. H., Bao, M. L., Sun, Y. Z., Yang, Y. J., Xu, X. H., Wang, J. H., et al. (2011). Regulation of auxin response by miR393-targeted transport inhibitor response protein 1 is involved in normal development in Arabidopsis. *Plant Mol. Biol.* 77, 619–629. doi: 10.1007/s11103-011-9838-1

Chi, X. Y., Yang, Q. L., Chen, X. P., Wang, J. Y., Pan, L. J., Chen, M. N., et al. (2011). Identification and characterization of microRNAs from peanut (*Arachis hypogaea* L.) by high-throughput sequencing. *PLoS ONE* 6:e27530. doi: 10.1371/journal.pone.0027530

Chinnusamy, V., Zhu, J., and Zhu, J. K. (2007). Cold stress regulation of gene expression in plants. *Trends Plant Sci.* 12, 444–451. doi: 10.1016/j.tplants.2007.07.002

Constabel, C. P., Yip, L., Patton, J. J., and Christopher, M. E. (2000). Polyphenol oxidase from hybrid poplar. Cloning and expression in response to wounding and herbivory. *Plant Physiol.* 124, 285–295. doi: 10.1104/pp.124.1.285

Dalton-Morgan, J., Hayward, A., Alamery, S., Tollenaere, R., Mason, A. S., Campbell, E., et al. (2014). A high-throughput SNP array in the amphidiploid species *Brassica napus* shows diversity in resistance genes. *Funct. Integr. Genomics* 14, 643–655. doi: 10.1007/s10142-014-0391-2

Dharmasiri, N., Dharmasiri, S., and Estelle, M. (2005). The F-box protein TIR1 is an auxin receptor. *Nature* 435, 441–445. doi: 10.1038/nature03543

Frazier, T. P., Sun, G. L., Burklew, C. E., and Zhang, B. H. (2011). Salt and drought stresses induce the aberrant expression of microRNA genes in tobacco. *Mol. Biotechnol.* 49, 159–165. doi: 10.1007/s12033-011-9387-5

Fujii, H., Chiou, T. J., Lin, S. I., Aung, K., and Zhu, J. K. (2005). A miRNA involved in phosphate-starvation response in Arabidopsis. *Curr. Biol.* 15, 2038–2043. doi: 10.1016/j.cub.2005.10.016

Fujita, M., Fujita, Y., Noutoshi, Y., Takahashi, F., Narusaka, Y., Yamaguchi-Shinozaki, K., et al. (2006). Crosstalk between abiotic and biotic stress responses: a current view from the points of convergence in the stress signaling networks. *Curr. Opin. Plant Biol.* 9, 436–442. doi: 10.1016/j.pbi.2006.05.014

Gao, Z. H., Shi, T., Luo, X. Y., Zhang, Z., Zhuang, W. B., and Wang, L. J. (2012). High-throughput sequencing of small RNAs and analysis of differentially expressed microRNAs associated with pistil development in Japanese apricot. *BMC Genomics* 13:371. doi: 10.1186/1471-2164-13-371

Golldack, D., Luking, I., and Yang, O. (2011). Plant tolerance to drought and salinity: stress regulating transcription factors and their functional significance in the cellular transcriptional network. *Plant Cell Rep.* 30, 1383–1391. doi: 10.1007/s00299-011-1068-0

Griffiths-Jones, S., Moxon, S., Marshall, M., Khanna, A., Eddy, S. R., and Bateman, A. (2005). Rfam: annotating non-coding RNAs in complete genomes. *Nucleic Acids Res.* 33, D121–D124. doi: 10.1093/nar/gki081

Griffiths-Jones, S., Saini, H. K., van Dongen, S., and Enright, A. J. (2008). miRBase: tools for microRNA genomics. *Nucleic Acids Res.* 36, D154–D158. doi: 10.1093/nar/gkm952

Guo, H. S., Xie, Q., Fei, J. F., and Chua, N. H. (2005). MicroRNA directs mRNA cleavage of the transcription factor NAC1 to downregulate auxin signals for Arabidopsis lateral root development. *Plant Cell* 17, 1376–1386. doi: 10.1105/tpc.105.030841

Guo, W. X., Wu, G. T., Yan, F., Lu, Y. W., Zheng, H. Y., Lin, L., et al. (2012). Identification of novel *Oryza sativa* miRNAs in deep sequencing-based small RNA libraries of rice infected with rice stripe virus. *PLoS ONE* 7:e46443. doi: 10.1371/journal.pone.0046443

Gutierrez, L., Bussell, J. D., Pacurar, D. I., Schwambach, J., Pacurar, M., and Bellini, C. (2009). Phenotypic plasticity of adventitious rooting in arabidopsis is controlled by complex regulation of AUXIN RESPONSE FACTOR transcripts and MicroRNA abundance. *Plant Cell* 21, 3119–3132. doi: 10.1105/tpc.108.064758

Han, R., Jian, C., Lv, J. Y., Yan, Y., Chi, Q., Li, Z. J., et al. (2014). Identification and characterization of microRNAs in the flag leaf and developing seed of

wheat (*Triticum aestivum* L.). *BMC Genomics* 15:289. doi: 10.1186/1471-2164-15-289

Huang, S. Q., Peng, J., Qiu, C. X., and Yang, Z. M. (2009). Heavy metal-regulated new microRNAs from rice. *J. Inorg. Biochem.* 103, 282–287. doi: 10.1016/j.jinorgbio.2008.10.019

Huang, S. Q., Xiang, A. L., Che, L. L., Chen, S., Li, H., Song, J. B., et al. (2010). A set of miRNAs from *Brassica napus* in response to sulphate deficiency and cadmium stress. *Plant Biotechnol. J.* 8, 887–899. doi: 10.1111/j.1467-7652.2010.00517.x

Jin, W. B., Li, N. N., Zhang, B., Wu, F. L., Li, W. J., Guo, A. G., et al. (2008). Identification and verification of microRNA in wheat (*Triticum aestivum*). *J. Plant Res.* 121, 351–355. doi: 10.1007/s10265-007-0139-3

Jones-Rhoades, M. W., and Bartel, D. P. (2004). Computational identification of plant MicroRNAs and their targets, including a stress-induced miRNA. *Mol. Cell* 14, 787–799. doi: 10.1016/j.molcel.2004.05.027

Juarez, M. T., Kui, J. S., Thomas, J., Heller, B. A., and Timmermans, M. C. P. (2004). microRNA-mediated repression of rolled leaf1 specifies maize leaf polarity. *Nature* 428, 84–88. doi: 10.1038/nature02363

Jung, H. J., and Kang, H. (2007). Expression and functional analyses of microRNA417 in *Arabidopsis thaliana* under stress conditions. *Plant Physiol. Biochem.* 45, 805–811. doi: 10.1016/j.plaphy.2007.07.015

Kantar, M., Lucas, S. J., and Budak, H. (2011). miRNA expression patterns of *Triticum dicoccoides* in response to shock drought stress. *Planta* 233, 471–484. doi: 10.1007/s00425-010-1309-4

Kim, B., Yu, H. J., Park, S. G., Shin, J. Y., Oh, M., Kim, N., et al. (2012). Identification and profiling of novel microRNAs in the *Brassica rapa* genome based on small RNA deep sequencing. *BMC Plant Biol.* 12:218. doi: 10.1186/1471-2229-12-218

Kim, J. Y., Kwak, K. J., Jung, H. J., Lee, H. J., and Kang, H. (2010). MicroRNA402 affects seed germination of *Arabidopsis thaliana* under stress conditions via targeting DEMETER-LIKE Protein3 mRNA. *Plant Cell Physiol.* 51, 1079–1083. doi: 10.1093/pcp/pcq072

Knight, H., and Knight, M. R. (2001). Abiotic stress signalling pathways: specificity and cross-talk. *Trends Plant Sci.* 6, 262–267. doi: 10.1016/S1360-1385(01)01946-X

Korbes, A. P., Machado, R. D., Guzman, F., Almerao, M. P., de Oliveira, L. F. V., Loss-Morais, G., et al. (2012). Identifying conserved and novel MicroRNAs in developing seeds of *Brassica napus* using deep sequencing. *PLoS ONE* 7:e50663. doi: 10.1371/journal.pone.0050663

Kozomara, A., and Griffiths-Jones, S. (2014). miRBase: annotating high confidence microRNAs using deep sequencing data. *Nucleic Acids Res.* 42, D68–D73. doi: 10.1093/nar/gkt1181

Kulcheski, F. R., de Oliveira, L. F. V., Molina, L. G., Almerao, M. P., Rodrigues, F. A., Marcolino, J., et al. (2011). Identification of novel soybean microRNAs involved in abiotic and biotic stresses. *BMC Genomics* 12:307. doi: 10.1186/1471-2164-12-307

Lee, R. C., Feinbaum, R. L., and Ambros, V. (1993). The *C. elegans* heterochronic gene lin-4 encodes small RNAs with antisense complementarity to lin-14. *Cell* 75, 843–854. doi: 10.1016/0092-8674(93)90529-Y

Lertpanyasampatha, M., Gao, L., Kongsawadworakul, P., Viboonjun, U., Chrestin, H., Liu, R. Y., et al. (2012). Genome-wide analysis of microRNAs in rubber tree (*Hevea brasiliensis* L.) using high-throughput sequencing. *Planta* 236, 437–445. doi: 10.1007/s00425-012-1622-1

Li, D. T., Wang, L. W., Liu, X., Cui, D. Z., Chen, T. T., Zhang, H., et al. (2013). Deep sequencing of maize small RNAs reveals a diverse set of microRNA in dry and imbibed seeds. *PLoS ONE* 8:e55107. doi: 10.1371/journal.pone.0055107

Li, H. Y., Dong, Y. Y., Yin, H. L., Wang, N., Yang, J., Liu, X. M., et al. (2011). Characterization of the stress associated microRNAs in Glycine max by deep sequencing. *BMC Plant Biol.* 11:170. doi: 10.1186/1471-2229-11-170

Li, R. Q., Yu, C., Li, Y. R., Lam, T. W., Yiu, S. M., Kristiansen, K., et al. (2009). SOAP2: an improved ultrafast tool for short read alignment. *Bioinformatics* 25, 1966–1967. doi: 10.1093/bioinformatics/btp336

Li, W. X., Oono, Y., Zhu, J. H., He, X. J., Wu, J. M., Iida, K., et al. (2008). The Arabidopsis NFYA5 transcription factor is regulated transcriptionally and posttranscriptionally to promote drought resistance. *Plant Cell* 20, 2238–2251. doi: 10.1105/tpc.108.059444

Liang, C. W., Zhang, X. W., Zou, J., Xu, D., Su, F., and Ye, N. H. (2010). Identification of miRNA from *Porphyra yezoensis* by high-throughput sequencing and bioinformatics analysis. *PLoS ONE* 5:e10698. doi: 10.1371/journal.pone.0010698

Liu, H. H., Tian, X., Li, Y. J., Wu, C. A., and Zheng, C. C. (2008). Microarray-based analysis of stress-regulated microRNAs in *Arabidopsis thaliana*. *RNA* 14, 836–843. doi: 10.1261/rna.895308

Liu, P. P., Montgomery, T. A., Fahlgren, N., Kasschau, K. D., Nonogaki, H., and Carrington, J. C. (2007). Repression of AUXIN RESPONSE FACTOR10 by microRNA160 is critical for seed germination and post-germination stages. *Plant J.* 52, 133–146. doi: 10.1111/j.1365-313X.2007.03218.x

Liu, Q., Zhang, Y. C., Wang, C. Y., Luo, Y. C., Huang, Q. J., Chen, S. Y., et al. (2009). Expression analysis of phytohormone-regulated microRNAs in rice, implying their regulation roles in plant hormone signaling. *FEBS Lett.* 583, 723–728. doi: 10.1016/j.febslet.2009.01.020

Lu, S. F., Sun, Y. H., and Chiang, V. L. (2008). Stress-responsive microRNAs in Populus. *Plant J.* 55, 131–151. doi: 10.1111/j.1365-313X.2008.03497.x

Lu, S. F., Sun, Y. H., Shi, R., Clark, C., Li, L. G., and Chiang, V. L. (2005). Novel and mechanical stress-responsive microRNAs in *Populus trichocarpa* that are absent from Arabidopsis. *Plant Cell* 17, 2186–2203. doi: 10.1105/tpc.105.033456

Lv, S. Z., Nie, X. J., Wang, L., Du, X. H., Biradar, S. S., Jia, X. O., et al. (2012). Identification and characterization of microRNAs from Barley (*Hordeum vulgare* L.) by high-throughput sequencing. *Int. J. Mol. Sci.* 13, 2973–2984. doi: 10.3390/ijms13032973

Mallory, A. C., Bartel, D. P., and Bartel, B. (2005). MicroRNA-directed regulation of Arabidopsis AUXIN RESPONSE FACTOR17 is essential for proper development and modulates expression of early auxin response genes. *Plant Cell* 17, 1360–1375. doi: 10.1105/tpc.105.031716

Martin, R. C., Liu, P. P., Goloviznina, N. A., and Nonogaki, H. (2010). microRNA, seeds, and Darwin?: diverse function of miRNA in seed biology and plant responses to stress. *J. Exp. Bot.* 61, 2229–2234. doi: 10.1093/jxb/erq063

Morin, R. D., Aksay, G., Dolgosheina, E., Ebhardt, H. A., Magrini, V., Mardis, E. R., et al. (2008). Comparative analysis of the small RNA transcriptomes of *Pinus contorta* and *Oryza sativa*. *Genome Res.* 18, 571–584. doi: 10.1101/gr.6897308

Munns, R. (2005). Genes and salt tolerance: bringing them together. *New Phytol.* 167, 645–663. doi: 10.1111/j.1469-8137.2005.01487.x

Navarro, L., Dunoyer, P., Jay, F., Arnold, B., Dharmasiri, N., Estelle, M., et al. (2006). A plant miRNA contributes to antibacterial resistance by repressing auxin signaling. *Science* 312, 436–439. doi: 10.1126/science.1126088

Nonogaki, H. (2010). MicroRNA gene regulation cascades during early stages of plant development. *Plant Cell Physiol.* 51, 1840–1846. doi: 10.1093/pcp/pcq154

Ohashi-Ito, K., and Fukuda, H. (2003). HD-Zip III homeobox genes that include a novel member, ZeHB-13 (Zinnia)/ATHB-15 (Arabidopsis), are involved in procambium and xylem cell differentiation. *Plant Cell Physiol.* 44, 1350–1358. doi: 10.1093/pcp/pcg164

Pant, B. D., Buhtz, A., Kehr, J., and Scheible, W. R. (2008). MicroRNA399 is a long-distance signal for the regulation of plant phosphate homeostasis. *Plant J.* 53, 731–738. doi: 10.1111/j.1365-313X.2007.03363.x

Pant, B. D., Musialak-Lange, M., Nuc, P., May, P., Buhtz, A., Kehr, J., et al. (2009). Identification of nutrient-responsive Arabidopsis and rapeseed microRNAs by comprehensive real-time polymerase chain reaction profiling and small RNA sequencing. *Plant Physiol.* 150, 1541–1555. doi: 10.1104/pp.109.139139

Peng, Z., He, S. P., Gong, W. F., Sun, J. L., Pan, Z. E., Xu, F. F., et al. (2014). Comprehensive analysis of differentially expressed genes and transcriptional regulation induced by salt stress in two contrasting cotton genotypes. *BMC Genomics* 15:760. doi: 10.1186/1471-2164-15-760

Rajagopalan, R., Vaucheret, H., Trejo, J., and Bartel, D. P. (2006). A diverse and evolutionarily fluid set of microRNAs in *Arabidopsis thaliana*. *Genes Dev.* 20, 3407–3425. doi: 10.1101/gad.1476406

Reyes, J. L., and Chua, N. H. (2007). ABA induction of miR159 controls transcript levels of two MYB factors during Arabidopsis seed germination. *Plant J.* 49, 592–606. doi: 10.1111/j.1365-313X.2006.02980.x

Schreiber, A. W., Shi, B. J., Huang, C. Y., Langridge, P., and Baumann, U. (2011). Discovery of barley miRNAs through deep sequencing of short reads. *BMC Genomics* 12:129. doi: 10.1186/1471-2164-12-129

Shi, R., and Chiang, V. L. (2005). Facile means for quantifying microRNA expression by real-time PCR. *Biotechniques* 39, 519–525. doi: 10.2144/000112010

Shinozaki, K., and Yamaguchi-Shinozaki, K. (2007). Gene networks involved in drought stress response and tolerance. *J. Exp. Bot.* 58, 221–227. doi: 10.1093/jxb/erl164

Si-Ammour, A., Windels, D., Arn-Bouldoires, E., Kutter, C., Ailhas, J., Meins, F., et al. (2011). miR393 and secondary siRNAs regulate expression of the TIR1/AFB2 auxin receptor clade and auxin-related development of Arabidopsis leaves. *Plant Physiol.* 157, 683–691. doi: 10.1104/pp.111.180083

Song, Q. X., Liu, Y. F., Hu, X. Y., Zhang, W. K., Ma, B. A., Chen, S. Y., et al. (2011). Identification of miRNAs and their target genes in developing soybean seeds by deep sequencing. *BMC Plant Biol.* 11:5. doi: 10.1186/1471-2229-11-5

Srivastava, P. K., Moturu, T. R., Pandey, P., Baldwin, I. T., and Pandey, S. P. (2014). A comparison of performance of plant miRNA target prediction tools and the characterization of features for genome-wide target prediction. *BMC Genomics* 15:348. doi: 10.1186/1471-2164-15-348

Subramanian, S., Fu, Y., Sunkar, R., Barbazuk, W. B., Zhu, J. K., and Yu, O. (2008). Novel and nodulation-regulated microRNAs in soybean roots. *BMC Genomics* 9:160. doi: 10.1186/1471-2164-9-160

Sullivan, C. S., and Ganem, D. (2005). MicroRNAs and viral infection. *Mol. Cell* 20, 3–7. doi: 10.1016/j.molcel.2005.09.012

Sunkar, R. (2010). MicroRNAs with macro-effects on plant stress responses. *Semin. Cell Dev. Biol.* 21, 805–811. doi: 10.1016/j.semcdb.2010.04.001

Sunkar, R., Chinnusamy, V., Zhu, J. H., and Zhu, J. K. (2007). Small RNAs as big players in plant abiotic stress responses and nutrient deprivation. *Trends Plant Sci.* 12, 301–309. doi: 10.1016/j.tplants.2007.05.001

Sunkar, R., Girke, T., and Zhu, J. K. (2005). Identification and characterization of endogenous small interfering RNAs from rice. *Nucleic Acids Res.* 33, 4443–4454. doi: 10.1093/nar/gki758

Sunkar, R., Kapoor, A., and Zhu, J. K. (2006). Posttranscriptional induction of two Cu/Zn superoxide dismutase genes in Arabidopsis is mediated by downregulation of miR398 and important for oxidative stress tolerance. *Plant Cell* 18, 2415. doi: 10.1105/tpc.106.041673

Tahir, M., Law, D. A., and Stasolla, C. (2006). Molecular characterization of PgAGO, a novel conifer gene of the ARGONAUTE family expressed in apical cells and required for somatic embryo development in spruce. *Tree Physiol.* 26, 1257–1270. doi: 10.1093/treephys/26.10.1257

Vidal, E. A., Araus, V., Lu, C., Parry, G., Green, P. J., Coruzzi, G. M., et al. (2010). Nitrate-responsive miR393/AFB3 regulatory module controls root system architecture in *Arabidopsis thaliana*. *Proc. Natl. Acad. Sci. U.S.A.* 107, 4477–4482. doi: 10.1073/pnas.0909571107

Wang, C., Ying, S., Huang, H. J., Li, K., Wu, P., and Shou, H. X. (2009). Involvement of OsSPX1 in phosphate homeostasis in rice. *Plant J.* 57, 895–904. doi: 10.1111/j.1365-313X.2008.03734.x

Wang, F. D., Li, L. B., Liu, L. F., Li, H. Y., Zhang, Y. H., Yao, Y. Y., et al. (2012). High-throughput sequencing discovery of conserved and novel microRNAs in Chinese cabbage (*Brassica rapa* L. ssp pekinensis). *Mol. Genet. Genomics* 287, 555–563. doi: 10.1007/s00438-012-0699-3

Wang, J. W., Wang, L. J., Mao, Y. B., Cai, W. J., Xue, H. W., and Chen, X. Y. (2005). Control of root cap formation by microRNA-targeted auxin response factors in Arabidopsis. *Plant Cell* 17, 2204–2216. doi: 10.1105/tpc.105.033076

Wang, J. Y., Yang, X. D., Xu, H. B., Chi, X. Y., Zhang, M., and Hou, X. L. (2012). Identification and characterization of microRNAs and their target genes in *Brassica oleracea*. *Gene* 505, 300–308. doi: 10.1016/j.gene.2012.06.002

Wang, L. W., Liu, H. H., Li, D. T., and Chen, H. B. (2011). Identification and characterization of maize microRNAs involved in the very early stage of seed germination. *BMC Genomics* 12:154. doi: 10.1186/1471-2164-12-154

Weitbrecht, K., Muller, K., and Leubner-Metzger, G. (2011). First off the mark: early seed germination. *J. Exp. Bot.* 62, 3289–3309. doi: 10.1093/jxb/err030

Wiese, K. C., and Hendriks, A. (2006). Comparison of P-RnaPredict and mfold - algorithms for RNA secondary structure prediction. *Bioinformatics* 22, 934–942. doi: 10.1093/bioinformatics/btl043

Windels, D., and Vazquez, F. (2011). miR393: integrator of environmental cues in auxin signaling? *Plant Signal. Behav.* 6, 1672–1675. doi: 10.4161/psb.6.11.17900

Wu, G., Park, M. Y., Conway, S. R., Wang, J. W., Weigel, D., and Poethig, R. S. (2009). The sequential action of miR156 and miR172 regulates developmental timing in Arabidopsis. *Cell* 138, 750–759. doi: 10.1016/j.cell.2009.06.031

Wu, H. J., Ma, Y. K., Chen, T., Wang, M., and Wang, X. J. (2012). PsRobot: a web-based plant small RNA meta-analysis toolbox. *Nucleic Acids Res.* 40, W22–W28. doi: 10.1093/nar/gks554

Wu, M. F., Tian, Q., and Reed, J. W. (2006). Arabidopsis microRNA167 controls patterns of ARF6 and ARF8 expression, and regulates both female and male reproduction. *Development* 133, 4211–4218. doi: 10.1242/dev.02602

Xie, F. L., Huang, S. Q., Guo, K., Xiang, A. L., Zhu, Y. Y., Nie, L., et al. (2007). Computational identification of novel microRNAs and targets in *Brassica napus*. *FEBS Lett.* 581, 1464–1474. doi: 10.1016/j.febslet.2007.02.074

Xiong, L. M., Wang, R. G., Mao, G. H., and Koczan, J. M. (2006). Identification of drought tolerance determinants by genetic analysis of root response to drought stress and abscisic acid. *Plant Physiol.* 142, 1065–1074. doi: 10.1104/pp.106.084632

Xu, M. Y., Dong, Y., Zhang, Q. X., Zhang, L., Luo, Y. Z., Sun, J., et al. (2012). Identification of miRNAs and their targets from *Brassica napus* by high-throughput sequencing and degradome analysis. *BMC Genomics* 13:421. doi: 10.1186/1471-2164-13-421

Yang, J. H., Han, S. J., Yoon, E. K., and Lee, W. S. (2006). 'Evidence of an auxin signal pathway, microRNA167-ARF8-GH3, and its response to exogenous auxin in cultured rice cells'. *Nucleic Acids Res.* 34, 1892–1899. doi: 10.1093/nar/gkl118

Yang, J. H., Liu, X. Y., Xu, B. C., Zhao, N., Yang, X. D., and Zhang, M. F. (2013). Identification of miRNAs and their targets using high-throughput sequencing and degradome analysis in cytoplasmic male-sterile and its maintainer fertile lines of *Brassica juncea*. *BMC Genomics* 14:9. doi: 10.1186/1471-2164-14-9

Yang, L., Conway, S. R., and Poethig, R. S. (2011). Vegetative phase change is mediated by a leaf-derived signal that represses the transcription of miR156. *Development* 138, 245–249. doi: 10.1242/dev.058578

Yang, X. Y., Wang, L. C., Yuan, D. J., Lindsey, K., and Zhang, X. L. (2013). Small RNA and degradome sequencing reveal complex miRNA regulation during cotton somatic embryogenesis. *J. Exp. Bot.* 64, 1521–1536. doi: 10.1093/jxb/ert013

Yu, X., Wang, H., Lu, Y. Z., de Ruiter, M., Cariaso, M., Prins, M., et al. (2012). Identification of conserved and novel microRNAs that are responsive to heat stress in *Brassica rapa*. *J. Exp. Bot.* 63, 1025–1038. doi: 10.1093/jxb/err337

Zhang, B. H., Pan, X. P., Cox, S. B., Cobb, G. P., and Anderson, T. A. (2006). Evidence that miRNAs are different from other RNAs. *Cell. Mol. Life Sci.* 63, 246–254. doi: 10.1007/s00018-005-5467-7

Zhang, J. H., Zhang, S. G., Han, S. Y., Li, X. M., Tong, Z. K., and Qi, L. W. (2013). Deciphering small noncoding RNAs during the transition from dormant embryo to germinated embryo in larches (*Larix leptolepis*). *PLoS ONE* 8:e81452. doi: 10.1371/journal.pone.0081452

Zhang, L. F., Chia, J. M., Kumari, S., Stein, J. C., Liu, Z. J., Narechania, A., et al. (2009). A genome-wide characterization of microRNA genes in maize. *PLoS Genetics* 5:e1000716. doi: 10.1371/journal.pgen.1000716

Zhang, X. H., Zou, Z., Gong, P. J., Zhang, J. H., Ziaf, K., Li, H. X., et al. (2011). Over-expression of microRNA169 confers enhanced drought tolerance to tomato. *Biotechnol. Lett.* 33, 403–409. doi: 10.1007/s10529-010-0436-0

Zhao, B. T., Ge, L. F., Liang, R. Q., Li, W., Ruan, K. C., Lin, H. X., et al. (2009). Members of miR-169 family are induced by high salinity and transiently inhibit the NF-YA transcription factor. *BMC Mol. Biol.* 10:29. doi: 10.1186/1471-2199-10-29

Zhao, B. T., Liang, R. Q., Ge, L. F., Li, W., Xiao, H. S., Lin, H. X., et al. (2007). Identification of drought-induced microRNAs in rice. *Biochem. Biophys. Res. Commun.* 354, 585–590. doi: 10.1016/j.bbrc.2007.01.022

Zhao, C. Z., Xia, H., Frazier, T. P., Yao, Y. Y., Bi, Y. P., Li, A. Q., et al. (2010). Deep sequencing identifies novel and conserved microRNAs in peanuts (*Arachis hypogaea* L.). *BMC Plant Biol.* 10:3. doi: 10.1186/1471-2229-10-3

Zhao, Y. T., Wang, M., Fu, S. X., Yang, W. C., Qi, C. K., and Wang, X. J. (2012). Small RNA profiling in Two *Brassica napus* cultivars identifies microRNAs with oil production- and development-correlated expression and new small RNA classes. *Plant Physiol.* 158, 813–823. doi: 10.1104/pp.111.187666

Zhou, X. F., Wang, G. D., Sutoh, K., Zhu, J. K., and Zhang, W. X. (2008). Identification of cold-inducible microRNAs in plants by transcriptome analysis. *Biochim. Biophys. Acta* 1779, 780–788. doi: 10.1016/j.bbagrm.2008.04.005

Zhou, Z. S., Song, J. B., and Yang, Z. M. (2012). Genome-wide identification of *Brassica napus* microRNAs and their targets in response to cadmium. *J. Exp. Bot.* 63, 4597–4613. doi: 10.1093/jxb/ers136

Conflict of Interest Statement: The authors declare that the research was conducted in the absence of any commercial or financial relationships that could be construed as a potential conflict of interest.

The reviewer AVCR and handling Editor declared their shared affiliation, and the handling Editor states that the process nevertheless met the standards of a fair and objective review.

frontiers in Plant Science

ORIGINAL RESEARCH
published: 25 July 2016
doi: 10.3389/fpls.2016.01082

GmCLC1 Confers Enhanced Salt Tolerance through Regulating Chloride Accumulation in Soybean

Peipei Wei[1], Longchao Wang[1], Ailin Liu[2], Bingjun Yu[1] and Hon-Ming Lam[2]**

[1] College of Life Sciences, Nanjing Agricultural University, Nanjing, China, [2] Center for Soybean Research of the Partner State Key Laboratory of Agrobiotechnology and School of Life Sciences, The Chinese University of Hong Kong, Hong Kong, China

The family of chloride channel proteins that mediate Cl^- transportation play vital roles in plant nutrient supply, cellular action potential and turgor pressure adjustment, stomatal movement, hormone signal recognition and transduction, Cl^- homeostasis, and abiotic and biotic stress tolerance. The anionic toxicity, mainly caused by chloride ions (Cl^-), on plants under salt stress remains poorly understood. In this work, we investigated the function of soybean Cl^-/H^+ antiporter GmCLC1 under salt stress in transgenic *Arabidopsis thaliana*, soybean, and yeast. We found that *GmCLC1* enhanced salt tolerance in transgenic *A. thaliana* by reducing the Cl^- accumulation in shoots and hence released the negative impact of salt stress on plant growth. Overexpression of *GmCLC1* in the hairy roots of soybean sequestered more Cl^- in their roots and transferred less Cl^- to their shoots, leading to lower relative electrolyte leakage values in the roots and leaves. When either the soybean *GmCLC1* or the yeast chloride transporter gene, *GEF1*, was transformed into the yeast *gef1* mutant, and then treated with different chloride salts ($MnCl_2$, KCl, NaCl), enhanced survival rate was observed. The result indicates that *GmCLC1* and *GEF1* exerted similar effects on alleviating the stress of diverse chloride salts on the yeast *gef1* mutant. Together, this work suggests a protective function of GmCLC1 under Cl^- stress.

Keywords: chloride transporter, Cl^- toxicity, *GmCLC1*, salt stress, soybean root transformation, transgenic *Arabidopsis*

OPEN ACCESS

Edited by:
Urs Feller,
University of Bern, Switzerland

Reviewed by:
Amarendra Narayan Misra,
Central University of Jharkhand, India
Michiel Van Eijk,
KeyGene, Netherlands

****Correspondence:***
Bingjun Yu
bjyu@njau.edu.cn
Hon-Ming Lam
honming@cuhk.edu.hk

Specialty section:
This article was submitted to Agroecology and Land Use Systems, a section of the journal Frontiers in Plant Science

Received: *03 June 2016*
Accepted: *08 July 2016*
Published: *25 July 2016*

Citation:
Wei P, Wang L, Liu A, Yu B and Lam H-M (2016) GmCLC1 Confers Enhanced Salt Tolerance through Regulating Chloride Accumulation in Soybean. Front. Plant Sci. 7:1082. doi: 10.3389/fpls.2016.01082

INTRODUCTION

Ionic stress, osmotic stress, nutritional imbalance, and oxidative damage are the main causes for salt injury of plants, among which ionic stress is the primary factor (Xiao et al., 2013; Adem et al., 2014). Sodium chloride is the most common salt in environment. In salinized conditions, salt changed the water potential around the root first causing the osmotic stress, then inducing ionic stress by the accumulation of Na^+ and Cl^- (Deinlein et al., 2014; Gupta and Huang, 2014; Nguyen et al., 2015; Nie et al., 2015). Plants counter these stresses through strategies such as extracellular exclusion of excess ions across the plasma membrane or intracellular vacuolar compartmentalization to reduce the effective Na^+ and Cl^- levels inside the cell, especially in the aerial parts (Zhang et al., 2011; Hasegawa, 2013). In general, crops such as cotton, rice, and barley are more sensitive to Na^+ than Cl^- (Qu et al., 2009). So far, the researches on plant physiological and molecular mechanisms of salt tolerance have mostly focused on cation (Na^+) poisoning and adaptations, such as the NSCCs (non-selective cation channels) and HKTs (High-affinity K^+ Transporter), both controlling

Na^+ import into the cell, together with Na^+/H^+ antiporters, such as AtSOS1 (*Arabidopsis* Salt Overly Sensitive 1) located in the plasma membrane for excluding Na^+ from cells, and AtNHX1 (*Arabidopsis* vacuolar Na^+/H^+ antiporter) located in the tonoplast for compartmentalizing Na^+ mainly in the vacuoles (Adams and Shin, 2014; Deinlein et al., 2014; Nguyen et al., 2015). However, salt injuries to plants resulting from anions (mainly Cl^-) have long been under-investigated.

Cl^- is the main form of anions in plant cells besides nitrate (NO_3^-). As one of the essential micronutrient elements for higher plant growth and development, Cl^- is involved in photosynthesis, stomatal movement, cellular osmotic pressure maintenance, charge balance, and disease resistance (Jossier et al., 2010; Tealle and Tyerman, 2010; Guo et al., 2014). Excessive amount of Cl^- lead to various adverse effects, such as negatively impacting the absorption of macronutrient elements (nitrogen [N], phosphorus [P], and potassium [K]), leaf water potential, causing stomatal closure and the accumulation of reactive oxygen species (ROS) in chloroplasts, which severely affected crop quality and yield (Yu and Liu, 2004; Nguyen et al., 2015). Some studies reported that certain crops or woody species such as tobacco, tomato, barley, grapevine, citrus, *Glycine max*, *Lotus,* and poplar were more sensitive to Cl^- than to Na^+ under salt stress (Moya et al., 2003; Luo et al., 2005; Chen and Yu, 2007; Brumós et al., 2010; Tregeagle et al., 2010). The genetic differences in the control of Cl^- transport from roots to shoots or the ability to maintain a low shoot Cl^- level is the key determinant of Cl^-/salt tolerance (Zhang et al., 2011; Henderson et al., 2014). The anion channels or transporters, widely distributed in all types of organelle membranes (such as plasma membrane, tonoplast, endoplasmic reticulum, mitochondria, and chloroplasts, etc.), predominantly mediate Cl^- and NO_3^- flux across the membrane, playing a vital function in plant nutrition absorption and transportation, adjustment of cellular action potential and turgor pressure, stomatal movement, hormone signal recognition and transduction, Cl^- homeostasis under abiotic (salt, heavy metal, low temperature, etc.) or biotic stress conditions (Jossier et al., 2010; Barbier-Brygo et al., 2011; Wei et al., 2013; Guo et al., 2014; Nguyen et al., 2015). Among them, the *CLCs* (Chloride channel proteins) family mainly mediate Cl^- transport and have attracted the most research interests (Zifarelli and Pusch, 2010). Currently, plant *CLCs* have been identified in *Arabidopsis*, tobacco, rice, potato, corn, spinach, citrus, salt cress, soybean, and maize (Wei et al., 2013; Zhou et al., 2013; Li et al., 2014; Wang et al., 2015). In response to Cl^- toxicity under salt stress, the NaCl-treated plants utilize the anion transporters such as CLCs to adjust and reduce Cl^- accumulation in the cell cytoplasm. In soybean, Li et al. (2006) reported that the protein encoded by the salt- and polyethylene glycol-inducible *GmCLC1* gene (GenBank accession: AY972079, or Phytozome database: *Glyma05g14760*) localizes on tonoplast and can transport and sequester Cl^- into the vacuoles of plant cells. Wong et al. (2013) further found that the transmembrane Cl^- transfer activity of the GmCLC1 protein depends on the cytoplasmic pH value, suggesting that it is most likely a kind of Cl^-/H^+ antiporter that participates in the maintenance of intracellular Cl^- homeostasis and regulates Cl^-/salt tolerance.

In the current study, we further investigated the functions of how *GmCLC1* regulates Cl^- transportation in salt-stressed plants and yeast. We found that overexpressing *GmCLC1* in *Arabidopsis thaliana*, soybean hairy roots and composite plants, as well as yeast mutant could enhance salt tolerance by regulation Cl^- homeostasis.

MATERIALS AND METHODS

Plant Materials, Bacteria and Yeast Strains, and Plasmids

Plant seeds including wild-type (WT) *A. thaliana* (Columbia ecotype glabrous1), *G. max* (L.) Merr. cultivars Jackson (salt-sensitive), Lee68 (salt-tolerant) and N23674 (salt-tolerant), *Escherichia coli* DH5α, *Agrobacterium tumefaciens* strain GV3101, *Agrobacterium rhizogenes* strain K599, binary vector for plant transformation pCAMBIA1300, the yeast Δ*gef1* mutant (derived from *Saccharomyces cerevisiae* BY4741) and yeast expression plasmid pYES2 were used in this study.

GmCLC1 Gene Cloning and Vectors Construction

The seeds of *G. max* N23674 cultivar were surface-sterilized with 1 g dm^{-3} $HgCl_2$ for 5 min, then fully rinsed in distilled water, soaked in distilled water for 6 h, and finally germinated at 25°C in the dark. The germinated seeds were grown on vermiculite irrigated with 1/2 Hoagland solution in a greenhouse with temperature at 25 ± 2°C and humidity ranging from 60 to 70%. Total RNA was extracted from 10-days-old seedlings using the Trizol reagent (Invitrogen, USA). First-strand cDNAs were synthesized with 2 μg total RNAs using a PrimeScript™ II 1st Strand cDNA Synthesis Kit (TaKaRa, Dalian) according to the manufacturer's protocol. The full-length coding region of *GmCLC1* was amplified from the cDNA using the following PCR protocol: 94°C 3 min; 30 cycles of 94°C 30 s, 55°C 30 s, and 72°C 2 min 30 s; and 72°C 5 min in a 25 μL reaction mixture [2 μL of first strand cDNA, 0.15 mM $MgCl_2$, 0.2 mM dNTPs, 0.4 μM of each primer, 0.25 U Taq DNA polymerase (TaKaRa, Dalian) and 10× PCR buffer]. Primers used: 5′-ATGGGTGAGGAATCCAGTTT-3′ and 5′-CTTCCTCT TTGATTTTGCCAG-3′. The PCR products were then cloned into pMD19-T vector (TaKaRa, Dalian) for sequencing.

Subsequently, the open reading frame of *GmCLC1* was amplified from cDNA by PCR (95°C 3 min, 28 cycles of 95°C for 30 s, 55°C for 30 s, and 68°C for 2.5 min) with KOD-Plus (TOYOBO, Japan), and ligated into the plasmid pCAMBIA1300 or pYES2 to obtain the recombinant plasmid pCAMBIA1300-*GmCLC1* (primers used: 5′-GGGGTACCATGGGTGAGGAATC CAGTTT-3′ and 5′-GGACTAGTCTTCCTCTTTGATTTTGCC AG-3′) or pYES2-*GmCLC1* (primers used: 5′-CCGGAATTCA TGGGTGAGGAATCCAG-3′ and 5′-CCGCTCGAGTCACTT CCTCTTTGATTTTG-3′). After sequence verification, the recombinant plasmid pCAMBIA1300-*GmCLC1* was transformed into *A. tumefaciens* GV3101 or *A. rhizogenes* K599, respectively.

Seed Germination and Root Elongation Experiments with WT and *GmCLC1*-Transgenic *A. thaliana*

The binary vector pCambia1300-*GmCLC1* was transformed into WT *Arabidopsis* plants using the floral dip method mediated by *A. tumefaciens* (Clough and Bent, 1998). Transformants were selected by germination on Murashige and Skoog (MS) agar medium supplemented with 40 mg L^{-1} hygromycin B. Homozygous lines (L_1–L_5) of T_2 plants were identified by PCR. The seeds of *A. thaliana* WT and a homozygous *GmCLC1*-transgenic line (L_1) were sterilized and sown evenly on MS agar medium (pH = 5.8; Nie et al., 2015) containing 0, 150, and 200 mM NaCl, respectively. The agar plates were put in an illuminated growth chamber under a 14 h light/10 h dark cycle at 20 ± 2°C, with 60–70% relative humidity. The seed germination percentage (%) was recorded after 7 days. For measuring the root elongation of *A. thaliana* under salt stress, seeds of WT and *GmCLC1*-transgenic plants were cultured on MS agar medium (pH = 5.8) without NaCl for 5 days. Then seedlings with similar root lengths were selected and transferred onto MS agar medium (pH = 5.8) containing 0, 150, and 200 mM NaCl. After placing the agar plates vertically for 5 days, the seedlings of WT and *GmCLC1*-transgenics were photographed and the root lengths were measured.

Determination of Leaf Relative Water Content (RWC) and Chlorophyll Fluorescence (Fv/Fm), Root and Leaf Relative Electrolyte Leakage (REL) of WT and *GmCLC1*-Transgenic *A. thaliana*

Seeds of *A. thaliana* WT and *GmCLC1*-transgenic line (L_1) were sterilized and sown on MS agar medium (pH = 5.8), and then placed in a growth chamber under a 14 h light/10 h dark cycle at 20 ± 2°C, with 60–70% relative humidity. After 8 days, the seedlings were then transferred to pots containing a sterilized peat moss and vermiculite mixture and grown for 5 days. Then the seedlings were treated with increasing concentrations of NaCl (50 mM NaCl for 2 days, 100 mM NaCl for the next 2 days, 150 mM NaCl solution for another 7 days). Finally, leaf relative water content (RWC) was measured according to the method described by Hu et al. (2016). Leaf chlorophyll fluorescence (Fv/Fm) was measured at room temperature with a plant efficiency analyzer (Handy PEA Fluorometer, Hansatech Instruments, UK; (Tian et al., 2014). Root or leaf relative electrolyte leakage (REL) was assayed using the method described by Hu et al. (2016) with a digital conductivity meter (DDS-307, Shanghai, China).

Analyses of Cl^- Contents in Roots and Shoots of WT and *GmCLC1*-Transgenic *A. thaliana* Seedlings

Seeds of WT and *GmCLC1*-transgenic *A. thaliana* were sterilized and sown in pots containing a sterilized peat moss and vermiculite mixture and grown in a growth chamber under a 14 h light/10 h dark cycle at 20 ± 2°C, with 60–70% relative humidity. After 30 days, plants were treated with 1/2 X Hoagland solution containing 150 mM NaCl for 0, 4, 12, 24 h, 2, 4, and 6 days, respectively. Then the roots and shoots of *Arabidopsis* seedlings were sampled and Cl^- contents were measured with the method described (Zhou and Yu, 2009).

Assays of Maximum Lengths and Fresh Weights of the Hairy Roots of Transformed Soybean Cotyledons, and REL and Cl^- Contents of Soybean Hairy Roots Composite Plants

Hairy root transformation was performed according to Ali et al. (2012). *A. rhizogenes* strain K599 containing the recombinant binary vector pCAMBIA1300-*GmCLC1* was grown in yeast extract peptone (YEP) medium containing 50 mg/L ampicillin (Amp) and 200 μM acetosyringone at 28°C for 16 h. Then the bacterial culture was centrifuged, and the pellet was resuspended gently in 10 mM $MgSO_4$ solution followed by two washings, and adjusted to $OD_{600} \approx 0.5$.

The cotyledons of soybean (Jackson and Lee68 cultivars) were scored with a scalpel and the wounds were infected with the pCAMBIA-containing *A. rhizogenes* infection solution for 1 h in dark at room temperature, and then transferred to moist filter paper and incubated in the dark for 5 days (at 25 ± 2°C). After that, the infected cotyledons were transferred to a growth chamber under a 12 h light/12 h dark cycle at 25 ± 2°C. New hair roots that sprout from the infected cotyledons that were free of *Agrobacterium* as screened by PCR and at similar lengths were selected and transferred into 1/2 X Hoagland solution (pH = 6.5) containing 0, 100, and 150 mM NaCl, respectively Hairy roots infected with *A. rhizogenes* strain K599 containing the empty vector pCAMBIA1300 served as the control. After 5 days treatment, hairy root growth (maximum root length and root fresh weight) was photographed and measured (Qi et al., 2014).

For whole-plant transformation, surface-sterilized soybean seeds (Jackson and Lee68 cultivars) were sown in pots containing a sterilized peat moss and vermiculite mixture. When the first pair of true leaves had fully expanded, the cotyledon nodes of the soybean seedlings were infected with the *A. rhizogenes* strain K599 infection solution for 1 h at room temperature by injection. Then the wounds were covered with moist vermiculite and incubated for 5 days at 28°C under a 12 h light/12 h dark cycle. After 7 days, hairy root lines that were free of *Agrobacterium* as screened by PCR were selected and the original roots removed from the seedlings. These seedlings were then cultured in 1/2 X Hoagland solution. Seedlings infected with *A. rhizogenes* strain K599 containing the empty vector pCAMBIA1300 served as the negative control. After 10 days, Jackson and Lee68 seedlings with similar-length hairy roots were selected and treated with 1/2 X Hoagland solution containing 120 mM NaCl for 3 and 5 days, respectively, and seedlings grown in Hoagland solution without NaCl served as the untreated control. All the solutions listed above were replaced every 3 days throughout the experiments. REL and Cl^- contents in roots, stems, first true leaves, and the first and second trifoliates were measured accordingly.

Tolerance Tests Using the Δ*gef1* Yeast Mutant

The yeast expression vector pYES2-*GmCLC1* was transformed into Δ*gef1* mutant yeast (*S. cerevisiae*) using the PEG/LiAc procedure and transformants were screened by PCR (Gietz, 2014). Ten-fold serial dilutions (starting at $OD_{550} \approx 0.5$) of each yeast culture were plated on agar supplemented with YPD medium (1% yeast extract/2% peptone/2% dextrose), YPG medium (1% yeast extract/2% peptone/2% galactose), or YPG medium supplemented with 1 M NaCl, 1 M KCl, or 3 mM $MnCl_2$. Plates were then incubated at 30°C and photographs were taken after 60 h. For Cl^- content measurements, the above-mentioned yeast cells were grown in the liquid YPG medium plus 1.0 M NaCl, and collected during the exponential growth phase ($OD_{550} \approx 0.2$), and their Cl^- contents were assayed by $AgNO_3$ titration as described by Zhou and Yu (2009).

Statistical Analyses

Data were expressed as mean ± SD of three independent experiments and were analyzed using one-way analysis of variance by SPSS 19.0, and pairwise comparisons were performed using Duncan's test.

RESULTS

GmCLC1 Alleviates NaCl Stress on Transgenic *A. thaliana* by Reducing Cl^- Accumulation in Leaves

The cDNA of *GmCLC1* was cloned from *G. max* cultivar N23674. The encoded protein product has the same sequence as the annotated product of *Glyma05g14760*. We have constructed five independent transgenic lines expressing *GmCLC1*. All transgenic lines exhibited NaCl tolerance (**Supplementary Figure S1**) and hence we selected one typical line for detailed analysis. The *A. thaliana* plant was successfully transformed with *GmCLC1* as shown with genotyping by PCR (**Figure 1A**). When grown on plate containing 150 or 200 mM NaCl, the seed germination rates of both WT and *GmCLC1*-transgenic line (L_1) declined as the NaCl concentration increased. However, under 150 or

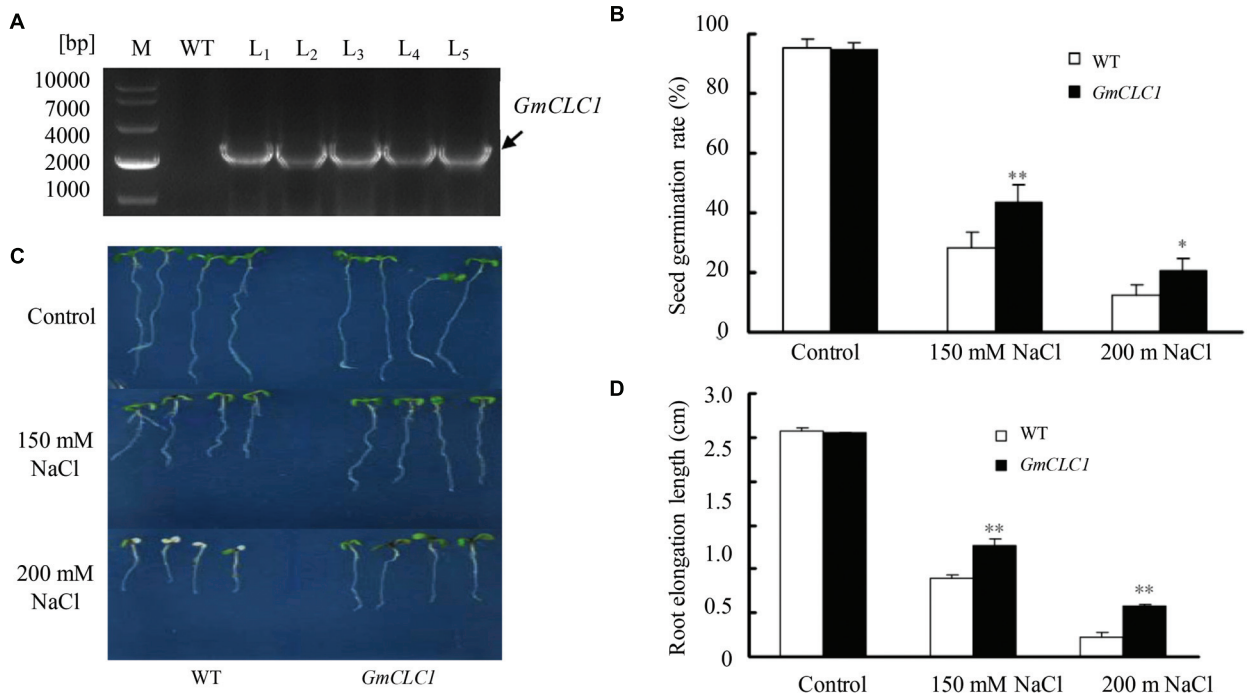

FIGURE 1 | Growth characteristics of *GmCLC1*-transgenic *Arabidopsis thaliana*. **(A)** Genotyping by PCR of *GmCLC1*-transgenic *A. thaliana* lines (L_1–L_5) to confirm success in transformation. All five lines contain the transgene. Comparison in **(B)** seed germination rate, **(C)** seedlings growth, and **(D)** root lengths between *A. thaliana* wild-type (WT) and transgenic plants (*GmCLC1*; using L_1 as the representative) sown on MS agar medium containing different concentrations of NaCl. **(B)** Seeds of WT and *GmCLC1* (30 seeds per plate each with three replicates) were surface-sterilized and stratified at 4°C for 2–4 days and then sown on MS medium supplemented with 150 or 200 mM NaCl. After 7 days of incubation, the seed germination rate (%) was measured. **(C,D)** 5-days-old WT and *GmCLC1* with nearly equal root lengths were transferred to MS agar medium supplemented with 0, 150, or 200 mM NaCl. After 5 days of vertical incubation, the seedlings' growth phenotypes were photographed and the root lengths measured. M: DNA markers. */**: The difference between WT and *GmCLC1* was significant at $p < 0.05$ and $p < 0.01$ respectively, using Duncan's test. Each bar represents the mean and SD of for **(C)** 30 seeds per plate each with three replicates; for **(D)** more than 10 plants for each treatment.

200 mM NaCl treatments, the transgenic line exhibited a higher germination rate than WT (**Figure 1B**). Also, under 200 mM NaCl treatment, the seedling growth of WT and *GmCLC1*-transgenic line in both roots and shoot were inhibited compared to the untreated control (**Figure 1C**). However, the root elongation of the *GmCLC1*-transgenic line was significantly higher than those of WT under either 150 or 200 mM NaCl stress ($p < 0.01$; **Figure 1D**). This indicates that ectopic expression of *GmCLC1* in *A. thaliana* could enhance seed germination and seedling growth under salt stress.

When WT and *GmCLC1*-transgenic seedlings were continuously exposed to NaCl stress with increasing concentrations (50 mM NaCl solution for 2 days, and 100 mM NaCl solution for next 2 days, followed by 150 mM NaCl solution for 7 days), the transgenic plants appeared to be healthier than WT (**Figure 2A**), and RWC and Fv/Fm were also significantly higher than those of WT ($p < 0.01$; **Figures 2B,C**), while the REL values were significantly lower than those of WT ($p < 0.01$ for root, $p < 0.05$ for leaf; **Figure 2D**). This further shows that the *GmCLC1*-transgenic *A. thaliana* plants suffered less leaf water loss, exhibited more stable photosynthetic capacity and had reduced salt injuries compared to untransformed WT when under salt stress.

During the 6-days treatment with 150 mM NaCl, the Cl^- contents in the roots of both WT and *GmCLC1*-transgenic seedlings increased significantly within the first 4 h and then leveled off (**Figure 3A**). However, the Cl^- contents in the shoots of both WT and transgenic seedlings increased steadily throughout the duration of the experiment, with the increase in the shoots of WT being significantly higher than in the transgenic plants ($p < 0.01$; **Figure 3B**), indicating that *GmCLC1* reduces salt stress partly by reducing the Cl^- accumulation in shoots.

GmCLC1 Alleviates NaCl Stress on Transgenic Soybean Hairy Root Growth and Composite Plants

The transformation of soybean cotyledon hairy roots with *GmCLC1* was shown to be successful through genotyping by PCR (**Figure 4A**). Under normal growing condition without

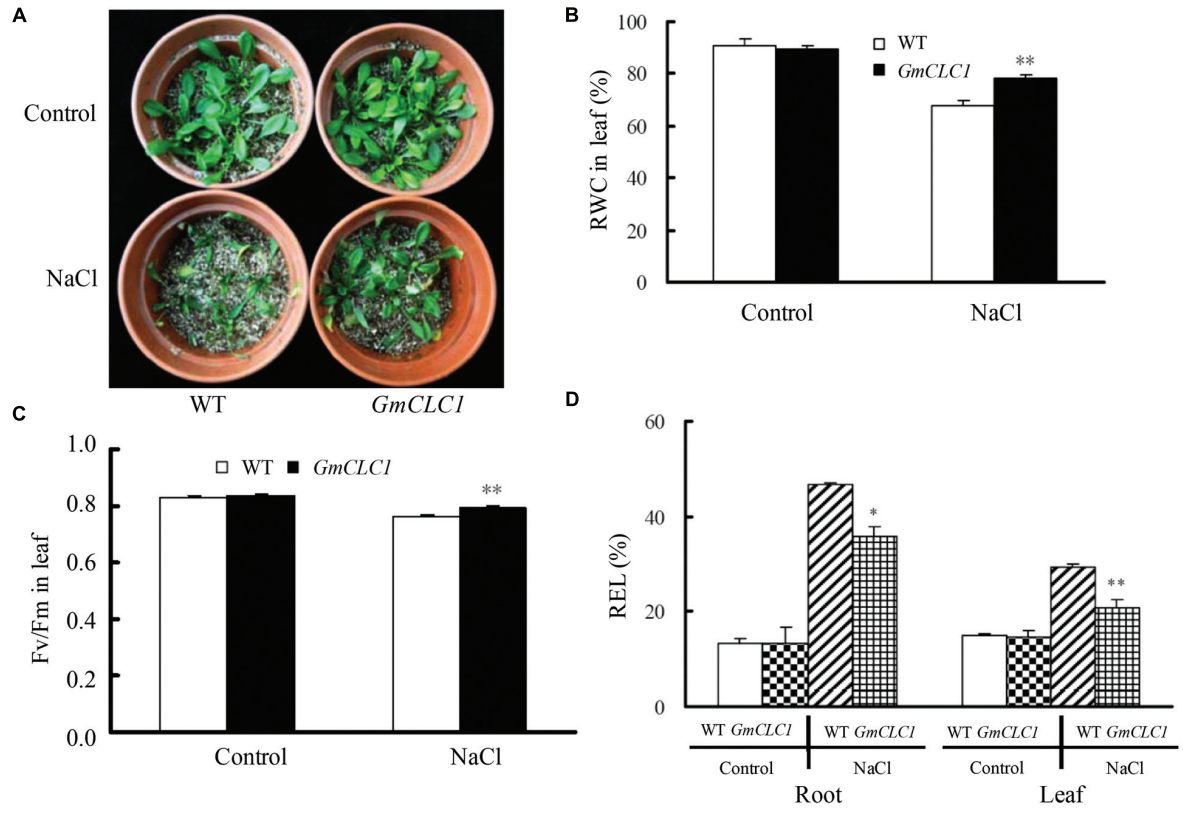

FIGURE 2 | Effects of NaCl treatment on (A) growth, (B) leaf relative water content (RWC), (C) chlorophyll fluorescence (Fv/Fm), and (D) relative electrolyte leakage (REL) in roots and leaves of *A. thaliana* WT and transgenic *GmCLC1* seedlings. Seeds of *Arabidopsis* WT and transgenic *GmCLC1* plants were surface-sterilized and kept at 4°C for 2–4 days and then sown on MS medium. After 8 days of incubation, the seedlings were transferred into plastic pots filled with a sterilized peat moss and vermiculite mixture, and fertilized with ½-strength Hoagland nutrient solution for 5 days in the greenhouse. The nutrient solution was continuously replaced with half-strength Hoagland solution containing 50 mM NaCl for 2 days, followed by 100 mM NaCl for 2 days, and finally 150 mM NaCl for 7 days. No NaCl was added to the nutrient solution for the control treatment. */**: The difference between WT and *GmCLC1* was significant at $p < 0.05/0.01$, respectively, using Duncan's test. Each bar represents the mean and SD of at least three replicates.

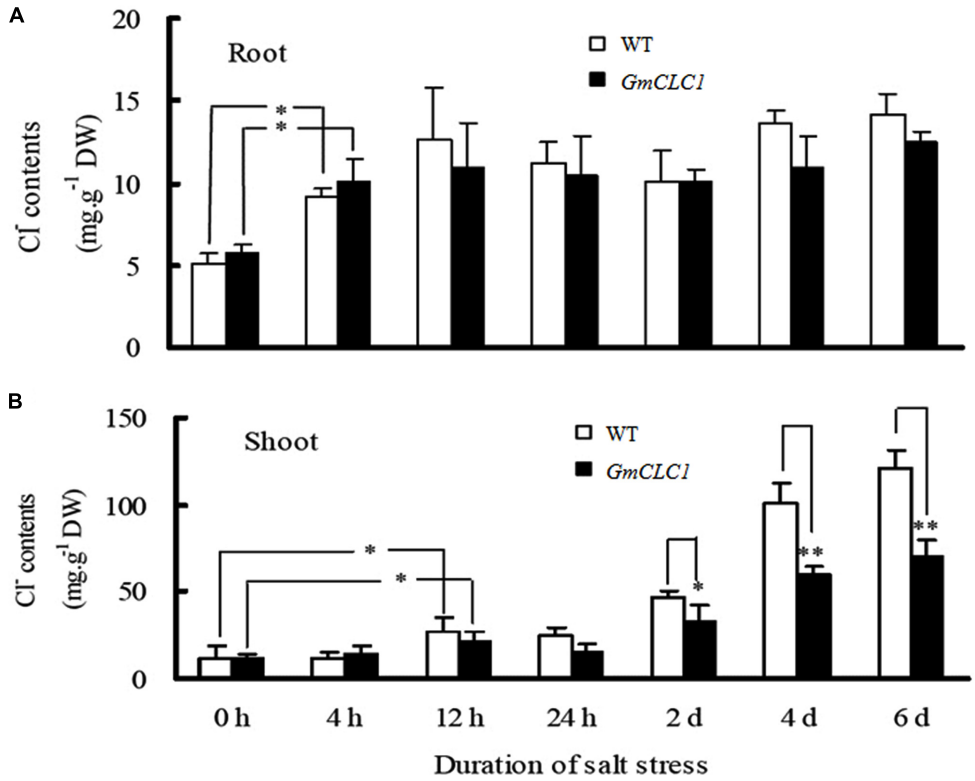

FIGURE 3 | Dynamic changes in the chloride (Cl^-) contents in (A) roots and (B) shoots of *A. thaliana* WT and transgenic *GmCLC1* seedlings under 150 mM NaCl stress for 6 days. Seeds of WT and *GmCLC1* transgenic *A. thaliana* were grown on pots containing the sterilized peat moss and vermiculite mixture and grown. After 30 days, plants were treated with 1/2 Hoagland solution containing 150 mM NaCl for 0, 4, 12, 24 h, 2, 4, and 6 days, respectively, then the roots **(A)** and shoot **(B)** of *Arabidopsis* seedlings were sampled and Cl^- contents were measured. */**: The difference between WT and the *GmCLC1* transgenic line was significant at $p < 0.05/0.01$, using Duncan's test. Each bar represents the mean and SD of at least three replicates.

additional NaCl, both empty vector- and *GmCLC1*-transformed hairy roots grew well, with no obvious difference (**Figure 4B**). However, under 100 mM NaCl stress, the growth of the hairy roots of both *GmCLC1*-transformed and empty vector-transformed lines were significantly inhibited, and the numbers of root branching were also reduced as compared to the untreated control. The maximum root lengths and fresh weights of empty vector-transformed hairy roots decreased more significantly than the *GmCLC1*-transformed ones ($p < 0.01$). At the NaCl concentration of 150 mM, the growth of the hairy roots of both *GmCLC1*- and empty vector-transformed cotyledons were inhibited, but there was no significant difference between the two (**Figures 4C,D**).

Building on the results we obtained using the *GmCLC1*-transgenic soybean cotyledon hairy root system, we further tested the response of whole *GmCLC1*-transgenic soybean hairy root composite plants to salt stress. First, the presence of the transgene in the soybean plants was confirmed by PCR (**Figure 5A**). Without any additional NaCl in the culture medium, there was no obvious phenotypic difference between the *GmCLC1*-transgenic soybean (including both Jackson and Lee68 cultivars) hairy root composite plants and the empty vector-transformed plants (**Figure 5B**). There was also no significant difference in the REL values of roots, first true leaves, the first and second trifoliate leaves among all the genotypes when grown in NaCl-free medium (**Figure 5C**).

When Jackson or Lee68 *GmCLC1*-transgenic soybean hairy root composite plants and the corresponding empty vector-transformed plants were exposed to 150 mM NaCl solution, the relatively salt-sensitive Jackson cultivar (both vector-only and *GmCLC1*) displayed obvious salt injury symptoms (with severely withered leaves) on the 3rd day, while the salt-tolerant Lee68 cultivar (both vector-only and *GmCLC1*) showed only mildly withered leaves up to the 5th day (**Figure 5B**). Furthermore, the hairy root composite plants of both cultivars that were transformed with *GmCLC1* showed better salt adaptation than their empty vector-transformed counterparts, especially for the more salt-tolerant Lee68 cultivar (**Figure 5B**). When examining the REL values in separate parts of the composite soybean plants, we found the REL values of roots, first true leaves, the first and second trifoliate leaves of *GmCLC1* were all significantly lower than their empty vector-transformed counterparts from the Lee68 cultivar ($p < 0.01$). The REL values of the second trifoliates of the *GmCLC1*-transgenic Lee68 cultivar, especially, were comparable to those of the water control. The REL values of the roots and second trifoliate leaves of *GmCLC1* of the

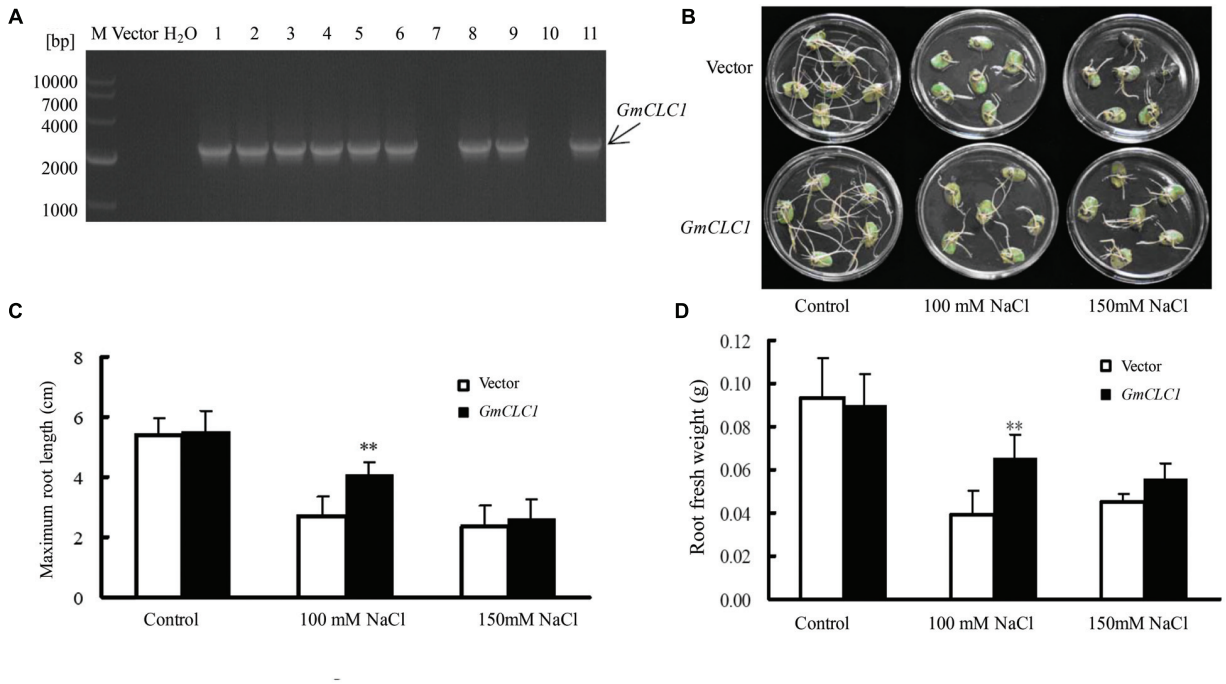

FIGURE 4 | Growth characteristics of transgenic soybean (hair root *GmCLC1*) under NaCl treatment. (A) PCR verification of the presence of the transgene, *GmCLC1*, in the transgenic soybean hairy roots (*GmCLC1*) that had undergone *Agrobacterium rhizogenes*-mediated cotyledon transformation. Nine out of the 11 lines were successfully transformed. M: DNA marker; Vector: empty vector, as negative control; ddH_2O: distilled deionized water, as negative control. Comparisons of **(B)** hairy root phenotype, **(C)** maximum root length, and **(D)** root fresh weight of empty vector-transformed control and *GmCLC1* grown in with 1/2 Hoagland solution containing 0, 100, and 150 mM NaCl for 5 days. Each bar represents the mean and SD of three replicates each with six soybean cotyledons. **: The difference between was significant at $p < 0.01$, using Duncan's test.

Jackson cultivar were also significantly lower than their empty vector-transformed counterparts ($p < 0.01$ and 0.05, respectively; **Figure 5C**).

In addition, under salt stress, the Cl^- contents in roots, stems, first true leaves and the first trifoliate leaves of both Jackson and Lee68 hairy root composite plants (including both *GmCLC1* and vector-only) were dramatically increased compared to the water control. It is clear that the *GmCLC1*-transgenic plants of the Lee68 cultivar, when compared to their empty vector-transformed counterparts, had significantly lower Cl^- accumulation in their stems, first true leaves and the first trifoliate leaves ($p < 0.01$), and *GmCLC1*-transgenic plants of the Jackson cultivar also had significantly lower Cl^- accumulation in the first trifoliates ($p < 0.01$; **Figure 5D**). This indicates that the ectopic expression of *GmCLC1* in Jackson or Lee68 hairy root composite plants can reduce the Cl^- transportation and accumulation in the aerial parts of the plant, especially for the salt-tolerant Lee68 cultivar.

GmCLC1 Enhances Survival of the Chloride-Channel-Deficient Yeast Mutant Δ*gef1* under $MnCl_2$, NaCl, or KCl

All the yeast strains, including the mutant Δ*gef1* (a *GEF1*-deficient mutant), and Δ*gef1* transformed with empty vector, *GEF1*, and *GmCLC1*, grew well on both YPD and YPG media under normal growing conditions. When cultured on YPG medium supplemented with 3 mM $MnCl_2$, the mutant Δ*gef1* and Δ*gef1*/Vector were unable to grow, but the mutants transformed with yeast *GEF1* or soybean *GmCLC1* could. Similarly, mutants transformed with yeast *GEF1* or soybean *GmCLC1* grew better on YPG medium supplemented with 1.0 M NaCl or 1.0 M KCl (**Figure 6A**). The Cl^- contents in the cells of Δ*gef1*/*GEF1* and Δ*gef1*/*GmCLC1* grown in liquid YPG medium plus 1.0 M NaCl were significantly higher than in the control cells without intracellular vesicle-localized *GEF1* transporter activity (Δ*gef1* and Δ*gef1*/Vector; $p < 0.01$; **Figure 6B**). Thus *GmCLC1* may have similar functions much like the yeast *GEF1*.

DISCUSSION

Ionic toxicity is the main cause of salt injury for plants or crops, and Cl^- is the main culprit. The predominant strategies for plants to reduce the effects of salt stress are via active Cl^- efflux or vacuolar Cl^- partitioning to reestablish intracellular Cl^- homeostasis (Tealle and Tyerman, 2010; Wei et al., 2013; Wong et al., 2013), especially for chloride-intolerant plants such as the cultivated soybean, citrus, grape, potato, tobacco, and so on (Moya et al., 2003; Henderson et al., 2014).

In the *Arabidopsis* genome, a total of seven genes (*AtCLCa-g*) encoding putative CLC proteins have been identified. For

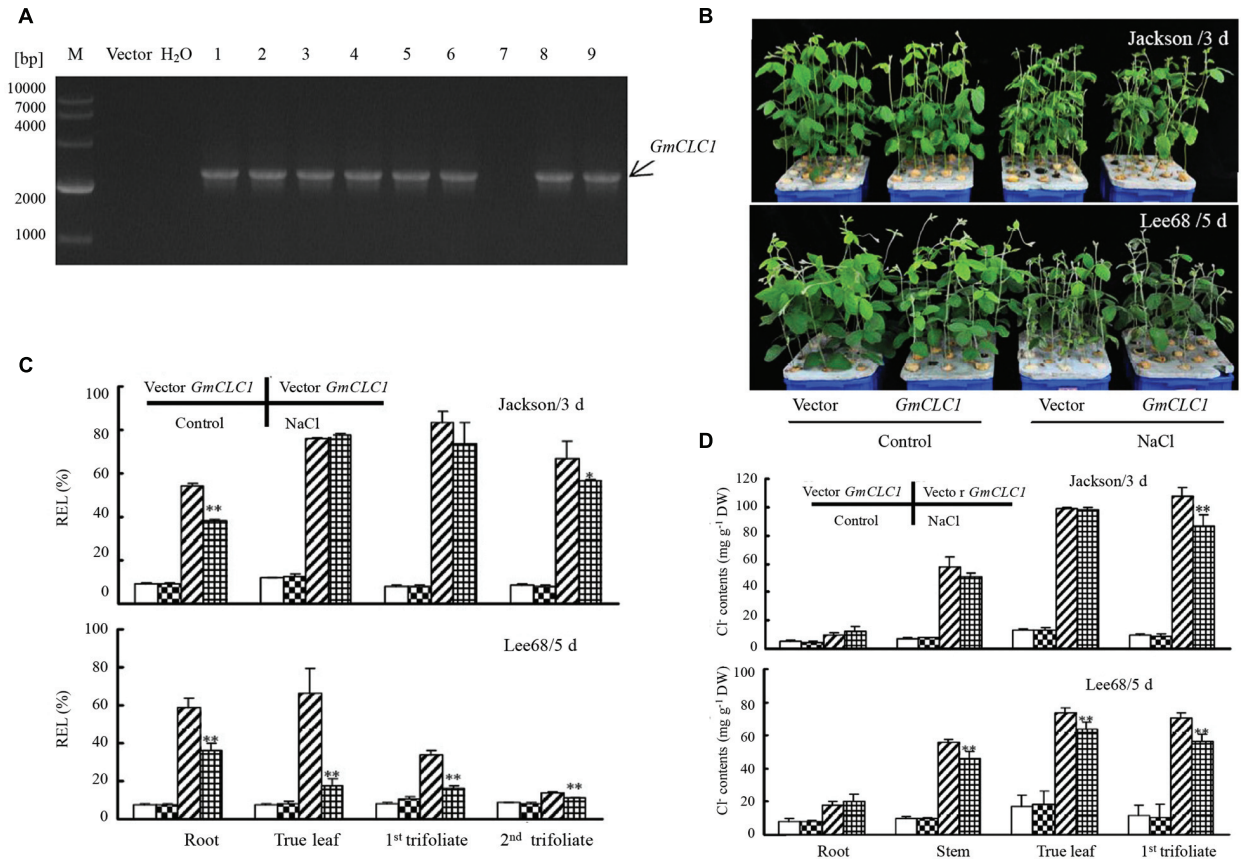

FIGURE 5 | Growth phenotype and physiological responses of soybean hairy root composite plants (*GmCLC1*) under NaCl treatment. (A) PCR verification of the presence of the transgene, *GmCLC1*, in the soybean hairy root composite plants (lines 1–6 and 8–9). M: DNA markers; Vector: Empty vector-transformed plants (negative control); ddH_2O: distilled deionized water (negative control). **(B)** Phenotypes of empty vector-transformed and *GmCLC1*-transgenic plants. Surface-sterilized soybean seeds were sown in container till the first pair of unifoliate leaves was fully expanded, the cotyledon node site of soybean seedlings were infected with the *A. rhizogenesin* K599 for 1 h at room temperature. The wound was then covered with moist vermiculite and co-cultivated with *A. rhizogenesin* K599 for 5 days at 25 ± 2°C under a 12/12 h light/dark cycle. After 7 days, hairy root lines were identified by PCR for free of bacterium. The original roots were removed and the seedlings with positive hairy roots were cultured in 1/2 Hoagland solution. After 10 days, seedlings were treated with 1/2 Hoagland solutions containing 120 mM NaCl for 3 or 5 days, respectively, and solutions without NaCl as the untreated control. **(C)** REL and **(D)** Cl^- content of *GmCLC1*-transgenic soybean plants versus empty vector-transformed controls (Vector) in different parts of the plant. Control: no NaCl was given to the growth medium; DW: dry weight; */**: The difference between was significant at $p < 0.05/0.01$, using Duncan's test. Each bar represents the mean and SD of three replicates.

example, *AtCLCc* is mainly expressed in stomatal guard cells, and the AtCLCc protein located in the tonoplast displays transmembrane Cl^--transporting activity, which not only aids in the regulation of stomatal movements, but also in enhancing salt tolerance (Lv et al., 2009; Jossier et al., 2010). Nguyen et al. (2015) reported that a knock-out mutant AtCLCg, a member of the *Arabidopsis* CLC family localized in the vacuolar membrane, showed a decrease in biomass and an accumulation of chloride in shoots when grown under NaCl stress. *AtCLCg* was expressed in mesophyll cells, hydathodes and phloem while AtCLCc (with 62% similarity to AtCLCg protein) was expressed in stomata. A *atclcc/atclccg* double mutant was not more sensitive to NaCl than the single mutants, which demonstrated that AtCLCc and AtCLCg formed part of a regulatory network controlling chloride sensitivity and were both important for chloride tolerance but not redundant.

The soybean genome has eight *CLC* genes in total: *Glyma01g44950*, *Glyma05g14760 (GmCLC1)*, *Glyma09g28620*, *Glyma11g00690*, *Glyma13g23080*, *Glyma16g06190*, *Glyma16-g33351,* and *Glyma19g25680* located on chromosomes 1, 5, 9, 11, 13, 16, and 19, respectively (Li et al., 2014).

We previously reported that *GmCLC1* encodes a putative Cl^-/H^+ antiporter (Wong et al., 2013) that is localized on tonoplast (Li et al., 2006). Protective functions of *GmCLC1* were only shown using transgenic tobacco cells (Li et al., 2006). In this study, we conducted functional tests *in planta*.

Our results showed that the ectopic expression of *GmCLC1* in *Arabidopsis* (**Figure 1A**) significantly enhanced the transgenic seeds germination rate and subsequent seedling growth (**Figures 1B–D**), and the transgenic plants were better able to adapt to NaCl stress (**Figure 2A**). Moreover, the alleviation of salt injuries to *GmCLC1*-transgenic *Arabidopsis* plants was

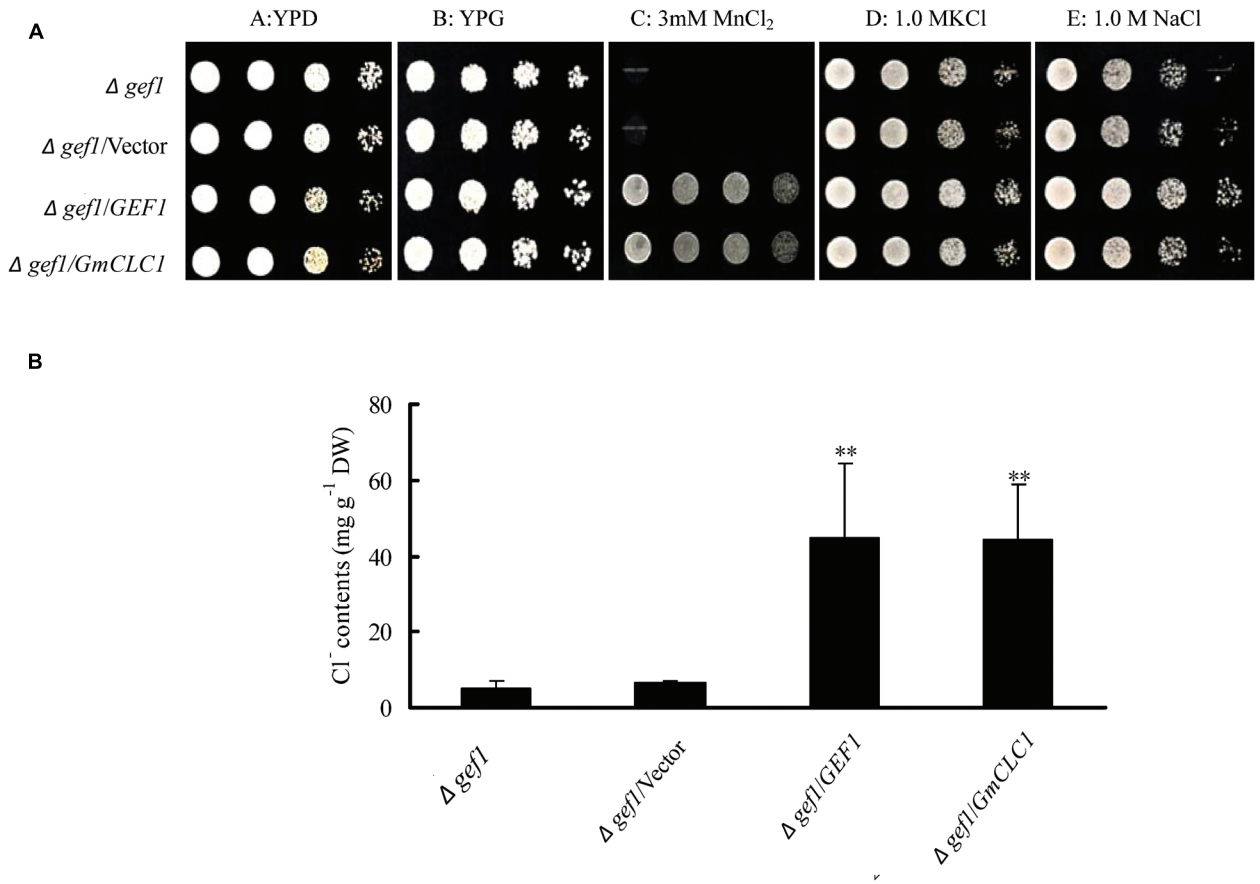

FIGURE 6 | Effects of expressing *GmCLC1* on the survival of the Δ*gef1* yeast mutant under $MnCl_2$, NaCl, or KCl. (A) *GmCLC1* could enhance the survival of the chloride channel-deficient Δ*gef1* yeast mutant in the same way as *GEF1*, when the yeast was grown in media supplemented with $MnCl_2$, KCl, and NaCl. The Δ*gef1* mutant was also transformed with an empty vector as a negative control. The expression vector pYES2 containing *GEF1* or *GmCLC1* was introduced into the Δ*gef1* mutant. Ten-fold serial dilutions (starting at $OD_{550} \approx 0.5$) of each sample were plated on media of YPD, YPG, or YPG supplemented with 3 mM $MnCl_2$, 1.0 M KCl, or 1.0 M NaCl. Plates were incubated at 30°C and photographs were taken after 60 h. **(B)** The expression of *GmCLC1* in the *gef1* yeast mutant increased Cl^- accumulation. Cells of the above-mentioned Δ*gef1* mutant, Δ*gef1/Vector*, Δ*gef1/GEF1*, or Δ*gef1/GmCLC1* were grown in liquid YPG medium with 1.0 M NaCl. When cultures reached $OD_{550} \approx 0.2$, cells were collected by filtration, and their Cl^- contents were determined. DW, dry weigh. Data shown are the means and standard deviations of ion contents of three independent cultures of each strain. **: The difference between was significant at $p < 0.01$, using Duncan's test.

correlated with reduction in Cl^- transport and accumulation in shoots compared to WT plants (**Figure 3B**). Since *GmCLC1* is tonoplast-localized, it is unlikely that this transporter will exclude Cl^- to prevent accumulating of this ion. Therefore, the root Cl^- concentration did not differ significantly by expressing *GmCLC1* (**Figure 3A**). In contrast, since *GmCLC1* may help to compartmentalize Cl^- into vacuole, it could delay Cl^- transporting from root to shoot and hence lead to a lower Cl^- concentration in the aerial part, in both transgenic *A. thaliana* (**Figure 3B**) and composite soybean plants (**Figure 5D**).

In a previous study Ali et al. (2012), it was found that over-expression of nine TFs (such as *GmWRKY*, *GmNAC2*, *GmbZIP110,* and *GmMYB92*) in hairy roots could enhance the survival or tolerance to 200 mM NaCl stress in mosaic or composite soybean plants. We also demonstrated that cotyledon hairy roots could be used as a rapid gain-of-function test for ion transporters (Qi et al., 2014). In this study, we employed soybean cotyledon hairy roots transformed with *GmCLC1* to investigate the role of this chloride transporter in enhancing salt tolerance (**Figures 4B–D**). We found that overexpression of *GmCLC1* in Jackson or Lee68 hairy root composite plants increased the Cl^- sequestering in roots, and, as a consequence, reduced Cl^- transportation and accumulation in aerial parts, and alleviated their salt injuries as represented by the REL values in roots and various stages of leaf development. This was especially true for the salt-tolerant Lee68 cultivar (**Figure 5**). All these findings inferred that in *GmCLC1* plays a vital role in enabling the soybean plant to adapt to chloride/salt stress.

To provide more understanding on how the GmCLC1 protein may function to control Cl^- accumulation, we made use of a yeast system. The yeast *GEF1* gene encodes a CLC-type chloride channel protein, which is co-localized with Ccc2 proteins to control Cu^{2+} in the intracellular vesicles, and drives Cl^- and H^+ transmembrane exchanges. Thus the yeast GEF1 protein is involved in the co-transport of Cu^{2+} or Fe^{3+}, the regulation of cation homeostasis and the growth of yeast cells. In the

Δ*gef1* loss-of-function yeast mutant, the Cl^- transport into the intracellular vesicles (vacuole or Golgi apparatus) was blocked, resulting in hypersensitivity to extracellular cations such as Cu^{2+}, Fe^{3+}, and Mn^{2+}, hygromycin B, tetramethyl ammonium chloride, and thus growth were hindered (Gaxiola et al., 1998; Lv et al., 2009; Sasvari et al., 2013). Among the seven *Arabidopsis CLC* paralogs (*AtCLCa-g*), over-expressions of *AtCLCa*, *AtCLCd,* and *AtCLCf* in the yeast *gef1* mutant could complement the deficiency in GEF1 protein functions or growth phenotype (Lv et al., 2009; Barbier-Brygo et al., 2011). When the soybean *GmCLC1* or the yeast *GEF1* gene was transformed into the Δ*gef1* mutant and cultured in YPG media containing different chloride salts ($MnCl_2$, KCl, NaCl), the growth of the transformed mutants was much enhanced compared to the original mutant. Therefore, *GmCLC1* may help restore the Cl^- transportation into intercellular vesicles.

AUTHOR CONTRIBUTIONS

PW and LW conducted the experiments, collected and analyzed all data. BY and H-ML designed the experiments. BY, H-ML, and AL interpreted the data and wrote the manuscript. All authors read and approved the final version of the manuscript.

FUNDING

This work was supported by the National Natural Science Foundation of China (No. 30871462) and the Transgenic Engineering Crops Breeding Special Funds of China (No. 2009ZX08004-008B) awarded to BY and grants from Hong Kong Research Grants Council (Collaborative Research Fund: CUHK3/CRF/11G; Area of Excellence: AoE/M-05/12) and Lo Kwee-Seong Biomedical Research Fund awarded to H-ML.

ACKNOWLEDGMENTS

We would like to thank Dr. Dayong Zhang (Institute of Biotechnolgy, Jiangsu Academy of Agricultural Sciences, China) for kindly providing the *A. rhizogenes* strain K599 and related technical guidance on soybean transformation. We also thank Ms. Jee-Yan Chu for copy-editing the manuscript.

SUPPLEMENTARY MATERIAL

The Supplementary Material for this article can be found online at: http://journal.frontiersin.org/article/10.3389/fpls.2016.01082

FIGURE S1 | Growth characteristics of *GmCLC1*-transgenic *Arabidopsis thaliana*. (A) Growth of WT and transgenic *Arabidopsis GmCLC1* (L_1–L_5) under salt stress. Comparison in **(B)** fresh weight (FW) and **(C)** shoot fresh weight (FW) of WT and *GmCLC1*-transgenic *Arabidopsis* plants (L_1, L_2, L_5). Seeds of WT and *Arabidopsis* transgenic *GmCLC1* plants were surface-sterilized and kept at 4°C for 2–4 days and then sown on MS medium. After 8 days of incubation, the seedlings were transferred into plastic pots filled with a sterilized peat moss and vermiculite mixture, and fertilized with 1/2-strength Hoagland nutrient solution for 5 days in the greenhouse. The nutrient solution was continuously replaced with half-strength Hoagland solution containing 50 mM NaCl for 2 days, followed by 100 mM NaCl for 2 days, and finally 150 mM NaCl for 6 days. No NaCl was added to the nutrient solution for the control treatment. */**: The difference between WT and *GmCLC1* was significant at $p < 0.05/0.01$, respectively, using Duncan's test. Each bar represents the mean and SD of at least three replicates.

REFERENCES

Adams, E., and Shin, R. (2014). Transport, signaling, and homeostasis of potassium and sodium in plants. *J. Integr. Plant Biol.* 56, 231–249. doi: 10.1111/jipb.12159

Adem, G. D., Roy, S. J., Zhou, M. X., Bowman, J. P., and Shabala, S. (2014). Evaluating contribution of ionic, osmotic and oxidative stress components towards salinity tolerance in barley. *BMC Plant Biol.* 14:113. doi: 10.1186/1471-2229-14-113

Ali, Z., Zhang, D. Y., Xu, Z. L., Xu, L., Yi, J. X., He, X. L., et al. (2012). Uncovering the salt response of soybean by unraveling its wild and cultivated functional genomes using tag sequencing. *PLoS ONE* 7:e48819. doi: 10.1371/journal.pone.0048819

Barbier-Brygo, H., Angeli, A. D., Filleur, S., Frachisse, J. M., Gambale, F., Thomine, S., et al. (2011). Anion channels/transporters in plants: from molecular bases to regulatory networks. *Annu. Rev. Plant Biol.* 62, 25–51. doi: 10.1146/annurev-arplant-042110-103741

Brumós, J., Talón, M., Bouhlal, R., and Colmenero-Flores, J. M. (2010). Cl-homeostasis in includer and excluder citrus rootstocks: transport mechanisms and identification of candidate genes. *Plant Cell Environ.* 33, 2012–2027. doi: 10.1111/j.1365-3040.2010.02202.x

Chen, X. Q., and Yu, B. J. (2007). Ionic effects of Na+ and Cl- on photosynthesis in *Glycine max* seedlings under isoosmotic salt stress. *J. Plant Physiol. Mol. Biol.* 33, 294–300.

Clough, S. J., and Bent, A. F. (1998). Floral dip: a simplified method for *Agrobacterium*-mediated transformation of *Arabidopsis thaliana*. *Plant J.* 16, 735–743. doi: 10.1046/j.1365-313x.1998.00343.x

Deinlein, U., Stephan, A. B., Horie, T., Luo, W., Xu, G. H., and Schroeder, J. I. (2014). Plant salt-tolerance mechanisms. *Trends Plant Sci.* 19, 371–379. doi: 10.1016/j.tplants.2014.02.001

Gaxiola, R. A., Yuan, D. S., Klausner, R. D., and Fink, G. R. (1998). The yeast CLC chloride channel functions in cation homeostasis. *Proc. Natl. Acad. Sci. U.S.A.* 95, 4046–4050. doi: 10.1073/pnas.95.7.4046

Gietz, R. D. (2014) "Yeast transformation by the LiAc/SS carrier DNA/PEG method," in *Yeast Protocols, Methods in Molecular Biology*. Vol. 1163, ed. W. Xiao (New York, NY: Springer Science+Business Media), 33–44.

Guo, W., Zuo, Z., Cheng, X., Sun, J., Li, H., Li, L., et al. (2014). The chloride channel family gene CLCd negatively regulates pathogen-associated molecular pattern (PAMP)-triggered immunity in *Arabidopsis*. *J. Exp. Bot.* 65, 1205–1215. doi: 10.1093/jxb/ert484

Gupta, B., and Huang, B. (2014). Mechanism of salinity tolerance in plants: physiological, biochemical, and molecular characterization. *Int. J. Genom.* 2014, 1–18. doi: 10.1155/2014/701596

Hasegawa, P. M. (2013). Sodium (Na+) homeostasis and salt tolerance of plants. *Environ. Exp. Bot.* 92, 19–31. doi: 10.1016/j.envexpbot.2013.03.001

Henderson, S. W., Baumann, U., Blackmore, D. H., Walker, A. R., Walker, R. R., and Gilliham, M. (2014). Shoot chloride exclusion and salt tolerance in grapevine is associated with differential ion transporter expression in roots. *BMC Plant Biol.* 14:273. doi: 10.1186/s12870-014-0273-8

Hu, S. B., Zhou, Q., An, J., and Yu, B. J. (2016). Cloning of *PIP* genes in drought-tolerant vetiver grass and responses of transgenic *VzPIP2;1* soybean plants to water stress. *Biol. Plant.* doi: 10.1007/s10535-016-0631-5

Jossier, M., Kroniewicz, L., Dalmas, F., Le Thiec, D., Ephritikhine, G., Thomine, S., et al. (2010). The *Arabidopsis* vacuolar anion transporter, AtCLCc, is involved

in the regulation of stomatal movements and contributes to salt tolerance. *Plant J.* 64, 563–576. doi: 10.1111/j.1365-313X.2010.04352.x

Li, W., Wang, L. C., and Yu, B. J. (2014). Bioinformatics analysis of CLC homologous genes family in soybean genome. *J. Nanjing Agric. Univ.* 37, 35–43.

Li, W. Y. F., Wong, F. L., Tsai, S. N., Phang, T. H., Shao, G. H., and Lam, H. M. (2006). Tonoplast-located GmCLC1 and GmNHX1 from soybean enhance NaCl tolerance in transgenic bright yellow (BY)-2 cells. *Plant Cell Environ.* 29, 1122–1137. doi: 10.1111/j.1365-3040.2005.01487.x

Luo, Q. Y., Yu, B. J., and Liu, Y. L. (2005). Differential sensitivity to chloride and sodium ions in seedlings of *Glycine max* and *G. soja* under NaCl stress. *J. Plant Physiol.* 162, 1003–1012. doi: 10.1016/j.jplph.2004.11.008

Lv, Q. D., Tang, R. J., Liu, H., Gao, X. S., Li, Y. Z., Zheng, H. Q., et al. (2009). Cloning and molecular analyses of the *Arabidopsis thaliana* chloride channel gene family. *Plant Sci.* 176, 650–661. doi: 10.1016/j.plantsci.2009.02.006

Moya, J. L., Gómez-Cadenas, A., Primo-Millo, E., and Talon, M. (2003). Chloride absorption in salt-sensitive Carrizo citrange and salt-tolerant *Cleopatra mandarin* citrus rootstocks is linked to water use. *J. Exp. Bot.* 54, 825–833. doi: 10.1093/jxb/erg064

Nguyen, C. T., Agorio, A., Jossier, M., Depré, S., Thomine, S., and Filleur, S. (2015). Characterization of the chloride channel-like, AtCLCg, involved in chloride tolerance in *Arabidopsis thaliana*. *Plant Cell Physiol.* 57, 764–775. doi: 10.1093/pcp/pcv169

Nie, W. X., Xu, L., and Yu, B. J. (2015). A putative soybean GmsSOS1 confers enhanced salt tolerance to transgenic *Arabidopsis* sos1-1 mutant. *Protoplasma* 252, 127–134. doi: 10.1007/s00709-014-0663-7

Qi, X. P., Li, M. W., Xie, M., Liu, X., Ni, M., Shao, G. H., et al. (2014). Identification of a novel salt tolerance gene in wild soybean by whole-genome sequencing. *Nat. Commun.* 5:4340. doi: 10.1038/ncomms5340

Qu, Y. N., Zhou, Q., and Yu, B. J. (2009). Effects of Zn2+ and niflumic acid on photosynthesis in *Glycine soja* and *Glycine max* seedlings under NaCl stress. *Environ. Exp. Bot.* 65, 304–309. doi: 10.1016/j.envexpbot.2008.11.005

Sasvari, Z., Kovalev, N., and Nagy, P. D. (2013). The GEF1 Proton-Chloride exchanger affects *Tombusvirus* replication via regulation of copper metabolism in yeast. *J. Virol.* 87, 1800–1810. doi: 10.1128/JVI.02003-12

Tealle, N. L., and Tyerman, S. D. (2010). Mechanisms of Cl- transport contributing to salt tolerance. *Plant Cell Environ.* 33, 566–589. doi: 10.1111/j.1365-3040.2009.02060.x

Tian, F., Jia, T. J., and Yu, B. J. (2014). Physiological regulation of seed soaking with soybean isoflavones on drought tolerance of *Glycine max* and *Glycine soja*. *Plant Growth Regul.* 74, 229–237. doi: 10.1007/s10725-014-9914-z

Tregeagle, J. M., Tisdall, J. M., Tester, M., and Walker, R. R. (2010). Cl– uptake, transport and accumulation in grapevine rootstocks of differing capacity for Cl—exclusion. *Funct. Plant Biol.* 37, 665–673. doi: 10.1071/FP09300

Wang, S., Su, S. Z., Wu, Y., Li, S. P., Shan, X. H., Liu, H. K., et al. (2015). Overexpression of maize chloride channel gene ZmCLC-d in *Arabidopsis thaliana* improved its stress resistance. *Biol. Plant.* 59, 55–64. doi: 10.1007/s10535-014-0468-8

Wei, Q. J., Liu, Y. Z., Zhou, G. F., Li, Q. H., Yang, C. Q., and Peng, S. A. (2013). Overexpression of CsCLCc, a chloride channel gene from *Poncirus trifoliata*, enhances salt tolerance in *Arabidopsis*. *Plant Mol. Biol. Rep.* 31, 1548–1557. doi: 10.1007/s11105-013-0592-1

Wong, T. H., Li, M. W., Yao, X. Q., and Lam, H. M. (2013). The GmCLC1 protein from soybean functions as a chloride ion transporter. *J. Plant Physiol.* 170, 101–104. doi: 10.1016/j.jplph.2012.08.003

Xiao, Y. H., Xi, H., Shen, Y. Z., and Huang, Z. J. (2013). A novel wheat alpha-amylase inhibitor gene, TaHPS, significantly improves the salt and drought tolerance of transgenic *Arabidopsis*. *Physiol. Plant.* 148, 273–283. doi: 10.1111/j.1399-3054.2012.01707.x

Yu, B. J., and Liu, Y. L. (2004). Chlorine, chloride channel and chlorine tolerance in plants. *Chin. Bull. Bot.* 21, 402–410.

Zhang, X. K., Zhou, Q. H., Cao, J. H., and Yu, B. J. (2011). Differential Cl-/Salt tolerance and NaCl-induced alternations of tissue and cellular ion fluxes in *Glycine max*, *Glycine soja* and their hybrid seedlings. *J. Agron. Crop Sci.* 197, 329–339. doi: 10.1111/j.1439-037X.2011.00467.x

Zhou, C., Wang, H. P., Zhu, J., and Liu, Z. X. (2013). Molecular cloning, subcellular localization and functional analysis of thclc-a from *Thellungiella Halophila*. *Plant Mol. Biol. Rep.* 31, 783–790. doi: 10.1007/s11105-012-0545-0

Zhou, Q., and Yu, B. J. (2009). Accumulation of inorganic and organic osmolytes and their role in osmotic adjustment in nacl-stressed vetiver grass seedlings. *Russ. J. Plant Physiol.* 56, 678–875. doi: 10.1134/S1021443709050148

Zifarelli, G., and Pusch, M. (2010). CLC transport proteins in plants. *FEBS Lett.* 584, 2122–2127. doi: 10.1016/j.febslet.2009.12.042

Conflict of Interest Statement: The authors declare that the research was conducted in the absence of any commercial or financial relationships that could be construed as a potential conflict of interest.

frontiers in Plant Science

ORIGINAL RESEARCH
published: 06 October 2015
doi: 10.3389/fpls.2015.00820

Impact of high temperature stress on floret fertility and individual grain weight of grain sorghum: sensitive stages and thresholds for temperature and duration

P. V. V. Prasad[1], Maduraimuthu Djanaguiraman[1], Ramasamy Perumal[2] and Ignacio A. Ciampitti[1]*

[1] Department of Agronomy, Throckmorton Plant Science Center, Kansas State University, Manhattan, KS, USA, [2] Agricultural Research Center – Hays, Hays, KS, USA

OPEN ACCESS

Edited by:
Urs Feller,
University of Bern, Switzerland

Reviewed by:
Mirza Hasanuzzaman,
Sher-e-Bangla Agricultural University, Bangladesh
Edmundo Acevedo,
University of California, Davis, USA

***Correspondence:**
P. V. V. Prasad,
Department of Agronomy, Throckmorton Plant Science Center, Kansas State University, Room 2004, 1712 Claflin Road, Manhattan, KS 66506, USA
vara@ksu.edu

Specialty section:
This article was submitted to Agroecology and Land Use Systems, a section of the journal Frontiers in Plant Science

Received: *28 July 2015*
Accepted: *18 September 2015*
Published: *06 October 2015*

Citation:
Prasad PVV, Djanaguiraman M, Perumal R and Ciampitti IA (2015) Impact of high temperature stress on floret fertility and individual grain weight of grain sorghum: sensitive stages and thresholds for temperature and duration. Front. Plant Sci. 6:820. doi: 10.3389/fpls.2015.00820

Sorghum [*Sorghum bicolor* (L.) Moench] yield formation is severely affected by high temperature stress during reproductive stages. This study pursues to (i) identify the growth stage(s) most sensitive to high temperature stress during reproductive development, (ii) determine threshold temperature and duration of high temperature stress that decreases floret fertility and individual grain weight, and (iii) quantify impact of high daytime temperature during floret development, flowering and grain filling on reproductive traits and grain yield under field conditions. Periods between 10 and 5 d before anthesis; and between 5 d before- and 5 d after-anthesis were most sensitive to high temperatures causing maximum decreases in floret fertility. Mean daily temperatures >25°C quadratically decreased floret fertility (reaching 0% at 37°C) when imposed at the start of panicle emergence. Temperatures ranging from 25 to 37°C quadratically decreased individual grain weight when imposed at the start of grain filling. Both floret fertility and individual grain weights decreased quadratically with increasing duration (0–35 d or 49 d during floret development or grain filling stage, respectively) of high temperature stress. In field conditions, imposition of temperature stress (using heat tents) during floret development or grain filling stage also decreased floret fertility, individual grain weight, and grain weight per panicle.

Keywords: abiotic stress, floret fertility, grain size, reproductive success, sensitive stage, spikelet fertility, sporogenesis

Introduction

Grain sorghum [*Sorghum bicolor* (L.) Moench] is an important dryland crop for food, feed, and fuel. In the semi-arid tropics the mean crop growing season temperatures are already close to optimum or above optimum for grain sorghum growth and development (Prasad et al., 2006a; Singh et al., 2014). The optimum range of air temperature for sorghum during the vegetative period is 26–34°C (Hammer et al., 1993); and during the reproductive period is 25–28°C (Prasad et al., 2006a, 2008a). Future projected changes in temperature could severely impact sorghum yields in several parts of the world. Srivastava et al. (2010) projected that climate change (HadCM3 model, A2a scenario) in different parts of India will decrease rainy season sorghum yields up to 14%

and post rainy season sorghum yields up to 7% by 2020. Similarly, Butt et al. (2005) projected a decrease in sorghum yield from 11 to 17% in Mali by 2030. Several other simulation models projected decrease in sorghum yield under future climate scenarios in Africa (Chipanshi et al., 2003; Tingem et al., 2008; Sultan et al., 2013, 2014). Projections for middle and end of the century are more severe.

Sorghum yield potential is often limited by short high temperature stress episodes occurring primarily during the reproductive period (Prasad et al., 2008a). Occurrence and intensity of high-temperature episodes is likely to increase in future climates (IPCC, 2013). Increased frequency of high temperature stress can cause significant yield losses depending on timing (sensitive growth stages), intensity and duration. Thus, it is critical to precisely: (i) quantify temperature responses, (ii) determine threshold for absolute temperature values and its duration, and (iii) define sensitive growth stages. Such information is needed to accurately estimate implications of climate variability and understand impact of short episodes of high temperature events on sorghum grain yield and its components.

Grain crops are generally more sensitive to high temperatures during reproductive than vegetative stages of crop development (Farooq et al., 2011); primarily impacting yield formation. The two major yield components of grain crops are grain numbers and individual grain weight (grain size), both of which are sensitive to high temperatures. Grain numbers are a result of successful fertilization (seed-set), which mainly depends on the functionality of male (pollen) and female (ovule) gametes. Adverse environmental conditions during floral development and anthesis can negatively influence viability and functionality of gametes leading to decreases in floret fertility and, consequently, seed set. Similarly, high temperatures during the grain filling period decrease individual grain size due to shorter grain filling duration (Prasad et al., 2008a) and/or grain filling rate (Prasad et al., 2006a, 2008b; Dias and Lidon, 2009). Decreases in grain number and individual grain weight leads to lower grain yields.

High temperature stress during pre-anthesis (sporogenesis) decreases pollen viability and fewer pollen grains, resulting in decreased seed set in grain sorghum (Prasad et al., 2008a). High temperature stress during floret development alters pollen morphology and results in an abnormal exine wall, degeneration of tapetum cells, and membrane damage, leading to pollen sterility in grain sorghum (Djanaguiraman et al., 2014), wheat (Prasad and Djanaguiraman, 2014), and soybean (Djanaguiraman et al., 2013a,b). Similarly, high temperature stress during anthesis decreases seed set in many cereal crops including sorghum (Prasad et al., 2008a; Jain et al., 2010; Prasad and Djanaguiraman, 2011; Nguyen et al., 2013; Djanaguiraman et al., 2014; Singh et al., 2015), wheat (*Triticum aestivum* L.) (Prasad et al., 2008b; Narayanan et al., 2015), rice (*Oryza sativa* L.) (Jagadish et al., 2007, 2010); and legume crops such as peanut (*Arachis hypogaea* L.) (Prasad et al., 1999, 2001), and soybean (*Glycine max* L. Merr.) (Djanaguiraman et al., 2013a,b) resulting in lower grain numbers and grain yield. High temperature stress during anthesis causes poor anther dehiscence and impairs pollen tube growth and hampers fertilization, resulting in lower seed set (Prasad et al., 2006b; Jagadish et al., 2007).

Although studies have shown that in grain sorghum episodes of high temperature stress (>36°C; daytime maximum temperature) decreases floret fertility (Prasad et al., 2008a; Jain et al., 2010), the relative sensitivity of various reproductive growth stages (panicle emergence, anthesis, and grain filling), critical thresholds for temperatures, and duration of stress have not been thoroughly quantified. In addition, the effect of high temperature stress on field grown sorghum is not well documented. The specific objectives of this research were to (i) identify the growth stage(s) most sensitive to high temperature stress during reproductive development, (ii) determine threshold temperature and duration of high temperature stress that decreases floret fertility and individual grain weight, and (iii) quantify impact of high daytime temperature during floret development, flowering and grain filling on reproductive traits and yield components for grain sorghum grown under field conditions.

Materials and Methods

This research was conducted at facilities established in the Department of Agronomy at Kansas State University, Manhattan, KS, USA. A series of experiments, under controlled environment and field condition, were conducted to quantify impact of high temperature stress on reproductive traits and grain yield of grain sorghum crop.

Plant Husbandry and Growth Conditions

Photoperiod-insensitive grain sorghum hybrid DK28E (short stature, early maturity, short duration, and stands well under stress conditions; DeKalb company) was used in this study due its sensitivity to high temperature stress (Prasad et al., 2006a, 2008a). Seeds were treated with fungicide (Captan, Hummert International, Earth City, MO, USA) as a precautionary measure against seed-borne diseases and sown at 4-cm depth in 15-L pots (pot diameter at the top and bottom was 27.5 and 26 cm, respectively; pot depth was 22 cm) containing commercial potting soil (Metro Mix 350, Hummert International, Topeka, KS, USA). After emergence, plants were thinned to one plant per pot and maintained until maturity. A systemic insecticide, Marathon 1%G (granules) (a.i. Imidacloprid 1-[(6-Chloro-3-pyridinyl) methyl]-N-nitro-2-imidazolidinimine, Hummert International, KS, USA) was applied to each pot at 4 g per pot. Each pot was fertilized with Osmocote (controlled release plant food, 14:14:14%, N: P_2O_5: K_2O, respectively; Hummert International, KS, USA) at 5 g per pot; applied before sowing and at flowering. To avoid water stress, all pots were irrigated daily from sowing to maturity.

Sorghum plants were grown in four large growth chambers (PGW 36, about 249 cm wide, 137 cm deep, and 180 cm high, Conviron, Winnipeg, MB, Canada) from sowing to start of high temperature stress treatments. Five pots were transferred for implementing various temperature and duration treatments to six other similar but slightly smaller growth chambers (PGW 15, about 184 cm wide, 78 cm deep, and

130 cm tall, Conviron, Winnipeg, MB, Canada). The quality of environmental conditions was similar in all growth chambers. After the temperature treatment, pots were returned back to the original growth chamber where they remained until final harvest at maturity. The pots were randomly arranged within each growth chamber. Plants in each growth chamber were moved randomly every 7–10 d during non-stress and every 1–2 d during the stress periods to avoid positional effects within the chamber. Temperatures in growth chambers were maintained in a square wave fashion. In all temperature regimes, daytime and nighttime temperatures were held for 12 h and the transition period between the daytime maximum and nighttime minimum temperatures was 6 h, and vice versa. Relative humidity (RH) in all growth chambers was set at 80% to avoid any confounding effects of dry air (drought stress). The photoperiod was 12 h (from 0800 to 2000 h). Such temperature conditions often occurs during sensitive stages of crop development in semi-arid, arid and humid regions of US, Africa and Asia (Prasad et al., 2006a, 2008a). In all the growth chambers, the canopy level photon flux density (400–700 nm) was close to 900 μmol m^{-2} s^{-1} provided by cool white fluorescent lamps (Philips Lighting Co., Somerset, NJ, USA). Air temperature and RH were continuously monitored at 15-min intervals in all growth chambers throughout the experiment using HOBO data loggers (Onset Computer Corporation, Bourne, MA, USA).

Treatments and Observations

Impact of High Temperature Stress: Sensitive Stages during Reproductive Development

Grain sorghum plants were grown under optimum temperature (30/20°C, daytime maximum and nighttime minimum temperature; 12 h photoperiod, and 80% humidity) from seedling emergence until onset of panicle emergence (about 15 d before anthesis). Thereafter, a set of five pots was transferred from the optimum temperature to high temperature stress conditions (36/26°C daytime maximum/nighttime minimum, 12 h photoperiod, and 80% humidity) at 5-days intervals, starting from 15 d before anthesis to 30 d after anthesis (a total of 10 treatments). The duration of high temperature stress for each treatment was 5 d. After the stress period, each set of five pots corresponding to a different treatment was returned to optimum temperature, where it remained until final harvest at maturity. Control plants (five pots) remained under optimum temperature from seedling emergence to final harvest at maturity.

In each treatment, florets on the middle portion of the panicle on each plant were tagged with cotton thread. This portion covered about 15–20 branches on each panicle. On each panicle about 80–100 florets were marked with permanent ink marker and used to determine floret fertility. At maturity, the tagged florets were hand-harvested and dried at 40°C for 7 d. Individual marked florets were checked for grain by pressing the floret between the thumb and the index finger. Both partially and fully filled tagged florets were used to determine floret fertility. Floret fertility percentage was estimated as the ratio of the total number of tagged florets to the number of grains from the tagged florets. The tagged florets were hand-threshed, counted, and weighted. Individual grain weight was calculated by dividing the total grain weight by number of grains from the tagged florets. Data on floret fertility and individual grain weight of various high temperature treatments are presented as percentage of control treatment (optimum temperature).

Impact of High Temperature Stress: Threshold Temperature during Floret Development and Grain Filling

Threshold temperatures during floret development were evaluated in growth chamber conditions with sorghum plants growing under optimum temperature (30/20°C, daytime maximum/nighttime minimum; 12 h photoperiod, and 80% humidity) from seedling emergence to start of panicle emergence (about 15 d before anthesis). Thereafter, a set of five pots was transferred from optimum temperature to six different temperature treatments (32/22, 36/26, 38/28, 40/30, 42/32, and 45/35°C, daytime maximum/nighttime minimum temperature, giving daily mean temperatures of 27, 31, 33, 35, 37, and 40°C) for a duration of 10 d. After the stress period, each set of five pots corresponding to different treatments was returned to optimum temperature, where they stayed until final harvest at maturity. Control plants (five pots) remained under optimum temperature from seedling emergence until final harvest at maturity. The procedure of tagging and determining of floret fertility and individual grain weight was similar to as detailed above.

Threshold temperatures during grain filling were quantified with sorghum plants grown in growth chambers under optimum temperature from seedling emergence to start of grain filling (7 d after full anthesis in the middle portion of the panicle). Thereafter, the plants were exposed to different temperature treatments as mentioned above (six treatment combinations). Tagging and floret fertility was determined following a similar procedures detailed above.

Impact of High Temperature Stress: Threshold Duration during Floret Development and Grain Filling

To determine threshold duration of high temperature stress during floret development and its subsequent effects on floret fertility, sorghum plants were grown under optimum temperature (30/20°C, daytime maximum/nighttime minimum temperature; 12 h photoperiod, and 80% humidity) from seedling emergence to the start of panicle emergence (about 15 d before anthesis). Thereafter, a set of five pots was transferred from optimum temperature to high temperature (36/26°C, daytime maximum/nighttime minimum temperature) for five different duration treatments (7, 14, 21, 28, and 35 d). After the stress period, each set of five pots corresponding to each treatment was returned to optimum temperature, and remained until maturity. Control plants (five pots) remained under optimum temperature from seedling emergence to maturity. Other procedures for tagging and determining of floret fertility and individual grain weight measurements were similar as detailed in the previous section.

To determine threshold duration of high temperature during grain filling, plants were grown under optimum temperature

from seedling emergence to start of grain filling (7 d after full anthesis). The temperature treatments, durations of stress, and procedure of tagging and determination, and presentation of floret fertility and individual grain weight were similar to those mentioned above.

Impact of High Temperature Stress: Field Studies using Heat Tents during Floret Development and Grain Filling

To determine the impact of high temperature stress under field conditions, plants of grain sorghum hybrid DK28E were planted at North Farm research field station in Manhattan, Kansas. Standard field crop management practices [76 cm spacing between rows and target plant population of 12 plants m^{-2}; 10 g N m^{-2} as urea granules (46% N)] were followed for planting the crop. Pre-emergence herbicide application and hand weeding were done when necessary to keep the plots weed free. Fields were flood irrigated as necessary to ensure that there was no water stress throughout the crop growing season until maturity.

To impose high temperature stress during floret development, three heat tents were placed on the field grown sorghum crop at the start of panicle emergence stage and remained until start of grain filling (about 7 d after full anthesis). Similarly, for imposition of high temperature stress during grain filling, three heat tents were placed on the field grown sorghum crop at the start of grain filling (7 d after full anthesis) and remained until maturity. The procedure of tagging and determination of floret fertility and individual grain weight were similar to those mentioned in previous sections. In addition, data on total number of florets, seeds per panicle, and grain weight per panicle were measured from five tagged plants in each tent (randomly selected).

Each heat tent was built on galvanized steel frame work with additional frame (0.6 m) only on the top that can open and close. The steel frame work is covered by clear polyethylene film which transmits 85% of the incoming solar radiation. Each heat tent was 5.4 m wide, 7.2 m long, and 3.0 m high at the apex. There are no artificial heating systems, heat tents are heated via natural solar radiation (greenhouse effect). Temperature increases inside the heat tents are dependent on the intensity of solar radiation and outside ambient temperatures. On a clear sunny day, the temperature inside the heat tent can be up to 10°C warmer than the outside ambient temperature. Each heat tent was equipped with a solar-powered battery to operate the actuators to open and close the additional frame on the top when temperatures were too high (the maximum was set at 45°C) to avoid excessive heating. Each heat tent has a 15 cm clearance on all four sides to allow circulation of air within the heat tent. Air temperature and RH were measured using WatchDog data loggers (1000 Series Micro Station, Spectrum Technologies, Aurora, IL, USA) at 30 min intervals. Similarly, incoming solar radiation was measured using PAR sensors (LightScout Quantum Light Sensor, Spectrum Technologies, Aurora, IL, USA). Volumetric soil water content was measured at 30 cm depth using soil moisture sensors (WaterScout SM 100 moisture sensor, Spectrum Technologies, Aurora, IL, USA). Environmental measurements were measured inside and outside heat tents.

Data Analyses

Data from all the experiments were statistically analyzed by using PROC GLM in the SAS software (SAS Institute, Cary, NC, USA). The experimental design for each experiment was a randomized complete block. The temperature of each growth chamber was assigned randomly, and plants (pots) were replicated within the chamber. There were five replications (five pots) for all measurements. Standard error was shown as an estimate of variability, and where appropriate means of different variables were separated by LSD at a probability level of 0.05. The response of floret fertility and individual grain weight to different temperatures and durations was tested for linear or quadratic relationships and significance using regression analysis in SAS and the best fit was identified and presented.

Results

Quality Control of Growth Chambers

Mean daytime and nighttime temperatures in the optimum temperature and high temperature treatments were ± 0.5°C of the target temperatures, and RH was within ± 10%. Quality of the temperature control and chamber performance was previously published (Pradhan et al., 2012).

Impact of High Temperature Stress: Sensitive Stages during Reproductive Development

Exposure to high temperature stress (36/26°C daytime maximum/nighttime minimum temperature; mean daily temperature, 31°C) for 5 d significantly decreased floret fertility compared to optimum temperature (30/20°C; daytime maximum/nighttime minimum temperature; mean daily temperature, 25°C) when imposed at 15, 10, 5, or 0 d before anthesis and 5 and 10 d after anthesis (**Figure 1A**). Maximum decreases in floret fertility (43–58% of control) occurred when stress was imposed at 10, 5, or 0 d before anthesis. High temperature stress imposed at 15 d before anthesis slightly decreased floret fertility (85% of control) and 5 and 10 d after anthesis (83–92% of control). Heat stress had no influence on floret fertility when stress was imposed at stages occurring beyond 10 d after anthesis (**Figure 1A**).

Exposure to high temperature stress from 15 d before- to 5 d after-anthesis did not influence individual grain weight (**Figure 1B**). However, high temperature stress occurring from 10 to 30 d after anthesis significantly decreased individual grain weight to a similar extent (78–85% of control), except at 15 d after anthesis, which has the maximum decrease (70% of control).

Impact of High Temperature Stress: Threshold Temperature during Floret Development and Grain Filling

Floret fertility decreased significantly with increasing mean daily temperatures in the range of 25–40°C when imposed for a duration of 10 d at the start of panicle emergence. Floret fertility

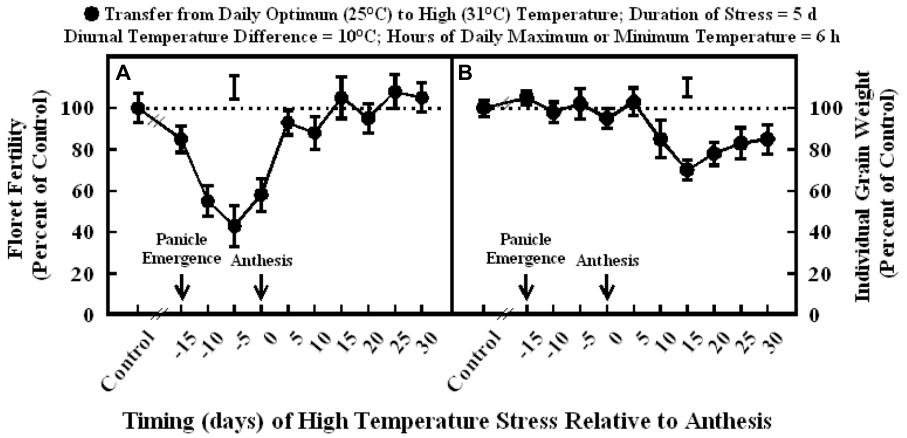

FIGURE 1 | Impact of high temperature stress (36/26°C daytime maximum/nighttime minimum temperature, for 5 days) at different times relative to anthesis on (A) floret fertility, and (B) individual grain weight. Each datum is expressed as percentage of control at optimum temperature (30/20°C, daytime maximum/nighttime minimum temperature) and shown with ± SE. Vertical bars above the lines denote LSD for comparison of treatment means. The dotted line provides reference to control means.

response to temperature fit a quadratic model (**Figure 2A**) Floret fertility decreased from about 100% of control at 25°C mean daily temperature to 0% of control at 37.4°C. Mean daily temperature in the specific range (25 through 37°C) imposed at the start of panicle emergence did not decrease individual grain weight (**Figure 2B**).

In the experiment where high temperature stress was imposed at the start of grain filling, there were no significant differences in the floret fertility in all plants and it was within the range of control (**Figure 3A**). Whereas, individual grain weight decreased significantly with increasing mean temperatures in the range of 25–40°C, when imposed for a duration of 10 d at the start of grain filling stage (**Figure 3B**). The grain weight response to temperature was also described with a quadratic model. Individual grain weight decreased by 62% from 25 to 40°C mean daily temperatures (100% of control to about 38% of control at 40°C).

Impact of High Temperature Stress: Threshold Duration during Floret Development and Grain Filling

Plants exposure to high temperature stress (36/26°C; daytime maximum/nighttime minimum temperature; mean daily temperature of 31°C) at the start of panicle emergence caused significant decreases in floret fertility (**Figure 4A**). The response of floret fertility to duration was best described with a quadratic function across all data points (**Figure 4A**). Exposure to high temperature stress for 7 and 14 d periods decreased floret fertility to 76 and 37% of control, respectively. Thereafter, extended duration of the heat stress to 21 and 35 d did not further decrease floret fertility, which remained in the range of 32 and 43% of the control. Individual grain weight was similar between 0, 7, and 14 d of high temperature stress, but further increase in durations to 21, 28, and 35 d decreased individual grain weight to 87, 82, and 68% of control, respectively (**Figure 4B**).

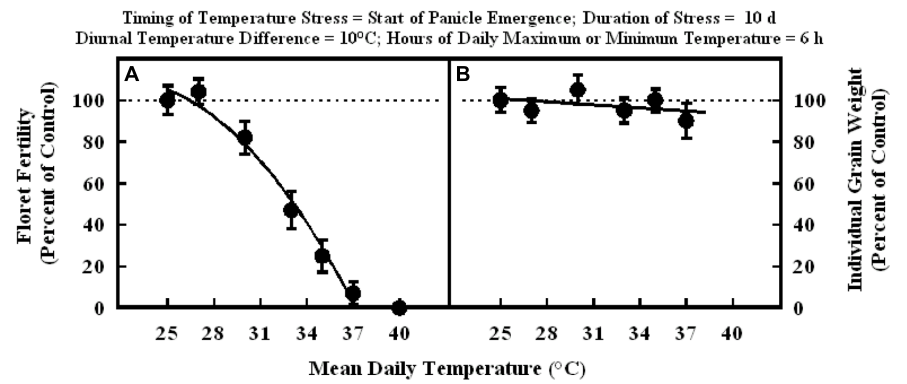

FIGURE 2 | Impact of different mean daily temperatures (°C) when imposed at start of panicle emergence for a duration of 10 d on (A) floret fertility, fitted line $Y = -119.7 + 20.8X - 0.47X^2$; $r^2 = 0.98$ ($P < 0.001$), and (B) individual grain weight, fitted line $Y = +112.5 - 0.48X$; $r^2 = 0.18$ (NS). Each datum is expressed as percentage of control at optimum temperature (30/20°C, daytime maximum/nighttime minimum) and shown with ± SE.

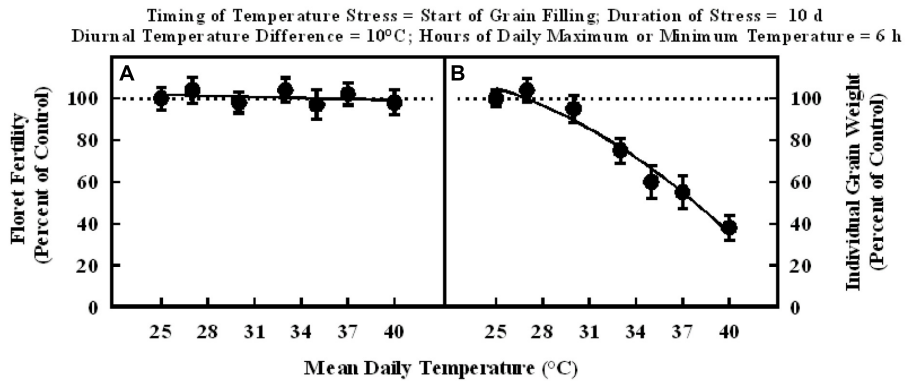

FIGURE 3 | Impact of different mean daily temperatures (°C) at the start of grain filling for a duration of 10 d on (A) floret fertility, fitted line $Y = +105.6 - 0.16X$; $r^2 = 0.09$ (NS), and (B) individual grain weight, fitted line $Y = +66.3 + 5.38X - 0.15X^2$; $r^2 = 0.97$ ($P < 0.001$). Each datum is expressed as percentage of control at optimum temperature (30/20°C, daytime maximum/nighttime minimum) and shown with ± SE.

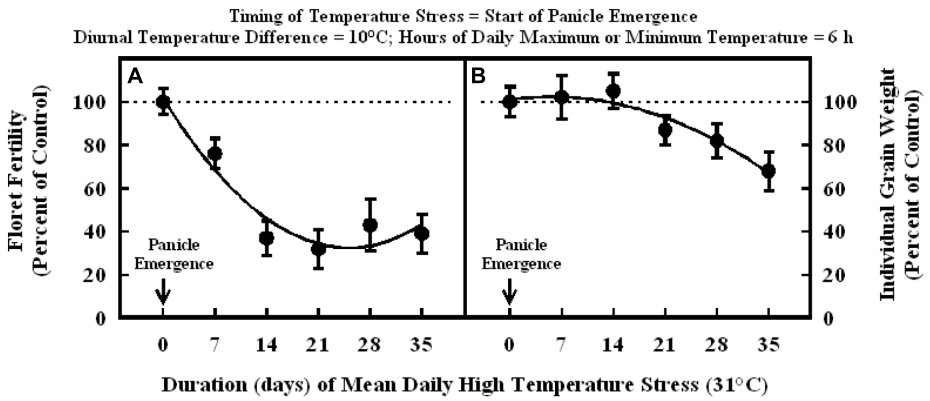

FIGURE 4 | Impact of high temperature stress (36/26°C, daytime maximum/nighttime minimum) for different durations when imposed at the start of panicle emergence on (A) floret fertility, fitted line $Y = +101.6 - 5.4X + 0.11X^2$; $r^2 = 0.93$ ($P < 0.001$), and (B) individual grain weight, fitted line $Y = +101 + 0.45X - 0.041X^2$; $r^2 = 0.94$ ($P < 0.001$). Each datum is expressed as percentage of control at optimum temperature (30/20°C, daytime maximum/nighttime minimum) and shown with ± SE.

In the experiment where high temperature stress was imposed at the start of grain filling, there were no significant differences in the floret fertility in all plants and it was within the range of control (**Figure 5A**). Individual grain weight decreased significantly in a quadratic fashion with increasing duration of high temperature stress from 7 to 49 d (**Figure 5B**). Individual grain weights after 7, 14, and 21 d of high temperature stress were in the range of 87 to 93% of control, but when high temperature stress extended to 28 and 35 d, individual grain weight decreased to 75 and 68% of control, respectively. Further increase in the duration of high temperature stress to 42 and 49 d did promote a decrease on individual grain weight to 49 and 42% of control, respectively.

Impact of High Temperature Stress: Field Studies using Heat Tents during Floret Development and Grain Filling

The daytime hourly mean maximum temperatures from the start of panicle emergence to the start of grain filling outside the heat tent (ambient) was 37°C, while inside the heat tent (high temperature) was 43°C (**Figure 6A**). However, the nighttime hourly mean minimum temperatures outside (ambient) and inside the heat tent were comparable (23–24°C) (**Figure 6B**). These daytime high temperatures above ambient did not cause any difference in number of florets per panicle and individual grain weight, but significantly decreased floret fertility (**Figure 7C**), seeds per panicle (**Figure 7B**), and grain weight panicle (**Figure 7E**) by 36, 40, and 41%, respectively.

Similarly, in the experiment where high temperature stress was imposed during grain filling, daytime hourly mean maximum temperature outside the heat tent (ambient) was 30°C, while inside heat tent (high temperature) was 40°C (**Figure 8A**). However, the nighttime hourly mean minimum temperature outside (ambient) and inside heat tent were comparable (15–16°C) (**Figure 8B**). The daytime high temperature stress did not cause any difference in the number of florets per panicle, seeds per panicle

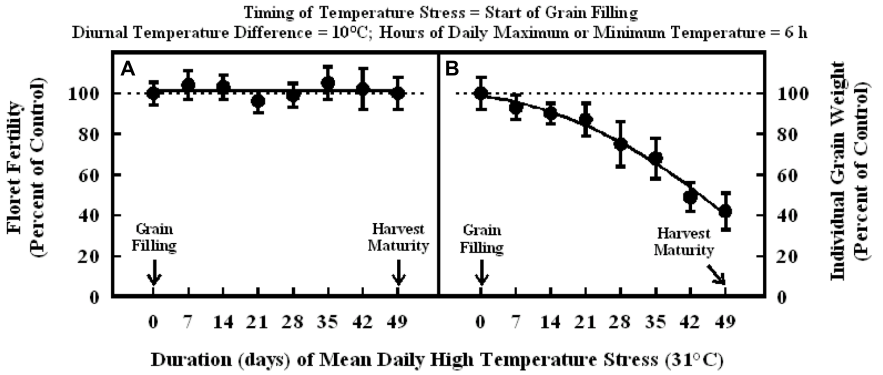

FIGURE 5 | Impact of high temperature stress (36/26°C, daytime maximum/nighttime minimum) for different durations at the start of grain filling on (A) floret fertility, fitted line $Y = +101 - 0.0017X$; $r^2 = 0.001$ (NS), and (B) individual grain weight, fitted line $Y = +98.7 - 0.32X - 0.018X^2$; $r^2 = 0.98$ ($P < 0.001$). Each datum is expressed as percentage of control at optimum temperature (30/20°C, daytime maximum/nighttime minimum) and shown with ± SE.

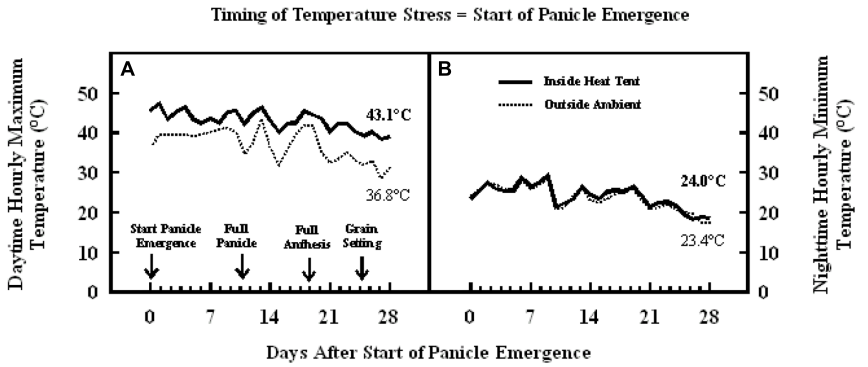

FIGURE 6 | Data on (A) daytime hourly maximum temperature; and (B) nighttime hourly minimum temperature outside heat tents (ambient, dotted lines) and inside heat tent (high temperature stress, solid lines) from start of panicle emergence to start of grain filling period on field grown sorghum plants during 2011 in Manhattan, KS, USA.

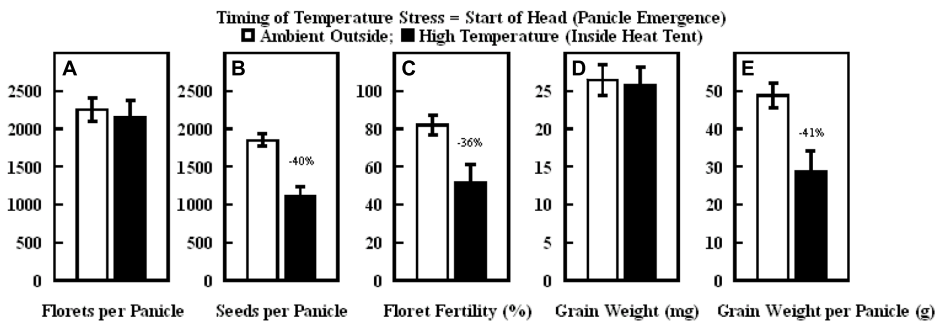

FIGURE 7 | Impact of high temperature stress imposed by heat tents (43/24°C, daytime maximum/nighttime minimum temperature) relative outside ambient conditions (37/23°C, daytime maximum/nighttime minimum temperature) from start of panicle emergence to start of flowering on (A) number of florets per panicle, (B) number of seeds per panicle, (C) floret fertility (%), (D) individual grain weight (mg), and (E) grain weight per panicle (g). Each datum is shown with ± SE. Numbers on top of the bars shows the percentage decline under high temperature stress conditions (inside heat tents) from outside ambient conditions.

or floret fertility, but significantly decreased individual grain weight by 15% and grain weight per panicle by 20% as compared with outside ambient temperatures (**Figure 9**).

Discussion

In grain sorghum, the most sensitive periods (maximum decreases in floret fertility) to high temperature stress were

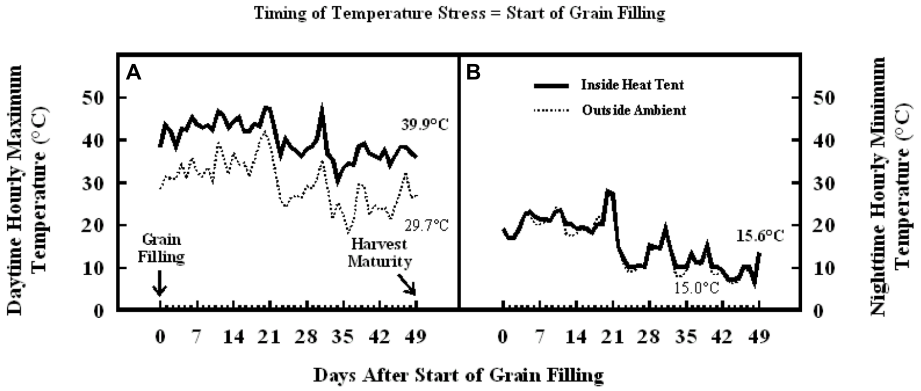

FIGURE 8 | Data on (A) daytime hourly maximum temperature; and (B) nighttime hourly minimum temperature outside heat tents (ambient, dotted lines) and inside heat tent (high temperature stress, solid lines) from start of grain filling to harvest maturity on field grown sorghum plants during 2011 in Manhattan, KS, USA.

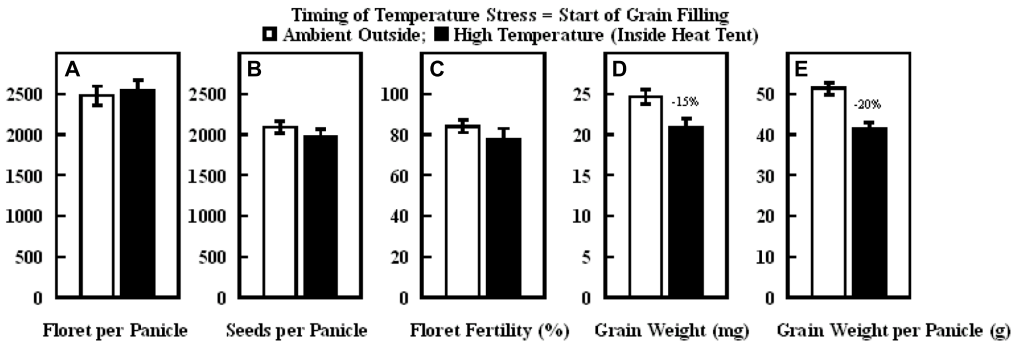

FIGURE 9 | Impact of high temperature stress imposed by heat tents (40/16°C, daytime maximum/nighttime minimum) relative outside heat tent ambient conditions (30/15°C, daytime maximum/nighttime minimum) from start of grain filling to harvest maturity on (A) number of florets per panicle, (B) number of seeds per panicle, (C) floret fertility (%), (D) individual grain weight (mg), and (E) grain weight per panicle (g). Each datum is shown with ± SE. Numbers on top of the bars shows the percentage decline under high temperature stress conditions (inside heat tents) from outside ambient conditions.

between 10 and 5 d before anthesis (**Figure 1A**), which coincides with meiosis and tetrad formation stage of sporogenesis, and between 5 d before anthesis and 5 d after anthesis which coincides with anthesis, fertilization, and embryo formation. These periods are similar to those identified in a previous study where the duration of stress was 10 d (Prasad et al., 2008a). A recent study in wheat also showed that the two periods (first at 8–6 d before anthesis and second at 2–0 d before anthesis) during reproductive development were most sensitive to short episodes (2 or 5 d) of high temperature stress, causing maximum decreases in floret fertility (Prasad and Djanaguiraman, 2014). The temperature-sensitive period for cowpea (*Vigna unguiculata* L. Walp.) was from 7 to 9 d before anthesis (Ahmed et al., 1992), for common bean (*Phaseolus vulgaris* L.) from 10 to 12 d before anthesis (Gross and Kigel, 1994), and for peanut about 4 d before anthesis (Prasad et al., 2001).

The loss of floret fertility under high temperature stress during sporogenesis is a result of loss of pollen or ovule viability and/or stigma receptivity (Prasad et al., 2008a; Nguyen et al., 2013; Djanaguiraman et al., 2014; Prasad and Djanaguiraman, 2014). High temperature stress during floret development (sporogenesis) results in several abnormalities in reproductive structures such as the formation of abnormal exines with deeply pitted and non-smooth surface regions and shriveled pollen grains; and desiccated stigma, style, and ovaries (Prasad and Djanaguiraman, 2014). Exine originates from the tapetal cells, and the altered exine ornamentation under high temperature stress is an indication of disruption to tapetal cells. Tapetal cells provide nourishment to the developing pollen, and early degeneration of tapetal cells under high temperature stress affects translocation of nutrients to the developing pollen grains, leading to loss of pollen viability (Hess and Hesse, 1994). These structural and functional abnormalities in reproductive organs lead to floret sterility and failure of fertilization and seed-set leading to lower grain numbers. In addition, studies on grain sorghum showed that high temperature stress causes changes in composition and concentrations of carbohydrates (Jain et al., 2007), structural abnormalities and oxidative damage in pollen gains resulting in pollen sterility and decreased seed-set (Djanaguiraman et al., 2014).

After completion of sporogenesis, the processes of anthesis, fertilization, and embryo formation are also sensitive to high temperature stress. The main processes occurring during this period include dehiscence of anthers, pollination, pollen reception by stigma, pollen germination, pollen tube growth in the style, fertilization, and embryo formation. High temperature stress at the time of anthesis (0 days prior to anthesis or after complete panicle emergence) can decrease floret fertility even when the pollen is viable (Prasad and Djanaguiraman, 2014). The decreased floret fertility under such conditions is commonly due to poor receptivity and dryness of the stigma, poor pollen germination and decreased rate of pollen tube growth, leading to unsuccessful fertilization and lower seed-set (Kakani et al., 2002; Prasad and Djanaguiraman, 2011; Djanaguiraman et al., 2014).

When high temperature stress was imposed for periods of 5 to 14 d during panicle emergence (sporogenesis and anthesis), despite resulting in lower floret fertility (lower grain number) it did not cause any significant increase in subsequent individual grain weights which remained unchanged relative to control plants at optimum temperature either under growth chamber conditions (**Figures 1B, 2B,** and **4B**) or field conditions under heat tents (**Figure 7**). This shows lack of compensation for fewer grain numbers with increased grain size in this sorghum hybrid. Furthermore, it also suggests that these short periods of high temperature stress during panicle emergence did not trigger subsequent increases in either grain filling rate or grain filling duration, leading to similar grain size. However, when high temperature stress was imposed after embryo formation (with similar seed set and grain numbers), at the start of the grain filling period, there was a quadratic decrease in individual grain weights with increasing temperature stress (**Figure 3B**) or duration of stress (**Figure 5B**). As the duration of high temperature stress increased, individual grain weight decreased in a quadratic fashion (**Figure 4B**). Similar observations were also made when high temperature stress was imposed during grain filling period under field conditions using heat tents (**Figure 9**). This is mainly because final individual grain weight is determined by the rate and duration of grain filling. Decreases in individual grain weight occurs when decreases in grain filling duration is not compensated by increases in grain filling rate. In the research presented here, the responses in grain numbers and grain size to high temperature stress followed a similar trend either in controlled environment growth chambers or field conditions (**Figures 1–3**, **7** and **9**). Our prior research on sorghum showed that season-long high temperature stress did not have a large impact on the rate of grain filling, but it significantly decreased the grain filling duration, leading to smaller individual grain weights (Prasad et al., 2006a). Recent studies on sorghum response to short episodes of high temperature stress under controlled environments and field conditions also showed decreased seed-set and seed numbers; and the response of seed set to high temperature in the field study was well correlated to that of controlled environments (Singh et al., 2015). Furthermore, decreased seed set and seed numbers were not compensated by increased seed size in either controlled environment or field conditions (Singh et al., 2015). There was genetic variability in response to short episodes of high temperature stress in grain sorghum (Nguyen et al., 2013; Singh et al., 2015). Similar results were also observed in wheat (Prasad et al., 2008b). While, decreases in both seed filling rate and seed filling duration were observed in peanut (Prasad et al., 2003).

The results presented on the sensitive stages and thresholds for temperature and duration are from the plants grown in pots and high temperature stress was imposed in growth chambers for fixed duration and following a 10°C diurnal difference between daytime maximum and nighttime minimum temperatures. This was done to ensure full control of temperature regime and avoid confounding effect of other environmental factors. We acknowledge that under field conditions the duration, intensity of temperature stress, daily fluctuations, and diurnal differences of the temperature stress may be highly variable (low or high), but could often be more acute. Although the sensitive stages or periods to high temperature stress may not be different under field conditions, they may have different thresholds. The results of the field studies, following field natural diurnal variations (in the semi-arid environment of Manhattan, Kansas), also showed that high temperature stress induced using heat tents from start of panicle emergence through anthesis decreased floret fertility and consequently grain number, leading to a significant reduction in grain yield (**Figures 7B,C**). Whereas, when high temperature stress was induced during grain filling it resulted in decreased individual grain weight to lower grain yield (**Figures 9D,E**). There were larger diurnal differences under field conditions in heat tents, as heat tents could only increase daytime temperature, while night temperatures were similar (**Figures 6B** and **8B**). The results of these field studies complemented growth chambers results presented here and our previous research findings with decreased floret fertility, seed-set percentage, grain numbers and individual grain weight under high temperature stress (Jain et al., 2007, 2010; Prasad et al., 2008a; Nguyen et al., 2013; Djanaguiraman et al., 2014). Studies have shown that increase in nighttime temperatures can cause decreases in sorghum floret fertility, individual grain size, and grain yield (Prasad and Djanaguiraman, 2011). Comparison of daytime and nighttime temperature stress on wheat showed similar decreases in yield and its components (Narayanan et al., 2015). However, more targeted studies to compare influence of day versus night temperatures using appropriate diurnal variations need further investigations. The results presented here are on single genotype, and research has shown that genotypes are known to respond differently to high temperature stress (Nguyen et al., 2013; Djanaguiraman et al., 2014; Singh et al., 2015). Identified sensitive stages will remain the same, but impact on floret fertility and grain weight may change in tolerant versus susceptible sorghum hybrids. There is limited tolerance to high temperature stress in germplasm that is currently being used in breeding programs and there is urgent need for exploiting genotypic resources and systematically evaluating parental lines for tolerance. In addition, there is a critical need for development of high throughput phenotyping techniques to screen large number of germplasm collection and develop biochemical or genetic markers to facilitate efficient breeding for high temperature tolerance.

Summary and Conclusion

In summary, our research showed that the periods between 10 and 5 d before anthesis (coinciding with sporogenesis) and 5 d before to 5 d after anthesis (coinciding with anthesis, fertilization and embryo formation) were the most sensitive to short episodes (5 d) of high temperature stress (mean daily temperature of 31°C), causing maximum decreases in floret fertility. Mid-duration episodes (10 d) of mean daily temperatures >25°C quadratically decreased floret fertility with the values reaching 0% at 37°C when imposed at start of panicle emergence. Similar increases in mean daily temperatures also quadratically decreased individual grain weight when imposed at start of grain filling. Both floret fertility and individual grain weights decreased quadratically with increasing duration (in the range of 0 to 35 d) of high temperature stress (mean daily temperature of 31°C) when imposed at the start of panicle emergence. Increases in duration (in the range of 0–49 d) of high temperature stress when imposed at the start of grain filling also quadratically decreased individual grain weight. A complementary field study where high daytime temperature stress was imposed using heat tents during floret development decreased floret fertility, seeds per panicle, and grain weight per panicle. Whereas, high daytime temperature stress imposed during grain filling decreased individual grain weight and grain weight per panicle. Further research is underway and required to identify potential parental lines with tolerance to high temperature stress during pre- and post-flowering stages of crop development. In addition, we are focused on determining biochemical or genetic marker(s) that can be used for high throughput phenotyping and facilitate identification of genotypes or parental lines that can be used in breeding for high temperature tolerance. Future research should focus on searching for genotypic variability to be used in breeding programs for building resilience and adaptation to climate change.

Author Contributions

PP and MD conceived, designed, carried out the experiments and drafted the manuscript. RP and IC made substantial contributions to measurements, data interpretation and edited the manuscript.

Acknowledgments

We thank the Kansas Grain Sorghum Commission and K-State Center for Sorghum Improvement and the USAID Feed the Future Sustainable Intensification Innovation Lab (Grant no. AID-OAA-L-14-00006) for financial support. We thank summer intern students of Crop Physiology Laboratory for their help in conducting these experiments. We thank Tamil Nadu Agricultural University, India, for permitting Dr. MD to conduct post-doctoral research at Kansas State University, USA. This is contribution no. 16-054-J from the Kansas Agricultural Experiment Station.

References

Ahmed, F. E., Hall, A. E., and DeMason, D. A. (1992). Heat injury during floral development in cowpea (*Vigna unguiculata*. Fabaceae). *Am. J. Bot.* 79, 784–791. doi: 10.2307/2444945

Butt, T. A., McCarl, B. A., Angerer, J., Dyke, P. T., and Stuth, J. W. (2005). The economic and food security implications for climate change in Mali. *Clim. Change* 68, 355–378. doi: 10.1007/s10584-005-6014-0

Chipanshi, A. C., Chanda, R., and Totolo, O. (2003). Vulnerability assessment of the maize and sorghum crops to climate change in Botswana. *Clim. Change* 61, 339–360. doi: 10.1023/B:CLIM.0000004551.55871.eb

Dias, A. S., and Lidon, F. C. (2009). Evaluation of grain filling rate and duration in bread and durum wheat, under heat stress after anthesis. *J. Agron. Crop Sci.* 195, 137–147. doi: 10.1111/j.1439-037X.2008.00347.x

Djanaguiraman, M., Prasad, P. V. V., Boyle, D. L., and Schapaugh, W. T. (2013a). Soybean pollen anatomy, viability and pod set under high temperature stress. *J. Agron. Crop Sci.* 199, 171–177. doi: 10.1111/jac.12005

Djanaguiraman, M., Prasad, P. V. V., and Schapaugh, W. T. (2013b). High day- or nighttime temperature alters leaf assimilation, reproductive success, and phosphotidic acid of pollen grain in soybean [*Glycine max* (L.) Merr.]. *Crop Sci.* 53, 1594–1604. doi: 10.2135/cropsci2012.07.0441

Djanaguiraman, M., Prasad, P. V. V., Murugan, M., Perumal, M., and Reddy, U. K. (2014). Physiological differences among sorghum (*Sorghum bicolor* L. Moench) genotypes under high temperature stress. *Environ. Exp. Bot.* 100, 43–54.

Farooq, M., Bramley, H., Palta, J. A., and Siddique, K. H. M. (2011). Heat stress in wheat during reproductive and grain-filling phases. *Crit. Rev. Plant Sci.* 30, 491–507. doi: 10.1080/07352689.2011.615687

Gross, Y., and Kigel, J. (1994). Differential sensitivity of high temperature of stages in the reproductive development of common bean (*Phaseolus vulgaris* L.). *Field Crop Res.* 36, 201–212. doi: 10.1016/0378-4290(94)90112-0

Hammer, G. L., Carberry, P. S., and Muchow, R. C. (1993). Modeling genotypic and environmental control of leaf area dynamics in grain sorghum. Whole plant level. *Field Crops Res.* 33, 293–310. doi: 10.1016/0378-4290(93)90087-4

Hess, M., and Hesse, M. (1994). Ultrastructural observations on anther tapetum development of freeze-fixed *Ledebouria socialis* Roth (Hyacinthaceae). *Planta* 192, 421–430. doi: 10.1007/BF00198579

IPCC (2013). "Summary for policymakers," in *Climate Change 2013: The Physical Science Basis. Contribution of Working Group I to the Fifth Assessment Report of the Intergovernmental Panel on Climate Change*, eds T. F. Stocker, G. K. Qin, M. Plattner, S. K. Tignor, J. Allen, A. Boschung et al. (Cambridge: Cambridge University Press).

Jagadish, S. V. K., Craufurd, P. Q., and Wheeler, T. R. (2007). High temperature stress and spikelet fertility in rice (*Oryza sativa* L.). *J. Exp. Bot.* 58, 1627–1635. doi: 10.1093/jxb/erm003

Jagadish, S. V. K., Muthurajan, R., Oane, R., Wheeler, T. R., Heuer, S., Bennett, J., et al. (2010). Physiological and proteomic approaches to dissect reproductive stage heat tolerance in rice (*Oryza sativa* L.). *J. Exp. Bot.* 61, 143–156. doi: 10.1093/jxb/erp289

Jain, M., Chourey, P. S., Boote, K. J., and Allen, L. H. Jr. (2010). Short-term high temperature growth conditions during vegetative-to-reproductive phase transition irreversibly compromise cell wall invertase-mediated sucrose catalysis and microspore meiosis in grain sorghum (*Sorghum bicolor*). *J. Plant Physiol.* 167, 578–582. doi: 10.1016/j.jplph.2009.11.007

Jain, M., Prasad, P. V. V., Boote, K. J., Allen, L. H. Jr., and Chourey, P. S. (2007). Effect of season-long high temperature growth conditions on sugar-to-starch metabolism in developing microspores of grain sorghum (*Sorghum bicolor* L. Moench). *Planta* 227, 67–69. doi: 10.1007/s00425-007-0595-y

Kakani, V. G., Prasad, P. V. V., Craufurd, P. Q., and Wheeler, T. R. (2002). Response of in vitro pollen germination and pollen tube growth of groundnut (*Arachis hypogaea* L.) genotypes to temperature. *Plant Cell Environ.* 25, 1651–1661. doi: 10.1046/j.1365-3040.2002.00943.x

Narayanan, S., Prasad, P. V. V., Fritz, A. K., Boyle, D. L., and Gill, B. S. (2015). Impact of high nighttime and high daytime temperature stress on winter wheat. *J. Agron. Crop Sci.* 201, 206–218. doi: 10.1111/jac.12101

Nguyen, C. T., Singh, V., van Oosterom, E. J., Chapman, S. C., Jordan, D. R., and Hammer, G. L. (2013). Genetic variability in high temperature effects on seed-set in sorghum. *Funct. Plant Biol.* 40, 439–448. doi: 10.1071/FP12264

Pradhan, G. P., Prasad, P. V. V., Fritz, A. K., Kirkham, M. B., and Gill, B. S. (2012). High temperature tolerance in *Aegilops* species and its potential transfer to wheat. *Crop Sci.* 52, 292–304. doi: 10.2135/cropsci2011.04.0186

Prasad, P. V. V., Boote, K. J., and Allen, L. H. Jr. (2006a). Adverse high temperature effects on pollen viability, seed-set, seed yield and harvest index of grain-sorghum (*Sorghum bicolor* L. Moench) are more severe at elevated carbon dioxide due to higher tissue temperatures. *Agric. For. Meteorol.* 139, 237–251.

Prasad, P. V. V., Boote, K. J., Allen, L. H. Jr., and Sheehy, J. E. (2006b). Species, ecotype and cultivar differences in spikelet fertility and harvest index of rice in response to high temperature stress. *Field Crops Res.* 95, 398–411. doi: 10.1016/j.fcr.2005.04.008

Prasad, P. V. V., Boote, K. J., Allen, L. H. Jr., and Thomas, J. M. G. (2003). Super-optimal temperatures are detrimental to peanut (*Arachis hypogaea* L.*)* reproductive processes and yield under both ambient and elevated carbon dioxide. *Global Change Biol.* 9, 1775–1787. doi: 10.1046/j.1365-2486.2003.00708.x

Prasad, P. V. V., Craufurd, P. Q., Kakani, V. G., Wheeler, T. R., and Boote, K. J. (2001). Influence of high temperature during pre- and post-anthesis stages of floral development on fruit-set and pollen germination in peanut. *Aust. J. Plant Physiol.* 28, 233–240.

Prasad, P. V. V., Craufurd, P. Q., and Summerfield, R. J. (1999). Fruit number in relation to pollen production and viability in groundnut exposed to short episodes of heat stress. *Ann. Bot.* 84, 381–386. doi: 10.1006/anbo.1999.0926

Prasad, P. V. V., and Djanaguiraman, M. (2011). High night temperature decreases leaf photosynthesis and pollen function in grain sorghum. *Funct. Plant Biol.* 38, 993–1003. doi: 10.1071/FP11035

Prasad, P. V. V., and Djanaguiraman, M. (2014). Response of floret fertility and individual grain weight of wheat to high temperature stress: sensitive stages and thresholds for temperature and duration. *Funct. Plant Biol.* 41, 1261–1269. doi: 10.1071/FP14061

Prasad, P. V. V., Pisipati, S. R., Mutava, R. N., and Tuinstra, M. R. (2008a). Sensitivity of grain sorghum to high temperature stress during reproductive development. *Crop Sci.* 48, 1911–1917. doi: 10.1016/j.jplph.2009.11.007

Prasad, P. V. V., Pisipati, S. R., Ristic, Z., Bukovnik, U., and Fritz, A. K. (2008b). Impact of night time temperature on physiology and growth of spring wheat. *Crop Sci.* 48, 2372–2380. doi: 10.2135/cropsci2007.12.0717

Singh, P., Nedumaran, S., Traore, P. C. S., Boote, K. J., Rattunde, H. F. W., Prasad, P. V. V., et al. (2014). Quantifying potential benefits of drought and heat tolerance in rainy season sorghum for adapting to climate change. *Agric. For. Meteorol.* 185, 37–48. doi: 10.1016/j.agrformet.2013.10.012

Singh, V., Nguyen, C. T., van Oosterom, E. J., Chapman, S. C., Jordan, D. R., and Hammer, G. L. (2015). Sorghum genotypes differ in high temperature responses for seed set. *Field Crops Res.* 171, 32–40. doi: 10.1016/j.fcr.2014.11.003

Srivastava, A., Kumar, S. N., and Aggrawal, P. K. (2010). Assessment on vulnerability of sorghum to climate change in India. *Agric. Ecosyst. Environ.* 138, 160–169. doi: 10.1016/j.agee.2010.04.012

Sultan, B., Guan, K., Kouressy, M., Biasutti, M., Piani, C., Hammer, G. L., et al. (2014). Robust features of future climate change impacts on sorghum yields in West Africa. *Environ. Res. Lett.* 9:104006. doi: 10.1088/1748-9326/9/10/104006

Sultan, B., Roudier, P., Quirion, P., Alhassane, A., Muller, B., Dingkuhn, M., et al. (2013). Assessing climate change impacts on sorghum and millet yields in the Sudanian and Sahelian savannas of West Africa. *Environ. Res. Lett.* 8:014040. doi: 10.1088/1748-9326/8/1/014040

Tingem, M., Ravington, M., Bellocchi, G., Azam-Ali, S., and Collis, J. (2008). Effect of climate change on crop production in Cameroon. *Clim. Res.* 36, 65–77. doi: 10.3354/cr00733

Conflict of Interest Statement: The authors declare that the research was conducted in the absence of any commercial or financial relationships that could be construed as a potential conflict of interest.

frontiers in Plant Science

PERSPECTIVE
published: 27 July 2016
doi: 10.3389/fpls.2016.01130

Limitation of Grassland Productivity by Low Temperature and Seasonality of Growth

Astrid Wingler[1] and Deirdre Hennessy[2]*

[1] School of Biological, Earth and Environmental Sciences, University College Cork, Cork, Ireland, [2] Teagasc-The Agriculture and Food Development Authority, Moorepark Animal & Grassland Research and Innovation Centre, Fermoy, Ireland

The productivity of temperate grassland is limited by the response of plants to low temperature, affecting winter persistence and seasonal growth rates. During the winter, the growth of perennial grasses is restricted by a combination of low temperature and the lack of available light, but during early spring low ground temperature is the main limiting factor. Once temperature increases, growth is stimulated, resulting in a peak in growth in spring before growth rates decline later in the season. Growth is not primarily limited by the ability to photosynthesize, but controlled by active regulatory processes that, e.g., enable plants to restrict growth and conserve resources for cold acclimation and winter survival. An insufficient ability to cold acclimate can affect winter persistence, thereby also reducing grassland productivity. While some mechanistic knowledge is available that explains how low temperature limits plant growth, the seasonal mechanisms that promote growth in response to increasing spring temperatures but restrict growth later in the season are only partially understood. Here, we assess the available knowledge of the physiological and signaling processes that determine growth, including hormonal effects, on cellular growth and on carbohydrate metabolism. Using data for grass growth in Ireland, we identify environmental factors that limit growth at different times of the year. Ideas are proposed how developmental factors, e.g., epigenetic changes, can lead to seasonality of the growth response to temperature. We also discuss perspectives for modeling grass growth and breeding to improve grassland productivity in a changing climate.

Keywords: brassinosteroids, gibberellins, grass breeding, growth modeling, perennial ryegrass (*Lolium perenne* L.), phytohormones, seasonality, winter persistence

OPEN ACCESS

Edited by:
Alison Kingston-Smith, Aberystwyth University, UK

Reviewed by:
Ricardo Cruz De Carvalho, University of Lisbon, Portugal
Anthony John Parsons, Massey University, New Zealand

****Correspondence:***
Astrid Wingler
astrid.wingler@ucc.ie

Specialty section:
This article was submitted to Agroecology and Land Use Systems, a section of the journal Frontiers in Plant Science

Received: *26 April 2016*
Accepted: *15 July 2016*
Published: *27 July 2016*

Citation:
Wingler A and Hennessy D (2016) Limitation of Grassland Productivity by Low Temperature and Seasonality of Growth. Front. Plant Sci. 7:1130. doi: 10.3389/fpls.2016.01130

INTRODUCTION

The growth response of forage grass species to temperature has been studied extensively since the 1970s. More recently, improved understanding of the growth physiology of grass has been gained, but knowledge is still lacking how the temperature response of grassland species can be improved to allow sustained growth throughout the year. Work with model species and recent progress in grass genetics can improve our understanding of the processes that determine growth and identify targets for breeding. Knowledge gained will also be important for grassland management, e.g., for deciding how long and extensively pastures should be grazed for maximum productivity. Developing models for grass growth in response to temperature may enable forecasting of growth

dependent on season and temperature, and also how grassland productivity may be affected by climate change.

SEASONAL PATTERNS OF GRASS GROWTH

Temperature has a major impact on the growth of temperate forage grasses, such as perennial ryegrass (*Lolium perenne*). For example, soil temperature was identified as the main determinant of growth in the South of Ireland (Hurtado-Uria et al., 2013a; see Monitoring Grassland Productivity). While low rates of growth can occur at temperatures down to 0°C, leaf elongation of perennial ryegrass was shown to increase strongly at temperatures above 5°C (Peacock, 1975). More recent work (Nagelmüller et al., 2016) also demonstrates low rates of leaf elongation in winter wheat, summer barley and perennial ryegrass at temperatures down to 0°C, with an abrupt increase above 5°C. Minor, but significant genotype-specific differences were found for growth at low temperatures, which could be exploited in breeding.

In addition to environmental conditions, developmental factors determine the growth of grass: productivity is highest in late spring and early summer and declines later in the summer (Hurtado-Uria et al., 2013a). Although, productivity is determined not only by the growth of individual leaves, but also by leaf production/tillering, measurement of leaf elongation can provide useful physiological information about the processes that determine biomass production. Often, there is a distinct peak of leaf extension in spring (Peacock, 1975; Parsons and Robson, 1980; Davies et al., 1989). These seasonal effects are demonstrated by transfer from cold into warm conditions. For example, a growth spurt was found after transfer of Italian and perennial ryegrass to warm conditions in February, but growth was lower after transfer in mid-April (Davies et al., 1989). This shows that ryegrass has the highest potential for growth early in the year, whereas developmental factors limit the temperature response later in the season. Furthermore, mild frost in winter and early spring can stimulate compensatory dry matter (DM) production in perennial grasses (Østrem et al., 2010).

COLD ACCLIMATION AND WINTER PERSISTENCE

An important factor for grassland productivity is winter persistence. Even in mild climates loss of biomass can occur during the winter (e.g., Hennessy et al., 2006), and lack of persistence can also affect the relative abundance of species and cultivars after the winter, e.g., resulting in a loss of the biomass of clover, which is often grown with grass in mixed swards (Wachendorf et al., 2001) and loss of perennial ryegrass tillers (Hennessy et al., 2008).

The process of cold acclimation that results in winter hardiness has been well characterized in temperate forage grasses. Fructans, which accumulate during summer and autumn and peak in December (Pollock and Jones, 1979), can protect the plants against stress (Sandve et al., 2011) and serve as a carbon source for regrowth in spring (Pollock and Jones, 1979; Tamura et al., 2014). The C-repeat binding factor (CBF) dependent cold acclimation pathway that was originally identified in *Arabidopsis thaliana* is also active during cold acclimation in perennial ryegrass (Xiong and Fei, 2006). More recently, analysis of changes in the transcriptome of perennial ryegrass showed disruption of the circadian rhythm network during cold acclimation in a variety adapted to warmer climates (Abeynayake et al., 2015). Candidate gene association mapping identified alleles of genes associated with winter survival and spring regrowth, including a *CBF* gene (Yu et al., 2015).

Compared to forage grasses, the information about processes underlying cold acclimation is limited for white clover (*Trifolium repens*), which can show lack of persistence during the winter. White clover requires slightly higher temperatures for growth than perennial ryegrass, thus limiting its persistence in mixed swards at temperatures below 10°C (Collins and Rhodes, 1995). In addition to low temperature alone, shading by grass tillers has a negative impact on the clover content of mixed swards, but only in combination with low spring and winter temperatures (Wachendorf et al., 2001). In white clover carbon accumulates in the form of pinitol and sucrose in the stolons during winter (Turner and Pollock, 1998), and cold exposure results in the accumulation of vegetative storage proteins in the roots and stolons. These vegetative storage proteins have a role as nitrogen store, but they may also be involved in the cold acclimation process (Goulas et al., 2003).

There are trade-offs between cold acclimation and growth during the winter – the synthesis of compounds required for cold hardiness limits carbon availability for growth. As discussed by Parsons et al. (2013) growth of perennial grasses may be limited not by resource availability but by maximizing long-term fitness. Breeding for increased frost hardiness can therefore result in low growth rates, whereas cultivars with increased growth at low temperature may be more susceptible to damage by frost. Growth and frost hardiness therefore both need to be optimized together for future climatic conditions.

PHYSIOLOGICAL MECHANISMS UNDERLYING GRASSLAND PRODUCTIVITY DURING THE GROWING SEASON

In humid temperate climates, uptake of CO_2 by grassland can continue throughout the year (Peichl et al., 2011), even at below-zero temperatures (Skinner, 2007), although solar radiation and daylength may be limiting photosynthesis during the winter months. Once light conditions become more favorable, growth can be actively restricted by processes that inhibit cell division and expansion at low temperature. Thus, instead of being source-limited, growth becomes sink-limited (Wingler, 2015). Hormone signaling pathways play an important role in this regulation, in particular gibberellic

acid (GA) signaling. For *Arabidopsis* it has been shown that GA stimulates growth by targeting growth-inhibiting DELLA proteins for degradation. At low temperature, CBF-dependent cold acclimation reduces GA content, resulting in DELLA accumulation and growth inhibition (Achard et al., 2008).

Gibberellic acid also determines the growth of grass species; for example, it can promote leaf extension of perennial ryegrass (Stapleton and Jones, 1987). It was proposed that GA plays a role in the induction of the fructan-degrading enzyme fructan exohydrolase to promote growth after defoliation (Morvan et al., 1997). As carbohydrate content declines, expression of the gene for the GA activating GA3 oxidase increases and that of the gene for the inactivating GA2 oxidase decreases (Liu et al., 2015). It was therefore proposed that an interaction between sugar and GA metabolism is responsible for the growth response to defoliation. In an association mapping study it was demonstrated that polymorphism of a gene for the DELLA protein *GAI* (GA insensitive) can explain differences in leaf elongation in perennial ryegrass (Auzanneau et al., 2011), demonstrating that not just the synthesis of active GA, but also GA signaling is involved in the growth response.

Similar to GA, brassinosteroids stimulate cell division and expansion (Fridman and Savaldi-Goldstein, 2013), and brassinosteroid insensitivity results in increased cold tolerance in *Arabidopsis* (Kim et al., 2010). Recently, brassinosteroids have been shown to regulate GA production, thus integrating both hormone signaling pathways in *Arabidopsis* (Unterholzner et al., 2015). Work with the model *Brachypodium distachyon* demonstrated that brassinosteroid signaling also determines growth in a grass species (Thole et al., 2012) and that down-regulation of brassinosteroid signaling results in increased drought tolerance (Feng et al., 2015). However, the importance of brassinosteroids in temperature-dependent growth and possible interactions with GA have not been reported in grass species. Jasmonic acid inhibits growth in response to low temperature in dicot species, such as *Arabidopsis* (Wingler, 2015), and also seems to have a growth inhibitory effect in grasses, although its role is less well-explored than in dicots (Shyu and Brutnell, 2015).

WHAT DETERMINES THE SEASONALITY OF GRASS GROWTH?

In spring, grass has a higher capacity to respond to warm temperature than later in the season. Peacock (1975) proposed that developmental instead of environmental factors are responsible for these seasonal differences in grass growth. Later work provided some insight into the nature of these factors. Reproductive tillers were found to have higher rates of leaf extension than those that remain vegetative (Davies et al., 1989). This is in agreement with the finding that vernalization stimulates leaf extension (Stapleton and Jones, 1987). Seasonal differences in the growth response to GA that may explain the seasonality of growth were identified (Ball et al., 2012; Parsons et al., 2013): perennial ryegrass plants taken from the field in winter showed a stronger increase in DM production in response to treatment with GA than plants taken from the field in summer. Similar to the growth promotion by vernalization (Stapleton and Jones, 1987), these differences are independent of daylength (Parsons et al., 2013). It is thus likely that epigenetic changes that occur during vernalization determine GA response, but the mechanisms that underlie this interaction have not been explored.

APPROACHES FOR ANALYZING THE GENETIC BASIS OF THE GROWTH RESPONSE OF GRASS SPECIES

Molecular tools enabling identification of genes and their variants that are responsible for plant growth in response to environmental and developmental factors are now available for model grass species. *B. distachyon* has emerged as a useful model for molecular studies to identify gene function in grasses. *B. distachyon* can easily be genetically modified, and T-DNA mutant collections are available (Thole et al., 2012). However, *B. distachyon* is annual and not adapted to cold climates (Li et al., 2012), which limits its use as model for perennial cool season forage grasses. In contrast, the relative *B. sylvaticum,* combines many of the advantages of *B. distachyon* with perenniality and growth at higher latitudes. It would therefore be an ideal model system to investigate aspects of temperature-dependent growth and seasonality. The ease with which transgenic lines can be created and self-fertility of *Brachypodium* species make them easier to use in functional studies than out-breeding forage grasses.

Association genetics now allows the identification of genetic polymorphisms that determine important traits. In forage grasses, association mapping has so far mainly been limited to candidate genes, e.g., establishing associations between polymorphisms in the *GAI* gene and leaf elongation (Auzanneau et al., 2011) and in a C-repeat binding factor (*CBF*) gene with winter survival (Yu et al., 2015). Further development of the genetic tools and approaches (Kopecký and Studer, 2014) should make genome-wide association studies (GWAS) in forage grasses possible in the near future. The knowledge gained can then be directly used in breeding by marker-assisted selection or genomic selection (Hayes et al., 2013; Grinberg et al., 2016).

MONITORING GRASSLAND PRODUCTIVITY

Monitoring grassland productivity provides valuable information for scientists, advisors and researchers. There is a long history of recording grassland production through cutting and weighing grass samples in the field (e.g., Davies and Simons, 1979; Binnie et al., 2001; O'Connor et al., 2012). For physiological research that requires recording of subtle differences in grass growth under controlled conditions or in the field, the Leaf Length Tracker (Nagelmüller et al., 2016) provides accurate information for leaf elongation which could, e.g., be used to

determine the genetic basis of physiological responses. However, this technology was not developed with the aim of determining biomass production under management regimes such as cutting and grazing.

The small-plot cutting method is the most widely used research technique (Hopkins, 2000) which attempts to simulate grazing or forage conservation management with different intervals, typically of 3 or 4 weeks. There are a range of methods available for measurement. The method developed by Corral and Fenlon (1978) involves recording the yield from four series of plots harvested in rotation, 1 week apart. Grass growth is estimated using a simple quadratic function which accelerates grass growth steadily from zero immediately after harvest.

Hurtado-Uria et al. (2013a) used multiple regression analysis to examine the relationship between grass growth measured using the Corral and Fenlon (1978) methodology and meteorological data at Teagasc, Animal and Grassland Research and Innovation Centre (AGRIC), Moorepark, Fermoy, County Cork in the south of Ireland from 1982 to 2010. Those authors found that the effects of a number of meteorological factors on grass growth varied depending on season (**Table 1**). Temperature has a significant effect in all seasons, as does evapotranspiration.

Plot based estimates of grassland production are useful but somewhat artificial in the context of grass-based ruminant production systems in which grazing comprises the predominant method of feeding. Techniques such as the rising platemeter, cut and weigh, and visual estimation can be used on farm (O'Donovan, 2000). Monitoring grassland production using these techniques provides farmers with reliable information with which to make decisions around managing grass supply, selection of paddocks for grazing or silage, feeding, supplementation, and fertilizer.

Collecting herbage production data from commercial dairy, beef and sheep farms in a database will allow the evaluation of the effects of various management, soil and meteorological factors on grass production. Recently, Teagasc, AGRIC, Moorepark, Fermoy, County Cork, Ireland developed PastureBase Ireland[1] for this purpose. O'Donovan et al. (2016) used the database to examine the effects of spring nitrogen fertilizer application and autumn closing date on spring herbage production.

Other methods for measuring grassland productivity include remote sensing and eddy covariance analysis. Remote sensing is potentially useful for comparing the current state of grass growth to the average, to the same time the previous year, or between regions. Different methods can be used to analyze satellite images with different levels of accuracy (Ali et al., 2016). The main limitations of remote sensing include the image resolution and noise associated with the satellite observations. Eddy covariance (eddy flux) analysis can be used to monitor grassland CO_2 exchange. While this method does not provide a direct measure of grass growth, measurement of net ecosystem CO_2 exchange in intensively managed grassland in Ireland indicated highest productivity in April and May (Peichl et al., 2011), which is in agreement with grass biomass production (Hurtado-Uria et al., 2013a). However, in contrast to foliage production (**Table 1**), net ecosystem CO_2 exchange was not correlated with spring temperature (Peichl et al., 2011), which indicates differences in the response of leaf growth and below-ground processes to temperature.

[1]https://www.pasturebase.teagasc.ie/

TABLE 1 | Meteorological factors influencing grass growth based on an analysis of grass growth and meteorological conditions recorded at Teagasc, AGRIC, Moorepark, Fermoy, County Cork, Ireland by Hurtado-Uria et al. (2013a).

Season	Variable
(1) January to March	Evapotranspiration
	Soil temperature at 100 mm
(2) April to mid-June	Soil temperature at 50 mm
(3) Mid-June to August	Maximum temperature
	Evapotranspiration
	Minimum temperature
	Sunshine hours
(4) September to December	Evapotranspiration
	Minimum temperature

MODELING GRASS GROWTH IN A CHANGING CLIMATE

In the last number of decades many models that describe grass growth have been developed, varying from simple empirical (e.g., Brereton et al., 1996) to more complex mechanistic models (e.g., Thornley, 1998; Jouven et al., 2006; Johnson et al., 2008). Such models provide increased understanding of the processes involved in grass growth and its interaction with farm management, as well as examining the environmental impact on grassland. Grass growth models are often a sub-model or component of larger farm system models, e.g., in APSIM (Keating et al., 2003), PaSim (Soussana et al., 2004; Graux et al., 2011), EcoMod, DairyMod and the SGS Pasture Model (Johnson et al., 2008), and as such are fully integrated with animal intake, grazing behavior and production, as well as N and C balances and other environmental impacts. Integrated models can be used to examine the effects of a changing climate on grass production and the impacts on animal production systems; e.g., Graux et al. (2011) used the PaSim model to assess climate change effects on pasture and herbivore production. Evaluation of models is important to ensure that a model selected for use in a particular region or scenario is useful (Hurtado-Uria et al., 2013b).

User-friendly grass growth prediction models that provide real time information using forecasted meteorological data and farm management data to predict grass growth and hence herbage supply can allow farmers to manage a key resource on their farms. Incorporating machine learning techniques into a grass growth predictor would increase the accuracy of the prediction for individual farms. Combining mechanistic grass growth models with remote sensing analysis of grass production is likely to improve the accuracy of grass growth prediction.

CONSEQUENCES FOR BREEDING TO IMPROVE GRASSLAND PRODUCTIVITY

While grass breeders have traditionally focused on total annual DM production when breeding grasses, there is an increasing realization that seasonal DM production is important. O'Donovan et al. (2011) highlighted the importance of early spring grass in pasture-based ruminant production systems. McEvoy et al. (2010) reported that winter DM yield is worth up to five times the value of spring and summer DM yield in Irish pasture-based dairy production systems. As highlighted here, a key trait that should be focused on in breeding is overwinter and early spring growth. This will require a focus on the response to environmental and internal (metabolic and hormone) signals in breeding to overcome the conservative utilization of resources that limits growth (Parsons et al., 2011, 2013). However, breeding grasses with increased overwinter growth must be undertaken with care, especially when the grasses are used in areas that experience even occasional cold winters (Stewart and Hayes, 2011). Stewart and Hayes (2011) suggest that it may be possible to combine strong early spring growth with a suitable level of winter hardiness even for colder winter regions (see Cold Acclimation and Winter Persistence).

Advances in plant breeding to meet the requirements for various traits depends on the type and quality of the germplasm/genetic resources available, and while selecting for a particular trait, breeders have to be aware of the other key plant traits required for the environment and system they are breeding for. Using traditional methods, the timescale for delivering a new grass cultivar to the market is up to 18 years. Adoption of new technologies, such as GWAS and genomic selection (Hayes et al., 2013; Kopecký and Studer, 2014; Grinberg et al., 2016) may increase this rate of delivery, which is vital in view of the current rapid change in climate.

AUTHOR CONTRIBUTIONS

AW wrote Section "Introduction, Seasonal Patterns of Grass Growth, Cold Acclimation and Winter Persistence, Physiological Mechanisms Underlying Grassland Productivity During the Growing Season, What Determines the Seasonality of Grass Growth?, Approaches for Analyzing the Genetic Basis of the Growth Response of Grass Species" and coordinated submission of the manuscript. DH wrote Section "Monitoring Grassland Productivity, Modeling Grass Growth in a Changing Climate, Consequences for Breeding to Improve Grassland Productivity" and provided **Table 1**. Both authors read and approved the whole manuscript.

REFERENCES

Abeynayake, S. W., Byrne, S., Nagy, I., Jonaviciene, K., Etzerodt, T. P., Boelt, B., et al. (2015). Changes in *Lolium perenne* transcriptome during cold acclimation in two genotypes adapted to different climatic conditions. *BMC Plant Biol.* 15:250. doi: 10.1186/s12870-015-0643-x

Achard, P., Gong, F., Cheminant, S., Alioua, M., Hedden, P., and Genschik, P. (2008). The cold-inducible CBF1 factor-dependent signaling pathway modulates the accumulation of the growth-repressing DELLA proteins via its effect on gibberellin metabolism. *Plant Cell* 20, 2117–2129. doi: 10.1105/tpc.108.058941

Ali, I., Cawkwell, F., Dwyer, E., and Green, S. (2016). Modeling managed grassland biomass estimation by using multitemporal remote sensing data—A machine learning approach. *IEEE J. Sel. Top. Appl. Earth Obs. Remote Sens.* 99, 1–16. doi: 10.1109/JSTARS.2016.2561618

Auzanneau, J., Huyghe, C., Escobar-Gutiérrez, A. J., Julier, B., Gastal, F., and Barre, P. (2011). Association study between the gibberellic acid insensitive gene and leaf length in a *Lolium perenne* L. synthetic variety. *BMC Plant Biol.* 11:183. doi: 10.1186/1471-2229-11-183

Ball, C. C., Parsons, A. J., Rasmussen, S., Shaw, C., and Rowarth, J. S. (2012). Seasonal differences in the capacity of perennial ryegrass to respond to gibberellin explained. *Proc. N. Z. Grassl. Assoc.* 74, 183–188. doi: 10.1104/pp.114.239004

Binnie, R. C., Mayne, C. S., and Laidlaw, A. S. (2001). The effects of rate and timing of application of fertiliser nitrogen in late summer on herbage mass and chemical composition of perennial ryegrass swards over the winter period in Northern Ireland. *Grass Forage Sci.* 56, 46–56. doi: 10.1046/j.1365-2494.2001.00245.x

Brereton, A. J., Danielov, S. A., and Scott, T. D. (1996). *Agrometeorology of Grass and Grasslands for Middle Latitudes: Technical Note No.* 197. Geneva: World Meteorological Organisation.

Collins, R. P., and Rhodes, I. (1995). Stolon characteristics related to winter survival in white clover. *J. Agric. Sci.* 124, 11–16. doi: 10.1017/S0021859600071197

Corral, J., and Fenlon, J. S. (1978). A comparative method for describing the seasonal distribution of production from grasses. *J. Agric. Sci.* 91, 61–67. doi: 10.1017/S0021859600056628

Davies, A., Evans, M. E., and Pollock, C. J. (1989). Influence of date of tiller origin on leaf extension rates in perennial and Italian ryegrass at 15 (C in relation to flowering propensity and carbohydrate status. *Ann. Bot.* 63, 377–384.

Davies, A., and Simons, R. G. (1979). Effect of autumn cutting regime on developmental morphology and spring growth of perennial ryegrass. *J. Agric. Sci.* 92, 457–469. doi: 10.1017/S0021859600063000

Feng, Y., Yin, Y., and Fei, S. (2015). Down-regulation of *BdBRI1*, a putative brassinosteroid receptor gene produces a dwarf phenotype with enhanced drought tolerance in *Brachypodium distachyon*. *Plant Sci.* 234, 163–173. doi: 10.1016/j.plantsci.2015.02.015

Fridman, Y., and Savaldi-Goldstein, S. (2013). Brassinosteroids in growth control: how, when and where. *Plant Sci.* 209, 24–31. doi: 10.1016/j.plantsci.2013.04.002

Goulas, E., Le Dily, F., Ozouf, J., and Ourry, A. (2003). Effects of a cold treatment of the root system on white clover (*Trifolium repens* L.) morphogenesis and nitrogen reserve accumulation. *J. Plant Physiol.* 160, 893–902. doi: 10.1078/0176-1617-00937

Graux, A.-I., Gaurut, M., Agabriel, J., Baumont, R., Delagarde, R., Delaby, L., et al. (2011). Development of the Pasture Simulation Model for assessing livestock production under climate change. *Agric. Ecosyst. Environ.* 144, 69–91. doi: 10.1016/j.agee.2011.07.001

Grinberg, N. F., Lovatt, A., Hegarty, M., Lovatt, A., Skøt, K. P., Kelly, R., et al. (2016). Implementation of genomic prediction in *Lolium perenne* L. breeding populations. *Front. Plant Sci.* 7:133. doi: 10.3389/fpls.2016.00133

Hayes, B. J., Cogan, N. O. I., Pembleton, L. W., Goddard, M. E., Wang, J., Spangenberg, G. C., et al. (2013). Prospects for genomic selection in forage plant species. *Plant Breed.* 132, 133–143. doi: 10.1111/pbr.12037

Hennessy, D., O'Donovan, M., French, P., and Laidlaw, A. S. (2006). The effects of date of autumn closing and timing of winter grazing on herbage production in winter and spring. *Grass Forage Sci.* 61, 363–374. doi: 10.1111/j.1365-2494.2006.00543.x

Hennessy, D., O'Donovan, M., French, P., and Laidlaw, A. S. (2008). Factors influencing tissue turnover during winter in perennial ryegrass dominated swards. *Grass Forage Sci.* 63, 202–211. doi: 10.1111/j.1365-2494.2007.00625.x

Hopkins, A. (2000). "Chapter 4: Herbage production," in *Grass its Production and Utilization*, 3rd Edn, ed. A. Hopkins (Oxford: Blackwell Science Ltd), 90–110.

Hurtado-Uria, C., Hennessy, D., Shalloo, L., O'Connor, D., and Delaby, L. (2013a). Relationships between meteorological data and grass growth over time in the south of Ireland. *Ir. Geogr.* 46, 175–201. doi: 10.1080/00750778.2013.865364

Hurtado-Uria, C., Hennessy, D., Shalloo, L., Schulte, R. P. O., Delaby, L., and O'Connor, D. (2013b). Evaluation of three grass growth models to predict grass growth in Ireland. *J. Agric. Sci.* 151, 91–104. doi: 10.1017/S0021859612000317

Johnson, I. R., Chapman, D. F., Snow, V. O., Eckard, R. J., Parsons, A. J., Lambert, M. G., et al. (2008). DairyMod and EcoMod: biophysical pasture-simulation models for Australia and New Zealand. *Austr. J. Exp. Agric.* 48, 621–631. doi: 10.1071/EA07133

Jouven, M., Carrére, P., and Baumont, R. (2006). Model predicting dynamics of biomass, structure and digestibility of herbage in managed permanent pastures. 1. Model description. *Grass Forage Sci.* 61, 112–124. doi: 10.1111/j.1365-2494.2006.00515.x

Keating, B. A., Carberry, P. S., Hammer, G. L., Probert, M. E., Robertson, M. J., Holzworth, D., et al. (2003). An overview of APSIM, a model designed for farming systems simulation. *Eur. J. Agron.* 18, 267–288. doi: 10.1016/S1161-0301(02)00108-9

Kim, S. Y., Kim, B. H., Lim, C. J., Lim, C. O., and Nam, K. H. (2010). Constitutive activation of stress-inducible genes in a brassinosteroid-insensitive 1 (bri1) mutant results in higher tolerance to cold. *Physiol. Plant.* 138, 191–204. doi: 10.1111/j.1399-3054.2009.01304.x

Kopecký, D., and Studer, B. (2014). Emerging technologies advancing forage and turf grass genomics. *Biotechnol. Adv.* 32, 190–199. doi: 10.1016/j.biotechadv.2013.11.010

Li, C., Rudi, H., Stockinger, E. J., Cheng, H., Cao, M., Fox, S. E., et al. (2012). Comparative analyses reveal potential uses of *Brachypodium distachyon* as a model for cold stress responses in temperate grasses. *BMC Plant Biol.* 12:65. doi: 10.1186/1471-2229-12-65

Liu, Q., Jones, C. S., Parsons, A. J., Xue, H., and Rasmussen, S. (2015). Does gibberellin biosynthesis play a critical role in the growth of *Lolium perenne*? Evidence from a transcriptional analysis of gibberellin and carbohydrate metabolic genes after defoliation. *Front. Plant Sci.* 6:944. doi: 10.3389/fpls.2015.00944

McEvoy, M., O'Donovan, M., and Shalloo, L. (2010). Evaluating the economic performance of grass varieties. *Adv. Anim. Biosci.* 1, 328. doi: 10.1017/S2040470010004711

Morvan, A., Challe, G., Prud'Homme, M.-P., Le Saos, J., and Boucaud, J. (1997). Rise of fructan exohydrolase activity in stubble of *Lolium perenne* after defoliation is decreased by uniconazole, an inhibitor of the biosynthesis of gibberellins. *New Phytol.* 136, 81–88. doi: 10.1046/j.1469-8137.1997.00713.x

Nagelmüller, S., Kirchgessner, N., Yates, S., Hiltpold, M., and Walter, A. (2016). Leaf Length Tracker: a novel approach to analyse leaf elongation close to the thermal limit of growth in the field. *J. Exp. Bot.* 67, 1897–1906. doi: 10.1093/jxb/erw003

O'Connor, P. J., Hennessy, D., Brophy, C., O'Donovan, M., and Lynch, M. B. (2012). The effect of the nitrification inhibitor dicyandiamide (DCD) on herbage production when applied at different times and rates in the autumn and winter. *Agr. Ecosyst. Environ.* 152, 79–89. doi: 10.1016/j.agee.2012.02.014

O'Donovan, M. (2000). *The Relationship between the Performance of Dairy Cows and Grassland Management on Intensive Dairy Farms in Ireland*. Ph.D. thesis, National University of Ireland, Dublin.

O'Donovan, M., Geoghegan, A., Hennessy, D., and O'Leary, M. (2016). "Lessons from PastureBase Ireland -Improving our focus on spring grass," in *Proceedings of the Irish Grassland Association Dairy Conference*, Limerick, 5–22.

O'Donovan, M., Lewis, E., and O'Kiely, P. (2011). Requirements of future grass-based ruminant production systems in Ireland. *Ir. J. Agric. Food Res.* 50, 1–21.

Østrem, L., Rapacz, M., Jørgensen, M., and Höglind, M. (2010). Impact of frost and plant age on compensatory growth in timothy and perennial ryegrass during winter. *Grass Forage Sci.* 65, 15–22. doi: 10.1111/j.1365-2494.2009.00715.x

Parsons, A. J., Edwards, G. R., Newton, P. C. D., Chapman, D. F., Caradus, J. R., Rasmussen, S., et al. (2011). Past lessons and future prospects: plant breeding for yield and persistence in cool-temperate pastures. *Grass Forage Sci.* 66, 153–172. doi: 10.1111/j.1365-2494.2011.00785.x

Parsons, A. J., Rasmussen, S., Liu, Q., Xue, H., Ball, C., and Shaw, C. (2013). Plant growth – resource or strategy limited: insights from responses to gibberellin. *Grass Forage Sci.* 68, 577–588. doi: 10.1111/gfs.12035

Parsons, A. J., and Robson, M. R. (1980). Seasonal changes in the physiology of S24 perennial ryegrass (*Lolium perenne* L.). 1. Response of leaf extension to temperature during the transition from vegetative to reproductive growth. *Ann. Bot.* 46, 435–444.

Peacock, J. M. (1975). Temperature and leaf growth in *Lolium perenne*. III. Factors affecting seasonal differences. *J. Appl. Biol.* 12, 685–697. doi: 10.2307/2402182

Peichl, M., Leahy, P., and Kiely, G. (2011). Six-year stable annual uptake of carbon dioxide in intensively managed humid temperate grassland. *Ecosystems* 14, 112–126. doi: 10.1007/s10021-010-9398-2

Pollock, C. J., and Jones, T. (1979). Seasonal patterns of fructan metabolism in forage grasses. *New Phytol.* 83, 9–15. doi: 10.1111/j.1469-8137.1979.tb00720.x

Sandve, S. R., Kosmala, A., Rudi, H., Fjellheim, S., Rapacz, M., Yamada, T., et al. (2011). Molecular mechanisms underlying frost tolerance in perennial grasses adapted to cold climates. *Plant Sci.* 180, 69–77. doi: 10.1016/j.plantsci.2010.07.011

Shyu, C., and Brutnell, T. P. (2015). Growth-defence balance in grass biomass production: the role of jasmonates. *J. Exp. Bot.* 66, 4165–4176. doi: 10.1093/jxb/erv011

Skinner, H. (2007). Winter carbon dioxide fluxes in humid-temperate pastures. *Agric. For. Meteorol.* 144, 32–43. doi: 10.1016/j.agrformet.2007.01.010

Soussana, J.-F., Loiseau, P., Vuichard, N., Ceschia, E., Balesdent, J., Chevallier, T., et al. (2004). Carbon cycling and sequestration opportunities in temperate grasslands. *Soil Use Manage.* 20, 219–230. doi: 10.1079/SUM2003234

Stapleton, J., and Jones, M. B. (1987). Effects of vernalization on the subsequent rates of leaf extension and photosynthesis of perennial ryegrass (*Lolium perenne* L.). *Grass Forage Sci.* 47, 27–31. doi: 10.1111/j.1365-2494.1987.tb02087.x

Stewart, A., and Hayes, R. (2011). Ryegrass breeding – balancing trait priorities. *Ir. J. Agric. Food Res.* 50, 31–46.

Tamura, K., Sanada, Y., Tase, K., and Yoshida, M. (2014). Fructan metabolism and expression of genes coding fructan metabolic enzymes during cold acclimation and overwintering in timothy (*Phleum pratense*). *J. Plant Physiol.* 171, 951–958. doi: 10.1016/j.jplph.2014.02.007

Thole, V., Peraldi, A., Worland, B., Nicholson, P., Doonan, J. H., and Vain, P. (2012). T-DNA mutagenesis in *Brachypodium distachyon*. *J. Exp. Bot.* 63, 567–576. doi: 10.1093/jxb/err333

Thornley, J. H. M. (1998). *Grassland Dynamics: An Ecosystem Simulation Model*. Wallingford: CAB International, 241.

Turner, L. B., and Pollock, C. J. (1998). Changes in stolon carbohydrates during the winter in four varieties of white clover (*Trifolium repens* L.) with contrasting hardiness. *Ann. Bot.* 81, 97–107. doi: 10.1006/anbo.1997.0534

Unterholzner, S. J., Rozhon, W., Papacek, M., Ciomas, J., Lange, T., Kugler, K. G., et al. (2015). Brassinosteroids are master regulators of gibberellin biosynthesis in *Arabidopsis*. *Plant Cell* 27, 2261–2272. doi: 10.1105/tpc.15.00433

Wachendorf, M., Collins, R. P., Elgersma, A., Fothergill, M., Frankow-Lindberg, B. E., Ghesquiere, A., et al. (2001). Overwintering and growing season dynamics of *Trifolium repens* L. in mixture with *Lolium perenne* L.: a model approach to plant-environment interactions. *Ann. Bot.* 88, 683–702. doi: 10.1006/anbo.2001.1496

Wingler, A. (2015). Comparison of signalling interactions determining annual and perennial plant growth in response to low temperature. *Front. Plant Sci.* 5:794. doi: 10.3389/fpls.2014.00794

Xiong, Y., and Fei, S.-Z. (2006). Functional and phylogenetic analysis of a DREB/CBF-like gene in perennial ryegrass (*Lolium perenne* L.). *Planta* 224, 878–888. doi: 10.1007/s00425-006-0273-5

Yu, X., Pijut, P. M., Byrne, S., Asp, T., Bai, G., and Jiang, Y. (2015). Candidate gene association mapping for winter survival and spring regrowth in perennial ryegrass. *Plant Sci.* 235, 37–45. doi: 10.1016/j.plantsci.2015.03.003

Conflict of Interest Statement: The authors declare that the research was conducted in the absence of any commercial or financial relationships that could be construed as a potential conflict of interest.

frontiers in Environmental Science

OPINION
published: 15 June 2016
doi: 10.3389/fenvs.2016.00044

Increased Risk of Freeze Damage in Woody Perennials *VIS-À-VIS* Climate Change: Importance of Deacclimation and Dormancy Response

Rajeev Arora[1]* *and Kari Taulavuori*[2]

[1] Department of Horticulture, Iowa State University, Ames, IA, USA, [2] Department of Biology, University of Oulu, Oulu, Finland

Keywords: winter hardiness, freezing tolerance, deacclimation, dormancy, climate change, spring phenology, chilling brequirement, heat-units

Winter survial during an annual cycle of temperate- and boreal-zone woody perennials is a multi-component response. Two of these components are: (1) the timing, rate, and extent of cold acclimation (CA; **Box 1**), and (2) plants' ability to sufficiently maintain its freezing tolerance (FT) until the danger of killing frosts is passed which is determined by, among other factors, plants' ability to resist any *premature/unseasonal* deacclimation (DA; **Box 1**), which, under a predictable seasonal pattern, typically occurs during spring-warming.

OPEN ACCESS

Edited by:
Urs Feller,
University of Bern, Switzerland

Reviewed by:
Gary Coleman,
University of Maryland, USA
Dominique Job,
Centre National de la Recherche Scientifique, France

***Correspondence:**
Rajeev Arora
rarora@iastate.edu

Specialty section:
This article was submitted to Agroecology and Land Use Systems, a section of the journal Frontiers in Environmental Science

Received: *22 April 2016*
Accepted: *30 May 2016*
Published: *15 June 2016*

Citation:
Arora R and Taulavuori K (2016) Increased Risk of Freeze Damage in Woody Perennials VIS-À-VIS Climate Change: Importance of Deacclimation and Dormancy Response. Front. Environ. Sci. 4:44. doi: 10.3389/fenvs.2016.00044

DA RESPONSE IS MORE CRITICAL THAN CA UNDER CLIMATE CHANGE SCENARIO

CA is primarily initiated by the shortening day-length in autumn but further enhanced by cold temperatures by mid-winter. Research shows that short-days alone are sufficient to induce significant FT in woody perennials. Following are just of many examples that support this observation: (1) *Pinus sylvestris* acclimated to −22°C under short-days alone compared to −40°C under both the short-days and cold (Smit-Spinks et al., 1985), (2) Taulavuori et al. (2000) reported significant induction of FT in pine seedlings by short-days at 20°C, and (3) *Fagus sylvatica* are already hardy to below −15°C in October for an average year (Tranquillini and Plank, 1989). Moreover, FT of overwintering tissues in mid-winter is generally much higher than the absolute minimum temperatures typically encountered in nature (Vitasse et al., 2014). Therefore, the timing or capacity of CA does not constitute a critical factor regarding the risk of freeze-damage unless, however, an unusually early freeze in autumn causes premature leaf-loss and interferes with the preparation for maximal CA.

The dominant driver of DA, on the other hand, is warm temperature, and DA proceeds much faster (hours to days) than autumnal CA (weeks to months) (Fuchigami et al., 1982; Taulavuori et al., 2004; Kalberer et al., 2006). Consequently, erratic temperature fluctuations, i.e., "unseasonal" spring-like conditions followed by a freeze, could render partially or fully deacclimated tissues vulnerable to freeze-damage. Indeed, magnitude and frequency of such fluctuations have been on the rise in recent years (Jentsch et al., 2007; IPCC, 2014), and some of the most devastating killer-frosts across North America are attributed to such vagaries of climate, e.g., Easter freeze of 2007 (Gu et al., 2008), Mother's Day freeze of 2010, killer frost of 2012, and polar vortex of 2014. Field simulations of winter-warming events have also confirmed their damaging effects on overwintering perennials (Taulavuori et al., 1997; Bokhorst et al., 2009, 2010). We, therefore, opine that under

a climate change scenario, the rate and extent of premature DA is a particularly critical factor determining overall winter-hardiness, and a genotype/tissue with relatively greater DA-resistance during "unseasonal" warm spells may be resilient to temperature extremes.

Notably, diurnal fluctuations in temperature impact FT differently than do the constant temperatures because while warm days might induce DA, cold nights could promote reacclimation (RA; **Box 1**), (provided DA is not totally irreversible) which could potentially serve as a "safety-net" against premature DA (Kalberer et al., 2006, 2007a,b). For example, a constant 6°C exposure caused steady DA of Scots pine needles whereas a temperature-cycle averaging 6°C, i.e., 11°C/1°C (D/N), caused DA and RA whereby the colder phase resulted in reacclimation of up to 10°C (Leinonen et al., 1997). Such DA/RA cycling and its potential significance in winter-survival are often ignored in studies undertaken to model winter-hardiness response vis-à-vis climate change.

BUD DORMANCY STATUS IMPACTS DA

Limited research shows that DA kinetics (timing and extent) is not a single-dimension response, and regulated by factors such as, climate, genotype, and the bud dormancy status (endodormancy vs. ecodormancy; **Box 2**) (Ögren, 2001; Taulavuori et al., 2004; Kalberer et al., 2006; Arora and Rowland, 2011; Pagter and Arora, 2013; Ferguson et al., 2014; Vitasse et al., 2014). In endodormant (END) state, buds are relatively resistant to deacclimation whereas ecodormant (ECD) buds are "physiologically primed" for growth resumption (spring phenology) and accompanying deacclimation under conducive temperatures (Litzow and Pellett, 1980; Wolf and Cook, 1992; Kalberer et al., 2006). For example, fully cold acclimated buds of *Rhododendron viscosum* var. *montanum* deacclimated by ∼40% in February (chilling requirement; CR met; **Box 2**) when exposed to elevated temperatures but the same dose of warming in December (CR not met) resulted in only 19% DA (Kalberer et al., 2007a).

Physiology

Physiological rationale for why plants are less prone to deacclimation in END state is not well understood. Conceivably, symplastic-isolation of shoot apices due to down-regulated cell-to-cell communication (Rinne et al., 2011; Paul et al., 2014) and/or reduced content and mobility of water in END tissues (low free to bound water ratio, Fennell and Line, 2001, lower aquaporin activity/expression, Yooyongwech et al., 2008) are non-conducive for DA biochemistry, such as the loss of soluble sugars. Sugar depletion is believed to be a primary physiological explanation for DA (Ögren, 2001; Pagter and Arora, 2013). Growth regulator dynamics is also a likely factor. ABA, a growth-suppressing hormone, is widely known to accumulate in END tissues (Tanino, 2004). While bud-swell/opening is positively correlated with DA (Arora et al., 2004; Rowland et al., 2008), conditions prevailing during END are not favorable for cell expansion or bud-swell. For example, the level/perception of active GA, a hormone needed for bud burst, is lower in END tissues (Cooke et al., 2012, and references therein). ECD tissues, on the other hand, can and do deacclimate even in mid-winter if exposed to conducive warm. Such mid-winter DA is known as "passive DA" and requires ecologically unrealistic warming (Taulavuori et al., 2002) as opposed to "active DA" that occurs during spring-like conditions (Kalberer et al., 2006). Even though the temperature is typically too cold during early ECD stage to initiate ontogenetic development or deacclimation, the risk of damaging events exists and is not fixed in calendar, i.e., sudden deacclimation followed by extreme cold, absence of snow cover and hastened spring followed by nocturnal frosts (Taulavuori, 2013). Other stresses (UV, nutrient etc.) may also accelerate DA by diverting carbon allocation toward stress protection instead of cryoprotective compounds (Taulavuori et al., 2013).

Chilling Requirement (CR)

Fulfillment of CR is dependent on prevailing chilling temperatures during autumn. Elevated winter temperatures may result in chilling-deficit and thus delay the transition from END to ECD, especially at the southern and coastal edges of species' ranges in northern latitudes due to typically milder winters (Harrington and Gould, 2015). Indeed, atypical warming (15°C) during autumn delayed END induction in birch seedlings leading to delayed budbreak next spring (Skre et al., 2008). However, such chilling-deficit is unlikely in regions currently experiencing cold winters (high elevation or latitudes). These

BOX 1 | DEFINITIONS (IN PRESENT CONTEXT):

Cold acclimation (CA): a seasonal increase in overwintering perennials' freezing tolerance during each autumn reaching the maximum by winter. **Deacclimation (DA):** loss of the freezing tolerance that was acquired during CA. **Reacclimation (RA):** Regain of some or most of the freezing tolerance (lost during DA) when deacclimated tissues are exposed to cold acclimating conditions, e.g., cold.

BOX 2 | DEFINITIONS:

Endodormancy (END): the deepest state of dormancy in autumn during which buds must meet their chilling requirement (CR) in order to begin growth upon return of conducive environment; also called physiological dormancy, winter-dormancy or rest. **Chilling requirement (CR):** exposure of buds to a minimum number of chill-units (CUs) to overcome END; **CUs**: number of hours that buds are exposed to chilling temperatures, generally taken to be between 0 and 7°C. **Ecodormancy (ECD):** inability of non-endodormant buds to grow due exclusively to non-conducive environment, such as too cold or hot, drought etc.; also called imposed dormancy or quiescence (for detailed definitions of END and ECD, readers are referred to Lang et al. (1987). **Heat units (HUs):** accumulated dose of conducive heat (time × temperature above a certain threshold) required by non-endodormant buds to break/grow.

areas, on the contrary, could possibly experience even greater chilling since winter warming could convert sub-freezing temperatures with less effectiveness in fulfilling CR to slightly >0°C temperatures with high chilling effectiveness, thereby, advancing the exit from END and potentially exposing tissues to spring frost damage (Hänninen, 2006). CR, a genetically determined trait with evolutionary background, varies greatly across species and ecotypes. Though exceptions occur, the northern species and ecotypes tend to have relatively low CR (Taulavuori et al., 2004, and references therein). Rationale for this may be the lack of selection pressure for evolving high CR in regions where winter temperatures are usually <0°C. These species and populations are expected to meet their CR despite warming winters, which would predispose ECD tissues to deacclimation under unseasonal warming and render vulnerable to early spring freeze. On the other hand, such liability may not be an issue in regions with cold but stable climates (Kalberer et al., 2007b). **Figure 1A** illustrates the responsiveness (susceptibility) of deacclimation to environmental, genetic and physiological factors over a dormancy continuum. Due to the dormancy's impact on the propensity (or lack thereof) to deacclimate, it is critically important to include dormancy-status as a key parameter in the models for predicting plants' FT vis-a-vis climate change.

TEMPERATURE IMPACTS DA KINETICS

Arguably, the extent and rate of DA depends on the total "dose" of warm temperatures, a "degree x duration" response, akin to classic degree-day calculations. The "threshold dose" required to induce DA in ECD tissues varies with species and regulated by genotype x temperature interaction. Moreover, "threshold minimum" temperature (i.e., degree) required for DA varies with species, and, in many perennials, is found to be ∼ +5°C (Bigras et al., 2001; Pagter et al., 2011). For example, DA rate in *Vaccinium myrtillus* was higher in plants kept at +20°C for 10 days, compared to those kept at +10°C for 24 days, and essentially no DA occurred in plants exposed to +5°C up to 24 days (Taulavuori et al., 2002). Relationship between the warming duration and deacclimation rate, however, is not always linear. Whereas some plants rapidly deacclimate followed by gradually decreasing rate, others deacclimate more stably and at moderate rates for relatively longer (Kalberer et al., 2006; Pagter and Arora, 2013).

PROPENSITY TO SLOW VS. FAST DA—POSSIBLE ENVIRONMENTAL OR BIOLOGICAL DRIVERS

In light of above discussion, species better able to resist deacclimation under unseasonal warming are expected to be resilient against temperature extremes and freeze-damage. Question then arises: what environmental/biological factors might promote such a trait, and at what cost?

Selection Pressure by Fluctuating Temperature Extremes and the Role of Carbohydrate Pool

DA-resistance may possibly be a function of temperature fluctuations (frequency and magnitude) to which plants are exposed in their native habitats. Arguably, plants experiencing relatively stable temperatures may be under little evolutionary pressure to develop DA-resistance to unseasonal warming. For example, when exposed to a warming regime, azalea genotypes native to Appalachian mountains (a fluctuating temperature climate) deacclimated much slower than those from lowland, coastal regions of the northeastern U.S. (cooler and stable temperatures) which is less likely to cause sudden DA (Kalberer et al., 2007a). It may also be argued that the genotypes with greater mid-winter freezing tolerance may experience less selective pressure for resisting DA than do less-hardy ones, because the former can safely undergo significant deacclimation before becoming vulnerable to cold injury. Ecotypic differences in DA-resistance of mountain birch support this viewpoint whereby alpine ecotypes deacclimated at much faster rate than the oceanic ones (Taulavuori et al., 2004). We opine that the data on warming dose ("degree-duration") should be compared with the climatic history and plant survival of a region/provenance in question to determine if indeed genotypes exposed more frequently to DA-inducing warm-dose also tend to be slow deacclimators. Such information should be useful in "simulation studies" to provide robust parameters for modeling winter-hardiness vis-à-vis climate change scenarios.

To resist DA, in spite of conducive environment, plant conceivably requires special physiology/biochemistry. Ögren (2001) proposed that an inherently higher respiration rate and therefore the sugar expenditure may explain higher temperature sensitivity of lodgepole pine to deacclimation compared to Norway spruce and Scots pine. Ögren hypothesized that while lodgepole pine (native to colder region) may rely on cold suppression of respiration in winter, those native to milder climates (Norway spruce, Scots pine) perhaps *actively* down-regulate respiration. Such active adjustment may incur metabolic cost but a relatively larger carbohydrate reserve may favor slower deacclimation under transient warming. An accelerated deacclimation in those bilberry tissues with relatively smaller carbohydrate pool (Taulavuori et al., 1997) supports this notion. Slow deacclimators will likely also need to maintain CA associated genes (e.g., *cor* genes) and compounds sufficiently up-regulated despite the transient warming, which too may incur metabolic cost. Lower carbohydrate status, resulting from warmer winters, may also be mal-adaptive for any possible reacclimation. Notably, the size of carbohydrate pool will also be influenced by the weather conditions in autumn, with sunny days favoring its production and storage.

Spring Phenology

Exposure to sufficient "degree and duration" of warming (heat-units; HUs; **Box 2**) by ECD buds is the most important factor in regulating the timing and extent of ontogenetic development to budburst (spring phenology) (Menzel et al., 2001; Harrington

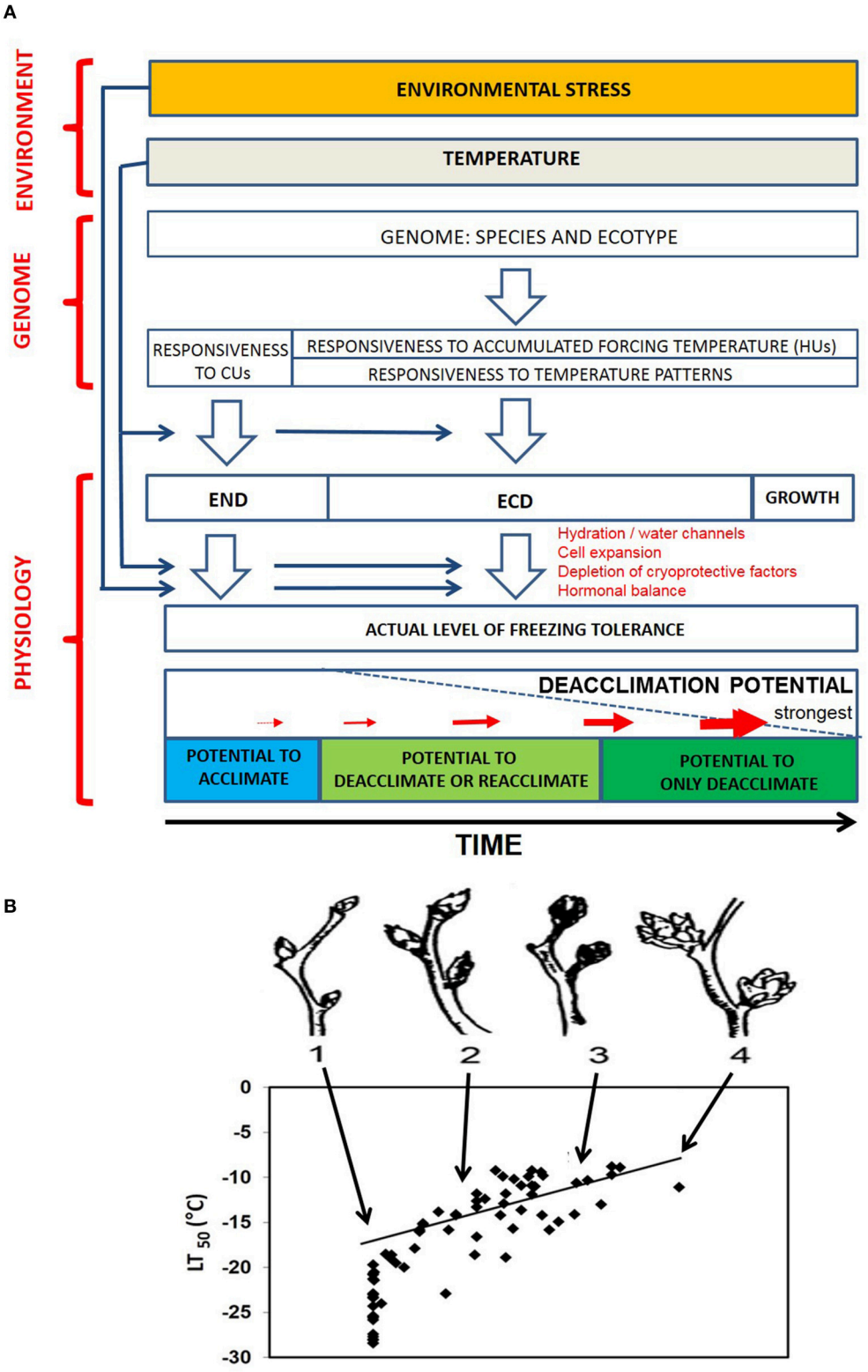

FIGURE 1 | (A). Basic concepts of plant deacclimation (DA) potential in response to interaction between environmental, genetic and physiological factors. Temperature, through genetics, determines the state of dormancy (END, ECD), and the level of freezing tolerance, which is also prone to environmental stress. Plant genome affects responsiveness to accumulating chilling units (CUs). Genotypic responsiveness to accumulating chilling units (CUs; **Box 2**) refers to DA resistance (strong/weak). Responsiveness to temperature patterns reflects genetic variation in DA kinetics at different times of winter. DA potential varies during the

(Continued)

FIGURE 1 | Continued
dormancy continuum, with being weakest during END and progressively becoming stronger toward and during ECD due to physiological changes. Reacclimation (RA) potential exists during early ECD but decreases with accumulating HUs; **(B)**. correlation ($r = 0.84$) between freezing tolerance and stage of opening in blueberry buds (drawn using the data extracted from Rowland et al. (2008); bud stages 1–4) 1: dormant bud with no visible sign of swelling; 2: visible bud swelling; 3: bud scales noticeably separated and flower tips becoming visible; and 4: bud scales dropped and corollas of individual flowers beginning to elongate.

et al., 2010). However, some reports have also suggested for photoperiodic control of phenology (Körner and Basler, 2010). Genetic variation exists for the HU requirement across and within species conceivably explained by the climate, latitude, altitude etc. of origin. HU requirement can also be regulated by a supposedly poorly understood relationship between chilling and HUs (Charrier et al., 2011; Polgar and Primack, 2011; Vitasse and Basler, 2013; Dantec et al., 2014) whereby HU requirement is negatively correlated to chilling accumulation (Harrington et al., 2010; Junttila and Hänninen, 2012; Laube et al., 2014). That chill- and heat-units can be satisfied by the same temperatures for some species (Cooke et al., 2012 and references therein) further adds to the complexity to this relationship.

Advance in spring phenology as a consequence of climate change/global warming has been widely reported (Peñuelas and Filella, 2001; Menzel et al., 2006; McEwan et al., 2011; Fu et al., 2014). It is amply evident that growth and development can lead directly or indirectly to irreversible DA (Leinonen et al., 1997; Mahfoozi et al., 2001; Rapacz, 2002a,b) and that FT is negatively correlated with bud-swell and budburst (Rowland et al., 2008; **Figure 1B**). Therefore, plants with somewhat delayed spring phenology, i.e., those with deeper ECD or higher HU-requirement, would be expected to better maintain FT despite the transient warming or be slow deacclimators. How does ontogenetic development modulate FT is not well understood. Conceivably, growth (cell expansion)-associated increased cellular hydration compromises FT by rendering tissues susceptible to mechanical damage from extracellular ice (Levitt, 1980) or active growth interferes with FT-maintenance by competing for energy resources (Levitt, 1980; Rapacz, 2002a,b). Growth initiation involves developmental reprogramming requiring *de novo* gene expression that may preclude maintenance of FT. However, it must be recognized that delayed spring phenology could shorten the growing season (and reduce productivity) of tree species in northern climates.

CONCLUDING REMARKS

Molecular genetic understanding of the cross-talk between loss of FT, i.e., DA, bud dormancy status, and growth/budbreak is needed in order to inform the selection of cultivars/genotypes with predictable responses to unseasonal warming episodes. A recent study by Wisniewski et al. (2015) is an important step in this direction. It is also important to include species-specific requirements for CR vs. HUs and both the magnitude and frequency of physiologically and regionally/locally relevant temperature fluctuations (rather than averages) in simulation experiments/modeling studies in order to infer about FT responses under a changing climate. While logistically it may be the best option available, caution should be exercised in drawing such conclusions from experiments using juvenile plants since their phenological responses may not accurately reflect the response of mature trees (Wolkovich et al., 2012; Vitasse, 2013; Lim et al., 2014).

AUTHOR CONTRIBUTIONS

Both the authors contributed to writing the manuscript which involved discussion of the themes, ideas to be projected, literature to be cited, and Figure development.

ACKNOWLEDGMENTS

We thank Dr. Mark Ehlenfeldt (USDA Fruit Lab, Chattsworth, N.J., USA) for helping with **Figure 1B**. We gratefully acknowledge the funding for this work from Iowa Agriculture and Home Economics Experiment Station project 3601, Iowa State University, and the Academy of Finland project no. 278364.

REFERENCES

Arora, R., and Rowland, L. J. (2011). Physiological research on winter-hardiness: deacclimation resistance, reacclimation ability, photoprotection strategies, and a cold acclimation protocol design. *HortScience* 46, 1070–1078. doi: 10.17660/ActaHortic.2013.990.6

Arora, R., Rowland, L. J., Ogden, E. L., Dhanaraj, A. L., Marian, C. O., Ehlenfeldt, M. K., et al. (2004). Rate of dehardening, stage of bud opening, and changes in dehydrin metabolism in blueberry (*Vaccinium* spp.) cultivars during deacclimation at constant, warm temperatures. *J. Am. Soc. Hort. Sci.* 129, 667–674

Bigras, J. F., Ryyppö, A., Lindstrom, A., and Stattin, E. (2001). "Cold acclimation and deacclimation of shoots and roots of conifer seedlings," in *Conifer Cold Hardiness,* eds J. F. Bigras and S. J. Colombo (Dordrecht: Kluwer Academic Publishers), 57–88.

Bokhorst, S., Bjerke, J. W., Davey, M. P., Taulavuori, K., Taulavuori, E., Laine, K., et al. (2010). Impacts of extreme winter warming events on plant physiology in a sub-arctic heath community. *Physiol. Plant.* 140, 128–140. doi: 10.1111/j.1399-3054.2010.01386.x

Bokhorst, S., Bjerke, J. W., Tommervik, H., Callaghan, T. V., and Phoenix, G. K. (2009). Winter warming events damage sub-arctic vegetation: consistent evidence from an experimental manipulation and natural event. *J. Ecol.* 97, 1408–1415. doi: 10.1111/j.1365-2745.2009.01554.x

Charrier, G., Bonhomme, M., Lacointe, A., and Ameglio, A. (2011). Are budburst dates, dormancy and cold acclimation in walnut trees (*Juglans regia* L.) under mainly genotypic or environmental control? *Int. J. Biometeorol.* 55, 763–774. doi: 10.1007/s00484-011-0470-1

Cooke, J. E., Eriksson, M. E., and Juntilla, O. (2012). The dynamic nature of bud dormancy in trees: environmental control and molecular mechanisms. *Plant Cell Environ.* 35, 1707–1728. doi: 10.1111/j.1365-3040.2012.02552.x

Dantec, C. F., Vitasse, Y., Bonhomme, M., Louvet, J-M., Kremer, A., and Delzon, S. (2014). Chilling and heat unit requirements for leaf unfolding in Europen beech and sesile oak populations at the southern limit of their distributions range. *Int. J. Biometeorol.* 58, 1853–1864. doi: 10.1007/s00484-014-0787-7

Fennell, A., and Line, M. J. (2001). Identifying differential tissue response in grape (*Vitis riparia*) during induction of endodormancy using nuclear magnetic resonance imaging. *J. Am. Soc. Hort. Sci.* 126, 681–688.

Ferguson, J. C., Moyer, M. M., Mills, L. J., Hoogenboom, G., and Keller, M. (2014). Modeling dormant bud cold hardiness and budbreak in twenty-three *Vitis* genotypes reveals variation by region of origin. *Am. J. Enol. Vitic.* 65, 59–71. doi: 10.5344/ajev.2013.13098

Fu, Y. H., Piao, S., Op de Beeck, M., Cong, N., Zhao, H., Zhang, Y., et al. (2014). Recent spring phenology shifts in western Central Europe based on mutiscale observations. *Glob. Ecol. Biogeogr.* 23, 1255–1263. doi: 10.1111/geb.12210

Fuchigami, L. H., Weiser, C. J., Kobayashi, K., Timmis, R., and Gusta, L. V. (1982). "A degree growth stage (°GS) model and cold acclimation in temperate woody plants," in *Plant Cold Hardiness and Freezing Stress Mechanisms and Crop Implications,* Vol. 2, eds P. H. Li and A. Sakai (New York, NY: Academic Press), 93–116.

Gu, L., Hanson, P. J., Post, W. M., Kaiser, D. P., Yang B., Nemani, R., et al. (2008). The 2007 eastern US spring freeze: increased cold damage in a warming world? *BioScience* 58, 253–262. doi: 10.1641/B580311

Hänninen, H. (2006). Climate warming and the risk of frost damage to boreal forest trees: identification of critical ecophysiological traits. *Tree Physiol.* 26, 889–898. doi: 10.1093/treephys/26.7.889

Harrington, C. A., and Gould, P. J. (2015). Tradeoffs between chilling and forcing in satisfying dormancy requirements for Pacific Northwest tree species. *Front. Plant Sci.* 6:120. doi: 10.3389/fpls.2015.00120

Harrington, C. A., Gould, P. J., and St. Clair, J. B. (2010). Modeling the effects of winter environment on dormancy release of Douglas-fir. *For. Ecol. Manage.* 259, 798–808. doi: 10.1016/j.foreco.2009.06.018

IPCC (2014). *Impacts, Adaptation, and Vulnerability. Part A: Global and SectoralAspects. Contribution of Working Group II of the Fifth Assessment Report of theIntergovernmental Panel on Climate Change*, eds C. B. Field, V. R. Barros, D. J. Dokken, K. J. Mach, M. D. Mastrandrea, T. E. Bilir, M. Chatterjee, K. L. Ebi, Y. O. Estrada, R. C. Genova, B. Girma, E. S. Kissel, A. N. Levy, S. MacCracken, P. R. Mastrandrea, and L. L. White (Cambridge; New York, NY: Cambridge Universiy Press), 1–32.

Jentsch, A., Kreyling, J., and Beierkuhnlein, C. (2007). A new generation of climate-change experiments: events, not trends. *Front. Ecol. Environ.* 5, 365–374. doi: 10.1890/1540-9295(2007)5[365:ANGOCE]2.0.CO;2

Junttila, O., and Hänninen, H. (2012). The minimum temperature for budburst in Betula depends on the state of dormancy. *Tree Physiol.* 32, 337–345. doi: 10.1093/treephys/tps010

Kalberer, S. R, Leyva-Estrada, N., Krebs, S. L., and Arora, R. (2007a). Cold hardiness of floral buds of deciduous azaleas: dehardening, rehardening, and endodormancy in late winter. *J. Am. Soc. Hort. Sci.* 132, 73–79.

Kalberer, S. R, Leyva-Estrada, N., Krebs, S. L., and Arora, R. (2007b). Frost dehardening and rehardening of floral buds of deciduous azaleas depend on genotypic biogeography. *Environ. Exp. Bot.* 59, 264–275. doi: 10.1016/j.envexpbot.2006.02.001

Kalberer, S. R., Wisniewski, M, and Arora, R. (2006). Deacclimation and reacclimation of cold-hardy plants: current understanding and emerging concepts. *Plant Sci.* 171, 3–16. doi: 10.1016/j.plantsci.2006.02.013

Körner, C., and Basler, D. (2010). Phenology under global warming. *Science* 327, 1461–462. doi: 10.1126/science.1186473

Lang, G. A., Early, J. D., Martin, G. C., and Darnell, R. L. (1987). Endo-, para-, and ecodormancy: physiological terminology and classification for dormancy research. *HortScience* 22, 371–377.

Laube, J., Sparks, T. H., Estrella, N., Höfler, J. F., Ankerst, D. P., and menzel, A. (2014). Chilling outweigs photoperiod in preventing precocious spring development. *Glob. Change Biol.* 20, 170–182. doi: 10.1111/gcb.12360

Leinonen, I., Repo, T., and Hanninen, H. (1997). Changing environmental effects on frost hardiness of scots pine during dehardening. *Ann. Bot.* 79, 133–138. doi: 10.1006/anbo.1996.0321

Levitt, J. (1980). *Responses of Plants to Environmental Stresses, 2nd Edn,* Vol. 1, New York, NY: Academic Press.

Lim, C.-C., Krebs, S. L., and Arora, R. (2014). Cold hardiness increases with age in juvenile Rhododendron populations. *Front. Plant Sci.* 5:542. doi: 10.3389/fpls.2014.00542

Litzow, M., and Pellett, H. (1980). Relationship of rest to dehardening in red-osier dogwood. *HortScience* 15, 92–93.

Mahfoozi, S., Limin, A. E., and Fowler, D. B. (2001). Developmental regulation of low-temperature tolerance in winter wheat. *Ann. Bot.* 87, 751–757. doi: 10.1006/anbo.2001.1403

McEwan, R. W., Brecha, R. J., Geiger, D. R., and John, G. P. (2011). Flowering phenology change and climate warming in southwestern Ohio. *Plant Ecol.* 212, 55–61. doi: 10.1007/s11258-010-9801-2

Menzel, A., Estrella, N., and Fabian, P. (2001). Spatial and temporal variability of the phenological seasons in Germany from 1951 to 1996. *Glob. Change Biol.* 7, 657–666. doi: 10.1046/j.1365-2486.2001.00430.x

Menzel, A., Sparks, T. H., Estrella, N., Koch, E., Aasa, A., Ahas, R., et al. (2006). European phenological response to climate change matches the warming pattern. *Glob. Change Biol.* 12, 1969–1976. doi: 10.1111/j.1365-2486.2006.01193.x

Ögren, E. (2001). Effects of climatic warming on cold hardiness of some northern woody plants assessed from simulation experiments. *Physiol. Plantarum.* 112, 71–77. doi: 10.1034/j.1399-3054.2001.1120110.x

Pagter, M., and Arora, R. (2013). Winter survival and deacclimation of perennials under warming climate: physiological perspectives. *Physiol. Plant.* 147, 75–87. doi: 10.1111/j.1399-3054.2012.01650.x

Pagter, M., Lefèvre, I., Arora, R., and Hausman, J.-F. (2011). Quantitative and qualitative changes in carbohydrates associated with spring deacclimation in contrasting *Hydrangea* species. *Environ. Exp. Bot.* 72, 358–367. doi: 10.1016/j.envexpbot.2011.02.019

Paul, L. K., Rinne, P. L., and van der Schoot, C. (2014). Shoot meristems of deciduous woody perennials: self organization and morphogenetic transituions. *Curr. Opin. Plant Biol.* 17, 86–95. doi: 10.1016/j.pbi.2013.11.009

Peñuelas, J., and Filella, I. (2001). Responses to a warming world. *Science* 294, 793–795. doi: 10.1126/science.1066860

Polgar, C. A., and Primack, R. B. (2011). Leaf-out phenology of temperate woody plants: from trees to ecosystems. *New Phytol.* 191, 926–941. doi: 10.1111/j.1469-8137.2011.03803.x

Rapacz, M. (2002a). Cold-deacclimation of oilseed rape (*Brassica napus* var. *oleifera*) in response to fluctuating temperatures and photoperiod. *Ann. Bot.* 89, 543–549. doi: 10.1093/aob/mcf090

Rapacz, M. (2002b). Regulation of frost resistance during cold de-acclimation and re-acclimation in oilseed rape. A possible role of PSII redox state. *Physiol. Plant.* 115, 236–243. doi: 10.1034/j.1399-3054.2002.1150209.x

Rinne, P. L. H., Welling, A., Vahala, J., Ripel, L., Ruonala, R., Kangasjarvi, J, et al. (2011). Chilling of dormant bud hyperinduces FLOWERING LOCUS T and recruits GA-inducible 1,3 beta glucanases to reopen signal conduits and release dormancy in *Populus*. *Plant Cell* 23, 130–146. doi: 10.1105/tpc.110.081307

Rowland, L. J., Ogden, E. L., Ehlenfeldt, M. K., and Arora, R. (2008). Cold tolerance of blueberry genotypes throughout the dormant period from acclimation to deacclimation. *HortScience* 43, 1970–1974.

Skre, O., Taulavuori, K., Taulavuori, E., Nilsen, J., Igeland, B., and Laine, K. (2008). The importance of hardening and winter temperature for growth in mountain birch populations. *Environ. Exp. Bot.* 62, 254–266. doi: 10.1016/j.envexpbot.2007.09.005

Smit-Spinks, B., Swanson, B. T, and Markhart, A. H. III (1985). The effect of photoperiod and thermoperiod on cold acclimation and growth of *Pinus sylvestris*. *Can. J. For. Res.* 15, 453–460. doi: 10.1139/x85-072

Tanino, K. (2004). "The role of hormones in endodormancy induction," in *Adaptations and Responses of Woody Plants to Environmental Stresses,* ed R. Arora (New York, NY: Haworth Press Inc.), 157–199.

Taulavuori, K. (2013). "Vegetation at high latitudes under global warming," in *Causes, Impacts and Solutions to Global Warming*, eds I. Ibrahim, C. O. Dincer, Colpan, and F. Kadioglu (New York, NY: Springer), 3–16.

Taulavuori, K., Laine, K., and Taulavuori, E. (2013). A review: experimental studies on *Vaccinium* species in relation to air pollution and global change. *Environ. Exp. Bot.* 87, 191–196. doi: 10.1016/j.envexpbot.2012.10.002

Taulavuori, K., Laine, K., Taulavuori, E., Pakonen, T., and Saari, E. (1997). Accelerated dehardening in the bilberry (*Vaccinium myrtillus* L.) induced by a small elevation in air temperature. *Environ. Pollut.* 98, 91–95. doi: 10.1016/S0269-7491(97)00115-2

Taulavuori, K., Taulavuori, E., and Laine, K. (2002). Artificial deacclimation response *of Vaccinium myrtillu*s (L.) in mid-winter. *Ann. Bot. Fenn*. 39, 143–147.

Taulavuori, K., Taulavuori, E., Sarjala, T., Savonen, E.-M., Pietiläinen, P., Lähdesmäki, P., et al. (2000). *In vivo* chlorophyll fluorescence is not always a good indicator of cold hardiness. *J. Plant Physiol.* 157, 227–229. doi: 10.1016/S0176-1617(00)80195-9

Taulavuori, K., Taulavuori, E., Skre, O., Nilsen, J., Igeland, B., and Laine, K. (2004). Dehardening of mountain birch (*Betula pubescens* ssp. *czerepanovii*) ecotypes at elevated winter temperatures. *New Phytol.* 162, 427–436. doi: 10.1111/j.1469-8137.2004.01042.x

Tranquillini, W., and Plank, A. (1989). Ökophysiologische untersuchungen an rotbuchen (*Fagus sylvatica* L.) in verschiedenen Höhenlagen Nord- und Südtirols. *Cent. Gesamte Forstwes.* 3, 225–246.

Vitasse, Y. (2013). Ontogenetic changes rather than difference in temperature cause understory trees to leaf out earlier. *New Phytol.* 198, 149–155. doi: 10.1111/nph.12130

Vitasse, Y., and Basler, D. (2013). What role for photoperiod in the bud burstphenology of European beech. *J. For. Res.* 132, 1–8. doi: 10.1007/s10342-012-0661-2

Vitasse, Y., Lenz, A., and Körner, C. (2014). The interaction between freezing tolerance and phenology in temperate deciduous trees. *Front. Plant Sci.* 5:541. doi: 10.3389/fpls.2014.00541

Wisniewski, M., Norelli, J., and Artlip, T. (2015). Overexpression of a peach CBF gene in apple: a model for understanding the integration of growth, dormancy, and cold hardiness in woody plants. *Front. Plant Sci.* 6:85. doi: 10.3389/fpls.2015.00085

Wolf, T. K., and Cook, M. K. (1992). Seasonal deacclimation patterns of three grape cultivars at constant, warm temperature. *Am. J. Enol. Viticult.* 43, 171–179.

Wolkovich, E. M., Cook, B. I., Allen, J. M., Crimmins, T. M., Betancourt, J. L., Travers, S. E., et al. (2012). Warming experiments underpredict plant phenological responses to climate change. *Nature* 485, 494–497. doi: 10.1038/nature 11014

Yooyongwech, S., Horigane, A. K., Yoshida, M., Yamaguchi, M., Sekozawa, Y., Sugaya, S., et al. (2008). Changes in aquaporin gene expression and magnetic resonance imaging of water status in peach tree flower buds during dormancy. *Physiol. Plant.* 134, 522–533. doi: 10.1111/j.1399-3054.2008.01143.x

Conflict of Interest Statement: The authors declare that the research was conducted in the absence of any commercial or financial relationships that could be construed as a potential conflict of interest.

frontiers in Environmental Science

ORIGINAL RESEARCH
published: 07 October 2016
doi: 10.3389/fenvs.2016.00063

Cytokinins Induce Transcriptional Reprograming and Improve *Arabidopsis* Plant Performance under Drought and Salt Stress Conditions

Yelena Golan[1†], Natali Shirron[1†], Avishi Avni[1], Michael Shmoish[2] and Shimon Gepstein[1]*

[1] Faculty of Biology, Technion – Israel Institute of Technology, Haifa, Israel, [2] Bioinformatics Knowledge Unit, The Lorry I. Lokey Interdisciplinary Center for Life Sciences and Engineering, Technion – Israel Institute of Technology, Haifa, Israel

In nature, annual plants respond to abiotic stresses by activating a specific genetic program leading to early flowering and accelerated senescence. Although, in nature, this phenomenon supports survival under unfavorable environmental conditions, it may have negative agro-economic impacts on crop productivity. Overcoming this genetic programing by cytokinins (CK) has recently been shown in transgenic plants that overproduce CK. These transgenic plants displayed a significant increase in plant productivity under drought stress conditions. We investigated the role of CK in reverting the transcriptional program that is activated under abiotic stress conditions and allowing sustainable plant growth. We employed 2 complementary approaches: Ectopic overexpression of CK, and applying exogenous CK to detached *Arabidopsis* leaves. Transgenic *Arabidopsis* plants transformed with the isopentyltransferase (*IPT*) gene under the regulation of the senescence associated receptor kinase (SARK) promoter displayed a significant drought resistance. A transcriptomic analysis using RNA sequencing was performed to explore the response mechanisms under elevated CK levels during salinity stress. This analysis showed that under such stress, CK triggered transcriptional reprograming that resulted in attenuated stress-dependent inhibition of vegetative growth and delayed premature plant senescence. Our data suggest that elevated CK levels led to stress tolerance by retaining the expression of genes associated with plant growth and metabolism whose expression typically decreases under stress conditions. In conclusion, we hypothesize that CK allows sustainable plant growth under unfavorable environmental conditions by activating gene expression related to growth processes and by preventing the expression of genes related to the activation of premature senescence.

Keywords: abiotic stress, cytokinins, RNA-sequencing, stress tolerance, transgenic plants

OPEN ACCESS

Edited by:
Urs Feller,
University of Bern, Switzerland

Reviewed by:
Autar Krishen Mattoo,
United States Department of Agriculture, USA
Jose M. Garcia-Mina,
University of Navarra, Spain

****Correspondence:***
Shimon Gepstein
gepstein@tx.technion.ac.il

[†] These authors have contributed equally to this work.

Specialty section:
This article was submitted to Agroecology and Land Use Systems, a section of the journal Frontiers in Environmental Science

Received: *06 June 2016*
Accepted: *21 September 2016*
Published: *07 October 2016*

Citation:
Golan Y, Shirron N, Avni A, Shmoish M and Gepstein S (2016) Cytokinins Induce Transcriptional Reprograming and Improve Arabidopsis Plant Performance under Drought and Salt Stress Conditions. Front. Environ. Sci. 4:63. doi: 10.3389/fenvs.2016.00063

INTRODUCTION

In nature, annual plants frequently encounter abiotic stresses that adversely affect growth, development, or productivity. Such stresses trigger a wide range of plant responses including a specific genetic program leading to growth retardation, early flowering, and accelerated senescence. Although, such responses may support survival in nature under severe stresses, they have negative agro-economic impact on crop productivity. Cytokinins (CKs; a class of phytohormones) have

a role in maintaining plant health and their biosynthesis is decreased under water deficit stress (Chernyad'ev, 2005). Low CK levels are associated with inhibition of growth, and acceleration of senescence onset (Roitsch and Ehneß, 2000; Gepstein and Glick, 2013), whereas applying exogenous CK delays leaf senescence (Chernyad'ev, 2005). Also, in transgenic plants that overproduce CK, the aforementioned stress-induced responses are attenuated (Rivero et al., 2007).

The first committed and rate-limiting step in the biosynthesis of CK is catalyzed by the enzyme isopentenyltransferase (IPT). In transgenic tobacco where IPT was expressed under the regulation of promoter of the senescence gene *SARK* from *Phaseolus vulgaris* (Hajouj et al., 2000), CK was maintained at high levels under water deficit stress, leading to improved drought tolerance (Rivero et al., 2007). These studies were later extended to other crops such as rice (Peleg et al., 2011). Notably, not only did these transgenic plants survive, they also displayed a significantly increased plant productivity under drought stress conditions (Rivero et al., 2007).

The genetic reprograming of plants under abiotic stresses involves reducing water demand by stomatal closure, decreased photosynthesis, reduced leaf evaporative area, as well as by premature termination of vegetative growth followed by a reproductive phase and plant senescence (Roitsch and Ehneß, 2000; Gepstein and Glick, 2013). However, not reducing transpiration and maintaining photosynthetic capacity is advantageous under moderate stress conditions, since it allows sustainable vegetative growth.

Drought resistance involves multiple responses and the interactions thereof. Reprograming of genomic expression leads to developmental and morphological changes, osmotic adjustment, and biochemical responses, ultimately resulting in a new homoeostatic state. Signaling pathways activated in response to abiotic stress include components related to phosphorylation/dephosphrylation activities such as protein kinases, protein phosphatases, activation of reactive oxygen species (ROS), and signaling of various transcriptional regulators (Arnholdt-Schmitt, 2004). Phytohormones are also key factors in the regulation of adaptive responses to drought and other stresses.

Among the major hormones produced by plants, Abscisic acid (ABA) is known to playing a key role in mediating abiotic stresses. Typically, environmental conditions such as drought and salinity are known to trigger increase in ABA levels. Increased ABA levels lead to stomatal closure which, in turn, minimizes water loss by reducing transpiration, but also reduces photosynthetic activity and accelerates premature senescence (Verma et al., 2016). ABA elevation during abiotic stresses, such as drought, has been proven beneficial for plant survival (Fujita et al., 2011). Many genes associated with ABA synthesis and genes encoding receptors and downstream signaling components through ABA response elements (ABRE) and dehydration-response element-binding proteins (DRE) motifs, have been identified (Mishra et al., 2014). Gene regulatory networks derived from genomic studies revealed that ABA is a universal hormone involved in massive transcriptional reprograming events leading to stress adaptation responses (Sreenivasulu et al., 2012).

Until a decade ago, CKs were not considered important stress-response hormones. CKs and ABA have antagonistic effects on stomatal opening, transpiration, and photosynthesis. Most of the studies support the notion that during stress response, CK levels decrease and that stress response is controlled by ABA and ethylene (Wang et al., 2011). However, recent studies using genetic manipulation of CK demonstrate a more complicated picture. We previously reported on the development of transgenic plants carrying the autoregulatory system of IPT activation and showed that CK plays a role in delaying tobacco plant senescence (Hajouj et al., 2000). We later found that these transgenic plants also displayed a significant drought tolerance (Rivero et al., 2007). Not only did these plants survive longer under water deficit, they also grew throughout the growth period on just 30% of the optimal watering regimes with almost no loss of plant yield (Rivero et al., 2007). Thus, we hypothesized that induction of CK biosynthesis during stress could enhance stress tolerance. Indeed, studies using the aforementioned transgenic tobacco plants showed that during water deficit stress, the protection of biochemical processes associated with photosynthesis increased alongside the induction of photorespiration (Rivero et al., 2007). The transcriptome of these plants during water deficit revealed that the expression of genes encoding components of the carotenoid pathway leading to ABA biosynthesis was enhanced in wild-type (w.t.) plants and repressed in the transgenic plants, suggesting that the photosynthetic apparatus was degraded in w.t. plants and unaffected in the transgenic plants (Rivero et al., 2010). This specific CK induction approach was successfully demonstrated in dicots and monocots (Rivero et al., 2007; Peleg et al., 2011), and could potentially serve as a generic system. However, several studies pointed at a negative effect of CKs on the stress tolerance. Constitutive expression of CK dehydrogenase (CKX, which degrades CK in plants) or multiple mutation of IPT 1, 3, 5, and 7 in tobacco showed significant resistance to drought, which was attributed to changes in membrane durability and integrity as manifested by a decrease in electrolyte leakage. These CK deficient mutants displayed ABA hypersensitivity which suggests that decreased CK content increased ABA sensitivity and ABA response in the context of improved stress tolerance (Nishiyama et al., 2011). The effect of silencing CK receptors AHK3 and AHK2 on stress resistance in plants indicated an improved resistance to drought and salt stress (Tran et al., 2007). Many stress- and ABA-controlled genes were upregulated at the mutant plants. Furthermore, some ABA-controlled genes were upregulated even under non-stress conditions, suggesting that AHK3- and AHK2 negatively regulate plant response to osmotic stress (Tran et al., 2007). Combined, these studies demonstrate that during stress, high CK levels affect plant metabolism at different levels, depending on the stress severity.

CKs are involved in plant development and metabolism; yet, very little is known about the molecular nature of CK signaling that mediates abiotic stress tolerance. Identifying genes that are regulated by CK during stress is key for enhancing our molecular understanding the role of CK in stress response and drought tolerance. Analyses of drought-induced genes have demonstrated the existence of ABA-independent signal transduction cascades

between the initial signal of water deficit and the expression of specific genes (Shinozaki and Yamaguchi-Shinozaki, 2000).

The goal of the current study was to investigate CK signaling under drought and salinity stress, to understand the overall effect of CK under such conditions, and to identify key genes involved in these processes.

MATERIALS AND METHODS

Plant Material and Growing Conditions

Arabidopsis thaliana plants (Columbia ecotype) were grown on soaked peat pellets (Jiffy 7, Kappa Forenade Well) in temperature-controlled growth room at 23°C (±25°C) under fluorescent lamps (75 $\mu E \times m^{-2} \times s^{-1}$) at long-day conditions (18 h light, 8 h dark).

Plasmid Construction and Plant Transformation

The pSARK:IPT vector contains the SARK:IPT:NOS cassette which carries the *IPT* gene under the regulation of the SARK promoter and the nopaline synthase (NOS) terminator as previously described (Rivero et al., 2007). The *Arabidopsis* transgenic lines were produced by infiltrating Col-0 using floral-dip method (Clough and Bent, 1998). Transgenic lines were screened and confirmed by PCR analysis.

Salinity and Drought Stress Experiments

Arabidopsis plants were grown for 40 days and irrigated with tap water. Then, plants were subjected to salinity stress by watering with 300 mM NaCl solution for 3 weeks. For the drought experiments, *Arabidopsis* plants were watered daily to keep the soil near 100% field capacity until 40 days after germination. Then, plants were divided into two groups: a control with daily irrigation and the stress group where water was withheld for 5 days. Applying exogenous CK under salinity stress was performed by excising fully expanded *Arabidopsis* leaves (non-yellowing) from the plant and incubating them in water for 1 h. After that, the leaves were divided into 4 treatments: Control (water), salinity (100–150 mM NaCl), synthetic CK (6-benzylaminopurine [BAP]; 10 μm), and salinity plus BAP. The exogenous application of CK's may suffer possible limitations such as penetration problems and using non-physiological concentration. However, this approach complements and supports the alternative approach of activation on endogenous CK's.

RNA Extraction and Quantitative RT-PCR (qRT-PCR)

Total RNA was isolated from ∼150 mg plant material using SV Total RNA Isolation kit (Promega, Madison, WI), according to the manufacturer's instructions. Concentration, integrity, and extent of contamination by ribosomal RNA were monitored using the ND-1000 spectrophotometer (Thermo Fisher Scientific, Waltham, MA). cDNA was prepared from the total RNA with qScript cDNA Synthesis Kit (Quanta, Beverly, MA) as described by the manufacturer. qRT-PCR was performed using teal-time SYBR Green FastMix ROX (Quanta, Beverly, MA). Primers used are listed in Supplementary Table 1. In each case, three biological samples were analyzed in triplicates. The expression of candidate genes was normalized to cyclophilin (At2g36130). Comparative C_t values were determined using Applied Biosystems, User Bulletin #2, (http://home.appliedbiosystems.com/). Results were statistically processed by the One Way Analysis of Variance (ANOVA) method using SPSS Statistics 19.0. $P \leq 0.05$ was considered significant. Error bars represent standard error (SE) of the mean of the 3 samples.

RNA Sequencing

Total RNA was extracted from 12 samples of rosette leaves of w.t plants, 3 samples for each of the 4 treatments: water, salt (NaCl 120 Mm), water plus BAP (10 μm), or salt (NaCl 120 Mm) plus BAP (10 μm). The 12 samples were treated with DNAse and sent to the Technion Genome Center (TGC) where cDNA libraries were constructed with TruSeq RNA Sample Prep Kit v2 (Illumina, San Diego, CA). High-throughput sequencing was performed using the Illumina HiSeq 2500 with 50 bp single-reads and barcoding. TGC personnel performed the initial analysis of results, and the quality of the reads was tested using the FastQC software with a phred score of +33. The short reads alignment/mapping was performed by the "TopHat2/Bowtie2" software (version 2.0.6) against the *A. thaliana* genome (version TAIR10) allowing 3 mismatches per read. Minimum and maximum intron sizes were set to 10 and 11,000, respectively, and the Bowtie2 mapping option –b2-sensitive was set. Furthermore, the aligned reads were processed by the Python package "HTSeq" version 0.5.3 p1 to get raw counts for each gene in TAIR10. The following *A. thaliana* reference genome was used: ftp://ftp.arabidopsis.org/home/tair/Genes/TAIR10_genome_release/TAIR10_chromosome_files/TAIR10_chr_all.fa. The annotation file ftp://ftp.arabidopsis.org/home/tair/Genes/TAIR10_genome_release/TAIR10_gff3/TAIR10_GFF3_genes.gff was modified to contain genes and not transcripts.

Differential Expression

The normalization of raw counts was performed using R-package DESeq2 with the default parameters and the Wald test (which serves in DESeq2 as a substitute for *t*-test and one-way ANOVA) was chosen for the detection of statistically significant differentially expressed genes. Results of DESeq2 were subject to advanced bioinformatics analysis by the Technion Bioinformatics Knowledge Unit.

Clustering Analysis and GO Functional Enrichment Analysis

The output of the initial analysis performed at the TGC was further analyzed with the EXPANDER 6.4 (EXpression Analyzer and DisplayER) suite of tools for bioinformatics analysis of microarray and RNA-seq data.

The SOM clustering algorithm was applied to produce a partition of the gene profiles into several clusters and to visualize the mean pattern of the cluster (clusters were then refined by manual inspection and re-clustering); the TANGO tool was used

for GO (Group by pattern similarity) functional enrichment analysis that was employed to identify genes with coordinated behavior across experimental conditions. The latter analysis was also performed using the QuickGO tool at EBI (https://www.ebi.ac.uk/QuickGO).

RESULTS

Drought Tolerance of Transgenic Sark::IPT *Arabidopsis* Plants

We cloned the *IPT* gene under senescence-induced promoter to produce SARK::IPT transgenic *Arabidopsis* plants. The presence of the *IPT* transgene in each of the lines was confirmed by PCR. After 5 days of water withholding, the w.t. plants showed symptoms of withering and senescence, whereas, the transgenic plants seemed to overcome the severe drought treatment as reflected by leaf turgidity and the greener color (**Figure 1**). Even after re-watering for a week, w.t. plants displayed senescence symptoms (yellowing and wilting), whereas, the transgenic plants seemed to overcome the severe drought treatment.

We then assessed, under normal and drought conditions (after 7 days of water withholding), the expression of candidate genes in w.t. vs. transgenic plants. First, we assessed 2 antioxidant genes: *cat1* (catalase 1) and *apx1* (ascorbate peroxidase 1; **Figure 2**). As expected, the expression of both genes increased under drought stress in the w.t. plants. In the transgenic plants, expression of these genes was lower relative to the w.t. plants under normal as well as drought conditions. To test whether the observed drought resistance is associated with known drought cell signals, we tested the expression of the early responsive dehydration (*ERD1*) gene, which is a known drought marker gene encoding a protein with homology to the ATP binding subunit of the Clp ATP-dependent protease of *E. coli* (Simpson et al., 2003), and is a known component of the ABA-independent pathway of drought response. Expression of the *erd1* gene was upregulated under drought stress in w.t. plants suggesting a classical induction of the stress response associated with the ABA independent pathway (**Figure 2**). In contrast, the transgenic plants displayed reduced *ERD1* expression compared to w.t. plants, with no upregulation under drought conditions.

Influence of Exogenous Application of CK on Expression of Candidate Genes in Response to Salinity Stress

Next, we tested expression of candidate genes (*APX1*, *CAT1*, *ERD1*) after adding exogenous CK to excised leaves of plants with and without salinity stress (100–150 nM NaCl). In leaves

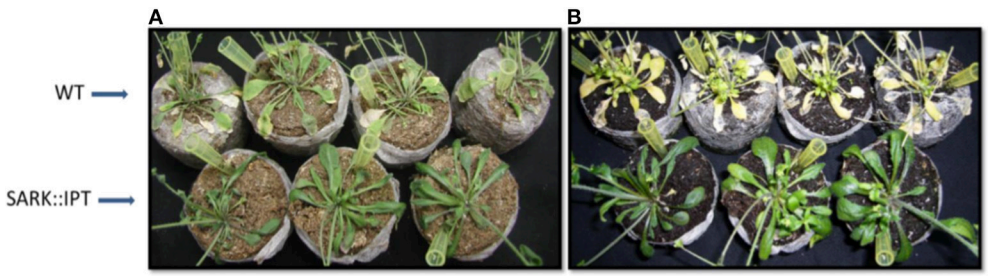

FIGURE 1 | Responses of SARK::IPT transgenic *Arabidopsis* plants to drought conditions followed by re-watering. *Arabidopsis* plants were grown for 40 days under long day regimes (16 h light, 8 h darkness) and were then subjected to drought stress by withholding water for 5 days. **(A)** w.t. and transgenic plants SARK::IPT after 5 days of drought. **(B)** w.t. and transgenic plants SARK::IPT after 7 days of re-watering.

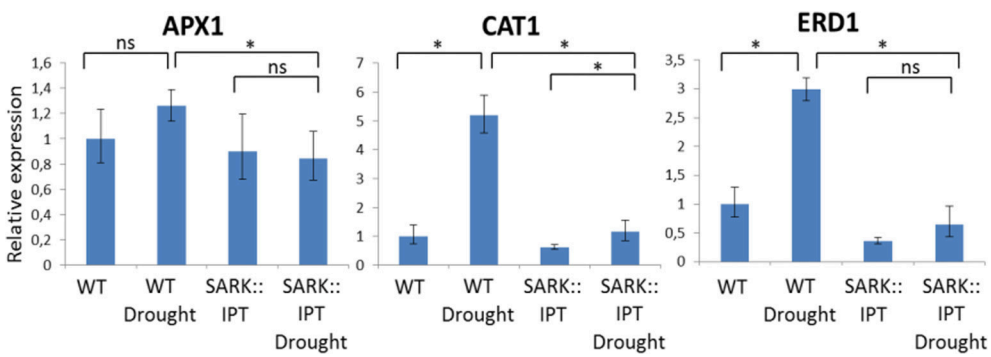

FIGURE 2 | Relative expression of *APX1*, *CAT1,* and *ERD1* genes in w.t. and transgenic SARK::IPT plants during drought stress. *Arabidopsis* plants were grown for 40 days in optimal conditions and were then transferred to drought stress for 7 days. Controls were well-watered plants (w.t. and transgenic). The qPCR assay reflects relative expression levels for each gene and was performed in triplicate for each of the three independent biological samples. Expression of each of the tested genes in the control treatment of w.t. plants was used as the basis for comparison (relative expression = 1). Horizontal brackets denote significance of $P < 0.05$ (*, statistical significance; ns, no significance).

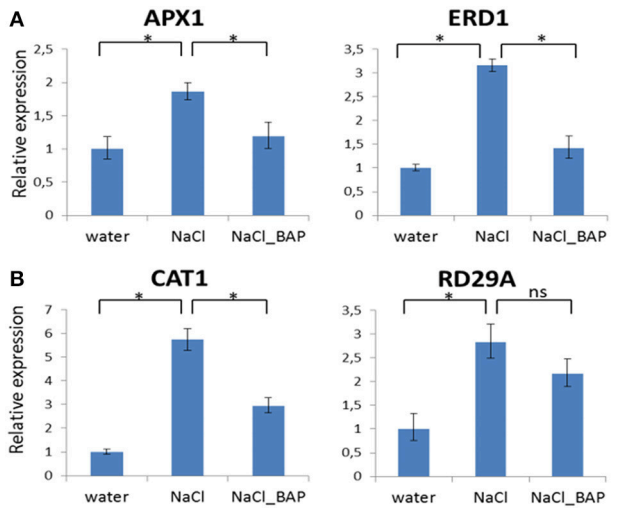

FIGURE 3 | Effect of CK on relative expression of the *APX1, ERD1* (A), *and CAT1, RD29A* (B) genes in *Arabidopsis* plants under salinity stress. *Arabidopsis* w.t. plants were grown for 30 days in optimal conditions and then leaves were detached and exposed to salinity stress of 100 mM NaCl or salinity plus 10 μm CK (BAP) for 24 h. Controls were detached leaves in water treatment. Samples (3 for each treatment) were collected from control and stressed leaves. Relative expression was measured by qRT- PCR. Expression of each gene in w.t. control plants was used for comparison (relative expression = 1). Horizontal brackets denote significance of $P < 0.05$ (*, statistical significance; ns, no significance).

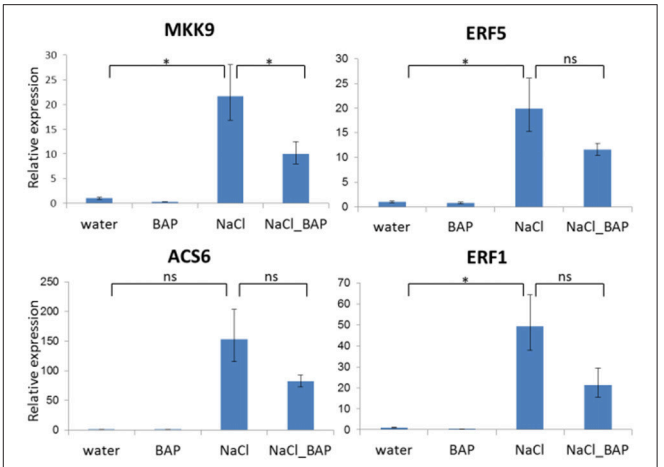

FIGURE 4 | Influence of exogenous CK on expression of genes related to ethylene biosynthesis and signaling during salt stress. *Arabidopsis* w.t. plants were grown for 30 days in optimal conditions and then leaves were detached and exposed to salinity stress of 120 mM NaCl in the presence of CK (BAP) for 24 h. Controls were detached leaves in water or BAP treatments. Relative expression of *MKK9*, *ACS6*, *ERF1*, and *ERF5* genes was assessed. Samples (3 for each treatment) were collected from controls and stressed leaves. Relative expression was measured by qRT-PCR. Expression of each gene in w.t. control plants was used for comparison (relative expression = 1). Horizontal brackets denote with significance of $P < 0.05$ (*, statistical significance; ns, no significance).

under salinity stress and without CK, increased expression of the 3 tested genes was observed (**Figure 3**). Adding CK (BAP) resulted in a significantly lower gene expression relative to the salinity treatment (**Figure 3**). We also tested the expression of the *rd29A* gene (which, like the *cat1* gene is controlled by ABA; Yamaguchi-Shinozaki and Shinozaki, 1994; Xing et al., 2008). The expression pattern for *rd29A* was similar to that of *APX1*, *CAT1*, and *ERD1* (**Figure 3**). These findings suggest that during stress, CK downregulated the expression of genes encoding components involved in the ABA dependent or independent plant stress responses.

We used the same experimental design to test the effect of exogenous CK on expression of components of the ethylene-signaling pathway (the MKK6-MKK9 kinase cascade) as ethylene also plays a role in plant stress response (Xu et al., 2008). Four genes were evaluated: mitogen kinase (*MKK9*), ACC synthase 6 (*ACS6*), and ethylene response factors (*ERF1* and *ERF5*). The expression of all 4 genes increased under salinity stress, but this increase was attenuated with exogenous CK (**Figure 4**), suggesting that CK reduced ethylene signal transduction during stress. These findings may explain the delay of premature senescence known to be regulated by ethylene and ABA.

Transcriptomic Analysis of *Arabidopsis* Leaves Treated with CK under Salinity Stress

We performed a transcriptomic analysis using next-generation sequencing in order to gain an overall understanding of CK-induced transcription reprograming in *Arabidopsis* leaves under salinity stress. The initial RNA sequencing analysis revealed, 28,775 genes which were then filtered using four criteria: At least 3 out of 12 samples showing minimum 20 results; expression that was significantly different between control and salt treatment ($P < 0.05$); expression that differed by ≥1.5-fold between control and salt treatment; a change (increase or decrease) in gene expression of ≥30% due to the addition BAP. A total of 5084 genes met the selection criteria. The EXPANDER 6.4 tool was used for the division of clusters according to the expression patterns in the 4 treatment groups using the SOM clustering algorithm (**Figure 5**). Two clusters (2 and 8) were removed from the analysis as they included only few genes and did not yield additional results. The remaining clusters were divided into 2 super groups based on similarity in expression patters: Super-group 1 (clusters 1, 3, and 4) and super-group 2 (clusters 5, 6, and 7). We analyzed the enrichment of differentially expressed genes in the different treatments to search for over-represented Gene Ontology functional terms using the TANGO tool of the Expander 6.4 (Supplementary Tables 2–8). Supplementary Table 2 describes the functional groups in the 2 super-groups each with a typical and distinctive expression pattern. The first super-group displayed an expression pattern that included upregulation of gene expression under salt treatment as well as partial downregulation due to the addition of exogenous CK. In the context of functional categories as defined in GO, 20 functional groups ($P < 0.05$) were determined. This super-group included genes involved in "defense response," "response to water stimulus," "cellular response to abscisic acid stimulus," and "cellular response to jasmonic acid stimulus" (**Figure 6**), (from the GO database or from published data; Supplementary

Table 2). Although this super-group is characterized by down-regulation due to addition of CK during salinity stress, these results are consistent with our previous findings showing that CK decreased the levels of stress-protective factors. In the second super-group, which was characterized by downregulation of genes under salinity stress and upregulation by adding CK under salinity stress, 81 functional groups were identified (Supplementary Table 2). Most of these were not directly related to stress response, but rather to CK-dependent growth processes under normal conditions (i.e., genes involved in normal homeostasis in the context of cell energy, metabolism, growth, and photosynthesis; **Figure 7A**). This group also included genes related to the perception and responses to light in the context of photomorphogenesis (i.e., phytochrome and blue-light pigments; **Figure 7B**) and components associated with general gene expression and translation (**Figure 7C**). These findings suggest a promotive effect of CK on cell normal functioning during stress that may allow normal growth even under stress conditions. Thus, the contribution of CK to stress resistance may be related to sustaining growth capacity and maintaining metabolic processes that are otherwise disabled under stress conditions.

The Expression Patterns of the DEAD-Box ATP-Dependent RNA Helicases

We used a bioinformatics scan (DESeq 2) to identify functional groups that could contribute to the observed CK-induced stress resistance. Expression of 7 DEAD-box ATP-dependent RNA helicase genes was found to be significantly changed under salinity stress and upon CK addition ($P < 0.05$; **Figure 8**). This group of RNA helicases was previously demonstrated to have a positive or negative effect on stress resistance (Luo et al., 2009; Tuteja et al., 2014). We found that 3 out of the 7 genes were upregulated under salinity stress. All 7 genes had increased expression in salt plus BAP conditions compared to treatment with water; however, six had increased expression in salt plus BAP relative to salt treatment alone, suggesting that for one gene (AT3G58570), salt-induced activation was attenuated by CK.

The Expression Patterns of Type A and B Response Regulators (ARR)

Signal transduction of CK includes a 2-component system (TCS), by which a histidine protein kinase is auto-phosphorylated and the phosphate is transferred to a response regulator protein

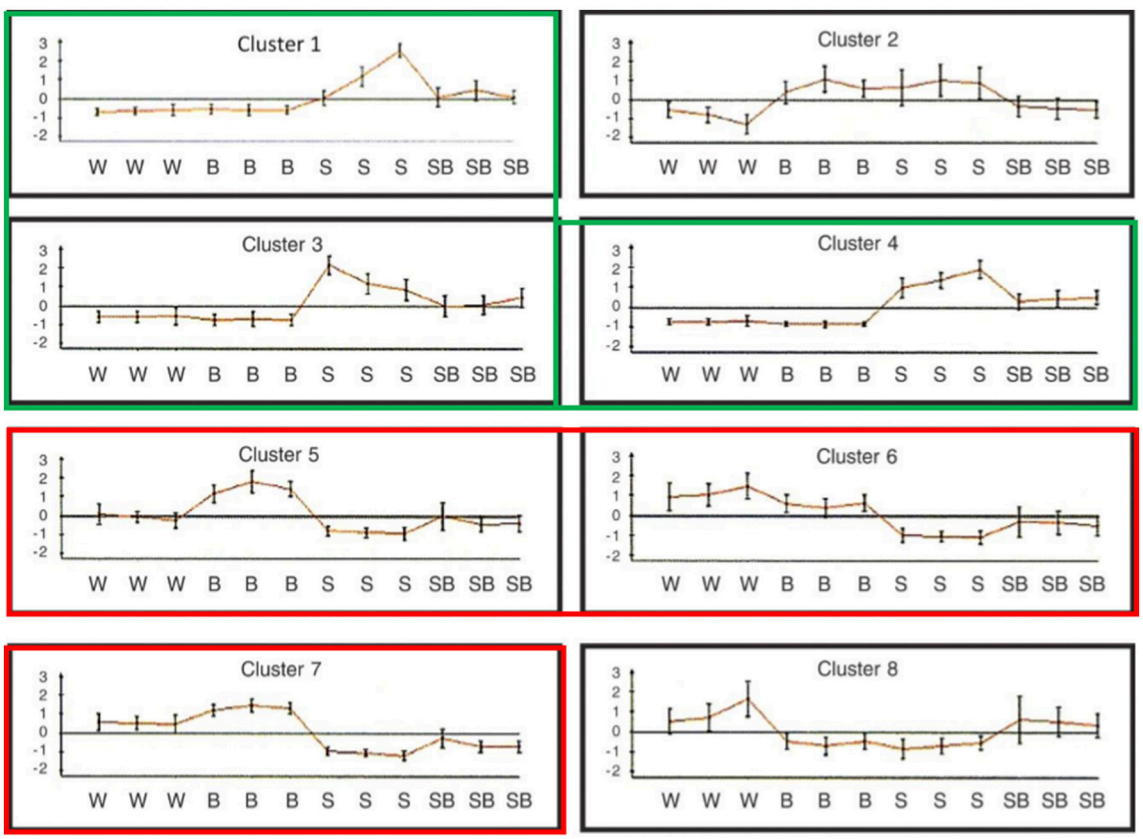

FIGURE 5 | Graphic representation of the expression patterns of gene clusters under salinity stress with and without adding CK. Genes were divided into 8 clusters according to the expression pattern. Each graph presents one cluster with 12 samples: 4 treatments (W, water; B, 10 μm BAP; S, 120 mM NaCl; SB, NaCl plus BAP) in three biological replicates for each treatment. Gene clusters: cluster 1 contained 710 probes; cluster 2, 32 probes; cluster 3, 487 probes; cluster 4, 1405 probes; cluster 5, 342 probes; cluster 6, 553 probes; cluster 7, 1517 probes; and cluster 8, 38 probes. The red (clusters 1,3,4) and green (clusters 5,6,7) colors represent gene clusters displaying similar expression.

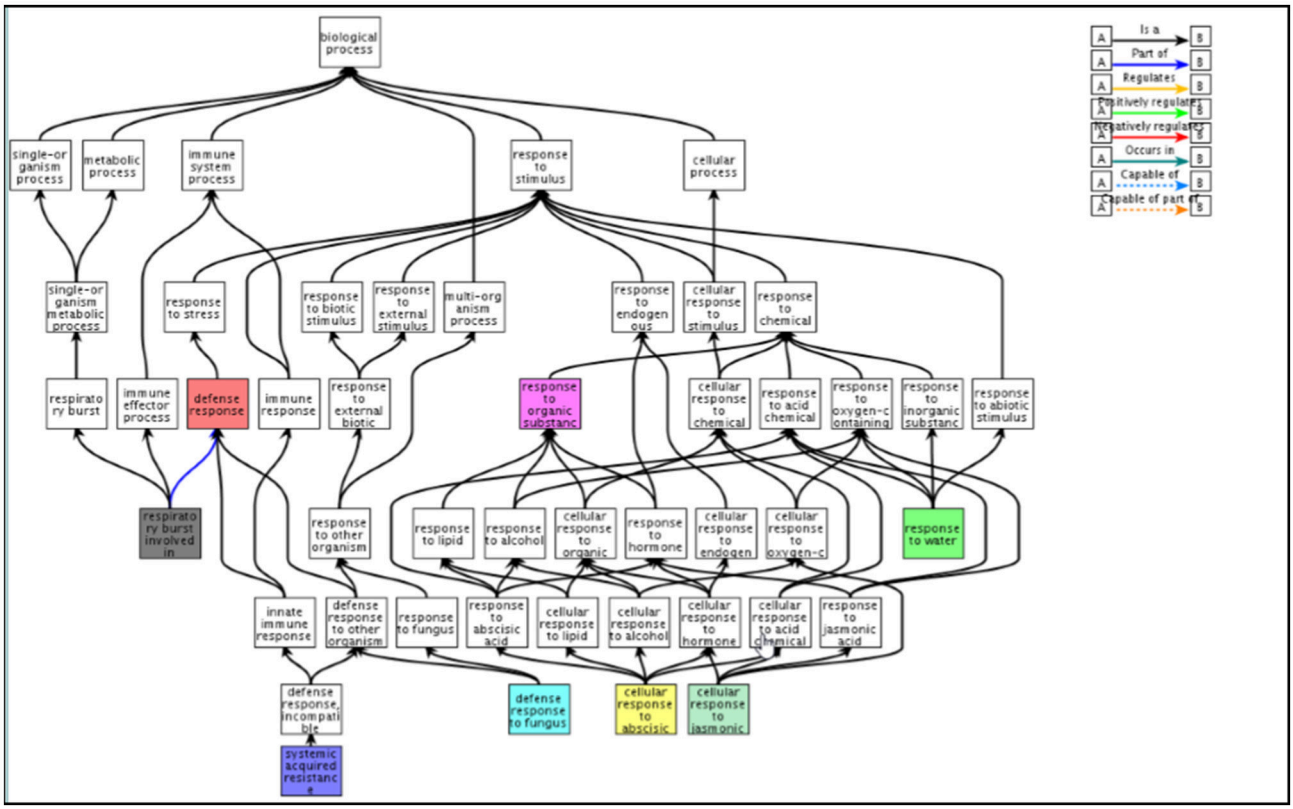

FIGURE 6 | Functional classification of gene clusters displaying reduced expression with CK treatment under salinity stress. QuickGo representation of down-regulated Gene Ontology groups identified by the enrichment analysis of the RNA sequencing data. Clusters were characterized by upregulation of gene expression under salinity which was attenuated with CK (clusters 1,3,4). The functional classification was performed with the QuickGo platform https://www.ebi.ac.uk/QuickGO/GMultiTerm#a=64%2400ft01ie02J702MR02Sn0CQG0.HOl0HRZ&tab=chart&c=.

(Ishida et al., 2008). Bioinformatics enrichment analysis of our RNA sequencing data showed 8 TCS genes (type A and type B response regulator proteins) whose expression was significantly changed ($P < 0.05$) with salt treatment with or without exogenous CK treatment. Type A genes were found to be upregulated with salt treatment and by CK addition (**Figure 9A**), whereas type B genes were downregulated by CK (as their expression with salt treatment plus CK was decreased compared to their expression with salt treatment alone; **Figure 9B**).

Expression of Cell Wall Modification Genes

We scanned the transcriptome for other genes whose expression pattern suggest regulation by CK, by looking for genes with an expression pattern similar to that of *ARR5*, a known important negative regulator of CK signal transduction (To et al., 2007). In CK addition experiments on detached leaves, *ARR5* was indeed shown to have increased levels under salt conditions and with CK (**Figure 10**). Overall, 1000 genes were selected based on similarity in expression to *ARR5* and its homologs. We then searched for functional groups (GO database) in these 1000 genes and identified 5 such groups ($P < 0.01$; Supplementary Table 3). One of these groups was the "cell wall organization or biogenesis" group (Supplementary Table 4), that can be divided into three families: plant invertase/pectin methylesterase inhibitor superfamily, expansins, and xyloglucan endotransglusylase/hydrolases (XTH). In *Arabidopsis,* there are 33 genes in the XTH group (Rose et al., 2002), which are involved in softening and increasing the flexibility of the cell wall. We identified 11 of these genes in our analysis and divided them into 3 subgroups based on their gene expression pattern: Genes that were induced more under salt conditions than by CK plus salt conditions (*XTH2, XTH11, XTH14, XTH24*, and *XTH26*, **Figure 11A**); genes that were induced more by CK in water than by salt alone or by CK plus salt conditions (*XTH8*, *XTH31*, and *XTH32*; **Figure 11B**); and genes that were induced more by CK plus salt conditions than by either CK or salt conditions alone (*XTH19*, *XTH29*, and *XTH33*; **Figure 11C**). Expansins also participate in softening the cell wall. There are 38 expansins in *Arabidopsis* (Li et al., 2012), of which 13 were identified in our analysis. These 13 genes were also divided into 3 subgroups based on their expression pattern: Genes that were induced in salt treatment and had a reduced induction in salt conditions plus CK (*EXPA2, EXPA20, EXPB1*; **Figure 12A**); genes that were strongly induced with CK and had a reduced induction in salt conditions plus CK (*EXPA1, EXPA3, EXPA4, EXPA11, EXPA15*;

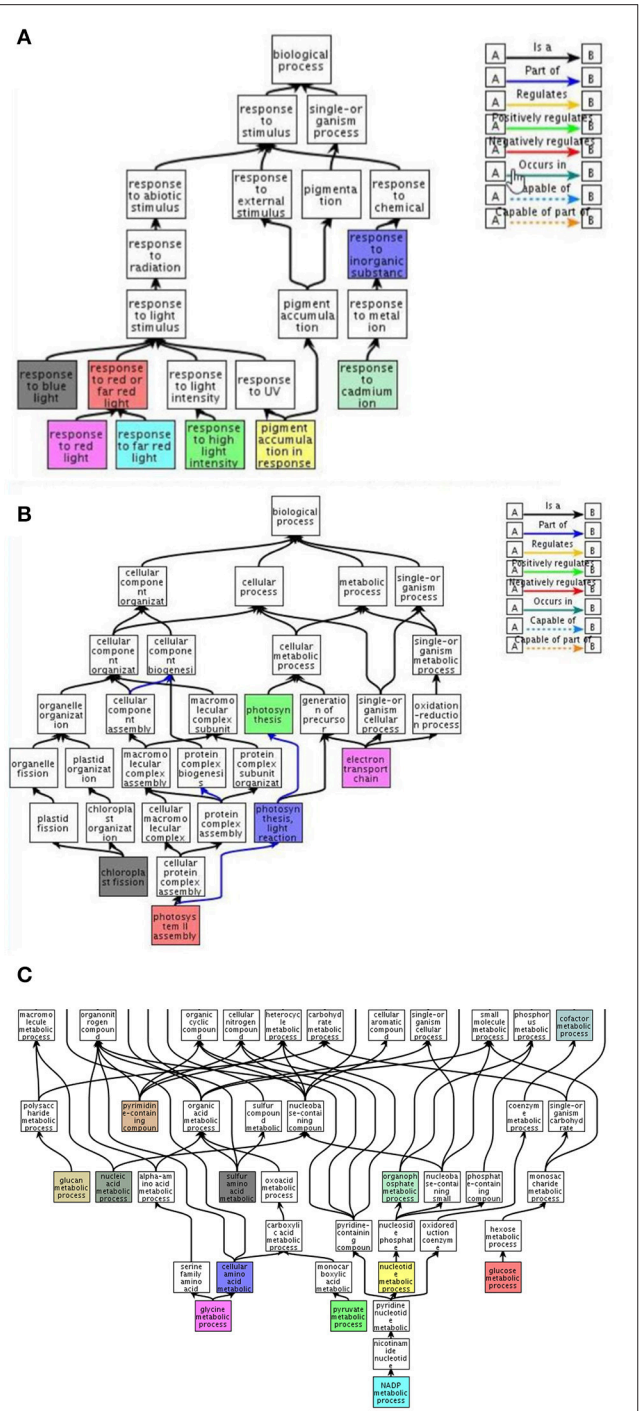

FIGURE 7 | Functional classification of gene clusters displaying CK-dependent increased expression under salinity stress. QuickGo representation of up-regulated Gene Ontology groups identified by the enrichment analysis of the RNA sequencing data. These gene clusters are characterized by transcriptional suppression under salinity stress and moderate suppression with CK (clusters 5, 6, and 7). Functional identification was performed with the QuickGO platform **(A)** https://www.ebi.ac.uk/QuickGO/GMultiTerm#a=64%2402Mb02Md02Mi02Sp02U202Vg0AdM0BPU&tab=chart&c=; **(B)** https://www.ebi.ac.uk/QuickGO/GMultiTerm#a=64%2402Sa02VV03vh04pa05 bq&tab=chart&c=; **(C)** https://www.ebi.ac.uk/QuickGO/GMultiTerm#a=64%24001W01Ts01VA01cG01fJ01g602ET04or0AmA0CVo0HjF0M30&tab=chart&c=.

(Continued)

Figure 12B); and genes that were induced in salt conditions and further induced by salt conditions plus CK (*EXPA5*, *EXPA10*, *EXPA12*, *EXPA14*, and *EXPA16*; **Figure 12C**). In *Arabidopsis,* there are >100 genes related to the plant invertase/pectin methylesterase inhibitor superfamily, although data on their function are lacking. We identified 7 genes from this family and divided them into 3 subgroups based on their expression pattern: Genes that were induced in salt conditions and had a reduced induction with salt conditions plus CK (AT3G05620, AT3G47380, and AT1G62760; **Figure 13A**); genes that were strongly induced in CK in water and were upregulated in salt conditions plus CK (AT3G10720 and AT5G20740; **Figure 13B**); and genes that were slightly upregulated in salt conditions and strongly induced upon adding CK (AT3G43270 and AT5G64640; **Figure 13C**).

qRT-PCR Validation of Differentially Expressed Transcripts from RNA Sequencing

We confirmed the RNA sequencing results by performing qRT-PCR on select genes. The relative gene expression of RT-PCR was calculated using the $2^{-\Delta\Delta Ct}$ method. The expression trends of these genes agreed with the RNA sequencing data (Supplementary Figure 1). A significant correlation of the gene fold change was observed between BAP treatment (Pearsol = 0.74; Supplementary Figure 1A), salinity treatment (Pearsol = 0.78, Supplementary Figure 1B) and salt plus BAP experiment (Pearsol = 0.83, Supplementary Figure 1C; all the results were calculated in comparison to water). Furthermore, in qRT-PCR analyses of 2 representative genes (*EXPA5* and *XTH19*) using the same experimental design as in the RNA sequencing experiments, we found expression patterns that were similar to those observed in the RNA sequencing analysis (**Figure 14**).

DISCUSSION

CKs, Homeostasis, and Drought Tolerance

Studies in recent years have shown that CKs regulate responses to environmental stresses. This regulation involves interaction and crosstalk with other phytohormones. CKs have both negative and positive influence on drought tolerance. CK levels may decrease or increase depending on stress severity and duration (Zwack and Rashotte, 2015). The positive effect of CKs on drought tolerance has been demonstrated by increasing endogenous CK levels in transgenic (SARK::IPT) tobacco plants and showing that it led to improved drought tolerance mainly through delaying plant senescence and enhancing photosynthesis activity (Rivero et al., 2007). The negative influence of CKs

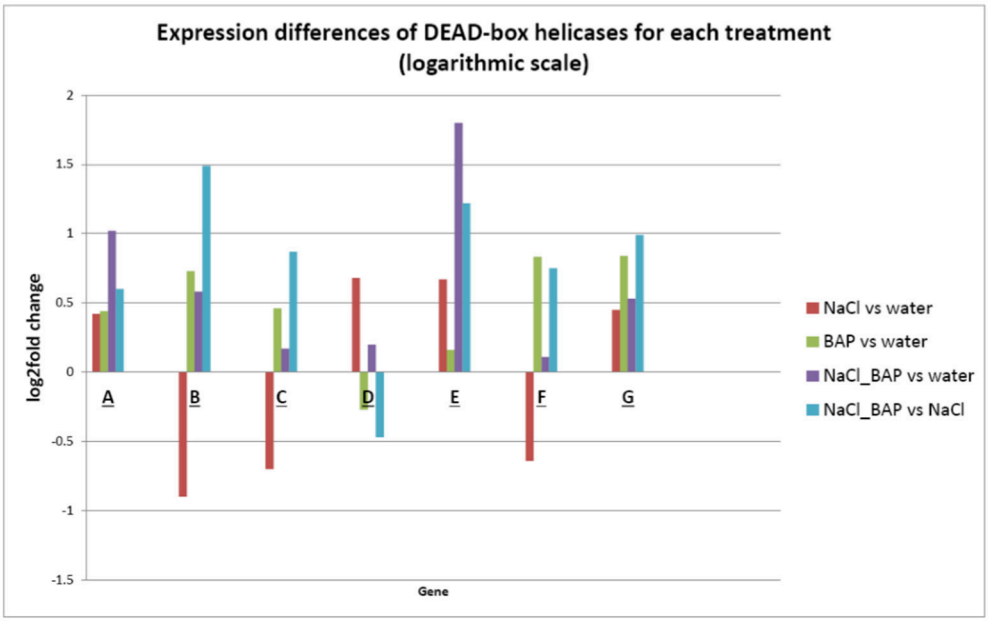

FIGURE 8 | Effect of CK on differential expression of DEAD-box helicases (logarithmic scale). A bioinformatics scan (DESeq 2 software) was employed to identify functional groups related to the CK-induced stress resistance mechanism. The expression of 7 DEAD-box ATP-dependent RNA helicases genes were significantly changed by CK under salt stress ($P < 0.05$). (A) DEAD-box RNA helicase family protein (AT4G16630); (B) DEAD-box RNA helicase family protein (AT3G18600); (C) STRS1 (AT1G31970); (D) DEAD-box RNA helicase family protein (AT3G58570); (E) AtRH9 (AT3G22310); (F) PRH75 (AT5G62190); and (G) AtRH2/STRS2 (AT5G08620).

is demonstrated by studies showing that reduced CK levels improve drought tolerance (Werner et al., 2010; Nishiyama et al., 2011, 2013). The contradicting evidence suggests that a complex CK-controlled network is involved in drought tolerance. The negative effect of CKs can derive from its effects on shoot and root growth. A decrease in the content of cytokinin, a hormone favoring shoot growth while inhibiting lateral root proliferation, can lead to increased water absorption in roots and decreased water loss under drought conditions (Ha et al., 2012).

This study focused on the molecular mechanisms underlying the positive influence of CKs on abiotic stress tolerance. We showed that CKs reverse the transcriptional programing that usually occurs in response to unfavorable abiotic stress conditions. We also showed that transgenic *Arabidopsis* with elevated CK levels display a significant drought resistance and maintain growth under unfavorable conditions without yield penalties. To understand how CKs influence yield under such conditions, we performed a transcriptomic analysis and showed that elevated CK levels led to stress tolerance by activating large set of genes that together maintain growth under unfavorable conditions while preventing premature senescence. All phytohormones are important for regulating every aspect of plant growth/development and in its adaptation to environmental stresses. However, phytohormones do not act in isolation and are interrelated by synergistic or antagonistic cross talk. Our data suggest the existence of cross talk between CKs and other phytohormones in the context of responses to abiotic stresses.

CK and ABA Cross-Talk

CK is antagonist of ABA: Exposing plants to water deficiency results in decreased CK levels. Exogenous ABA treatment leads to downregulation of the CK biosynthesis gene *IPT* (Wang et al., 2011). We demonstrated inhibition in the expression of the ABA responsive genes *CAT1* and *RD29A* in transgenic plants that are overproducing CK. This observation suggests that CK may have an inhibitory effect on ABA biosynthesis or ABA signaling. Our transcriptomic analysis also supports this notion, as expression of genes in the Gene Ontology group associated with "cellular response to abscisic acid stimulus," which is normally increased during stress, was inhibited by CK. Among the genes whose expression increased under salinity stress and was attenuated by CK we found the major regulatory ABA signaling component SnRK2.3 (Fujita et al., 2009) and ABF3 (Yoshida et al., 2010).

Prior studies also support the existence of cross-talk between CK and ABA signaling. For example, Rivero et al. demonstrated an increased expression of genes involved in ABA biosynthesis in w.t. plants under stress conditions but only moderate expression of the same genes in transgenic plants overproducing CK (Rivero et al., 2010). Another study reported that plants carrying 2 mutations in the CK signaling pathway (in ahk2 and ahk3) had increased expression of ABA-inducible genes (Tran et al., 2007), and a more recent study showed that CK-deficient *Arabidopsis* plants had increased sensitivity to exogenous ABA, causing

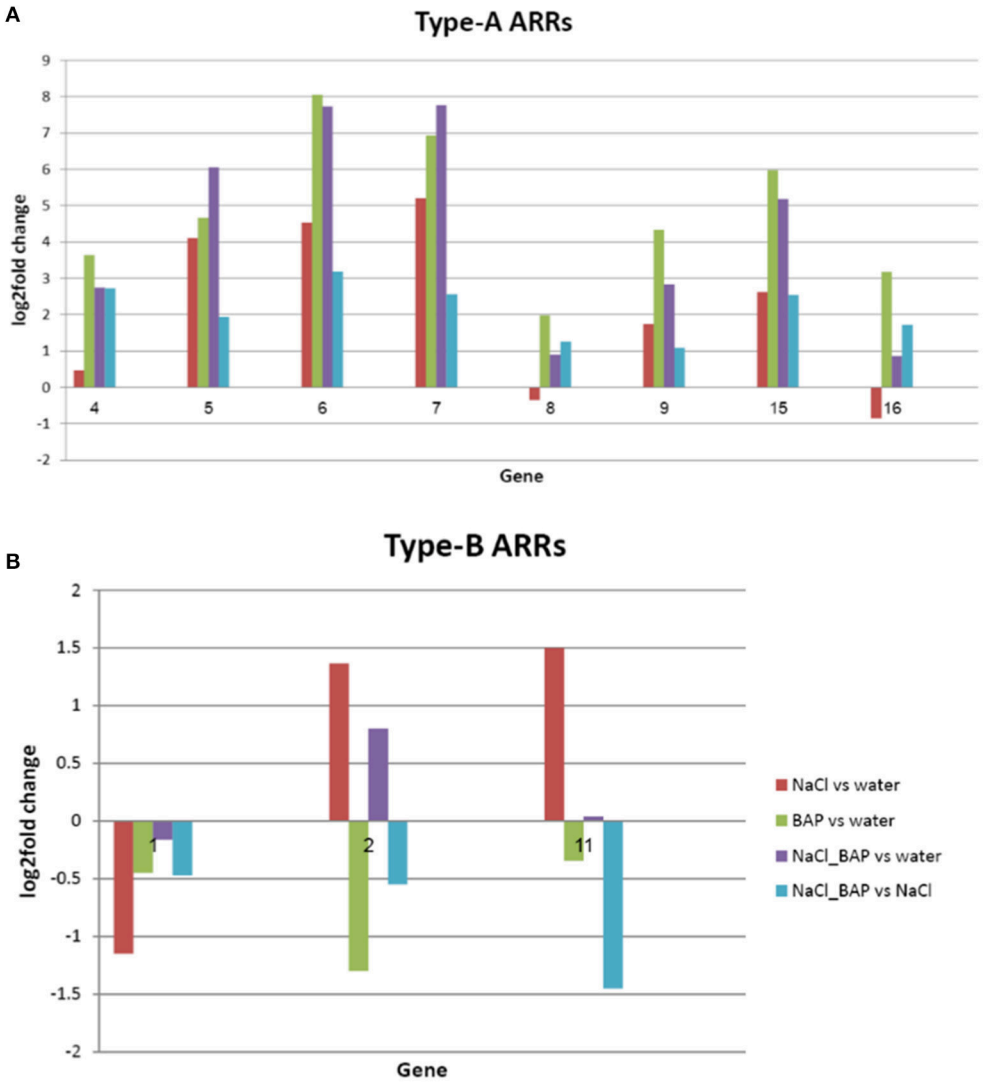

FIGURE 9 | Effect of CK on differential expression of (A) type-A and (B) type-B ARRs in plants under salinity stress (logarithmic scale). The bioinformatics enrichment analysis of our RNA sequencing data results, showed that 8 TCS genes (type A and type B response regulator proteins) had significantly different gene expression in salinity and salinity plus CK t ($P < 0.05$). 4. ARR4 (AT1G10470); 5. ARR5 (AT3G48100); 6. ARR6 (AT5G62920); 7. ARR7 (AT1G19050); 8. ARR8 (AT2G41310); 9. ARR9 (AT3G57040); 15. ARR15 (AT1G74890);16. ARR16 (AT2G40670); 1. ARR1 (AT3G16857); 2. ARR2 (AT4G16110); and 11. ARR11 (AT1G67710).

downregulation of key ABA biosynthetic genes, and a significant reduction in endogenous ABA levels (Nishiyama et al., 2011). Furthermore, recent data have shown that the ABA-to-CK ratio in xylem sap is important for stress signaling (Nishiyama et al., 2011), suggesting that modifying CK levels can change this ratio and consequently affect the expression of ABA-induced genes. Indeed, consistent with this notion, in our experiments, when endogenous CK levels were elevated or exogenous CK (BAP) was added, many ABA inducible genes known to inhibit growth were not activated.

The known antagonistic effects of ABA and CK (Gepstein and Thimann, 1980) on plant senescence are reflected by the delayed premature senescence of our SARK::IPT transgenic plants under stress. Also, in experiments where exogenous CK was added under salinity conditions, a reduced expression of the *erd1* gene, a known marker of the drought-induced senescence process (Simpson et al., 2003) was observed. Furthermore, our transcriptomic analysis revealed the Gene Ontology group designated as "defense response" whose expression was upregulated in salt conditions but downregulated when exogenous CK was added. Among the identified genes in this group were WRKY53, an important senescence regulator, and 2 senescence-associated genes (SAG13 and SAG101).

CK and Ethylene Cross-Talk

Ethylene and CK are antagonists: ethylene inhibits growth under stress and accelerates premature senescence and CKs reverse these 2 processes. Our observation that genes involved

in ethylene biosynthesis and signal transduction are upregulated in salt conditions and that this upregulation is attenuated with CK, may raise a question regarding a previous study demonstrating a CK-promotive effect on ethylene biosynthesis and signal transduction under stress conditions (Jones et al., 1995). The apparent discrepancy may stem from using plants at different developmental stages (matured plants in our study vs. young plants in prior studies). The inhibitory effect of CK on ethylene biosynthesis and signal transduction is supported by our transcriptomic analysis. The ethylene response factors *ERF1* and *ERF13* genes (involved in transcriptional regulation of several immune responsive genes; Cheng et al., 2013), and the *WRK33* gene (which encodes a transcription factor associated with plant responses to microbial infection (Mao et al., 2011), were significantly upregulated in salt conditions but were only moderately induced by exogenous CK. Our findings suggest a possible direct inhibitory effect of CK on ethylene–dependent responses, or an indirect effect on other hormones that are also related to the group associated with "cellular response to abscisic and jasmonic acids." Other findings supporting the cross talk between CK and ethylene include reduced expression of *MKK9* (a key regulator of ethylene biosynthesis (Kudryakova et al., 2001; Xu et al., 2008; An et al., 2010) and *MPK3* with CK treatment under salinity stress. Furthermore, *ARR2* (a type B response regulator that regulates both ethylene and CK signal transduction pathways; Hass et al., 2004), was upregulated under salinity stress, but this upregulation was attenuated with CK, suggesting that high CK levels during stress may antagonize the negative effect of ethylene through the inhibition of *ARR2* expression.

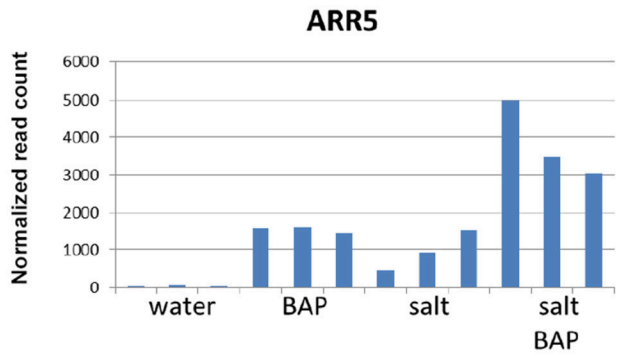

FIGURE 10 | Effect of CK on the differential expression of ARR5 under salinity stress. *Arabidopsis* w.t. plants were grown for 30 days in optimal conditions and then leaves were detached and exposed to10 μm BAP, 120 mM NaCl or salt plus BAP treatments for 24 h. Controls were detached leaves in water. Samples (3 for each treatment) were collected from controls and stressed leaves.

Transcriptional Re-Programing by CK under Salinity Stress

We performed a transcriptomic analysis to elucidate the molecular mechanisms underlying CK-induced abiotic stress tolerance, looking at both approaches of candidate genes and the entire *Arabidopsis* genome. Although candidate genes represent a select sample of genes, the 2 approaches yielded similar expression patterns reflecting the effects of CKs on plant growth under abiotic stress conditions. We used the EXPANDER tool to analyze gene expression, as it integrates all analysis steps and found it to be a superior platform. In the genes identified as having low expression under salinity stress and moderate expression with CK, we found genes involved in cell normal metabolism such as gene expression, translation, metabolism of nucleic and amino acids, and metabolism of mitochondria and chloroplasts. In addition, this group included genes related to the perception and response of plants to light. These results represent the normal influence of CK on growth processes under non-stress conditions. The second super-group of genes clusters included genes whose upregulation under salinity stress was attenuated by CKs. Overall, these genes are associated with stress responses, such as "defense response" mediated by plant hormones, "cellular response to abscisic acid stimulus," "response to water stimulus," and "cellular response to jasmonic acid stimulus." Interestingly, although reducing stress response, as observed for CK, could potentially diminish stress tolerance, the overall effect of CK is better tolerance as reflected by growth improvement. This observation may be partially explained by the anti-senescence action of CK. CK prevents premature senescence in stressed plants resulting in wilted but not dead leaves despite losing osmotic turgor, which facilitates recovery after the stress period ends (Zwack and Rashotte, 2013).

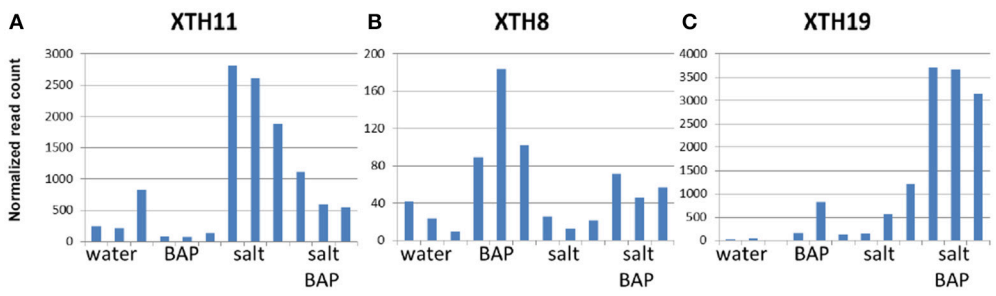

FIGURE 11 | Effect of CK on differential expression of *XTH11*, *XTH8*, and *XTH19* genes under salinity stress. (A) *XTH11* gene expression **(B)** *XTH8* gene expression **(C)** *XTH19* gene expression. *Arabidopsis* w.t. plants were grown for 30 days in optimal conditions and then leaves were detached and exposed to BAP 10 μm, 120 mM NaCl, or salt plus BAP for 24 h. Controls were detached leaves in water. Three samples were collected from the controls and stressed leaves.

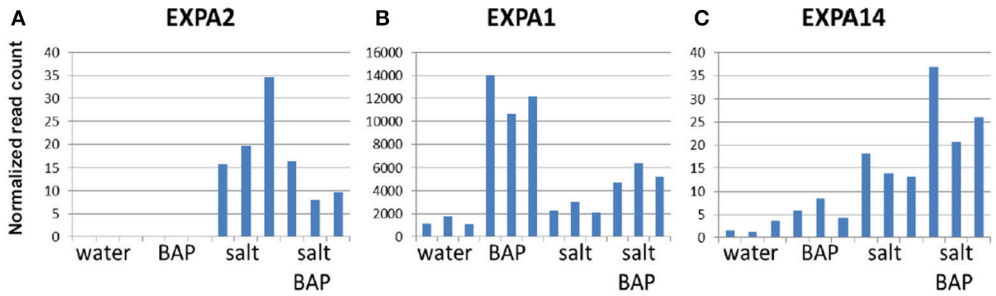

FIGURE 12 | Effect of CK on differential expression of expansins genes under salinity stress. (A) *EXPA2* gene expression **(B)** *EXPA1* gene expression **(C)** *EXPA14* gene expression. *Arabidopsis* w.t. plants were grown for 30 days in optimal conditions and then leaves were detached and exposed to BAP 10 μm, 120 mM NaCl, or salt plus BAP for 24 h. Controls were detached leaves in water. Three samples were collected from the controls and stressed leaves.

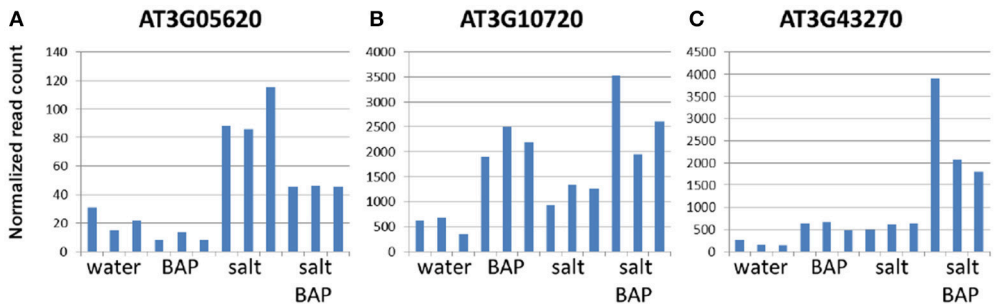

FIGURE 13 | Effect of CK on differential expression of plant invertase/pectin methylesterase inhibitor superfamily genes under salinity stress. (A) AT3G05620 gene expression. **(B)** AT3G10720 gene expression. **(C)** AT3G43270 gene expression. *Arabidopsis* w.t. plants were grown for 30 days in optimal conditions and then leaves were detached and exposed to BAP 10 μm, 120 mM NaCl, or salt plus BAP for 24 h. Controls were detached leaves in water. Three samples were collected from the controls and stressed leaves.

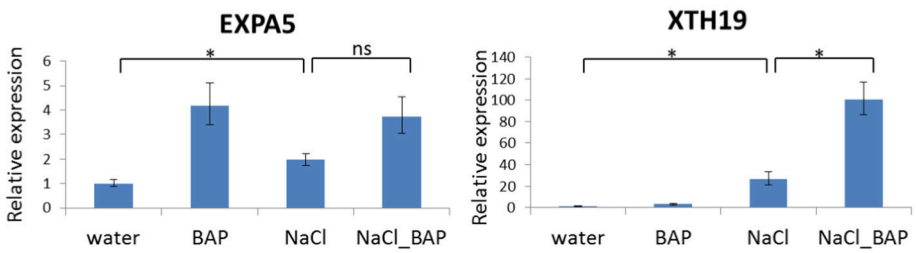

FIGURE 14 | Effect of CK on differential expression of the *EXPA5* and *XTH19* genes under salinity stress. *Arabidopsis* w.t. plants were grown for 30 days in optimal conditions and then leaves were detached and exposed to BAP 10 μm, 120 mM NaCl, or salt plus BAP for 24 h. Controls were detached leaves in water. Three samples were collected from the controls and stressed leaves. Expression of each gene in w.t. control plants was used for comparison (relative expression = 1). Horizontal brackets denote *t*-test with significance of $P < 0.05$ (*, statistical significance; ns, no significance).

However, the delay of premature senescence does not explain the observed improvement in plant growth under harsh conditions. Our results suggest that the known role of CK in promoting sustainable growth and photosynthetic activity during normal plant development also exists under stress conditions.

Interestingly, the genes in the clusters characterized by upregulation by CK included genes associated with "photosynthesis, light reaction," "photosystem II assembly," "chlorophyll biosynthetic process," and "protein targeting to chloroplast," suggesting that CK plays a role in reconstiting chloroplast components under stress conditions. This observation is supported by previous studies such as those demonstrating that CK has a role in increasing electron donation capacity of photosynthesis system II in drought conditions (Shao et al., 2010). The clusters also included cell wall proteins such as expansions and XTH, that may provide increased growth under stress conditions (Cho et al., 2006; Lü et al., 2013), and genes in the family of DEAD-box ATP-dependent RNA helicases, which are known to be involved in plant stress resistance (Luo et al., 2009; Tuteja et al., 2014).

CONCLUSIONS

We have shown that CK confers improved performance in *Arabidopsis* plants grown under abiotic stress by overcoming the genetic program that facilitates survival by growth retardation, early flowering, and accelerated senescence. Transcriptomic analysis suggested that CK triggers transcriptional reprograming leading to attenuation of the stress-dependent inhibition of vegetative growth and delaying the premature plant senescence under salt stress. We therefore hypothesize that CK allows sustainable plant growth under unfavorable environmental conditions by activating the expression of genes related to photosynthetic activity and growth. The agricultural applications of this study are under advanced developmental stages for biotechnology initiatives focused on producting transgenic crops that may grow under unfavorable water and salinit regimes.

AUTHOR CONTRIBUTIONS

All authors contributed extensively to the work presented in this paper. YG performed all the experiments and collected the data and did the analysis of the results; NS carried out with the data interpretation and wrote the manuscript; AA assisted with the Real time PCR experiments. MS assisted with the RNAseq data analysis. SG provided direction and guidance and did the critical revision of the article.

ACKNOWLEDGMENTS

This work was supported by the Nancy and Stephen Grand Technion Energy Program (GTEP), and comprises part of The Leona M. and Harry B. Helmsley Charitable Trust reports on Alternative Energy series of the Technion, Israel Institute of Technology, and the Weizmann Institute of Science. This research was also supported by the I-CORE (Israeli Centers for Research Excellence) Program of the Planning and Budgeting Committee and The Israel Science Foundation. The contribution of the KAMIN funding of the Office of the Chief Scientist (OCS) in the Ministry of Economy of Israel is also acknowledged.

SUPPLEMENTARY MATERIAL

The Supplementary Material for this article can be found online at: http://journal.frontiersin.org/article/10.3389/fenvs.2016.00063

REFERENCES

An, F., Zhao, Q., Ji, Y., Li, W., Jiang, Z., Yu, X., et al. (2010). Ethylene-induced stabilization of ETHYLENE INSENSITIVE3 and EIN3-LIKE1 is mediated by proteasomal degradation of EIN3 binding F-box 1 and 2 that requires EIN2 in Arabidopsis. *Plant Cell* 22, 2384–2401. doi: 10.1105/tpc.110.076588

Arnholdt-Schmitt, B. (2004). Stress-induced cell reprogramming. A role for global genome regulation? *Plant Physiol.* 136, 2579–2586. doi: 10.1104/pp.104.042531

Cheng, M. C., Liao, P. M., Kuo, W. W., and Lin, T. P. (2013). The Arabidopsis ETHYLENE RESPONSE FACTOR1 regulates abiotic stress-responsive gene expression by binding to different cis-acting elements in response to different stress signals. *Plant Physiol.* 162, 1566–1582. doi: 10.1104/pp.113.221911

Chernyad'ev, I. I. (2005). Effect of water stress on the photosynthetic apparatus of plants and the protective role of cytokinins: a review. *Appl. Biochem. Microbiol.* 41, 115–128. doi: 10.1007/s10438-005-0021-9

Cho, S. K., Kim, J. E., Park, J. A., Eom, T. J., and Kim, W. T. (2006). Constitutive expression of abiotic stress-inducible hot pepper CaXTH3, which encodes a xyloglucan endotransglucosylase/hydrolase homolog, improves drought and salt tolerance in transgenic Arabidopsis plants. *FEBS Lett.* 580, 3136–3144. doi: 10.1016/j.febslet.2006.04.062

Clough, S. J., and Bent, A. F. (1998). Floral dip: a simplified method for Agrobacterium-mediated transformation of *Arabidopsis thaliana*. *Plant J.* 16, 735–743 doi: 10.1046/j.1365-313x.1998.00343.x

Fujita, Y., Fujita, M., Shinozaki, K., and Yamaguchi-Shinozaki, K. (2011). ABA-mediated transcriptional regulation in response to osmotic stress in plants. *J. Plant Res.* 124, 509–525. doi: 10.1007/s10265-011-0412-3

Fujita, Y., Nakashima, K., Yoshida, T., Katagiri, T., Kidokoro, S., Kanamori, N., et al. (2009). Three SnRK2 protein kinases are the main positive regulators of abscisic acid signaling in response to water stress in *Arabidopsis*. *Plant Cell Physiol.* 50, 2123–2132. doi: 10.1093/pcp/pcp147

Gepstein, S., and Glick, B. R. (2013). Strategies to ameliorate abiotic stress-induced plant senescence. *Plant Mol. Biol.* 82, 623–633. doi: 10.1007/s11103-013-0038-z

Gepstein, S., and Thimann, K. V. (1980). Changes in the abscisic acid content of oat leaves during senescence. *Proc. Natl. Acad. Sci. U.S.A.* 77, 2050–2053. doi: 10.1073/pnas.77.4.2050

Ha, S., Vankova, R., Yamaguchi-Shinozaki, K., Shinozaki, K., and Tran, L. S. P. (2012). Cytokinins: metabolism and function in plant adaptation to environmental stresses. *Trends Plant Sci.* 17, 172–179. doi: 10.1016/j.tplants.2011.12.005

Hajouj, T., Michelis, R., and Gepstein, S. (2000). Cloning and characterization of a receptor-like protein kinase gene associated with senescence. *Plant Physiol.* 124, 1305–1314. doi: 10.1104/pp.124.3.1305

Hass, C., Lohrmann, J., Albrecht, V., Sweere, U., Hummel, F., Yoo, S. D., et al. (2004). The response regulator 2 mediates ethylene signalling and hormone signal integration in Arabidopsis. *EMBO J.* 23, 3290–3302. doi: 10.1038/sj.emboj.7600337

Ishida, K., Yamashino, T., Yokoyama, A., and Mizuno, T. (2008). Three type-B response regulators, ARR1, ARR10 and ARR12, play essential but redundant roles in cytokinin signal transduction throughout the life cycle of *Arabidopsis thaliana*. *Plant Cell Physiol.* 49, 47–57. doi: 10.1093/pcp/pcm165

Jones, M. L., Larsen, P. B., and Woodson, W. R. (1995). Ethylene-regulated expression of a carnation cysteine proteinase during flower petal senescence. *Plant Mol. Biol.* 28, 505–512. doi: 10.1007/BF00020397

Kudryakova, N. V., Burkhanova, E. A., Rakitin, V. Y., Yakovleva, L. A., Smith, A., Hall, M. A., et al. (2001). Ethylene and cytokinin in the control of senescence in detached leaves of *Arabidopsis thaliana* eti-5mutant and wild-type plants. *Russ. J. Plant Physiol.* 48, 624–627. doi: 10.1023/A:1016708002899

Li, G., Meng, X., Wang, R., Mao, G., Han, L., Liu, Y., et al. (2012). Dual-level regulation of ACC synthase activity by MPK3/MPK6 cascade and its downstream WRKY transcription factor during ethylene induction in Arabidopsis. *PLoS Genet.* 8:e1002767. doi: 10.1371/journal.pgen.1002767

Lü, P., Kang, M., Jiang, X., Dai, F., Gao, J., and Zhang, C. (2013). RhEXPA4, a rose expansin gene, modulates leaf growth and confers drought and salt tolerance to *Arabidopsis*. *Planta* 237, 1547–1559. doi: 10.1007/s00425-013-1867-3

Luo, Y., Liu, Y. B., Dong, Y. X., Gao, X. Q., and Zhang, X. S. (2009). Expression of a putative alfalfa helicase increases tolerance to abiotic stress in Arabidopsis by enhancing the capacities for ROS scavenging and osmotic adjustment. *J. Plant Physiol.* 166, 385–394. doi: 10.1016/j.jplph.2008.06.018

Mao, G., Meng, X., Liu, Y., Zheng, Z., Chen, Z., and Zhang, S. (2011). Phosphorylation of a WRKY transcription factor by two pathogen-responsive MAPKs drives phytoalexin biosynthesis in *Arabidopsis*. *Plant Cell* 23, 1639–1653. doi: 10.1105/tpc.111.084996

Mishra, S., Shukla, A., Upadhyay, S., Sanchita, Sharma, P., Singh, S., et al. (2014). Identification, occurrence, and validation of DRE and ABRE Cis-regulatory

motifs in the promoter regions of genes of *Arabidopsis thaliana*. *J. Integr. Plant Biol.* 56, 388–399. doi: 10.1111/jipb.12149

Nishiyama, R., Watanabe, Y., Fujita, Y., Le, D. T., Kojima, M., Werner, T., et al. (2011). Analysis of cytokinin mutants and regulation of cytokinin metabolic genes reveals important regulatory roles of cytokinins in drought, salt and abscisic acid responses, and abscisic acid biosynthesis. *Plant Cell Online* 23, 2169–2183. doi: 10.1105/tpc.111.087395

Nishiyama, R., Watanabe, Y., Leyva-Gonzalez, M. A., Ha, C. V., Fujita, Y., Tanaka, M., et al. (2013). Arabidopsis AHP2, AHP3, and AHP5 histidine phosphotransfer proteins function as redundant negative regulators of drought stress response. *Proc. Natl. Acad. Sci. U.S.A.* 110, 4840–4845. doi: 10.1073/pnas.1302265110

Peleg, Z., Reguera, M., Tumimbang, E., Walia, H., and Blumwald, E. (2011). Cytokinin-mediated source/sink modifications improve drought tolerance and increase grain yield in rice under water-stress. *Plant Biotechnol. J.* 9, 747–758. doi: 10.1111/j.1467-7652.2010.00584.x

Rivero, R. M., Gimeno, J., Van Deynze, A., Walia, H., and Blumwald, E. (2010). Enhanced cytokinin synthesis in tobacco plants expressing PSARK::IPT prevents the degradation of photosynthetic protein complexes during drought. *Plant Cell Physiol.* 51, 1929. doi: 10.1093/pcp/pcq143

Rivero, R. M., Kojima, M., Gepstein, A., Sakakibara, H., Mittler, R., Gepstein, S., et al. (2007). Delayed leaf senescence induces extreme drought tolerance in a flowering plant. *Proc. Natl. Acad. Sci. U.S.A.* 104, 19631. doi: 10.1073/pnas.0709453104

Roitsch, T., and Ehneß, R. (2000). Regulation of source/sink relations by cytokinins. *Plant Growth Regul.* 32, 359–367. doi: 10.1023/A:1010781500705

Rose, J. K., Braam, J., Fry, S. C., and Nishitani, K. (2002). The XTH family of enzymes involved in xyloglucan endotransglucosylation and endohydrolysis: current perspectives and a new unifying nomenclature. *Plant Cell Physiol.* 43, 1421–1435. doi: 10.1093/pcp/pcf171

Shao, R., Wang, K., and Shangguan, Z. (2010). Cytokinin-induced photosynthetic adaptability of *Zea mays* L. to drought stress associated with nitric oxide signal: Probed by ESR spectroscopy and fast OJIP fluorescence rise. *J. Plant Physiol.* 167, 472–479. doi: 10.1016/j.jplph.2009.10.020

Shinozaki, K., and Yamaguchi-Shinozaki, K. (2000). Molecular responses to dehydration and low temperature: differences and cross-talk between two stress signaling pathways. *Curr. Opin. Plant Biol.* 3, 217–223. doi: 10.1016/S1369-5266(00)00067-4

Simpson, S. D., Nakashima, K., Narusaka, Y., Seki, M., Shinozaki, K., and Yamaguchi-Shinozaki, K. (2003). Two different novel cis-acting elements of erd1, a clpA homologous Arabidopsis gene function in induction by dehydration stress and dark-induced senescence. *Plant J.* 33, 259–270. doi: 10.1046/j.1365-313X.2003.01624.x

Sreenivasulu, N., Harshavardhan, V. T., Govind, G., Seiler, C., and Kohli, A. (2012). Contrapuntal role of ABA: does it mediate stress tolerance or plant growth retardation under long-term drought stress? *Gene* 506, 265–273. doi: 10.1016/j.gene.2012.06.076

To, J. P. C., Deruère, J., Maxwell, B. B., Morris, V. F., Hutchison, C. E., Ferreira, F. J., et al. (2007). Cytokinin regulates type-A arabidopsis response regulator activity and protein stability via two-component phosphorelay. *Plant Cell* 19, 3901–3914. doi: 10.1105/tpc.107.052662

Tran, L. S. P., Urao, T., Qin, F., Maruyama, K., Kakimoto, T., Shinozaki, K., et al. (2007). Functional analysis of AHK1/ATHK1 and cytokinin receptor histidine kinases in response to abscisic acid, drought, and salt stress in *Arabidopsis*. *Proc. Natl. Acad. Sci. U.S.A.* 104, 20623. doi: 10.1073/pnas.0706547105

Tuteja, N., Banu, M. S., Huda, K. M., Gill, S. S., Jain, P., Pham, X. H., et al. (2014). Pea p68, a DEAD-box helicase, provides salinity stress tolerance in transgenic tobacco by reducing oxidative stress and improving photosynthesis machinery. *PLoS ONE* 9:e98287. doi: 10.1371/journal.pone.0098287

Verma, V., Ravindran, P., and Kumar, P. P. (2016). Plant hormone-mediated regulation of stress responses. *BMC Plant Biol.* 16, 1–10. doi: 10.1186/s12870-016-0771-y

Wang, Y., Li, L., Ye, T., Zhao, S., Liu, Z., Feng, Y. Q., et al. (2011). Cytokinin antagonizes ABA suppression to seed germination of Arabidopsis by downregulating ABI5 expression. *Plant J.* 68, 249–261. doi: 10.1111/j.1365-313X.2011.04683.x

Werner, T., Nehnevajova, E., Kollmer, I., Novák, O., Strnad, M., Krämer, U., et al. (2010). Root-specific reduction of cytokinin causes enhanced root growth, drought tolerance, and leaf mineral enrichment in Arabidopsis and tobacco. *Plant Cell* 22, 3905–3920. doi: 10.1105/tpc.109.072694

Xing, Y., Jia, W., and Zhang, J. (2008). AtMKK1 mediates ABA-induced CAT1 expression and H2O2 production via AtMPK6-coupled signaling in Arabidopsis. *Plant J.* 54, 440–451. doi: 10.1111/j.1365-313X.2008.03433.x

Xu, J., Li, Y., Wang, Y., Liu, H., Lei, L., Yang, H., et al. (2008). Activation of MAPK kinase 9 induces ethylene and camalexin biosynthesis and enhances sensitivity to salt stress in Arabidopsis. *J. Biol. Chem.* 283, 26996–27006. doi: 10.1074/jbc.M801392200

Yamaguchi-Shinozaki, K., and Shinozaki, K. (1994). A novel cis-acting element in an Arabidopsis gene is involved in responsiveness to drought, low-temperature, or high-salt stress. *Plant Cell Online* 6, 251–264. doi: 10.1105/tpc.6.2.251

Yoshida, T., Fujita, Y., Sayama, H., Kidokoro, S., Maruyama, K., Mizoi, J., et al. (2010). AREB1, AREB2, and ABF3 are master transcription factors that cooperatively regulate ABRE-dependent ABA signaling involved in drought stress tolerance and require ABA for full activation. *Plant J.* 61, 672–685. doi: 10.1111/j.1365-313X.2009.04092.x

Zwack, P. J., and Rashotte, A. M. (2013). Cytokinin inhibition of leaf senescence. *Plant Signal. Behav.* 8:e24737. doi: 10.4161/psb.24737

Zwack, P. J., and Rashotte, A. M. (2015). Interactions between cytokinin signalling and abiotic stress responses. *J. Exp. Bot.* 66, 4863–4871. doi: 10.1093/jxb/erv172

Conflict of Interest Statement: The authors declare that the research was conducted in the absence of any commercial or financial relationships that could be construed as a potential conflict of interest.

frontiers in Plant Science

ORIGINAL RESEARCH
published: 13 May 2016
doi: 10.3389/fpls.2016.00652

Tissue- and Cell-Specific Cytokinin Activity in *Populus* × *canescens* Monitored by *ARR5::GUS* Reporter Lines in Summer and Winter

Shanty Paul[1], Henning Wildhagen[1], Dennis Janz[1], Thomas Teichmann[1†], Robert Hänsch[2] and Andrea Polle[1]*

[1] Department of Forest Botany and Tree Physiology, Georg-August-Universität Göttingen, Göttingen, Germany, [2] Department of Molecular and Cell Biology of Plants, Institute for Plant Biology, University of Technology, Braunschweig, Germany

OPEN ACCESS

Edited by:
Alison Kingston-Smith, Aberystwyth University, UK

Reviewed by:
Amarendra Narayan Misra, Central University of Jharkhand, India
Richard Napier, University of Warwick, UK

***Correspondence:**
Andrea Polle
apolle@gwdg.de

†Present address:
Thomas Teichmann, Department of Plant Cell Biology, Albrecht-von-Haller-Institute of Plant Sciences, Georg-August-Universität Göttingen, Göttingen, Germany

Specialty section:
This article was submitted to Agroecology and Land Use Systems, a section of the journal Frontiers in Plant Science

Received: *03 November 2015*
Accepted: *28 April 2016*
Published: *13 May 2016*

Citation:
Paul S, Wildhagen H, Janz D, Teichmann T, Hänsch R and Polle A (2016) Tissue- and Cell-Specific Cytokinin Activity in Populus × canescens Monitored by ARR5::GUS Reporter Lines in Summer and Winter. Front. Plant Sci. 7:652. doi: 10.3389/fpls.2016.00652

Cytokinins play an important role in vascular development. But knowledge on the cellular localization of this growth hormone in the stem and other organs of woody plants is lacking. The main focus of this study was to investigate the occurrence and cellular localization of active cytokinins in leaves, roots, and along the stem of *Populus* × *canescens* and to find out how the pattern is changed between summer and winter. An *ARR5::GUS* reporter construct was used to monitor distribution of active cytokinins in different tissues of transgenic poplar lines. Three transgenic lines tested under outdoor conditions showed no influence of *ARR5::GUS* reporter construct on the growth performance compared with the wild-type, but one line lost the reporter activity. *ARR5::GUS* activity indicated changes in the tissue- and cell type-specific pattern of cytokinin activity during dormancy compared with the growth phase. *ARR5::GUS* activity, which was present in the root tips in the growing season, disappeared in winter. In the stem apex ground tissue, *ARR5::GUS* activity was higher in winter than in summer. Immature leaves from tissue-culture grown plants showed inducible *ARR5::GUS* activity. Leaf primordia in summer showed *ARR5::GUS* activity, but not the expanded leaves of outdoor plants or leaf primordia in winter. In stem cross sections, the most prominent *ARR5::GUS* activity was detected in the cortex region and in the rays of bark in summer and in winter. In the cambial zone the *ARR5::GUS* activity was more pronounced in the dormant than in growth phase. The pith and the ray cells adjacent to the vessels also displayed *ARR5::GUS* activity. *In silico* analyses of the tissue-specific expression patterns of the whole PtRR type-A family of poplar showed that *PtRR10*, the closest ortholog to the *Arabidopsis ARR5* gene, was usually the most highly expressed gene in all tissues. In conclusion, gene expression and tissue-localization indicate high activity of cytokinins not only in summer, but also in winter. The presence of the signal in meristematic tissues supports their role in meristem maintenance. The reporter lines will be useful to study the involvement of cytokinins in acclimation of poplar growth to stress.

Keywords: cytokinin, localization, *ARR5*, summer, winter, dormancy, wood

INTRODUCTION

Cytokinins are adenine derivatives that act as master regulators of plant growth and development. They are synthesized mainly in the root tips (Dieleman et al., 1997; Miyawaki et al., 2004; Aloni et al., 2005), but also locally in shoot tissues (Sakakibara, 2006; Tanaka et al., 2006; Hirose et al., 2008; Kamada-Nobusada and Sakakibara, 2009). Root-derived cytokinins are transported acropetally through xylem sap by the transpirational pull (Aloni et al., 2005), while shoot-derived cytokinins are transported through phloem (Bishopp et al., 2011). Active and inactive forms of cytokinins occur as free bases and as ribosides, ribotides, or glucose conjugates, respectively (Mok and Mok, 2001; Romanov et al., 2006).

Cytokinins have roles in almost all aspects of plant growth and development including cell division, shoot initiation and growth, sink/source relationships, nutrient uptake, breaking of bud dormancy, delay of leaf senescence, and regulation of vascular development (Hwang et al., 2012; Kieber and Schaller, 2014). Cytokinins determine vascular cell identities, except those of the protoxylem (Mähönen et al., 2000; Hutchison et al., 2006; Yokoyama et al., 2007; Argyros et al., 2008) and promote the development of vascular cambium (Matsumoto-Kitano et al., 2008; Nieminen et al., 2008). Cytokinins specify the vascular pattern by regulating the level of PIN auxin efflux proteins (Bishopp et al., 2011). Cytokinins increase the sensitivity of the cambium to the auxin signal thereby determining wood quantity and quality (Aloni, 1991, 2001).

Cytokinin perception and signaling in plants has been extensively studied in *Arabidopsis* and involves a His-Asp phosphorelay that mediates the signal transmission (Mizuno, 2005; Schaller et al., 2008). Among the response regulators in this pathway, type-A *ARRs* (*Arabidopsis* Response Regulators), i.e., genes which contain the highly conserved Lys and two Asp residues in their receiver domains, are the primary response genes for cytokinins (D'Agostino et al., 2000). Ten type-A *ARR* genes are described in *Arabidopsis* (D'Agostino et al., 2000; Schaller et al., 2008; Pils and Heyl, 2009) and eleven in *Populus trichocarpa* (Ramírez-Carvajal et al., 2008; Immanen et al., 2013). The *ARR* genes are transcriptionally regulated and can be induced by exogenous cytokinin treatment (D'Agostino et al., 2000; Taniguchi et al., 1998).

In trees, changes in endogenous cytokinin levels in relation to seasonality have been studied for a long time. Most of these studies focused on the endogenous cytokinin levels in xylem or phloem sap of the trees (Hewett and Wareing, 1973; Alvim et al., 1976; Weiler and Ziegler, 1981; Tromp and Ovaa, 1990; Cook et al., 2001) or reported the endogenous cytokinin concentrations in different organs (Hewett and Wareing, 1973; Van Staden and Dimalla, 1981; Cook et al., 2001). Furthermore active and inactive forms of cytokinins were distinguished (Hewett and Wareing, 1973; Van Staden and Dimalla, 1981; Tromp and Ovaa, 1990) and their changes were related to seasonal fluctuations (Tromp and Ovaa, 1990). For example, in the xylem sap of apple trees, the active *trans*-zeatin type (tZ) levels were high during the growing season, dropped during dormancy and showed an increase during bud burst, whereas continued to increase during the growing season (Tromp and Ovaa, 1990). Despite the importance of cytokinins in vascular development, knowledge on the cellular localization of this growth hormone in the stem and other organs of woody plants is still lacking. Furthermore, it is unclear how the tissue-specific distribution of active cytokinins is influenced by dormancy.

The goal of this study was to investigate the occurrence and cellular localization of active cytokinins in leaves, roots and along the stem of poplar and to find out how the pattern is changed between the active growth phase in summer and dormancy in winter. Our hypothesis was that cytokinin activity was present in actively growing tissues in summer and lacking in winter, except in those tissues, where cells have to be kept in the meristematic stage. Tissue-specific localization patterns of cytokinin activity were also compared with expression of genes belonging to the type-A Response Regulator (RR) family in poplar. In *Arabidopsis*, the *ARR5::GUS* (β-glucuronidase) reporter construct has been used to monitor the distribution of active cytokinins in different tissues (D'Agostino et al., 2000). *ARR5* has high homology to the cytokinin-inducible gene *PtRR10* of *Populus trichocarpa* (Ramírez-Carvajal et al., 2008; Immanen et al., 2013). Here, we employed the *ARR5::GUS* construct as a tool to investigate the localization pattern of active cytokinins in poplar. The transgenic poplar cytokinin reporter lines were grown outdoors under ambient conditions and used to map *ARR5* activity in summer and winter.

MATERIALS AND METHODS

Plant Transformation

The *ARR5::GUS* construct described in D'Agostino et al. (2000) was provided by Prof. Kieber (University of North Carolina, Chapel Hill, NC, USA), cloned, transformed into *Agrobacterium tumefaciens* strain C58C1/MP90 and then used to transform *Populus* × *canescens* [INRA (Institut National de la Recherche Agronomique) clone 717-1B4] as described by Teichmann et al. (2008). Plantlets were regenerated, maintained on Murashige and Skoog (MS) medium containing 50 mg l^{-1} kanamycin and micropropagated after Leple et al. (1992).

Selection of Transgenic Reporter Lines

Leaves from 3-week-old transformed plantlets were collected and GUS staining was performed according to Jefferson et al. (1987) as modified by Teichmann et al. (2008). Briefly, the presence of GUS activity was investigated in intact leaves that were vacuum-infiltrated with GUS buffer (100 mM NaH_2PO_4, pH 7.0, 10 mM Na_4EDTA, 0.05% Triton X-100) containing 1 mg ml^{-1} 5-bromo-4-chloro-3-indolyl-β-D-glucuronic acid (Duchefa, Haarlem, The Netherlands). The leaves were then incubated in the dark at 37 °C for 24 h and chlorophyll was removed by ethanol treatment. The *ARR5::GUS* activity was observed mainly in the petiole and primary veins of these leaves. The leaves were viewed and photographed directly. From the regenerated plantlets which were maintained on MS medium containing kanamycin, 17 lines showed GUS activity after GUS staining, mainly in the veins (**Figures 1A,B**).

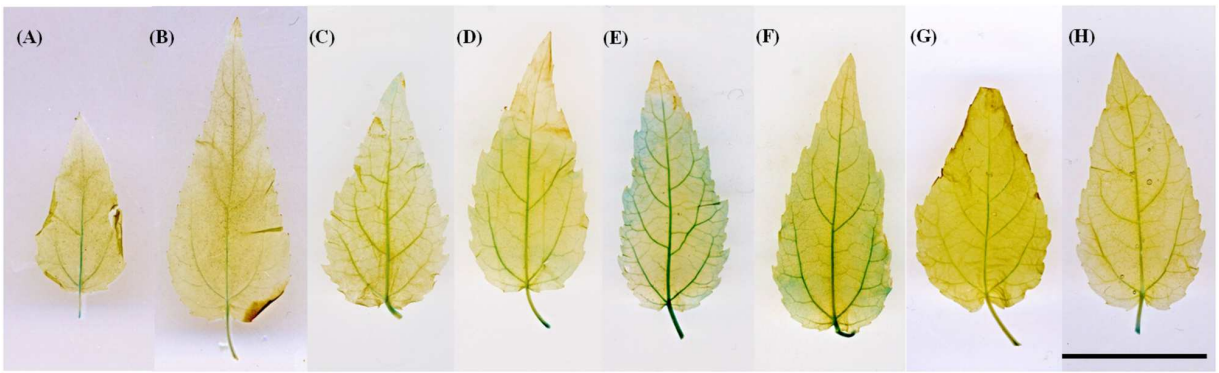

FIGURE 1 | *ARR5::GUS* activity in leaves of *ARR5::GUS* poplar reporter line. The leaves of line 80 were incubated directly in GUS staining solution **(A,B)** or GUS staining was performed after mock-incubated in 0.1% DMSO (solvent control; **C,D**). **(E,F)** show *ARR5::GUS* activity in leaves after petiole-feeding with 5 μM thidiazuron and BAP, respectively, while **(G,H)** show *ARR5::GUS* activity in leaves after petiole feeding with 5 μM adenine in the light (200 μmol quanta m^{-2} s^{-1} PAR) for 24 h. Scale bar = 2 cm

The pattern was similar to that of mock treated leaves (**Figures 1C,D**).

All plantlets from these 17 lines showed similar morphology and growth *in vitro* when compared to the wild-type (WT). Plantlets from each line were propagated *in vitro*. The leaves from these lines were also treated with an exogenous cytokinin supply in order to monitor the response of *ARR5::GUS* construct to cytokinin. For this purpose, leaves from 3-week-old *in vitro* micropropagated plantlets were fed by the petioles with a solution containing 5 μM thidiazuron (Duchefa, Haarlem, The Netherlands) or 5 μM 6-benzylaminopurine (BAP, Sigma–Aldrich Chemie, Steinheim, Germany) in 0.1% DMSO (Merck KGaA, Darmstadt, Germany), both active cytokinin analogs or 5 μM adenine (Sigma–Aldrich Chemie, Steinheim, Germany), which is an inactive cytokinin analog. A solution of 0.1 % DMSO (Merck KGaA, Darmstadt, Germany) was used as the solvent control. During the treatment the leaves were kept inside a sealed glass jar at high humidity to avoid desiccation stress. The leaves were allowed to transpire under 200 μmol quanta m^{-2} s^{-1} photosynthetically active radiation (PAR) for 24 h. Afterward, the leaves were directly used for GUS staining as above. Examples for cytokinin induction of the *ARR5* promoter in thidiazuron- or BAP-fed leaves are shown in **Figures 1E,F**. When compared to controls, the thidiazuron-treated leaves showed a strong induction in *ARR5::GUS* activity over the leaf blade and in tertiary veins (**Figure 1E**). On the other hand, the leaves treated with the inactive cytokinin analog adenine did not show an induction (**Figures 1G,H**). For documentation of staining pattern, the leaves were laid flat in a petri dish filled with distilled water and were scanned (Canoscan 4400F, Canon Inc., China).

From the lines that showed an increased *ARR5::GUS* activity under exogenous cytokinin treatment, three lines (line 9, 32, and 80) were selected for the study.

Plant Cultivation

In vitro micropropagated plantlets of the lines 9, 32, and 80 along with WT, were grown in hydroponics for 3 weeks and then transferred into pots with soil (Fruhstorfer Erde Type N, Hawite Gruppe GmbH, Vechta, Germany) as described by Müller et al. (2013). The plants were grown in a greenhouse for 3 months under controlled environmental conditions: 16 h day length, 200 μmol quanta m^{-2} s^{-1} PAR, 20 °C air temperature and 55% relative air humidity. Afterward, the potted plants were transferred from the greenhouse to a caged area outdoors (Göttingen, Germany, 51.55739°N, 9.95857°E, 293 m above sea level) and acclimated to ambient light and temperature (after Müller et al., 2013). On 18th July 2011, the poplars were planted in four boxes (3.5 m length × 3 m width × 0.7 m height) filled with a compost soil and sand mixture (1:1) (Vogteier Erdenwerk GmbH, Niederdorla, Germany). The WT and transgenic lines were planted in a mixed design. Each box was equipped with a total of 42 plants comprising 10 plants each of WT, line 9 and 80, and 12 plants of line 32. The first row of plants near to the box edges was not included in any of the analyses to avoid edge effects.

During the growing season, plants were watered with tap water every second day or daily on warm days. Air temperature, relative humidity, and PAR for every hour per day were recorded during the whole study period using MeteoLOG TDL 14 data logger (Adolf Thies GmbH & Co. KG, Göttingen, Germany).

Harvest

Harvests were conducted in the growing season (August, 2012) when the mean temperature was 22.4 °C and during dormancy (January, 2013) when the mean temperature was −5.0 °C. In the growing season harvest, four plants each from WT, line 9, 32, and 80 were harvested. In the dormancy harvest, one plant from WT and two plants from each line 9, 32, and 80 were harvested. Roots, bark, wood, and leaves were separated and fresh mass was determined for each fraction. Aliquots of these plant tissues were oven dried at 60 °C for 7 days for measurement of dry mass. Tissue dry mass (g) was calculated as:

$$\frac{\text{Dry mass of the aliquot (g)} \times \text{total tissue fresh mass (g)}}{\text{fresh mass of the aliquot (g)}}$$

During harvest, the following fresh tissues were collected for GUS staining: one half of the apical bud, leaf disks (diameter 5 mm) from the first fully developed leaf from the apex, stem cross sections (2 mm thickness) at three positions: top (50 mm beneath the stem apex), middle (the position in the stem exactly in the center between the apex and the shoot–root junction) and bottom (50 mm above the root–shoot junction), and fine root tips. The stem cross sections were cut using a micro-saw (Proxxon, Föhren, Germany). The materials were directly transferred into the GUS buffer and GUS staining was performed as described above.

GUS Activity Analyses at Tissue and Cellular Level

Tissue staining patterns were documented by photos, which were taken with a digital camera (DFC420 C, Leica Microsystems Ltd., Germany) attached to a stereomicroscope (M205 FA, Leica Microsystems Ltd., Wetzlar, Germany). The stained tissues were fixed in a solution of 1 part of 37% formaldehyde, 1 part of 100% acetic acid, and 18 parts of 70% ethanol. Subsequently, the fixed tissues were dehydrated in a series of ethanol solutions (70, 80, 90, and 96% (v/v)) for 2 h each at room temperature. The tissues were embedded in Technovit 7100 resin (Heraeus Kulzer GmbH & Co. KG, Germany) according to manufacturer's instructions with the following modifications: The dehydrated samples were infiltrated in 1:1 (v/v) solutions of 96% ethanol and Technovit 7100 basic solution for 5 h. Then the samples were infiltrated in 1:2 and then in 1:3 (v/v) solutions of 96% ethanol and Technovit 7100 basic solution for 12 and 5 h, respectively. Thereafter, the samples were treated with Technovit 7100 infiltration medium consisting of 1 g Hardner I in 100 ml Technovit 7100 basic solution (provided by the manufacturer) for 24 h. A reduced pressure of 20 kPa for 15 min was applied at each step during infiltration. Finally, the tissues were embedded in the embedding medium (prepared by mixing 30 ml infiltration medium and 1.5 ml Hardner II provided by the manufacturer). Sections of 15 μm thickness were cut with a rotarymicrotome (RM 2265, Leica Microsystems, Wetzlar, Germany) and viewed under a microscope (Axioplan Observer.Z1, Carl Zeiss GmbH, Germany). Photographs were taken at 100× and 200× magnification with a digital camera (Axio Cam MRC, Carl Zeiss Microimaging GmbH, Göttingen, Germany) attached to the microscope (Axioplan Observer.Z1, Carl Zeiss GmbH, Germany).

Gene Expression Analyses of PtRR Type-A Family

For the analysis of tissue specific expression patterns of poplar genes belonging to the two component RR type-A gene family of cytokinin signaling pathway, the gene list as reported by Ramírez-Carvajal et al. (2008) was used. The genomic sequence of each gene was obtained from Joint Genome Institute, JGI[1] and the respective gene IDs were obtained by blasting the genomic sequences in Phytozome v10.1[2] (Goodstein et al., 2012). The homolog of each gene in *Arabidopsis* was obtained by blasting the protein sequence taken from Phytozome, in TAIR[3]. The gene names and gene IDs of the genes used for the expression analyses have been compiled in **Table 1**. Microarrays were downloaded from the EMBL-EBI ArrayExpress database (Kolesnikov et al., 2015). For *P.* × *canescens*: E-GEOD-16495 (shoot apex; Yordanov et al., 2014), E-MEXP-1928 (mature leaves; Janz et al., 2010), E-MEXP-2120 (mature leaves), E-MEXP-3741(bark; He et al., 2013), E-MEXP-2031 (developing xylem; Janz et al., 2012), E-GEOD-33977 (rays- summer and winter; Larisch et al., 2012), E-MEXP-1874 (fine roots; Luo et al., 2009), E-GEOD-43162 (fine roots; Wei et al., 2013), and for *P. trichocarpa*: E-GEOD-30507 (stem, shoot and leaf primordia, mature leaves, developing xylem, cambium, bark; Ko et al., 2012), E-MEXP-3910 (young leaves; Bai et al., 2013), E-GEOD-49983 (bark), E-MTAB-1483 (developing xylem and elongation zone; Euring et al., 2014), E-GEOD-21480 (stem- summer and winter); E-MEXP-3909 (young roots; Bai et al., 2013).

For the annotation of the microarray ID to the best gene model, the annotation file downloaded from Aspen Database (Tsai et al., 2011) was used.

Statistical Analyses

Statistical analyses were performed using the free statistical software R (version 3.1.1, R Core Team, 2014). One-way ANOVA was conducted for dry biomass data with plant lines (transgenic reporter lines and WT) as factor. Normality and homogeneity of variance were tested visually by plotting residuals and the data was transformed logarithmically ($\log_2$) if needed. Data shown are mean ± SE. Means were considered to be significantly different with a p-value ≤ 0.05.

For the analyses of expression data, to summarize and normalize the array probes, 'rma' function from the R package 'affy' (Gautier et al., 2004) obtained from Bioconductor (Kauffmann et al., 2009) was used. Mean transcript abundance of the biological replicates was calculated for each gene in each

[1]http://genome.jgi-psf.org/Poptr1_1/Poptr1_1.home.html

[2]http://phytozome.jgi.doe.gov/pz/portal.html

[3]www.arabidopsis.org

TABLE 1 | Poplar genes belonging to the two component type-A response regulator gene family (Ramírez-Carvajal et al., 2008) that were used for analysis of tissue-specific expression pattern.

Populus trichocarpa gene name	*Populus trichocarpa* gene ID	*Arabidopsis* gene name	AGI
PtRR1	Potri.010G037800	*ARR3*	AT1G59940
PtRR2	Potri.008G193000	*ARR3*	AT1G59940
PtRR3	Potri.002G082200	*ARR9*	AT3G57040
PtRR4	Potri.003G197500	*ARR9/ARR8*	AT3G57040/ AT2G41310
PtRR5	Potri.001G027000	*ARR9/ARR8*	AT3G57040/ AT2G41310
PtRR6	Potri.006G041100	*ARR9*	AT3G57040
PtRR7	Potri.016G038000	*ARR8*	AT2G41310
PtRR8	Potri.019G058900	*ARR17*	AT3G56380
PtRR9	Potri.013G157700	*UCP030365*	AT5G05240
PtRR10	Potri.015G070000	*ARR5*	AT3G48100
PtRR11	Potri.019G133600	*ARR17*	AT3G56380

tissue. When more than one probe set was present for one gene, all probe sets were used to calculate the mean value. The means were used for creating a heatmap with the 'heatmap.2' function from the R package 'gplots' (Warnes et al., 2012).

RESULTS

The *ARR5::GUS* Reporter Lines Showed No Growth Differences Compared to Wild-type Poplars

The poplar lines 9, 32, and 80 were grown in ambient conditions, along with WT plants for 1.5 years. The determination of the dry mass did not show any significant difference among the lines (**Table 2**). There were no apparent visual differences neither in summer nor in winter (**Figure 2**) suggesting that the transformation with the *ARR5::GUS* gene construct did not hit any gene that was relevant for growth and that the expression of the construct had no influence on the plant stature.

ARR5::GUS Activity Reports a Tissue- and Cell-type Specific Pattern of Cytokinin Activity in Poplar in the Growth Phase

The localization pattern of *ARR5::GUS* activity during growing season was investigated in apical buds, leaf disks, root tips and in stem cross sections at three positions, i.e., top, middle, and bottom. Plants from line 9 did not display a *GUS* signal in any of the samples from the outdoor grown plants, suggesting that silencing had occurred. Therefore, the pictures of these samples were not considered.

In the growing season, line 32 and 80 exhibited *ARR5::GUS* activity in all tissues (**Figure 3**), except in mature leaves (not shown). In the apical buds, the *ARR5::GUS* activity was localized in the leaf primordia and also in the apical bud base from where the leaf primordia started (**Figure 3A**). *ARR5::GUS* was also expressed in root tips (**Figure 3E**). Higher magnification showed that the staining was concentrated in the root cap region, decreased in the cell division zone and was stronger again at the onset of the cell elongation zone (**Figure 4**). The signal showed a gradual decrease toward the direction of the shoot (**Figure 4**).

Examination of cytokinin activity along the stem revealed strong staining in pith in the region of the stem elongation zone, while the signal in the pith disappeared in the stem middle and at the stem bottom, where the pith was compressed by secondary growth (**Figures 3B–D**). In the stem middle and at the bottom the bark region below the periderm also showed a strong *GUS* staining (**Figures 3C,D**).

To investigate the cellular localization pattern of *ARR5::GUS* activity, stem cross sections were analyzed at a higher magnification. In the elongation zone strong *ARR5::GUS* activity in the pith was confirmed, but no staining was detected in the cortex or primary xylem (**Figure 5A**). In the middle

TABLE 2 | Biomass of 1-year-old *Populus* × *canescens* wild-type and *ARR5::GUS* reporter lines in the growing season.

	WT	Line 9	Line 32	Line 80
Parameter				
Stem + branches (g dry wt)	162.1 ± 18.1	124.0 ± 16.2	159.2 ± 38.2	228.0 ± 13.8
Coarse root (g dry wt)	74.8 ± 12.3	59.8 ± 10.6	63.7 ± 10.1	84.7 ± 3.3
Fine root (g dry wt)	5.7 ± 1.0	4.7 ± 0.6	6.6 ± 1.3	5.3 ± 1.0
Below-ground (g dry wt)	80.4 ± 12.4	64.5 ± 10.8	70.3 ± 11.2	90.0 ± 2.3

One-year-old whole poplar trees were harvested in August, 2012. Data indicate mean ± SE (n = 4). One-way ANOVA conducted for dry mass of the plant lines did not reveal any significant differences (p > 0.05).

FIGURE 2 | *Populus* × *canescens* wild-type (WT) and *ARR5::GUS* transgenic reporter lines before harvest in the growth phase (A; August, 2012) and before harvest during dormancy (B; January, 2013).

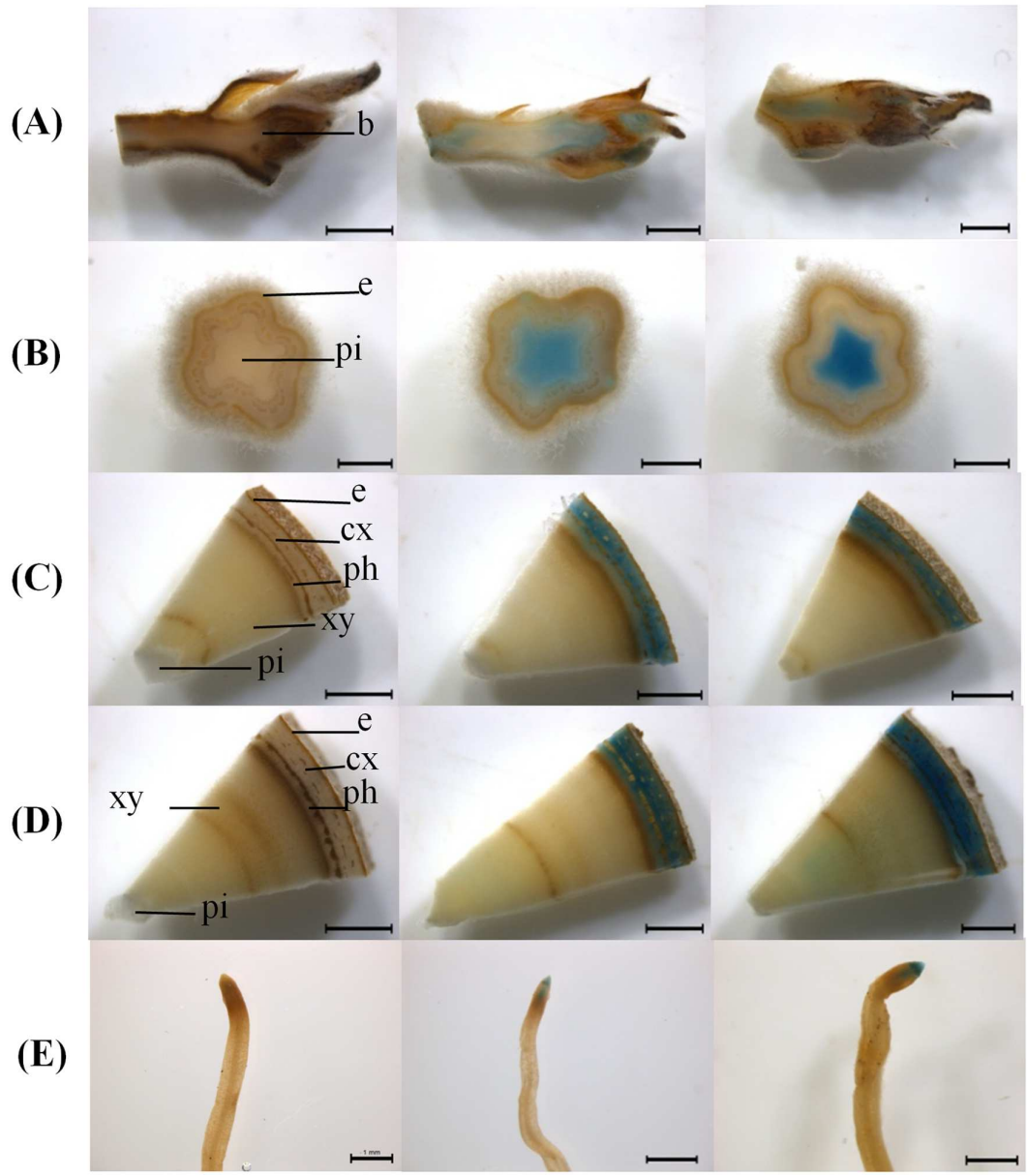

FIGURE 3 | *ARR5::GUS* activity observed in different tissues of *Populus* × *canescens* reporter lines and WT in the growing season. Representative pictures of $n = 4$ replicates per line are shown. Rows **(A–E)** represent apical bud, stem sections from top, middle, and bottom positions, and the root tips, respectively. Tissues are indicated by the following abbreviations: b, apical bud base; e, epidermis; cx, cortex; ph, phloem; xy, xylem; and pi, pith. Scale bar = 2 mm for apical bud, stem middle and stem bottom. Scale bar = 1 mm for stem top and root tip.

of the stem strong GUS staining was observed only in the cortex between strands of phloem fiber cells (**Figure 5B**). The stem bottom sections showed a strong staining in the cortex and also in the phloem, especially at the position of the primary rays (**Figure 5C**). Detailed analysis in the mature xylem showed *ARR5::GUS* activity in the ray cells adjacent to vessels (**Figure 6A**). *ARR5::GUS* activity was also detected in the cambial zone (**Figure 6C**).

ARR5::GUS Activity Reports Changes in the Tissue- and Cell-type Specific Pattern of Cytokinin Activity during Dormancy Compared with the Growth Phase

During winter dormancy the apical buds showed no *ARR5::GUS* activity in the leaf primordia, but a very strong signal in the

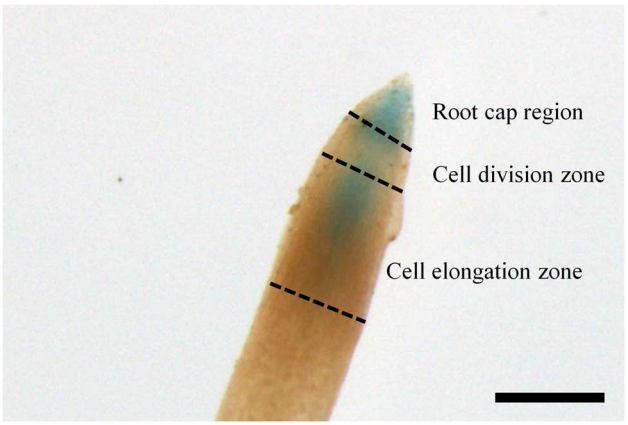

FIGURE 4 | *ARR5::GUS* activity in the root tip of the *Populus* × *canescens* reporter line 32 during the growth phase. Scale bar = 250 μm.

ground tissue below the bud base (**Figure 7A**). *ARR5::GUS* activity below the bud base extended into a larger area of the ground tissue of the stem than that observed during the growing season.

Below the apex, at the stem top *ARR5::GUS* activity was detected in the pith, however, with weaker intensity than in summer (**Figure 7B**). This signal disappeared in the stem middle and bottom (**Figures 7C,D**). The stem middle and bottom cross sections showed a strong staining in the bark region (**Figures 7C,D**). In the root tips *ARR5::GUS* activity was absent in winter (**Figure 7E**).

Cellular localization of *ARR5::GUS* activity was also monitored along the dormant stem (**Figure 8**). The stem top section, which was collected at the same position below the apex as in summer, showed a fully developed circular ring of secondary xylem, indicating that secondary growth had already started in this zone (**Figure 8A**). The reason is that after bud set in fall, elongation growth stops and the undifferentiated ground tissues continue to develop for some

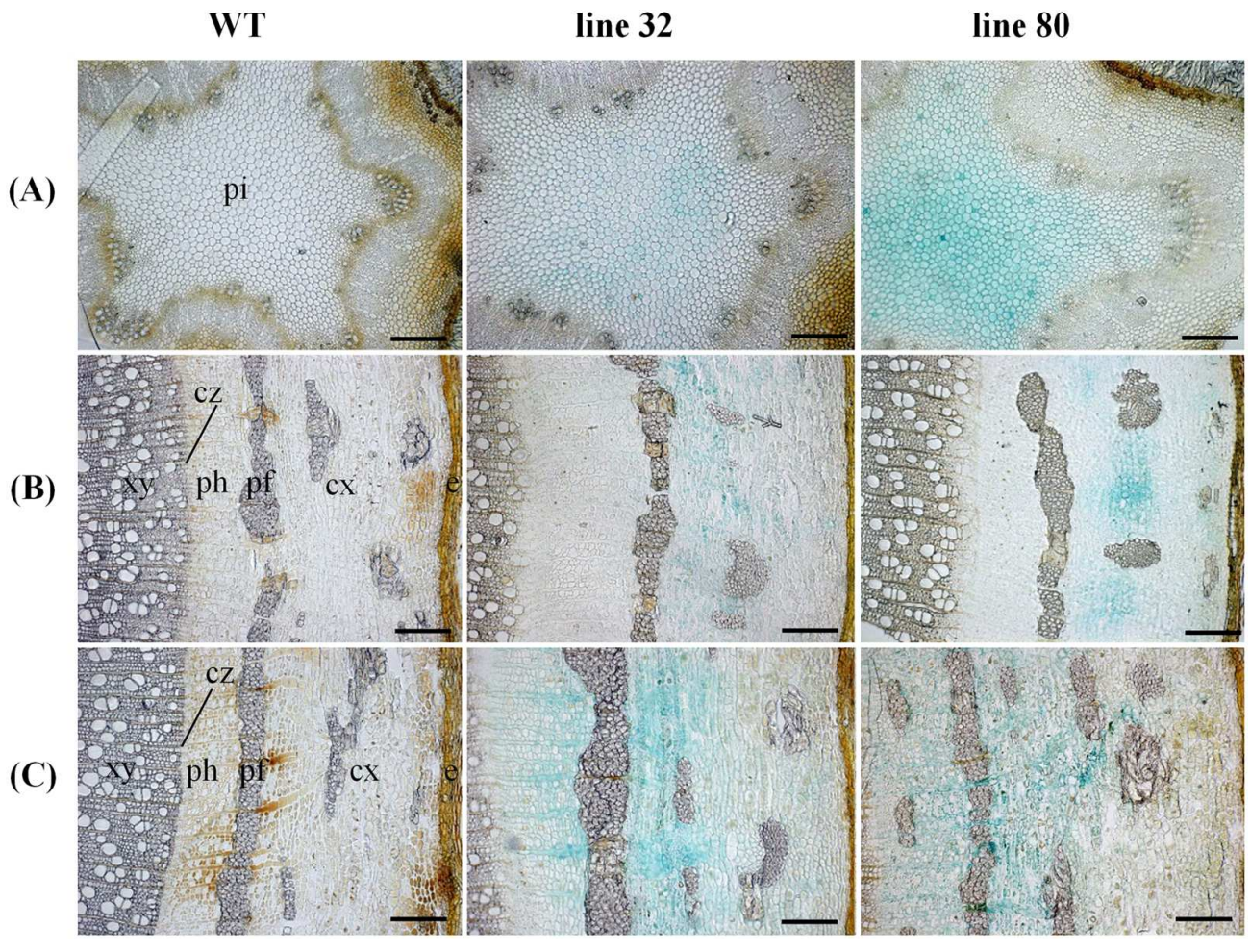

FIGURE 5 | Cellular localization of *ARR5::GUS* activity in different stem sections of *Populus* × *canescens* reporter lines and the WT in the growth phase. Representative pictures of $n = 4$ replicates per line are shown. Rows **(A–C)** represent stem top, stem middle, and stem bottom sections, respectively. Here, e, epidermis; cx, cortex; pf, phloem fibers; ph, phloem; cz, cambial zone; xy, xylem; and pi, pith. Scale bar = 200 μm.

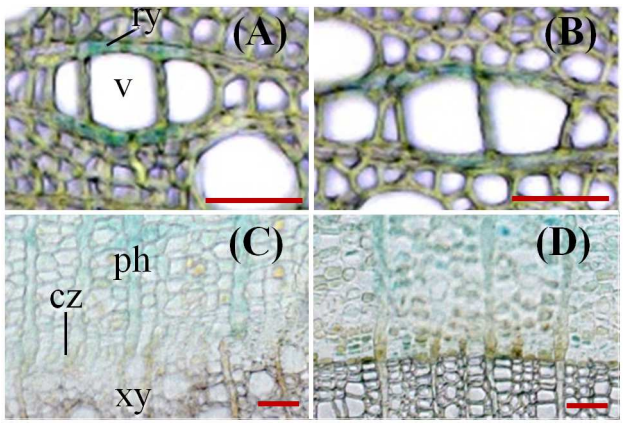

FIGURE 6 | *ARR5::GUS* activity observed in the xylem rays (A,B) and in cambium (C,D) at the stem bottom of *Populus* × *canescens* in the growth phase and during dormancy. (A,C) represent samples from growth phase and **(B,D)** represent samples during dormancy of line 32. The following abbreviations were used: ry, ray cell; v, vessel; ph, phloem; cz, cambial zone; and xy, xylem. Scale bar = 50 μm.

time. In winter, *ARR5::GUS* activity was present mainly in the outer pith region, the perimedullary zone (**Figure 8A**), whereas in the stem top sections from the growth phase most of the *ARR5::GUS* activity was localized in the center of the pith. In the stem middle, anatomy and the pattern of *ARR5::GUS* activity were similar to that at the stem bottom (**Figures 8B,C**). The *ARR5::GUS* activity extended across the whole cortex region of the bark and therefore, was stronger than in summer in this tissue (**Figures 8B,C**). Similar as in summer, the staining was pronounced in cell files that were connected with xylem rays (**Figures 8B,C**). *ARR5::GUS* activity was also localized in the cambial zone at the stem bottom during dormancy with a stronger signal than that detected in summer (**Figure 6D**).

Similar as in summer, the ray cells adjacent to vessels showed *ARR5::GUS* activity (**Figure 6B**), but the stain was less pronounced than in summer (**Figure 6A**). The *ARR5::GUS* activity in distinct locations of the xylem rays was only present at the stem bottom.

Tissue Specific Expression Pattern of PtRR Type-A Genes

The expression of genes belonging to the type-A RR family in poplar was analyzed in different tissues employing microarray data (**Figure 9**). Each of the 11 genes identified in poplar (Ramírez-Carvajal et al., 2008, cf. **Table 1**) had a probe set on the microarrays and therefore could be included here. There was no clustering of the *PtRR* transcriptional pattern according to tissues (not shown), but all tissues showed an expression of all *PtRR* type-A genes (**Figure 9**). The *PtRR* transcriptional pattern clearly clustered the genes in two categories, one comprising genes with low expression *(PtRR8*, *9,* and *11*) and the other with genes that showed variable expression across the tissues and season (*PtRR1*, *2*, *3*, *4*, *5*, *6*, *7,* and *10*). *PtRR10*, the ortholog of *ARR5*, was expressed in all tissues under study, especially in the phloem and elongation zone in the growth phase (**Figure 9**), thus supporting consistency between *PtRR10* expression and our reporter lines. In the fine roots from the growth phase, mainly *PtRR10* was expressed while in the young roots *PtRR5* was also expressed. *PtRR5*, *3,* and *1* showed strong expression in the phloem during the growth phase. In the cambium tissues during summer, *PtRR10* and *5* were mainly expressed. In developing xylem, during growth phase, *PtRR10*, *5,* and *6* showed strong expression. *PtRR5* showed a strong expression in the developing xylem in summer followed by *PtRR10* and *4*. In the summer rays, *PtRR10* and *1* showed strong expression. *PtRR7* was also expressed in summer ray cells. But in winter rays, only *PtRR1* showed strong expression. In the elongation zone of the stem, during the growth phase, *PtRR10*, *5*, *3*, *6*, *1*, and *5* were strongly expressed. In the shoot apex only *PtRR10* was strongly expressed.

DISCUSSION

The *ARR5::GUS* Construct Is Functional in Poplar

Many of the biological and developmental phenomena shared by herbaceous and woody plants are regulated by the same molecular mechanism. Besides having the same cytokinin signal transduction components, the type-*ARR* gene family found in *Arabidopsis* and poplar is well conserved in these two plant species (Immanen et al., 2013) with the highest similarity between *PtRR10* and *ARR5* (Ramírez-Carvajal et al., 2008; Immanen et al., 2013). Here, we show that the *ARR5::GUS* reporter construct was functional in poplar because it was inducible by the cytokinin analogs, thidiazuron and BAP and not by adenine, an inactive cytokinin analog. Thus, *ARR5::GUS* transformed poplar lines record the distribution of active cytokinins selectively. However, quantification of the signal is not possible because of the unknown turnover of GUS and the produced indigo dye.

Normal growth of the transgenic poplars indicated that there was no significant non-target effect of the biotechnological modification on plant performance. However, in one of the three reporter lines, *ARR5::GUS* construct was apparently silenced during long-term growth under ambient conditions. Silencing is not uncommon in transgenic plants and can have a number of different reasons (Stam et al., 1997; Fagard and Vaucheret, 2000). The synthetic promoter construct *TCS::GFP* for monitoring cytokinin in *Arabidopsis* was also subjected to silencing (Zürcher et al., 2013). Here, the two active reporter lines showed similar patterns of the *ARR5::GUS* activity in those tissues that also showed *PtRR10* expression, thus, supporting that they confidently recorded cytokinin activity.

The Localization of *ARR5::GUS* Identifies Novel Cytokinin-Active Cell Types in Poplar

In the growing phase, the main tissues with strong *ARR5::GUS* activity included the apical bud base, the root tips, pith in stem elongation zone, and bark in the stem middle and bottom. The localization of active cytokinins in the apical bud base and in

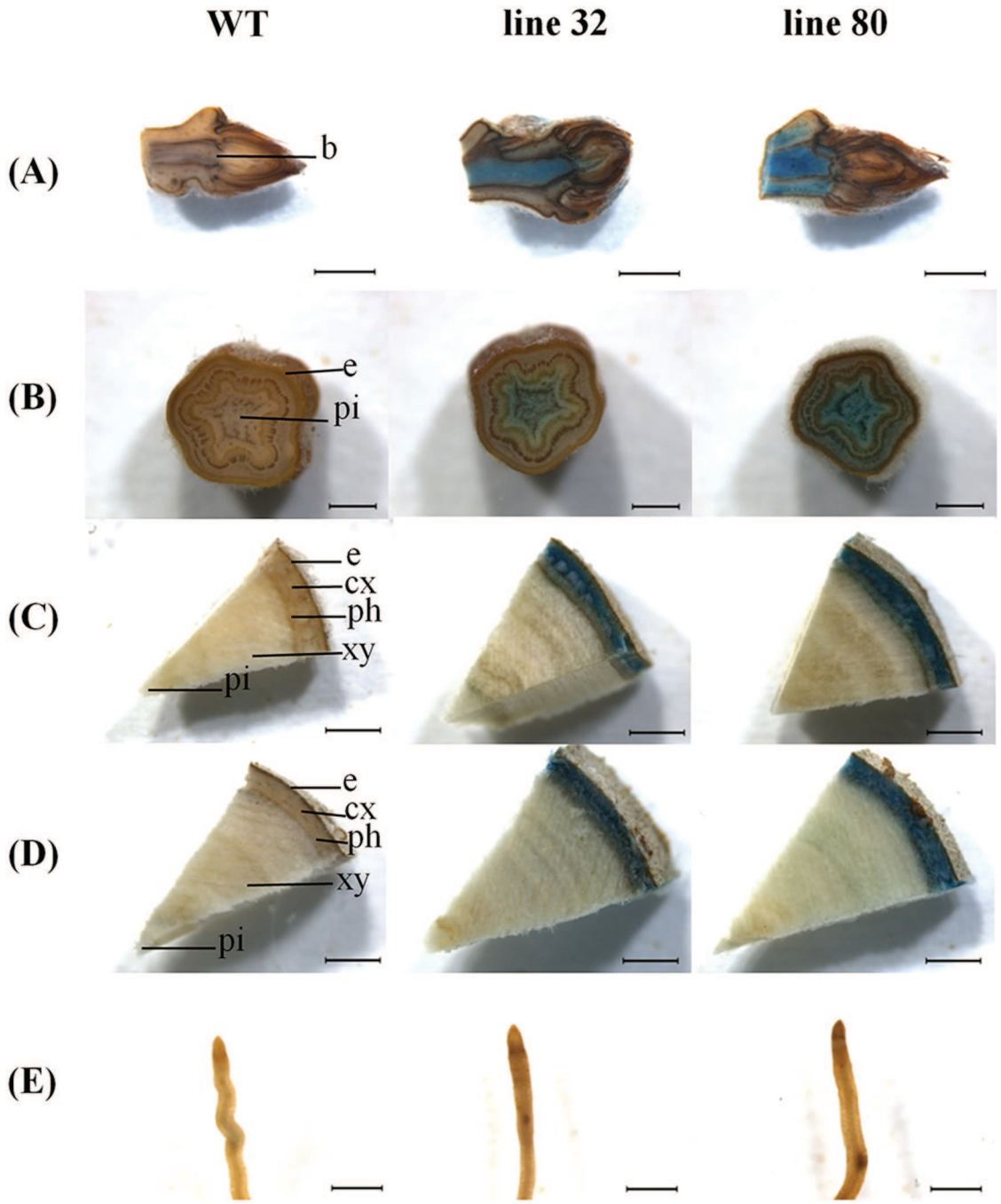

FIGURE 7 | *ARR5::GUS* activity observed in different tissues of *Populus* × *canescens* reporter lines and WT in winter. Representative pictures of $n = 2$ replicates per line are shown. Rows **(A–E)** represent apical bud, stem sections from top, middle, and bottom positions, and the root tips, respectively. In the pictures, b, apical bud base; e, epidermis; cx, cortex; ph, phloem; xy, xylem; and pi, pith. Scale bar = 2 mm for apical bud, stem middle, and stem bottom. Scale bar = 1 mm for stem top and root tip.

root tips shows strong similarity to that observed in *ARR5::GUS* expressing *Arabidopsis* seedlings (D'Agostino et al., 2000). In *Arabidopsis* seedlings, the primary and lateral root tips showed strong *ARR5::GUS* activity in the root cap region as well as in the cell division region and elongation zone with a gradual decrease toward the direction of the shoot apex (D'Agostino et al., 2000). This staining pattern was also evident in the growing season in poplar root tips in our study. Aloni et al. (2004) reported that the *ARR5::GUS* signal in *Arabidopsis* roots was produced in the statocytes.

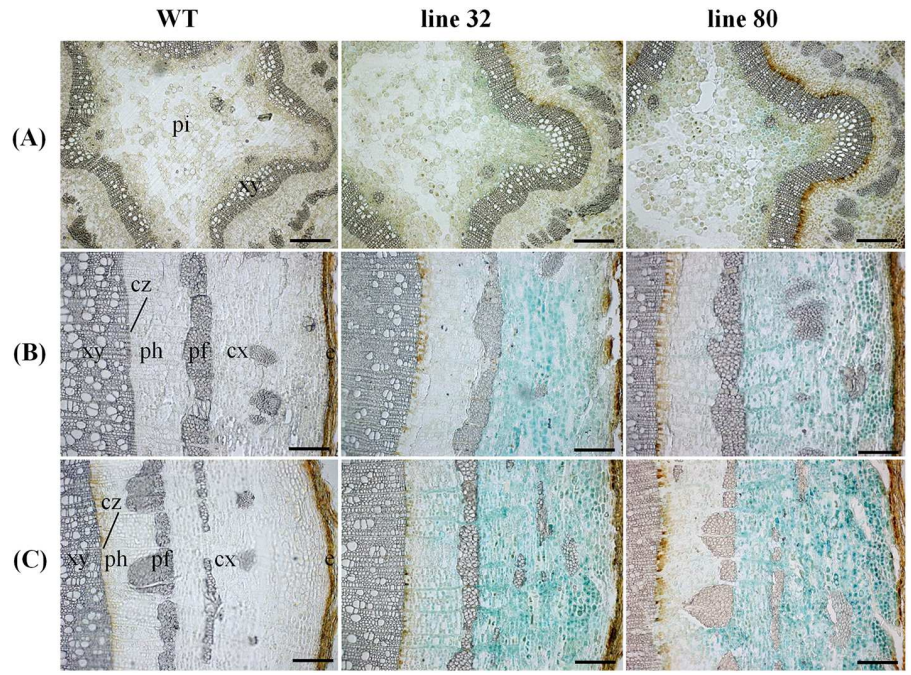

FIGURE 8 | Cellular localization of *ARR5::GUS* activity in different stem sections of *Populus* × *canescens* reporter lines and the WT in the growth phase. Representative pictures of $n = 2$ replicates per transgenic line. Rows **(A–C)** represent stem top, stem middle, and stem bottom sections, respectively. Here e, epidermis; cx, cortex; pf, phloem fibers; ph, phloem; cz, cambial zone; xy, xylem; and pi, pith. Scale bar = 200 μm.

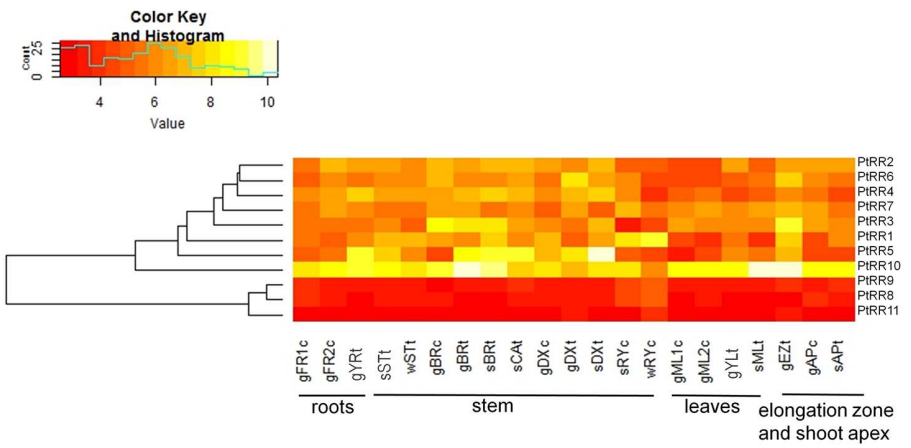

FIGURE 9 | Tissue-specific expression pattern of poplar genes belonging to the two component response regulator (*PtRR*) type-A gene family of cytokinin signaling pathway. The following abbreviations were used: FR, fine roots; YR, young roots; ST, stem bottom; BR, bark; CA, cambium; DX, developing xylem; RY, ray cells; ML, mature leaves; YL, young leaves; EZ, elongation zone; AP, shoot apex. The prefixes g, growing plants in controlled conditions; s, summer; and w, winter. The suffix c, tissues from *P.* × *canescens* and t, tissues from *P. trichocarpa*. The numbers 1 and 2 represent two different experiments. *PtRR9* has no assigned ARR name in *Arabidopsis* (see **Table 1**)

In the stem top, the observation of *ARR5::GUS* activity in the pith was unexpected, but similarly Teichmann et al. (2008) also had found auxin activity in this tissue. This finding suggests that the pith may have an important function for the hormone supply in the young stem, where the vascular system is not yet fully differentiated. Active cytokinins were also detected in the cambial zone of poplar, in agreement with studies showing that cytokinins are important regulators of cambial activity in growing poplars (Matsumoto-Kitano et al., 2008; Nieminen et al., 2008).

The presence of active cytokinins in the xylem ray cells, which was detected here, has not been reported so far, but was underpinned by high expression of poplar *PtRR10*, *PtRR1,* and *PtRR7* in this cell type. A noteworthy finding was that

the *ARR5::GUS* activity in the ray cells was seen only in parts associated with vessels. The biological significance of high cytokinin activity close to the vessels is unknown. However, root-derived cytokinin that are transported with the xylem sap through the vessel, are likely to be supplied by this route to the rays.

The *ARR5::GUS* staining pattern observed in the bark cortical cells, primary rays and in the cambium support previous studies reporting that cytokinins are necessary for determining vascular cell identities (Mähönen et al., 2000; Hutchison et al., 2006; Yokoyama et al., 2007; Argyros et al., 2008) and stimulate growth (Werner et al., 2003). The positional pattern of active cytokinin found here agrees with strong expression of the type-*ARR* genes *PtRR3, PtRR5,* and *PtRR10*) in the phloem of greenhouse grown *P. trichocarpa* (Ramírez-Carvajal et al., 2008). Furthermore, we found strong expression of *PtRR10*, *PtRR5*, *PtRR3,* and *PtRR1* in bark tissues. In the cambium *PtRR10* and *PtRR5* were highly expressed indicating responsiveness to cytokinins.

The reporter lines generally show expected localization pattern, but an exception was also noted. Although *PtRR10* was expressed in mature leaves, no *ARR5::GUS* activity was found in these tissues. One possibility is that *PtRR10* transcription is regulated by further signals to which *ARR5* is not responsive or the *ARR5::GUS* reporter construct is insensitive to cytokinins in fully expanded leaves in summer. Similar cases have been reported for poplar auxin reporter lines transformed with *GH3::GUS* (Teichmann et al., 2008) and *DR5::GUS* (Chen et al., 2013), where no activity of these constructs was noted in the cambium, a tissue in which an auxin maximum is expected. However, in our study *ARR5::GUS* activity was detected in the leaf primordia, where cytokinin levels determine leaf size (Holst et al., 2011) A comparison of *ARR5::GUS* activity along the stem with that of auxin reporter lines (*GH3::GUS*, *DR5::GUS*, Teichmann et al., 2008; Chen et al., 2013) shows overlap of the hormone activities in the elongation zone, but contrasting intensities in the bark. In *ARR5::GUS* poplars, the staining in bark was stronger toward the stem base, whereas that of auxin reporter lines decreased toward the base. These observations indicate that the phytohormone reporter lines also truly reflect the hormone gradients installed by the opposite apical production sites in roots for cytokinins and in the stem for auxin and the inverse transport pattern of these phytohormones along the stem (Jones and Ljung, 2011).

Cytokinin Activity Is Subject to Seasonal Fluctuations in Distinct Tissues

Seasonal fluctuation of cytokinin activity was most notable in the root tips, the major site of cytokinin synthesis (Aloni et al., 2004, 2005). The absence of *ARR5::GUS* activity in the root tips during dormancy together with a strong presence of *ARR5::GUS* activity in the apical bud base, in the pith, and in the bark suggests that the active cytokinins in these shoot tissues may be shoot-derived rather than root-derived. Cytokinins from different production sites have been distinguished by their chemical composition. Root-derived cytokinins are mainly of the *trans*-zeatin (tZ) type (Aloni et al., 2005), whereas phloem-transported isopentenyladenine (iP) type cytokinins are considered to be shoot-derived (Bishopp et al., 2011). In winter, the concentration of tZ is low in the xylem sap of willows, probably because of their decreased root production (Alvim et al., 1976), which corresponds to the lacking *ARR5::GUS* signal in our study. At the start of dormancy very high levels of the iP type are present in the phloem sap of 14 different tree species (Weiler and Ziegler, 1981). The studies with excised twigs of *Populus* × *robusta* and rootless almond shoots also confirm the presence of cytokinin after chilling (Hewett and Wareing, 1973; Van Staden and Dimalla, 1981). Increased cytokinin levels of the bark and in buds before the bud burst were further reported in artificially chilled, excised apple shoots (Cook et al., 2001). All these studies suggested that shoot derived cytokinins play a role in dormancy and the following bud burst in spring. The source of these cytokinins could be *de novo* biosynthesis or conversion of storage forms to their active forms (Skene, 1972; Kannangara and Booth, 1974; Van Staden and Brown, 1978; Van Staden, 1979; Van Staden and Dimalla, 1981). Collectively, these studies show that cytokinins are present in the dormant phase and together with our results on *ARR5::GUS* activity, it is clear that they are active in distinct cell types such as cortical and ray cells in the bark, pith, and ray cells next to vessels and in the shoot apex. In the cambial zone, a strong staining was also detected during dormancy. This observation may suggest a role of cytokinins in cambial cell maintenance in winter.

CONCLUSION

Employing an *ARR5::GUS* reporter, we monitored seasonal differences and similarities of cytokinin activity at the tissue and cellular level in poplar. Since cytokinins increase the sensitivity of the cambium to the auxin signal, they are important regulators of wood quantity and quality (Aloni, 1991, 2001). Therefore, the reporter lines can be used to investigate the involvement of cytokinins in mediating growth constraints and growth-promoting treatments for vascular development and cell type identities in the future. Thereby, these poplars may become an important tool to enhance our understanding of woody biomass production.

AUTHOR CONTRIBUTIONS

SP conducted field and laboratory experiments, analyzed data, and wrote the manuscript. HW supervised experiments, analyzed data, and commented on manuscript. DJ analyzed bioinformatic data and commented on the manuscript. TT constructed the vectors, characterized transformants, and commented on the manuscript. RH transformed plants, tested the transformants, and commented on the manuscript. AP designed the experiments, analyzed data, and wrote the manuscript. All authors contributed to the final version of the manuscript.

FUNDING

We are grateful to the German Science Foundation for financial support for the generation of the poplar lines in the frame of Poplar Research Group Germany (PRG, FOR546, Po362-12, Po362-13). SP thanks the European Commission for the Ph.D. scholarship in the Erasmus Mundus (India4EU II) program. The outdoor study was conducted in the frame of WATBIO (Development of improved perennial non-food biomass and bioproduct crops for water-stressed environments) which is a collaborative research project funded from the European Union's Seventh Programme for research, technological development and demonstration under grant agreement No. 311929. The publication fund of the University of Göttingen and the Deutsche Forschungsgemeinschaft supported open access publication of this article. This publication reflects the views only of the authors, and the European commission cannot be held responsible for any use which may be made of the information contained therein.

ACKNOWLEDGMENTS

We thank Merle Fastenrath, Marion Kay, Christine Kettner, Marianne Smiatacz, Giesbert Langer, and Monika Franke-Klein for maintenance of the stock cultures and for their excellent technical support of the outdoor study and Mareike Kavka for introducing array analyses using R to SP.

REFERENCES

Aloni, R. (1991). "Wood formation in deciduous hardwood trees," in *Physiology of Trees*, ed. A. S. Raghavendra (New York, NY: Wiley), 175–197.

Aloni, R. (2001). Foliar and axial aspects of vascular differentiation: hypotheses and evidence. *J. Plant Growth Regul.* 20, 22–34. doi: 10.1007/s003440010001

Aloni, R., Langhans, M., Aloni, E., Dreieicher, E., and Ullrich, C. I. (2005). Root-synthesized cytokinin in *Arabidopsis* is distributed in the shoot by the transpiration stream. *J. Exp. Bot.* 56, 1535–1544. doi: 10.1093/jxb/eri148

Aloni, R., Langhans, M., Aloni, E., and Ullrich, C. I. (2004). Role of cytokinin in the regulation of root gravitropism. *Planta* 220, 177–182. doi: 10.1007/s00425-004-1381-8

Alvim, R., Hewett, E. W., and Saunders, P. F. (1976). Seasonal variation in the hormone content of Willow: I. changes in abscisic acid content and cytokinin activity in the xylem Sap 1. *Plant physiol.* 57, 474–476. doi: 10.1104/pp.57.4.474

Argyros, R. D., Mathews, D. E., Chiang, Y.-H., Palmer, C. M., Thibault, D. M., Etheridge, N., et al. (2008). Type B response regulators of *Arabidopsis* play key roles in cytokinin signaling and plant development. *The Plant Cell Online* 20, 2102–2116. doi: 10.1105/tpc.108.059584

Bai, H., Euring, D., Volmer, K., Janz, D., and Polle, A. (2013). The nitrate transporter (NRT) gene family in poplar. *PLoS ONE* 8:e72126. doi: 10.1371/journal.pone.0072126

Bishopp, A., Help, H., El-Showk, S., Weijers, D., Scheres, B., Friml, J., et al. (2011). A mutually inhibitory interaction between auxin and cytokinin specifies vascular pattern in roots. *Curr. Biol.* 21, 917–926. doi: 10.1016/j.cub.2011.04.017

Chen, Y., Yordanov, Y. S., Ma, C., Strauss, S., and Busov, V. B. (2013). DR5 as a reporter system to study auxin response in *Populus*. *Plant Cell Rep.* 32, 453–463. doi: 10.1007/s00299-012-1378-x

Cook, N. C., Bellstedt, D. U., and Jacobs, G. (2001). Endogenous cytokinin distribution patterns at budburst in Granny Smith and Braeburn apple shoots in relation to bud growth. *Sci. Hortic.* 87, 53–63. doi: 10.1016/S0304-4238(00)00161-8

D'Agostino, I. B., Deruère, J., and Kieber, J. J. (2000). Characterization of the response of the *Arabidopsis* response regulator gene family to cytokinin. *Plant Physiol.* 124, 1706–1717. doi: 10.1104/pp.124.4.1706

Dieleman, J. A., Verstappen, F. W. A., Nicander, B., Kuiper, D., Tillberg, E., and Tromp, J. (1997). Cytokinins in *Rosa hybrida* in relation to bud break. *Physiol. Plant.* 99, 456–464. doi: 10.1111/j.1399-3054.1997.tb00560.x

Euring, D., Bai, H., Janz, D., and Polle, A. (2014). Nitrogen-driven stem elongation in poplar is linked with wood modification and gene clusters for stress, photosynthesis and cell wall formation. *BMC Plant Biol.* 14:391. doi: 10.1186/s12870-014-0391-3

Fagard, M., and Vaucheret, H. (2000). (Trans) gene silencing in plants: how many mechanisms? *Annu. Rev. Plant Physiol. Plant Mol. Biol.* 51, 167–194. doi: 10.1146/annurev.arplant.51.1.167

Gautier, L., Cope, L., Bolstad, B. M., and Irizarry, R. A. (2004). Affy-analysis of Affymetrix GeneChip data at the probe level. *Bioinformatics* 20, 307–315. doi: 10.1093/bioinformatics/btg405

Goodstein, D. M., Shu, S., Howson, R., Neupane, R., Hayes, R. D., Fazo, J., et al. (2012). Phytozome: a comparative platform for green plant genomics. *Nucleic Acids Res.* 40, D1178–D1186. doi: 10.1093/nar/gkr944

He, J., Li, H., Luo, J., Ma, C., Li, S., Qu, L., et al. (2013). A transcriptomic network underlies microstructural and physiological responses to cadmium in *Populus* × *canescens*. *Plant Physiol.* 162, 424–439. doi: 10.1104/pp.113.215681

Hewett, E. W., and Wareing, P. F. (1973). Cytokinins in *Populus* × *robusta* Schneid: a complex in leaves. *Planta* 112, 225–233. doi: 10.1007/BF00385326

Hirose, N., Takei, K., Kuroha, T., Kamada-Nobusada, T., Hayashi, H., and Sakakibara, H. (2008). Regulation of cytokinin biosynthesis, compartmentalization and translocation. *J. Exp. Bot.* 59, 75–83. doi: 10.1093/jxb/erm157

Holst, K., Schmülling, T., and Werner, T. (2011). Enhanced cytokinin degradation in leaf primordia of transgenic *Arabidopsis* plants reduces leaf size and shoot organ primordia formation. *J. Plant Physiol.* 168, 1328–1334. doi: 10.1016/j.jplph.2011.03.003

Hutchison, C. E., Li, J., Argueso, C., Gonzalez, M., Lee, E., Lewis, M. W., et al. (2006). The *Arabidopsis* histidine phosphotransfer proteins are redundant positive regulators of cytokinin signaling. *Plant Cell Online* 18, 3073–3087. doi: 10.1105/tpc.106.045674

Hwang, I., Sheen, J., and Müller, B. (2012). Cytokinin signaling networks. *Annu. Rev. Plant Biol.* 63, 353–380. doi: 10.1146/annurev-arplant-042811-105503

Immanen, J., Nieminen, K., Silva, H. D., Rojas, F. R., Meisel, L. A., Silva, H., et al. (2013). Characterization of cytokinin signaling and homeostasis gene families in two hardwood tree species: *Populus trichocarpa* and *Prunus persica*. *BMC Genomics* 14:885. doi: 10.1186/1471-2164-14-885

Janz, D., Behnke, K., Schnitzler, J.-P., Kanawati, B., Schmitt-Kopplin, P., and Polle, A. (2010). Pathway analysis of the transcriptome and metabolome of salt sensitive and tolerant poplar species reveals evolutionary adaption of stress tolerance mechanisms. *BMC Plant Biol.* 10:150. doi: 10.1186/1471-2229-10-150

Janz, D., Lautner, S., Wildhagen, H., Behnke, K., Schnitzler, J.-P., Rennenberg, H., et al. (2012). Salt stress induces the formation of a novel type of pressure wood in two *Populus* species. *New Phytol.* 194, 129–141. doi: 10.1111/j.1469-8137.2011.03975.x

Jefferson, R. A., Kavanagh, T. A., and Bevan, M. W. (1987). GUS fusions: β-Glucuronidase as a sensitive and versatile gene fusion marker in higher plants. *EMBO J.* 6, 3901–3907.

Jones, B., and Ljung, K. (2011). Auxin and cytokinin regulate each other's levels via a metabolic feedback loop. *Plant Signal. Behav.* 6, 901–904. doi: 10.4161/psb.6.6.15323

Kamada-Nobusada, T., and Sakakibara, H. (2009). Molecular basis for cytokinin biosynthesis. *Phytochemistry* 70, 444–449. doi: 10.1016/j.phytochem.2009.02.007

Kannangara, T., and Booth, A. (1974). Diffusible cytokinins in shoot apices of *Dahlia variabilis*. *J. Exp. Bot.* 25, 459–467. doi: 10.1093/jxb/25.2.459

Kauffmann, A., Rayner, T. F., Parkinson, H., Kapushesky, M., Lukk, M., Brazma, A., et al. (2009). Importing ARRAYEXPRESS datasets into R/ bioconductor. *Bioinformatics* 25, 2092–2094. doi: 10.1093/bioinformatics/btp354

Kieber, J. J., and Schaller, G. E. (2014). Cytokinins. *Arabidopsis Book* 12:e0168. doi: 10.1199/tab.0168

Ko, J.-H., Kim, H.-T., Hwang, I., and Han, K.-H. (2012). Tissue-type-specific transcriptome analysis identifies developing xylem-specific promoters in poplar: xylem-specificutility promoters in poplar. *Plant Biotechnol. J.* 10, 587–596. doi: 10.1111/j.1467-7652.2012.00690.x

Kolesnikov, N., Hastings, E., Keays, M., Melnichuk, O., Tang, Y. A., Williams, E., et al. (2015). ArrayExpress update-simplifying data submissions. *Nucleic Acids Res.* 43, D1113–D1116. doi: 10.1093/nar/gku1057

Larisch, C., Dittrich, M., Wildhagen, H., Lautner, S., Fromm, J., Polle, A., et al. (2012). Poplar wood rays are involved in seasonal remodeling of tree physiology. *Plant Physiol.* 160, 1515–1529. doi: 10.1104/pp.112.202291

Leple, J. C., Brasileiro, A. C. M., Michel, M. F., Delmotte, F., and Jouanin, L. (1992). Transgenic poplars: expression of chimeric genes using four different constructs. *Plant Cell Rep.* 11, 137–141. doi: 10.1007/BF00232166

Luo, Z.-B., Janz, D., Jiang, X., Gobel, C., Wildhagen, H., Tan, Y., et al. (2009). Upgrading root physiology for stress tolerance by ectomycorrhizas: insights from metabolite and transcriptional profiling into reprogramming for stress anticipation. *Plant Physiol.* 151, 1902–1917. doi: 10.1104/pp.109.143735

Mähönen, A. P., Bonke, M., Kauppinen, L., Riikonen, M., Benfey, P. N., and Helariutta, Y. (2000). A novel two-component hybrid molecule regulates vascular morphogenesis of the *Arabidopsis* root. *Genes Dev.* 14, 2938–2943. doi: 10.1101/gad.189200

Matsumoto-Kitano, M., Kusumoto, T., Tarkowski, P., Kinoshita-Tsujimura, K., Václavíková, K., Miyawaki, K., et al. (2008). Cytokinins are central regulators of cambial activity. *Proc. Natl. Acad. Sci. U.S.A.* 105, 20027–20031. doi: 10.1073/pnas.0805619105

Miyawaki, K., Matsumoto-Kitano, M., and Kakimoto, T. (2004). Expression of cytokinin biosynthetic isopentenyltransferase genes in *Arabidopsis*: tissue specificity and regulation by auxin, cytokinin, and nitrate. *Plant J.* 37, 128–138. doi: 10.1046/j.1365-313X.2003.01945.x

Mizuno, T. (2005). Two-component phosphorelay signal transduction systems in plants: from hormone responses to circadian rhythms. *Biosci. Biotechnol. Biochem.* 69, 2263–2276. doi: 10.1271/bbb.69.2263

Mok, D. W., and Mok, M. C. (2001). Cytokinin metabolism and action. *Annu. Rev. Plant Physiol. Plant Mol. Biol.* 52, 89–118. doi: 10.1146/annurev.arplant.52.1.89

Müller, A., Volmer, K., Mishra-Knyrim, M., and Polle, A. (2013). Growing poplars for research with and without mycorrhizas. *Front. Plant Sci.* 4:332. doi: 10.3389/fpls.2013.00332

Nieminen, K., Immanen, J., Laxell, M., Kauppinen, L., Tarkowski, P., Dolezal, K., et al. (2008). Cytokinin signaling regulates cambial development in poplar. *Proc. Natl. Acad. Sci. U.S.A.* 105, 20032–20037. doi: 10.1073/pnas.0805617106

Pils, B., and Heyl, A. (2009). Unraveling the evolution of cytokinin signaling. *Plant Physiol.* 151, 782–791. doi: 10.1104/pp.109.139188

R Core Team (2014). *R: A Language and Environment for Statistical Computing*. Vienna: R foundation for statistical computing. Available at: http://www.R-project.org/

Ramírez-Carvajal, G. A., Morse, A. M., and Davis, J. M. (2008). Transcript profiles of the cytokinin response regulator gene family in *Populus* imply diverse roles in plant development. *New Phytol.* 177, 77–89. doi: 10.1111/j.1469-8137.2007.02240.x

Romanov, G. A., Lomin, S. N., and Schmulling, T. (2006). Biochemical characteristics and ligand-binding properties of *Arabidopsis* cytokinin receptor AHK3 compared to CRE1/AHK4 as revealed by a direct binding assay. *J. Exp. Bot.* 57, 4051–4058. doi: 10.1093/jxb/erl179

Sakakibara, H. (2006). Cytokinins: activity, biosynthesis, and translocation. *Annu. Rev. Plant Biol.* 57, 431–449. doi: 10.1146/annurev.arplant.57.032905.105231

Schaller, G. E., Kieber, J. J., and Shiu, S.-H. (2008). Two-component signaling elements and histidyl-aspartyl phosphorelays. *Arabidopsis Book* 6:e0112. doi: 10.1199/tab.0112

Skene, K. G. (1972). Cytokinins in the xylem sap of grape vine canes: changes in activity during cold-storage. *Planta* 104, 89–92. doi: 10.1007/BF00387686

Stam, M., Mol, J. N., and Kooter, J. M. (1997). The silence of genes in transgenic plants. *Ann. Bot.* 79, 3–12. doi: 10.1006/anbo.1996.0295

Tanaka, M., Takei, K., Kojima, M., Sakakibara, H., and Mori, H. (2006). Auxin controls local cytokinin biosynthesis in the nodal stem in apical dominance. *Plant J.* 45, 1028–1036. doi: 10.1111/j.1365-313X.2006.02656.x

Taniguchi, M., Kiba, T., Sakakibara, H., Ueguchi, C., Mizuno, T., and Sugiyama, T. (1998). Expression of *Arabidopsis* response regulator homologs is induced by cytokinins and nitrate. *FEBS Lett.* 429, 259–262. doi: 10.1016/S0014-5793(98)00611-5

Teichmann, T., Bolu-Arianto, W. H., Olbrich, A., Langenfeld-Heyser, R., Göbel, C., Grzeganek, P., et al. (2008). GH3::GUS reflects cell-specific developmental patterns and stress-induced changes in wood anatomy in the poplar stem. *Tree Physiol.* 28, 1305–1315. doi: 10.1093/treephys/28.9.1305

Tromp, J., and Ovaa, J. C. (1990). Seasonal changes in the cytokinin composition of xylem sap of Apple. *J. Plant Physiol.* 136, 606–610. doi: 10.1016/S0176-1617(11)80221-X

Tsai, C. J., Ranjan, P., DiFazio, S. P., Tuskan, G. A., and Johnson, V. (2011). "Poplar genome microarrays," in *Genetics, Genomics and Breeding of Poplars*, eds C. P. Joshi, S. P. DiFazio, and C. Kole (Enfield: Science Publishers), 112–127.

Van Staden, J. (1979). Changes in the endogenous cytokinin levels of excised buds of *Salix babylonica* L., cultured aseptically. *Bot. Gaz.* 140, 138–141. doi: 10.1086/337069

Van Staden, J., and Brown, N. A. C. (1978). Changes in the endogenous cytokinins of bark and buds of *Salix babylonica* as a result of stem girdling. *Physiol. Plant.* 43, 148–153. doi: 10.1111/j.1399-3054.1978.tb01583.x

Van Staden, J., and Dimalla, G. G. (1981). The production and utilisation of cytokinins in rootless, dormant Almond shoots maintained at low temperature. *Z. Pflanzenphysiol.* 103, 121–129. doi: 10.1016/S0044-328X(81)80141-9

Warnes, G. R., Bolker, B., Bonebakker, L., Gentleman, R., Liaw, W. H. A., Lumley, T., et al. (2012). *Gplots: Various R Programming Tools for Plotting Data*. Available at: http://CRAN.R-project.org/package=gplots

Wei, H., Yordanov, Y. S., Georgieva, T., Li, X., and Busov, V. (2013). Nitrogen deprivation promotes *Populus* root growth through global transcriptome reprogramming and activation of hierarchical genetic networks. *New Phytol.* 200, 483–497. doi: 10.1111/nph.12375

Weiler, E. W., and Ziegler, H. (1981). Determination of phytohormones in phloem exudate from tree species by radioimmunoassay. *Planta* 152, 168–170. doi: 10.1007/BF00391189

Werner, T., Motyka, V., Laucou, V., Smets, R., Van Onckelen, H., and Schmülling, T. (2003). Cytokinin-deficient transgenic *Arabidopsis* plants show multiple developmental alterations indicating opposite functions of cytokinins in the regulation of shoot and root meristem activity. *Plant Cell Online* 15, 2532–2550. doi: 10.1105/tpc.014928

Yokoyama, A., Yamashino, T., Amano, Y.-I., Tajima, Y., Imamura, A., Sakakibara, H., et al. (2007). Type-B ARR transcription factors, ARR10 and ARR12, are implicated in cytokinin-mediated regulation of protoxylem differentiation in roots of *Arabidopsis thaliana*. *Plant Cell Physiol.* 48, 84–96. doi: 10.1093/pcp/pcl040

Yordanov, Y. S., Ma, C., Strauss, S. H., and Busov, V. B. (2014). EARLY BUD-BREAK 1 (EBB1) is a regulator of release from seasonal dormancy in poplar trees. *Proc. Natl. Acad. Sci. U.S.A.* 111, 10001–10006. doi: 10.1073/pnas.1405621111

Zürcher, E., Tavor-Deslex, D., Lituiev, D., Enkerli, K., Tarr, P. T., and Müller, B. (2013). A robust and sensitive synthetic sensor to monitor the transcriptional output of the cytokinin signaling network in planta. *Plant Physiol.* 161, 1066–1075. doi: 10.1104/pp.112.211763

Conflict of Interest Statement: The authors declare that the research was conducted in the absence of any commercial or financial relationships that could be construed as a potential conflict of interest.

frontiers in Plant Science

ORIGINAL RESEARCH
published: 22 August 2016
doi: 10.3389/fpls.2016.01228

Enhanced Tolerance of Transgenic Potato Plants Over-Expressing Non-specific Lipid Transfer Protein-1 (*StnsLTP1*) against Multiple Abiotic Stresses

Baniekal H. Gangadhar[1]†, Kappachery Sajeesh[2], Jelli Venkatesh[1†], Venkidasamy Baskar[1], Kumar Abhinandan[3], Jae W. Yu[1], Ram Prasad[4]* and Raghvendra K. Mishra[5]**

[1] Department of Molecular Biotechnology, Konkuk University, Seoul, South Korea, [2] School of Applied Biosciences, Kyungpook National University, Daegu. South Korea, [3] Department of Biological Sciences, University of Calgary, Calgary, AB, Canada, [4] Amity Institute of Microbial Technology, Amity University, Noida, India, [5] Amity Institute of Biotechnology, Amity University, Gwalior, India

Abiotic stresses such as heat, drought, and salinity are major environmental constraints that limit potato (*Solanum tuberosum* L.) production worldwide. Previously, we found a potential thermo-tolerance gene, named *StnsLTP1* from potato using yeast functional screening. Here, we report the functional characterization of *StnsLTP1* and its role in multiple abiotic stresses in potato plants. Computational analysis of StnsLTP1 with other plant LTPs showed eight conserved cysteine residues, and four α-helices stabilized by four disulfide bridges. Expression analysis of *StnsLTP1* gene showed differential expression under heat, water-deficit and salt stresses. Transgenic potato lines over-expressing *StnsLTP1* gene displayed enhanced cell membrane integrity under stress conditions, as indicated by reduced membrane lipid per-oxidation, and hydrogen peroxide content relative to untransformed (UT) control plants. In addition, transgenic lines over-expressing *StLTP1* also exhibited increased antioxidant enzyme activity with enhanced accumulation of ascorbates, and up-regulation of stress-related genes including *StAPX*, *StCAT*, *StSOD*, *StHsfA3, StHSP70,* and *StsHSP20* compared with the UT plants. These results suggests that *StnsLTP1* transgenic plants acquired improved tolerance to multiple abiotic stresses through enhanced activation of antioxidative defense mechanisms via cyclic scavenging of reactive oxygen species and regulated expression of stress-related genes.

Keywords: abiotic stress-tolerance, drought, heat stress, non-specific lipid transfer protein, salinity, *Solanum tuberosum*

OPEN ACCESS

Edited by:
Mauro Centritto, National Research Council, Italy

Reviewed by:
Aldo Ceriotti, National Research Council, Italy
Guzel Kudoyarova, Institute of Biology, Russia
Mukhtar Ahmed, Pir Mehr Ali Shah Arid Agriculture University, Pakistan

****Correspondence:***
Baniekal H. Gangadhar
gangubhm@gmail.com
Raghvendra K. Mishra
raghy_mishra@yahoo.com
Ram Prasad
rprasad@amity.edu

†Present address:
Baniekal H. Gangadhar, Department of Biotechnology and Crop Improvement, University of Horticultural Sciences, Bagalkot, India
Jelli Venkatesh, Department of Plant Science and Vegetable Breeding Research Center, Seoul National University, Seoul, South Korea

Specialty section:
This article was submitted to Agroecology and Land Use Systems, a section of the journal Frontiers in Plant Science

Received: *08 April 2016*
Accepted: *02 August 2016*
Published: *22 August 2016*

Citation:
Gangadhar BH, Sajeesh K, Venkatesh J, Baskar V, Abhinandan K, Yu JW, Prasad R and Mishra RK (2016) Enhanced Tolerance of Transgenic Potato Plants Over-Expressing Non-specific Lipid Transfer Protein-1 (StnsLTP1) against Multiple Abiotic Stresses. Front. Plant Sci. 7:1228. doi: 10.3389/fpls.2016.01228

INTRODUCTION

Plants growing in natural habitats are continuously subjected to multiple abiotic stresses such as drought, salinity, heat, cold and heavy metal stress. Adaptation and response to these stresses is extremely intricate and involve changes at molecular, cellular, and physiological levels. Among abiotic stresses, factors such as heat, drought, and salinity have a major impact on cultivated potato

(*Solanum tuberosum* L.), affecting yield, tuber quality, and market value (Levy and Veilleux, 2007). In order to counter the negative effects of these abiotic stresses, scientists around the globe are engaged in developing broad-spectrum abiotic stress tolerant potatoes, but efforts have met with varying degree of success due to limited understanding of molecular mechanisms involved in abiotic stress-tolerance (Levy and Veilleux, 2007; Kappachery et al., 2015). In this scenario, it is important to identify potential candidate genes or gene networks associated with broad-spectrum multiple abiotic stress-tolerance. In our earlier publications, we reported 95 potential candidate genes responsible for imparting thermo-tolerance in potato using yeast functional screening approach (Gangadhar et al., 2014). Among 95 genes, 11 were found to be associated with multiple stress-tolerance (drought, salt and heat stress) in potato. The functional relevance of previously identified genes, *GLP1* (Germin-like protein 1), *nsLTP*1 (Non-specific lipid transfer protein1), *PI-PLC* (phosphoinositide-specific phospholipase-c), *CHP* (Conserved hypothetical protein) and *RPL4* (60 S Ribosomal L4/L1 protein) genes in improving abiotic stress-tolerance was confirmed by using virus induced gene silencing (VIGS) (Gangadhar et al., 2016). Herein, *StnsLTP1* is used as candidate gene for developing broad-spectrum multiple abiotic stress tolerant potato using genetic engineering.

Plant non-specific lipid transfer protein (nsLTPs) are low molecular mass basic proteins belong to the plant specific prolamin super family (Kader, 1997). To date a large number of LTPs have been described from various species, such as *Arabidopsis*, cotton, wheat, rice, and tobacco (Kinlaw et al., 1994; Feng et al., 2004; Liu et al., 2006; Boutrot et al., 2008). Besides mediating phospholipid transfer, plant LTPs have been implicated with the various biological functions, such as seed storage, lipid mobilization, cuticle synthesis, somatic embryogenesis and pollen tube adhesion (Carvalho and Gomes, 2007). LTPs have been found to modulate plant tolerance brought-out by environmental changes such as drought, cold, salt stress and also infection with bacterial and fungal pathogen (Sarowar et al., 2009; Choi et al., 2012; Guo et al., 2013). For instance, over-expression of pepper LTPs, *CALTP1* and *CALTP2* genes enhanced resistance to oomycete pathogen, *Phytophthora nicotianae* and bacterial pathogen, *Pseudomonas syringae* (Sarowar et al., 2009). More recently, over-expression of *Arabidopsis* nsLTP (*AtLTP3*) gene exhibited improved performance of *Arabidopsis* seedlings under salt, drought, and cold stress (Guo et al., 2013; Zou et al., 2013). However, the biological role of LTPs in improving abiotic stress-tolerance of potato is still an unsolved question. To date best evidence for the role of *StnsLTP1* in abiotic stress-tolerance came from our previous reports in which the heterologous expression of *StnsLTP1* in yeast cells (*Saccharomyces cerevisiae*) was found to enhance resistance to yeast cells to severe heat stress (Gangadhar et al., 2014). Later we confirmed its role in imparting improved thermo-tolerance in higher plants using VIGS (Gangadhar et al., 2016). The objectives of this study are to express a *StnsLTP1* gene in potato and to investigate its potentially increased resistance to multiple abiotic stress induced oxidative stresses by over-produced H_2O_2 via induction of antioxidant enzymes.

MATERIALS AND METHODS

Plant Material and Growth Conditions

In vitro cultures of potato (*S. tuberosum*) cv. 'Desiree' were initiated from nodal segments and cultured in standard flat bottom culture boxes (100 mm × 110 mm) on Murashige and Skoog (MS) basal medium containing 2% (w/v) sucrose and gelled with 0.8% (w/v) plant agar (Duchefa, Germany). After every 4 weeks, nodal segments were excised and sub cultured on fresh MS medium for multiplication. The cultures were maintained at 24 ± 1°C with light: dark regime of 16: 8 h and light intensity of 40 μmol m^{-2} s^{-1} in growth chambers.

Isolation and Gateway Cloning of *StnsLTP1* Gene

Full length cDNA encoding potato *StnsLTP1* (345 bp; Genbank accession- JX576237) was isolated from back transformed *Escherichia coli* plasmids containing specific cDNAs using gene specific prepared previously in our lab (Gangadhar et al., 2014; Supplementary Table S1). The coding region of *StnsLTP1*gene was prepared through PCR (95°C for 5 min, followed by 30 cycles of 95°C for 1 min, 55°C for 45 s and 72 °C for 5 min) using forward primer, 5- CACCATGGAAATGTTTGGCAAAATTGCAT-3 and the reverse primer, 5- TTACTGGAC CTTGGAGCAATCAGTG -3 containing CACC over hang at 5 end of the forward primer in order to clone into pENTR™ /D-TOPO® vector. The desired *StnsLTP1* DNA was PCR eluted according to manual instructions of FavorPrep GEL/PCR Purification Kit. Cloning of *StnsLTP1* was carried out using PCR amplification-based Gateway cloning method as described by Kumar et al. (2013). The purified *StnsLTP1* DNA fragments were cloned into pENTR™ /D-TOPO® vector using pENTR™ Directional TOPO® Cloning Kit (Invitrogen, Carlsbad, CA, USA), and the positive entry clones containing *StnsLTP1* gene was confirmed by colony PCR using M13 forward (−20) and M13 reverse primers (Supplementary Table S1). After confirming the sequence, entry clone including *StnsLTP1* gene was further mobilized into a plant expression vector PMDC32 using LR Clonase II™ enzyme mix, (Invitrogen, Carlsbad, CA, USA), orientation and cloning of *StnsLTP1* gene was confirmed by colony PCR and DNA sequencing using PMDC32 specific forward and reverse primers as provided in Supplementary Table S1. The resulting construct, *StnsLTP1* gene under the control of the 2 × 35 S CaMV (cauliflower mosaic virus) promoter, were transferred into *Agrobacterium tumefaciens* GV3101 by using the gene pulser (Bio-Rad, Hercules, CA, USA).

Development of *StnsLTP1* Over-Expression Potato Transgenic Lines

Transgenic potato plants expressing *StnsLTP1* gene were generated using *A. tumefaciens* mediated transformation according to the protocol described by Kappachery et al. (2015). Hygromycin resistant shoots were excised and transferred to the rooting medium (MS basal, 20 g l^{-1} sucrose, 250 mg l^{-1} cefotaxime, 25 mg l^{-1} hygromycin). Putative transformants

were multiplied by nodal culture, and the insertion of the cassette carrying the transgene into genomic DNA was confirmed by PCR, Southern blotting and quantitative real-time reverse transcription PCR (qPCR). Genomic DNA was isolated from control and putative transgenic potato leaves according to Allen et al. (2006), and its purity was evaluated using Nano Drop ND-100 Spectrophotometer (Nano Drop Technologies, USA). Putative transgenic lines of potato were identified using hygromycin phosphotransferase (*hpt)* gene and pMDC32 vector specific primer flanking *StnsLTP1* gene (Supplementary Table S1). For Southern blotting, genomic DNA (30 μg) isolated from wild-type and putative transgenic plants were restrict digested with *EcoRI*, and separated on a 0.8% agarose gel. DNA was transferred onto a nylon membrane (Bio-Rad, USA) and hybridized with a probe for *hpt* gene. The probe was labeled using a Biotin DecaLabel kit (K0652, Fermentas, EU), and the membrane was then detected using the Biotin Chromogenic Detection Kit (K0661, Fermentas, EU), according to the manufacturer's instructions.

To evaluate the possible role of the *StnsLTP1* gene in imparting tolerance to multiple abiotic stresses, we monitored expression levels of mRNA from different tissue of potato plantlets (leaf, stem, root, whole plant) subjected to heat, drought, and salinity stress treatments using qPCR. Total RNA was isolated from young leaves using Nucleo-Spin RNA plant mini prep kit (Macherey–Nagel, Germany) and genomic DNA contamination was removed with RNAse-free DNAse I (New England Biolabs, USA) treatment. First strand cDNA was prepared from 1 μg of total RNA using Accu-power rocket script RT premix kit (Bioneer, Korea). Real-time PCR amplification of the *StnsLTP1* gene was carried out using SYBR green master mix in Bio-Rad CFX96 real-time PCR system at 95°C for 10 min, followed by 29 cycles of 95°C for 20 s, 60°C for 45 s. Later, the products were analyzed through a melt curve analysis to check the specificity of PCR amplification. Each reaction was performed in triplicates, and the relative expression ratio was calculated using the $2^{-\Delta\Delta ct}$ method employing the *S. tuberosum actin* gene as the reference. The primers used in this study have been listed in (Supplementary Table S1).

Stress Treatments

To assess the physiological and biochemical changes in plants under stress, 4-week old *StnsLTP1* transgenic and wild-type control plants grown in glasshouse conditions were subjected to different abiotic stress treatments. To assess thermo-tolerance, plants were initially acclimated by gradual increase in the temperature by 5°C in every 3 h, reaching to 30, 35, 40°C and finally maintained at 45°C for 24 h. For the salt stress, the plants were watered through trays underneath the pots with 200 mM NaCl solution for 15 days and drought stress was initiated by suspending watering the plants for 12 days. Non-stress treatment plants were maintained at 23 ± 1°C with regular irrigation with water (**Supplementary Figure S1**). All of the measurements of the physiological and biochemical parameters were performed on the fully expanded leaves. Cell membrane stability, cell viability, chlorophyll content, lipid per-oxidation [malondialdehyde (MDA) contents] and tissue-specific expression under different stress using qPCR was assessed from *StnsLTP1* transgenic and UT plants as described earlier (Gangadhar et al., 2016). Detailed protocol can be found in Supplementary Table S2.

Quantification of Relevant Antioxidant Compounds

Total ascorbic acid was measured according to Davies and Masten (1991), as ascorbates acts as scavenger of toxic reactive oxygen species (ROS) including the superoxide radical (O_2^-), the hydroxyl radical (OH^-) and hydrogen peroxide (H_2O_2). *StnsLTP1* transgenic and UT leaf samples (1 g) collected from stress and non-stress treatments was extracted using 1% of phosphate citrate buffer pH 3.5 using chilled mortar and pestle. The homogenate was then centrifuged at 10000 rpm at 4°C for 10 min. One milliliter of 2 mM 2,6- dichloroindophenol (2,6-DCPIP) was added to supernatant and the absorbance was recorded at 518 nm. The concentration of total ascorbic acid content was expressed as mg g^{-1} FW. For determination of reduced glutathione (GSH) content, the leaves of potato plants were homogenized in an ice bath with 5% (w/v) sulfosalicylic acid and centrifuged at 10000 rpm for 10 min. The supernatant was used for reduced glutathione (GSH) estimation and the GSH content was assayed following the change in absorbance at 412 nm after the addition of 5,5′-dithio-2,2′-dinitrobenzoic acid (DTNB) according to the method of Griffith (1980). The concentration of GSH content was expressed as μmol g^{-1} FW.

Estimation of Hydrogen Peroxide Levels and Antioxidant Enzyme Activities

The hydrogen peroxide (H_2O_2) content in leaves collected from *StnsLTP1* transgenic and UT plants was determined by the ferrous ammonium sulfate/xylenol orange method as described by Cheeseman (2006). A standard curve was prepared from serial dilutions of H_2O_2 with concentration ranging from 100 to 1000 μmol ml^{-1} and R^2 coefficient of 0.94. Data were normalized and expressed as micro-molar H_2O_2 g^{-1} FW of leaves.

To understand the signaling roles of *StnsLTP1* mediated up-regulation of antioxidant enzyme activities by providing tolerance to abiotic stresses induced oxidative damage was tested by measuring activities of antioxidant enzymes. Leaf samples (1 g) from the *StnsLTP1* over-expressed and UT potato plants subjected to different heat stress treatments as well as non-stress conditions were collected and homogenized using liquid N_2. Protein was extracted using 0.1 M potassium phosphate extraction buffer (pH 7.5) containing 50% (v/v) glycerol, 16 mM $MgSO_4$, 0.2 mM PMSF and 0.2% PVP at 4°C. The homogenate was centrifuged at 13,000 × g for 30 min at 4°C. Activities of ascorbate peroxidase (APX), catalase (CAT), superoxide dismutase (SOD) and Glutathione reductase (GR) were measured as described earlier (Hemavathi et al., 2011). The protein content of these enzyme extracts was determined using coomasive brilliant blue according to the method of Bradford (1976).

Expression Profiling of Antioxidant and Stress-Responsive Genes Using Quantitative Real-Time PCR (qRT-PCR)

Total RNA isolation and cDNA synthesis was performed as described earlier from *StnsLTP1* transgenic and UT potato plants subjected to stress and non-stress conditions. All gene specific qPCR primers were designed based on their cDNA sequences are listed in Supplementary Table S3. The expression of genes encoding heat stress-responsive proteins and antioxidant enzymes such as *StHSP70* (encoding 70-kD heat shock protein), *StHSFA3* (encoding heat stress transcription factor A3), *StHSP90* (encoding 90-kD heat shock protein), *StsHSP20* (encoding class I small heat shock protein 20.1), *StAPX*, *StCAT*, *StSOD* and *StGR* was qPCR assayed using SYBR green qPCR kit as previously described (Gangadhar et al., 2014).

Sequence Analysis of *StnsLTP1*

The pI (isoelectric point) and Mw (molecular weight) predictions were performed using the Compute pI/Mw tool[1]. The signal peptide was predicted using online SignalP, version 4.0[2]; Petersen et al., 2011). Multiple sequence alignments were carried out with ClustalX, version 1.83 (Thompson et al., 1997). Three dimensional structures (3D) of StnsLTP1 were generated using the SWISS-MODEL server ([3]Arnold et al., 2006). The details of sequences used for multiple sequence alignment analysis can be found in Supplementary Table S4.

Statistical Analysis

All the experiments were independently carried out at least three times with transgenic and UT control lines, and each time with three replicates for all measurements. The means were analyzed using the Origin 8.1 program. The statistical differences between the treatment means were determined using one-way analysis of variance followed by Turkey's test ($P < 0.05$), and standard error was calculated.

RESULTS

Isolation and Sequence Analysis of *StnsLTP1* cDNA from Potato

Full length cDNA encoding *StnsLTP1* was isolated from potato cDNA expression library (Gangadhar et al., 2014) using gene specific primers. The deduced aminoacid sequence of *StnsLTP1*encodes an open reading frame containing 114 amino acids. The putative polypeptide of *StnsLTP1* contains a typical signal peptide of 24 amino acid residues at the N terminus and molecular mass of 8.7 kDa with theoretical pI of 8.8. Multiple amino acid sequence alignments showed that *StnsLTP1* contains the conserved lipid binding motifs such as DRQ and CGV and the eight conserved cysteine residues involved in formation of four disulfide bridges, following typical pattern of type I *nsLTP* {C X_2 V X_6 C [L] XY [L] X_{12} CC X G X_{12} DR [K] X_2 CXC X_{20} P X_2 C X_{13} C} as reported by Wang et al. (2012; **Figure 1**). Further sequence analysis with other plant *nsLTPs* revealed that *StnsLTP1* shares 83% sequence homology with *Solanum lycopersicum LTP* (*SlTSW12*; CAA39512) and more than 50 % homology with *Spinacia oleracea LTP* (*SoLTP*; AAA34032), *Beta vulgaris LTP* (*BvLTP*; Q 43748), *Betula platyphylla LTP* (*BPLTP*; AFR31532), which recently has been reported to be involved in imparting tolerance to several abiotic and biotic stresses in plants. The 3D structure of *StnsLTP1* was predicted using maize nsLTP (PDB Code: 1FK5) as a template, whose 3D structure has been determined by X-ray crystallography (Han et al., 2001). The hypothetical 3D structural model of *StnsLTP1* shows a protein that contains four α-helices, with a secondary structure compacted by four disulfide bridges and a C-terminal tail. The four bridges are formed by Cys27 and Cys73, Cys37 and Cys50, Cys51 and Cys26, and Cys71 and Cys110 (**Figure 1**). These results allow us to propose that this potato nsLTP (i.e., *StnsLTP1*) gene belongs to the type 1 nsLTP family.

Tissue-Specific Expression Patterns of *StnsLTP1* under Various Abiotic Stresses

The results of qPCR analysis showed that the expression level of *StnsLTP1* was significantly different in different tissues under stress and non-stress conditions in UT potato plants (**Figure 1**). In absence of abiotic stress (heat, drought, and salt stress), *StnsLTP1* transcript accumulation was low in almost all organs tested, while its expression increased significantly upon heat stress in the leaves, stem and whole plant except roots. Whereas, upon drought or salt stress, expression of *StnsLTP1* was significantly higher in whole plant and roots compared other tissues tested. Thus, indicating that expression of *StnsLTP1* gene might responsible for inducing tolerance to multiple abiotic stresses.

Molecular Analysis of Transgenic Potato Plants Over-Expressing *StnsLTP1*

Agrobacterium-mediated transformation of *StnsLTP1* gene and selection of hygromycin resistant transgenic plants produced 15 independent transformants. All of the 15 putative regenerated plants were PCR positive for both *StnsLTP1* (*StnsLTP1*gene flanked with pMDC32 vector) and *hpt* genes. Among them three representative transgenic lines (L1, L2, and L3) were selected for further studies (**Figures 2A,B**). Southern blot analysis of three transgenic lines showed successful integration of T-DNA into transgenic plant genomes, whereas no hybridization signal was detected in UT control plants. The variable size of gene on the blot indicated independent integration events in different transgenic plants (**Figure 2C**). The mRNA expression levels of *StnsLTP1* gene in putative transgenic lines is confirmed using qPCR. As shown **Figure 2D**, we noted that the expression of *StnsLTP1* in transgenic plants under different abiotic stresses (heat, drought, and salinity stress) was relatively higher in transgenic lines compared to UT control plants. Whereas, the levels of *StnsLTP1* expression was slightly increased in all three transgenic lines compared to UT control plants under normal growth conditions.

[1]http://web.expasy.org/compute_pi/

[2]http://www.cbs.dtu.dk/services/SignalP/

[3]http://swissmodel.expasy.org/

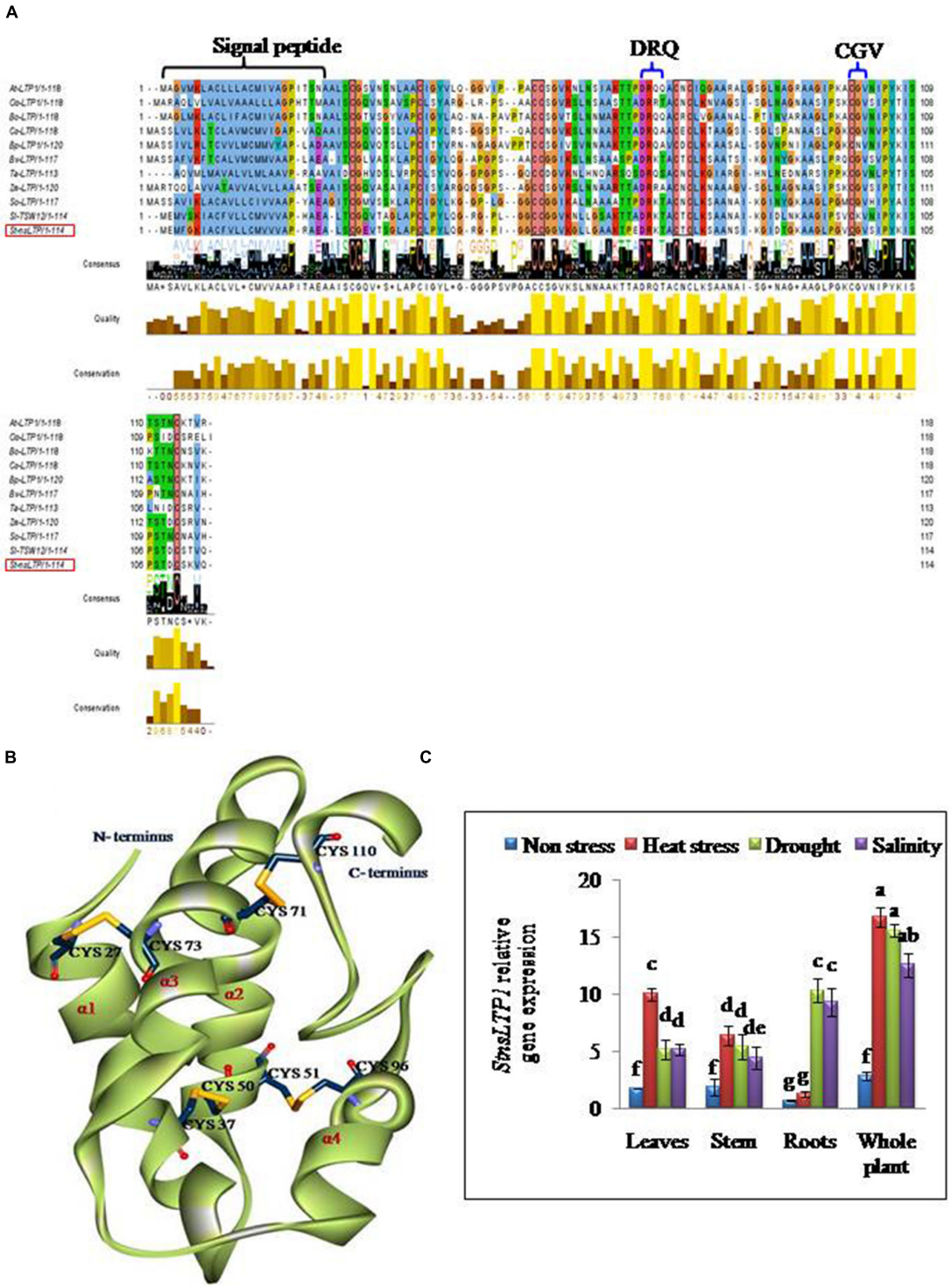

FIGURE 1 | *StnsLTP1* sequence analysis and stress specific expression in wild-type potato plants. (A) Alignment of the deduced StnsLTP1 sequence with other known plant nsLTP sequences. The amino acid sequences used in the alignment were from *Arabidopsis thaliana* (NP_181388.1), *Oryza sativa* (AAP92127), *Brassica oleracea* (AAA73948), *Castanea sativa* (ADK60918), *Betula platyphylla* (AFR31532), *Beta vulgaris* (Q43748), *Triticum aestivum* (P24296), *Spinacia oleracea* (AAA34032), *Solanum lycopersicum* (CAA39512), and *Zea mays* (P19656). The probable signal peptide sequence and lipid binding motifs (DRQ and CGV) in StnsLTP1 are indicated by flower bracket. The eight strictly conserved cysteine residues are boxed in black. **(B)** A 3D model of putative StnsLTP1 protein is shown as a ribbon model. The N-terminal and C-terminal are marked and the four α-helices are labeled α1–α4. The cysteine side chains forming the four disulfide bridges are showed as stick models. **(C)** Tissue-specific expression pattern of the *StnsLTP1* gene in control potato plants under heat, drought and salinity stress and non-stress using qRT-PCR.

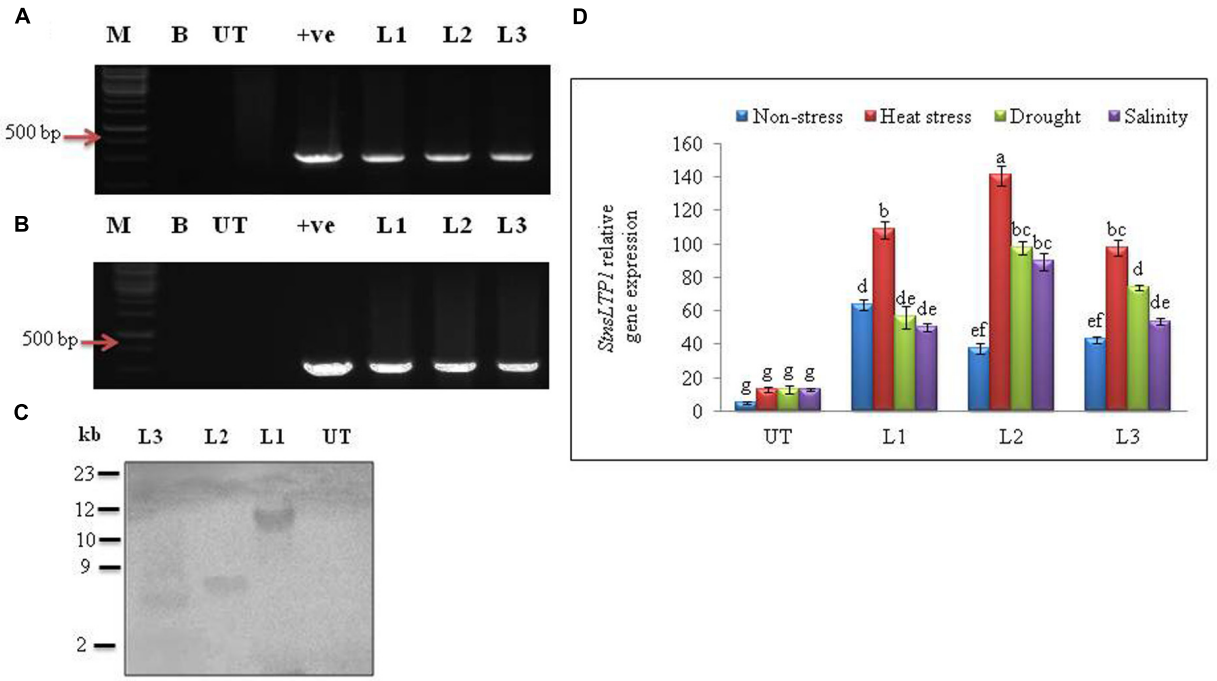

FIGURE 2 | Molecular analysis of putative transgenic potato lines over-expressing *StnsLTP1*. (A) PCR amplification of *StnsLTP1* gene using gene specific primers. **(B)** PCR amplification using hygromycin phosphotransferase (*hpt*) gene. **(C)** Southern blot analysis of different independent potato control (Untransformed-UT), putative *StnsLTP1* transgenic lines (L1, L2, and L3). **(D)** The relative *StnsLTP1* expression levels in UT and transgenic lines (L1, L2, and L3) under non-stress as well as heat, drought and salinity stress conditions. M: 1000 bp DNA Ladder (+): positive control PCR from pMDC32 plasmid and B- water blank. Means of three independent samples and standard errors are presented. The same letters above the columns indicate no significant difference at $P < 0.05$.

Over-Expression of *StnsLTP1* Gene Enhances Tolerance to Heat, Drought, and Salt in Transgenic Potato

In the thermo-tolerance test, the *StnsLTP1* transgenic lines had higher survival rates than UT control plants. The survival rate of *StnsLTP1* transgenic plants (lines L1, L2, and L3) were 72, 89, and 70%, respectively, whereas UT control survival was only 10%. Drought induced by withholding watering produced similar results. In the salt tolerance test, *StnsLTP1* transgenic plants (lines L2 and L3) had survival rates of 77 and 54%, respectively, whereas the UT control plants had a survival rate of 7% (**Table 1**). These data suggest that *StnsLTP1* is a functional protein that improves the tolerance to multiple abiotic stresses in potato. To further confirm the multiple abiotic stress-tolerances observed in *StnsLTP1* over-expression lines, we carried out a quantitative assay for abiotic stress-tolerance based on cell membrane stability, cell viability and chlorophyll content of transgenic and UT plants subjected to stress and non-stress conditions (**Table 1**; **Figures 3A,B**). Upon abiotic stress, *StnsLTP1* over-expression lines (L2 and L3) showed notable improvements of cell viability, membrane stability index and reduced chlorophyll degradation than UT control plants. In summary, enhanced survival rates of *StnsLTP1* transgenic lines were associated with higher cell viability, membrane stability index and reduced chlorophyll degradation.

Over-Expression of *StnsLTP1* Gene Enhanced the Ability of ROS Scavenging under Multiple Abiotic Stresses

Abiotic stresses result in the accumulation of ROS in plants. H_2O_2 is one of the most common ROS produced in the plants and its levels were found significantly higher in UT control plants as compared to the *StnsLTP1* transgenic potato plants under stress conditions (**Figure 4A**). *StnsLTP1* transgenic lines (L1 and L2) showed significantly reduced H_2O_2 production under heat and drought stress compared to UT control plants. In all the applied stress (heat, drought, and salinity stress) conditions as well as non-stress condition, UT control plants showed almost threefold higher levels of H_2O_2 as compared to the corresponding *StnsLTP1* transgenic plants. MDA, which causes membrane lipid per-oxidation, is a final product of the accumulation of ROS under stresses. Therefore MDA content in under stress can directly indicate the damage of the plants. The level of MDA as a consequence of heat, drought, and salinity stresses was increased in both *StnsLTP1* transgenic lines and UT plants. However, the transgenic lines accumulated less than three times (20–34 nmolg^{-1} FW) of MDA compared to UT control plants (90–102 nmolg^{-1} FW) under multiple abiotic stress conditions (**Figure 4B**). The specific activity of APX was increased 3.3, 2.8 and 3.0 times higher in *StnsLTP1* transgenic line (L2) compared to UT control plants when treated with heat, drought, and salinity stress respectively. Highest APX specific activity was

TABLE 1 | Estimation of growth and biochemical parameters of *StnsLTP1* transgenic lines (L1, L2, and L3) and UT potato plants, during non-stress, heat, drought and salinity stress conditions.

Treatment	Shoot length (cm)	Root length (cm)	Survival rate (%)	Chlorophyll (mg g^{-1} FW)	Ascorbate content (mg g^{-1} FW)	GSH content (μmol g^{-1} FW)
Non-stress						
L1	14.0 ± 0.5b	9.1 ± 0.7a	96.4 ± 0.5a	9.2 ± 0.2ab	8.3 ± 0.1b	0.2 ± 0.01ab
L2	16.5 ± 0.1a	9.5 ± 0.8a	96.4 ± 0.7a	9.9 ± 0.2a	10.5 ± 0.8a	0.3 ± 0.02ab
L3	15.5 ± 0.5a	8.9 ± 0.3a	98.5 ± 0.6a	9.4 ± 0.1a	7.4 ± 0.7bc	0.2 ± 0.01a
UT	10.0 ± 0.5c	5.2 ± 0.8b	96.5 ± 0.3a	5.0 ± 0.4a	4.5 ± 0.3d	0.2 ± 0.01ab
Heat stress						
L1	11.0 ± 0.3c	6.7 ± 0.3c	72.6 ± 0.8b	5.2 ± 0.1c	14.3 ± 0.7b	1.0 ± 0.02a
L2	15.5 ± 0.9a	8.5 ± 0.3a	89.5 ± 0.4a	6.9 ± 0.6a	19.8 ± 0.2a	1.5 ± 0.03a
L3	13.5 ± 0.6b	7.5 ± 0.3b	70.6 ± 0.9bc	6.2 ± 0.9ab	18.9 ± 0.8a	0.8 ± 0.03ab
UT	2.0 ± 0.9d	1.0 ± 0.3c	10.7 ± 0.2d	2.2 ± 0.6d	5.2 ± 0.7c	0.3 ± 0.01c
Drought						
L1	7.5 ± 0.6b	4.5 ± 0.3b	66.4 ± 0.6b	4.4 ± 0.8c	10.6 ± 0.2c	0.9 ± 0.02ab
L2	11.0 ± 0.2a	7.3 ± 0.4a	78.4 ± 0.4a	7.3 ± 0.36ab	16.5 ± 0.9a	1.1 ± 0.01a
L3	11.0 ± 0.1a	7.5 ± 0.5a	76.4 ± 0.7a	7.6 ± 1.1a	14.7 ± 0.3ab	1.0 ± 0.01a
UT	2.1 ± 0.5c	0.8 ± 0.5c	12.5 ± 0.6c	1.7 ± 0.2d	4.9 ± 1.7d	0.2 ± 0.02c
Salinity						
L1	3.5 ± 0.8c	1.5 ± 0.3c	25.9 ± 0.9c	4.1 ± 1.1c	4.8 ± 0.3b	0.3 ± 0.01b
L2	10.5 ± 0.1a	6.3 ± 0.4a	77.1 ± 0.4a	5.7 ± 0.8a	12.7 ± 0.2a	1.2 ± 0.01a
L3	7.1 ± 0.2b	4.5 ± 0.5b	54.6 ± 0.2b	4.6 ± 0.4b	11.3 ± 0.3a	0.9 ± 0.02a
UT	2.0 ± 0.4d	0.8 ± 0.6d	7.7 ± 0.3d	1.7 ± 0.7d	4.7 ± 0.9b	0.3 ± 0.01b

Means of three independent samples and standard errors are presented. The same letter indicates no significant difference at $P < 0.05$.

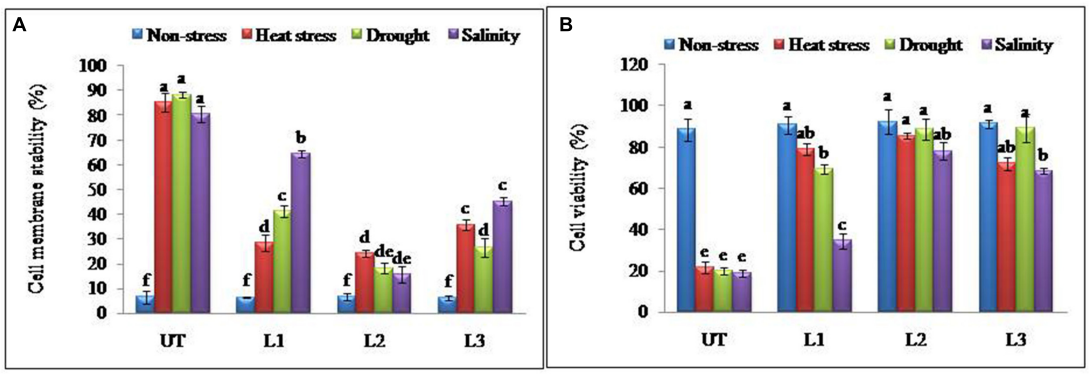

FIGURE 3 | Enhanced cellular adjustments in *StnsLTP1* transgenic lines (A) Percent membrane damage and (B) percent cell viability indicated by TTC reduction in *StnsLTP1* transgenic lines (L1, L2, and L3) and UT potato plants under, non-stress, heat, drought and salinity stress conditions. Means of three independent samples and standard errors are presented. The same letter above the column indicates no significant difference at $P < 0.05$.

recorded in *StnsLTP1* transgenic lines (L2 and L3) plants under heat stress while least activity was found in *StnsLTP1* transgenic lines (Ll) plants treated with 200 mM NaCl (**Figure 4C**). The specific activity of CAT was found 4.9 times higher in *StnsLTP1* transgenic line (L2) plants compared to UT control plants under all three abiotic stresses (**Figure 4D**). Highest SOD specific activity was recorded in *StnsLTP1* transgenic lines (L2) plants subjected to heat stress while least SOD activity was found in *StnsLTP1* transgenic lines (Ll) under salinity stress induced by 200 mM NaCl (**Figure 4E**). Similarly, specific enzyme activity of another major ROS scavenging enzyme, GR was measured and similar trends were observed (2.4–5.8 times increased activity) with highest GR activity recorded in *StnsLTP1* transgenic lines subjected to salinity stress induced by 200 mM NaCl, and least GR activity in control plants under salinity stress induced by 200 mM NaCl (**Figure 4F**).

Over-Expression of *StnsLTP1* Gene Enhanced the Accumulation Antioxidant Compounds under Multiple Abiotic Stress Conditions

The ascorbate contents were measured in leaves of *StnsLTP1* transgenic lines (L1, L2, and L3) and the UT control plants grown

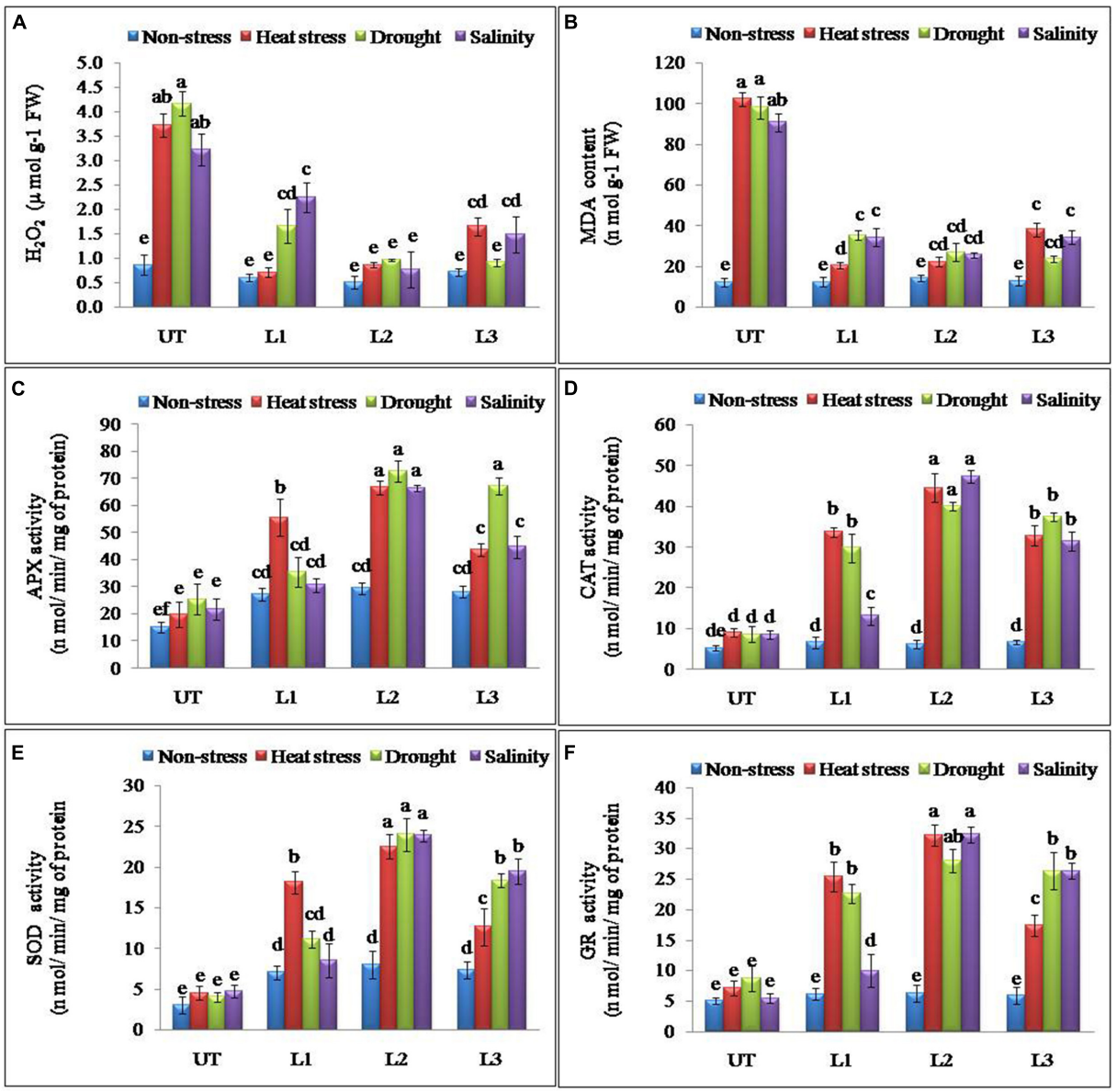

FIGURE 4 | Enhanced performance of *StnsLTP1* transgenic lines in scavenging ROS (A) H_2O_2 accumulation, (B) MDA contents and antioxidant enzyme activity of (C) APX, (D) CAT, (E) SOD and (F) GR in *StnsLTP1* transgenic lines (L1, L2, and L3) and untransformed (UT) potato plants under, non-stress, heat, drought and salinity stress conditions. Means of three independent samples and standard errors are presented. The same letter above the column indicates no significant difference at $P < 0.05$.

under heat, drought, salinity and non-stress conditions (**Table 1**). Under heat, drought, and salt stress *StnsLTP1* transgenic line L2 registered 3.8, 3.3, and 2.7 fold higher accumulation of ascorbate compared to UT control plants, respectively. Similar to ascorbate, the reduced glutathione (GSH) contents in leaves of *StnsLTP1* transgenic lines grown under non-stress showed a slight increase over those of UT control plants (**Table 1**) and their levels dramatically increased with the application of heat, drought, and salinity stresses in *StnsLTP1* transgenic lines. This demonstrates that over-expression of *StnsLTP1* contributed to reduce the accumulation of ROS (H_2O_2) generated by stress mediated via enhanced accumulation of ascorbate and GSH in *StnsLTP1* transgenic lines.

Over-Expression of *StnsLTP1* Gene Altered Expression of Antioxidant and Abiotic Stress-Responsive Genes

Antioxidant and ROS scavenging enzyme activities suggested that enhanced multiple abiotic stress-tolerance observed in *StnsLTP1* over-expression lines may involve in the selective up-regulation of antioxidant genes. To further support this observation,

expression analysis of *StAPX*, *StCAT*, *StSOD* and *StGR* genes involved in ROS scavenging activities were studied under the multiple abiotic stress (heat, drought, and salt) treatments. Expression of genes *StAPX*, *StCAT*, *StSOD* and *StGR* were up-regulated in *StnsLTP1* transgenic lines compared to UT control plants under multiple abiotic stress (**Figures 5A–D**). Among different abiotic stress, *StSOD* and *StGR* genes showed maximum up-regulation under drought stress, whereas expression of *StAPX* and *StCAT* genes registered maximum up-regulation under heat stress (**Figures 5A–D**). Among the *StnsLTP1* transgenic lines, L2 showed about 9, 8, 7 and 9-fold higher expression of *StAPX*, *StCAT*, *StSOD* and *StGR* genes respectively, compared to their respective UT control plants under different abiotic stresses. Moreover, the mRNA expression levels of these antioxidant enzymes were positively correlated with their specific activities (**Figures 4C–F** and **5A–D**). To further investigate the molecular mechanism of stress-tolerance via *StnsLTP1* we analyzed the expression of down-stream genes (*StHsfA3, StHSP70*, *StHSP90* and *StsHSP20*) in transgenic potato. In the non-stress conditions, transcript levels of *StHsfA3, StHSP70*, *StHSP90* and *StsHSP20* were apparently enhanced in the three *StnsLTP1* transgenic lines compared with those of UT control. The expression of the *StHsfA3* gene improved concomitantly with stress treatments (except transgenic line L1 under NaCl) in transgenic lines compared to UT control plants (**Figure 5E**). About 11-fold expression (*StHsfA3*) was observed in L2 line under heat and salinity stress, while about ninefold expression was detected under drought stress compared to non-stress condition. Remaining L1 and L3 lines demonstrated relatively higher expression of *StHsfA3* gene under different abiotic stress conditions compared to UT control plants. Relative fold expression of *StHSP70* gene was found higher in *StnsLTP1* transgenic lines compared to UT plants under drought and heat stress treatments (**Figure 5F**). Compared to UT control plants, *StnsLTP1* transgenic line L2 showed maximum *StHSP70* gene expression about 6, 5, and 4-fold under drought, heat and salinity stress, respectively. However, *StHSP90* gene expression was up-regulated by sixfold in all three *StnsLTP1* transgenic lines under heat stress, while expression was increased by fourfold during drought and salinity stress (**Figure 5G**). Elevated *StsHSP20* gene expression about 2–3 fold was observed in *StnsLTP1* transgenic lines (except L1 under salinity and drought) compared to UT control plants under heat, drought and salinity stress conditions (**Figure 5H**). These data point out that over-expression of *StnsLTP1* in potato led to change in the transcript levels of endogenous stress-related and antioxidant genes.

DISCUSSION

Our previous study revealed that heterologous expression of *StnsLTP1* gene imparted enhanced tolerance to heat, drought, and salinity stress in wild-type yeast cells (Gangadhar et al., 2014). Further, we confirmed the functional role of *StnsLTP1* gene in imparting broad-spectrum thermo-tolerance to *Nicotiana benthamiana* using VIGS (Gangadhar et al., 2016). Herein, we demonstrated enhanced tolerance to multiple abiotic stresses (heat, drought, and salinity) through over-expression of *StnsLTP1* gene in potato for the first time. *StnsLTP1* encodes a small protein with eight highly conserved cysteine residues involved in formation of four disulphide bridges, as well as a 25-amino acid N-terminal signal peptide predicted to target proteins to the secretory pathway (Kader, 1997; Carvalho and Gomes, 2007). The compact and globular 3D structure of *StnsLTP1,* comprises of four α-helices and a flexible hydrophobic pocket with a distinctive ability to accommodate fatty acids, acyl-CoA, and other phospholipids (Kader, 1997; Carvalho and Gomes, 2007). The estimated molecular mass of mature *StnsLTP1 was* approximately 9 kDa, suggesting that this protein belongs to the type I LTP family (Kader, 1997; Carvalho and Gomes, 2007). In addition, *StnsLTP1* gene showed high similarity to the tomato LTP (*SlTSW12*), which is highly induced by various abiotic stresses such as NaCl, mannitol and ABA (Torres-Schumann et al., 1992). A homolog of *StnsLTP1* gene, *Betula platyphylla LTP* (*BPLTP*), which found to enhance the resistance of *E. coli* strain BL21 to salt (induced by NaCl) and drought (polyethylene glycol) stress upon its heterologus expression (Guan et al., 2013). Consistent with these results, *StnsLTP1* gene expression was found to be highly inducible in potato plants subjected to heat, drought, and salinity stress (**Figure 1C**). To gain further insight into the function of *StnsLTP1*, we generated transgenic potato plants over-expressing *StnsLTP1*. Over-expression of *StnsLTP1* in potato enhanced survivability during multiple abiotic stress and also suppressed the heat, drought, and salt-induced leaf damages by maintaining higher leaf chlorophyll content, antioxidant enzyme activity, and lower electrolyte leakage, H_2O_2 and MDA content (**Figures 3** and **4**; **Table 1**). Furthermore, cell death associated with cell structural damages, such as disruption of cell membranes and cell walls, which are typical heat and drought stress symptoms were high in UT control plants compared to *StnsLTP1* transgenic lines. These results indicated that over-expression of *StnsLTP1* facilitated better cellular survivability during multiple abiotic stress induced heat, drought, and salinity stresses and possibly be linked to the enhanced membrane integrity through reduced lipid per-oxidation, and accumulation of ROS such as H_2O_2 (**Figures 3** and **4**). In the present study, higher activities and transcripts of antioxidant enzymes *StAPX*, *StCAT*, *StSOD* and *StGR* were recorded in the transgenic lines (L1, L2, and L3) compared to UT control under normal growth conditions (**Figure 4**), suggesting that antioxidative defense system has been up-regulated by the over-expressed *StnsLTP1*. On the other hand, the expression of antioxidant enzymes (SOD, CAT, APX and GR) was increased by 5–9 folds in *StnsLTP1* transgenic lines subjected to multiple abiotic stresses as compared to UT control, suggesting that various components of ROS scavenging systems were co-regulated to induce the tolerance to multiple abiotic stresses in *StnsLTP1* transgenic lines (**Figure 4**). These results are consistent with our previous reports (Gangadhar et al., 2016), where silencing of *StnsLTP1* ortholog gene in *N. benthamiana* using VIGS produced hypertensive phenotype under heat stress with increased cell death and cell membrane damage. This finding demonstrates that *StnsLTP1* over-expression contribute

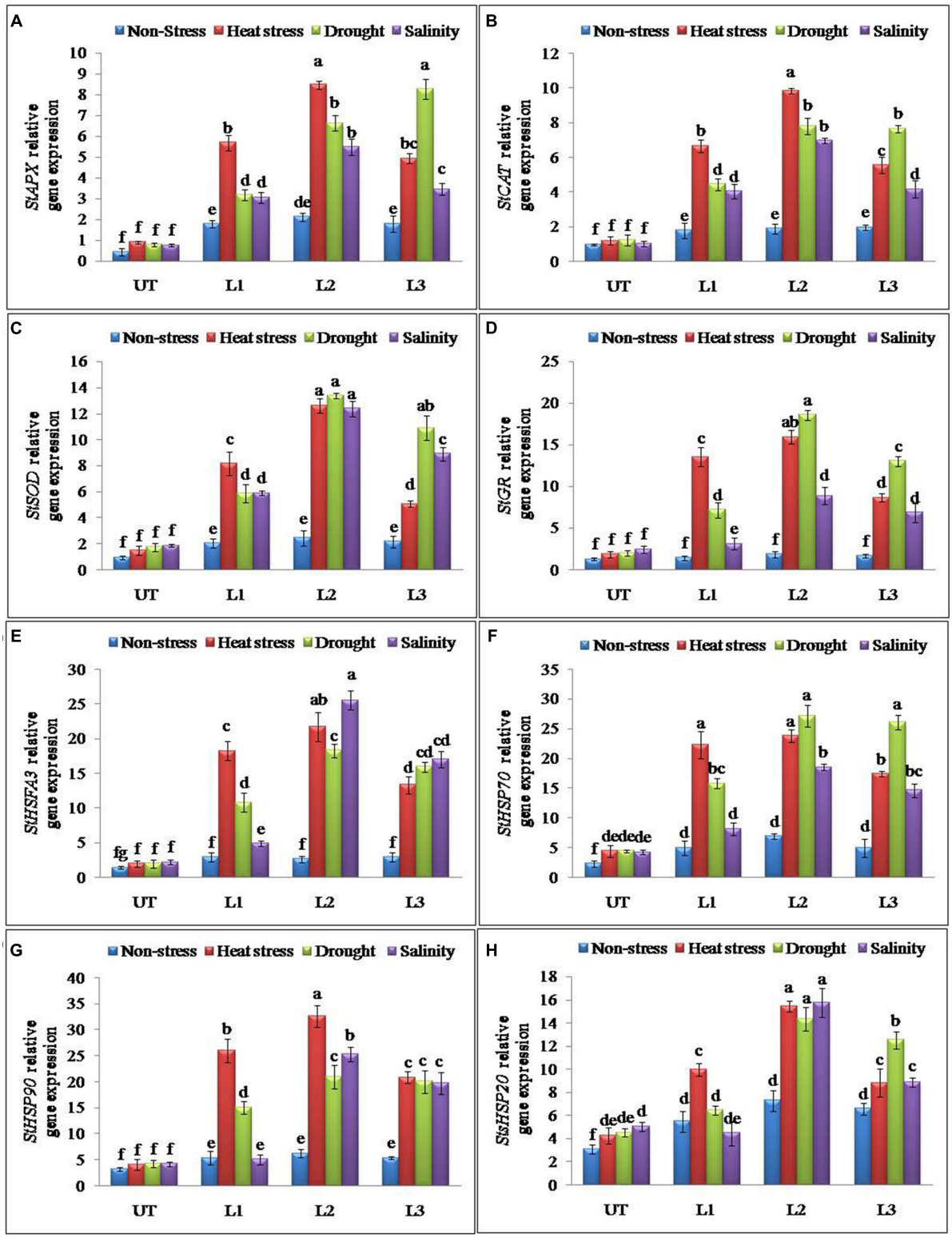

FIGURE 5 | Relative expression of antioxidant and genes encoding different stress-responsive proteins in *StnsLTP1* transgenic lines (L1, L2, and L3) and untransformed (UT) potato plants under, non-stress, heat, drought and salinity stress conditions. (A) *StAPX,* **(B)** *StCAT*, **(C)** *StSOD*, **(D)** *StGR,* **(E)** *StHSFA3,* **(F)** *StHSP70*, **(G)** *StHSP90*, and **(H)** *StsHSP20.* Means of three independent samples and standard errors are presented. The same letter above the column indicates no significant difference at $P < 0.05$.

to the reduce accumulation of ROS (H_2O_2) generated by stress through up-regulated expression of antioxidant enzyme genes, which in turn result in the elevated tolerance to heat, drought, and high salt-induced oxidative stresses. The negative effects of abiotic stress induced ROS accumulation is also counteracted by non-enzymatic low molecular weight metabolites such as ascorbate and glutathione. Furthermore, the enhanced accumulation of ascorbate and glutathione in potato is believed to play key role in modulating tolerance to various environmental stresses (Hemavathi et al., 2011). As a scavenger of ROS, both these metabolites (ascorbate and glutathione) accumulated in higher concentrations in *StnsLTP1* transgenic lines, which in turn helped plants to withstand the H_2O_2-mediated oxidative stress induced by different abiotic stress. Taken together, these observations suggests that over-expression of *StnsLTP1* gene resulted in decreased accumulation of ROS species (H_2O_2) mediated via increased accumulation of ascorbate and glutathione is proved to be an important factor for inducing multiple abiotic stress-tolerance. This is in agreement with the previous reports of Safi et al. (2015), over-expression of wheat LTP gene improved tolerance to oxidative stress induced by abiotic stress factors (100 mM NaCl, 50 mM JA and 20 mM ABA) through improved accumulation of ascorbates in *Arabidopsis*. Recently, the hypothesis that LTPs mediated expression of HSPs could be involved; in plant stress-tolerance induced by abiotic stress had emerged. It has been shown that over-expression of wheat LTP (*TaLTP3*) conferred thermo-tolerance through early accumulation of HSPs (AtHSP101and AtHSA32; Wang et al., 2014). Here, we tested *StnsLTP1* induced expression of HSPs such as *StHsfA3, StHSP70*, *StHSP90* and *StsHSP20* in transgenic lines over-expressed *StnsLTP1* subjected to different abiotic stress. Our results indicated that *StHsfA3* was up-regulated by 5-11-fold in *StnsLTP1* transgenic lines (L2 and L3) as compared to UT control (0.8–1 fold) under abiotic stress generated by heat, drought, or salinity stress. On the other hand, expression pattern of *StHSP70*, *StHSP90* and *StsHSP20* genes followed similar trend of expression with 3–4 fold higher expression in *StnsLTP1* transgenic lines compared to UT control potato plants. Based on these results, we suggest *StnsLTP1* mediated expression of *StHsfA3* may play important role in imparting tolerance to different abiotic stress in potato plants (**Figures 5E–H**). However, the molecular relationship between the putative protective roles of *StnsLTP1* induced expression of heat shock factors to various stress conditions needs to be determined.

In summary, *StnsLTP1* cloned from potato was classified as type I LTP and closely related to LTP genes in other Solanaceae species. Over-expression of *StnsLTP1* in potato alleviated cellular damages and growth inhibition due to multiple abiotic stresses such as heat, drought, and salinity stress. The improved tolerance to multiple abiotic stresses in *StnsLTP1* over-expressing lines of potato is manifested by greater survivability, chlorophyll content, and Cell membrane stability, as well as lower level of membrane lipid per-oxidation. Moreover, the multiple abiotic stress-tolerances exhibited in *StnsLTP1* transgenic lines is attributed to more robust activation of ROS scavenging system and coordinated activation of an array of stress-responsive genes at molecular level, leading to synthesis of a broad range of protective compounds such as ascorbate and glutathione. These results are warranted that *StnsLTP1* could be a candidate for improving the plant tolerance to environmental stress in other Solanaceae species using genetic engineering. Over-expression of *StnsLTP1* provides a novel strategy for endogenously adjusting H_2O_2 signaling during heat stress, induction of ROS scavenging system against cellular ROS accumulation for protection of crops from abiotic stress induced oxidative stress injury and future research into role of cross-talk among ROS and heat stress response signaling pathways in other crops could be a promising avenue.

AUTHOR CONTRIBUTIONS

BG, KS, JV, and VB performed wet lab experiments; BG, KS, JV, and JY performed computational analysis; BG, KS, JV, VB, KA, and JY. interpreted the results; BG, KS, JV, VB, KA, JY, RP, and RM wrote the manuscript.

ACKNOWLEDGMENTS

This work was supported by the next-Generation Bio Green 21 Program (PJ008182), Rural Development Administration, Republic of Korea. We express our appreciation to the late Prof. Se Won Park, whose contribution to this work was of great significance.

SUPPLEMENTARY MATERIAL

The Supplementary Material for this article can be found online at: http://journal.frontiersin.org/article/10.3389/fpls.2016.01228

FIGURE S1 | Enhanced plant growth performances of *StnsLTP1* transgenic lines (L1, L2, and L3) and UT potato plants under, non-stress, heat, drought, and salinity stress conditions. (A) Non-stress treatment plants were maintained at 23 ± 1°C with regular irrigation with water. **(B)** Heat stress was assessed by gradual increase in the temperature by 5°C in every 3 h, reaching to 30, 35, 40°C and finally maintained at 45°C for 24 h. **(C)** Drought stress was initiated by suspending watering the plants for 12 days. **(D)** Salt stress was assessed by irrigating the plants with 200 mM NaCl solution for 15 days. UT, untransformed plants; L1–L3, transgenic potato plants expressing *StnsLTP1* gene.

REFERENCES

Allen, G. C., Flores-Vergara, M. A., Krasynanski, S., Kumar, S., and Thompson, W. F. (2006). A modified protocol for rapid DNA isolation from plant tissues using cetyltrimethylammonium bromide. *Nat. Protoc.* 1, 2320–2325. doi: 10.1038/nprot.2006.384

Arnold, K., Bordoli, L., Kopp, J., and Schwede, T. (2006). The SWISS-MODEL workspace: a web-based environment for protein structure homology modeling. *Bioinformatics* 22, 195–201. doi: 10.1093/bioinformatics/bti770

Boutrot, F., Chantret, N., and Gautier, M. F. (2008). Genomewide analysis of the rice and *Arabidopsis* non-specific lipid transfer protein (nsLtp) gene families

and identification of wheat nsLtp genes by EST data mining. *BMC Genomics* 9:86. doi: 10.1186/1471-2164-9-86

Bradford, M. M. (1976). A rapid and sensitive method for the quantitation of microgram protein utilizing the principle of protein-dye binding. *Anal. Biochem.* 72, 248–254. doi: 10.1016/0003-2697(76)90527-3

Carvalho, A. O., and Gomes, V. M. (2007). Role of plant LTPs in plant cell physiology: a concise review. *Peptides* 28, 1144–1153. doi: 10.1016/j.peptides.2007.03.004

Cheeseman, J. M. (2006). Hydrogen peroxide concentrations in leaves under natural conditions. *J. Exp. Bot.* 57, 2435–2444. doi: 10.1093/jxb/erl004

Choi, Y. E., Lim, S., Kim, H. J., Han, J. Y., Lee, M. H., Yang, Y., et al. (2012). Tobacco NtLTP1, a glandular-specific lipid transfer protein, is required for lipid secretion from glandular trichomes. *Plant J.* 70, 480–491. doi: 10.1111/j.1365-313X.2011.04886.x

Davies, S. H. R., and Masten, S. J. (1991). Spectrophotometric method for ascorbic acid using dic hlorophenolindophenol: elimination of the interference due to iron. *Anal. Chim. Acta* 248, 225–227. doi: 10.1016/S0003-2670(00)80888-0

Feng, J. X., Ji, S. J., Shi, Y. H., Wei, G., and Zhu, Y. X. (2004). Analysis of five differentially expressed gene families in fast elongating cotton fiber. *Acta Biochim. Biophys. Sin.* 36, 51–57. doi: 10.1093/abbs/36.1.51

Gangadhar, B. H., Sajeesh, K., Venkatesh, J., Baskar, V., Abhinandan, K., Moon, S. H., et al. (2016). Identification and characterization of genes associated with thermo-tolerance using virus induced gene silencing in *Nicotiana benthamiana*. *Plant Growth Regul.* 1–12. doi: 10.1007/s10725-016-0175-x

Gangadhar, B. H., Yu, J. W., Sajeesh, K., and Park, S. W. (2014). A systematic exploration of high-temperature stress-responsive genes in potato using large-scale yeast functional screening. *Mol. Genet. Genomics* 289, 185–201. doi: 10.1007/s00438-013-0795-z

Griffith, O. W. (1980). Determination of glutathione and glutathione disulfide using glutath ione reductase and 2-vinylpyridine. *Anal. Biochem.* 106, 207–212. doi: 10.1016/0003-2697(80)90139-6

Guan, M. X., Chai, R. H., Kong, X., and Liu, X. M. (2013). Isolation and characterization of a lipid transfer protein gene (BplLTP1) from *Betula platyphylla*. *Plant Mol. Biol. Report.* 31, 991–1001. doi: 10.1007/s11105-013-0571-6

Guo, L., Yang, H., Zhang, X., and Yang, S. (2013). Lipid transfer protein 3 as a target of MYB96 mediates freezing and drought stress in *Arabidopsis*. *J. Exp. Bot.* 64, 1755–1767. doi: 10.1093/jxb/ert040

Han, G. W., Lee, J. Y., Song, H. K., Chang, C., Min, K., Moon, J., et al. (2001). Structural basis of non-specific lipid binding in maize lipid transfer protein complexes revealed by high-resolution X-ray crystallography. *J. Mol. Bio.* 308, 263–278. doi: 10.1006/jmbi.2001.4559

Hemavathi, Upadhyaya, C. P., Akula, N., Kim, H. S., Kim, J. H., Ho, O. M., et al. (2011). Biochemical analysis of enhanced tolerance in transgenic potato plants over-expressing d-galacturonic acid reductase gene in response to various abiotic stresses. *Mol. Breed.* 28, 105–115. doi: 10.1007/s11032-010-9465-6

Kader, J. C. (1997). Lipid transfer proteins: a puzzling family of plant proteins. *Trends Plant Sci.* 2, 66–70. doi: 10.1016/S1360-1385(97)82565-4

Kappachery, S., Baniekal Hiremath, G., Yu, J. W., and Park, S. W. (2015). Effect of over-and under-expression of glyceraldehyde3-phosphate dehydrogenase on tolerance of plants to water-deficit stress. *Plant Cell Tissue Organ Cult.* 121, 97–107. doi: 10.1007/s11240-014-0684-0

Kinlaw, C. S., Gerttula, S. M., and Carter, M. C. (1994). Lipid transfer protein genes of loblolly pine are members of a complex gene family. *Plant Mol. Biol.* 26, 1213–1216. doi: 10.1007/BF00040702

Kumar, K., Yadav, S., Purayannur, S., and Verma, P. K. (2013). An alternative approach in Gateway (®) cloning when the bacterial antibiotic selection cassettes of the entry clone and destination vector are the same. *Mol. Biotechnol.* 54, 133–140. doi: 10.1007/s12033-012-9549-0

Levy, D., and Veilleux, R. E. (2007). Adaptation of potato to high tempera-tures and salinity—a review. *Am. J. Potato Res.* 84, 487–506. doi: 10.1038/hdy.2008.132

Liu, K., Jiang, H., Moore, S., Watkins, C., and Jahn, M. (2006). Isolation and characterization of a lipid transfer protein expressed in ripening fruit of Capsicum chinense. *Planta* 223, 672–683. doi: 10.1007/s00425-005-0120-0

Petersen, T. N., Brunak, S., von-Heijne, G., and Nielsen, H. (2011). SignalP 4.0: discriminating signal peptides from transmembrane regions. *Nat. Methods* 8, 785–786. doi: 10.1038/nmeth.1701

Safi, H., Saibi, W., Alaoui, M. M., Hmyene, A., Masmoudi, K., Hanin, M., et al. (2015). A wheat lipid transfer protein (TdLTP4) promotes tolerance to abiotic and biotic stress in *Arabidopsis thaliana*. *Plant Physiol. Biochem.* 89, 64–75. doi: 10.1016/j.plaphy.2015.02.008

Sarowar, S., Kim, Y. J., Kim, K. D., Hwang, B. K., Ok, S. H., and Shin, J. S. (2009). Over-expression of LTP genes enhances resistance to plant pathogens and LTP functions in long-distance systemic signaling in tobacco. *Plant Cell Rep.* 28, 419–427. doi: 10.1007/s00299-008-0653-3

Thompson, J. D., Gibson, T. J., Plewniak, F., Jeanmougin, F., and Higgins, D. G. (1997). The ClustalX windows interface: flexible strategies for multiple sequence alignment aided by quality analysis tools. *Nucleic Acids Res.* 25, 4876–4882. doi: 10.1093/nar/25.24.4876

Torres-Schumann, S., Godoy, J. A., and Pintor-Toro, J. A. (1992). A probable lipid transfer protein gene is induced by NaCl in stems of tomato plants. *Plant Mol. Biol.* 18, 749–757. doi: 10.1007/BF00020016

Wang, F., Zang, X. S., Kabir, M. R., Liu, K. L., Liu, Z. S., Ni, Z. F., et al. (2014). A wheat lipid transfer protein 3 could enhance the basal thermotolerance and oxidative stress resistance of *Arabidopsis*. *Gene* 550, 18–26. doi: 10.1016/j.gene.2014.08.007

Wang, N. J., Lee, C. C., Cheng, C. S., Lo, W. C., Yang, Y. F., Chen, M. N., et al. (2012). Construction and analysis of a plant non-specific lipid transfer protein database (nsLTPDB). *BMC Genomics* 13(Suppl. 1):S9. doi: 10.1186/1471-2164-13-S1-S9

Zou, H. W., Tian, X. H., Ma, G. H., and Li, Z. X. (2013). Isolation and functional analysis of ZmLTP3, a homologue to *Arabidopsis* LTP3.*Int. J. Mol. Sci.* 14, 5025–5035. doi: 10.3390/ijms14035025

Conflict of Interest Statement: The authors declare that the research was conducted in the absence of any commercial or financial relationships that could be construed as a potential conflict of interest.

The reviewer AC and handling Editor declared their shared affiliation, and the handling Editor states that the process nevertheless met the standards of a fair and objective review.

frontiers in Environmental Science

ORIGINAL RESEARCH
published: 14 October 2016
doi: 10.3389/fenvs.2016.00066

An Increasing Need for Productive and Stress Resilient *Festulolium* Amphiploids: What Can Be Learnt from the Stable Genomic Composition of *Festuca pratensis subsp.* apennina (De Not.) Hegi?

*David Kopecký[1], John Harper[2], Jan Bartoš[1], Dagmara Gasior[2], Jan Vrána[1], Eva Hřibová[1], Beat Boller[3], Nicola M. G. Ardenghi[4], Denisa Šimoníková[1], Jaroslav Doležel[1] and Mike W. Humphreys[2]**

[1] Centre of Plant Structural and Functional Genomics, Institute of Experimental Botany, Olomouc-Holice, Czechia, [2] Institute of Biological, Environmental and Rural Sciences, Gogerddan Aberystwyth University, Aberystwyth, Wales, UK, [3] Agroscope INH, Zürich, Switzerland, [4] Department of Earth and Environmental Sciences, University of Pavia, Pavia, Italy

OPEN ACCESS

Edited by:
Mauro Centritto,
National Research Council, Italy

Reviewed by:
Luigi Frusciante,
University of Naples Federico II, Italy
Domenico Pignone,
National Research Council, Italy

***Correspondence:**
Mike W. Humphreys
mkh@aber.ac.uk

Specialty section:
This article was submitted to Agroecology and Land Use Systems, a section of the journal Frontiers in Environmental Science

Received: 01 June 2016
Accepted: 26 September 2016
Published: 14 October 2016

Citation:
Kopecký D, Harper J, Bartoš J, Gasior D, Vrána J, Hřibová E, Boller B, Ardenghi NMG, Šimoníková D, Doležel J and Humphreys MW (2016) An Increasing Need for Productive and Stress Resilient Festulolium Amphiploids: What Can Be Learnt from the Stable Genomic Composition of Festuca pratensis subsp. apennina (De Not.) Hegi? Front. Environ. Sci. 4:66. doi: 10.3389/fenvs.2016.00066

Genome composition of *Festuca pratensis* subsp. *apennina* (De Not.) Hegi, a tetraploid fescue species native to the tall forbs communities of south-eastern Europe at altitudes between 1100 and 2200 m a.s.l. has been the subject of some debate by grass taxonomists. Our cytogenetic analyses including fluorescence *in situ* hybridization with probes for genomic DNA and selected DNA repeats revealed the species to be allotetraploid and derived from interspecific hybridization between *F. pratensis* Huds., a species confined to grassland at lower altitudes, and a so far unknown *Festuca* species. Besides tetraploids, triploids, and pentaploids were found growing in Alpine meadows in close association with *F. pratensis* subsp. *apennina*. Triploid cytotypes predominated at many sites in Switzerland and Romania, and in some localities, they were the only cytotypes observed. Cytogenetic analyses revealed the triploids to be hybrids between diploid *F. pratensis* and tetraploid *F. pratensis* subsp. *apennina,* while the pentaploid cytotypes originated from hybridization between *F. pratensis* subsp. *apennina* and hexaploid *F. arundinacea* Schreb., a closely-related species growing in a close vicinity to *F. pratensis* subsp. *apennina*. Parental genomes of *F. pratensis* subsp. *apennina* and of the triploid and pentaploid hybrids showed no evidence of homoeologous chromosome pairing and interspecific recombination, supporting previous observation of a disomic inheritance at meiosis, where chromosome pairing was restricted to bivalent associations. A hypothesis is presented that a chromosome pairing regulator(s), reported previously in other polyploid broad-leaved fescue species of the *Festuca* subg. *Schedonorus*, is present and functional in *F. pratensis* subsp. *apennina*. It is likely that a common ancestors' genome that carries the chromosome pairing regulator(s) is present in all polyploid broad-leaved fescue species, and its acquisition was a key event that enabled speciation, and development of a polyploid series within

Festuca. Identification of a functional chromosome pairing regulator capable of stabilizing advantageous genome combinations in hybrids within the *Lolium-Festuca* complex would greatly assist in development of stable *Festulolium* cultivars. Its expression within *Festulolium* amphiploid cultivars would assist strategies aimed at climate-proofing productive European grasslands to combat exposures to stress conditions.

Keywords: amphiploidy, *Festuca pratensis subsp. apennina* (De Not.) Hegi, chromosome pairing, diploidization, *Festulolium* breeding

INTRODUCTION

Climate-smart strategies are required to ensure sustainability of European-based grassland management systems suitable for livestock agriculture in the face of increasing external environmental pressures. These arrive from increased requirements for improved resilience to extreme weather events and from governments and policy makers seeking some assurance of greater efficiencies and environmental safeguards. *Festulolium* grasses, defined as hybrids between any ryegrass (*Lolium*) and fescue (*Festuca*) species, are considered an effective response by providing combinations of high yields of nutritious fodder from *Lolium* together with added resilience to abiotic and biotic stress from *Festuca* (Humphreys et al., 2006, 2014). Whilst *Festulolium* have hitherto been used quite widely in Central and Eastern Europe, in the case of the UK, the acceptance of the IBERS' bred *Festulolium* cultivar "AberNiche" onto the UK National Recommended Lists represented a change in mind-set by the commercial sector. There is a growing belief that *Festulolium* cultivars capable of providing effective and appropriate stress resilience when conditions require, should now become more widely available commercially, to underpin future food security, and grassland agriculture.

Festulolium are marketed either as amphiploids, (where entire *Lolium* and *Festuca* genomes are combined), or as introgressive forms [where specific genes from one species (usually from *Festuca*) are incorporated into the genome of another; Ghesquiere et al., 2010]. Whilst maintaining fertility and genome stability through use of an introgression breeding approach has not thus far presented significant difficulties, the more widely used amphiploid breeding approach which for several quantitative traits may be deemed more appropriate has proved to be more problematic (Ghesquiere et al., 2010). One example where *Festulolium* amphiploids were required was reported recently where in order to assist efficient ruminant nutrition, the maintenance of complete and balanced *Lolium* and *Festuca* genome complements was seen as an essential prerequisite in order to combat plant-mediated proteolysis within ingested fodder (Humphreys et al., 2014). Unfortunately, for such a breeding approach the outcome reported from all cytogenetic studies that involved amphiploid *Festulolium* varieties was that unbalanced genome complements had arisen over generations of seed multiplication which had resulted in a shift toward a *Lolium* genome, accompanied by loss of *Festuca* chromosomes (Canter et al., 1999; Kopecký et al., 2006; Zwierzykowski et al., 2006). This outcome was aided by frequent homoeologous pairing and recombination between *Festuca* and *Lolium* chromosomes and possibly by the self-incompatibility of the species involved (Kopecký et al., 2008a, 2010; Harper et al., 2011).

A stable and balanced genome composition could it is thought be achieved by the incorporation of a diploid-like chromosome pairing mechanism in *Festulolium* hybrids, such as *Ph1* found in wheat, capable of encouraging homologous and preventing homoeologous chromosome pairing. However, the agriculturally desirable diploid grass species (such as *F. pratensis* Huds., *Lolium perenne* L., and *Lolium multiflorum* Lam.) widely used in *Festulolium* amphiploid varieties lack such a functional system (Kopecký et al., 2009). However, an equivalent diploidizing chromosome pairing mechanism to *Ph1* has been identified in closely related polyploid broad-leaved fescues of subg. *Schedonorus*, such as *F. arundinacea* Schreb. subsp. *arundinacea*, *F. arundinacea* var. *glaucescens* Boiss. (≡*F. arundinacea* subsp. *fenas* (Lag.; here-after referred to as *F. glaucescens* Arcang.), and *F. mairei* St. Yves (Jauhar, 1975, 1993; Kopecký et al., 2009) and is considered essential in their evolution and speciation. If the chromosome pairing regulator was incorporated successfully into synthetic *Festulolium* hybrids and its function maintained, it should provide for regular chromosome disjunction, consistent disomic inheritance, and the levels of genome stability over generations required to fully exploit the benefits to be derived from use of *Festulolium* amphiploids in agriculture, and adherence to the strict requirements for genome uniformity and stability necessary for variety status within the UK.

Unlike the *Lolium* genus, where species are all diploids, polyploidy is a prominent feature amongst related *Festuca* species including the broad-leaved fescues of the subg. *Schedonorus*. The polyploids of this sub-genus, whose genome origins have previously been reported (e.g., Jauhar, 1993), are believed to derive as a consequence of species' hybridization and through assemblies of novel advantageous genome combinations that gave enhanced adaptations absent in their parental species. An excellent example was the result of the hybridization between the North and Central European grass *Festuca pratensis* Huds. ($2n = 2x = 14$) and the Mediterranean-based *Festuca glaucescens* Arcang. ($2n = 4x = 28$) that gave rise to the now widely dispersed hexaploid tall fescue (*Festuca arundinacea* Schreb.) ($2n = 6x = 42$), used widely in grassland agriculture and in particular where abiotic stresses are too severe for less well adapted *Lolium* varieties (Humphreys et al., 1995).

Key events in the evolution and speciation of these hybrids were their initial chromosome doubling and the subsequent restricted preferential chromosome pairing between homologous partners at meiosis, encouraged by a chromosome pairing

regulator (Jauhar, 1975). These events led to hybrid genome stabilization and maintained intact their adaptive advantages, a situation sought but unfortunately not so far replicated to the same extent within current synthetic *Festulolium* cultivars.

One of the progenitors of *F. arundinacea*, the tetraploid fescue *F. glaucescens* is a mid to high altitude species found in the southern part of the Iberian Peninsula and north-western Africa (Devesa et al., 2013). It has been used for the development of three drought-tolerant *Festulolium* cultivars (*L. multiflorum* × *F. glaucescens*), which were released and registered in France (Ghesquiere et al., 2010). The hybrid combination has more recently also been produced independently at IBERS together with an equivalent amphiploid hybrid involving *F. glaucescens* and *L. perenne*. Both hybrid combinations have demonstrated excellent potential as fodder and as aides to efficient ruminant nutrition considered likely to reduce greenhouse gas emissions by livestock (Humphreys et al., 2014). Other novel amphiploid *Festulolium* hybrids with high agronomic potential, large root systems, and significant stress tolerance generated at IBERS include *L. multiflorum* and *L. perenne* combinations with tetraploid Atlas fescue (*Festuca mairei*; Humphreys et al., 2014).

The focus of the research described herein is on another fescue from subg. *Schedonorus*, the little-studied tetraploid species *F. pratensis* Huds. subsp. *apennina* (De Not.) Hegi [also classified as *Schedonorus pratensis* subsp. *apenninus* (De Not.) H. Scholtz and Valdès]. The *Festuca* species henceforth referred to as *F. apennina* was described by De Notaris (1844) and St. Yves (1913) from the locality of Santo Stefano d'Aveto and is probably the same species as *F. pratensis* var. *megalostachys* (Stebler, 1904; Foggi and Müller, 2009). The genomic composition of the species has been a matter of some conjecture. The close relationship between *F. apennina* and the diploid fescue *F. pratensis*, a species having wider distribution throughout Eurasia and north-western Africa (Foggi and Müller, 2009), has long been known. Alternative claims have been made that *F. apennina* is an autotetraploid cytotype of *F. pratensis*, or now and more widely accepted, an allotetraploid species derived from two ancestral progenitor species (Lewis, 1977; Jauhar, 1993). Borrill et al. (1976) reported a different ecological and altitudinal distribution for the two fescue species with *F. apennina* absent below 1300 m above sea level (a.s.l.), sometimes accompanied by *F. pratensis* in regions between 1300 and 1600 m a.s.l., but to its exclusion at higher altitudes. The adaptation of *F. apennina* to high altitudes derives from its vegetative growth being confined to summer months, followed by a protracted growth quiescence and complete leaf senescence when winter stresses are evident from October to May (Tyler and Chorlton, 1974). Besides diploids and tetraploids, Tyler (1988) discovered the existence of triploid cytotypes and considered them as putative natural hybrids between *F. pratensis* and *F. apennina* at the mid-altitude locations where both species coexist.

The current research provides compelling evidence for the genome composition of *F. apennina*, and for its putative progenitors. Through cytogenetic studies of plant collections abstracted from Alpine meadows, including putative natural hybrids involving *F. apennina*, a hypothesis is proposed of how the region may have played a pivotal role in events that led to the evolution of polyploidy within the *Festuca* subg. *Schedonorus*. Through enhanced understanding of such key events and their genetic controls, it may be possible to replicate in similar fashion in hybrid genomes within *Festulolium* and thereby achieve desirable and productive grass varieties combined with the essential safeguards required to combat climate change.

MATERIALS AND METHODS

Plant Materials

The plant materials derived from two sources: from a genebank maintained at IBERS and from newly sourced plant material. Their origins including GPS coordinates and altitudes from where they were collected are summarized in **Table 1** and **Figure 1**. The initial IBERS *F. apennina* collection was established from Swiss accessions Bf 967 and Bf 1248 and three accessions from Romania (Bf 1575, Bf 1213, Bf 1214). In addition, an accession of *F. pratensis* (Bf 970) and of *F. arundinacea* (Bn 950) were included both collected from locations in close proximity to the sources of Swiss accessions Bf 967 and Bf 1248. Seed storage at IBERS included periods at 2°C with a Relative Humidity of 20% (to maintain viability for an estimated 25 years), but also from unique seed storage facilities where seed was maintained in sealed foil laminate pouches following drying to circa6% moisture content at −20°C (where viability was predicted for circa 100 years).

A synthetic triploid hybrid P127/200 ($2n = 3x = 21$) produced by crossing tetraploid *F. apennina* and diploid *F. pratensis* was used to verify the provenance of the unknown triploids collected. Another synthetic hybrid developed from the cross of tetraploid *L. multiflorum* and *F. apennina* has been used in this study.

New plant collections were made in May and September 2015 in order to collect new *F. apennina* genotypes. In May 2015, entire plants were collected from various localities in Switzerland and Italy (Alps and Apennines), including the *locus classicus* of *F. apennina* (Santo Stefano d'Aveto; see Ardenghi and Foggi, 2015). In September 2015, two sets of single leaves representing individual plants were collected from three Swiss localities and stored in wet paper towel until the flow cytometry analyses was carried out (10 days after collection). The first set of plants represented a random sample. The second set, were of leaves from selected plants whose morphology (large plants with broad leaves and brown-red bases of the leaves) was considered as consistent with expectations for a tetraploid cytotype. The collection sites in Switzerland and Italy differed; in Switzerland, plants were collected from mountain meadows and grazed-lands near farmsteads; in Italy the collection sites at Santo Stefano d'Aveto were in shaded woodland-cleared and water-logged areas.

Ploidy Level Determination

The ploidy level of each accession from the sampling expedition and plants grown from seed obtained from IBERS gene bank was estimated by flow cytometry (Doležel et al., 2007). Nuclear suspensions were prepared from 50 mg leaf tissues of each grass sample with *Pisum sativum* cv. Ctirad used as standard

TABLE 1 | Ploidy level of all plants analyzed in this study.

Accession/locality	GPS	Altitude (meters a.s.l.)	Number of plants			
			2×	3×	4×	5×
Bf 967 (Kandersteg, SUI)	46°49′5.7″N, 7°67′3.6″E	1650	0	**10**	8	8
Bf 1248 (Moleson, SUI)	46°55′5.0″N, 7°02′0.0″E	1420	0	0	**8**	0
Bf 1575 (Nou Sasesc, ROM)	47°12′2.5″N, 24°60′6.6″E	No detail given	0	0	**5**	0
Bf 1213 (Baile Borsa, ROM)	47°66′6.2″N, 24°65′0.0″E	1220	0	**6**	4	2
Bf 1214 (Borsa, ROM)	46°93′1.6″N, 23°66′8.1″E	1400	0	0	**2**	**2**
Mörlialp (SUI)	46°49′29.831″N, 8°6′33.691″E	1355	2	**9**	0	0
Glaubenbielen (SUI)	46°49′9.322″N, 8°5′6.227″E	1568	3	**11**	1	0
Fontanen (SUI)	46°48′25.780″N, 8°6′1.054″E	1703	0	0	**7**	0
Küblisbiehlschwand (SUI)	46°48′7.049″N, 7°58′20.928″E	1250	5	**11**	0	0
Stoos (SUI)	46°58′33.861″N, 8°39′8.480″E	1651	0	0	**1**	0
	46°58′33.756″N, 8°38′51.331″E	1717	0	**1**	0	0
	46°58′29.434″N, 8°38′33.951″E	1783	0	0	**4**	0
	46°58′13.674″N, 8°38′19.042″E	1865	0	0	**2**	0
Moleson (SUI)	46°33′54.005″N, 7°1′36.008″E	1401	0	**4**	1	0
	46°33′40.475″N, 7°1′27.395″E	1416	0	**1**	0	0
	46°33′16.041″N, 7°0′56.109″E	1516	0	**2**	0	0
	46°33′14.023″N, 7°0′41.123″E	1533	0	0	**1**	0
	46°33′3.133″N, 7°0′32.317″E	1634	0	0	**2**	0
	46°32′53.251″N, 7°0′43.595″E	1810	0	**2**	0	0
	46°32′45.070″N, 7°0′49.389″E	1743	0	0	**3**	0
	46°32′53.464″N, 7°1′32.261″E	1515	0	**1**	**1**	0
Gsteig (SUI)	46°23′15.657″N, 7°15′6.528″E	1737	0	**5**	0	0
	46°23′19.493″N, 7°15′11.936″E	1703	0	**5**	0	0
	46°23′17.948″N, 7°15′26.999″E	1541	0	**5**	0	0
La Para (SUI)	46°22′27.216″N, 7°10′24.343″E	2006	0	0	**5**	0
	46°22′18.769″N, 7°10′57.096″E	1907	0	0	**6**	0
	46°22′14.931″N, 7°11′23.823″E	1895	0	**4**	1	0
	46°21′39.263″N, 7°11′52.926″E	1710	0	**3**	0	0
Crissolo (SUI)	44°42′6.845″N, 7°8′54.079″E	1415	**5**	0	0	0
	44°42′9.487″N, 7°8′8.387″E	1603	**5**	0	0	0
	44°42′10.750″N, 7°8′59.370″E	1497	**4**	0	0	0
Santo Stefano d'–Aveto (IT)	44°33′33.621″N, 9°29′6.615″E	1596	0	0	**8**	0
	44°33′12.209″N, 9°29′5.997″E	1583	0	0	**5**	0

The altitude of the localities is highlighted by the gray scale. The most frequent cytotype is bolded.

having 2C = 9.09 pg (Doležel et al., 1998). The tissues were homogenized with a razor blade in a Petri dish containing 0.5 ml of Otto I solution (0.1M citric acid, 0.5% Tween 20). The nuclear suspension was filtered through 42 µm nylon mesh and stained with 1 ml Otto II solution (0.4M Na_2HPO_4.12 H_2O) containing 2 mg/ml ß-mercaptoethanol, and 2 µg/ml DAPI (4′,6-diamidino-2-phenylindole). Samples were analyzed using a CyFlow Space flow cytometer (Sysmex Partec GmbH., Görlitz, Germany) equipped with a UV led diode array. At least 5000 events were acquired per sample and only measurements with

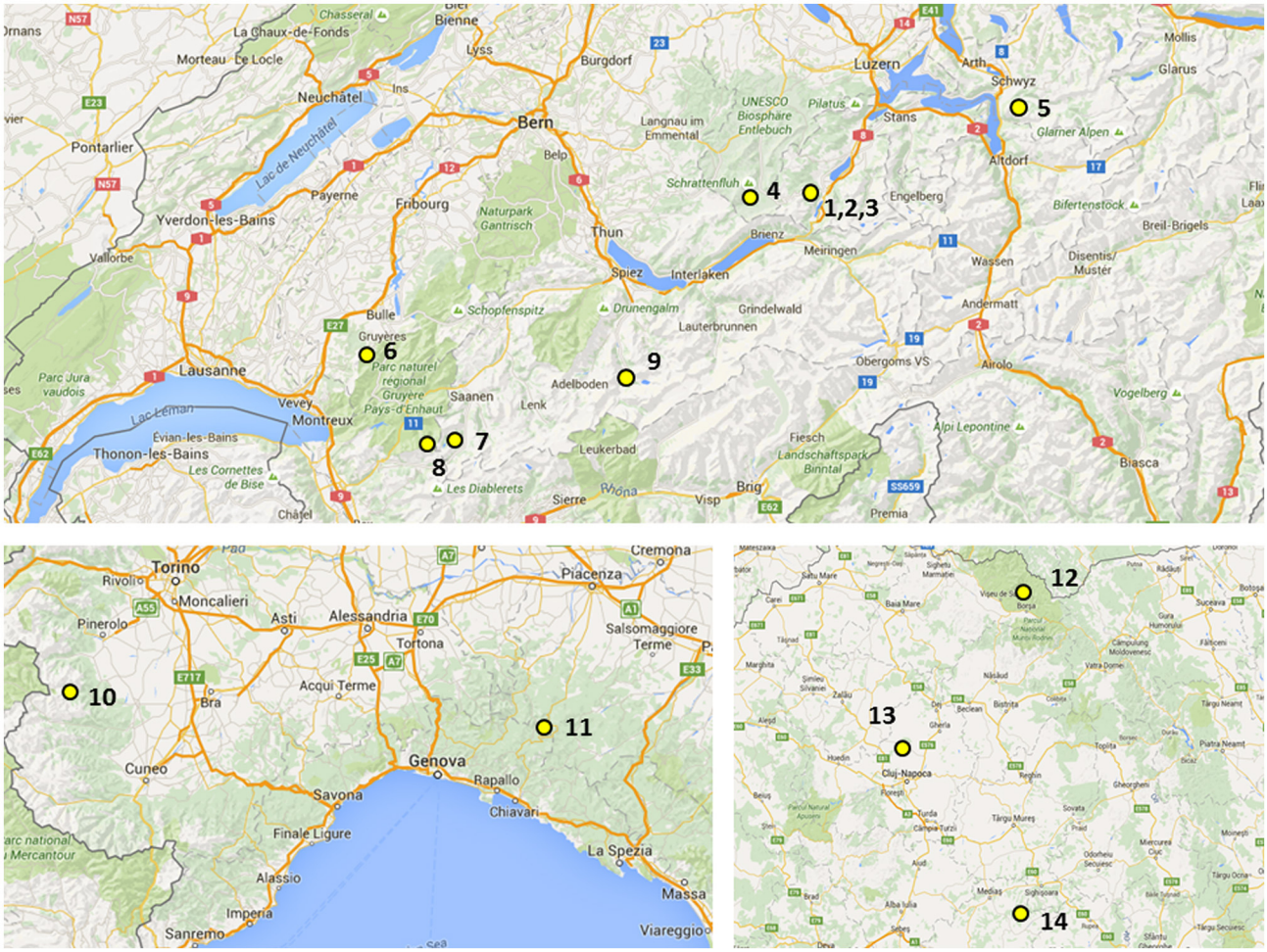

FIGURE 1 | Geographical distribution of localities in Switzerland (up), Italy (bottom, left), and Romania (bottom, right): (1) Mörlialp, (2) Glaubenbielen, (3) Fontanen (4) Küblisbiehlschwand, (5) Stoos, (6) Moleson, (7) Gsteig, (8) La Para, (9) Kandersteg, (10) Crisollo, (11) Santo Stefano d'–Aveto, (12) Baile Borsa, (13) Borsa, and (14) Nou Sasesc.

coefficient of variation for G0/G1 peaks <2.5% were accepted. Two representative plants from each tetraploid, triploid, and pentaploid cytotypes were checked by chromosome squash preparations and counting as described in Ahloowalia (1965) to verify the flow cytometric results.

Genomic *In situ* Hybridization (GISH) and Fluorescence *In situ* Hybridization (FISH) Analyses

A GISH analysis was undertaken on representative triploid, tetraploid, and pentaploid plants. In total, we analyzed five tetraploid plants: two plants from accession Bf 967, and one each from Bf 1248, Bf 1575, and Bf 1213, three pentaploids: two plants from Bf 967 and one from Bf 1213 and three triploid plants: one each from Bf 967, Bf 1213, and Bf 1214. In addition, the synthetic triploid hybrid *F. pratensis* × *F. apennina* P127/200 ($2n = 3x = 21$) and the synthetic tetraploid hybrid *L. multiflorum* × *F. apennina* developed from the cross of autotetraploid *L. multiflorum* with *F. apennina* were used for GISH analysis. GISH was done as described in Anamthawat-Jónsson and Reader (1995). In the first experiment, total genomic DNAs (gDNA) of *F. pratensis* and *F. apennina* were labeled with tetramethyl-rhodamine-5dUTP and fluorescein-12-dCTP, respectively. Both probes had been preannealed and thereafter hybridized with chromosomes of triploid and tetraploid cytotypes and also the synthetic hybrids squashed on microscopic slides. The same approach was used for GISH with the pentaploid cytotype, except the total gDNAs of *F. glaucescens* and *F. pratensis* were used as probes. In the case of the synthetic *L. multiflorum* × *F. apennina* hybrid, both probe combinations (*F. pratensis*–*F. apennina* and *F. pratensis*–*F. glaucescens*) were applied.

In the second experiment, probe made from total gDNA of *F. pratensis* by Nick-translations with Dig-Nick Translation Mix (Roche) and blocking DNA developed by shearing total gDNA of *F. glaucescens* were used. Probe hybridization signals were detected by anti-DIG-FITC conjugate.

In order to support the GISH results, FISH analyses (as described in Thomas et al., 1996; Harper et al., 2004) were undertaken with probes for 5S and 45S rDNA and tandem repeats (see below). Probes for 5S rDNA and 45S rDNA were prepared as described in Thomas et al. (1997). The rDNA probes were used in an initial FISH experiment with triploid, tetraploid, and pentaploid cytotypes and their possible progenitors represented by *F. arundinacea* Bn 950 and *F. pratensis* Bf 970.

Additionally, FISH probes were prepared from four tandem repeats (fpTR4, fpTR7, fpTR12, and fpTR15) identified in our previous work (Kopecký et al., 2013) using PCR labeling with biotin- or digoxigenin-labeled nucleotides (Roche) and pairs of specific primers. In addition, a 45S rDNA probe was used in this subsequent experiment. Probe hybridization signals were detected by anti-DIG-FITC and streptavidin-Cy3 conjugates. In total, 20 plants representing all identified ploidy levels were analyzed, each group comprising five genotypes identified as either having diploid (*F. pratensis*), triploid, or and tetraploid (*F. apennina*) genome compositions (localities Fontanen and Küblisbiehlschwand), and an additional five tetraploid *F. apennina* genotypes from Italy. In all experiments, the chromosomes were counterstained with 1.5 μg/ml DAPI in Vectashield antifade solution (Vector Laboratories). Slides were evaluated with an Olympus AX70 microscope equipped with epi-fluorescence and a SensiCam B/W camera and a Leica DM/RB epifluorescence microscope. ScionImage and Adobe Photoshop software were used for processing of the color pictures.

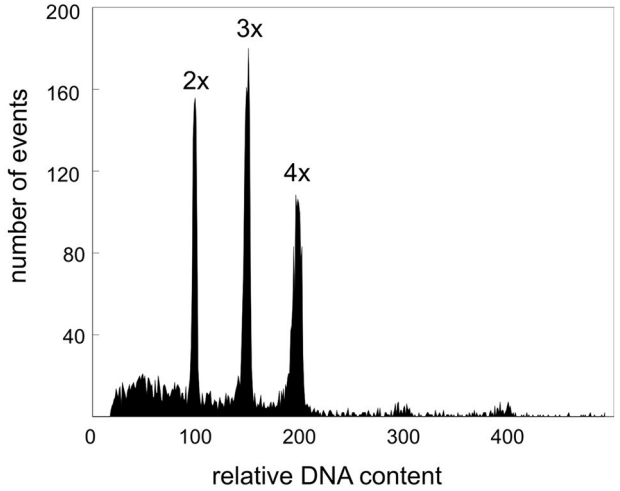

FIGURE 2 | Histogram of relative DNA content (DAPI fluorescence intensity) obtained after simultaneous analysis of nuclei isolated from diploid, triploid, and tetraploid plants collected in Glaubenbielen.

RESULTS AND DISCUSSION

Mitotic chromosome counts in 26 plants randomly selected from Swiss accession Bf 967 indicated large variation in chromosome number. Ten plants had 21 chromosomes (including several plants possessing B chromosomes), eight plants had 35 chromosomes, and only eight plants had the anticipated 28 chromosome constitution. All eight analyzed plants of another accession from Switzerland (Bf 1248) were confirmed as tetraploids. Among 12 plants of Romanian accession Bf 1213, six were triploid, two were pentaploid ($2n = 35$), whilst the remaining four plants carried the anticipated 28 chromosome complement. In another Romanian Accession (Bf 1214), two plants with 35 chromosomes and another two plants with 28 chromosomes were detected. All five plants of accession Bf 1575 from Romania were tetraploid (**Table 1**).

Large variation in ploidy level from location to location and at different altitudes has also been found among the plants sampled in Switzerland and Italy. In total, 136 plants were analyzed and 24 diploid (*F. pratensis*), 64 triploid and 48 tetraploid (*F. apennina*) genotypes were identified (**Figure 2**). Surprisingly, unlike the Swiss and Romanian accessions described above, no pentaploid plants were found amongst the newly collected Swiss and Italian ecotypes. The diploids were detected primarily at lower altitudes, and no diploids were detected above 1750 m a.s.l. Plants having triploid chromosome complements were found growing together with diploids in a sympatric manner, but only up to 1900 m a.s.l. Tetraploids were usually detected above 1500 m a.s.l., but one tetraploid plant from the Moleson locality was recovered at 1401 m a.s.l. In most of the Swiss localities, two or three cytotypes were found growing sympatrically. However, in the Italian locality Crissolo, only diploids were detected. In contrast, only tetraploid genotypes were found in the Italian locality Santo Stefano d'Aveto. Triploids predominated in many Swiss localities and in several sites they were the only cytotypes identified (e.g., localities in Gsteig and one La Para locality). Ploidy levels of plants from all sites and localities are given in **Table 1**.

In order to achieve a more accurate and representative view of ploidy compositions, as the initial plant numbers sampled were small (up to 15 plants per site), a further collection was taken from the three sites where previously two or three cytotypes had been detected. Random sampling of 85 plants in Mörlialp (1355 m a.s.l.) revealed 11.8% of plants as diploids, 88.2% as triploids, and with no tetraploid genotype detected. Random sampling of one hundred genotypes in Glaubenbielen (1568 m a.s.l.) identified 15% of plants as diploids, 52% as triploids, and 33% as tetraploids. When preferential sampling was undertaken on 20 plants considered from their morphology as likely to be tetraploid cytotypes of *F. apennina*, three diploids, and 13 triploids were identified, whilst only four plants had an expected tetraploid genome complement. Flow cytometric analysis of 89 randomly sampled plants from Küblisbiehlschwand locality (1250 m a.s.l.) revealed 92.1% diploids, and 7.9% triploids. Attempts at preferential sampling for 20 plants with tetraploid-like growth morphology proved totally inadequate as cytological studies revealed 14 as diploids and 6 as triploids. It is evident that preferential sampling for tetraploid-like plants based only on their morphological characters is not practical as it was impossible to distinguish diploids, triploids and tetraploids at the vegetative stage.

Flow cytometry showed that triploid cytotypes predominated and moreover they were the only cytotype found at some

localities. Previous sampling had revealed only diploids and tetraploid cytotypes (Borrill et al., 1976; Tyler et al., 1978), but one report mentioned the recovery of triploid cytotypes (Tyler, 1988). Whilst the fertility of the triploid cytotypes was not assessed, it is expected that they had high sterility relying primarily on vegetative propagation for their widespread establishment. Clarke et al. (1976) developed synthetic triploid hybrids of *F. pratensis* × *F. apennina* which they found to be sterile. In this case, fertility was restored by chromosome doubling to encourage preferential homologous chromosome pairing in the resulting hexaploid genotype. The predominance of the triploid cytotype is intriguing, and implies they have an adaptive selection advantage compared to the diploid and tetraploid cytotypes. In the Küblisbiehlschwand and Mörlialp localities, over one hundred individuals were sampled, and no tetraploid detected. A somewhat similar finding was reported by Humphreys and Harper (2008). They reported the presence of triploid hybrids of *Festulolium loliaceum* (Huds.) P. Fourn., a natural *Festulolium* hybrid species derived from hybridization between diploid *F. pratensis* and *L. perenne*. The triploid cytotypes (which had two alternative genome combinations; either having two genomes of *Lolium* or two of *Festuca*) were found growing on heavily waterlogged soils where neither parental species was generally found, suggesting that their enhanced genome dosage and consequent genome interactions had provided them a certain adaptive advantage. However, diploid cytotypes of *Festulolium loliaceum* are also found growing in waterlogged soils at the same locations as the triploid cytotypes, which might indicate, at least in this instance, that it is more the extent of intergeneric genome activity between the *Lolium* and *Festuca* genomes that is responsible for the adaptive advantage found over the parental species. Both diploid and triploid cytotypes of *Festulolium loliaceum* show high male and female sterility (Humphreys and Harper, 2008).

The triploid cytotypes of *F. apennina* and of *Festulolium loliaceum* arose probably from the interspecific hybridization of diploid and tetraploid cytotypes (triploid *F. apennina*) or as a consequence of the presence of unreduced gametes within their diploid parental (either *F. pratensis* or *L. perenne*) species (triploid *Festulolium loliaceum*). The occurrence of unreduced gametes is believed to be a common feature found in various *Festulolium* species (Morgan et al., 1988), and is likely within the genus to be an important component part in the events that led to the evolution of a polyploid series and through these, the perpetuation of interspecific hybrids. Through genome duplication in interspecific hybrids preferential intraspecific homologous chromosome pairing becomes possible leading to disomic inheritance, genome stability and to improved fertility. However, on its own, in hybrids between the closely related species of the *Lolium-Festuca* genome complex, the extent of intraspecific homologous chromosome pairing is insufficient to reliably maintain over generations stable and balanced genome complements. Indeed, if preferential chromosome pairing was sufficient on its own to ensure genome perpetuity, then the consistent difficulties reported by *Festulolium* breeders in maintaining intact and stable hybrid genomes would not have arisen (Ghesquiere et al., 2010). An additional requirement was necessary in the evolution of *Festuca* polyploids in order to obtain consistent disomic inheritance in their natural amphiploid hybrid genome complements; the chromosome pairing regulator first identified in *F. arundinacea* (Jauhar, 1975; Lewis et al., 1980). The event(s) that allowed acquisition of the supplementary diploidising mechanism present in polyploid fescues is likely to have played a pivotal role in the evolution of a polyploid series in *Festuca*.

It would seem unlikely that such an otherwise unique diploidising mechanism had evolved to function in the same manner through independent events in different polyploid fescue species. The system may have evolved only once and subsequently been distributed by interspecific hybridization events between various fescue species. The mechanism is presumably sited on a common subgenome found in all polyploid fescues. The system in polyploid *Festuca* species differs from the *Ph1* of wheat and the system found in polyploid oats by the haplo-insufficiency or hemizygous-ineffectiveness, which means that the system is inactive in single-dose. From a *Festulolium* plant breeding perspective strategies need to be developed whereby gene(s) that confer a functional diploid like chromosome -pairing system are present in two copies in order that stable *Festulolium* genomes are achieved.

Genomic *In situ* Hybridization (GISH) and Fluorescence *In situ* Hybridization (FISH) Analysis of *Festuca apennina* Cytotypes

GISH was used to determine the genomic composition of tetraploid *F. apennina*, and also the triploid and pentaploid cytotypes found growing in close association. Hybridization of *F. apennina* chromosomes with differentially labeled probes of gDNA of *F. pratensis* and *F. apennina* resulted in the painting of 14 chromosomes by gDNA of *F. pratensis* and of all chromosomes by the gDNA of *F. apennina* (data not shown). When *F. pratensis* gDNA probe was used together with blocking DNA from *F. glaucescens* onto tetraploid *F. apennina* chromosomes, 14 chromosomes became labeled with 14 chromosomes remaining unlabeled (**Figure 3G**). From this, it can be concluded that *F. apennina* is an allotetraploid species having derived from at least two ancestral progenitors, one of which was *F. pratensis*. The second diploid species progenitor of *F. apennina* is unknown. This is not surprising as *F. pratensis* is the only diploid species found in the European clade of *Festuca* subg. *Schedonorus*. GISH provided no evidence for any interspecific chromosome recombination between the constituent genomes in *F. apennina* giving support to previous meiotic studies where strict homologous bivalent chromosome pairing and disomic inheritance of the parental genomes was reported (Lewis, 1977).

Conclusions drawn from the GISH results over the genomic constitution of *F. apennina* gained further support from the FISH study where rDNA and tandem repeats were used as probes. In *F. pratensis*, two 45S rDNA loci were detected each at homologous sites on the short arm of chromosome 3. Two 5S rDNA loci were located at a pericentromeric region on the short arm of chromosome 2 (**Figure 3A**). These findings are in agreement

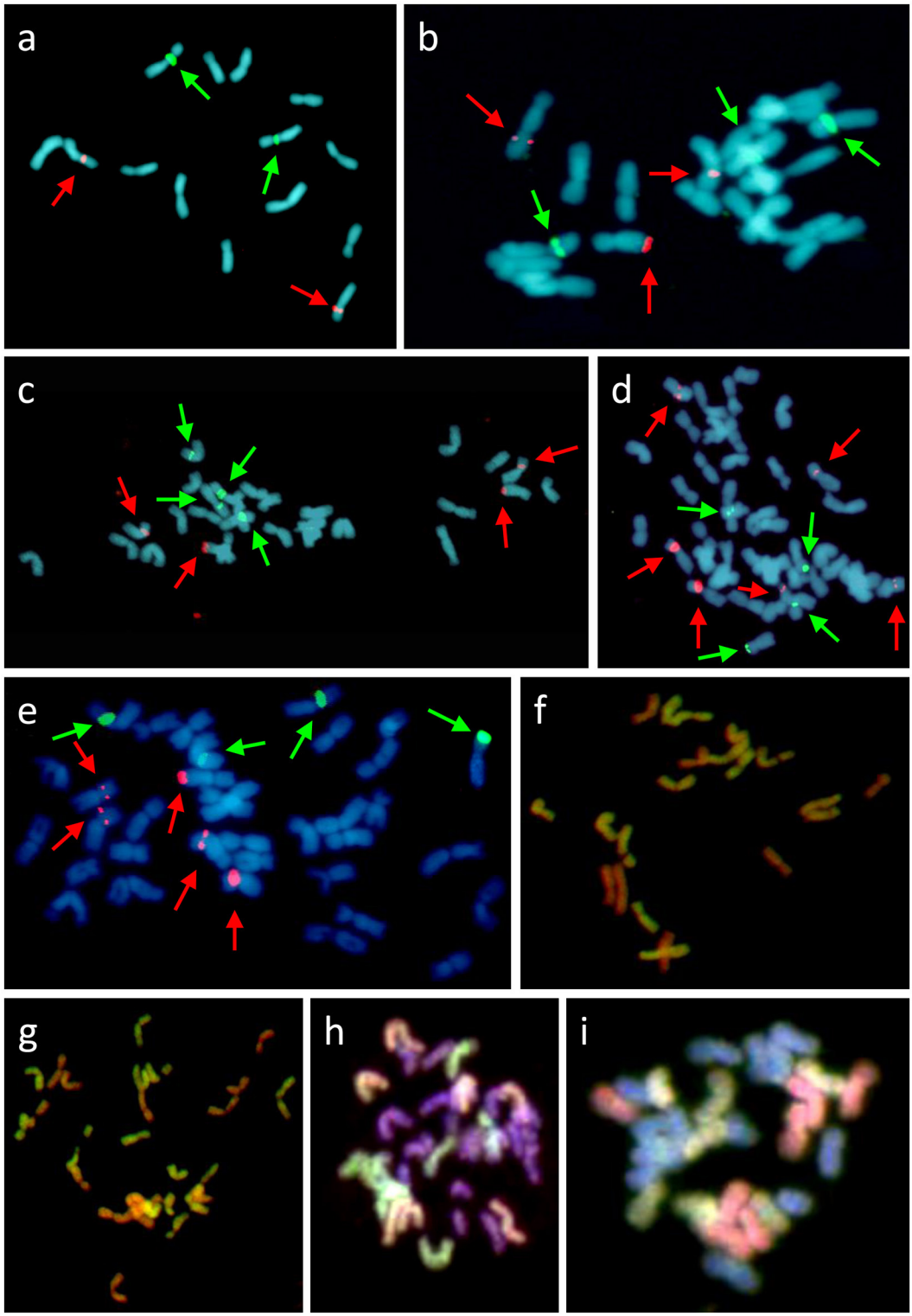

FIGURE 3 | Cytogenetic analysis of *F. pratensis*/*F. apennina*/*F. arundinacea* complex (A–G) and *L. multiflorum* × *F. apennina* hybrid (H,I). FISH with probes for 5S rDNA (red color, highlighted with red arrows) and 45S rDNA (green color, highlighted with green arrows) on metaphase spreads of diploid *F. pratensis* **(A)**, triploid hybrid **(B)**, tetraploid *F. apennina* **(C)**, pentaploid hybrid **(D)**, and hexaploid *F. arundinacea* **(E)**. GISH with probe made from labeled gDNA of *F. pratensis* and blocking DNA from sheared gDNA of *F. glaucescens* in triploid **(F)** and tetraploid **(G)** revealed hybrid origin of both cytotypes. Additional GISH analysis of tetraploid *L. multiflorum* × *F. apennina* hybrid with two probe combinations: **(H)** gDNA of *F. pratensis* (red color) and gDNA of *F. apennina* (green color) and **(I)** gDNA of *F. pratensis* (green color) and *F. glaucescens* (red color). Chromosomes were counterstained with DAPI (blue color).

with previous results of Thomas et al. (1997) and Kopecký et al. (2008a). In *F. apennina*, four 45S rDNA loci were detected on two pairs of chromosomes. In addition, a pair of chromosomes carried 5S rDNA loci at proximal regions, whilst another pair of chromosomes carried 5S rDNA loci in telomeric or subtelomeric regions (**Figure 3C**). This supports expectations that *F. pratensis* was one of the progenitor species found in *F. apennina*. However, FISH studies where four tandem repeats were used as probes revealed that in the years subsequent to speciation, the subgenome of *F. pratensis* present in *F. apennina* had undergone substantial chromosome reconstruction (**Figure 4**).

A similar approach was applied to the triploid and pentaploid cytotypes. In triploid plants ($2n = 3x = 21$), 14 chromosomes were found to be labeled by a gDNA probe of *F. pratensis* and the other seven chromosomes by a gDNA probe of *F. apennina*. When *F. pratensis* gDNA probe was applied together with blocking DNA from *F. glaucescens* again 14 chromosomes were labeled (**Figure 3F**). This was evidence that the triploid cytotype was a consequence of the hybridization of tetraploid *F. apennina* and diploid *F. pratensis*. The numbers and position of rDNA loci (**Figure 3B**) and tandem repeats (**Figure 4**) detected were consistent with expectations based on their number and positions in *F. apennina* and *F. pratensis* and that these were the parental species supporting the GISH results. Given the same GISH and FISH treatments, the synthetic triploid hybrid P217/200 (*F. apennina* × *F. pratensis*) produced an identical result to those obtained in the natural triploid hybrids. No evidence for homoeologous recombination events was detected, which implies either that the triploids were sterile F_1 hybrids, or that they were *de novo* and had not yet passed through a flowering stage.

The identification of a pentaploid cytotype involving *F. apennina* was a new discovery. It may have arisen from an unreduced gamete of the triploid cytotype that hybridized with a normally reduced gamete of tetraploid *F. apennina*. Alternatively, the pentaploid may have arisen following interspecific hybridization of tetraploid *F. apennina* and a closely related hexaploid fescue, probably *F. arundinacea* subsp. *arundinacea*. This species was found growing nearby and could have inter-pollinated with tetraploid *F. apennina*. The latter scenario was tested. *F. arundinacea* subsp. *arundinacea* Shreb. is an allohexaploid species developed from hybridization of *F. pratensis* and tetraploid *F. glaucescens* (Humphreys et al., 1995). Consequently, labeled gDNAs of *F. glaucescens* and *F. pratensis* were selected as probes for GISH and applied to denatured chromosomes of the pentaploid plants. The results supported expectation that the pentaploid genotypes had arisen following the hybridization of *F. apennina* by *F. arundinacea* subsp. *arundinacea*. The *F. pratensis* probe labeled 14 chromosomes expected to have derived from one genome of *F. pratensis* chromosome complement from *F. arundinacea* and another from *F. apennina*. The *F. glaucescens* gDNA probe hybridized to 14 chromosomes, expected to have derived from *F. arundinacea* subsp. *arundinacea*. The remaining seven chromosomes in the pentaploid hybrid were weakly hybridized to the *F. glaucescens* gDNA probe (**Figure 4**). Through further detailed GISH analysis of the pentaploid hybrid its origin was confirmed (**Figure 5**). In this case two probe combinations were used: (1) gDNA of *F. pratensis* in combination with 45S rDNA with sheared DNA from *F. glaucescens* used as blocking gDNA; (2) gDNA of *F. glaucescens* with sheared *F. pratensis* used as blocking DNA. Chromosomes were counterstained with DAPI. The *F. pratensis* gDNA probe hybridized onto 14 chromosomes (representing one *F. pratensis* genome from its putative *F. apennina* parent and one from *F. arundinacea*). The remaining 21 chromosomes were unlabeled. The gDNA probe of *F. glaucescens* hybridized onto 21 chromosomes. These represented the two ancestral genomes of *F. glaucescens* found in *F. arundinacea* together with the single *F. glaucescens* genome in *F. apennina*. The signal intensity of the *F. glaucescens* probe over the pentaploid hybrid chromosomes varied with 14 chromosomes having a stronger signal compared to the other seven chromosomes. It is proposed that the stronger hybridization was onto the two chromosome sets derived from *F. arundinacea* whilst the inferior signal derived from the chromosomes of the so far unknown subgenome of *F. apennina*. It is likely that this subgenome has a common origin to that of one of the subgenomes of *F. glaucescens*. As current *F. glaucescens* shares greater genome homology to the two *F. glaucescens* subgenomes of *F. arundinacea* than to the *F. glaucescens* genome present in *F. apennina* it can be speculated that the speciation events that gave rise to the allotetraploid *F. apennina* may have occurred at an earlier date than those that led to the hexaploid *F. arundinacea.* In that event, it can be further speculated, the speciation of *F. apennina* may represent a key intervening stage during the evolution of *F. arundinacea.*

The 5S rDNA loci found in *F. arundinacea* subsp. *arundinacea* accession Bf 950 (**Figure 3E**) differed in their position as compared to those reported previously in another genotype of *F. arundinacea* subsp. *arundinacea* (Thomas et al., 1997). In accession Bf 950, all three pairs of 5S rDNA loci were located proximally. This contrasted with the previous report where one pair of 5S rDNA loci was located in telomeric region of long arm of one chromosome pair. The number and distribution of 45S rDNA loci found in accession Bf 950 agreed with previous reports (Thomas et al., 1997). As in the case of the triploids, the distribution and number of rDNA sites in the pentaploid plants was completely consistent with expectations based on their presumed parentage (*F. apennina* and *F. arundinacea* subsp. *arundinacea*) (**Figure 3D**) drawn from the GISH analyses. All FISH results are summarized in **Table 2** and in **Figure 6**.

GISH analysis of a synthetic tetraploid hybrid *L. multiflorum* × *F. apennina* ($2n = 4x = 28$) supported the conclusions drawn from cytogenetic studies involving the natural *F. apennina* cytotypes. GISH analysis using gDNA probes of *F. pratensis* and of *F. apennina* identified seven chromosomes when labeled by the *F. pratensis* probe (one of the two genomes of *F. apennina*) and 14 chromosomes when labeled by the *F. apennina* probe (both genomes of *F. apennina*). Fourteen chromosomes remained unlabeled and were the chromosome complement derived from *L. multiflorum* (**Figure 3H**). Similarly when gDNA probes of *F. pratensis* and of *F. glaucescens* were applied in

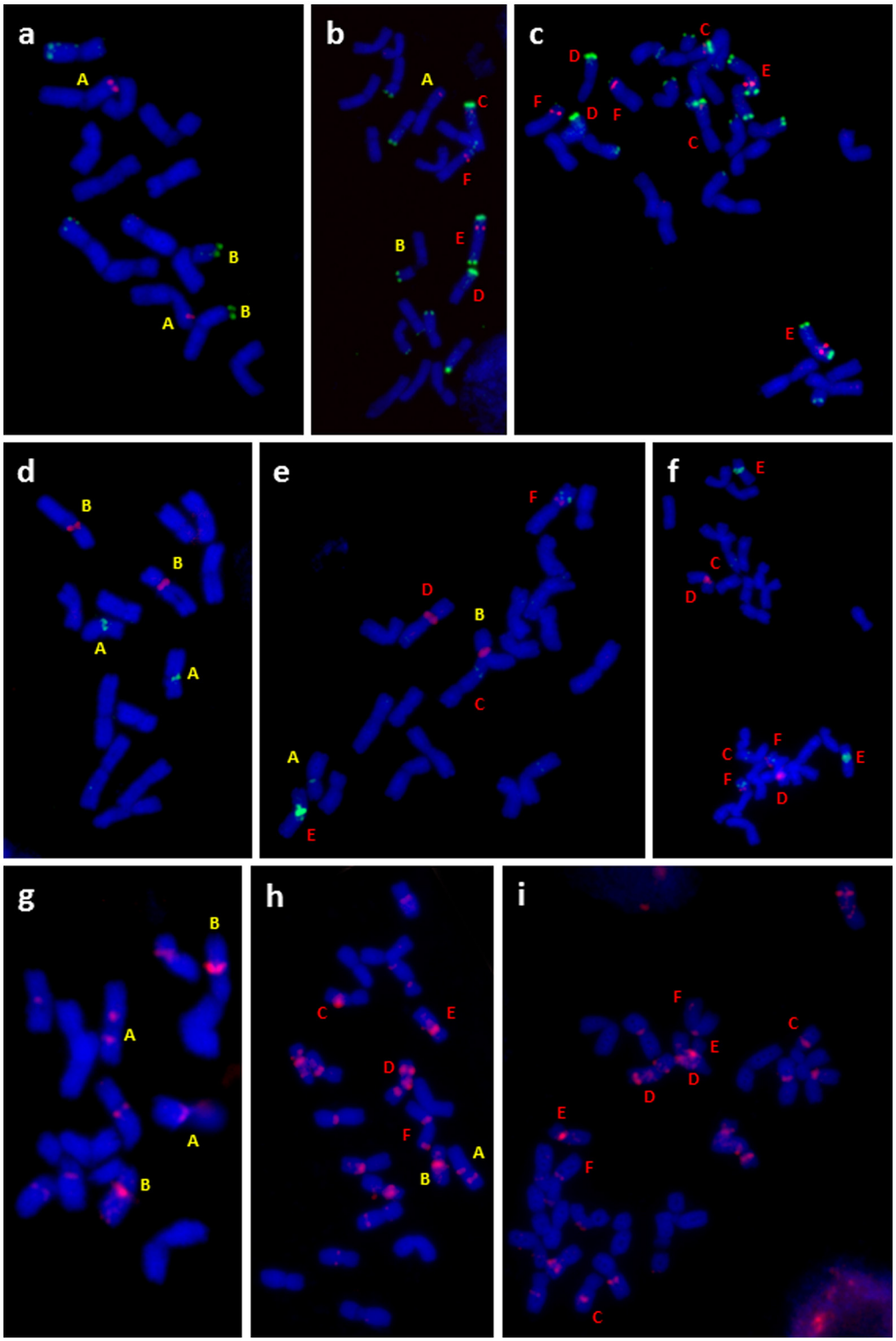

FIGURE 4 | Cytogenetic analysis of diploid *F. pratensis* (A,D,G), triploid hybrid (B,E,H), and tetraploid *F. apennina* (C,F,I). FISH was done on metaphase spreads with probes for: **(A,B,C)** tandem repeats fpTR12 (green color) and fpTR4 (red color), **(D,E,F)** fpTR15 (green color) and 45S rDNA (red color) and **(G,H,I)** fpTR7 (red color). Chromosomes with unique fluorescent signals present in diploid *F. pratensis*, tetraploid *F. apennina* and their triploid hybrid are marked by letters. Chromosomes were counterstained with DAPI (blue color).

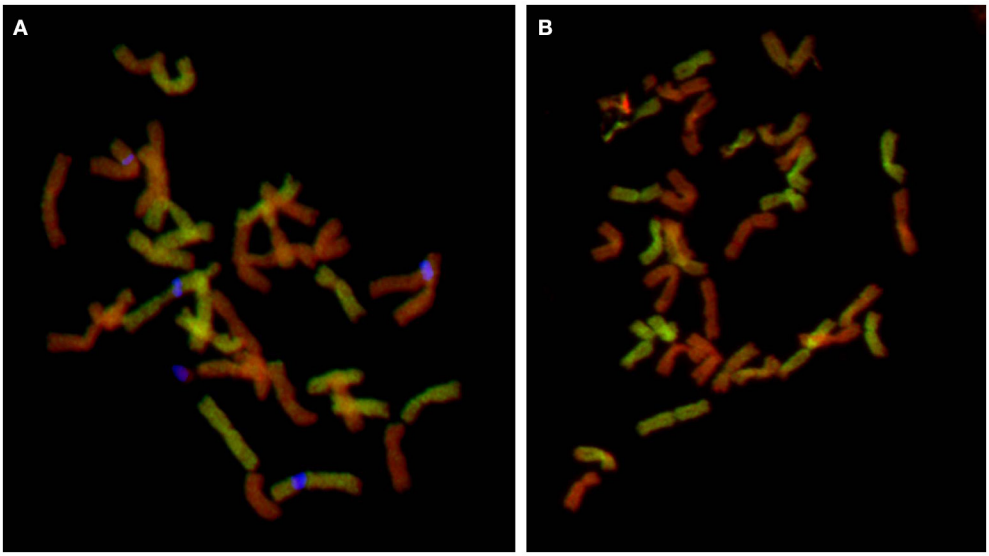

FIGURE 5 | Cytogenetic analysis of pentaploid hybrid. GISH with two probe combinations: **(A)** gDNA of *F. pratensis* (green color) and 45S rDNA (blue pseudocolor) and blocking DNA from sheared gDNA of *F. glaucescens* and **(B)** gDNA of *F. glaucescens* (green color) and blocking DNA from sheared gDNA of *F. pratensis*. Chromosomes were counterstained with DAPI (red pseudocolor). In the first combination, *F. pratensis* probe produced signal over 14 chromosomes (representing two sets of *F. pratensis* chromosomes: one from *F. apennina* and other from *F. arundinacea*) and other 21 chromosomes remained unlabeled (one set from the second subgenome of *F. apennina* and two sets representing subgenomes of *F. glaucescens* present in *F. arundinacea*). The second probe combination supports the previous findings: 14 chromosomes were unlabeled and represent two sets of *F. pratensis* chromosomes (one coming from *F. arundinacea* and the second from *F. apennina*) and 21 chromosomes were labeled with *F. glaucescens* probe. However, there was a variation in the signal intensity—signal over 14 chromosomes was much stronger (representing two chromosome sets of *F. glaucescens* coming from *F. arundinacea*) than other seven poorly labeled chromosomes, which are probably from the so far unknown subgenome of *F. apennina*. This subgenome is probably related to *F. glaucescens*, but has diversified during its evolution.

TABLE 2 | Localization of four tandem repeats and rDNAs by FISH.

Ploidy	Number of chromosomes with fluorescent signal (s) per mitotic metaphase plate					
	5S rDNA	45S rDNA	fpTR4	fpTR7	fpTR12	fpTR15
Diploid (*F. pratensis*)	2	2	2	8	4	2
Triploid	3	3	3	14–15	11	3–5
Tetraploid (Romania)	4	4	N/A	N/A	N/A	N/A
Tetraploid (Switzerland)	4	4	6	20–21	18	6
Tetraploid (Italy)	N/A	4	6	20	14	6
Pentaploid	5	4	N/A	N/A	N/A	N/A
Hexaploid (*F. arundinacea*)	6	4	N/A	N/A	N/A	N/A

conjunction to chromosomes of the synthetic *L. multiflorum* × *F. apennina* tetraploid hybrid, the *F. pratensis* probe labeled seven chromosomes, and the *F. glaucescens* gDNA probe labeled further seven chromosomes (the two species' genomes in combination believed to represent the complete *F. apennina* haplotype). Fourteen chromosomes representing *L. multiflorum* genome remained unlabeled (**Figure 3I**). The GISH study of the synthetic *Festulolium* hybrid revealed the close relationship between a subgenome of tetraploid *F. glaucescens* and of *F. apennina* and it is hypothesized here that they share a common progenitor.

The development of the cytogenetic techniques GISH and FISH for applications with the grasses of the *Lolium-Festuca* complex has enabled the effective discrimination between genomes of several species (Thomas et al., 1994; reviewed in Kopecký et al., 2008b) and allowed determination of the progenitors of certain polyploid *Festuca* species. A good example was the determination of the ancestry of *F. arundinacea* Schreb. (Humphreys et al., 1995). Using FISH with rDNA probes, Ezquerro-Lopez et al. (personal communication) identified *F. mairei* and *F. glaucescens* to be potential progenitors of octoploid *F. arundinacea* subsp. *atlantigena* (St.-Yves) Auquier and decaploid *F. arundinacea* var. *letourneuxiana* (St.-Yves) Torrec. & Catalán. In a similar approach, the combined GISH and FISH analysis reported here reveals for the first time the genomic constitution of *F. apennina*.

In addition to the hybridization that has occurred naturally between species within *Festuca* subg. *Schedonorus*, there are equivalent occurrences between these *Festuca* species and representatives of genus *Lolium*. An example is *Festulolium holmbergii* (Dőrfl.) P. Fourn., a tetraploid grass hybrid formed between *Lolium perenne* and *F. arundinacea* subsp. *arundinacea*. Similarly, *Festulolium braunii* (K.Richt.) A.Camus (*L. multiflorum* × *F. pratensis*) and the previously mentioned *Festulolium loliaceum* (Huds.) P.Fourn. (*L. perenne* × *F. pratensis*). All these *Festulolium* hybrids are well known and as synthetic combinations have been bred for agricultural

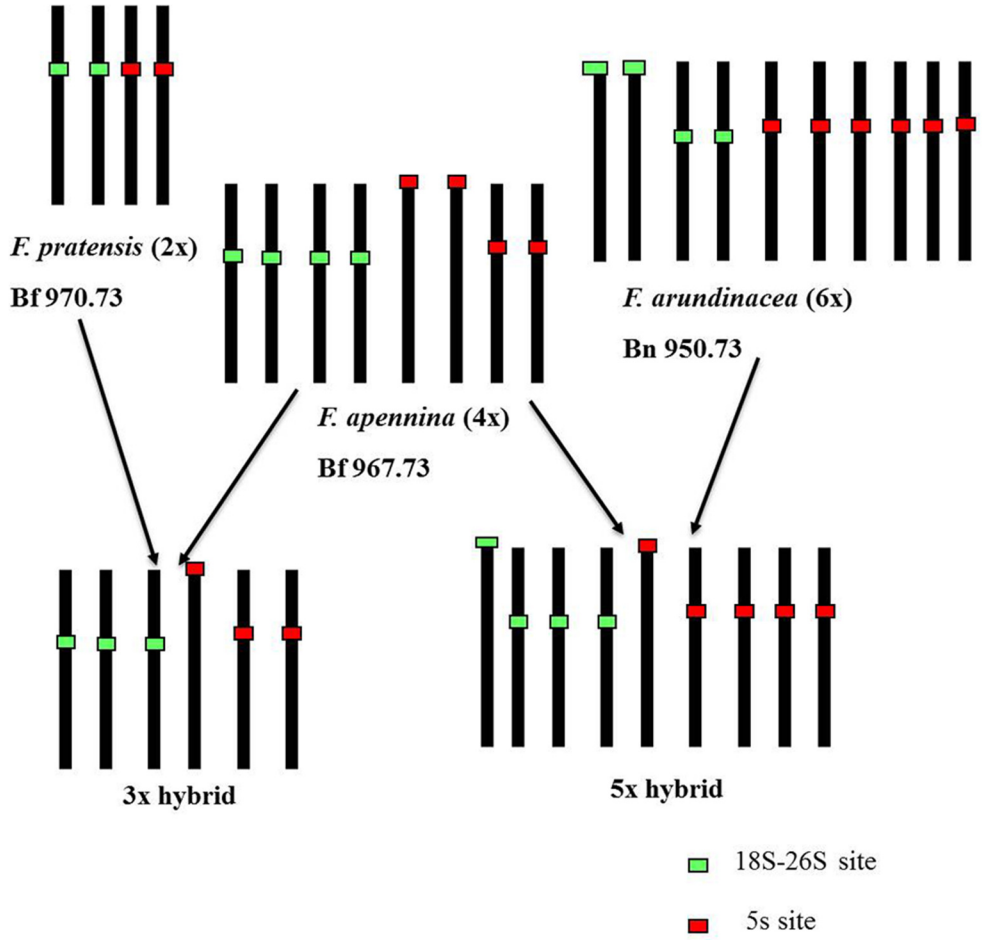

FIGURE 6 | The relationship between the *Festuca* species and their hybrids based on rDNA sites.

production with the aim to combine the attributes of their parent species (Ghesquiere et al., 2010).

How Can Plant Breeders Benefit from Improved Understanding of the Genomic Constitution of *F. apennina* and Its Hybrids?

It has long been an aim for grass breeders to combine the complementary characters found in *Lolium* (high growth rates and forage quality) with those found in *Festuca* (stress tolerance, deeper rooting) species (Ghesquiere et al., 2010) to ensure that grass varieties are both productive and resilient to climate-change. The additional novel ecosystem service properties found recently in certain *Festulolium* hybrids, such as for flood mitigation (Macleod et al., 2013), or for improved ruminant nutrition with potential for lowering greenhouse gas emissions by livestock (Humphreys et al., 2014) only serve to reinforce the view. Genetically stable, productive, and resilient high quality *Festulolium* varieties are necessary to ensure we have in place future safeguards in grassland agriculture sufficient to withstand extreme weather events and to achieve consistent and sustainable fodder for use by livestock to help feed an increasing global population. Introgressive forms of *Festulolium*, where limited numbers of targeted genes were transferred from a wild-relative into the genomes of existing high quality varieties have been successful. They have proven to be genetically stable and have led to advances in the breeding of drought tolerant or disease resistant cultivars (Humphreys et al., 2006).

However, evolution and speciation within the broad-leaved fescues of the *Festuca* subgenus *Schedonorus* has demonstrated consistently that hybridization followed by the retention of intact species' genomes in combination is an essential prerequisite for ensuring consistent adaptations to stresses encountered regularly by grasses that grow in extreme climates. It is clearly of advantage that once a hybrid form and desirable genome combination has been achieved, that it is stabilized and perpetuated into subsequent generations. Incidents of heterosis abound within the species of the *Lolium-Festuca* complex capable of providing adaptive traits that otherwise are unavailable to their parental genotypes. The hexaploid species *F. arundinacea* is a good example (Humphreys et al., 1995).

The hexaploid fescue, as shown here, shares two common genomes with tetraploid *F. apeninna*. Their progenitors are the northern European and cold-tolerant species *F. pratensis* and an ancestral southern European or Mediterranean based drought and heat-tolerant species also found in *F. glaucescens*. These species' genomes of *F. apennina* in combination provide the appropriate stress-tolerance adaptations necessary for grasses to grow and perpetuate at high altitude in Alpine meadows. The species *F. glaucescens* in Mediterranean regions avoids extreme temperatures and desiccation by undergoing complete growth quiescence (Humphreys et al., 1997) during the summer months. *F. apennina* undergoes an equivalent growth cessation and induced senescence stage that offers it protection against freezing temperatures and desiccation throughout the winter months (Tyler and Chorlton, 1974). From a plant breeding perspective, any prolonged cessation in foliar growth is far from ideal from the perspective of satisfying requirements for achieving sustainable agricultural production and sufficient fodder provision for livestock. However, the incorporation of genes for drought and heat tolerance from *F. glaucescens* into *Lolium* has been achieved without recourse to summer growth cessation (Humphreys et al., 2005) showing that drought avoidance alone is not the only strategy available to *F. glaucescens* to combat drought stresses. As it shares common ancestral genomes, the findings by Humphreys et al. (2005) provide hope that equivalent physiological mechanisms for stress-tolerance may be available to *F. apennina* that may provide benefits to *Lolium* spp. in certain synthetic hybrid combinations.

The evolution of the polyploid series of *Festuca* species within the subgenus *Schedonorus* provides us with an insight as to how optimal *Lolium* and *Festuca* species' genome combinations may be retained over generations. An essential prerequisite appears to be the incorporation of an intact and functional diploidising mechanism present in polyploid *Festuca* spp. within the genomes of a synthetic amphiploid *Festulolium* hybrid. As far as is known diploid species within the *Lolium/Festuca* complex lack such a functional system (Kopecký et al., 2009). As *F. pratensis* provides a subgenome for *F. apennina*, its chromosome regulator must reside on the other species' subgenome, one that may well be common in all polyploid species within the subgenus *Schedonorus*. From a practical *Festulolium* plant breeding perspective, this provides *F. apennina* with an advantage over all other *Festuca* polyploids. The location of the chromosome pairing regulator in these other polyploid fescues is unknown as it may reside anywhere in two or more subgenomes making its selection in breeding programmes in a functional homozygous form very problematic. The substitution of the *F. pratensis* genome of *F. apennina* by one from a *Lolium* spp. whilst also maintaining intact the integrity of the second *F. apennina* subgenome should provide opportunities to select genotypes that contain a functional chromosome pairing regulator to thereby restrict chromosome pairing to intraspecific homologous associations. Using conventional plant breeding technologies and interpollination of *Lolium* spp. × *F. apennina* amphiploid ($2n = 4x = 28$) hybrids and incorporating selections over generations for disomic inheritance, aided hopefully by future inclusion of relevant gene marker technologies, the attributes of both *Lolium* and *Festuca* may be combined in a stable and consistent form with the full potential for assemblies of complementary *Lolium* and *Festuca* traits within a single *Festulolium* genome be achieved.

Future genomic investigations may reveal candidate gene(s) for the chromosome pairing regulator known to occur in *F. apennina* and other related polyploid fescues. Its successful transfer and operation in a homozygous form in *Lolium* × *Festuca* hybrids would mark a significant progress into achieving climate-smart grasses and for procedures to safeguard future grassland agriculture by the creation of *Festulolium* cultivars with fescue-derived adaptations to abiotic stresses.

AUTHOR CONTRIBUTIONS

DK, JH, JD, and MH designed the project and experiments; JH, DG, and MH established the initial seed collection; DK, BB, and NA realized sampling expeditions; NA checked taxonomic and nomenclatural aspects; JB, JV, and DŠ made cytometric analyses; JH performed chromosome counting; JH and DG made GISH experiments and FISH with rDNAs; DK, EH, and DŠ performed FISH with tandem repeats. DK, JH, and MH drafted the manuscript. All authors revised the text and approved the final version of the manuscript.

ACKNOWLEDGMENTS

DK, JB, JV, EH, DŠ, and JD has been partially supported by the grant LO1204 from the National Program of Sustainability I. MH, JH, and DG are funded by the Biotechnology and Biological Sciences Research Council. MH is also part funded by the BBSRC-LINK Programme SUREROOT which in addition to BBSRC is supported by partners from the UK's grass seed, grassland, and livestock industries. MH is part of the Climate-Smart Grass Consortium. Funding to support this work was provided by the Welsh Government and HEFCW through the Sêr Cymru National Research Network for Low Carbon, Energy, and Environment.

REFERENCES

Ahloowalia, B. S. (1965). A root tip squash technique for screening chromosome number in *Lolium*. *Euphytica* 14, 170–172. doi: 10.1007/BF00038983

Anamthawat-Jónsson, K., and Reader, S. M. (1995). Pre-annealing of total genomic DNA probes for simultaneous genomic *in situ* hybridization. *Genome* 38, 814–816. doi: 10.1139/g95-104

Ardenghi, N. M. G., and Foggi, B. (2015). Lectotypification and combination of *Festuca apennina* (Poaceae). *Taxon* 64, 1038–1041. doi: 10.12705/645.14

Borrill, M., Tyler, B. F., and Morgan, W. G. (1976). Studies in *Festuca* 7. Chromosome atlas (Part 2), an appraisal of chromosome race distribution and ecology, including *F. pratensis* var. *apennina* (De Not.) Hack– tetraploid. *Cytologia* 41, 219–236. doi: 10.1508/cytologia.41.219

Canter, P. H., Pašakinskiene, I., Jones, R. N., and Humphreys, M. W. (1999). Chromosome substitution and recombination in the amphiploid *Lolium*

perenne x *Festuca pratensis* cv. Prior (2n=4x=28). *Theor. Appl. Genet.* 98, 809–814. doi: 10.1007/s001220050087

Clarke, J., Chandrasekharan, P., and Thomas, H. (1976). Studies in *Festuca* 9. Cytological studies of *Festuca pratensis* var. *apennina* (De Not) Hack. (2n=28). *Z. Pflanzenzüchtg.* 77, 205–214.

De Notaris, G. (1844). *Repertorium Florae Ligusticae*. Taurini [Turin]: Ex Regio Typographeo.

Devesa, J. A., Catalán, P., Müller, J., Cebolla, C., and Ortúñez, E. (2013). Checklist of *Festuca* L. (Poaceae) in the Iberian Peninsula. *Lagascalia* 33, 183–274.

Doležel, J., Greilhuber, J., Lucretti, S., Meister, A., Lysák, M., Nardi, L., et al. (1998). Plant genome size estimation by flow cytometry: interlaboratory comparison. *Ann. Bot.* 82, 17–26. doi: 10.1006/anbo.1998.0730

Doležel, J., Greilhuber, J., and Suda, J. (2007). Estimation of nuclear DNA content in plants using flow cytometry. *Nat. Protocols* 2, 2233–2244. doi: 10.1038/nprot.2007.310

Foggi, B., and Müller, J. (2009). (last updated Apr 2015). "Schedonorus," in *Poaceae. Euro+Med Plantbase - The Information Resource for Euro-Mediterranean Plant Diversity*, eds B. Valdés and H. Scholz, Available online at: http://ww2.bgbm.org/EuroPlusMed/ (Accessed on May 28, 2016).

Ghesquiere, M., Humphreys, M. W., and Zwierzykowski, Z. (2010). "Festulolium," in *Fodder Crops and Amenity Grasses, Book Series: Handbook of Plant Breeding*, Vol. 5, eds B. Boller, U. K. Posselt, and F. Veronesi (New York, NY; Dordrecht; Heidelberg; London: Springer Science+Business Media), 293–316.

Harper, J. A., Thomas, A., Armstead, I. P., James, C., Gasior, D., Bisaga, M., et al. (2011). Alien introgression in the grasses *Lolium perenne* (perennial ryegrass) and *Festuca pratensis* (meadow fescue) - the development of seven monosomic substitution lines and their molecular and cytological characterisation. *Ann. Bot.* 107, 1313–1321. doi: 10.1093/aob/mcr083

Harper, J. A., Thomas, I. D., Lovatt, J. A., and Thomas, H. M. (2004). Physical mapping of rDNA sites in possible diploid progenitors of polyploid Festuca species. *Plant Syst. Evol.* 245, 163–168. doi: 10.1007/s00606-003-0110-2

Humphreys, J., Harper, J. A., Armstead, I. P., and Humphreys, M. W. (2005). Introgression-mapping of genes for drought resistance transferred from *Festuca arundinacea* var. *glaucescens* into *Lolium multiflorum*. *Theor. Appl. Genet.* 110, 579–587. doi: 10.1007/s00122-004-1879-2

Humphreys, M. W., and Harper, J. A. (2008). Festulolium loliaceum, an understudied natural UK grass hybrid species that may provide benefits to UK grasslands withstanding the onsets of climate change. *Crop Wild Rel.* 6, 7–9.

Humphreys, M. W., O'Donovan, S. A., Farrell, M. S., Gay, A. P., and Kingston-Smith, A. H. (2014). The potential of novel Festulolium (2n=4x=28) hybrids as productive, nutrient-use-efficient fodder for ruminants. *Food Ener. Security* 3, 98–110. doi: 10.1002/fes3.50

Humphreys, M., Thomas, H. M., Harper, J., Morgan, G., James, A., Zare, A. G., et al. (1997). Dissecting drought- and cold-tolerance traits in the Lolium-Festuca complex by introgression mapping. *New Phytol.* 137, 55–60. doi: 10.1046/j.1469-8137.1997.00832.x

Humphreys, M. W., Thomas, H. M., Morgan, W. G., Meredith, M. R., Harper, J. A., Thomas, H., et al. (1995). Discriminating the ancestral progenitors of hexaploid *Festuca arundinacea* using genomic *in situ* hybridization. *Heredity* 75, 171–174. doi: 10.1038/hdy.1995.120

Humphreys, M. W., Yadav, R. S., Cairns, A. J., Turner, L. B., Humphreys, J., and Skøt, L. (2006). A changing climate for grassland research. *New Phytol.* 169, 9–26. doi: 10.1111/j.1469-8137.2005.01549.x

Jauhar, P. P. (1975). Genetic control of diploid-like meiosis in hexaploid tall fescue. *Nature* 254, 595–597. doi: 10.1038/254595a0

Jauhar, P. P. (1993). *Cytogenetics of the Festuca-Lolium Complex. Relevance to Breeding.* Monographs on Theoretical and Applied Genetics No. 18. Berlin: Springer-Verlag.

Kopecký, D., Bartoš, J., Zwierzykowski, Z., and Doležel, J. (2009). Chromosome pairing of individual genomes in tall fescue (*Festuca arundinacea* Schreb.), its progenitors, and hybrids with Italian ryegrass (*Lolium multiflorum* Lam.). *Cytogenet. Genome Res.* 124, 170–178. doi: 10.1159/000207525

Kopecký, D., Havránková, M., Loureiro, J., Castro, S., Lukaszewski, A. J., Bartoš, J., et al. (2010). Physical distribution of homoeologous recombination in individual chromosomes of *Festuca pratensis* in *Lolium multiflorum*. *Cytogenet. Genome Res.* 129, 162–172. doi: 10.1159/000313379

Kopecký, D., Loureiro, J., Zwierzykowski, Z., Ghesquière, M., and Doležel, J. (2006). Genome constitution and evolution in *Lolium* x *Festuca* hybrid cultivars (Festulolium). *Theor. Appl. Genet.* 113, 731–742. doi: 10.1007/s00122-006-0341-z

Kopecký, D., Lukaszewski, A. J., and Doležel, J. (2008a). Meiotic behavior of individual chromosomes of *Festuca pratensis* in tetraploid *Lolium multiflorum*. *Chromosome Res.* 16, 987–998. doi: 10.1007/s10577-008-1256-0

Kopecký, D., Lukaszewski, A. J., and Doležel, J. (2008b). Cytogenetics of Festulolium (*Festuca* × *Lolium* hybrids). *Cytogenet. Genome Res.* 120, 370–383. doi: 10.1159/000121086

Kopecký, D., Martis, M., Cíhalíková, J., Hřibová, E., Vrána, J., Bartoš, J., et al. (2013). Flow sorting and sequencing meadow fescue chromosome 4F. *Plant Physiol.* 163, 1323–1337. doi: 10.1104/pp.113.224105

Lewis, E. J. (1977). Studies in *Festuca*, I. V. A phyletic study of *Festuca pratensis* var. *apennina* (De Not.) Hack., hybridization with synthetic tetraploid *F. pratensis* Huds. *Genetica* 47, 59–64. doi: 10.1007/BF00122440

Lewis, E. J., Humphreys, M. W., and Caton, M. P. (1980). Disomic inheritance in *Festuca arundinacea* Schreb. *Z. Pflanzenzüchtg.* 84, 335–341.

Macleod, C. J. A., Humphreys, M. W., Whalley, W. R., Turner, L., Binley, A., Watts, C. W., et al. (2013). A novel grass hybrid to reduce flood generation in temperate regions. *Sci. Rep.* 3:1683. doi: 10.1038/srep01683

Morgan, W. G., Thomas, H., and Lewis, E. J. (1988). Cytogenetic studies of hybrids between *Festuca gigantea* Vill. and Lolium multiflorum Lam. *Plant Breed.* 101, 335–343. doi: 10.1111/j.1439-0523.1988.tb00306.x

Stebler, F. G. (1904). Jahresbericht der Schweizerischen Samenuntersuchungs- und Kontrollstation Zürich. *Schweiz. Landw. Jahrbuch* 18, 43.

Thomas, H. M., Harper, J. A., Meredith, M. R., Morgan, W. G., and King, I. P. (1997). Physical mapping of ribosomal DNA sites in *Festuca arundinacea* and related species by *in situ* hybridization. *Genome* 40, 406–410. doi: 10.1139/g97-054

Thomas, H. M., Harper, J. A., Meredith, M. R., Morgan, W. G., Thomas, I. D., Timms, E., et al. (1996). Comparison of ribosomal DNA sites in Lolium species by fluorescence *in situ* hybridization. *Chromosome Res.* 4, 486–490. doi: 10.1007/BF02261775

Thomas, H. M., Morgan, W. G., Meredith, M. R., Humphreys, M. W., and Leggett, J. M. (1994). Identification of parental and recombined chromosomes in hybrid derivatives of *Lolium multiflorum* x *Festuca pratensis* by genomic *in situ* hybridization. *Theor. Appl. Genet.* 88, 909–913. doi: 10.1007/BF00220795

Tyler, B. F. (1988). "Description and distribution of natural variation in forage grasses," in *Proceedings of the Eucarpia Fodder Crops Section Meeting* (Lusignan), 13–22.

Tyler, B. F., Borrill, H., and Chorlton, K. H. (1978). Studies in *Festuca pratensis* and tetraploid *F.* pratensis var. *apennina* in relation to their altitudinal distribution. *J. Appl. Ecol.* 15, 219–226. doi: 10.2307/2402932

Tyler, B. F., and Chorlton, K. H. (1974). Growth rhythm studies on Festuca collected in Western Europe in 1971. *Rep. Welsh Pl. Breed.* 1973, 21–22.

St. Yves, A. (1913). Les Festuca de la section Eu-Festuca et leurs variations dans les Alpes Maritimes. *Annuaire Conservatoire Jardin Botaniques Geneve* 42, 1–218.

Zwierzykowski, Z., Kosmala, A., Zwierzykowska, E., Jones, N., Joks, W., and Bocianowski, J. (2006). Genome balance in six successive generations of the allotetraploid *Festuca pratensis* x *Lolium perenne*. *Theor. Appl. Genet.* 113, 539–547. doi: 10.1007/s00122-006-0322-2

Conflict of Interest Statement: The authors declare that the research was conducted in the absence of any commercial or financial relationships that could be construed as a potential conflict of interest.

The reviewer DP and handling Editor declared their shared affiliation, and the handling Editor states that the process nevertheless met the standards of a fair and objective review.

Advantages of publishing in Frontiers

OPEN ACCESS
Articles are free to read, for greatest visibility

COLLABORATIVE PEER-REVIEW
Designed to be rigorous – yet also collaborative, fair and constructive

FAST PUBLICATION
Average 85 days from submission to publication (across all journals)

COPYRIGHT TO AUTHORS
No limit to article distribution and re-use

TRANSPARENT
Editors and reviewers acknowledged by name on published articles

SUPPORT
By our Swiss-based editorial team

IMPACT METRICS
Advanced metrics track your article's impact

GLOBAL SPREAD
5'100'000+ monthly article views and downloads

LOOP RESEARCH NETWORK
Our network increases readership for your article

Frontiers
EPFL Innovation Park, Building I • 1015 Lausanne • Switzerland
Tel +41 21 510 17 00 • Fax +41 21 510 17 01 • info@frontiersin.org
www.frontiersin.org

Find us on